

Cover
Type reversed
PIN 5261

UNITED STATES
DEPARTMENT OF THE INTERIOR
GEOLOGICAL SURVEY

PROCEEDINGS OF THE SYMPOSIUM ON
"THE NEW MADRID SEISMIC ZONE"

NOVEMBER 26, 1984
RESTON, VIRGINIA



This report is preliminary and has not been edited or reviewed for conformity with U.S. Geological Survey publication standards and stratigraphic nomenclature. The views and conclusions contained in this document are those of the authors and should not be interpreted as necessarily representing the official policies, either expressed or implied, of the United States Government. Any use of trade names and trademarks in this publication is for descriptive purposes only and does not constitute endorsement by the U.S. Geological Survey.

Reston, Virginia
1984

2011
**UNITED STATES
DEPARTMENT OF THE INTERIOR
GEOLOGICAL SURVEY**

**PROCEEDINGS OF THE SYMPOSIUM ON
"THE NEW MADRID SEISMIC ZONE"**

**November 26, 1984
Reston, Virginia**

**Convenor and Organizer
Otto W. Nuttli
St. Louis University
St. Louis, Missouri**

**Editors
Paula L. Gori and Walter W. Hays
U.S. Geological Survey
Reston, Virginia 22092**

Open File Report 84-770

**Compiled by
Carla J. Kitzmiller**

This report is preliminary and has not been edited or reviewed for conformity with U.S. Geological Survey publication standards and stratigraphic nomenclature. The views and conclusions contained in this document are those of the authors and should not be interpreted as necessarily representing the official policies, either expressed or implied, of the United States Government. Any use of trade names and trademarks in this publication is for descriptive purposes only and does not constitute endorsement by the U.S. Geological Survey.

**Reston, Virginia
1984**

①

Preface

The greatest sequence of earthquakes in the history of the United States occurred in the winter of 1811-1812 in New Madrid, Missouri. To commemorate the importance of these earthquakes, 150 scientists, professors, teachers, students, engineers, emergency planners, and private citizens attended a symposium on the "New Madrid Seismic Zone" at the Southeast Missouri State University in Cape Girardeau, Missouri, April 27-28, 1984. The purpose was to discuss these earthquakes and the geology, geophysics, and seismicity of the central Mississippi Valley area and to identify the increase in knowledge during the past decade.

The papers appearing in this open-file report were presented at the symposium which was held in conjunction with the annual meeting of the Missouri Academy of Sciences in Cape Girardeau. The symposium was sponsored by the Missouri Academy of Sciences and the U.S. Geological Survey (USGS). The symposium was organized by Otto Nuttli of Saint Louis University. Donald H. Froemsdorf, President-Elect of the Academy and Dean of the College of Science and Technology of Southeast Missouri State University, and Walter W. Hays and Paula L. Gori, Office of Earthquakes, Volcanoes, and Engineering of the USGS, provided assistance for the symposium and published this document.

Sponsorship of the symposium by the USGS represents one of the first activities conducted under the new USGS's "Regional Earthquake Hazards Assessment" element of the National Earthquake Hazards Reduction Program. The objectives of the element are:

- 1) Compile and synthesize geologic and geophysical data needed for evaluating the earthquake hazards of ground-shaking, ground failure, surface fault rupture, and tectonic deformation and for assessing the risk in broad geographic regions containing important urban areas.
- 2) Foster an environment for implementation, creating partnerships and providing high-quality scientific information that can be used by local governments to devise and implement loss-reduction measures, such as building codes, zoning ordinances, and personal preparedness.

The Regional Earthquake Hazards Assessment element has five interrelated components. They are:

- 1) Information Systems--The goal is to produce quality data along with a comprehensive information system, available to both internal and external users for use in earthquake hazards evaluations, risk assessment, and implementation of loss-reduction measures.
- 2) Synthesis of Geological and Geophysical Data for Evaluation of Earthquake Hazards--The goal is to produce synthesis reports describing the state-of-knowledge about earthquake hazards (ground shaking, surface faulting, earthquake-induced ground failure, and tectonic deformation) in the region and to recommend future research to increase the state-of-knowledge required for the creation and implementation of loss-reduction measures.
- 3) Ground Motion Modeling--The goal is to produce deterministic and probabilistic ground-motion models and maps of the ground-shaking hazard with commentaries on their use.

- 4) Loss Estimation Modeling--The goal is to devise economical methods for acquiring inventories of structures and lifeline systems in urban areas, to create a standard model and commentary for loss estimation, and to produce loss and casualty estimates for urban areas.
- 5) Implementation--The goal is to foster the creation and implementation of hazard-reduction measures in urban areas, providing high-quality scientific information that can be used by local government decisionmakers as a basis for calling for change.

Research focusing on one or more of the five components is presently being conducted in the following areas:

- | | |
|----------------------------|-------------------------------------|
| 1) Wasatch front, Utah | 6) Mississippi Valley |
| 2) Southern California | 7) Puerto Rico |
| 3) Northern California | 8) Charleston, South Carolina |
| 4) Anchorage, Alaska | 9) Buffalo-Rochester area, New York |
| 5) Puget Sound, Washington | 10) Boston area, Massachusetts |

In each area, the research is performed by using the resources of the USGS's internal and external program (the external program is implemented through grants and contracts awarded annually following a program announcement). The goal is to achieve maximum synergism of State, local, and Federal resources. Strategies for this element are to foster strong partnerships with universities, local government agencies, other State and Federal agencies, and the private sector, as well as to strengthen existing programs and partnerships. Another strategy is to take advantage of earthquakes, postearthquake investigations, past research studies, and other activities.

Walter W. Hays
Office of Earthquakes, Volcanoes
and Engineering
U.S. Geological Survey

Paula L. Gori
Office of Earthquakes, Volcanoes
and Engineering
U.S. Geological Survey

Otto W. Nuttli
Department of Earth and
Atmospheric Sciences
Saint Louis University

(3) (44)

(new odd pg)

Table of Contents

Evaluation of the Symposium on the New Madrid Seismic Zone
by Paula Gori..... 1

New Madrid Seismic Zone: Part I: Historical Review of Studies and Part II:
Contemporary Studies by the U.S. Geological Survey
by Frank McKeown..... 6

The Central Mississippi Valley Earthquakes of 1811-1812
by Ronald Street and Otto Nuttli..... 33

Sedimentary Geology of the New Madrid Seismic Zone
by Thomas Buschbach and H. R. Schwalb..... 64

Use of Earth Resistivity and Gravity with Drilling for Shallow Exploration
in the Reelfoot Lake Region
by Richard Stearns..... 97

Seismic-Refraction Studies of the Mississippi Embayment: An Overview
by Walter Mooney and Mary Andrews.....138

Rift Structures of the Northern Mississippi Embayment From the Analysis
of Gravity and Magnetic Data
by Thomas Hilderbrand.....168

Tectonic Development of the New Madrid Seismic Zone
by Lawrence Braile, William Hinze, John Sexton, G. Randy Keller,
and Edward Lidiak.....204

Anomalous Crust and Upper Mantle Properties in the New Madrid Area
by Brian Mitchell, James Kohsmann, and Haydar Al-Shukri.....234

The Seismicity of the New Madrid Seismic Zone
by Robert Herrmann.....267

Recurrence Rates and Probability Estimates for the New Madrid Seismic Zone
by Arch Johnston and Susan Nava.....279

Source Characteristics and Strong Ground Motion of New Madrid Earthquakes
by Otto Nuttli and Robert Herrmann.....330

Earthquake-Induced Landslide Potential for the Central Mississippi Valley,
Tennessee and Kentucky
by Randall Jibson and David Keefer.....353

Liquefaction Potential for the Central Mississippi Valley
by Stephen Obermeier.....391

A Look at the Present State-Of-Knowledge on Earthquake Hazards in the
New Madrid Seismic Zone and Suggestions for Future Research
by Walter Hays.....447

Participants List.....462

(5)

(64)

EVALUATION OF THE SYMPOSIUM ON THE NEW MADRID SEISMIC ZONE

by

Paula Gori

U.S. Geological Survey

Reston, Virginia 22092

At the conclusion of the one-and a-half day symposium on the New Madrid Seismic Zone, held in Cape Girardeau, Missouri, on April 27-28, 1984, participants were asked to evaluate the meeting, rating the value of the discussions and activities and the benefits to them and their organization. The symposium was designed to define the ground-shaking and ground failure hazards in terms of the geology, geophysics, and seismicity of the New Madrid Seismic Zone.

Responses were elicited on a five-point scale, 1 and 2 representing the lowest level of agreement, 3 moderate agreement, and 4 and 5 highest agreement (see Figure 1). Since not all respondents answered all the questions, percentages are based only on those who submitted evaluations (see Figure 2).

Evaluations returned by 51 participants indicated that the symposium was successful in meeting its goals. Eighty-six percent of the evaluators thought that the symposium did a "good to excellent" job of defining the geology of the New Madrid Seismic Zone. Ninety-four percent thought that the symposium did a "good to excellent" job of defining the geophysical parameters of the New Madrid Seismic Zone, and 92% of the evaluators thought that the symposium did a "good to excellent" job of defining the seismicity of the zone. Eighty-eight percent of the evaluators thought that the symposium did a "moderate to



excellent" job of defining the nature and extent of ground failure hazards. Clearly, the participants valued the technical information presented at the meeting.

Evaluators also felt that the symposium benefited them and their organization. Ninety-four percent agreed that the symposium provided new sources of information and expertise that could be used in the future, and 98% agreed that the symposium established better understanding of the extent of the earthquake ground-shaking and ground failure hazards in the Central United States.

To determine which activities were viewed as the most useful, in the communication process, participants were asked to rate formal presentations, follow-up discussions, informal discussions, and materials such as notebooks and abstracts. Formal presentations were rated very highly, with 76% of the evaluators giving a "good to excellent" rating and 18% giving a "moderate rating." Discussions following formal presentations were rated less favorably with 43% giving a "high rating" and 49% a "moderate rating." This rating documents the fact that insufficient time was programmed for questions and discussion. Since no time was set aside for breaks, informal discussions during breaks and after hours were given relatively "low marks" with 66% of the evaluators giving "moderate to high" ratings. Clearly, the notebooks containing abstracts of the presentations were considered valuable by the evaluators, with 84% rating them as "good to excellent."

The importance attached to this symposium is shown in the response of 98% of those submitting evaluation that they would, knowing what to expect, attend

a similar meeting. The same percentage of the respondents strongly agreed that future meetings should be planned to continue the work initiated at this symposium.

Individuals were given an opportunity to make comments and to criticize the symposium. The goal was to receive constructive suggestions of ways to improve future meetings. Many respondents took the time to personalize their suggestions. Most comments were enthusiastic about the subject matter and many of the presentations. However, a large number of evaluators commented on the apparent lack of preparations on the part of some speakers. Also the lack of an adequate sound system and the uncomfortable temperature and layout of the meeting facility detracted from the quality of many of the presentations.

Many of the participants noted that the symposium was an enriching educational experience, notable for the diversity of the subject matter and quality of research. Many felt that additional symposiums (or meetings) on the same subject as well as related subjects would be well attended, especially those dealing with engineering and design implications and emergency response and land-use planning issues in the Central United States.

FIGURE 1
Evaluations of the Symposium by Individual Participants

| | Low | | High | | |
|--|-------|---|------|-------|----|
| 1. Did you find the symposium to be useful for defining: | 1 & 2 | | 3 | 4 & 5 | |
| a. The geology of the New Madrid Seismic Zone | 1 | 2 | 4 | 26 | 18 |
| b. The geophysics of the New Madrid Seismic Zone | 1 | 1 | 7 | 19 | 24 |
| c. The seismicity of the New Madrid Seismic Zone | | 1 | 2 | 17 | 30 |
| d. The nature and extent of ground failure hazards in the New Madrid Seismic Zone | | 4 | 11 | 23 | 11 |
| 2. Did the symposium benefit you or your organization by: | | | | | |
| a. Providing new sources of information and expertise you might want to utilize in the future? | 1 | 2 | 9 | 6 | 23 |
| b. Establishing better understanding of the extent of the earthquake and ground failure hazards in the Central United States? | | 1 | 14 | 22 | 14 |
| 3. Did you find the following activities useful: | | | | | |
| a. Formal presentations? | 2 | | 9 | 13 | 26 |
| b. Discussions following the formal presentations? | 2 | 2 | 25 | 14 | 8 |
| c. Notebook and abstracts? | | 1 | 7 | 18 | 25 |
| d. Informal discussions during breaks and after hours? | | 7 | 14 | 15 | 5 |
| | | | Yes | No | |
| 4. If the clock were turned back and the decision to attend the symposium were given to you again, would you want to attend? | | | 50 | 1 | |
| 5. Should future symposiums be planned to continue the work initiated at this meeting? | | | 50 | | |
| 6. Use the remaining portion of this page and the back if necessary for comments and criticisms of the symposium and suggestions on how other meetings of this type might be improved. | | | | | |

FIGURE 2
Evaluation of the Symposium by Percentages of Participants

| | Low | | High |
|--|-------|-----|-------|
| | 1 & 2 | 3 | 4 & 5 |
| 1. Did you find the symposium to be useful for defining: | | | |
| a. The geology of the New Madrid Seismic Zone | 6% | 8% | 86% |
| b. The geophysics of the New Madrid Seismic Zone | 2% | 14% | 84% |
| c. The seismicity of the New Madrid Seismic Zone | 2% | 4% | 92% |
| d. The nature and extent of ground failure hazards in the New Madrid Seismic Zone | 8% | 22% | 66% |
| 2. Did the symposium benefit you or your organization by: | | | |
| a. Providing new sources of information and expertise you might want to utilize in the future? | 6% | 18% | 76% |
| b. Establishing better understanding of the extent of the earthquake and ground failure hazards in the Central United States? | 2% | 27% | 71% |
| 3. Did you find the following activities useful: | | | |
| a. Formal presentations? | 4% | 18% | 76% |
| b. Discussions following the formal presentations? | 8% | 49% | 43% |
| c. Notebook and abstracts? | 2% | 14% | 84% |
| d. Informal discussions during breaks and after hours? | 14% | 27% | 39% |
| | | Yes | No |
| 4. If the clock were turned back and the decision to attend the symposium were given to you again, would you want to attend? | | 98% | 2% |
| 5. Should future symposiums be planned to continue the work initiated at this meeting? | | 98% | |
| 6. Use the remaining portion of this page and the back if necessary for comments and criticisms of the symposium and suggestions on how other meetings of this type might be improved. | | | |

**NEW MADRID SEISMIC ZONE,
PART I: HISTORICAL REVIEW OF STUDIES
and
PART II: CONTEMPORARY STUDIES BY THE U.S. GEOLOGICAL SURVEY
by
F. A. McKeown
U.S. Geological Survey
Denver, Colorado 80225**

INTRODUCTION

This paper is a revision of a paper given by me at the New Madrid Seismic Zone Symposium at Cape Girardeau, Missouri, on April 27, 1984 and entitled "New Madrid Seismic Zone: Overall perspective and significance of studies." Because of the wide range in content of the Cape Girardeau version and resultant disparity in tenor of the subjects described in it, a clear division in the subject matter seemed necessary. This revision therefore is divided into two parts and is in essence two reports. The first part is an historical review of studies published before 1983; the second part is a review of studies recently completed or still in progress by U.S. Geological Survey personnel.

PART I: HISTORICAL REVIEW OF STUDIES

INTRODUCTION

The earliest description by a geologist of the effects of the New Madrid sequence of earthquakes was that of Sir Charles Lyell (1849). His description of the effects, some 38 years after the earthquakes, was probably as detailed and accurate as could be made. It contained little, however, that was useful in deciphering the geologic structure to which the earthquakes might be related. This was to be expected of much of the descriptive material by eyewitness accounts and by later observers. These old accounts have proved invaluable, however, to the construction of isoseismal maps such as by Nuttli (1973), Stearns and Wilson (1972) and Street (1982). It was not until 100 years after the earthquakes that Fuller (1912) suggested physically reasonable

explanations of many phenomena associated with the earthquake. His report contained not only much descriptive material, cited from the literature and from personal observation, but also a geologically plausible explanation of the origin of the earthquakes. The two most popular explanations until then were that the earthquakes were related to volcanism or electricity. Fuller recognized the importance of faulting and suggested the following origin.

"The best evidence of origin is that afforded by the distance to which the vibrations were felt. It does not seem possible to conceive of a shock originating in soft embayment deposits being transmitted to the hard rocks and thence across the Appalachians to the Atlantic Coast on the east and across the central coal basin to Chicago, Detroit, and Canada. The fact that the shocks were strongly felt at these localities seems to point conclusively to a deep-seated origin in rigid rocks. A faulting in the hard Paleozoic rocks seems, therefore, to be the only probable explanation."

Considering how little was known in 1912 about earthquake source zones and seismic waves Fuller's reasoning and explanation show remarkable insight. He also recognized that most of the disturbance from the earthquakes was in a linear zone, which in his terminology was the centrum. This linear zone is now well recognized from seismicity and geophysical studies. Lastly, he recognized, as we now do, the great amount of damage that could be caused by a repetition of the New Madrid sequence of earthquakes.

An important concept about the relationship of seismicity to an inferred major geologic structure in the central United States was suggested by Wollard (1958). In a discussion of the Mississippi Valley earthquakes he noted an alignment of them extended to the St. Lawrence River valley and suggested that a major "structural break" was related to the earthquakes. If such a structural break did exist and was related to earthquakes, it would have a great impact on assessments of seismic risk in central and northeastern United States. More recent data, however, do not support the existence of a continuous major structural break.

In a study of the Illinois-Kentucky mining district, Heyl and Brock (1961) suggested that the district was at the intersection of two major fault zones. One of these they defined as the New Madrid fault zone extending from near Vincennes, Ind., southwest to beyond New Madrid, Mo. The other is the Rough Creek-Shawneetown fault zone, which Heyl later incorporated into the 38th Parallel Lineament (1972). The evidence used to define the New Madrid zone is the northeast-trending faults in the Wabash valley area and in the Illinois-Kentucky mining district, which, if projected southwestward, is coextensive with the northeast alignment of epicenters in the northern Mississippi embayment. This concept of the New Madrid fault zone is a plausible explanation of a seismogenic structure particularly because earthquakes in the Wabash valley area seemed to be associated with the Wabash valley fault zone. Data now available, however, show that the earthquakes in the Wabash valley and the New Madrid area are related to a much more complex structural framework than a single fault zone.

In the 1960's, interpretations of geologic and geophysical data were not made in terms of plate tectonics or in terms of rifts if the area under study was in a so-called stable continental interior. However, the concept of an incipient rift in the upper Mississippi embayment was recorded at a meeting of the Society of Economic Geologists at the United Nations, New York, N.Y., on March 10, 1966 (White, 1967). The purpose of the meeting was to discuss the latest knowledge of the origin of lead-zinc-barite-fluorite deposits in carbonate rock. In response to a question about the possibility of there being a rift in the embayment, A. V. Heyl of the U.S. Geological Survey suggested on the basis of the distribution of alkalic rocks and a gravity high that perhaps an incipient rift was present in the embayment (White, 1967, p. 382). This concept, according to Heyl, was based in large part on an unrecorded interpretation of gravity data by the late Henry R. Joesting (1966) of the U.S. Geological Survey. Joesting's interpretation of the gravity high in the embayment was that it indicated that the earth's crust had thinned and that dense mantle material had upwelled to produce the gravity high (A. V. Heyl and L. E. Cordell, U.S. Geological Survey, oral commun., 1984). This interpretation of relatively scant gravity data is much the same as current interpretations of more recent and much more detailed gravity, magnetic, and seismic data.

That earthquakes in the New Madrid region may be related to a rift system similar to those in east Africa was suggested by Kumarapeli and Saull (1966). Part of their argument was similar to that of Wollard, namely that an alignment of epicenters runs from New Madrid to the St. Lawrence Valley. They included other evidence such as highly alkalic igneous rocks, diatremes, and carbonatites that are abundant in and near intracratonic rifts. Some or all of these features are common to the St. Lawrence Valley area, the Illinois-Kentucky mining district, igneous rock penetrated by exploratory oil test wells in the Mississippi embayment, and the Magnet Cove mining district of Arkansas. They also noted that the dimensions of the proposed rifts in North America are similar to those of most rift valleys worldwide. The rift system proposed by Kumarapeli and Saull in 1966 was imaginative, and had considerable merit, but was severely criticised. One of the most severe criticisms was that the St. Lawrence region is now under compression and not extension as they had proposed (Voight, 1969), and therefore contemporary earthquakes in the region could not be the results of an extensional stress regime that would cause rifting. In a subsequent paper, Kumarapeli (1976) recognized that seismicity in the region may be the result of release of compressional stresses on faults in an old rift system. This is a concept that is well accepted today for many seismically active areas, including the New Madrid region.

In 1973 the concept of a buried rift in the upper Mississippi embayment gained more stature when Burke and Dewey (1973) proposed that a triple junction was located near Jackson, Miss., during late Paleozoic time. They suggested that two of the arms of this junction became spreading centers and formed a continental edge. The third arm failed to spread and was thought to extend northward into the continent and to have become the Mississippi embayment. It should be remembered that until about 1974 very little geophysical data was available for the embayment that could provide a basis for interpreting subsurface structure. Furthermore, the data that did exist was generally not interpreted in the context of plate tectonics. Ervin and McGinnis (1975) were among the first to make a rigorous effort to integrate plate tectonic concepts with available geologic and geophysical data. They outlined the development of a rift, which they named the Reelfoot rift, that started in early Paleozoic time. Their interpretation of the available data was a major contribution to concepts and initial understanding of the structural history of the embayment. Briefly,

they proposed arching and rifting of the crust as the result of mantle upwelling in late Precambrian time. This was followed by isostatic subsidence in early Paleozoic, uplift in middle Paleozoic and Mesozoic times, and rift reactivation and intrusions in late Mesozoic time. Much new data have been acquired and interpreted since this structural history was proposed, but no fundamental changes in the concept have been made.

As indicated in the text of this paper thus far, concepts of the geologic framework of the New Madrid seismic zone evolved without much of the kind of data needed to define deep subsurface structure to which earthquakes may be related. Financial support from the Earthquake Hazards Reduction Program of the U.S. Geological Survey starting in 1974, and from the Nuclear Regulatory Commission starting in 1976, provided the means to undertake multidisciplinary studies on a scale never before possible in the New Madrid region. Impetus for the studies came from the growing awareness of the great amount of damage and probable loss of life should an earthquake sequence like that of 1811-12 occur today. Earlier Fuller (1912, p. 110) and a few other individuals had recognized this risk, but the means, expertise, and public interest were not adequate to initiate large scale projects. In order to mitigate the risk, more detailed understanding of the seismicity and geology of the region was needed. Seismic networks were established. Gravity surveys, aeromagnetic surveys, and a variety of geologic studies were conducted. And most recently, seismic exploration methods were used. As a result, the geologic framework with which the New Madrid earthquakes are associated is now well, though not perfectly understood. Also, estimates of the recurrence intervals have been made and the source mechanisms of the earthquakes are reasonably well known. The new data have provided a basis for revising source zones from which probabilistic estimates of ground motion can be made (Algermissen and others, 1982). Much of the new data have been published in scientific journals, in U.S. Geological Survey Professional Paper 1236, and in NUREG publications of the NRC. A detailed summary of these published data is not within the scope of this paper nor is it appropriate. Some of the most significant results in these studies are briefly stated below; all are described more fully in several chapters in Professional Paper 1236 (McKeown and Pakiser, 1982).

- 1) Aeromagnetic and gravity data indicate a buried rift in the upper Mississippi embayment about 70 km wide, more than 200 km long, and with 2-3 km of structural relief.
- 2) More than 90 percent of contemporary earthquakes in the region occurs along an axial zone within the rift.
- 3) A northeast extension of the rift in the Wabash valley region has been proposed.
- 4) Geomorphic studies indicate Holocene uplift and faulting in the Reelfoot Lake area. Of most significance, these studies also indicate a recurrence interval of about 600 years for earthquakes large enough to produce ground motion great enough to liquefy sand in the alluvium of the New Madrid region.
- 5) Seismicity studies show right lateral strike-slip movement on northeast-trending faults and reverse movement on northwest-trending faults; from these mechanisms the maximum principal stress is inferred to be oriented east-west. This stress direction is about 90° from that which produced the rift.

SIGNIFICANCE OF NEW MADRID SEISMIC ZONE STUDIES

It is appropriate in this part to consider the significance of New Madrid seismic zone studies. Hundreds of manyears and millions of dollars have been expended to reach the present level of understanding of New Madrid seismicity and application of this understanding to assesments of seismic hazard. The results and importance of this large expenditure is commonly not recognized by society for several reasons, apathy probably being formost. This is understandable because the lack of any large earthquakes in the region since the 1811-12 series quite naturally dulls societies perception of the damage and loss of life that would occur should a similar series occur in the near future.

It is worthwhile to consider some of the benefits to various segments of society that have resulted, or may yet result, from studies related to the New

Madrid seismic zone. Of most importance to everyone is the information on recurrence intervals of earthquakes and the extent of the active seismic zone, both of which are needed to make justifiable assessments of seismic hazards. Until about 1979 no strong arguments could be made for what the recurrence interval of large earthquakes in the New Madrid region might be. The current estimates of 600-700 years based independently on seismologic and geologic data may have a large uncertainty. If data were available to make additional estimates of recurrence intervals they very likely would show a greater range in time. Nevertheless, prior to these estimates no defensible arguments could be given for statements that a New Madrid type sequence of earthquake could occur within any particular range of time.

The problem of delimiting the extent of the active seismic zone is probably resolved better than the question of recurrence intervals. Interpretation of a rift and recognition that most seismicity in the New Madrid region occurs within the rift provides a strong argument to delimit the likely extent of the seismically active zone.

Of less tangible importance, the manner in which the New Madrid seismic zone studies were conducted is worthy of note. They are an excellent example of the value of large-scale, multidisciplinary efforts. The concept of a buried ancient rift in the upper Mississippi embayment had been suggested by several investigators when very little information was available. Strong support for, if not absolute proof of the rift, however came only after acquisition of a large amount of data and application of new techniques. Further, the close association of seismicity with the rift could only be recognized after operation of a seismographic network designed to improve greatly the accuracy of epicenters. These and results from other disciplines demonstrated the importance and effectiveness of large scale multidisciplinary efforts. No one discipline or small-scale effort could possibly be expected to provide the amount and kind of information needed to make defensible judgments on seismic hazards.

In addition to the importance of the New Madrid seismic zone studies to hazard assessments, the studies have been synergistic and of considerable importance to several fields of earth science. An academic perspective is that they have resulted in developing a fairly detailed understanding of a major

crustal structure that was at best a tentative hypothesis less than 20 years ago. The post-Cretaceous subsidence and depositional history of the Mississippi embayment had been reasonably well known for many years; the pre-Cretaceous history, however, was largely speculative.

As a serendipitous and synergistic byproduct of studies of the New Madrid seismic zone by the governmental and academic communities, a major effort by the oil industry was undertaken to explore for oil and gas reservoirs in the rift. Exploration in the Upper Mississippi embayment for oil and gas has been done very sporadically since about the late 1920's with little geologic bases for the location of exploratory drill holes. After the Reelfoot Rift was defined from aeromagnetic and gravity surveys, several individuals and companies in the oil industry recognized that the rift probably contains clastic rocks with the potential of being reservoirs for oil or gas. The results of their explorations have not been made public and the exploration activity has stopped. It is reasonable to expect new activity however if the price of oil and gas rise as they most surely will in the long term. Release of only a small part of the very large amount of seismic reflection surveying and some deep drilling information conducted by the oil industry, in turn, provided much general knowledge about crustal structure and some detail of the structural characteristics of the longest part of the most active seismic zone west of the Basin and Range province.

PART II: CONTEMPORARY STUDIES BY THE U.S. GEOLOGICAL SURVEY

INTRODUCTION

Since about 1982 studies related to seismicity in the New Madrid region have been as diverse as earlier studies but funding, therefore effort, has been decreasing. The symposium on the New Madrid seismic zone, sponsored by the Missouri Academy of Sciences and the U.S. Geological Survey (USGS) is the first major attempt to bring together a collection of papers that describe most of the latest information and concepts on the New Madrid seismic zone. These papers are given in this volume and it would be redundant to summarize their contents. In addition to these papers, it seems appropriate to include in this volume a brief

description of some studies in progress by USGS investigators that is quite relevant to the New Madrid seismic zone.

The first two studies to be described below are incomplete and have as a primary objective the detection of small amounts of crustal deformation in areas of several tens to hundreds of square kilometers. These two studies utilize level line data from the National Geodetic Survey (NGS) and digitized stream profile data. A third study involves the interpretation of seismic reflection profile data collected using marine methods on the Mississippi River. The principal objective is to locate geologically young faults. Part of this study is published and another part is nearly complete.

The fourth study has just been started and is the interpretation of about 320 km (200 mi) of seismic reflection profile data acquired recently for the area from near Caruthersville, Mo., to near Marked Tree, Ark. The tentative interpretations made to date in this study will be discussed in greater detail than any other study reported herein because of their direct relevance to the geologic characteristics of a large part of the New Madrid seismic source zone.

LEVEL LINE STUDY

The use of level line data is fraught with uncertainties and problems. Nevertheless, in areas where crustal strain must be changing as indicated by the occurrence of earthquakes, it may be helpful to examine the level line survey data available from the National Geodetic Survey (NGS) to detect significant changes in vertical strain. Accordingly, Richard Dart of the USGS has compiled all pertinent level line data in and around the Upper Mississippi embayment for the period from 1888 to 1981. Differences in elevations along most lines are small; a few have differences in elevation that appear to be significant but refraction and rod errors have not been applied. One of the largest rates of change in elevation within the embayment occurs along a line from New Madrid, Mo., to Markham, Tenn., which is on the Lake County uplift (Russ, 1982). The rate of change in elevation along this line is 80 mm/yr up towards Markham, and qualitatively agrees with geologic observations. A line from Clinton, Ky., in the highlands east of the embayment, to New Madrid, Mo., via Markham, Tenn., indicates that the Lake County uplift area is subsiding at a rate of about 100

mm/yr relative to the highlands but 80 mm of this subsidence is between Markham and New Madrid, which is consistent with the change along the New Madrid-Markam line.

A line 62 km long surveyed in 1935 and again in 1940 along Highway 8 between Steelville and Mineral Point in central Missouri appears to have a significant change in elevation in association with a fault zone (fig. 1). A change of 70 mm along 12 km of this line occurred within 5 years. The relatively high rate of change in elevation and its relationship to a fault zone suggests recent fault movement. The relatively long distance, 12 km, over which the displacement along the level line occurred, however, makes a relationship to faulting suspect. Field examination of benchmarks still in place proved them to be in stable ground and none appeared to have been reset because of road repairs, realignment or other reasons. Several other factors need to be considered in any interpretation of the displacement. One factor is that the Viburnum trend of lead-zinc mineralization crosses the zone of displacement. Another factor is that in the course of field inspection of the benchmarks it was noted that silicification of the limestone bedrock is much greater along the level line on the up side of the displacement than along the line where the displacement is downward. A third factor is that solution of limestone in the Ozark Mountains, where the level line is located, is a major phenomenon (for example, Harvey, 1982).

The available data are not adequate to support any explanation of the displacement. The author's speculation however is that it may best be explained by solution of limestone and that the amount of solution may be controlled by the amount of silicification of the limestone which may be related to mineralization along the viburnum trend.

The level line data must be examined for the effect of refraction and rod error. It seems unlikely, however, that the 70 mm change in elevation can be attributed to refraction error. This error is largely a function of topographic relief and is generally conformable with topography. The changes in elevation and topography in figure 1 do not suggest such conformability.

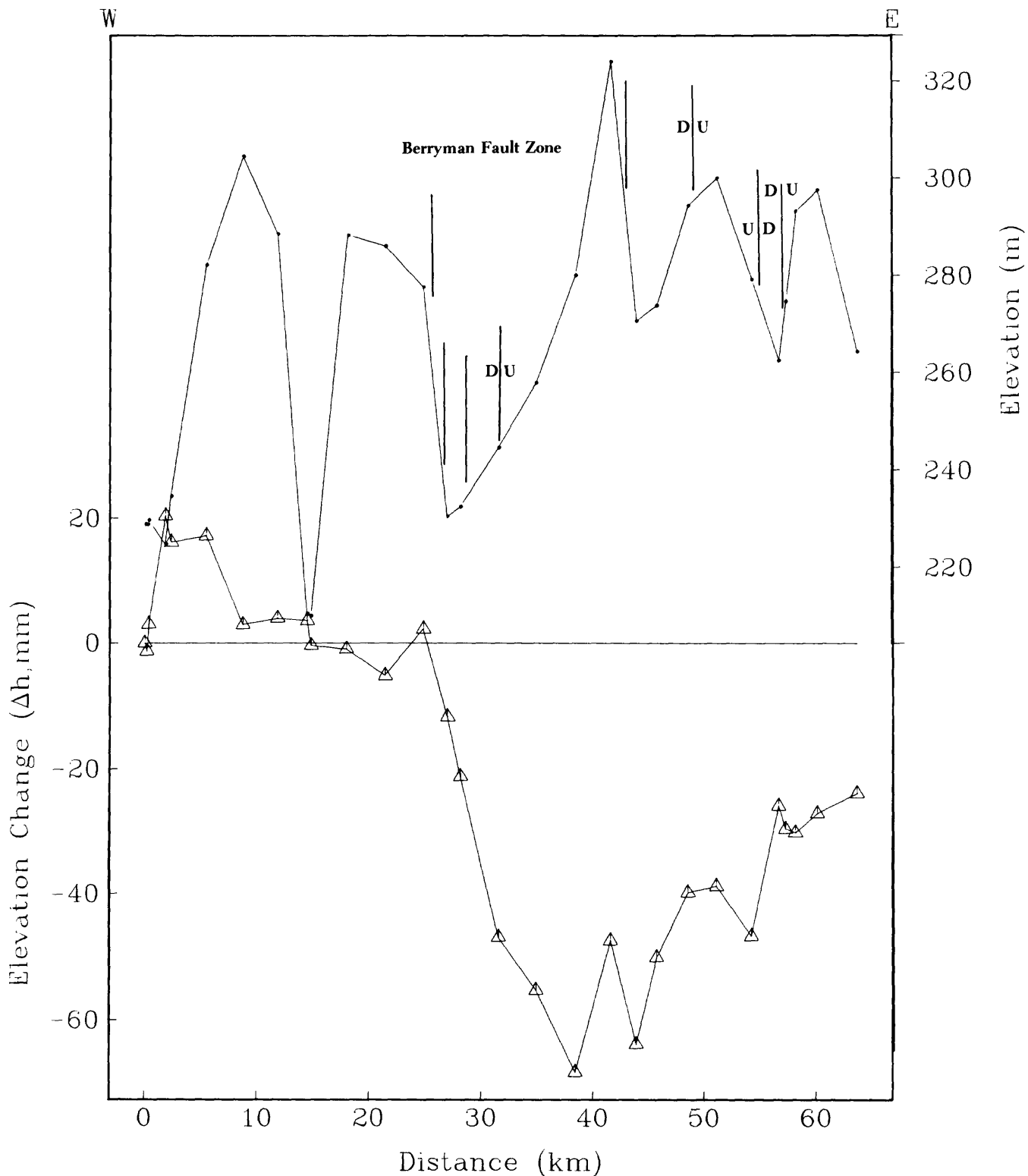


Figure 1.--Profiles of elevation changes during period of 1935-40 (bottom) and topography (top) along Route 8 from Steelville to Mineral Point, Mo. Heavy vertical lines on topographic profile are location of faults from Pratt (1982). D, down; U, up.

STREAM PROFILE STUDY

The author initiated this study in an effort to search for some geomorphic anomaly that could be related to the enigmatic central Arkansas earthquake swarm (Johnston, 1982). The scope and detail of the study gradually increased so that a number of scientists have made major contributions to it. In early stages of the study Bonny Askew and Michael McGrath did much of the computer programming. In later stages Meridee Jones Cecil managed nearly all of the computer work and has been involved with interpretation of the data, which is far from complete. In addition, contributions from E. E. Glick and Boyd Haley of the USGS provided detailed geology along nearly all of the stream profiles. The objective of the study is to identify areas of several hundred square kilometers with recent uplift or subsidence. Courses and elevations of 70 streams longer than 10 km in one hundred ninety-two 7 1/2-minute quadrangles were digitized. From these data plots were made of: stream courses, profiles in Cartesian and semilog coordinates, stream gradient indices (Hack, 1973), first derivatives of slope, and an innovative measure of erosion named pseudohypsometric value. Also, a subenvelope map was plotted.

Two examples of the products derived from the digitized stream courses and elevations are shown in figures 2 and 3. Figure 2 is a gray-tone scale plot of stream gradient index values that have been smoothed in their distribution by a gridding program. The actual values were calculated for each reach of a stream between every contour interval, regardless of the size of the interval. In general, most contour intervals were 20 feet. The figure shows that a greater area in the Salem Plateau has a high stream gradient index value than in the Boston Mountains and Ouachita Province. Figure 3 is a contour map of stream gradient index values, but the values are for the whole stream. That is, the total length of a stream is treated as a single reach, and only one value is calculated for the whole stream. The figure also shows the distribution of epicenters for the period June 29, 1974, through March 28, 1981, and the location of the epicentral area of the central Arkansas earthquake swarm which started in January 1982 (Johnston, 1982). At the present stage of interpretation no significance is attached to the distribution of epicenters in the Salem Plateau area. Interpretation of the data are not complete but some tentative conclusions include the following.

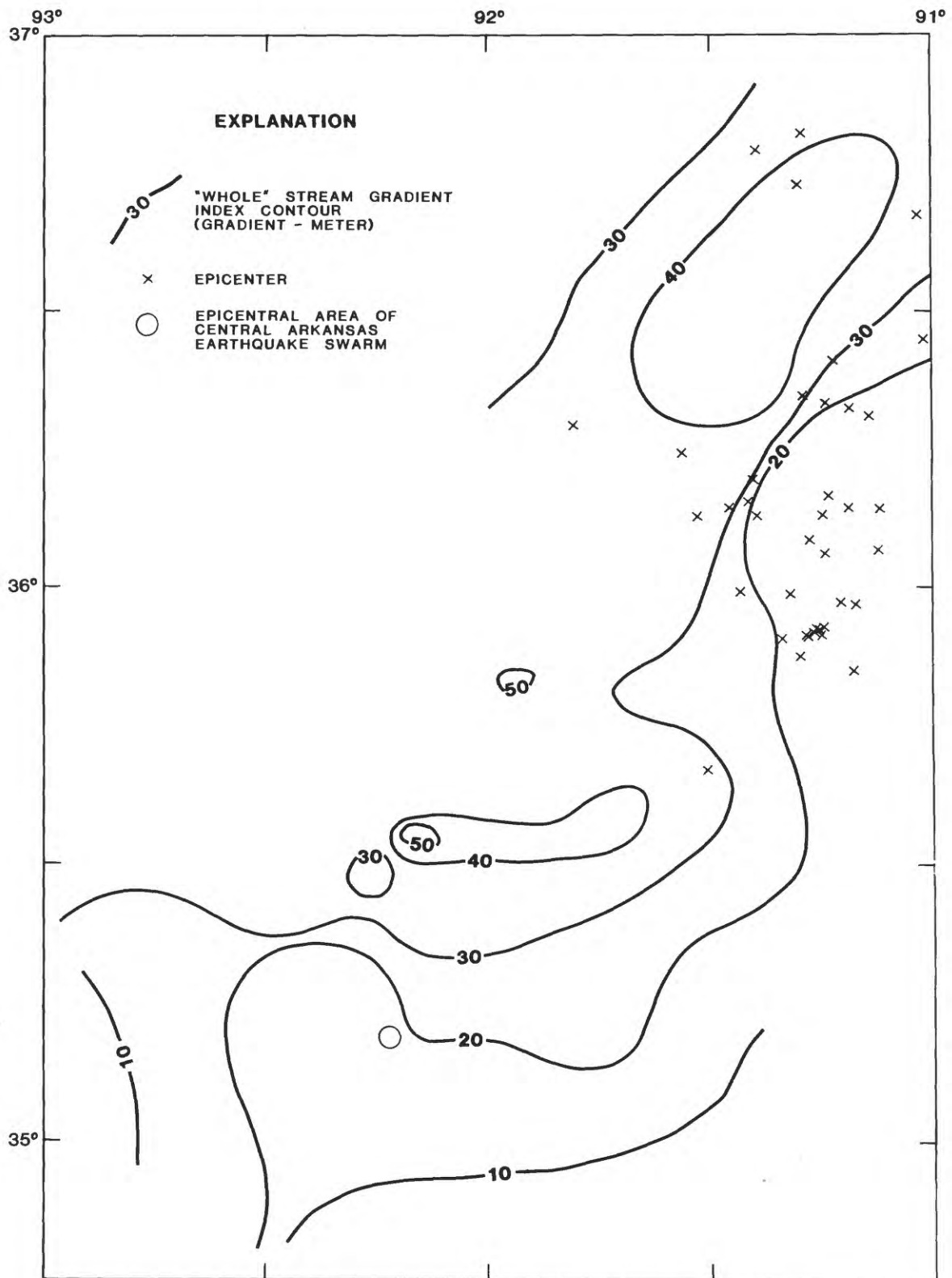


Figure 3.--Map showing relationship of earthquake epicenters to contours of stream gradient index values calculated for total length of streams. Epicenters are for the period June 29, 1974, through March 28, 1981.

93° 00'
37° 00'

90° 45'

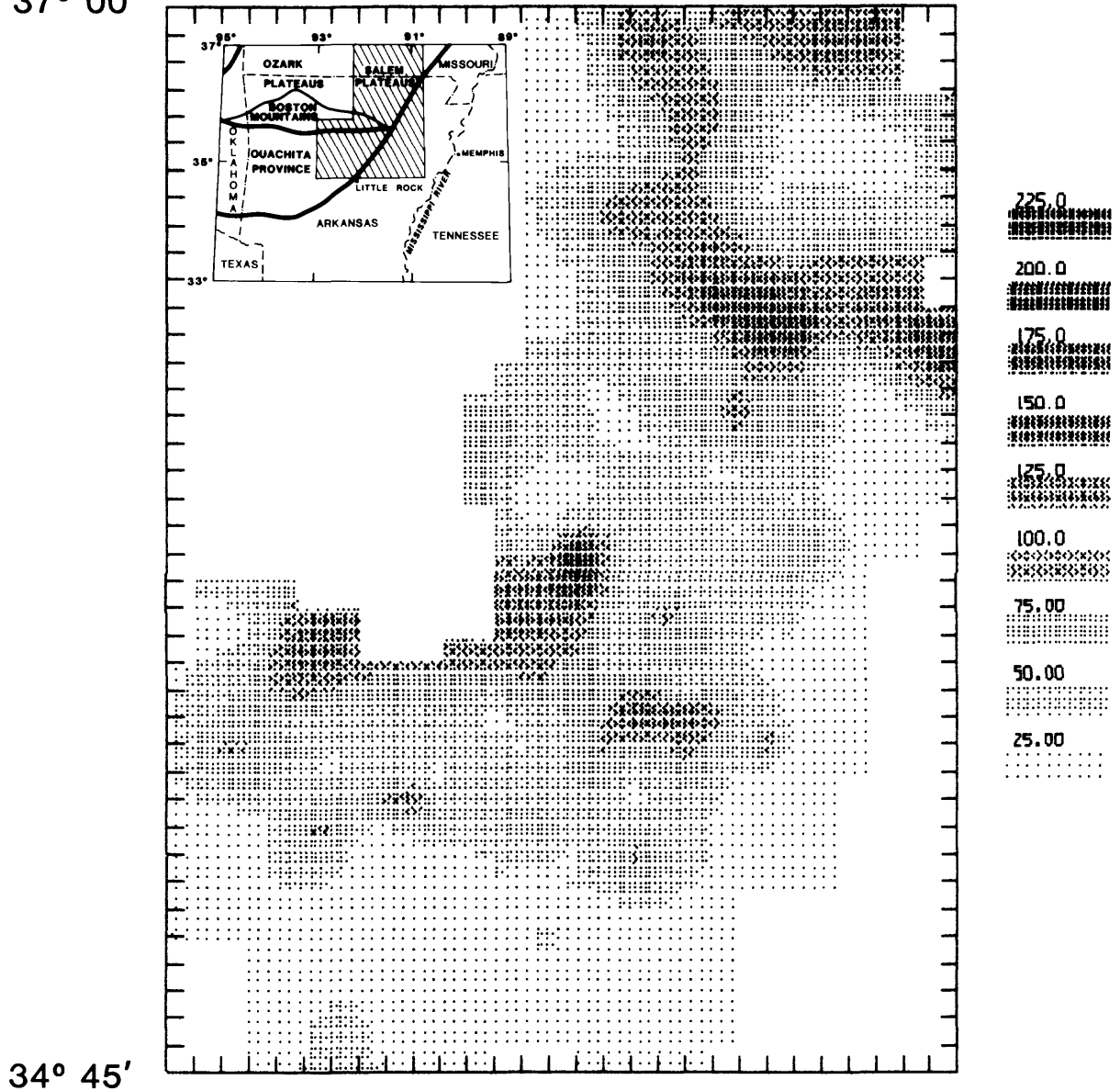


Figure 2.--Stream gradient index values calculated for reaches between every elevation contour and smoothed by a gridding program for plotting in gray scales. Grid size is 5.6 km; centers of grid cells indicated by ticks within the neat lines. Areas without pattern are outside of mapped area or have no data within a 10-km radius of the grid center.

- 1) Streams on the Salem Plateau commonly have steeper gradients and their profiles are less concave than streams draining the Boston Mountains and Ouachita physiographic provinces even though the Salem Plateau has lower elevation and less relief than the latter provinces.
- 2) The largest size of material in stream beds controls stream gradients much more than the rock type eroded by a stream. This observation is consistent with other studies of stream gradients (Hack, 1957) and with some theories of erosion (Shulits, 1936).
- 3) Meandering reaches of streams, particularly on the Salem Plateau, commonly have the steepest gradients, which is contradictory to most observations and theory of the meandering process. One explanation could be that in the Salem Plateau gradients have continued to increase since the meanders first developed, which was probably during the Tertiary Period.
- 4) Streams draining the Salem Plateau enter the Mississippi embayment lowlands at a much higher elevation relative to Pleistocene base level than streams draining the Boston Mountains and Ouachita provinces. This suggests that the Salem Plateau has not been eroded as deeply as the other provinces and has been uplifted more recently to account for the steeper gradients of the Plateau streams.

A number of the quantitative measures of stream profiles suggests that the Salem Plateau may be rising relative to surrounding areas since the Tertiary Period. Many variables must still be considered, however, before quantitative differences in the stream profile data can be confidently related to tectonic activity.

MISSISSIPPI RIVER REFLECTION PROFILE SURVEY

The principal investigators of this study are A. J. Crone, D. P. Russ, Kaye Shedlock, and S. T. Harding. The principal results of the Mississippi River seismic reflection profile survey between Osceola, Ark., and Wickcliffe, Ky., are the identification of a number of faults in the shallow subsurface

clearly offset Tertiary sediments; a few appear to offset alluvium of Pleistocene and possibly Holocene age. Vertical offset on all of the faults identified to date is less than 10 m with the exception of the southwestern extension of the Cottonwood Grove fault (Shedlock and Harding, 1982), first identified in a seismic reflection profile survey in the Ridgely, Tenn., area (Zoback and others, 1980).

SEISMIC REFLECTION PROFILES IN THE NEW MADRID SEISMIC ZONE

The recently purchased seismic reflection profile lines were selected mainly to show a major zone of structural disruption in the middle of the Reelfoot rift. The disrupted zone had been recognized on earlier reflection profiles to coincide with the seismicity (Zoback and others 1980; Hamilton and Zoback, 1982) but its extent could not be determined based on the limited amount of profiling available from the earlier surveys. Also, inspection of a large amount of the available reflection data prior to purchasing showed clearly that the zone could be delimited. The zone is of great importance because nearly all of the contemporary seismicity between Marked Tree, Ark., and Caruthersville, Mo., a distance of about 100 km, is within or very close to the boundaries of the zone. Furthermore, the greatest density of sandblows produced by the 1811-12 earthquakes overlies the subsurface position of the disturbed zone (fig. 4). The coincidence of contemporary seismicity, sandblows, and the disturbed zone strongly indicate a common genetic relationship. Because of this coincidence, delimiting and inferring the nature of the disrupted zone in the interpretation of the profiles is of first priority. A short report on interpretation of the profile data is in preparation for publication in *Geology*. The large amount of seismicity north of the disrupted zone (see index map on fig. 4) is not discussed herein, because no new data for the northern area have been acquired since the reports by Zoback and others (1980) and Hamilton and Zoback (1982). A summary of some of the principal results described in the report for *Geology* and some speculation by the author of this paper on the significance of igneous rocks in the zone follows.

Several reflectors below the eroded top of the Paleozoic section of rocks have been identified on the basis of cuttings and geophysical logs of

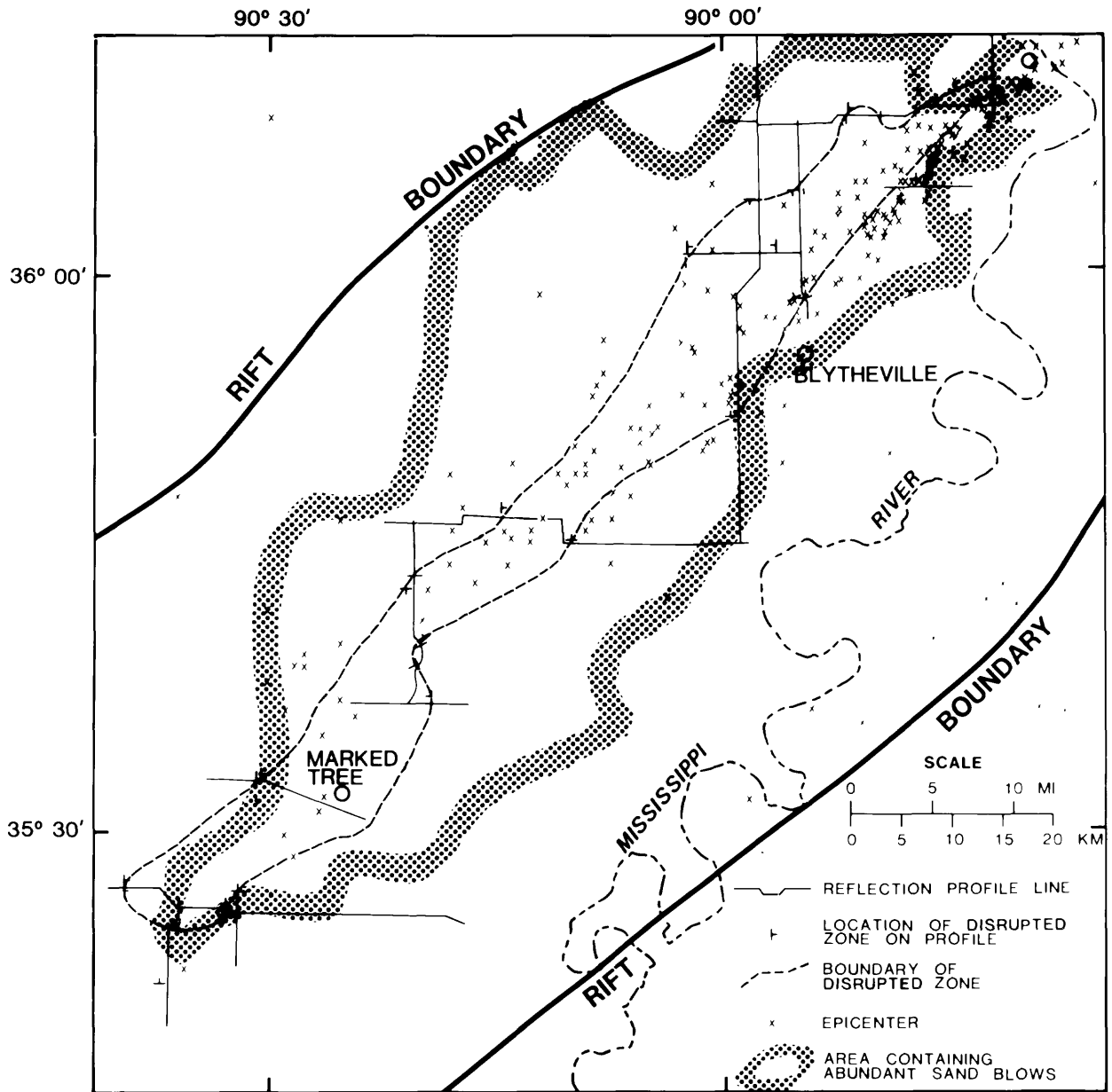


Figure 4.--Preliminary map showing relationship of seismicity to disturbed zone mapped at the depth of magnetic basement in the southern part of the New Madrid seismic zone. Epicenters are for the period June 29, 1974, through March 28, 1981, from R. B. Herrmann (written commun., 1981).

exploratory drill holes, and on the basis of depth of magnetic basement shown by Hildenbrand and others (1979). The two deepest and most important drill holes were located about 12 km southwest of Osceola and about 13 km southwest of Blytheville in Mississippi County, Ark. A brief description of the rocks penetrated by the drill hole near Blytheville has been published by Denison (1983). Preliminary examination of cuttings from both holes has been made by E. E. Glick (U.S. Geological Survey, oral commun., 1984).

Because of erosion of nearly all of the Paleozoic rocks during uplift of the Pascola arch in the northern part of the area for which reflection profiles were obtained, only a few of the deepest reflectors can be mapped throughout all of the area. South of about lat $35^{\circ}45'$, the four most useful reflectors are from the magnetic basement (MB), the middle (MC) and the top (TC) of an unnamed sequence of carbonate and clastic rocks, and the base of a carbonate sequence (BC), which may be the base of the Knox Megagroup. North of this latitude the BC reflector cannot always be identified.

In addition to the lack of continuous reflectors throughout the Paleozoic section of rocks, mapping of the disrupted zone is complicated by differences in structural characteristics within the zone. Locally the MB reflector occurs discontinuously and nearly horizontally through the zone, (fig. 5), particularly near the north and south ends of the zone. At places, midway between the ends of the disturbed zone, the MB reflector is absent in the zone and its attitude may be nearly horizontal or dipping downward as it approaches the zone. The downward dip is presumably caused by low velocity material above the reflector. Reflectors above the MB are commonly warped into an antiform (figs. 5 and 6); generally, the magnetic basement is not involved in the antiform except on one profile where it is warped upward (fig. 6). Only the MB reflector was used to map the disrupted zone as shown in figure 4.

Orgins considered for the disrupted zone are speculative as are the reasons for why the longest epicentral trend of earthquakes in the New Madrid region is coincident with the surface projection of the zone. Some characteristics of the zone which may be clues to an explanation are as follows.

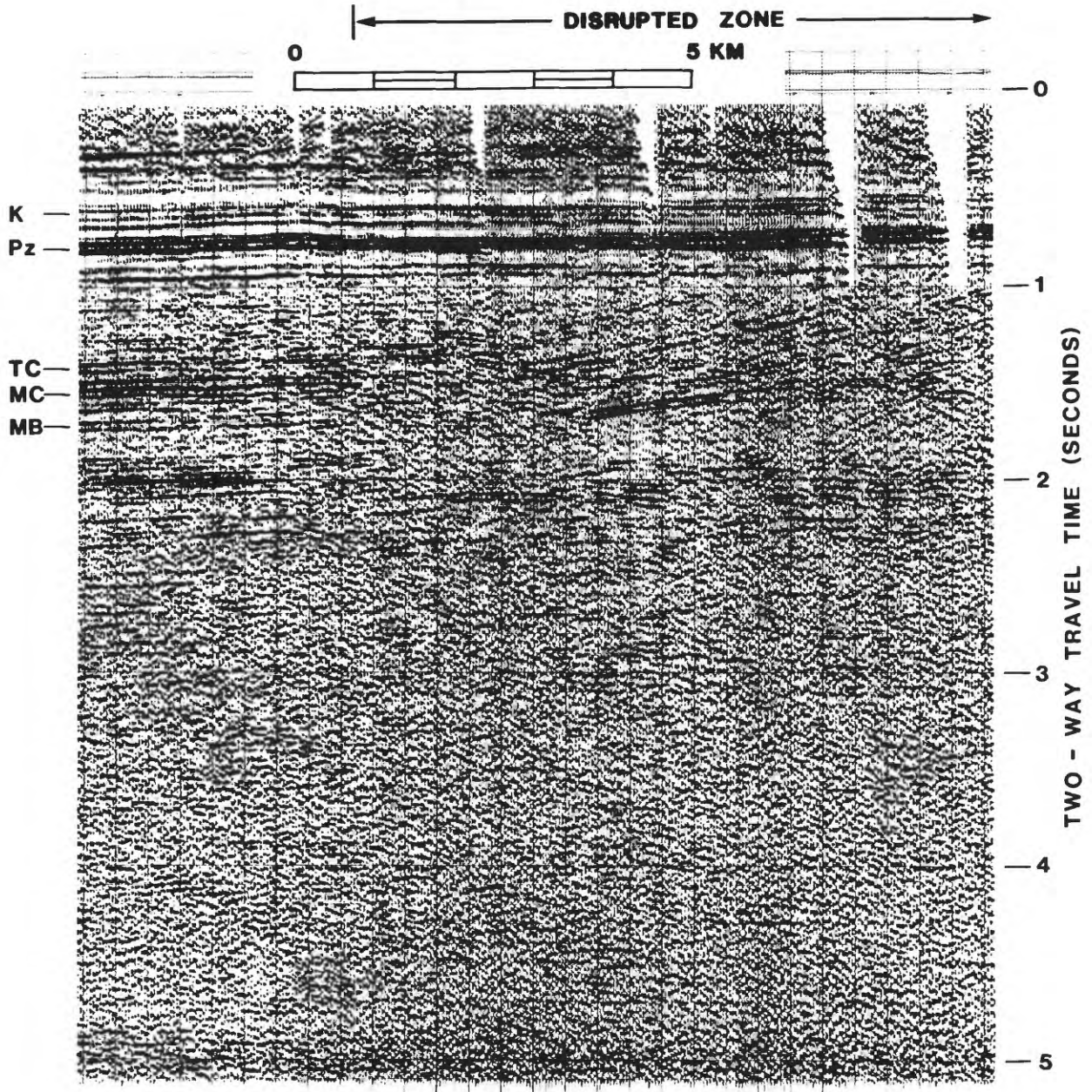


Figure 6.--Part of a seismic-reflection profile near center of the disturbed zone showing warping of MB, MC, and TC reflectors in the disrupted zone and layered sequence of reflectors under MB reflector. MB, magnetic basement; MC and TC, middle and top of unnamed carbonate and clastic rocks; PZ, Upper Cretaceous-Paleozoic contact; K, Tertiary-Upper Cretaceous contact.

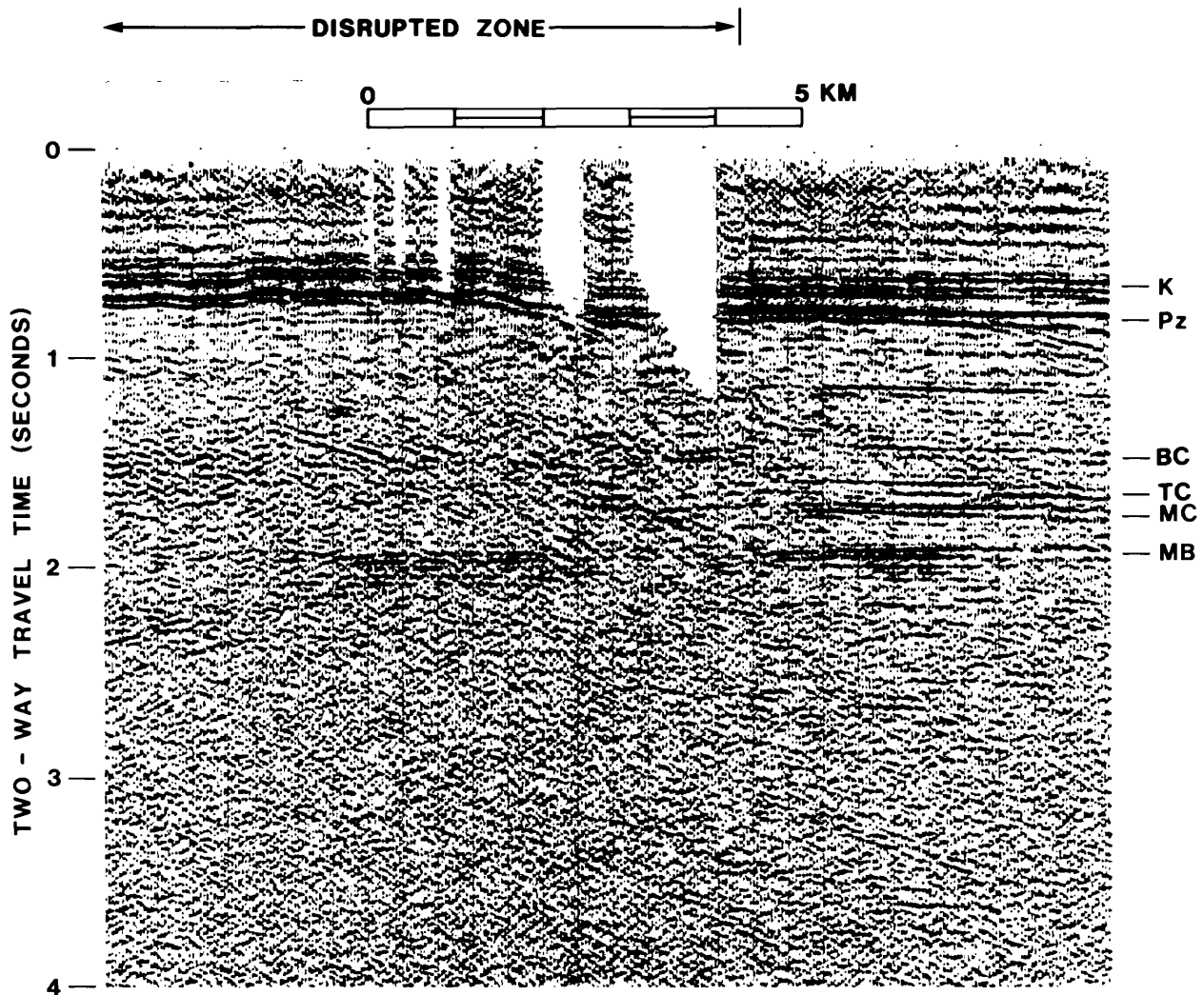


Figure 5.--Part of a seismic-reflection profile about 10 km north of Marked Tree, Ark., showing discontinuity and warping of reflectors used for mapping the disturbed zone. Warping of the Paleozoic surface, top of the Cretaceous and reflectors from Tertiary sediments are also shown. Warping of these post-Paleozoic sediments is not common to most reflection profiles. MB, magnetic basement; MC and TC, middle and top of unnamed carbonate and clastic rocks; BC, base of carbonate sequence; PZ, Upper Cretaceous-Paleozoic contact; K, Tertiary-Upper Cretaceous contact.

Reflectors below the magnetic basement, which range in depth from about 3 to 15 km, are generally continuous beneath the zone without the same great disruption and warping of these horizons above the magnetic basement. The warping of beds over but not below the disturbed zone suggests that it is caused by intrusion of some material. Diapiric ridges of salt, anhydrite, or of shale have been considered, but available data from aeromagnetic and gravity surveys, logs of drill holes, and interval velocities calculated from the reflection profile data do not support a salt or shale diapiric origin of the warping. Intrusion by magma of felsic composition in the form of laccoliths, sills, or some irregular subhorizontal body into sedimentary rocks above crystalline rocks seems the most likely cause of warping of Paleozoic and younger rocks. No available data preclude this explanation of warping; no direct evidence is known, however, to prove the existence of such intrusives in the center of the rift.

Below the MB in many of the profiles across the disrupted zone is a sequence of reflectors that also indicate layered rocks with a thickness ranging from about 1/2 to more than 1 km. The reflection profiles outside of the rift boundary do not indicate a layered sequence of rocks below the MB. It is unlikely that sedimentary rocks would occur below MB and as the layered rocks do not produce strong magnetic anomalies, basalt flows can probably be precluded. The layered rocks below MB are, therefore, inferred to be a sequence of volcanoclastic rocks with a felsic composition. The extrusion of such rocks is common during and following the tumescent stage of the crust that precedes a collapse to form calderas or rifts (see for example, Baker and others, 1971; Smith and others, 1961). It is quite possible that eruption and deposition of lava flows, ash flows and ash falls occurred in the pre-Reelfoot rift area at about the same time as the same kind of eruptive activity was occurring in the St. Francois Mountains some 150 km to the northwest, about 1.4 m.y. B.P. This interpretation is similar to that of Hildenbrand and others (1982) who suggest that a number of thermotectonic events occurred in the Central Province during the period 0.55-1.5 m.y. B.P.

Reflections from above the MB indicates a layered sequence of rocks as might be expected from sediments deposited early in the formation of the rift (fig. 5).

If the inferred explanation of warping of Paleozoic sedimentary rocks is correct, the age of many of the inferred intrusive rocks in the disrupted zone is much younger than the initial development of the rift. This conclusion is evident from the fact that Cambro-Ordovician (500 b.y. B.P.) sediments are warped wherever they overlies the disrupted zone, and provides an estimate of the maximum age of the inferred intrusive activity. The youngest age for this activity is pre-Late Cretaceous because rocks of this age are not warped, nor is the Paleozoic surface on which they were deposited warped.

In very general terms, the reason for earthquakes occurring primarily within the disrupted zone may simply be that the zone is more highly fractured and weaker than adjacent parts of the crust. This is too simplistic an answer however, and is relevant to a problem common to nearly all faults or fault zones with seismic activity. In brief, the problem is why is one fault or fault zone seismically active in a region and another is not active. The following reasoning and speculation might be considered.

If earthquakes are related in some way to highly fractured zones containing intrusive rocks, like the disrupted zone in the middle of Reelfoot rift, the rift boundary zones may also be expected to be seismically active. These zones on reflection profiles are also interpreted to be highly fractured over widths of several kilometers and appear to have intrusive rocks in them. Aeromagnetic and gravity data clearly show small plutons along the boundaries of the rift, particularly along the northwest boundary (Hildenbrand and others, 1982). The principal difference between the boundary zones and the disturbed zone is the composition of the igneous rocks as indicated by the aeromagnetic data. The plutons along the boundary zones are mafic; the intrusives in the disrupted zone are interpreted to be felsic because they do not produce strong magnetic anomalies.

Another difference between the boundary and disturbed zones, which may be relevant to the cause of seismicity, is the history of each. The disrupted zone has had a long history of igneous and fault activity. If the interpretation of volcanoclastic rocks below the MB is correct, igneous activity, and certainly some contemporaneous faulting, probably started before development of the rift. Reflection profiles show deformation and intrusives in and outside of the disrupted zone during Cambrian and Ordovician times,

locally during Cretaceous and possibly Tertiary times. Further, as stated above, most of the igneous rock emplaced during early development of the rift, and apparently concentrated near the axis of the developing rift, was likely to be alkalic felsic or rhyolitic in composition. In contrast the boundary zone is highly fractured but does not appear to have the abundant evidence of felsic rocks but has mafic rocks, which were injected as small plutons, dikes, or sills during the Permian and Cretaceous long after development of the rift.

In summary, therefore, the disturbed zone has probably had a long history of felsic igneous activity and faulting from late Precambrian to Tertiary time whereas the boundary zones formed later, during the main development of the rift, with mafic igneous activity starting no earlier than late Paleozoic time.

Given these contrasting environments in different parts of the Reelfoot rift, several lines of argument could be hypothesized to explain the cause of earthquakes in the rift. In addition to the highly fractured condition of the disrupted-zone, factors that should be considered are the gross difference in physical properties including the possibility of higher porosity, hence, weaker rock, and the possibility of higher radiogenic heat production and consequent thermal stress in felsic rocks compared to the mafic rocks in the boundary zone. Elaboration on these speculations, however, is beyond the scope of this report.

REFERENCES

- Algermissen, S. T., Perkins, D. M., Thenhaus, P. C., Hansen, S. L., and Bender, B. B., 1982, Probabilistic estimates of acceleration and velocity in the contiguous United States: U.S. Geological Survey Open-File Report 82-1033, 99 p., 6 pls., scale 1:750,000.
- Baker, B. H., Williams, L. A. J., Miller, J. A., and Fitch, F. J., 1971, Sequence and geochronology of the Kenya rift volcanics: *Tectonophysics*, v. 11, p. 191-215.

- Burke, Kevin, and Dewey, J. F., 1973, Plume-generated triple junctions; key indicators in applying plate tectonics to old rocks: *Journal of Geology*, v. 81, p. 406-433.
- Denison, R. E., 1983, Basement rocks in northern Arkansas: *Geological Society of America Abstracts with Programs*, v. 16, no. 2, p. 82.
- Erickson, R. L., and Blade, L. V., 1963, Geochemistry and petrology of the alkalic igneous complex at Magnet Cove, Arkansas: *U.S. Geological Survey Professional Paper 425*, 95 p.
- Ervin, C. P., and McGinnis, L. D., 1975, The Reelfoot rift--reactivated precursor of the Mississippi embayment: *Geological Society of America Bulletin*, v. 86, no. 9, p. 1287-1295.
- Fuller, M. L., 1912, The New Madrid earthquake: *U.S. Geological Survey Bulletin 494*, 119 p.
- Hack, J. T., 1957, Studies of longitudinal stream profiles in Virginia and Maryland: *U.S. Geological Survey Professional Paper 294-B*, p. 45-97.
- _____, 1973, Stream-profile analysis and stream-gradient index: *U.S. Geological Survey Journal of Research*, v. 1, no. 4, p. 421-429.
- Hamilton, R. M., and Zoback, M. D., 1982, Tectonic features of the New Madrid seismic zone from seismic-reflection profiles, in McKeown, F. A., and Pakiser, L. C., eds., 1982, *Investigations of the New Madrid, Missouri, earthquake region*: *U.S. Geological Survey Professional Paper 1236*, p. 55-82.
- Harvey, E. J., 1980, Ground water in the Springfield-Salem plateaus of southern Missouri and northern Arkansas: *U.S. Geological Survey, Water Investigations Report 80-101*, 66 p.
- Heyl, A. V., Jr., 1972, The 38th parallel lineament and its relationship to ore deposits: *Economic Geology*, v. 67, p. 879-894.

- Heyl, A. V., and Brock, M. R., 1961, Structural framework of the Illinois-Kentucky mining district and its relation to mineral deposits, in Short papers in the geologic and hydrologic sciences: U.S. Geological Survey Professional Paper 424-D, p. D3-D6.
- Hildenbrand, T. G., Kane, M. F., and Hendricks, J. D., 1982, Magnetic basement in the upper Mississippi embayment region--a preliminary report, in McKeown, F. A., and Pakiser, L. C., eds., Investigations of the New Madrid, Missouri, earthquake region: U.S. Geological Survey Professional Paper 1236, p. 39-53.
- Hildenbrand, T. G., Kucks, R. P., Kane, M. F., and Hendricks, J. D., 1979, Aeromagnetic map and associated depth map of the upper Mississippi Embayment region: U.S. Geological Survey Miscellaneous Field Studies Map MF-1158, scale 1:1,000,000.
- Johnston, A. C., 1982, A natural earthquake laboratory in Arkansas: EOS (American Geophysical Union Transactions), p. 1207-1210, December 14.
- Kumarapeli, P. S., 1976, The St. Lawrence rift system, related metallogeny, and plate tectonic models of Appalachian evolution: Geological Association of Canada Special Paper 14, p. 501-520.
- Kumarapeli, P. S., and Saull, V. A., 1966, The St. Lawrence Valley system--a North American equivalent of the East African rift system: Canadian Journal of Earth Sciences, v. 3, no. 5, p. 639-658.
- Lyell, Sir Charles, 1849, A second visit to the United States of North America: London, v. 2, p. 228-239.
- McKeown, F. A., and Pakiser, L. C., eds., 1982, Investigations of the New Madrid, Missouri, earthquake region: U.S. Geological Survey Professional Paper 1236, 201 p.
- Nuttli, O. W., 1973, The Mississippi Valley earthquakes of 1811 and 1812; intensities, ground motion, and magnitudes: Seismological Society of America Bulletin, v. 63, no. 1, p. 227-248.

- Pratt, W. P., 1982, Map showing geologic structures in the Rolla 1° by 2° quadrangle, Missouri: U.S. Geological Survey Miscellaneous Field Studies Map MF-1000-A, scale 1:250,000.
- Russ, D. P., 1982, Style and significance of surface deformation in the vicinity of New Madrid, Missouri, in McKeown, F. A., and Pakiser, L. C., eds., 1982, Investigations of the New Madrid, Missouri, earthquake region: U.S. Geological Survey Professional Paper 1236, p. 95-114.
- Shedlock, Kaye, and Harding, S. T., 1982, Mississippi River seismic survey: Geophysical Research Letters, v. 9, no. 11, p. 1275-1278.
- Shulits, Samuel, 1936, Fluvial morphology in terms of slope, abrasion, and bed-load: American Geophysical Union Transactions, v. 17, p. 440-444.
- Smith, R. L., Bailey, R. A., and Ross, C. S., 1961, Structural evolution of the Valles caldera, New Mexico, and its bearing on the emplacement of ring dikes, in Short papers in the geologic and hydrologic sciences: U.S. Geological Survey Professional Paper 424-D, p. D145-D149.
- Stearns, R. G., and Wilson, C. W., Jr., 1972, Relationships of earthquakes and geology in west Tennessee and adjacent areas: Tennessee Valley Authority, Tributary Area Development Research Paper, report prepared by Vanderbilt University, Nashville, Tenn. , 344 p.
- Street, R., 1982, A contribution to the documentation of the 1811-1812 Mississippi Valley earthquake sequence: Earthquake Notes, v. 53, no. 2.
- Voight, Barry, 1969, Evolution of North Ocean--Relevance of rock-pressure measurements, in Ray, M., ed., North Atlantic geology and continental drift: American Association of Petroleum Geologists Memoir 12, p. 955-962.

White, P.E., 1967, Outline of thermal and mineral waters as related to origin of Mississippi Valley ore deposits, with discussions, in Brown, J.S., ed., 1967, Genesis of stratiform lead-zinc-barite-flourite deposits in carbonate rocks (the so-called Mississippi Valley type deposits), a symposium: Economic Geology Monograph 3, p.379-382.

Woollard, G. P., 1958, Areas of tectonic activity in the United States as indicated by earthquake epicenters: American Geophysical Union Transactions, v. 39, p. 1135-1150.

Zartman, R. E., Brock, M. R., Heyl, A. V., and Thomas, H. H., 1967, K-Ar and Rb-Sr ages of some alkalic intrusive rocks from the central and eastern United States: American Journal of Science, v. 265, p. 848-876

Zoback, M. D., Hamilton, R. M., Crone, A. J., Russ, D. P., McKeown, F. A., and Brockman, S. R., 1980, Recurrent intraplate tectonism in the New Madrid seismic zone: Science, v. 209, no. 4460, p. 971-976.

THE CENTRAL MISSISSIPPI VALLEY EARTHQUAKES OF 1811-1812

by

**Ronald Street
University of Kentucky
Lexington, Kentucky**

and

**Otto Nuttli
University of St. Louis
St. Louis, Missouri**

ABSTRACT

Contemporary accounts of the central Mississippi river valley earthquakes that occurred during the winter of 1811-1812 are used to examine the four principal shocks, several of the stronger after-shocks, and the effects of the earthquakes along the Mississippi river.

The principal shocks on December 16, 1811 destroyed the Mississippi river settlements of Big Prairie and Little Prairie, while the principal shock on Feb. 7, 1812, destroyed New Madrid and created two temporary falls in the Mississippi river. The effects of these shocks are well documented over an extensive area by the accounts of several travelers along the Mississippi river.

INTRODUCTION

The earthquake sequence that began on December 16, 1811 and continued for at least a year thereafter, in what is now southeast Missouri and northeast Arkansas, is the greatest sequence of earthquakes ever to have occurred in the recorded history of eastern North America. The major earthquakes of this sequence, of which there were at least four, were felt as far away as Hartford, CT to the northeast, Charleston, SC to the east, and New Orleans, LA to the south. They caused ground failure (i.e., fissuring, sandblows, slides, subsidence, etc.) over an area of 48,000 square kilometers (an area slightly less than the state of West Virginia) that encompasses portions of six states; temporarily obstructed the flow of the Mississippi river in two places; and created innumerable navigational hazards on both the Mississippi and Ohio rivers for hundreds of kilometers. In addition, the earthquakes destroyed the Mississippi river settlements of New Madrid, Little Prairie and Big Prairie (located on the south side of the mouth of the St. Francis river) and caused minor structural damage to buildings as far away as Cincinnati, Ohio to the east, and St. Louis, Missouri to the north.

Due to the lack of inhabitants and the types of structures in use in the region at the time of the earthquakes, however, few deaths were reported. The population of New Madrid in 1810 was somewhat less than one thousand inhabitants, while that of Little

Prairie consisted of approximately twenty families and Big Prairie probably half that number. As summarized by Penick (1976), the only deaths generally reported as resulting from the earthquakes, are three individuals in and near New Madrid, six Indians who were in the vicinity of caving banks along the St. Francis river, a drowning on the White river in Arkansas, and a missing boy in the St. Francis swamps. A settler in New Madrid reported (The Lexington [KY] Reporter; Feb. 1, 1812) several individuals were injured by the earthquakes of Dec. 16, 1811, but that no one had been killed. The principal reason there were so few casualties in the settlements is the fact that nearly all of the inhabitants lived in log cabins that proved to be very resilient to ground motions (Berry, 1908).

On the other hand, several travelers along the Mississippi reported seeing empty canoes and rafts drifting, and assumed that many of their fellow travelers had been drowned. This is difficult to evaluate, since it was not uncommon for travelers to abandon their river craft for the supposed safety of the land (Latrobe, 1835), and it is likely that many of the empty canoes and rafts seen drifting along on the river were either deliberately abandoned or had broken loose from their moorings along the collapsing banks. Still, it is likely that several individuals did drown in the river, particularly as a result of the largest shock on February 07, 1812 earthquake that so severely disrupted flow of the Mississippi river and created two falls in the general vicinity of New Madrid. Indeed, Fr. Joseph who was traveling with Firmin La Roche (Shoemaker, 1928) mentions seeing several bodies of drowned persons in the Mississippi River.

There have been numerous papers written on the earthquakes that occurred during the winter of 1811-1812 in the central Mississippi river valley. Some of the more notable ones are the newspaper compilations by an anonymous author (1812) and Mitchill (1815), the observations and summary of effects of the earthquakes in the Ohio river valley by Drake (1815), the detailed study of epicentral region by Fuller (1912), and the body-wave magnitude scaling of the earthquakes by Nuttli (1973).

The purpose of this paper is to present a review of the principal facts of the earthquakes. In this context, a brief summary of the major earthquakes, the stronger aftershocks, and the first-hand observations along the Ohio and Mississippi rivers are given.

MAJOR EARTHQUAKES

Four major earthquakes occurred during the 1811-1812 sequence. Two occurred on Dec. 16, 1811 at 2:15 A.M. (all times are based on local times) and 8:15 A.M., one on Jan. 23, 1812 at 9 A.M., and one on Feb. 7, 1812 at 3:45 A.M. Based on the distribution of Modified Mercalli (MM) intensities similar to those shown in Figures 1 thru 4, Nuttli (1973) and Street (1982) estimate m_{bLg} magnitudes of 7.2, 7.0, 7.1 and 7.3 for the four events respectively. The abbreviations F and NF used in the figures indicate "felt" and "not felt". The "+" signs following the MM intensities in the figures are used to indicate a MM intensity value midway between the value shown and the next higher value.

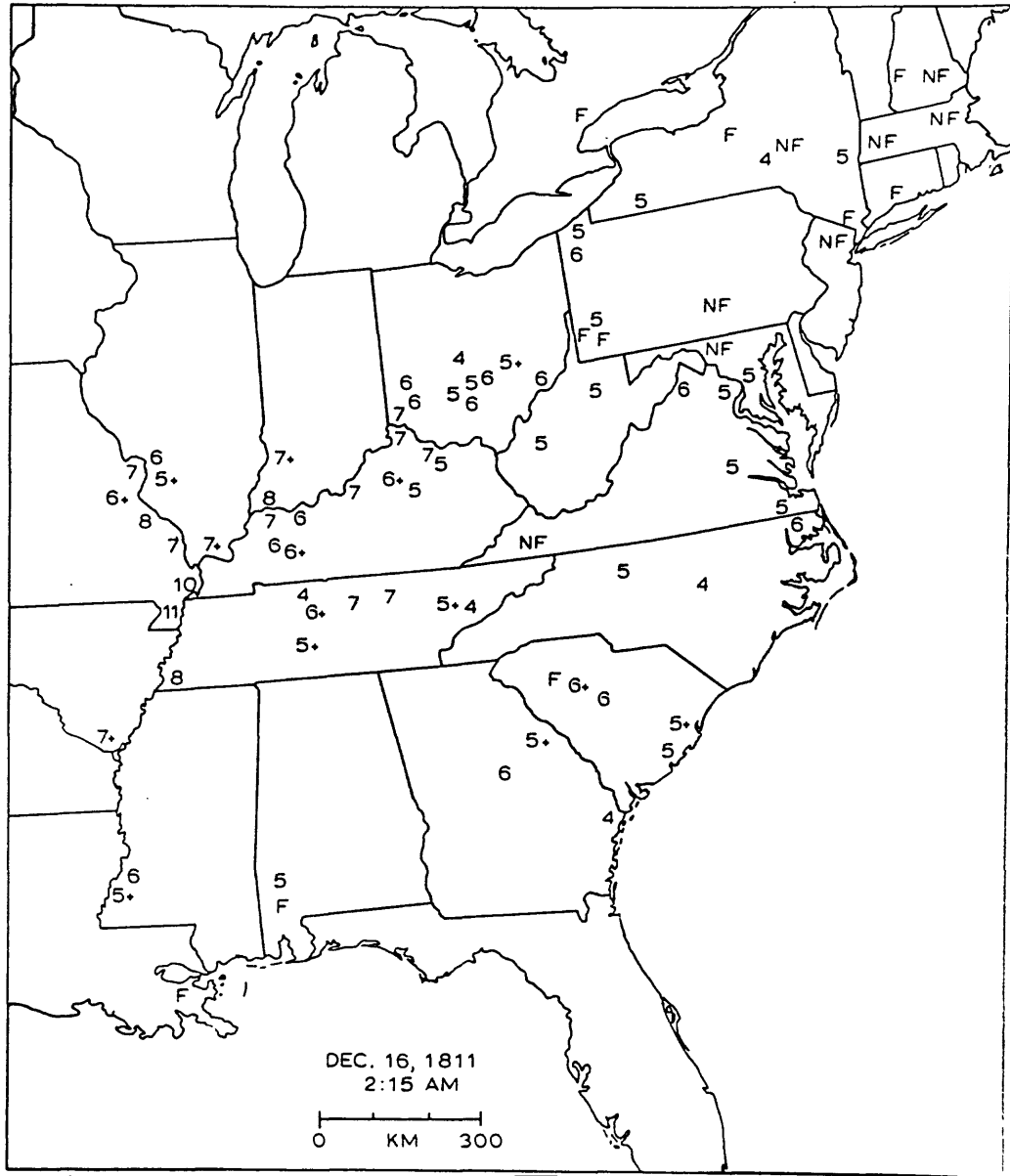


Figure 1.--The geographical distribution of the MM intensities for the central Mississippi river valley earthquake at 2:15 A.M., December 16, 1811, (taken from Street, 1982, which modifications).

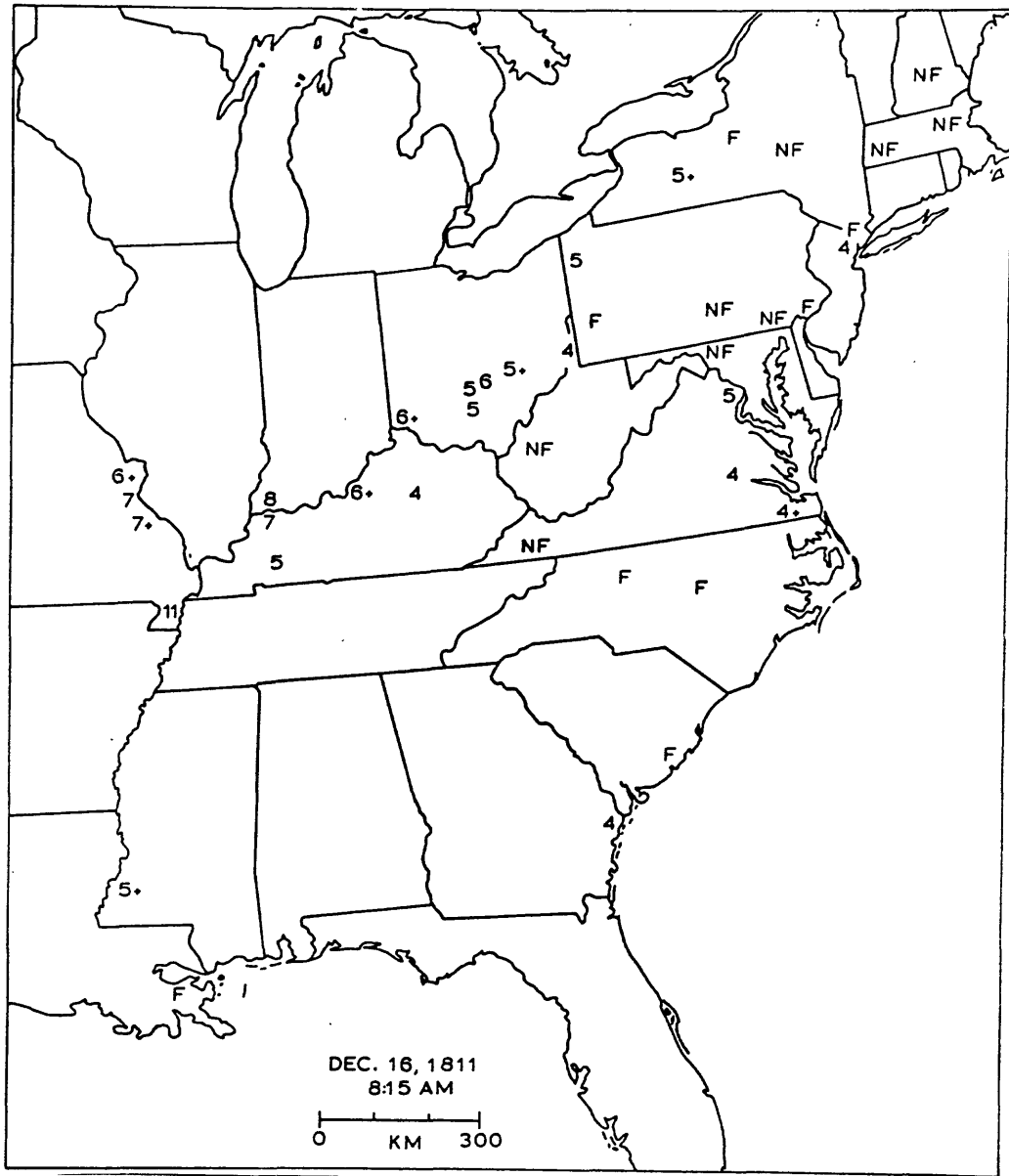


Figure 2.--The geographical distribution of the MM intensities for the central Mississippi river valley earthquake of 8:15 A.M., December 16, 1811. (taken from Street, 1982, with modifications).

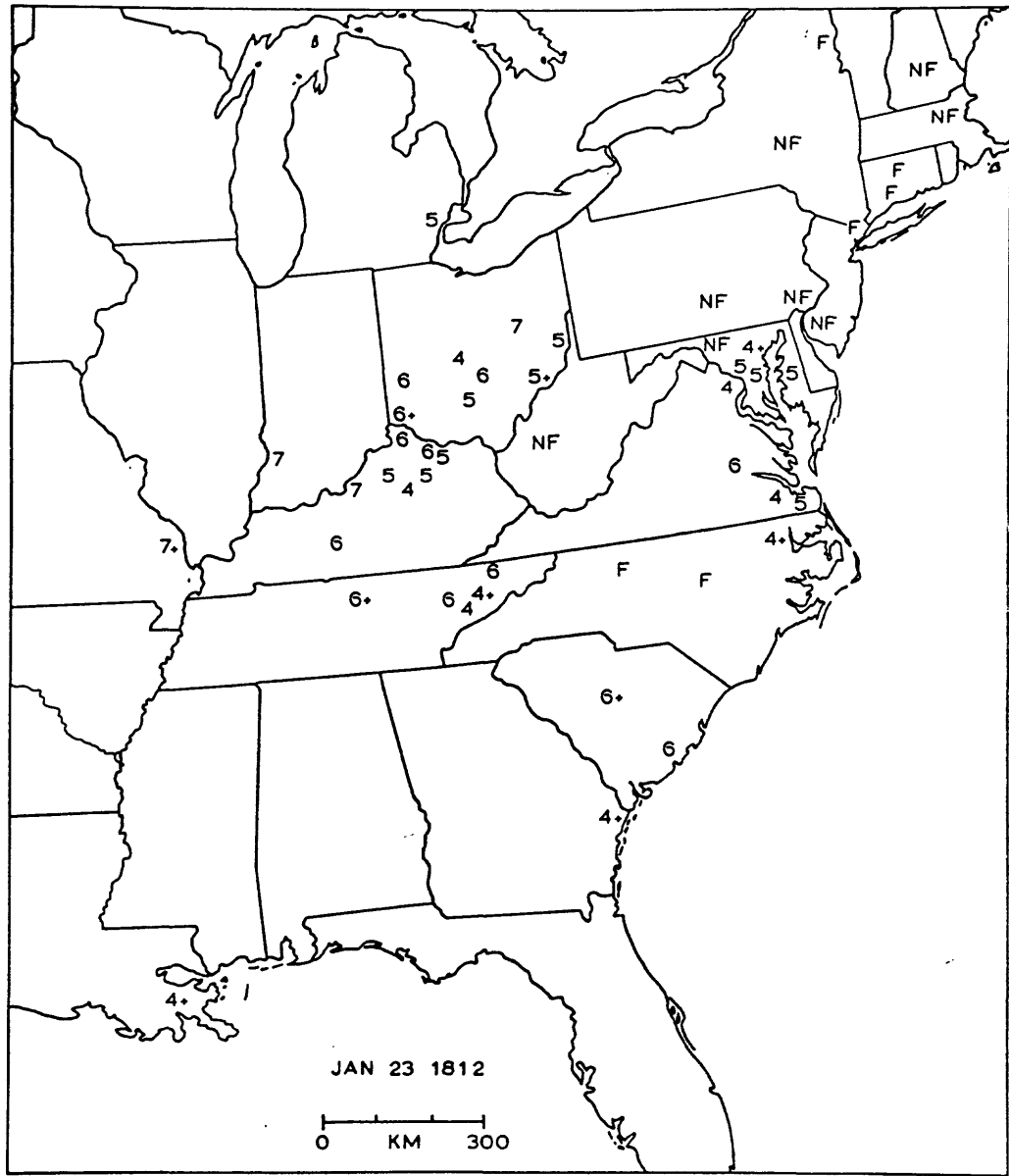


Figure 3.--The geographical distribution of the MM intensities for the central Mississippi river valley earthquake of Jan. 23, 1812 (taken from Street, 1982, with modifications).

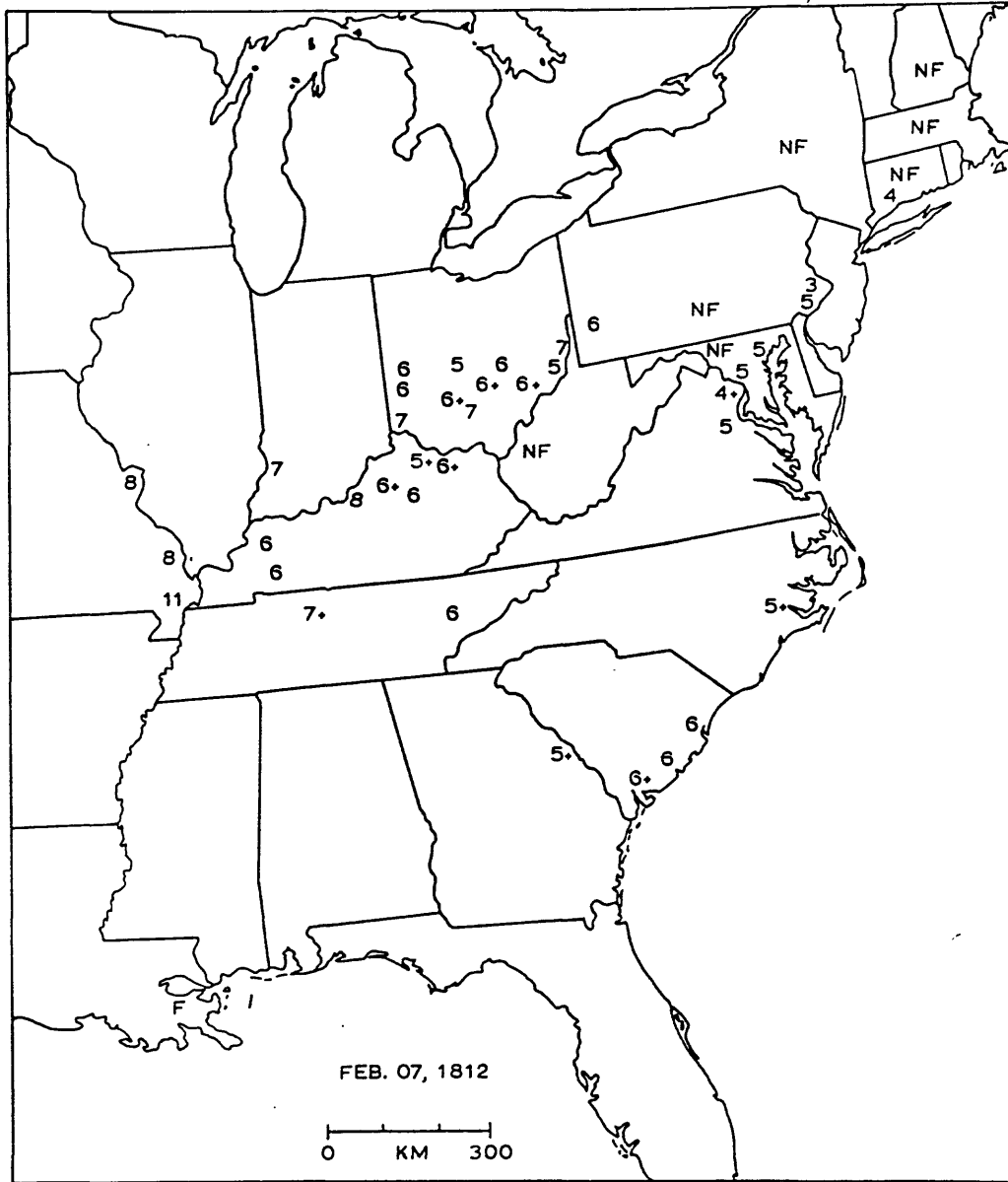


Figure 4.--The geographical distribution of the MM intensities for the central Mississippi river valley earthquake of February 7, 1812, with modifications).

An important fact about the 1811-1812 earthquake sequence, with respect to seismic hazard analysis, is the extent of the area in which ground failure occurred. One hundred years after the earthquakes, Fuller (1912), did a detailed investigation of the meizo-seismal area of the events, and outlined a 48,000 square kilometer area for which there was evidence of various types of ground failures (i.e., sand blows, slumping, landslides, fissures, etc.). Figure 5 is a slightly modified version of Fuller's work; the area within the dashed contour, what Fuller denotes as the area of disturbances, has been extended a short distance up the Wabash river valley on the basis of the work by Berry (1908).

Within the principal area of disturbances, indicated in Figure 5 by the shaded zone, large fissures, extensive and large sand blows, slumping and landslides, subsidence and uplifting, and caving of the river banks occurred as a result of the earthquakes. Many of these phenomena are also described in eye-witness accounts by individuals who were traveling down the Ohio and Mississippi rivers, and by settlers at Little Prairie and Big Prairie (see Figure 6a for the locations of these two settlements). At Little Prairie, for example, Fletcher (Wilson's Knoxville [TN] Gazette; Feb. 10, 1812), and a letter in the Kentucky Reporter (pub. in Lexington, KY; Feb. 1, 1812) and others describe the extensive ground failure that occurred in and nearby the settlement of Little Prairie during the earthquakes of Dec. 16, 1811. They tell of fish being left out of water on what once was lake and river bottoms, of large chasms and sand blows, of buildings tilting due to differential settling, and of trees being

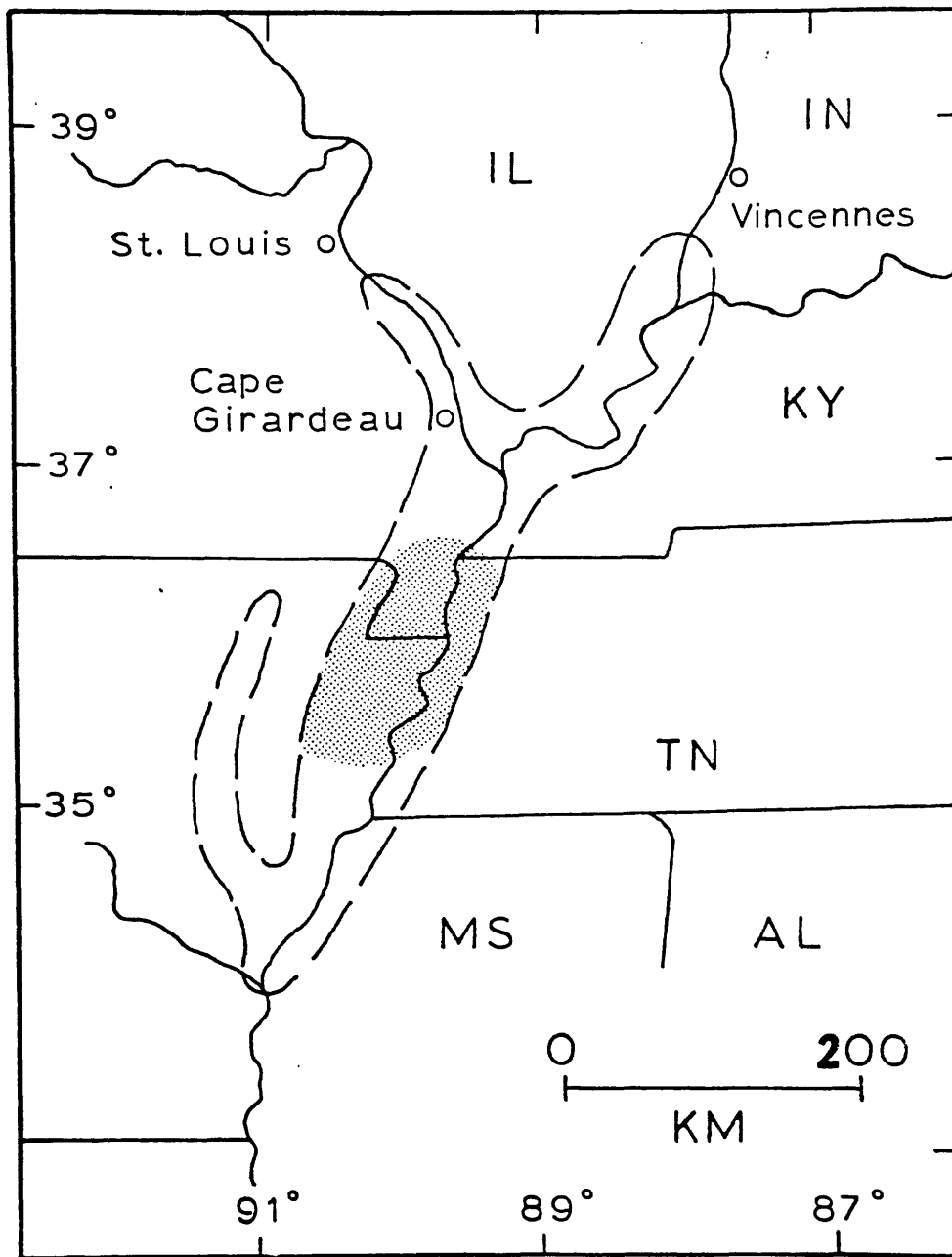


Figure 5.--Map showing the extent of the area of ground failures; shaded zone is the principal area of liquefaction, landslides, etc. (taken from Fuller, 1912, with modifications).

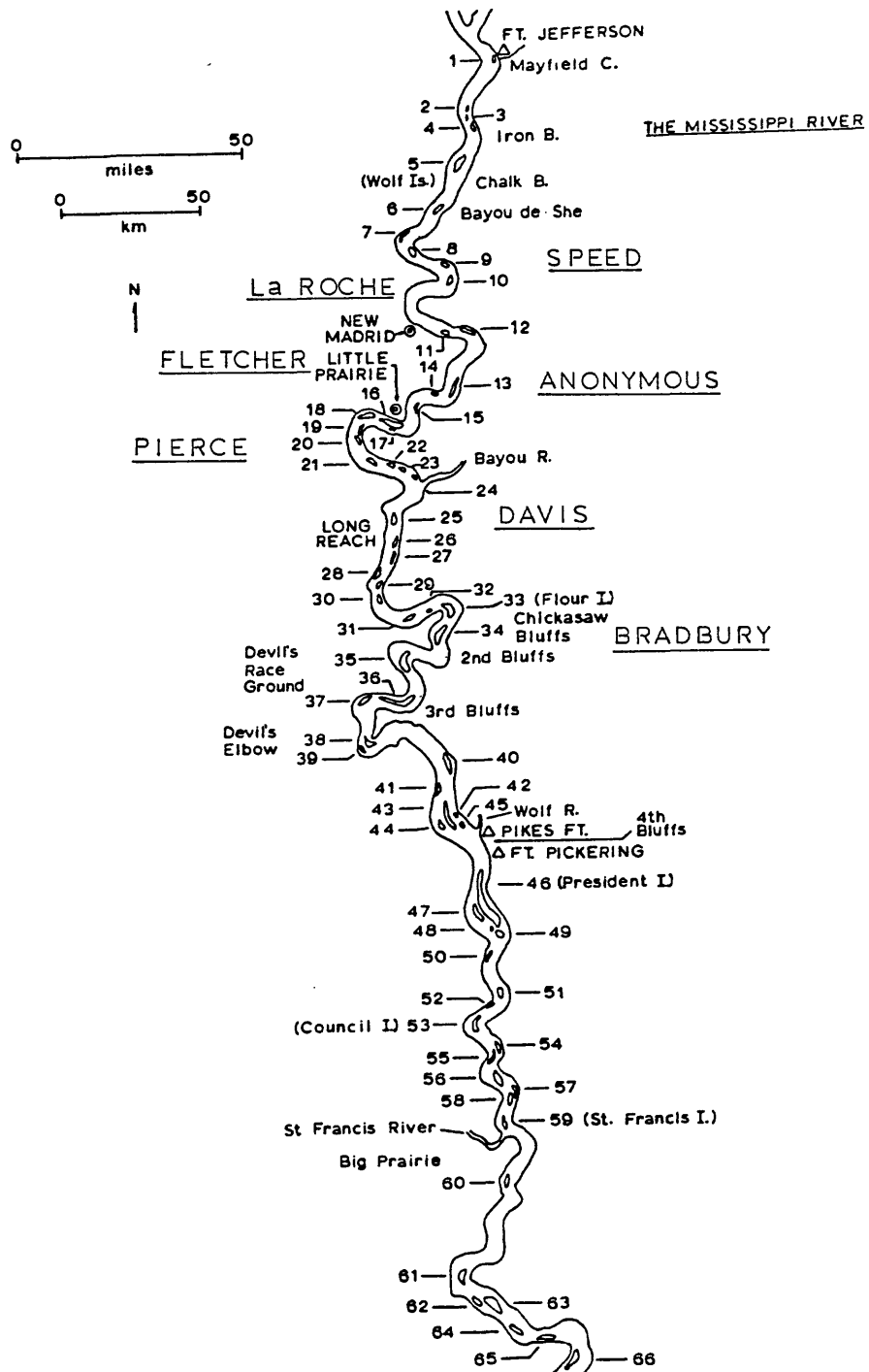


Figure 6a.--Map of the Mississippi river from Island 1 through Island 66, indicating geographical locations and island number (taken from Cramer, 1814). The underlined last names of individuals indicated on the figure refer to their locations on December 16, 1811, and February 07, 1812.

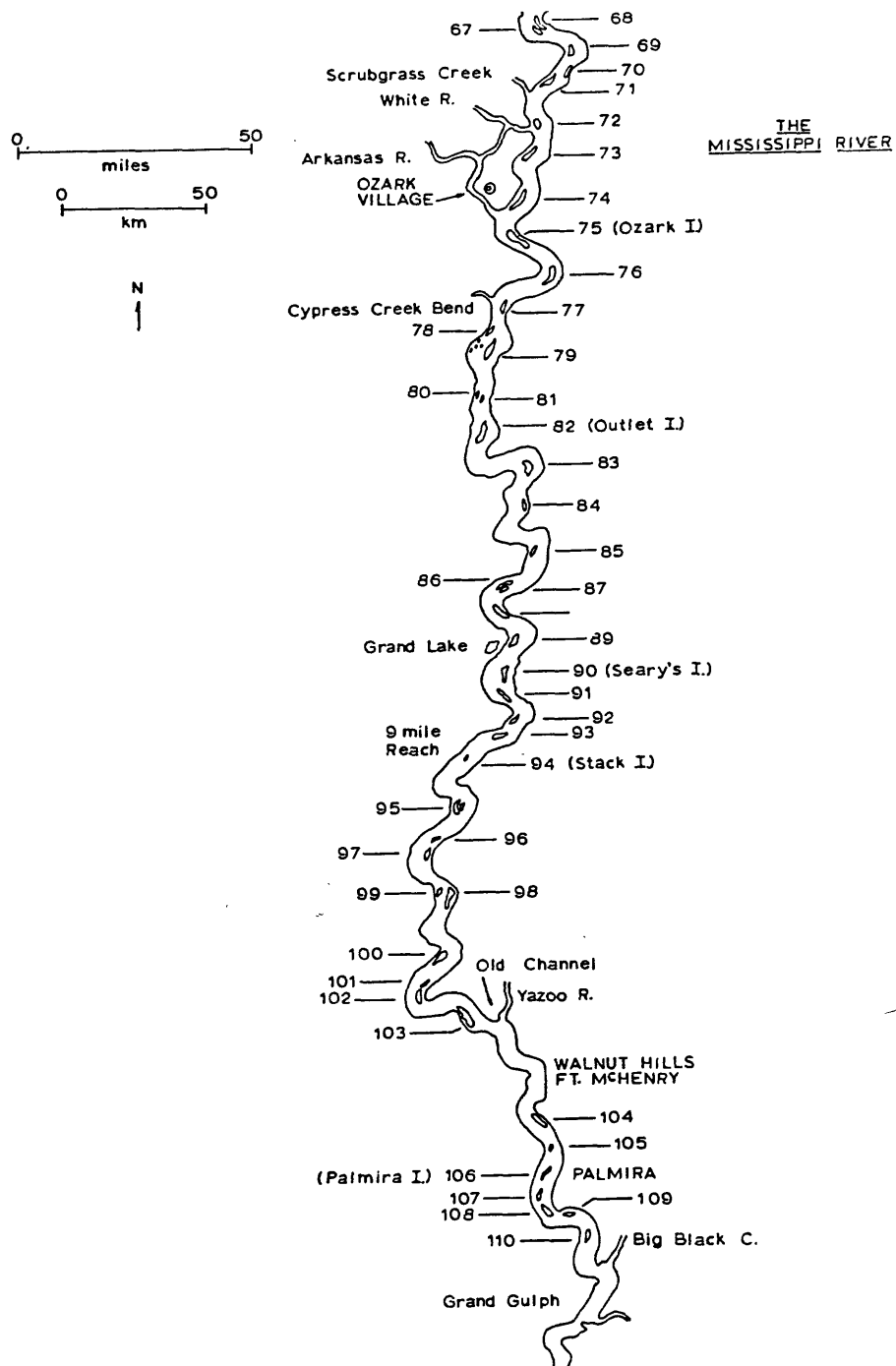


Figure 6b.--Map of the Mississippi river from Island 67 thru Island 110, indicating principal geographical locations and island numbers (taken from Cramer, 1814).

nearly submerged below the water's surface. At Big Prairie Mrs. Martha Eastwood (Joint Collection) tells of wide crevices, numerous sand blows, large trees being uprooted and extensive flooding.

Besides the general destruction and extensive ground failures within the shaded area of Figure 1, there are several reports of ground failures elsewhere. Twenty miles above New Madrid, it is reported in the American Statesman (pub. in Lexington, KY; Mar. 3, 1812) that sand blows and extensive flooding resulted from the Dec. 16, 1811 earthquake. Speed (Pennsylvania Gazette; Mar. 18, 1812) tells of seeing sand blows at Fort Massac on the Ohio river in southern Illinois, and as previously mentioned, Berry (1908) tells of sand blows and fissuring in White County, Illinois along the Wabash river.

The settlements of Little Prairie and Big Prairie were destroyed by the earthquakes of Dec. 16, 1811, whereas the settlement of New Madrid was destroyed by the earthquake of Feb. 07, 1812 (Robert McCoy; see Joint Collection).

AFTERSHOCKS

In addition to the four major earthquakes, there were hundreds of aftershocks felt as far away as Louisville, KY (McMurtrie, 1819), and Cincinnati, OH (Drake, 1815); and many of these were significant events in their own right. Table I, Section A, is a compilation of a few of those aftershocks that have been documented as being felt throughout the Ohio river valley and southeastern United States. The bases for the table are the newspaper accounts compiled by Street (1980), and summaries by McMurtrie (1819) and Drake (1815). Five of these shocks, those on Dec. 16, 1811 (at 3 A.M.); Dec. 17, 1811;

TABLE 1. Principal aftershocks: dates, times, and localities that reported the events.

| A. Aftershocks of the 1811-1812 Felt As Far East As The Atlantic Seaboard | | |
|--|------------|--|
| Date Day-Mo-Year | Time (EST) | Localities Reporting The Aftershock |
| 16 Dec. 1811 | 3 A.M. | Augusta (GA), Chillicothe (OH), Cincinnati (OH), Frankfort (KY), Knoxville (TN), Louisville (KY), Mount Gilead (KY)*, New Bourbon (MO)**, St. Louis (MO), and Savannah (GA). |
| 16 Dec. 1811 | 10 A.M. | Cincinnati (OH), Columbia (SC), Fort St. Stephens (AL), New Bourbon (MO), and St. Louis (MO). |
| 17 Dec. 1811 | Noon | Charleston (SC), Chillicothe (OH), Cincinnati (OH), Columbia (SC), Fort St. Stephens (AL), Georgetown (SC), Louisville (KY), Meadville (PA), Marietta (OH), Natchez (MS), New Bourbon (MO), St. Louis (MO), Savannah (GA), Wheeling (WV), and Zanesville (OH). |
| 07 Feb. 1812 | 10:40 P.M. | Augusta (GA), Dayton (OH), Knoxville (TN), Lancaster (OH), Louisville (KY), Mount Gilead (KY), Newbern (NC), New York (NY), Richmond (KY), and Wheeling (WV). |
| 10 Feb. 1812 | 4 P.M. | Charleston (SC), Cincinnati (OH), Louisville (KY). |
| 11 Feb. 1812 | 6 A.M. | Charleston (SC) and Cincinnati (OH). |
| B. Aftershocks of the 1811-1812 Sequence Felt Throughout The Mid-West | | |
| 16 Dec. 1811 | 7:15 A.M. | Chillicothe (OH), Cincinnati (OH), Louisville (KY), and New Bourbon (MO). |
| 16 Jan. 1812 | 11 P.M. | Cincinnati (OH) and Lexington (KY). |
| 23 Jan. 1812 | 11 P.M. | Lexington (KY) and Louisville (KY). |
| 27 Jan. 1812 | 9 A.M. | Cincinnati (OH), Dayton (OH), Louisville (KY), Mount Gilead (KY), Newport (KY), Wheeling (WV), and Zanesville (OH). |
| 04 Feb. 1812 | 5 P.M. | Cincinnati (OH), Columbia (SC), Louisville (KY), Marietta (OH), Mount Gilead (KY), and Zanesville (OH). |
| 07 Feb. 1812 | 8 P.M. | Cincinnati (OH), Dayton (OH), Knoxville (TN), Lancaster (OH), Louisville (KY), Mount Gilead (KY), Richmond (KY), and Wheeling (WV). |

*Mount Gilead (KY) - located three miles north of Hodgenville, KY.

**New Bourbon (MO) - a former small settlement of French Royalists located two miles south of Ste. Genevieve, MO.

Feb. 07, 1812 (at 10:40 P.M.); Feb. 10, 1812; and Feb. 11, 1812, were felt as far east as the eastern seaboard of the United States.

The aftershock at 3 A.M. on Dec. 16, 1811, was felt as far east as Augusta and Savannah, GA, as well as to some degree in several other central and eastern United States cities (see Table 1). The 6.2 m_{bLg} magnitude southeastern Missouri earthquake of Oct. 31, 1895 is described by Nuttli (1974) as being an intensity III (MM) event in Augusta. Since the two earthquakes were about equally severe at Augusta, and were felt over approximately the same area, the Dec. 16, 1811 aftershock at 3 A.M. is probably a magnitude 6 to 6½ m_{bLg} event.

The aftershock on Dec. 17, 1811 was felt in Charleston, SC where it is described as lasting less than thirty seconds. It was sensibly felt by those in their houses but not by those on the streets, and caused hanging articles to vibrate; i.e., an intensity III (MM) at Charleston, SC. By way of comparison, the 6.6 m_{bLg} (Nuttli et al, 1979) Charleston, SC earthquake of Aug. 13, 1886 is described by Bollinger and Stover (1976) as being an intensity III MM event at New Madrid, MO - reciprocity suggests that the two events are approximately equal in magnitude. The Dec. 17, 1811 earthquake, which also stopped clocks in Natchez (an epicentral distance of 510 kilometers) was reported as being severe at Georgetown, SC (an epicentral distance of 1,020 kilometers), and was described by Bradbury (1819), who was traveling down the Mississippi river, as a violent shock that greatly agitated the trees and river.

Another strong aftershock that can be somewhat documented is the one that was felt at approximately 10:40 P.M. on Feb. 07, 1812. This aftershock was felt as far away as New York city (an epicentral dis-

tance of 1,430 kilometers), is described in Louisville, KY as being "severe to tremendous", as being "smart" at Dayton, OH and Augusta, GA, as being "felt by many" in Newbern, NC, as "frightening children" in Wheeling, WV, and as of being of "considerable violence" in Knoxville, TN. This aftershock is not specifically mentioned in the Charleston, SC newspaper accounts of the earthquakes, but since it was felt in both Georgia and North Carolina, it was probably also felt in Charleston. Regardless, since the earthquake was felt as far away as New York city and is widely collaborated elsewhere, it too was probably on the same order of magnitude as the Charleston, SC earthquake of Aug. 31, 1886.

The aftershocks that occurred on Feb. 10, 1812 at 4 P.M. and Feb. 11, 1812, were also felt in Charleston, SC, where they were described as being "slight". At Louisville, KY the Feb. 10, 1812 aftershock was described as being "smart", while at Cincinnati, OH it was described as being a "gentle vibration". The magnitudes of both aftershocks are probably slightly less than that of the previous two, and more likely were on the order of the 1895 Charleston, MO earthquake's magnitude, $6.2 m_{bLg}$.

The aftershock listed in Section B of Table 1 were felt throughout most of the Ohio river valley and, in some instances, were reported as being felt as far east as Columbia, SC and Wheeling, WV. Based on the felt areas of the 1886 and 1895 earthquakes referenced above, and the south-central Illinois earthquake of Nov. 09, 1968 (Gorden et al, 1970), the aftershocks listed in section B are probably on the order of $5\frac{1}{2}$ to $6 m_{bLg}$ magnitude earthquakes.

The aftershocks listed in Table 1 are but a very few of the total number known to have occurred. In addition to those listed in the table, there are several other aftershocks that are reported in various eastern cities, but which are not included in the table since they could not be collaborated as being felt elsewhere. In addition, Brooks (McMurtrie, 1819) chronicled 191 other aftershocks that Nuttli (1973) classifies as MM intensity II at Louisville, KY. Based on recent earthquakes, for which there are available both instrumental and intensity data, southeastern Missouri earthquakes that are felt in Louisville generally have a m_{bLg} magnitude of 5.2 or greater.

Therefore, in summary with respect to the aftershocks, it can be concluded that between Dec. 16, 1811, when the first earthquake occurred, and March 15, 1812, when Brooks stopped recording the aftershocks, four earthquakes of magnitude 7 m_{bLg} or greater occurred, at least six aftershocks of magnitude 6.2 to 7.0 m_{bLg} occurred, and at least 197 aftershocks of magnitude 5.2 and 6.2 m_{bLg} occurred.

EFFECTS ALONG THE MISSISSIPPI RIVER

Some of the most dramatic eye-witness accounts of the 1811-1812 earthquakes are the observations noted by travelers going down the Ohio and Mississippi rivers during the winter of 1811-1812.

Eye Witness Accounts of the Earthquake of Dec. 16, 1811

On the evening of Dec. 16, 1811, Charles Latrobe (1835) was aboard the steam boat 'New Orleans' that was tied up on the Ohio river a short distance upriver from the present site of Owensboro, KY; Firmin La Roche, Fr. Joseph, and others (Shoemaker, 1928) were

on a boat tied up eight miles above New Madrid along the west bank of the Mississippi river; John Wiseman (New Madrid Record; Joint Collection) was on a boat tied up near New Madrid; an anonymous traveler (Farmer's Repository; Feb. 28, 1812) was on a boat moored to a sandbar 10 miles above Little Prairie; James Fletcher (Wilson's Knoxville Gazette; Feb. 10, 1812) was on a boat tied up at Little Prairie; William Pierce (New York Evening Post; Feb. 11, 1812) was on a boat tied up along the Mississippi river 116 miles below the mouth of the Ohio - i.e., near island 20; Captain John Davis (Otsego [NY] Herald; Mar. 28, 1812) was on a boat tied to island 25; and John Bradbury (1819) was on a boat tied up to an island in the Mississippi river - most likely island 34. Superimposed on Figure 6a are the approximate locations of the various travelers on the night of Dec. 15, 1811.

In general their accounts agree that the most extensive ground failures associated with the two major shocks on Dec. 16, 1811, and their immediate aftershocks, occurred along the Mississippi river beginning a few miles above New Madrid, MO to a point mid-way between Devil's Elbow and Fort Pickering. Less severe ground failure phenomena were observed along the Ohio river as far up river as a point somewhere between present day Henderson and Owensboro, KY (Latrobe, 1835), and as far south along the Mississippi river as the mouth of the St. Francis river. The following is a brief summary of their observations; as indicated previously, Figures 6a and 6b illustrate the geographic locations along the Mississippi river mentioned in the summary.

On board the steamboat 'New Orleans' that was tied up on the Ohio river a short distance above the present day site of Owensboro, KY, Latrobe did not feel the Dec. 16th earthquakes. The first time that those on board became aware of something unusual was when they landed on the Indiana side of the Ohio river opposite of Yellow Banks (Owensboro, KY) to take on a load of coal. While loading the coal, squatters in the area told them about the strange noises and shaking felt that morning.

On the 16th and 17th the steamboat continued its journey down the Ohio, during which time those on board frequently witnessed large portions of the shore falling into the river. On the second day (the 17th) they observed trees in the forests being shaken, and numerous trees obstructing the channels in the Ohio. Late that night they tied up to an island in the Ohio that was within sight of the Mississippi river. During the night they felt several after-shocks that were strong enough to jar loose articles on board the boat.

Eight miles above New Madrid on Dec. 16th, La Roche witnessed trees and banks falling into the river, and described how the boat he was on was pushed upriver by a great wave for a distance of about one mile before the river returned to its normal flow. He also described the death of one of his crewmen, a man named Ben, who was killed by a falling tree as they were landing at New Madrid later that morning. The falling tree also severely damaged their boat, but La Roche's crew apparently decided that they were better off on the river than remaining in New Madrid where houses were on fire,

the ground was badly cracked (fissures), and small earthquakes were continually being felt. Latrobe arrived at New Madrid on Dec. 18th aboard the 'New Orleans', and likewise mentions seeing many fissures in the settlement.

About twenty miles below New Madrid (or ten miles above Little Prairie) the anonymous traveler was tied up on a sandbar near island 13. The writer of the letter described seeing trees and banks caving into the river, large trees being snapped in two by the violence of the earthquakes, and seeing trees being torn up by their roots. And while this was happening on shore, he described large bodies of water, logs, etc. being thrown above the river to the height of several feet in places. The traveler also described the Mississippi river as rising 18 inches immediately after the first shock; he was afraid of being stuck on the sandbar and consequently sounded the water level beneath his boat at regular intervals throughout the night. On the morning of Dec. 16th, he got underway and arrived at Little Prairie shortly thereafter, where he was told that the fourth shock (the second major event; i.e., the one at 08:15 on the morning of the 16th) had destroyed that settlement.

James Fletcher, who had arrived at Little Prairie on the evening of the 15th, was most impressed by the many fissures and sand blows that developed in the nearby vicinity of that settlement. The largest fissures he observed were 3 to 10 feet in width, and exhibited differences in elevation between the two sides by as much as 12 feet. Fletcher also observed sand blows and described them as spouting water and sand out of the earth to a height of eight or ten feet.

William Pierce's boat was tied up along the left bank of the Mississippi river in the vicinity of island 20 on the evening of Dec. 15th. He reported seeing a large oak tree snap in two by the violence of the earthquake, of seeing water, sticks, mud, etc. being spouted into the air, extensive caving of the river banks, and tremendous explosions resembling discharges of artillery. The second major earthquake on the morning of the 16th caused still more extensive caving of the river banks, and Pierce witnessed water, mud, sticks, etc. spouting into the air to heights of thirty feet above the river. During the day of the 16th, he reported an almost continuous series of aftershocks between the first event shortly after 2 A.M. and daylight.

Shortly after dawn on the 16th, the boat Pierce was on casted off from the river bank, where it had been moored the night before, and floated 52 miles downriver before tying up to some willows at the extremity of a partially sunken island (probably somewhere in the vicinity of island 51). Throughout the day the aftershocks continued, and Pierce described them as ". . . a continued series of shocks, attended with innumerable explosions like the rolling of thunder; the bed of the river was incessantly disturbed, and the water boiled severely in every part." The effects of the aftershocks along the river banks were no less alarming; the river banks were continuously caving in, and large trees were being whipped back and forth with many being uprooted. Pierce's boat remained tied up to the island for two days (i.e., the 17th and 18th of December). On

the island itself, Pierce found many sand blows - the largest being 63 feet in circumference, 16 feet deep, and having extruded chunks of material weighing from 15 to 20 pounds for distances up to 160 measured paces.

Based on his own observations, Pierce stated that the worst destruction along the Mississippi river, due to the Dec. 16th earthquakes and their aftershocks, was along that stretch of the river from Bayou River to a point just down river from Devil's Elbow. The greatest destruction he observed was in the vicinity of Flour Island.

About 17 miles down river from Pierce, Captain John Davis, in company with forty other boats, was on a boat that was tied up to island 25. At the time of the first shock, he casted off and anchored on the right (west) side of the island where his boat remained until daylight. During the early morning hours, they experienced fifty additional shocks which greatly shook the boats. Shortly after 7 A.M., an aftershock occurred that Davis described as causing the islands, boats and mainland to become ". . . perfectly convulsed"; trees twisted together; the earth in all quarters sinking - thirty to forty acres of mainland falling into the river; and torrents of water "issuing" from the center of island 25 and running down its side. That afternoon, after floating thirty-five miles down river in five hours, his boat landed at the lower end of Flour Island. During their ordeal, Davis mentioned the sinking of three boats by logs, but does not mention any loss of life.

Down river from Davis, on Dec. 16, 1811, John Bradbury was on a boat moored to a small island (possibly island 34) at the head of Devil's Race Ground. The earthquake shortly after 2 A.M. caused vast portions of the river banks to fall into the river, trees to fall, and the river to be agitated as if by a severe storm. By daylight Bradbury had counted 27 aftershocks, the river was rising rapidly, and it had been decided to push off into the Devil's Race Ground. At 11 A.M. they experienced another severe shock that violently shook the trees, caused large portions of the river banks to collapse into the river, and greatly agitated the river. On the 17th of Dec. at noon, while (approximately) in the vicinity of island 40, they felt a severe shock of a very long duration. On the 18th, in the vicinity of Council Island, they felt a violent earthquake that threw a great number of trees into the river.

In summary with respect to the accounts by the travelers going down the Mississippi river on Dec. 16, 1811, the only inconsistency between the different accounts is the southern limit of the damaged area. Bradbury places the southern limit of the damaged area as island 53 (Council Island), the anonymous traveler places it at island 57, while La Rache claims to have seen cracks in the river banks forty to fifty miles south of the mouth of the Arkansas river (approximatley island 80).

Eye Witness accounts of the Earthquake of Feb. 07, 1812

The only available first-hand account of the effects of the Feb. 07, 1812 earthquake along the Mississippi river is that of Mathias M. Speed (Pennsylvania Gazette; Mar. 18, 1812). On the evening of

Feb. 6th, Speed's boat, in company with another, was tied up to a willow bar on the west bank of the Mississippi river opposite island no. 9 (see Figure 6a). At about three o'clock in the morning the travelers were awakened by the violent agitation of the boat and a tremendous noise reminiscent of the constant discharge of heavy cannon. At the same time the river began to rise, swells (nearly large enough to sink the boat) developed, and trees began to fall into the river. They cut loose the boats and drifted until daylight, at which time they found themselves four miles down river near the head of island 10. A short time later, while approaching New Madrid, the two boats still lashed together went over a falls, described by Speed as being about equal to height to those on the Ohio (i.e., the falls on the Ohio river near Louisville, KY).

Speed describes New Madrid, MO as being deserted, almost all of the buildings in ruins, and the elevation of the town as being sunk 12 to 13 feet. While at New Madrid (Speed remained there from the 7th to the 12th of February), he met a number of other travelers who had ascended the Mississippi and who had encountered a similar rapids 7 miles below the town.

Shaler (Mitchill, 1815) relates a second-hand account of the Feb. 7th earthquake as told to him by the patron (?) of a river boat. On the morning of the 7th, the patron's boat was tied to the river bank thirteen miles above New Madrid when the earthquake struck shortly after 3 A.M. At the time of the shock the mooring cables were cut, and the boat began drifting down river. At about daylight, a short distance above New Madrid, the boat passed over a falls that he (the patron) estimates to have been about six feet in height. Of the 30

boats he was aware of that attempted to pass over the falls, only two succeeded and many boatmen lost their lives in the river. Upon arriving at New Madrid, he found the settlement wrecked and being continuously shaken by aftershocks. Nonetheless, since another falls had formed eight miles below the town, he was forced to remain at New Madrid for five days before the lower falls had worn away sufficiently for the boat to pass over. The boat patron reported feeling aftershocks as far south as Flam Island (location - unknown).

Due to the similarities in the accounts, it is quite probable that Shaler either related to Mitchill a version of Speed's experiences, or an account of a crew member of his or the other boat that Speed mentioned being lashed together on the morning of Feb. 7th.

General Observations Along the Mississippi

Soon after the cessation of the major earthquakes in the central Mississippi river valley, two other travelers moving down river wrote lengthy and detailed accounts of their observations. The first of these, the letter by James McBride (1810), was written on April 1, 1812 and is based on his observations while barging barrels of flour, whiskey and pork down the Ohio and Mississippi rivers in early March. McBride told of seeing the effects of the earthquakes soon after entering the Mississippi, and of experiencing several considerable shocks every few hours for a distance of one hundred miles above and below the settlement at Little Prairie. He also told of a totally destroyed and abandoned Little Prairie, at which place he disembarked

and walked inland for a distance of two miles. In every direction along his walk he observed the ground to be badly broken by fissures, some almost too large for him to leap. In one area he also noted several sand blows ranging in diameter from 5 to 30 feet. In addition, he saw trees that had been split from their bases upwards to a height of 12 feet, with the two halves separated at the base by as much as 3 feet. Along the river, he saw badly cracked river banks, trees that had been broken in two, and acres of ground with trees still standing sunken well below their former level (as evidenced in some instances by trees with only their very tops remaining above the water).

Another first-hand account describing the cumulative effects of the earthquakes along the Mississippi river is that of Stephen Austin (1824), which is based on the log he wrote in May of 1812 while traveling down the Mississippi river from St. Louis, MO. At Cape Girardeau, MO, Austin described the earthquakes as having been very severe, judging from the fact that every chimney was either thrown down or cracked, and two partially completed brick buildings were wrecked. Further down river, Austin observed badly shattered river banks beginning at a point about twenty miles above New Madrid: he described the settlement as being shattered, and repeated a version of the account written by Shaler to Mitchill (1815) of many lives being lost among the boats that went over the falls in the Mississippi river above New Madrid shortly after the major earthquake on the morning of Feb. 7, 1812.

SUMMARY

Numerous papers and articles have been written on various aspects of the central Mississippi river valley earthquakes that occurred during the winter of 1811-1812. This paper is a review of what the authors believe to be the principal facts of the earthquakes; the major earthquakes, the stronger aftershocks, and the extent and severity of the ground failures.

By comparing the felt reports for some of the stronger aftershocks that were felt along the eastern seaboard of the United States to more recent earthquakes, m_{bLg} magnitudes of six aftershocks are estimated to be on the order of 6.2 to 7.0. The magnitudes of 197 other aftershocks that were felt as far east as Louisville, KY are estimated to be in the range of 5.2 and 6.2 m_{bLg} .

The four major earthquakes, along with the principal aftershocks, occurred over a period of time involving $3\frac{1}{2}$ months. Such a continuation of significant earthquake activity is in itself a major problem for the recovery of an area devastated by the initial shocks.

REFERENCES

- Anonymous (1812). Account of the earthquakes which occurred in the United States, North America on the 16th of December, 1811, the 23rd of January, and the 7th of February, 1812, Smith, Philadelphia, Pennsylvania, 84 p.
- Austin, Stephen F. (1924). "Stephen F. Austin's Diary", Annual Report of the American Historical Association, for the year 1919.
- Berry, Daniel L. (1908). "The Illinois earthquakes of 1811-1812," Transactions of the Illinois State Historical Society, 12, 74-78.
- Bollinger, G. A. and C. W. Stover (1976). "List of intensities for the 1886 Charleston, South Carolina earthquake", U.S. Dept. of Interior, Geological Survey, Open-file Report, 76-66, 31 p.
- Bradbury, John (1819). Travels in the interior of North America in the years 1809, 1810 and 1811, London.
- Cramer, Zadoc (1814). The Navigator, Pittsburgh, PA, 215 p.
- Drake, D. (1815). Natural and statistical view, a picture of Cincinnati and the Miami county, illustrated by maps, with an appendix, containing observations on the late earthquakes, the aurora borealis, and the south-west wind, Cincinnati, Ohio, 251 p.
- Fuller, M. L. (1912). "The New Madrid earthquakes", U.S. Geological Survey Bulletin, 494, Washington, D.C., 119 p.

Gordon, David W., Theron J. Bennett, Robert B. Herrmann, and Albert M. Rodgers (1970). "The south-central Illinois earthquake of November 9, 1968: Macroseismic studies", Bull. Seism. Soc. Am., 60, 953-971.

Joint Collection. Accounts of the 1811-1812 earthquakes attributed to Mrs. Martha Eastwood and Robert McCoy were found in a scrapbook in the Joint Collection of the University of Missouri Western Historical Manuscript Collection - Columbia and State Historical Society of Missouri Manuscripts.

Latrobe, Charles Joseph (1835). The Rambler in North America, 2nd edition, London, vol. 1, 107-108.

McBride, James (1910). "Voyage down the Mississippi river", Quarterly Publication of the Historical and Philosophical Society of Ohio, v. 27-31.

Mitchell, S. L. (1815). "A detailed narrative of the earthquakes which occurred on the 16th of December, 1811, and agitated the parts of North America that lie between the Atlantic ocean and Louisiana; and also a particular account of other quakings of the earth occasionally from that time to the 23rd and 30th of January, and the 7th and 16th of February, 1812, and subsequently to the 18th of December, 1813, and which shook the country from Detroit and the Lakes to New Orleans and the Gulf of Mexico, Trans. Literary Phil. Soc., vol. 1, 281-307.

- Nuttli, O. W. (1973). "The Mississippi valley earthquakes of 1811 and 1812: intensities, ground motion and magnitudes", Bull. Seism. Soc. Am., 63, 227-248.
- Nuttli, O. W. (1974). "Magnitude recurrence relation for central Mississippi valley earthquakes", Bull. Seism. Soc. Am., 64, 1189-1207.
- Nuttli, O. W., G. A. Bollinger, and D. W. Griffiths (1979). "On the relation between Modified Mercalli intensity and body-wave magnitude", Bull. Seism. Soc. Am., 69, 893-909.
- Penick, James, Jr. (1976). The New Madrid Earthquakes of 1811 and 1812, University of Missouri Press, Columbia, MO.
- Shoemaker, Floyd C. (1928). "A sailors record of the New Madrid earthquake", The Missouri Historical Review, 268-270.
- Street, R. (1980). A compilation of accounts describing the Mississippi valley earthquakes of 1811-1812: Part I, Dept. of Geology, University of Kentucky, Lexington, KY, 247 p.
- Street, R. (1982). "A contribution to the documentation of the 1811-1812 Mississippi valley earthquake sequence," Earthquake Notes, 53, 39-52.

ACKNOWLEDGMENTS

The authors wish to acknowledge the many helpful suggestions made to them over the years by Mr. Andrew Lacroix.

This research was supported in part by the U.S. Geological Survey under Contract No. 14-08-0001-21251. The opinions, findings, and conclusions, or recommendations expressed in this manuscript are those of the authors and do not necessarily reflect the views of the U.S. Geological Survey.

Ronald L. Street
Department of Geology
Bowman Hall
University of Kentucky
Lexington, KY 40506-0059

Otto Nuttli
Dept. of Earth & Atmospheric Sciences
P.O. Box 8099, Laclede Station
St. Louis University
St. Louis, MO 63156

SEDIMENTARY GEOLOGY OF THE NEW MADRID SEISMIC ZONE

by

T. C. Buschbach

Saint Louis University

and

H. R. Schwalb

Illinois State Geological Survey

ABSTRACT

Early and middle Cambrian sediments in the New Madrid area are restricted to two down-faulted structures, the Reelfoot Rift and the Rough Creek Graben. Both of these trenchlike features were apparently subjected to continued growth faulting, and they served as loci of sedimentary depocenters through the early Paleozoic. By Silurian time the depocenter had migrated northward to southern Illinois, where it probably remained until at least late Mississippian time. Late Mississippian and Pennsylvanian strata are preserved only in basinal parts of the New Madrid region, but many individual rock units appear to thicken southward to their truncated edges in southern Illinois.

Although the Ozark Uplift was covered by Paleozoic sediments from time to time, it has been a relatively positive feature since late in the Precambrian. The Nashville Dome, a southern extension of the Cincinnati Arch, was also a relatively positive feature in the region. The dome furnished almost no sediments to the New Madrid area, and in fact, was covered by shallow seas throughout most of the Paleozoic Era. The Pascola Arch, which was uplifted about 12,000 feet after Pennsylvanian deposition, created the southern margin of the Illinois Basin. The arch was eroded to a broad base level by late Cretaceous time and subsided into the Mississippi Embayment.

INTRODUCTION

In order to discuss stratigraphy of the New Madrid area without becoming immersed in details of correlations, facies relationships, and local names, it is necessary to combine units of similar rock types into major rock-stratigraphic units. The stratigraphic units are discussed here chronologically, but they are mapped on the basis of their gross lithology (Fig. 1).

This report draws freely on work released as contractors' reports by participants in the New Madrid Seismotectonic Study sponsored by the U.S. Nuclear Regulatory Commission. A review of this research was compiled by Buschbach (1983). Discussions of the Paleozoic rock units are summarized from a detailed report of the geology of the New Madrid area by Schwalb (1982). The regional aspects of some of the major rock-stratigraphic units in the region were discussed in reports for the National Petroleum Council study in Future Petroleum Provinces in the United States. Those studies were published by American Association of Petroleum Geologists as Memoir 15 (Cram, ed., 1971). From those studies the stratigraphy of the Eastern Interior Region of the United States was summarized by Buschbach (1971).

GEOLOGIC SETTING

The dominant tectonic features that exerted an influence on sedimentation in the New Madrid area are the Illinois Basin, the Cincinnati Arch, the Mississippi Embayment, and the Ozark Uplift (Fig. 2). Other features that also had significant effects on sedimentation in the area but were somewhat more

PALEOZOIC STRATIGRAPHIC COLUMN
(New Madrid study area)

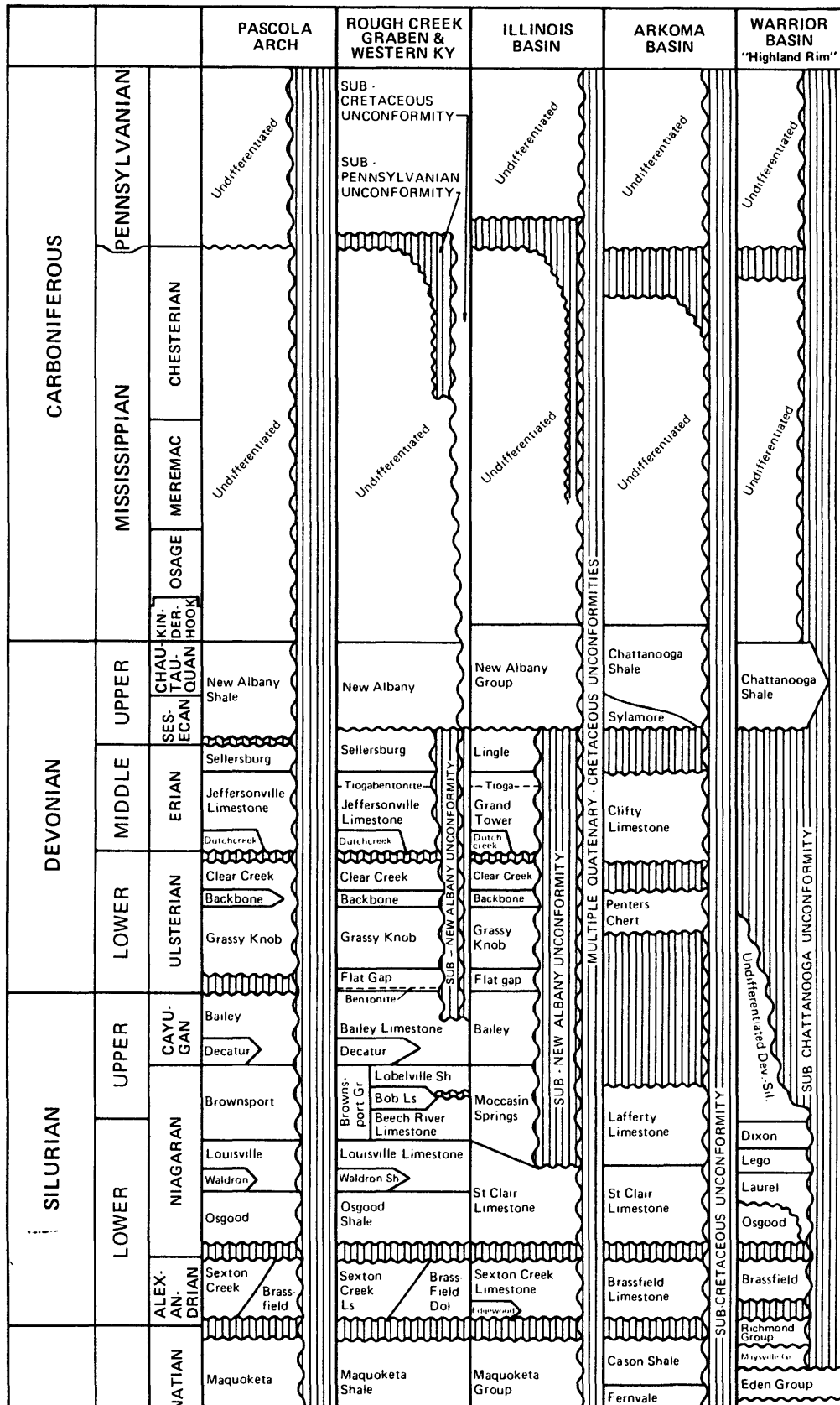


Figure 1. Geologic columns of study area
(from Schwalb, 1982).

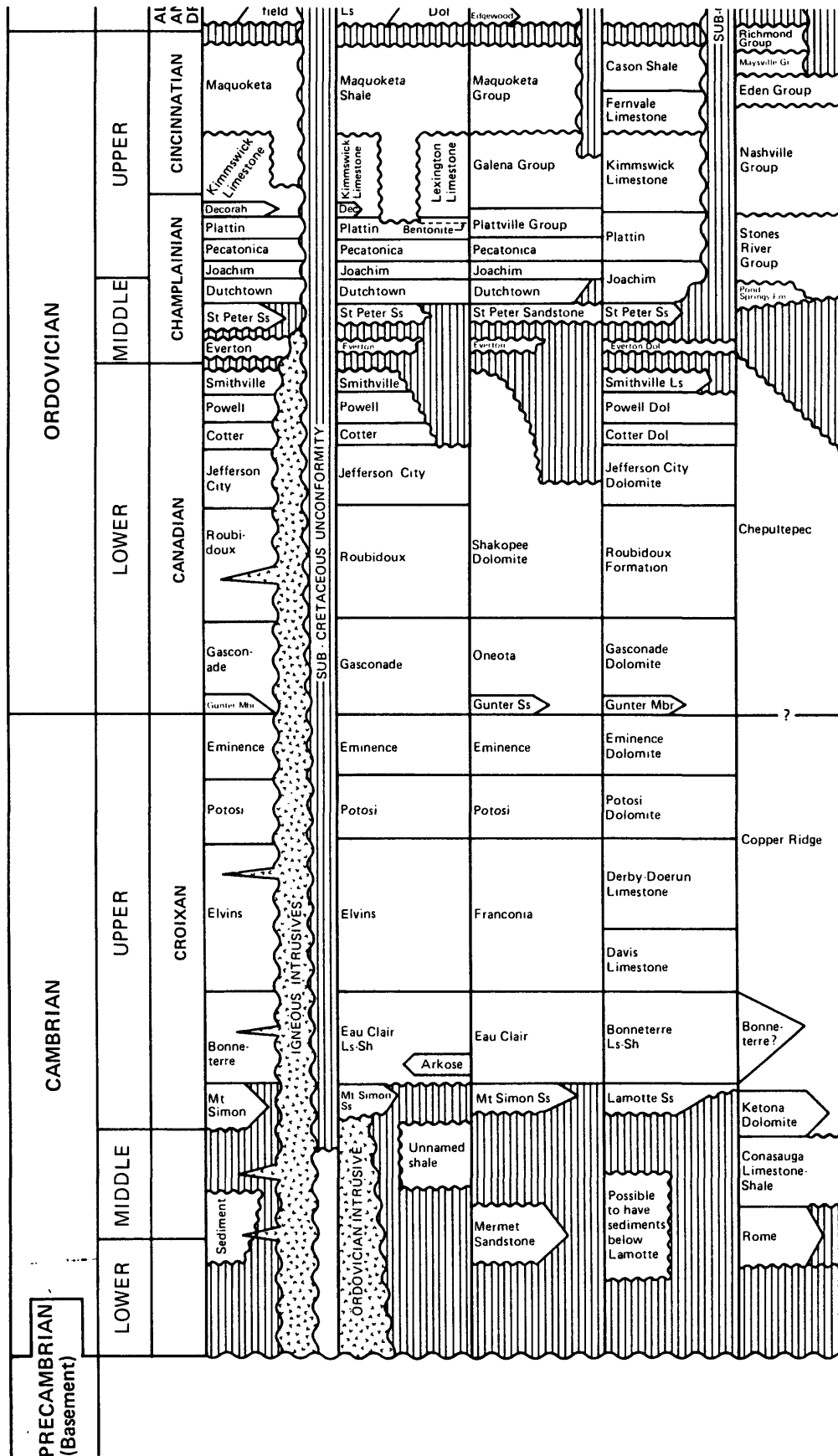


Figure 1, continued.

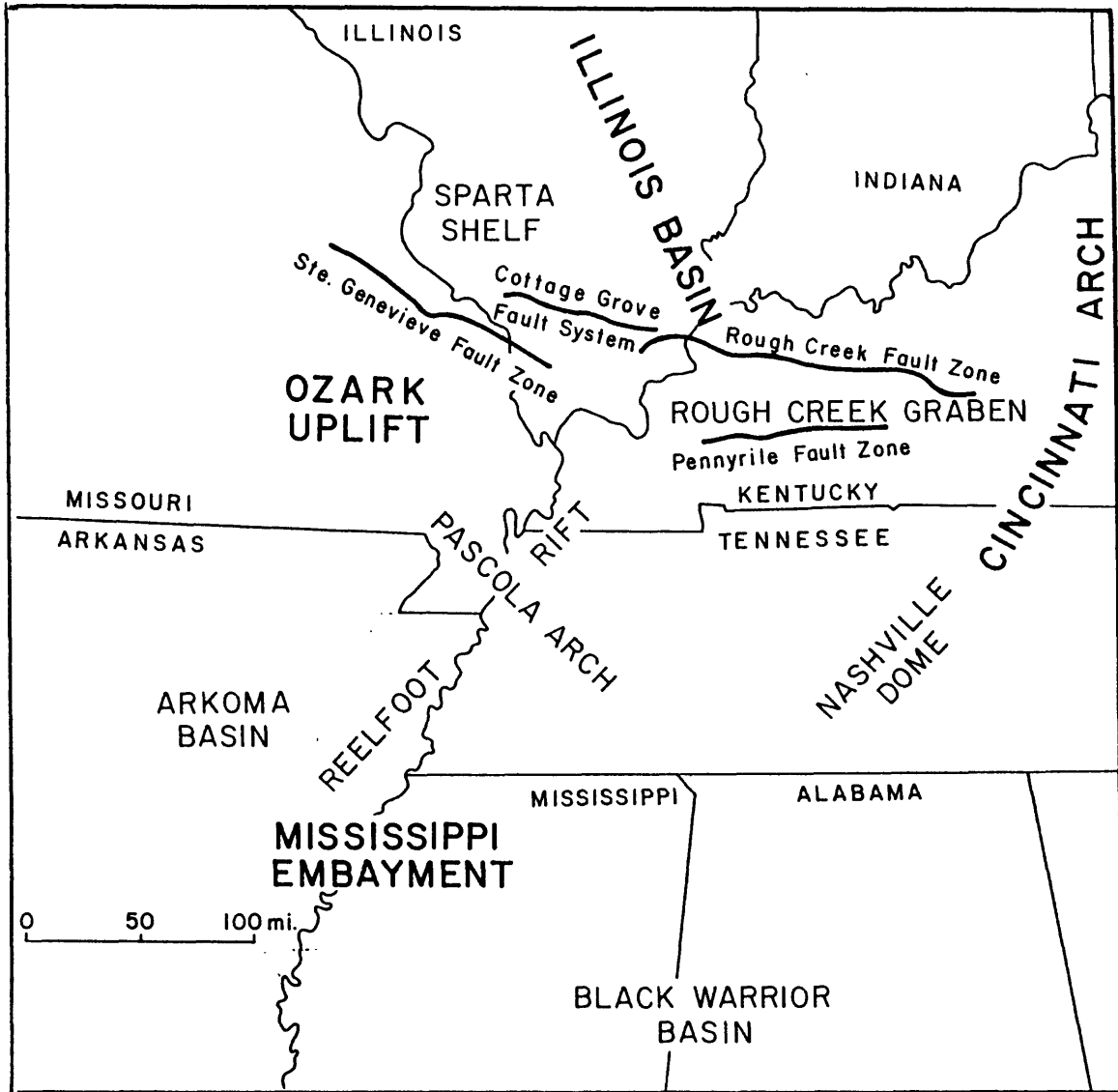


Figure 2. Structural features in the New Madrid area.

restricted in time or in geographical extent, were the Reelfoot Rift, the Rough Creek Graben, and the Pascola Arch.

The Illinois Basin is a spoon-shaped structure filled with more than 14,000 feet of Paleozoic sediments. The Cincinnati Arch is a broad uplift that separates the Illinois Basin from the Appalachian Basin. At its southern extension the arch includes the Lexington and Nashville Domes. Although the Cincinnati Arch apparently furnished no sediments to the New Madrid area, this positive structure influenced sedimentation throughout much of Paleozoic time. The Mississippi Embayment is a southward-plunging trough filled with Cretaceous and Tertiary sediments. The Ozark Uplift stood as a positive feature when Cambrian sediments first covered the area, but it subsided and was covered by Cambrian and early Ordovician sediments. By the beginning of middle Ordovician time the Ozarks again became a positive feature, and the crest of the uplift was not covered by significant deposits until middle Mississippian time and again in Pennsylvanian time. Throughout its long history as a positive element, the Ozark Uplift provided the source for only minor amounts of sandstone and shale in the New Madrid area.

The Reelfoot Rift and the Rough Creek Graben appear to be genetically related and were probably formed contemporaneously late in Precambrian or early in Cambrian time. At the base of the sedimentary succession both depressions contain several thousands of feet of clastic rocks dated or suspected of being middle and possibly early Cambrian age. These sediments appear to be restricted to the down-faulted structures in the area. Both of these trenchlike features have shown evidence of reactivation and have served as the loci of later sedimentary depocenters where total thicknesses of 15,000 to 20,000 feet of

sediments are present. The area of the Reelfoot Rift includes the Reelfoot Basin (Cambrian and Ordovician) and the Mississippi Embayment (Cretaceous and Tertiary); the area of the Rough Creek Graben includes the Moorman Syncline (Pennsylvanian-Permian).

The Pascola Arch is a circular uplift located between the Ozark Uplift and the Nashville Dome. The uplift, which occurred during the interval between the end of Pennsylvanian time and early in late Cretaceous time, caused the erosion of an estimated 12,000 feet of Paleozoic sediments from its crest (Fig. 3). In the New Madrid area, the coarse chert pebbles in the Tuscaloosa Formation of early late Cretaceous age are the only sediments present that resulted from the erosion of this uplift. Presumably most of the clastic material eroded from the Pascola Arch is incorporated in pre-late Cretaceous Mesozoic sediments of the Mississippi Embayment.

PRECAMBRIAN SURFACE

The top of Precambrian igneous rocks in the New Madrid area represents a major unconformity between the 1- to 1 1/2-billion-year-old Precambrian rocks and the overlying Cambrian sediments. The crystalline rocks were subjected to subaerial erosion, and a terrain with pronounced topographic relief was developed. As much as 1,500 feet of relief existed in the area of the Ozark Uplift, and more than 500 feet of relief is documented for hills and ridges in the Illinois Basin area. The Sparta Shelf appears to have stood as much as 1,000 feet above a low area to the east. Stream gradients were apparently steep enough to cause the removal of erosional debris because there has been no appreciable accumulation of a regolith or detritus zone in the region.

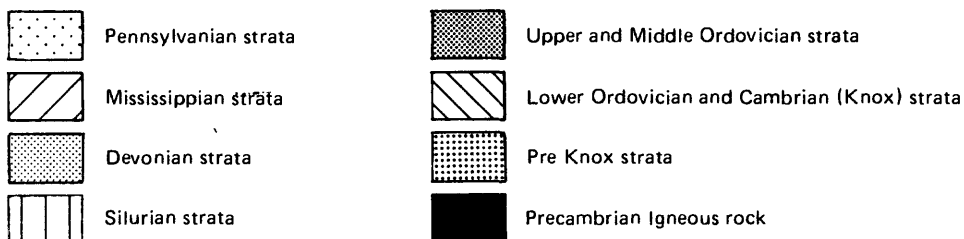
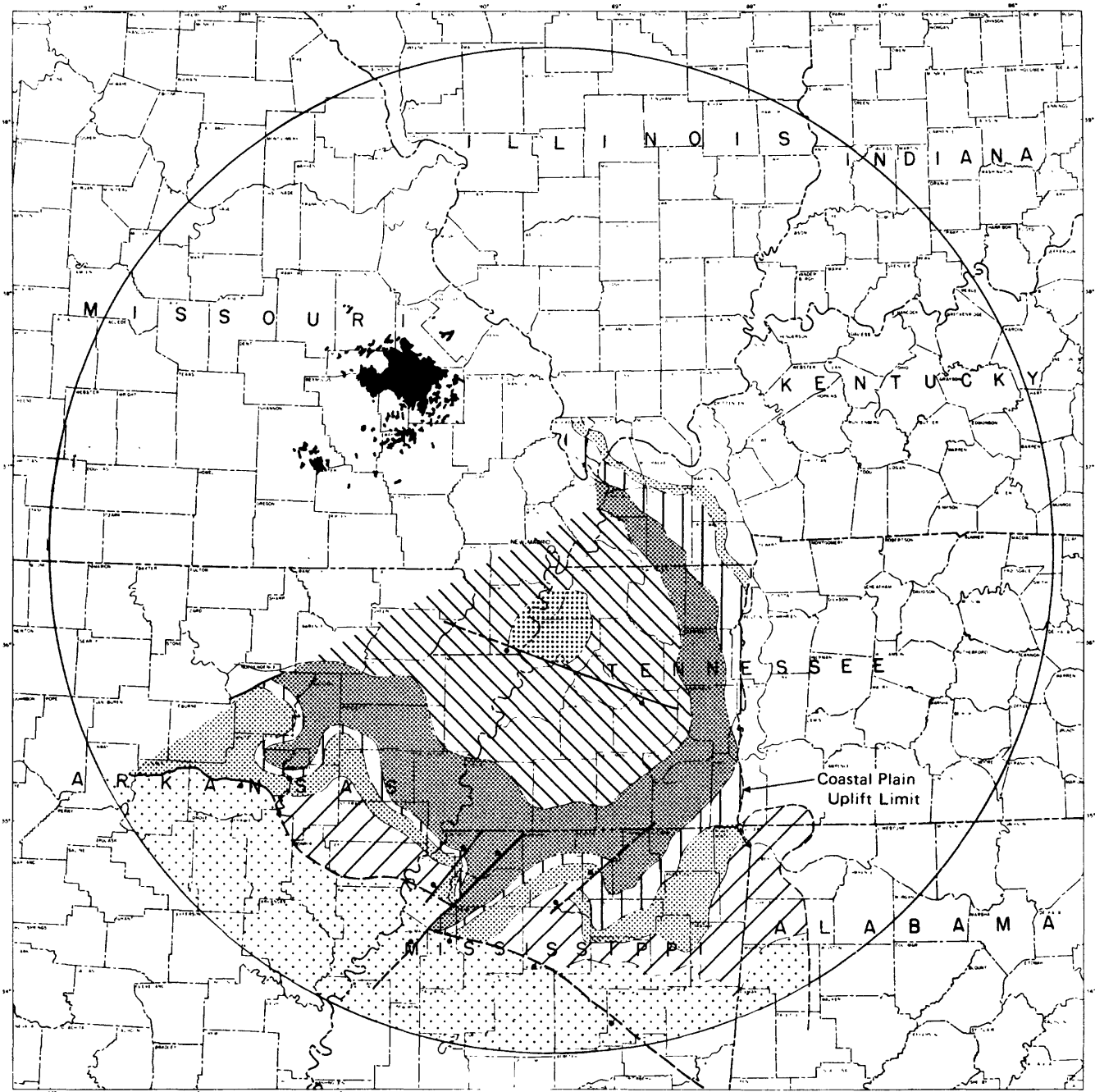


Figure 3. Subcrop pattern of Paleozoic rocks beneath Cretaceous cover (from Schwalb, 1982).

Precambrian rocks crop out in the St. Francois Mountains of the Ozark Uplift, where they have been extensively studied (Kisvarsanyi, 1976).

The unconformity at the top of the Precambrian igneous rocks is overlain by sedimentary rocks of various ages. In the Reelfoot Rift and Rough Creek Graben areas, the first sediments were probably of early Cambrian or Precambrian age. Early Cambrian sediments deposited on the eastern and southern edges of the ancestral Nashville Dome probably came from a different source than did the sediments in the New Madrid area. In the areas north of the Rough Creek Fault Zone and in the vicinity of the Ozark Uplift the basal sediments are late Cambrian in age. The tops of the highest Precambrian hills were probably covered by sediments at the end of Cambrian time, and the thickness of cover on Precambrian rocks at that time ranged from a few hundred to several thousands of feet.

To construct a map showing the configuration of the top of Precambrian rocks, we plotted the relatively small number of datum points, projected structural trends downward from shallower and better explored horizons, and considered the information gained from various geophysical surveys in the area. The map presented here (Fig. 4) was based on observations of surface exposures (in the Ozarks) and a considerable amount of drilling information, and therefore probably predicts, within reasonable limits, the elevations of Precambrian rocks in the areas of the Ozark Uplift, much of the Illinois Basin, and the Nashville Dome.

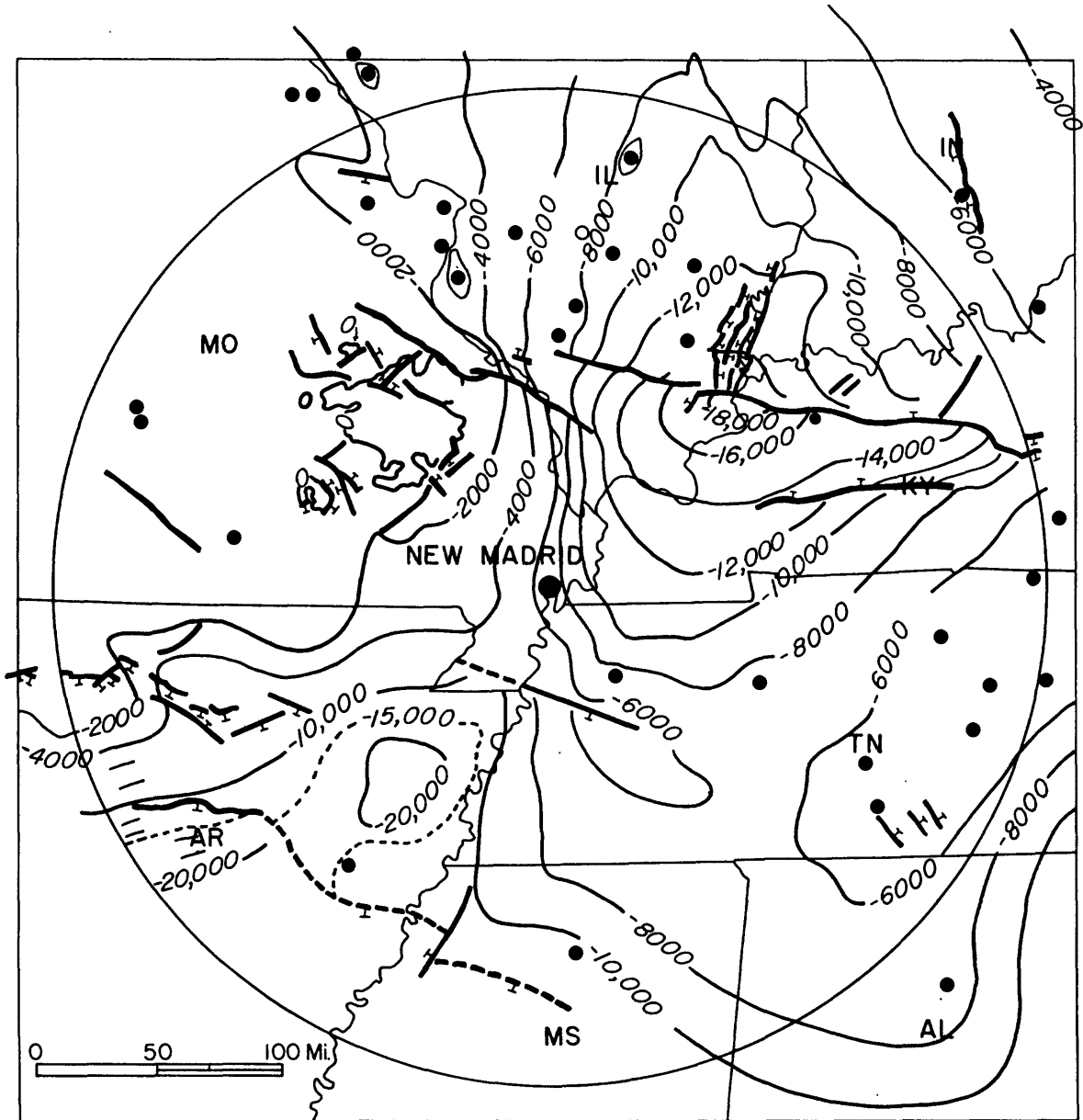


Figure 4. Top of Precambrian igneous rocks.

The Rough Creek Graben, bordered on the north by the Rough Creek Fault Zone, is clearly an ancient graben or half-graben with the basement rocks dropped down sharply to the south. Post-Pennsylvanian movement along the Rough Creek Fault Zone, however, is chiefly down to the north. The southern flank of the graben is less well-defined; it is drawn along the Pennyrile Fault Zone because those faults seem to be in about the right place with displacement in the right direction. Maximum depths to the Precambrian in the lowest part of the Rough Creek Graben could exceed 20,000 feet.

The Reelfoot Rift is vaguely indicated by the minus 15,000-foot contours from the Ouachita front northeastward to the southern flank of the Pascola Arch. Total depth to igneous rocks, types of igneous rocks, and age of sediments at the base of this trough are not known. Recent drilling in Mississippi County, Arkansas, confirms the depth of 15,000 feet to igneous rocks, and on the basis of aeromagnetic and seismic studies, depths of 20,000 feet appear reasonable in the deeper parts of the rift zone. Local seismic reflection surveys have detected deep layered reflectors in the rift, and the possibility that lava flows are interbedded with Precambrian sediments at the base of the sedimentary section in the central part of the rift cannot be ruled out.

Probably the least predictive part of the interpretation shown in Figure 4 is in the area of the Pascola Arch: portraying the intersection of a linear trough that was dropped downward at least 15,000 feet with an arch that was later uplifted about 12,000 feet poses a real challenge. The data are sparse, so there is a tendency to smooth the gradients when contouring. It is, however, anticipated that unmapped faulting contributed significantly to complex structural adjustments in the area, and as more data become available the local gradients will be determined to be much steeper than suggested here.

LOWER CAMBRIAN

Sedimentation began as a basal sandstone on the flanks of the Nashville Dome, which lapped onto the dome from the east and possibly from the south. Shale and sandy shale with some carbonates overlie these sands; reddish coloration is typical of this section. These clastic rocks are believed to be equivalent to the Rome of Appalachian outcrop.

A large graben (Reelfoot Rift) formed in the Mississippi Embayment, trending northeasterly into southern Illinois. A similar graben of smaller dimensions (Rough Creek Graben) formed, trending easterly from southern Illinois into western Kentucky. Deep wells in southern Illinois and western Tennessee encounter early sediments of unknown age. The Mermet Sandstone of Johnson County, Illinois, which may be of only local extent, was deposited as fluvial deltaic or pediment fans southward of the east-west trending Rough Creek fault scarp. Dolomite and siltstone of pre-late Cambrian age in Lake County, western Tennessee, may represent the first marine sediments in the Reelfoot Rift. Total thickness and exact age of early sediments is unknown, and they do not crop out. Houseknecht and Weaverling (1983) described a detrital unit at least several hundred feet thick near the axis of the Reelfoot Rift. The unit is reported to grade from arkosic sandstone in the north to a basinal shale southward. They correlate the detrital unit with the Rome (lower Cambrian) Formation of the Appalachian area.

MIDDLE CAMBRIAN

Limestone and shale of Conasuaga age overlie "Rome" sediments in the Appalachian area and thin to zero on the northern rim of Nashville Dome. Thick shale accumulated in the Rough Creek Graben while crystalline basement rock remained partly exposed to the north and south. Dolomite deposition in northern Mississippi and eastern Arkansas may be of middle Cambrian age; this dolomite rests on a varied terrain of granite and metamorphic rocks probably exposed to erosion during earlier Cambrian time. Near the axis of the Reelfoot Rift, Houseknecht and Weaverling (1983) found a carbonate unit more than 1,000 feet thick overlying their lower Cambrian detrital unit. They correlated this carbonate with the Conasuaga (middle Cambrian) Formation of the southern Appalachians. The Reelfoot Rift and Rough Creek Graben nearly filled with sediment by the end of middle Cambrian time, and growth faulting probably deepened these troughs during most of the early to middle Paleozoic Era.

UPPER CAMBRIAN

Deposits of limestone (since altered to dolomite in the Appalachian area), lap onto the Nashville Dome. Mt. Simon (Lamotte) Sandstone accumulated in the Ozark and central Illinois regions, where they rest on basement rock. Mt. Simon (Lamotte) Sands extend southward and overlie Mermet Sandstone in southern Illinois. The Mt. Simon Sandstone, present in northwestern Tennessee, rests on older carbonate rock in the Reelfoot Rift, but laps onto basement rocks on either side of the graben. The basement apparently remained exposed along the eastern end of the Rough Creek Fault Zone and created a large shadow zone in which no Mt. Simon sand accumulated. A transition zone at the top of the Mt. Simon grades

into the base of Eau Claire and Bonneterre limestone and dolomite, which accumulated as thick carbonate banks of oolites with some sandstone incursions in the Ozark Region. The Eau Claire-Bonneterre oolitic carbonate was deposited north of the Rough Creek Graben in southern Illinois and in the Missouri Ozark region as a shallow water facies, while Bonneterre shale accumulated in the deep water of the Rough Creek Graben and Reelfoot Rift in western Tennessee and southeastern Missouri, and extended into eastern Arkansas and northwestern Mississippi. The bordering faults of the old grabens continued to be displaced as growth faults which deepened the grabens and allowed the accumulation of thickened marine sediments of shale and siltstone (Fig. 5). Whether this clastic material was washed over the oolitic limestone banks flanking the graben areas or had a source from the south and southwest cannot be determined, but the northward coarsening of the Eau Claire Formation to sand and siltstone would indicate a source from that direction.

The Franconia Formation of Illinois is a southward-thickening unit of silty, glauconitic, and argillaceous sandstone with increasing amounts of dolomite toward the south. It is equivalent to the Elvins Group of Missouri and extends eastward into Kentucky where it is primarily dolomite with small amounts of black shale. In Kentucky it lacks the characteristic glauconite of areas to the north and west. In southern Illinois and western Kentucky the Elvins Group and Franconia Formation are included in the Knox Megagroup. Oolitic cherts and relict oolite structures in the dolomite indicate that the original lithology was predominantly an oolitic limestone of shallow water deposition.

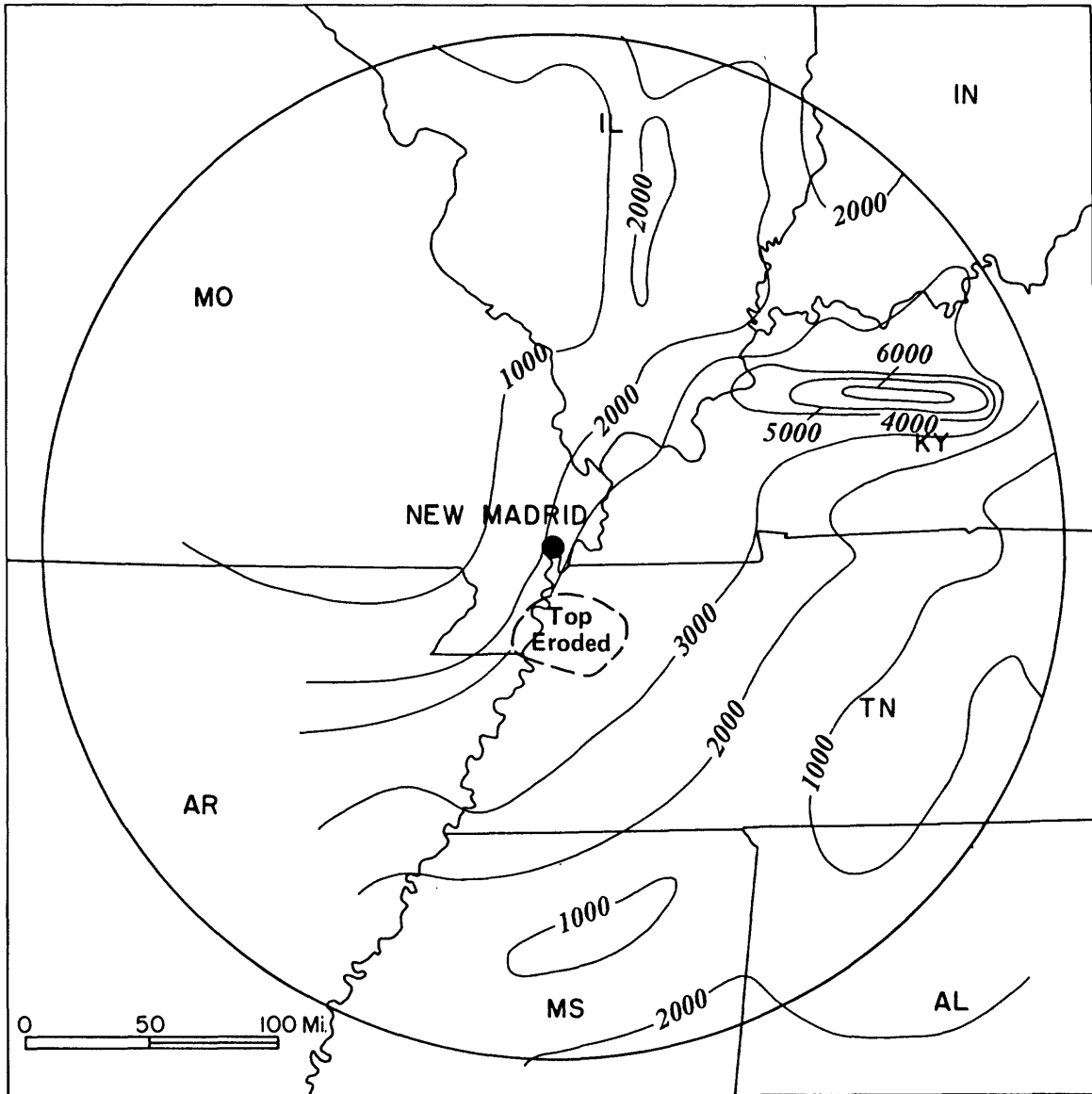


Figure 5. Thickness of pre-Knox sediments.

CAMBRIAN-ORDOVICIAN KNOX MEGAGROUP

The Knox Megagroup, a lower Ordovician and upper Cambrian carbonate unit, underlies sedimentary cover between outcrops in the Appalachian area and outcrops in Missouri around the Ozark Uplift. From east to west this unit in the subsurface gradually increases from about 1,000 to over 7,000 feet in thickness (Fig. 6). The maximum thickness occurs in the Reelfoot Basin of the upper Mississippi Embayment, although the entire section of Knox has been beveled by erosion over the Pascola Arch. West of the Mississippi River the thick Knox section extends into the Arkoma Basin and is called Arbuckle, which, in general, is correlated westward with the Ellenburger of Texas and Oklahoma.

In most areas the Knox has been subjected to subaerial erosion, and this surface represents one of the major unconformities within the Paleozoic sediments. The unconformity delineates the upper limit of the Sauk Sequence. Above the unconformity are sandstones, such as the St. Peter, and shale, limestone, and dolomite of middle Ordovician age. The Everton Dolomite partly covers the Knox unconformity in western Kentucky, Missouri, Arkansas, and southern Illinois. The Everton is included with the Knox on the isopach map (Fig. 6).

The original lithology of the Knox was shallow-water limestone containing very minor amounts of sand, shale, and chert. Most of the limestones were oolitic and probably rather porous, but dolomitization and replacement chert destroyed much of the original texture and porosity. The oolitic character of the formations is well-preserved in the cherts, and where dolomitization is not complete, the relict structure of oolites can be seen in sample cuttings. In the Ozark region there are abundant nonsilicified algal deposits and numerous sandy zones.

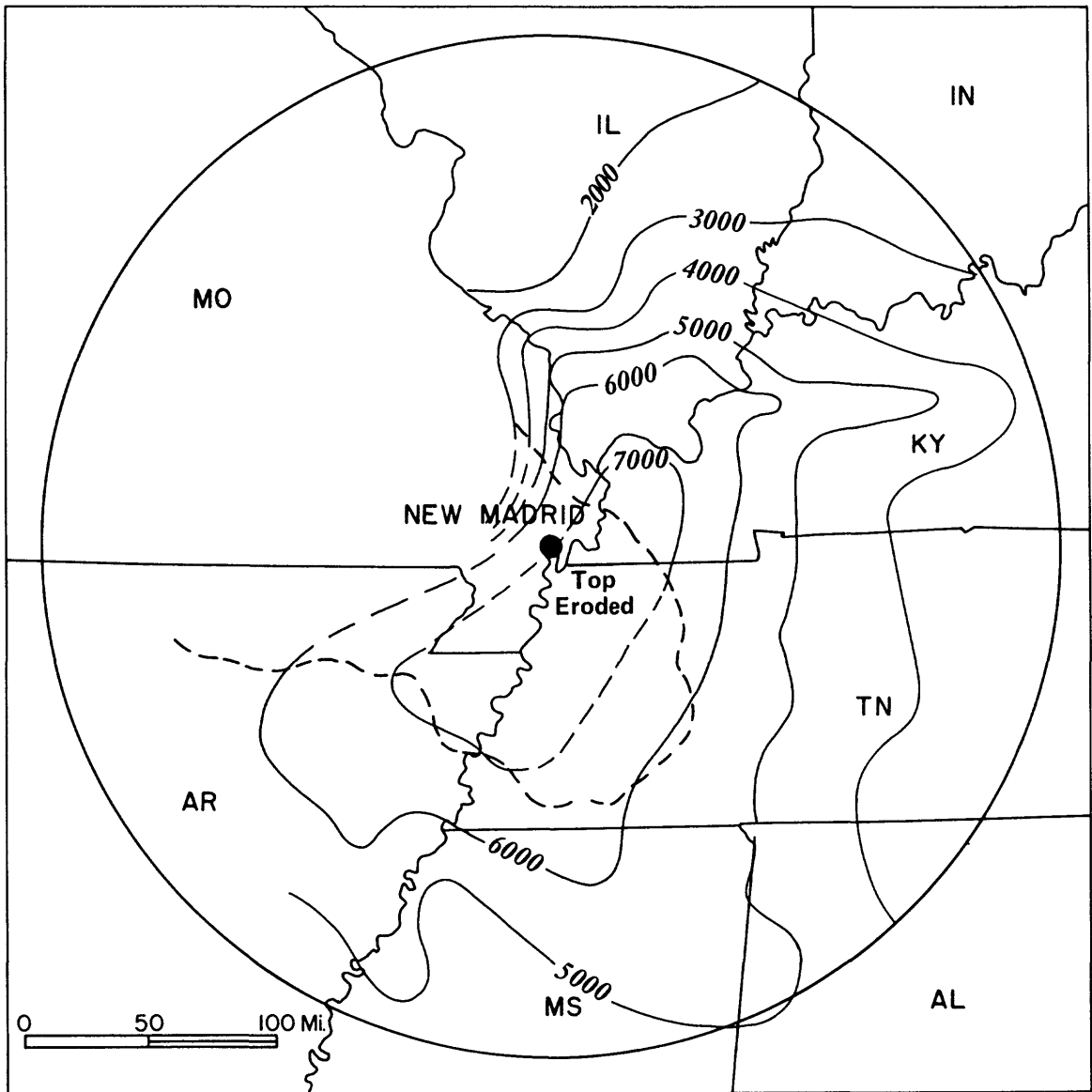


Figure 6. Thickness of Knox Megagroup.

The following characteristics of the Knox (based on data from wells drilled in the upper Mississippi Embayment area) are useful in defining formational units:

1. The upper Cambrian formations are the Eminence-Potosi-Elvins Group, which may have a combined overall thickness of more than 4,000 feet. These formations are dolomite containing less chert than the overlying formations and a decrease in sand and chert downward. The lower part of the section is nonsandy and has almost no chert. The typical glauconitic zones of the Elvins disappear basinward, and no clear distinction has been made between the formations where they are unusually thick.
2. The Gasconade (Oneota) is very cherty dolomite that contains floating sand, but there is a decrease in the sandiness from the overlying formation. The basal member of the Gasconade is the Gunter Sandstone, which also is used to define the base of the Ordovician system. Maximum thickness of the formation is 700 feet.
3. The Roubidoux is a very sandy, very cherty dolomite and dolomitic limestone containing an abundance of both oolitic and sandy chert. Sandiness is noted at the top and bottom of the formation, which may reach 500 feet in thickness.
4. The Jefferson City contains oolitic limestone, and the formation has usually been only moderately dolomitized; its maximum thickness is about 500 feet.

5. The Smithville-Powell-Cotter may attain a thickness of 2,000 feet where it has not been removed by erosion. It is represented by dolomite and dolomitic limestone having occasional sandy zones and minor amounts of chert. Limestone is present through much of this section in Arkansas.

MIDDLE ORDOVICIAN

Although included with the Knox in some areas, the Everton Dolomite overlies the major unconformity at the top of the Knox in much of the study area. The Everton is a sandy dolomite generally lacking chert, and it is not known to be oolitic. The Everton was deposited in a restricted sea that lapped onto Knox carbonates to the east and north; subaerial erosion continued to bevel the Knox in exposed areas farther north while the Everton was being deposited. The Everton is unconformably overlain by the St. Peter Sandstone, which is a more widespread formation that overlaps the Everton and covers the unconformity on top of the Knox to the north.

The St. Peter is composed predominantly of quartz sand with well-rounded and frosted grains. The sand is fine to medium grained and well-sorted, and throughout the region it lacks significant amounts of clay or shale. The St. Peter Sandstone is 100 to 200 feet thick in the northern part of the New Madrid area (Fig. 7), but is thin or absent to the east in Indiana and Kentucky where emergence continued to expose the Knox at that time.

The middle Ordovician carbonates that overlie the St. Peter represent a widespread marine invasion throughout the Midwest. These Trentonian and Black

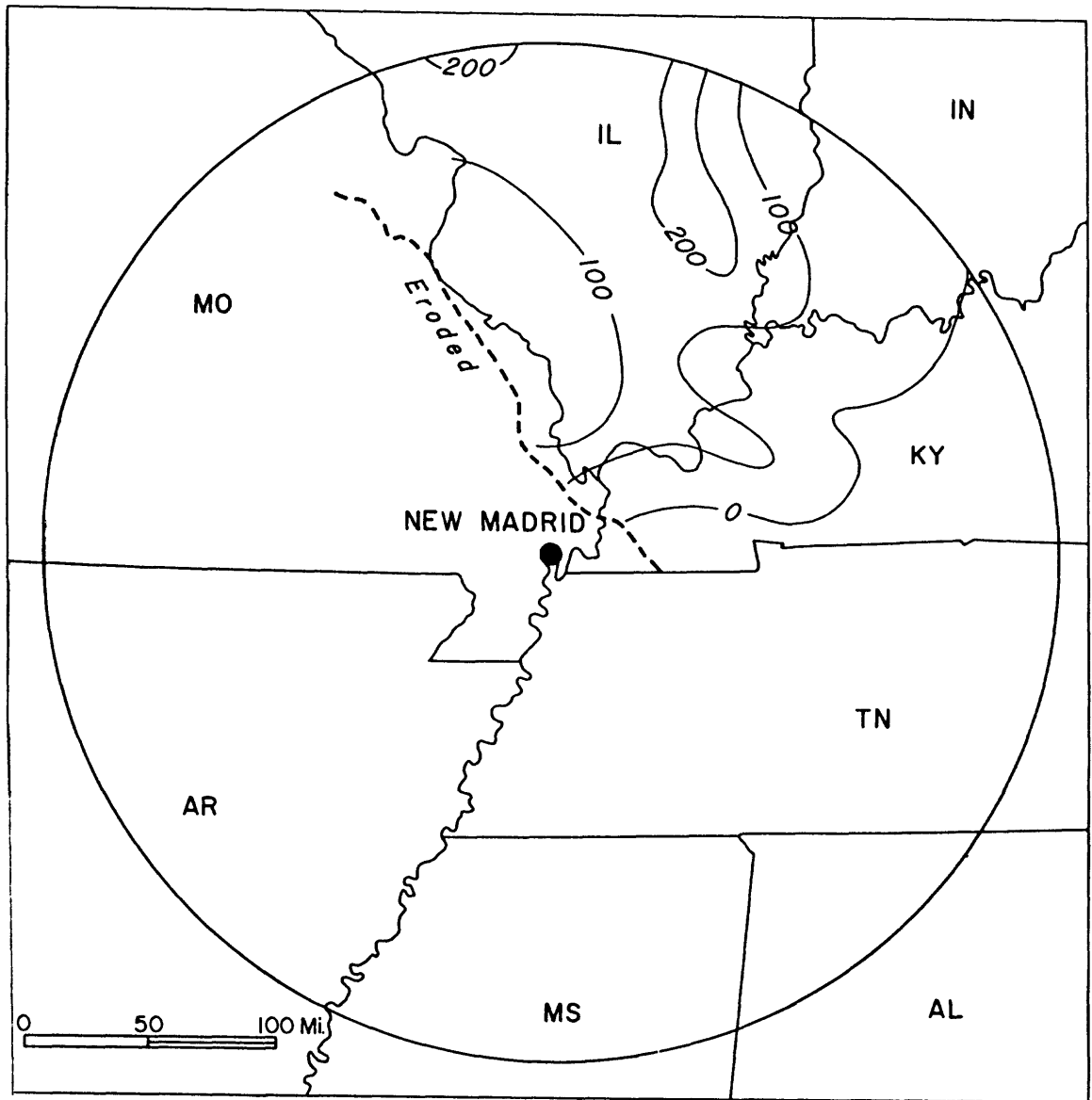


Figure 7. Thickness of St. Peter Sandstone.

Riveran carbonates are assigned to the Ottawa Megagroup. Recent studies have shown that the upper units of this megagroup are of Cincinnatian (late Ordovician) age. The Ottawa thickens southward to about 1,400 feet at the north edge of the Mississippi Embayment (Fig. 8); erosion has removed it from the Pascola Arch. The megagroup contains many persistent, widely traceable carbonate units. Volcanic activity, believed to be located to the east, produced numerous ash falls that have been preserved as metabentonites. The Ottawa consists chiefly of limestone that grades locally to dolomite, especially in the lower formations. Over much of its extent, the lower part of the Ottawa contains some silt, sand, and anhydrite.

UPPER ORDOVICIAN

The Maquoketa Group includes the relatively shaly strata of Cincinnatian (late Ordovician) age. The base of the Cincinnatian is difficult to establish in western parts of Kentucky and Tennessee because of the interfingering of shale and carbonate facies. In that area the isopach map (Fig. 9) includes some shaly strata that have been assigned a middle Ordovician age. The Maquoketa is about 200 feet thick in much of Illinois. In Indiana and Kentucky it thickens regularly eastward from 300 to 900 feet. The Maquoketa is absent by erosion over the Pacola Arch, the Nashville Dome, and the Lexington Dome. The Maquoketa consists chiefly of silty and dolomitic or calcitic shale containing some prominent limestone units; locally it contains beds of silty sandstone (Thebes Sandstone Member). The proportion of carbonate rocks increase southeastward, and in central Tennessee the upper Ordovician rocks are composed primarily of shaly limestone.

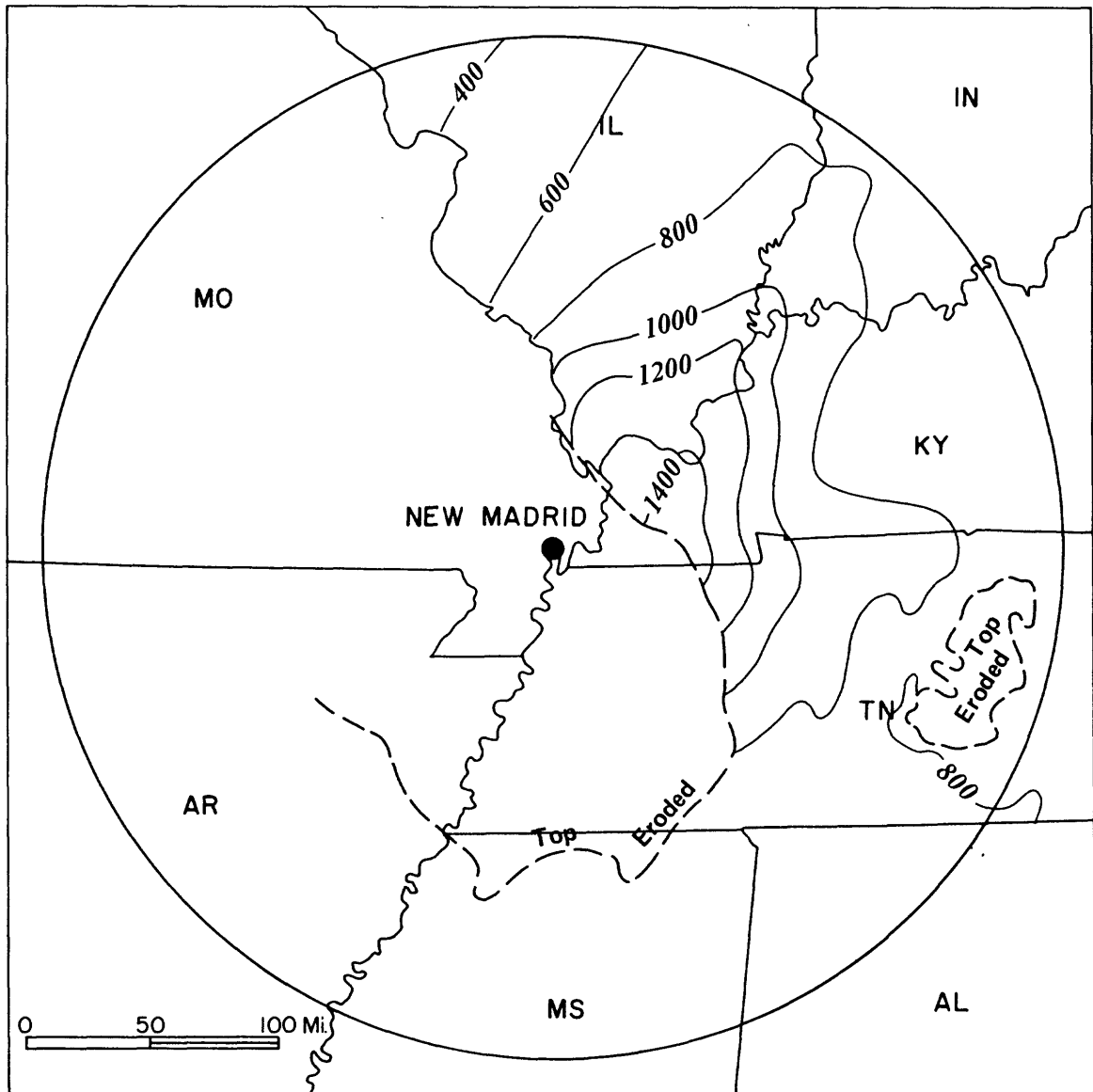


Figure 8. Thickness of Ottawa Megagroup.

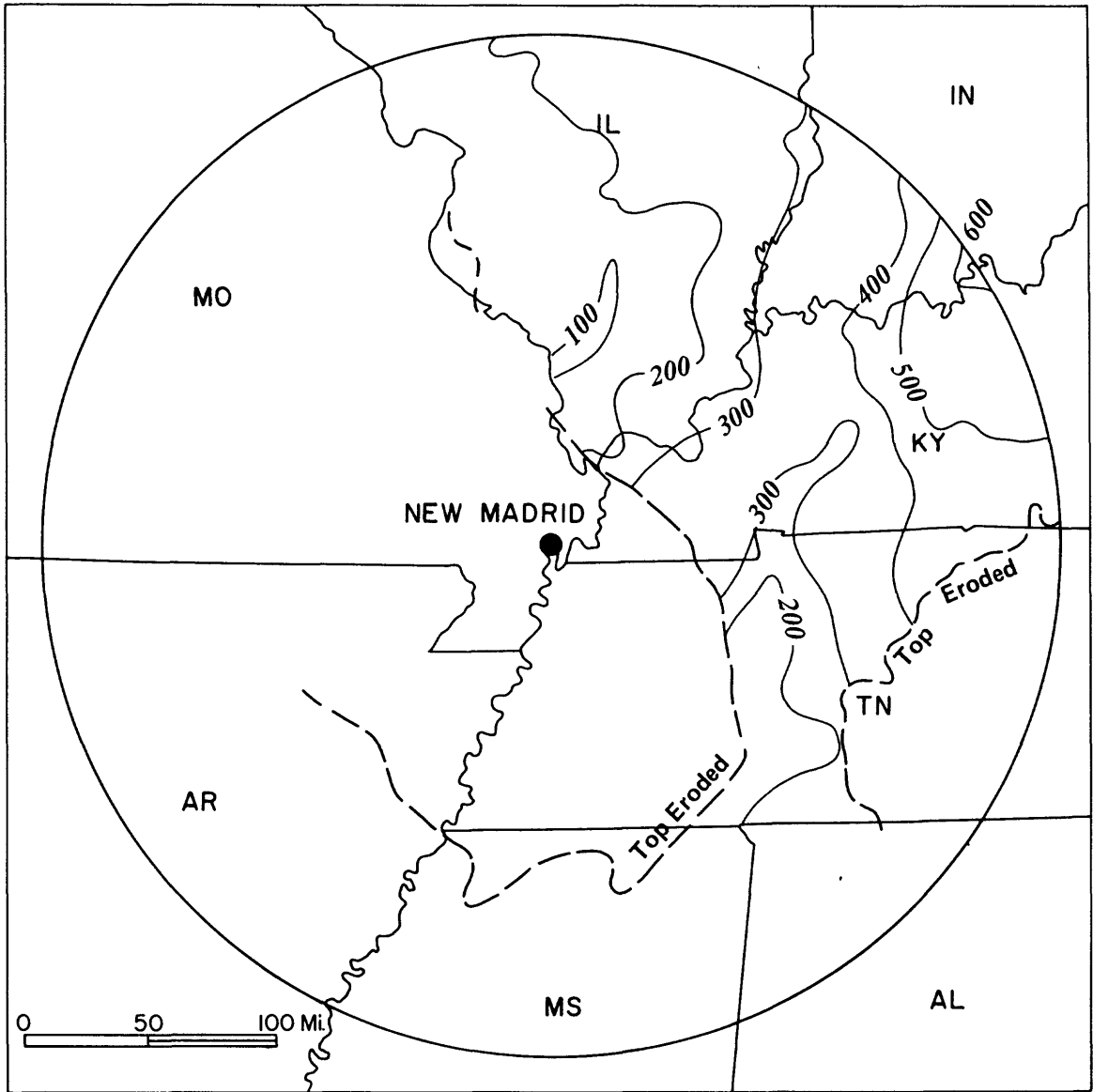


Figure 9. Thickness of Maquoketa Group.

Ordovician sedimentation ended with shallowing and partial withdrawal of the seas, which created an unconformity of low relief.

SILURIAN AND DEVONIAN

Virtually quartz sand-free Silurian carbonates were deposited throughout the region during a widespread marine advance that apparently had submerged clastic source areas. Thick carbonate banks surrounded the Illinois Basin except to the south, and bioherms developed in front of and on these banks.

Starved basin conditions existing during Silurian time in Illinois resulted in thin deposits in deep-water areas, and some marked facies changes occurred between contemporaneous deposits. Gradual subsidence seems to have been the only tectonic activity during the Silurian.

Cayugan (upper Silurian) and lower Devonian sediments that filled the starved basin are mostly sand-free limestone and dolomite. Some of these beds were extensively altered to chert in the northern part of the Mississippi Embayment, but the source of the silica is not known.

The end of early Devonian time was marked by pronounced uplift and reactivation of many local features. Sources of quartz sand were exposed, and the beginning of middle Devonian time is marked by the first widespread occurrence of mature sandstone and sandy limestone since the middle Ordovician. Dolomite and limestone are the principal rock types deposited during the balance of middle Devonian time.

The carbonate rocks of the Silurian System are combined with those of early and middle Devonian age to form the Hunton Megagroup. The Hunton has a maximum thickness of more than 1,800 feet in southern Illinois (Fig. 10).

Before deposition of the New Albany Shale Group (upper Devonian and lower Mississippian) another erosion surface developed on exposed rocks around the margins of the Illinois Basin. The seas then advanced in the most widespread inundation since Ordovician time. The various unconformities merge beneath the New Albany Shale toward the basin edges and other uplifted features, bringing the New Albany Shale in contact with strata as old as Champlainian (middle Ordovician).

MISSISSIPPIAN

Subsidence continued during Mississippian time with shale and siltstone deposition predominant in the early part of the period, and limestone deposition dominant toward the middle of the period. The shale, siltstone, and carbonate of the upper Devonian and the lower and middle Mississippian have been combined to make a single mapping unit; these strata reach a maximum thickness of more than 2,200 feet in southern Illinois (Fig. 11). They are absent by erosion over the Pascola Arch and the Nashville Dome.

Cyclic deposition of alternating beds of sandstone, shale, and limestone is typical of upper Mississippian strata. From a northeastern source, clastic sediments were carried by a southwestward-flowing river system across the Illinois Basin (Swann, 1964). Almost all of the 20 or so individual upper Mississippian formations thicken southward to their truncated edges in southern

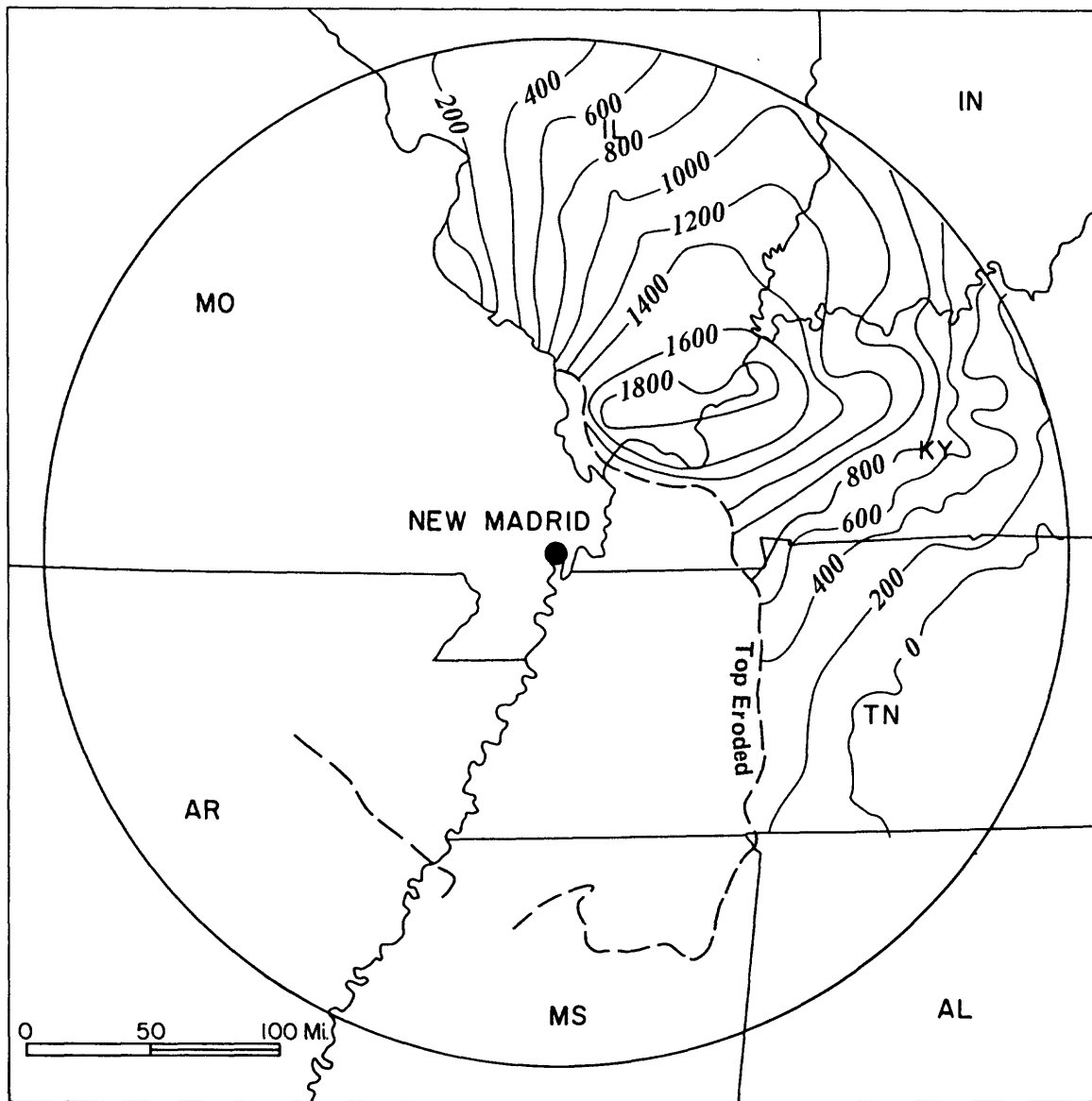


Figure 10. Thickness of Hunton Megagroup (Silurian-Lower and Middle Devonian).

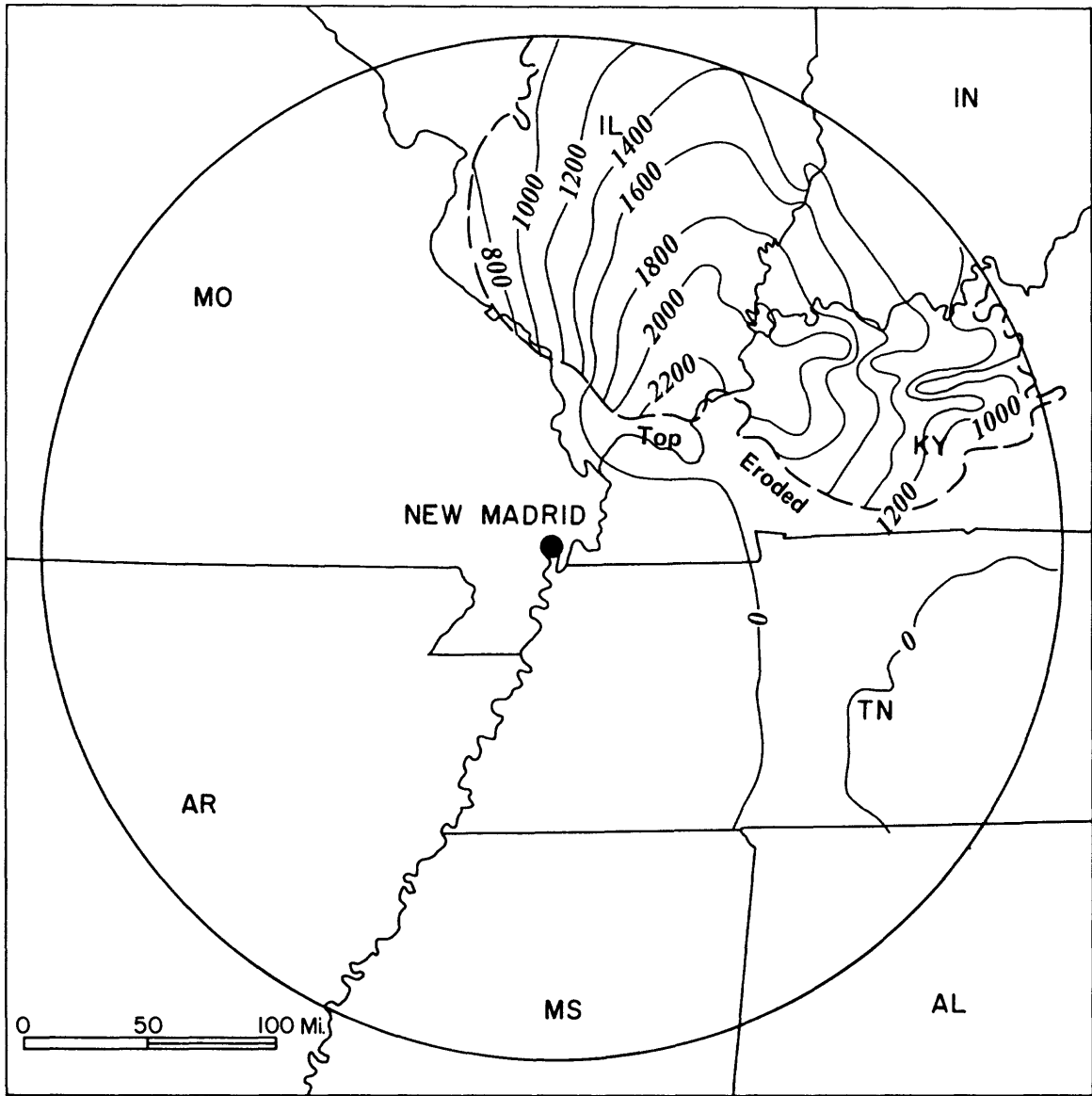


Figure 11. Thickness of Upper Devonian - Lower and Middle Mississippian.

Illinois and western Kentucky. Total thickness of upper Mississippian strata in southern Illinois is more than 1,400 feet (Fig. 12).

PENNSYLVANIAN AND PERMIAN

Southwestward-flowing streams incised a vast drainage pattern on Mississippian and older strata, which was subsequently buried by Pennsylvanian clastics. Coal, the chief economic mineral of the Illinois Basin, was formed in vast amounts, although coal beds represent less than 1 percent of the Pennsylvanian sedimentary column. Sandstone and shale are the major lithic types of Pennsylvanian strata; limestone constitutes only a minor portion. Something marine limestone and coal seams can be traced over large portions of the Illinois Basin. The thickest Pennsylvanian succession preserved north of the Pascola Arch is located just south of the Rough Creek Fault Zone in western Kentucky and in fault blocks within the fault zone (Fig. 13). Slightly more than 3,200 feet of Pennsylvanian strata occur in Union County, Kentucky (Smith and Smith, 1967), and include an almost continuous section of the very youngest Pennsylvanian.

In a down-dropped fault block within the Rough Creek Fault Zone, beds of lower Permian age have been identified (Douglas, 1979) on the basis of the study of fusulinids. All Paleozoic deposits younger than lower Permian are believed to have been entirely removed by erosion from the region.

The Illinois Basin remained opened to the south during Pennsylvanian time and was subjected to repeated marine flooding. Thinning of Pennsylvanian strata occurs over some anticlinal structures, but slow subsidence seems to have been the principal tectonic activity. Permian sediments were presumably deposited

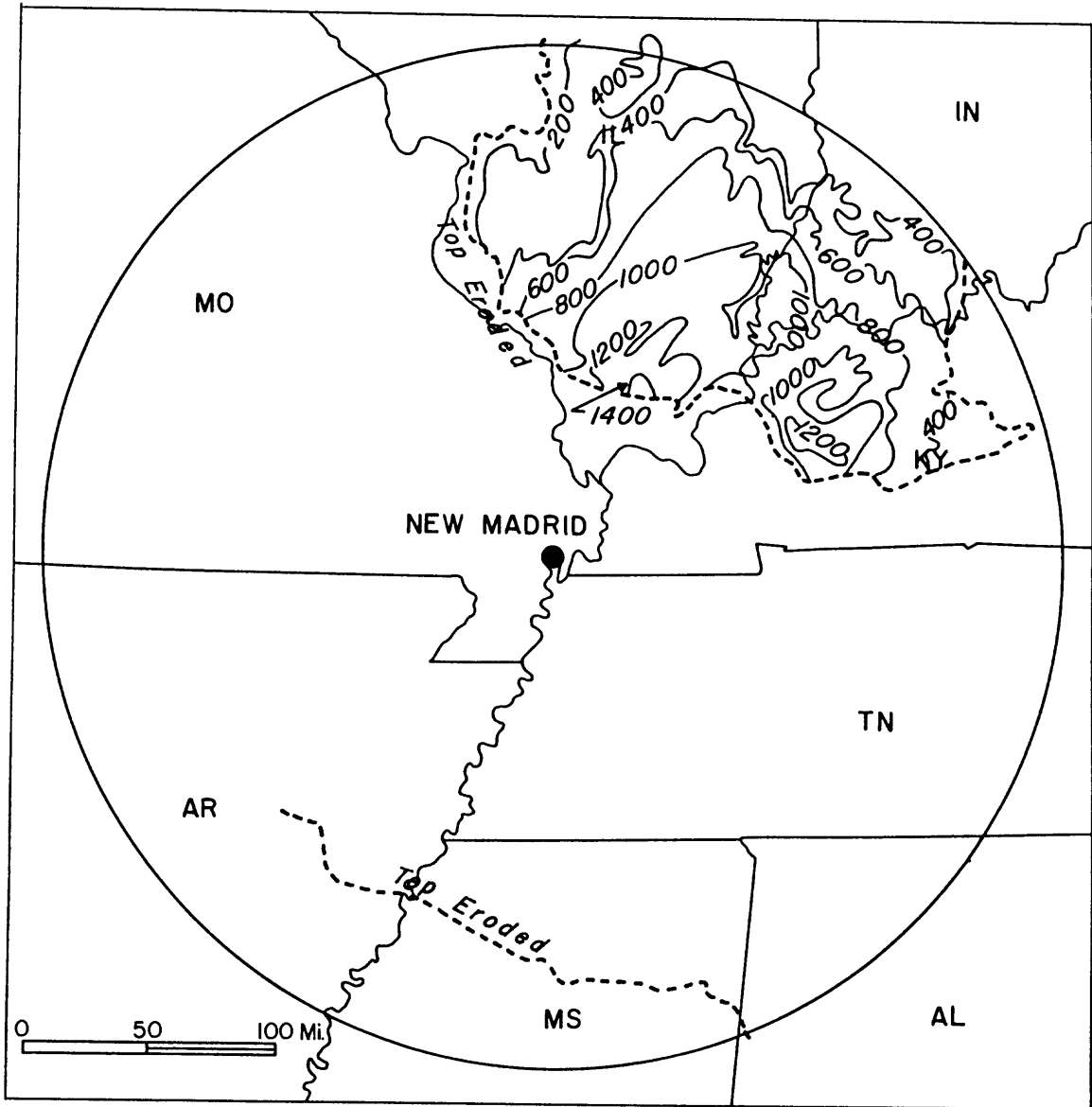


Figure 12. Thickness of Chesterian (Upper Mississippian).

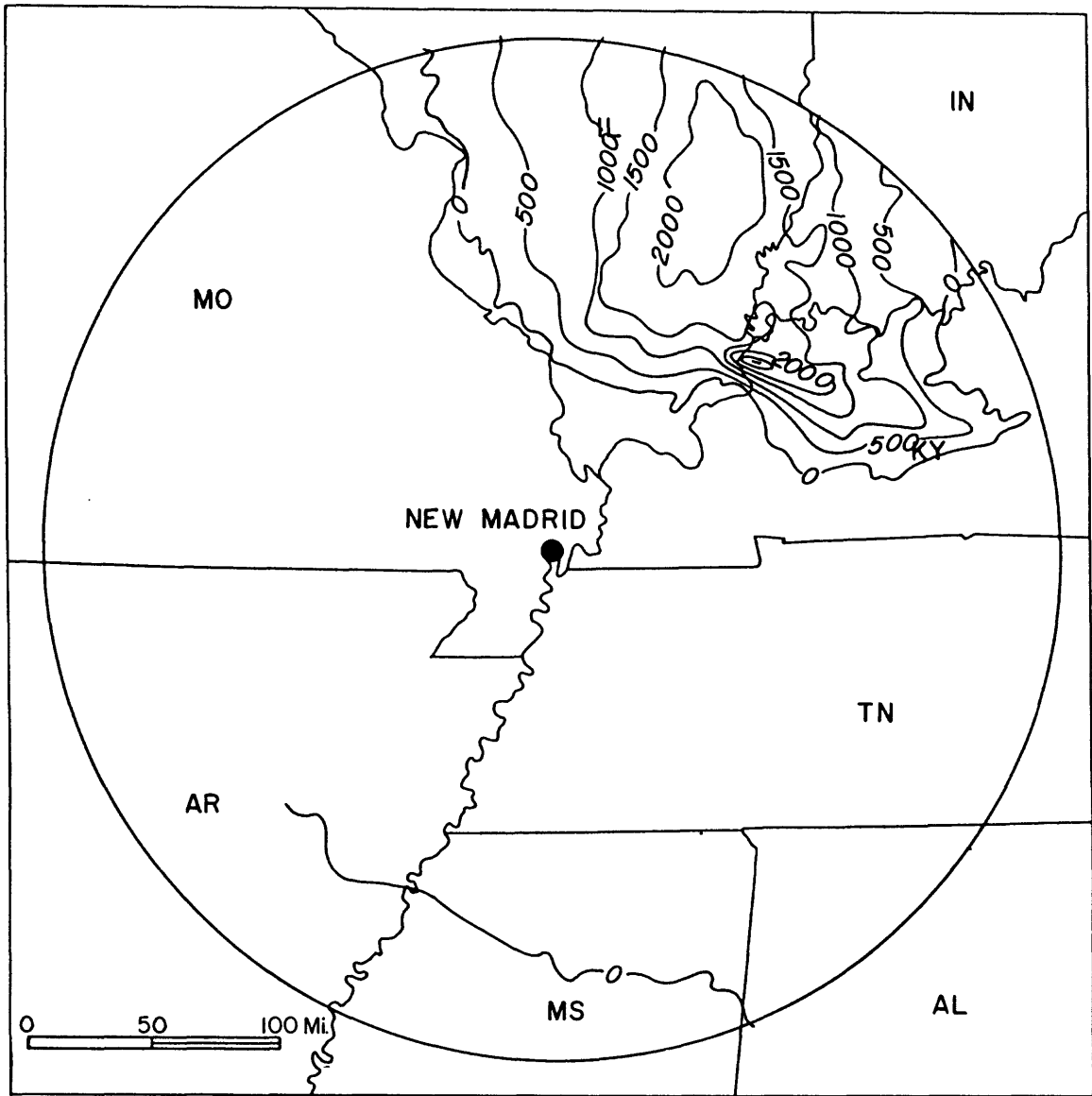


Figure 13. Thickness of Pennsylvanian sediments.

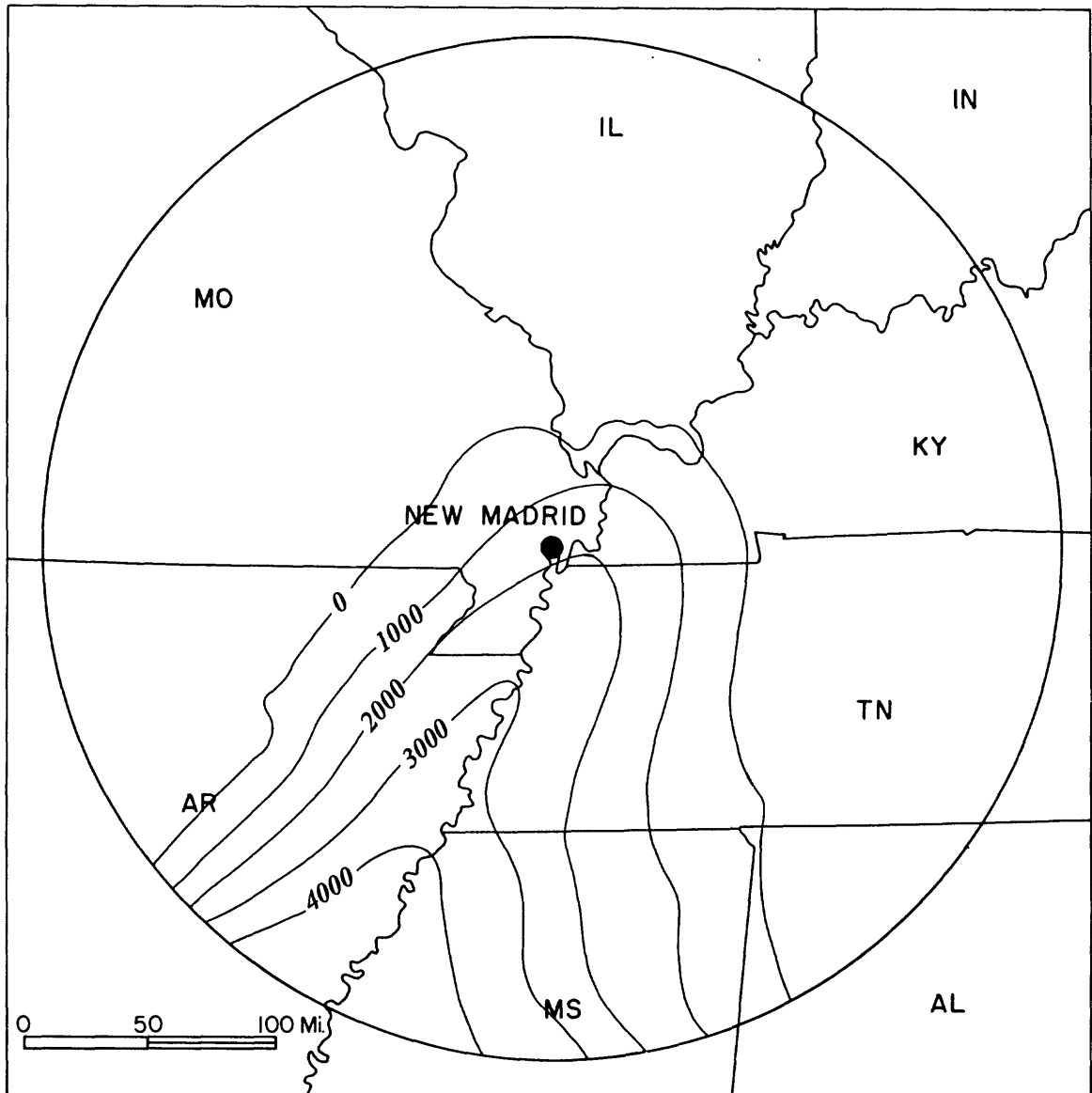


Figure 14. Thickness of Cretaceous-Tertiary sediments (Estimated from configuration map of the base of Cretaceous compiled by R. Stearns, 1981).

over at least a portion of southern Illinois and western Kentucky, but their thickness can only be surmised from the rank of the Pennsylvanian coal seams, which indicate a previous depth of burial by 4,000 feet of sedimentary cover (Damberger, 1971).

CRETACEOUS AND TERTIARY

A long hiatus occurred between the last Paleozoic sedimentation in the New Madrid area and the first Mesozoic deposits of Cretaceous age. During this time, a great amount of tectonic activity took place and changed the structural configuration of the region. From early Permian to late Cretaceous the sedimentary history of the New Madrid area is unknown. This interval is probably represented by uplift and erosion, and any sediments deposited have been completely removed. Drilling in the area indicates that a karst topography developed on the land surface; the sink holes were later filled with upper Cretaceous and younger sediments. The Tertiary and Cretaceous sediments are mostly sand and clay, but they include some lignite and impure limestone. The strata thicken southward from southernmost Illinois and are about 3,300 feet thick near Memphis, Tennessee (Fig. 14).

REFERENCES

- Buschbach, T.C., 1971, Stratigraphic setting of the Eastern Interior Region of the United States: Illinois State Geological Survey Illinois Petroleum 96, p. 3-20.
- Buschbach, T.C. ed. , 1983, New Madrid Seismotectonic Study--Summary of Activities from 1977 through 1981: U.S. Nuclear Regulatory Commission NUREG/CR-3173, p. 1-25.

- Cram, I.H. ed. , 1971, Future petroleum provinces of the United States--Their Geology and Potential: Amer. Assoc. Petroleum Geologists Memoir 15, v. 2, p. 1165-1218.
- Damberger, H.H., 1971, Coalification Pattern of the Illinois Basin: Econ. Geology, v. 66, no. 3, p. 488-494.
- Douglas, Raymond C., 1979, The distribution of fusulinids and their correlation between the Illinois Basin and the Appalachian Basin: in Palmer and Dutcher eds. , Depositional and Structural History of the Pennsylvanian System of the Illinois Basin, Part 2: invited papers, Field Trip No. 9/ Ninth International Congress of Carboniferous Stratigraphy and Geology, p. 15-20.
- Houseknecht, D.W. and Weaverling, P.H., 1983, Early Paleozoic sedimentation in Reelfoot Rift (abs.): 12th Annual Meeting of Eastern Section Amer. Assoc. of Petroleum Geologist, Carbondale, Illinois, October 1-4, 1983.
- Kisvarsanyi, Eva B. ed. , 1976, Studies in Precambrian Geology of Missouri: Missouri Geol. Survey, Contribution of Precambrian Geology No. 6, Rept. of Inv. 61, 190 p.
- Oder, Charles R.L., 1934, Preliminary Subdivision of the Knox Dolomite in East Tennessee, Jour. of Geol., v. 42, p. 469-497.
- Schwalb, H.R., 1982, Paleozoic geology of the New Madrid area: U.S. Nuclear Regulatory Commission NUREG/CR-2909, 61 p.
- Smith, W.H. and Smith, G.E., 1967, Description of Late Pennsylvanian strata from deep diamond drill cores in the southern part of the Illinois Basin: Illinois State Geological Survey Circular 411, 27 p.
- Stearns, R.G., 1983, Near-surface structure of the Reelfoot Lake District as estimated by gravity, earth resistivity, and drill data: in Buschbach, T.C. ed. , New Madrid seismotectonic study--Summary of activities from 1977 through 1981: U.S. Nuclear Regulatory Commission NUREG/CR-3173, p. 171-195.
- Swann, D.H., 1964, Late Mississippian rhythmic sediments of Mississippi Valley: Am. Assoc. of Petroleum Geologists Bull., v. 48, no. 5, p. 637-658.

**USE OF EARTH RESISTIVITY AND GRAVITY WITH DRILLING
FOR SHALLOW EXPLORATION IN THE REELFOOT LAKE REGION**

by

Richard G. Stearns

Vanderbilt University

Nashville, Tennessee

INTRODUCTION

In the New Madrid earthquake area, geological features are generally concealed, and so must be investigated by drilling, excavation, and geophysics. Earth resistivity is useful to investigate the extremely shallow subsurface (1 to hundreds of feet). Gravity, which is more commonly used mainly for deeper investigations (1000s of feet), can also focus on geology near the surface. Both techniques are related to information obtained from drill holes. Perhaps more important is their utility when related to each other.

Earth Resistivity

For earth resistivity, precision is reasonably good at shallow depths; equipment is inexpensive and easy to maintain; operators can be trained in a few hours under the eye of an experienced operator; and contrasts in resistivity correlate well with geological situations (faults, channels, inclined layers). Although deep penetration remains difficult, faults and features at the surface are well defined; and this shallow focus is important, because other techniques that probe deeper are not as readily or cheaply focused near the surface (reflection seismology). Field work, calculation and curve matching are laborious, but benefits seem to justify the effort. One of the more successful techniques (Barnes Layer profiling) uses the most straightforward calculations and a minimum of subjective interpretation.

Gravity

Gravity can also be focused on shallow depth, but at the expense of covering a small area with considerable effort in measuring elevations, placing observation points close together, and special handling of the meter. Gravity will also be shown to be useful with wider spacing (half a mile or so or more) to point up areas of potential faulting. This is possible in the New Madrid area because of the convenient great density change at the Paleozoic Mesozoic surface about half a mile down (from about 2 to over 2.6 gm/cm).

The Study Area (Figure 1)

The study area is on the Mississippi River alluvial plain and Loess Hills upland away from the river to the east. It is all underlain by unconsolidated sediments. Sufficient density and resistivity contrasts exist to give good definition, particularly between light conductive clay and denser resistive sand regardless of age.

EARTH RESISTIVITY

Earth Resistivity Values

Differences in resistivity permit the subsurface to be explored. In the study region unconsolidated sediments are partly or fully saturated with fresh water. Values vary considerably but are generally related to sediment size. Clay has a low resistivity; sand has a high resistivity. Table 1 lists some values determined in this investigation.

The values at Chickasaw Bluffs were determined by applying the electrodes to surface outcrops and measuring resistivity in situ. Those on the Mississippi River alluvial plain at Reelfoot Scarp were measured on samples taken by hand auger.

TABLE 1.--Resistivity values for nearsurface
Materials in the study area

Chickasaw Bluffs at the I-155 Lennox-Big Boy Intersection
(36°4.55'N, 89°29.82'W)

| <u>Material</u> | <u>Apparent Resistivity (ohm-feet)</u> |
|--|--|
| alluvial topsoil (Recent at foot of bluffs) | 100-150 |
| loess (Pleistocene) | 100-130 |
| sandy gravel not saturated (Pliocene Lafayette Fm.) | 250-1000 |
| water saturated gravel (Pliocene Lafayette Fm.) | 250-350 |
| carbonaceous siltstone (Eocene Jackson? Fm.) | 70-115 |
| gray stiltstone (Eocene Jackson? Fm.) | 120-140 |

Chickasaw Bluffs at the Samburg Gravel Pit
(36°29.27'N, 89°17.14'N)

| <u>Material</u> | <u>Apparent Resistivity (ohm-feet)</u> |
|--------------------------------------|--|
| yellow loess (Pleistocene) | 150-170 |
| reddish brown loess (Pleistocene) | 60-70 |
| red loess (Pleistocene) | 70-100 |
| gravel (Pliocene Lafayette Fm) | 200-500 |
| clay (Eocene Jackson? Fm.) | 20-30 |

Mississippi River Alluvial Plain. Five Auger Holes at
Reelfoot Scarp (36°25.5'N, 89°26.5'W)

| <u>Material (All Recent Alluvium)</u> | <u>Apparent Resistivity (ohm-feet)</u> |
|---------------------------------------|--|
| Sand | 355-970 |
| Sandy Silt | 128-150 |
| Clayey Silt | 82-105 |
| Silty Clay | 44-104 |
| Clay | 12-36 |

Main Techniques

General

The three general techniques for surface measurements involve varying one of these three factors--location, azimuth, and electrode spacing--while keeping the other two constant or fixed. All three techniques were tried in this study; they all yielded worthwhile results. An empirical system, known as Barnes Layer profiling also turned out to be particularly useful. The reader is referred to standard works on resistivity such as those by Zohdy, et al. (1974) and Orellana and Mooney (1966) for background.

Profiling - Variation of Station Location

This consists of taking measurements at successive locations while keeping the azimuth and the electrode spacing constant. The variations of resistivity in such a profile are due to lateral changes in resistivity.

Sounding - Variation of Electrode Spacings

For this technique, measurements are made by varying the electrode spacing while keeping the azimuth and the location constant. Increasing the spacings of the current electrodes will give rise to a large proportion of current penetrating deeper in the ground. The variation of resistivity along with the electrode spacing allows the approximate determination of thickness and depth of each electrically distinctive layer. This technique assumes the ground consists of horizontal layers each having an even thickness, and this is more or less true in most situations.

Circle Sounding - Variation of Azimuth

This technique (Zohdy, 1970) consists of taking measurements in different azimuths while keeping the center of the electrode array at the same place. Values are plotted on polar coordinate paper. Comparison of these with

Zohdy's theoretical polar plots allows the location and trend of a discontinuity (perhaps a fault) to be determined.

The Barnes Layer Technique (Barnes, 1954)

This empirical method is used to construct vertical resistivity sections along a line of soundings. This method turned out to be exceptionally useful. It is based on two concepts: first, the earth may be approximated as a stack of horizontal resistors, and total resistance of the resistors in parallel can be computed by summing the reciprocals of the resistance of individual resistors. The second premise is that the thickness probed is equal to the Wenner A spacing, and this is not true. All that is true, is that a fraction of the current is confined to a calculable depth. Consequently, the technique is theoretically useful only for a qualitative approximation of lateral changes in cases where lateral changes are likely to be more meaningful than thicknesses (for example, a steep fault). Practically it works; in the study area the depth of probing is coincidentally approximately equal to the A Wenner electrode spacing.

Test of Geologic Situations and Resistivity Techniques

Resistivity Profile across an Old Mississippi River Channel

An example profile is across an abandoned channel in the Ridgely Quadrangle (Saucier, 1964). It was designed to test profiling using a variable spacing of electrodes; the wider the spacing, the deeper the penetration (See Figure 2). As expected, high irregular resistivity values correspond to the natural levee beside the river channel. More homogeneous low values mark the channel. Note that resistivity is sensitive to A spacing. At the old levee higher values corresponding to wider spacings indicate a deeper high resistivity (probably natural levee fine sand) deposit.

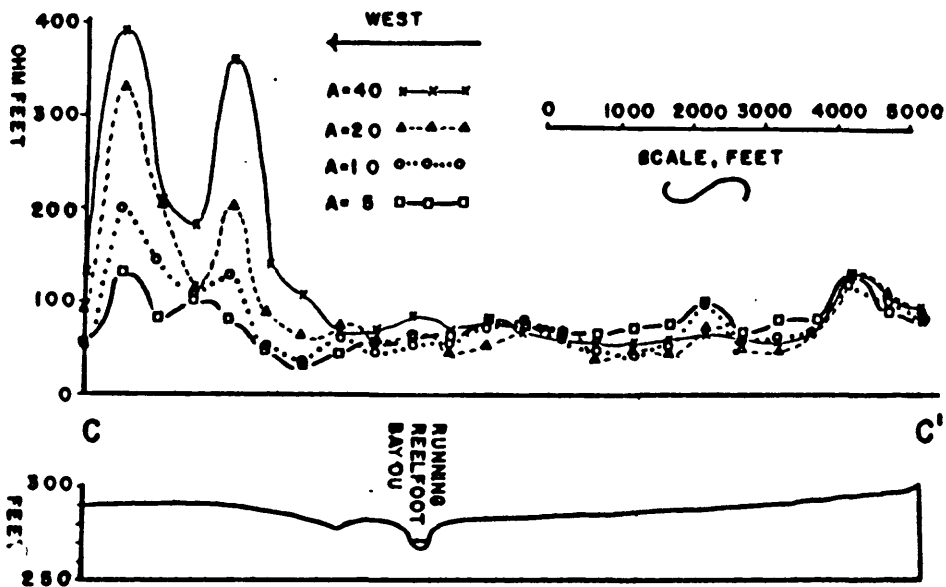


Figure 2 - Abandoned river channel profile south of Reelfoot Lake. Natural levee deposits, being sand and silt, have a higher resistivity than clay in the channel. In the channel resistivity of the clay is constant and low regardless of electrode spacing. On the old levee wider spacing gives higher resistivity showing more sand at depth, and more mud at the surface. From Stearns et al., 1982, Fig. 9.

Profiling and Mapping at Reelfoot Scarp

Geology and Background--Reelfoot Scarp at the eastern edge of the Tiptonville Dome drops eastward about 25 feet across a distance of about 500 feet. Tiptonville dome, the high side of the scarp, is an earthquake related feature, a region of localized uplift (Stearns, 1979; Russ, 1982). At the time this project was undertaken (1976-77), it was not certainly known whether the scarp marked a surface fault (it does). Here we made a series of parallel resistivity profiles for a map. Later, in conjunction with drilling, we made numerous soundings, and circle soundings.

Profile--First, a profile over a mile long was made perpendicular to the scarp on which irregular high resistivity values occurred on high ground west of the scarp, changing abruptly to low regular values to the east. This is typical of a natural levee flanking a clay plug, as just shown. Alternatively, the low ground to the right (east) could be sunk and covered by low resistivity flood deposited fine silt and clay (it is).

Resistivity Maps--Surveying continued for a series of parallel profiles to be contoured as a map. An example from several made at Reelfoot Scarp is Figure 3. The main significance of this is that the map pattern made manifest the old channel that cuts across the scarp. High resistivity marks the levee and low resistivity the clay plug. The levee is abruptly subdued at the scarp where it is buried beneath low resistivity material to the east. This does not prove faulting, but it does prove the offset of the channel at the scarp.

Surface Electric Soundings as Estimators of Subsurface Sections

General--Because clay and sand, that make up most of the nearsurface deposits in the study region, contrast strongly in resistivity, soundings should have a maximum chance to correctly predict subsurface sections. We made surface soundings (example on Figure 4) and compared results with a



Figure 3 - A resistivity contour map made from 19 parallel E-W profiles using a Wenner array with A spacing of 30 feet. The irregular high values to the west are on Tiptonville dome, and Reelfoot Scarp is the boundary with lower and more constant values to the east. To the east fine grained low resistivity recent flood deposits have buried such features as an old channel and levee that arcs across the map from lower right toward upper left. Burial results in an exponential decrease in resistivity contrasts. From Stearns et al., 1982, Fig. 12.

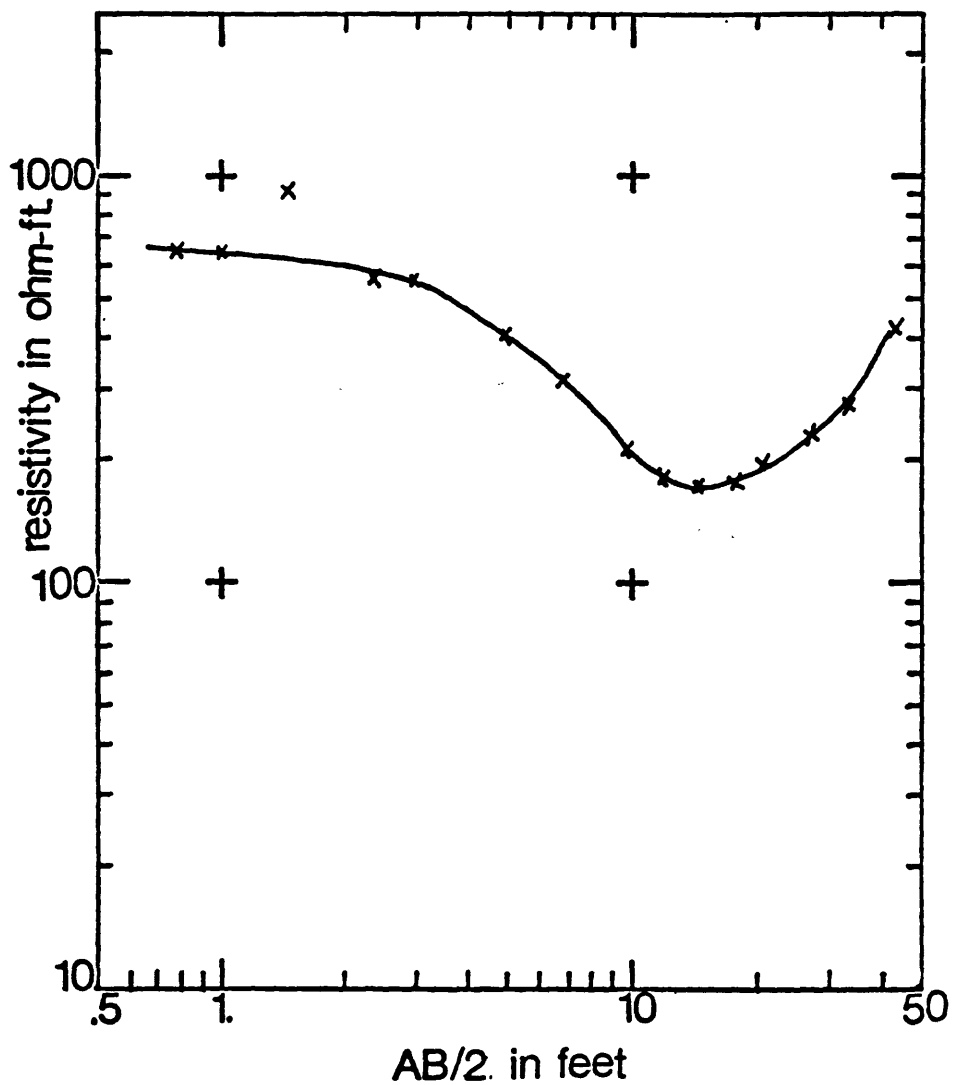


Figure 4 - A field sounding curve at Reelfoot Scarp. Curve matching gives four layers from this; the shallowest three are shown on the next figure. From Stearns et al., 1982, Fig. 21.

geoelectric column made by measuring resistivity of samples from hand auger holes, also some instances of electric logs of rotary-drilled holes. Results were mixed, and appear to depend on the electrode array: Wenner array sounding matched somewhat better than Schlumberger.

Schlumberger Soundings--These were compared two ways. Six holes were drilled by rotary at Reelfoot Scarp and resistivity was logged by a single point electrode. This allows thickness, but not resistivity, to be compared. Using depth to the base of a persistent clay layer for comparison, we found that for only 2 of the 6 holes did Schlumberger soundings predict depth within 25%. Others had errors up to 8 fold! For eight auger hole sites we measured resistivity of samples and made Schlumberger soundings (Figs. 4, 5). In these cases we were able to compare soundings with corresponding geoelectric measured sections using comparisons of Dar Zarrouk curves as recommended by Zohdy (1974). For these we obtained an average error of $31 \pm 21\%$ error in resistivity. For depth estimators to the base of the top 2 layers we obtained errors of $24 \pm 24\%$. At Reelfoot Scarp in 5 auger hole sites we obtained thickness estimates that differed from auger hole measurements by $27 \pm 21\%$, about like the Dar Zarrouk curve comparisons. Because of instrumental limits, we had to move the inner electrodes a lot during soundings. This requires nearly as much effort as Wenner soundings.

Wenner Soundings--These are compared one way only, that is by thickness of layers at Reelfoot Scarp at 6 auger hole sites. Here the average error is $29 \pm 33\%$, not much different from the statistical accuracy of Schlumberger soundings at the same sites. Because we had to move all the electrodes a lot anyway, and because the same Wenner array data can be used for the Barnes Layer system, we prefer Wenner over Schlumberger.

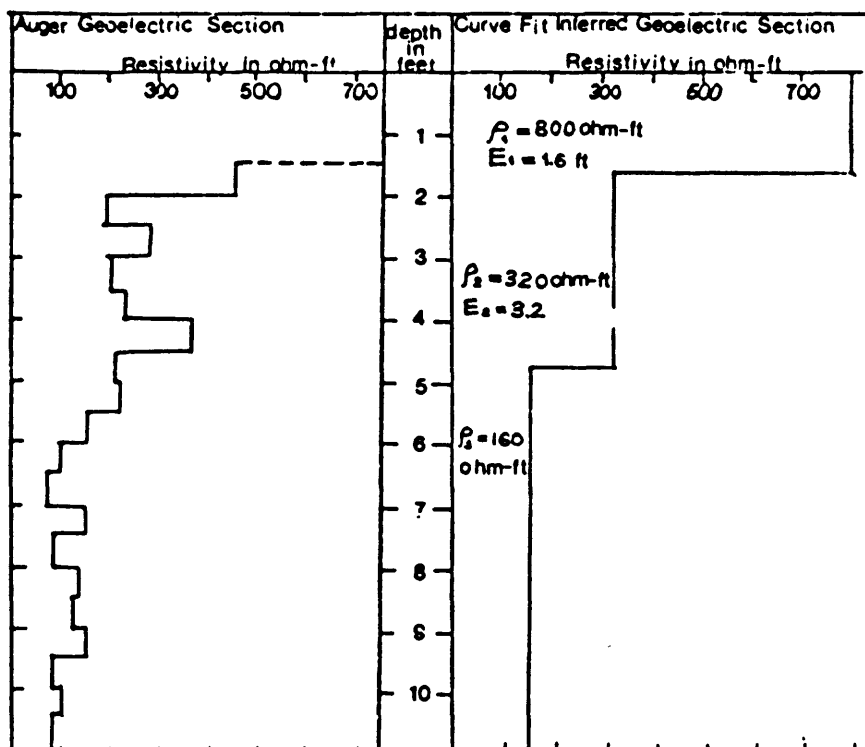


Figure 5 - Auger geoelectric section compared with curve match layers interpreted from the AUG-09 sounding. The deepest high resistivity layer is not shown, because we did not auger that deep. A meaningful rough comparison is evident in this case, but others gave a poorer correspondence. From Stearns et al., 1982, Fig. 22.

Circle Soundings as a Tool to Locate Faults

Circle soundings could yield information on both the location and the strike of faults if material of contrasting resistivity is juxtaposed across a steep boundary (Zohdy, 1970). To make the sounding, spacing of electrodes, in a Schlumberger array, is kept constant, and the electrodes are rotated about the array center. A series of circle soundings were made at two localities at the foot of Reelfoot Scarp where faults were known. These localities are at the site of the USGS-Vanderbilt trench and the site where the rotary test holes and hand auger holes were drilled. The 6 Test Holes were drilled in April 1977 before the trench was dug, since faulting was suspected because of abrupt lateral change in resistivity. Here there is about 20 feet of offset of layers between drill holes about 100 feet apart. Two months later, a fault was unearthed in the USGS-Vanderbilt trench about 2000 feet to the north in the same topographic position at the foot of the scarp. It was hoped that circle soundings would be verified by the observed fault in the trench, and so be used to locate the suspected fault in the line of drill holes, and they did.

The first trial was at the trench where we took measurements in 2 circles. We would like to have made more circles and taken more readings per circle, but the temperature was so cold that we had to penetrate frozen soil with a star drill and batteries weakened fast. The second test was run under better conditions near the test wells where we took measurements every 15 degrees in four circles. In both cases a solution was obtained from Zohdy's type curves. Figures 6 and 7 show the results. Faults were, in fact, located by this technique. There is, however, a distressingly small variation of resistivity with azimuth at the test well site, but here fault offset is small and so small changes are to be expected.

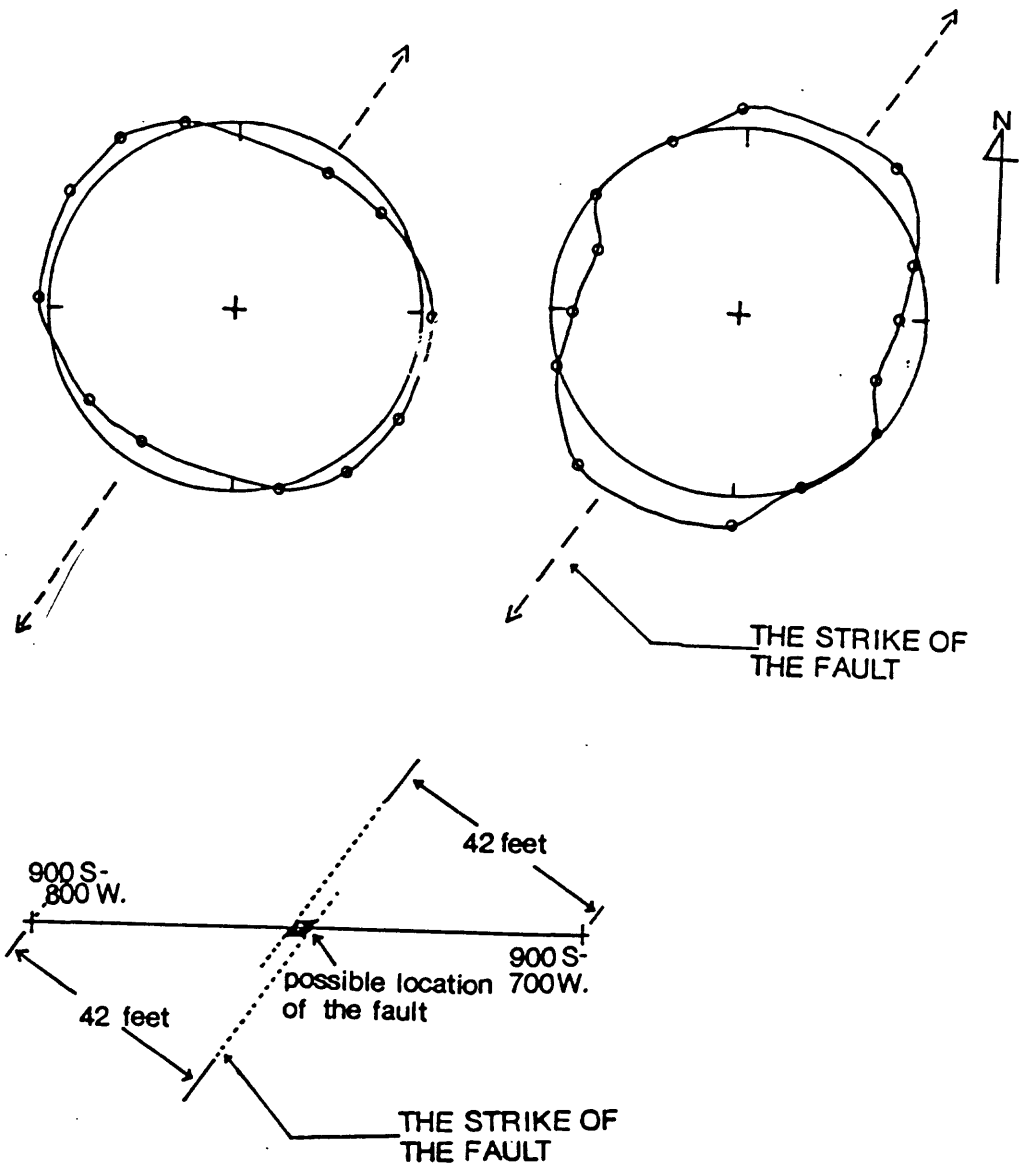


Figure 6 - Circle soundings on either side of the fault at Reelfoot Scarp unearthed in the USGS-Vanderbilt trench. The two soundings were 100 feet apart. The right one is east of the fault, and more than 42 feet away; the left one west of the fault, and more than 42 feet away. These combined distances locate the fault as shown below. This position is within 10 feet of its observed position in the trench. From Stearns et al., 1982, Figs. 30 and 31.

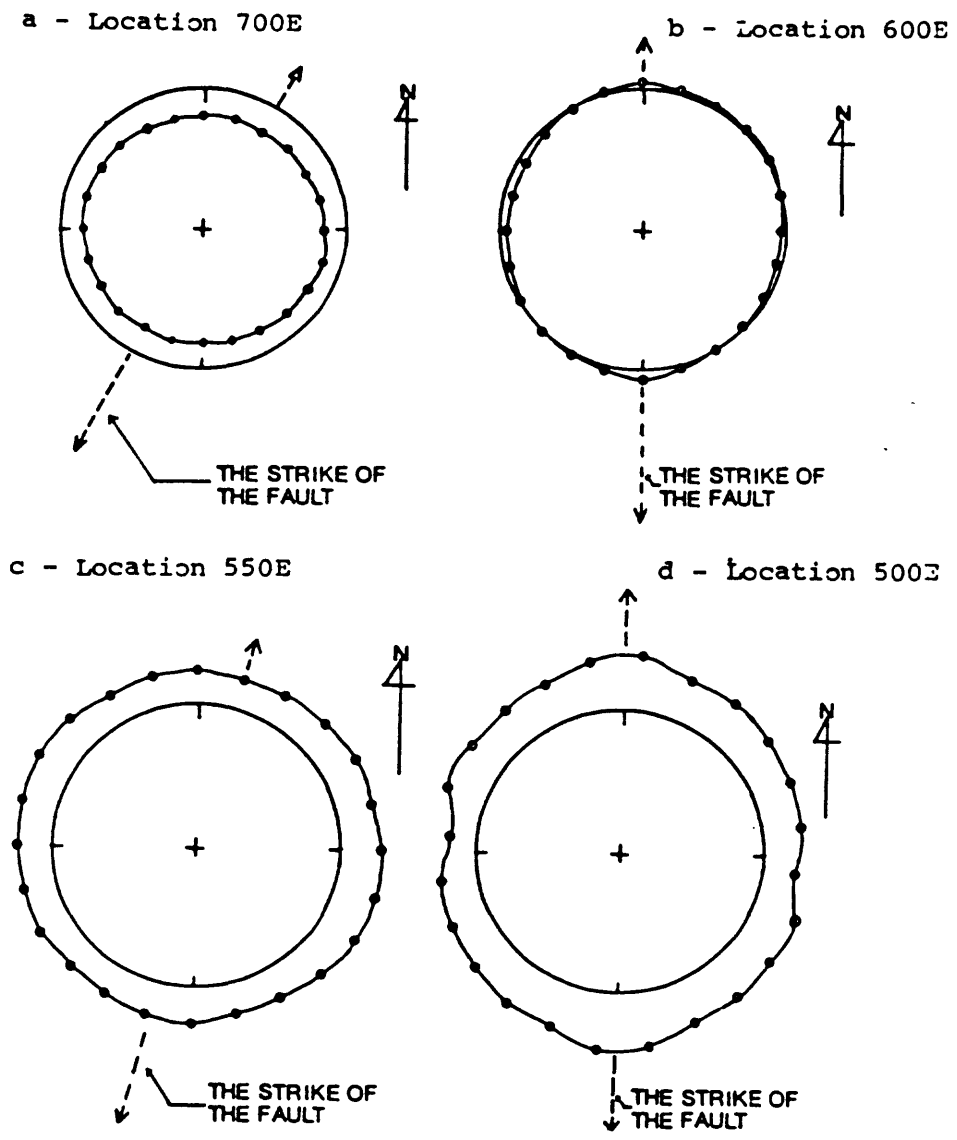


Figure 7 - Circle sounding diagrams at the Test well site. Top left is 100 feet east of an inferred fault. Top right is still east but close to the fault. Bottom left is about 50 feet west of the fault. Bottom right is about 100 feet west of the fault which probably strikes a bit east of N-S. Interpretation of this is made by comparison with type "Shapes" published by Zohdy (1974). Detailed drilling in fact proved this fault to be at about 590 E, a location consistent with all distance limits from all the circles (See Fig. 8 for the location at D-D'). From Stearns et al., 1982, Fig. 28.

Reelfoot Scarp Test Hole Area -- A Combined Test Using Drilling, and Resistivity

General--In 1978 and 1979, while structure at the foot of Reelfoot Scarp was being investigated by closely spaced shallow hand auger holes (located on Figure 8), resistivity data were also acquired. Resistivity results, particularly of Wenner soundings and use of the same electrical observations to construct a Barnes Layer cross section gave an excellent match to drill holes.

Fifteen hand auger holes were drilled. At the sites of all of the holes Wenner array soundings were made; at 12 sample resistivity was measured, and at 7 Schlumberger soundings were made. The Wenner array is the most useful way to make surface electrical observations here, because the same readings can be used for Barnes Layer profile calculations, and layer interpretation from curve matching.

As a result of this exercise, five techniques can be compared:

- 1) drill holes from which lithology and a standard geologic cross section is drawn;
- 2) measured sample resistivity from which "Electric Logs" are constructed on a cross section;
- 3) Barnes layer profile through the line of holes for direct comparison with the geologic and "Electric Log" cross sections; and
- 4) series of geoelectric sections from curve match of Soundings.

The Site--The site is line C-C' of Figure 8 at the foot of Reelfoot Scarp. The terrane is nearly flat here rising only 6 feet across a distance of 400 feet. This line crisscrosses the line along which three of the earlier Test Holes were drilled. It is also the line on which circle soundings were centered. Recall that a possible fault is located here between wells 1 and 2,

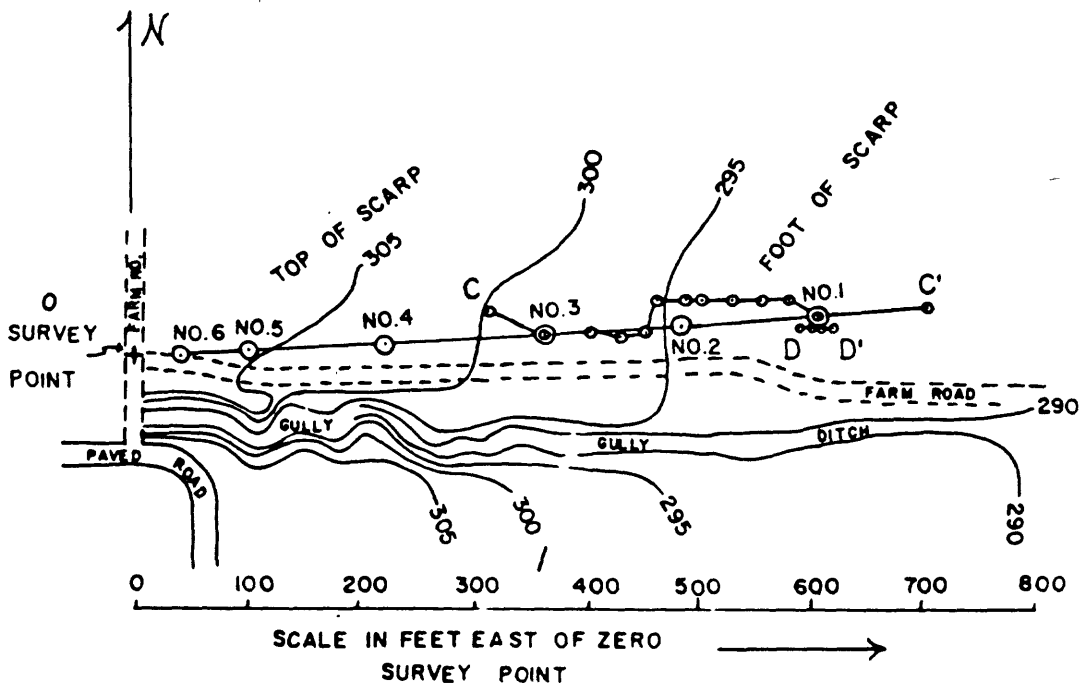


Figure 8 - Location of the auger holes and resistivity survey sites at the Test Hole Site. A fault was tentatively located just east of Well No. 1 before the closely spaced holes on D-D' were drilled, and it is present there though small.

based on a resistivity profile and circular soundings as well as apparent offset in the wells.

Line DD' close to the No. 1 well marks a line of closely spaced hand auger holes where a fault was clearly demonstrated after this survey was completed (Stearns, 1980).

General Results--The results will be presented with the Barnes Layer profile first, then the soundings, and last, the "truth" of auger hole lithology and resistivity; this is the order in which future investigations should be made. During the actual field operations, holes were drilled soon after surface resistivity observations were made. We had the lithologic information in some cases, before calculation, plotting and electrical interpretation was done.

Barnes Layer Section (Figure 9) --The section is dominated by a low resistivity zone (clay) descending eastward from a position nearly at the land surface at location 420 but 10 to 20 feet deep at location 700. There is also a high resistivity layer at the land surface that increases from little or nothing at location 520 to a considerable thickness from 580 eastward. A high resistivity layer at depth (sand) lowers eastward with a distinct "hump" at location 470. Theoretically, this is supposed to show vertical and lateral changes with no representation of accuracy for depths. However, all of these features turn out to be not too far off in depth, as well as being real.

Wenner Soundings (Figure 10)--These are related to the Barnes Layer section in that they used the same data from the same electrode arrangement. The line of soundings shows the same features as did the Barnes Layer section with some variations. It is much more laborious to construct this section than to construct the Barnes Layer section, and it is interesting that (in this case) it conveys no more information.

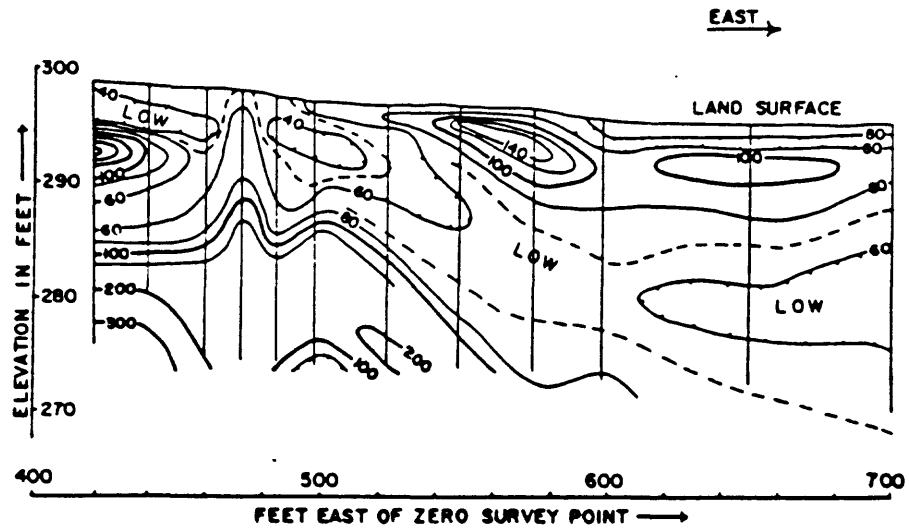


Figure 9 - Barnes Layer profile. The straight vertical lines are beneath the center of the electrode array during each Wenner Sounding. These are also locations of some of the geoelectric columns and auger holes shown in subsequent figures. The low resistivity zone descending eastward is clay. From Stearns et al., 1982, Fig. 33.

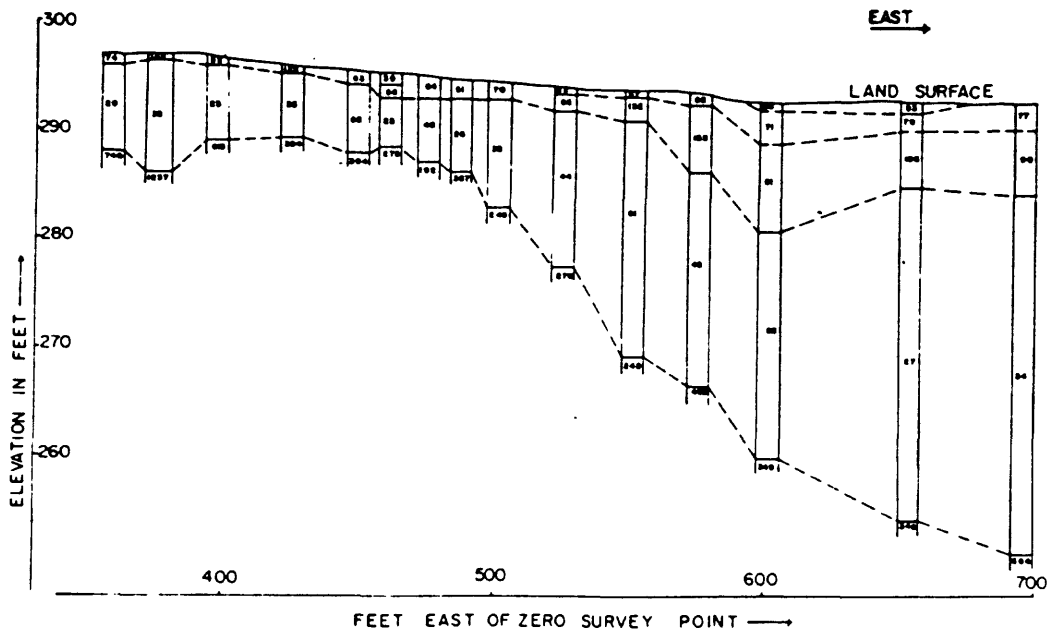


Figure 10 - A line of geoelectric columns interpreted from curve matching using Wenner Array. From Stearns et al., 1982, Fig. 34.

Auger Hole Resistivity--The sample resistivity (Figure 11) section shows a low resistivity layer (clay) close to and essentially parallel to the land surface from location 300 to location 500 from where it drops eastward. As it drops, a higher resistivity section appears, thickens to location 600, then continues eastward as an even layer at the land surface. At depth, a high resistivity layer (sand) roughly maintains a 10-foot depth eastward to location 520 where it drops off eastward. Note that the low resistivity layer is very close to the land surface from location 440 to location 500. This is a detail correctly predicted by the Barnes Layer and Wenner Sounding sections.

Auger Hole Lithology--Lithology (Figure 12) is closely related to resistivity. Clay is the low resistivity material with sand and silt having high resistivity. There is no clear difference in resistivity of silt and sand. All of the sample details are consistent with the Barnes layer profile. An interesting detail is the sand dike picked up by the Barnes Layer Profile at 470 which we dug into with a shovel and drilled.

GRAVITY

General

Gravity information is useful in interpretation of shallow geological features in the region, at depths ranging from the land surface (faults, clay-filled old Mississippi River channels), to the configuration of the Paleozoic-Cretaceous boundary 2000 feet or so below the land surface.

As is generally true, gravity data alone have a limited utility, but interpretation is enhanced when combined with other information. In the study area, data from drill holes and earth resistivity can be related to gravity.

Density of lithologic units must be known or estimated to use gravity variation for geologic interpretation. Table 2 shows densities of units in the study region.

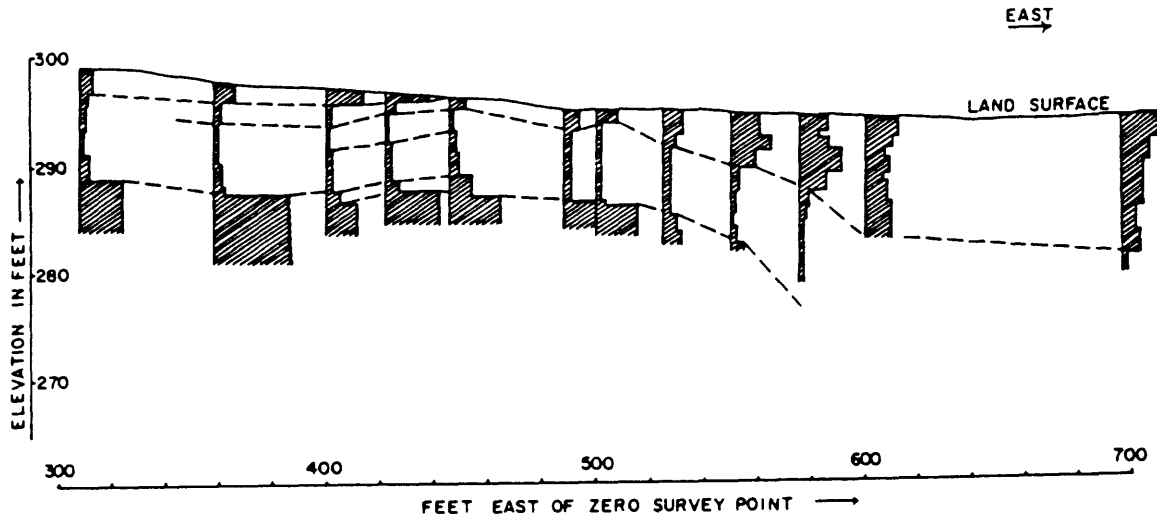


Figure 11 - Correlation section of auger hole sample resistivity. The auger hole is located at the vertical left side of each shaded block. These are histograms such that the wider the block the higher the resistivity. From Stearns et al., 1982, Fig. 36.

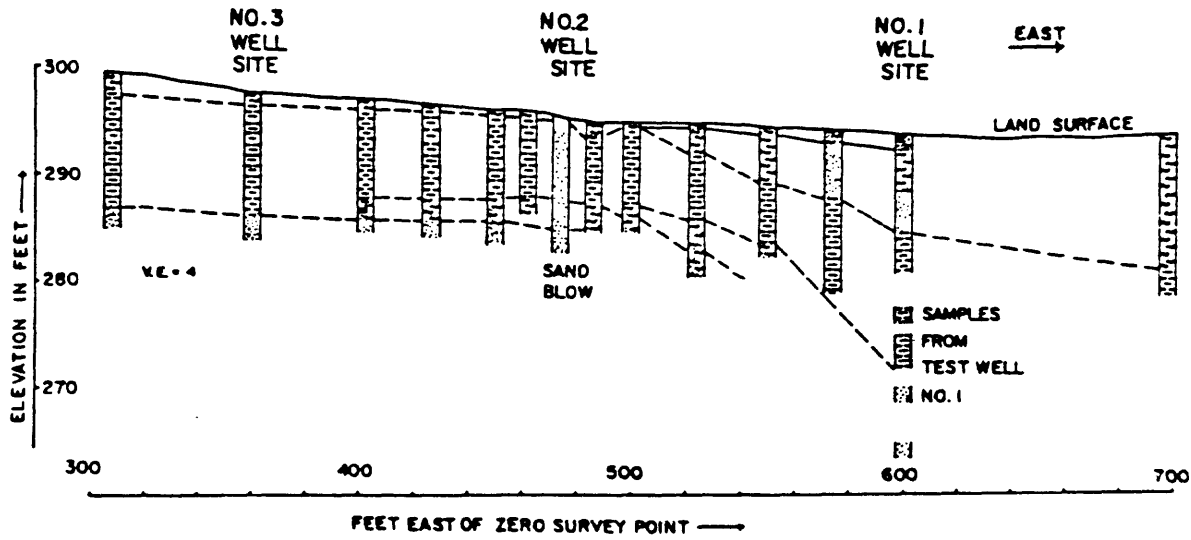


Figure 12 - Lithology encountered in the auger holes. Samples for Well No. 1 are included to show the depth of the base of the clay. Dots are sand; horizontal lines are clay; wavy lines are silt. From Stearns et al., 1982, Fig. 37.

TABLE 2.--Density Values in the Study Area
(From Stearns, et al., 1984, Table 1)

| Stratigraphic Unit | Generalized Description of Measured Lithologies (Number of Samples of Reported Densities) | Average or Estimated Density (\pm Standard Deviation) |
|--|--|--|
| Alluvium (including ancient upland alluvium) | | |
| High Plasticity Clay | "Fat" plastic clay (3) | 1.86 \pm 0.06 |
| Low Plasticity Clay | "Stiff" silty clay (40) | 1.93 \pm 0.08 |
| Silty Sand | Silty sand to poorly sorted sand (11) | 1.98 \pm 0.08 |
| Clayey Sand | Clayey sand (8) | 2.00 \pm 0.10 |
| Clean Sand | Water-bearing sand or gravel (no sample) | 2.32 calculated as 80% quartz, 20% water |
| Loess | Sandy, clayey, silt (74) | 1.89 \pm 0.13 |
| Jackson | Gray-blue sandy clay (24) | 1.98 \pm 0.12 |
| Claiborne and Wilcox | Interbedded clay, silt, sand (33) | 2.01 \pm 0.10 |
| Porter's Creek Clay and Clayton | Low-plasticity clay under- lain by a thin sand (35) | 1.95 \pm 0.14 |
| Owl Creek | Sandy clay (4) | 2.03 \pm 0.16 |
| Cretaceous other than Owl Creek | Mainly sand (2) | 2.07 \pm 0.11 |
| Knox Dolomite | Dolomite (4) | 2.76 \pm 0.03 |
| Pre-Knox Siltstone | Dolomitic or Calcareous siltstone (no sample) | 2.65 \pm (esti- mated from gamma-gamma density log) |
| Granite Basement | Granite (no sample) | 2.65 (esti- mated from density log) |

The northwest corner of Tennessee and adjacent Arkansas and Missouri (23 7-1/2 minute quadrangles) was surveyed through 1981 using about 1200 stations spaced about 1 mile apart. More detailed surveys were made at Reelfoot Scarp. The larger anomalies reflect density contrasts within Paleozoic and older rocks, but some small or narrow anomalies must have a shallow origin or young expression. A more detailed survey employing closely spaced stations (100 to 2000 feet) was made at Reelfoot Scarp and vicinity for the purpose of investigating structure.

Reelfoot Lake Area Survey

The survey is summarized by Figure 13, the Bouguer gravity anomaly map of the 22 quadrangle area. Among the features shown on this large scale map that deserve special mention as candidates for shallow structures are:

1. At and north of Caruthersville, Missouri, there is an imperfect but striking correspondence between directions of individual reaches of the Mississippi River, and the trends of contours of gravity anomalies. This suggests that shallow features (perhaps faults) relating to deeper density contrasts (perhaps fault blocks) control courses of the Mississippi River north of $36^{\circ}05'$.
2. The Tiptonville dome and related high ground there is a positive gravity anomaly, indicating uplift here of dense Paleozoic rocks.
3. A northeast-trending 1 mile wide negative anomaly extends through Bogota for about 10 miles to Cat Corner. At Cat Corner there is a northwest-trending scarp offsetting the Chickasaw Bluff line. It is interesting that this area coincides with numerous earthquakes. The northeast-trending gravity trough through Bogota to Cat Corner may well be a graben or half graben. East of the Bogota-Cat Corner gravity trough, there is a (2 x 5 mile) positive gravity anomaly.

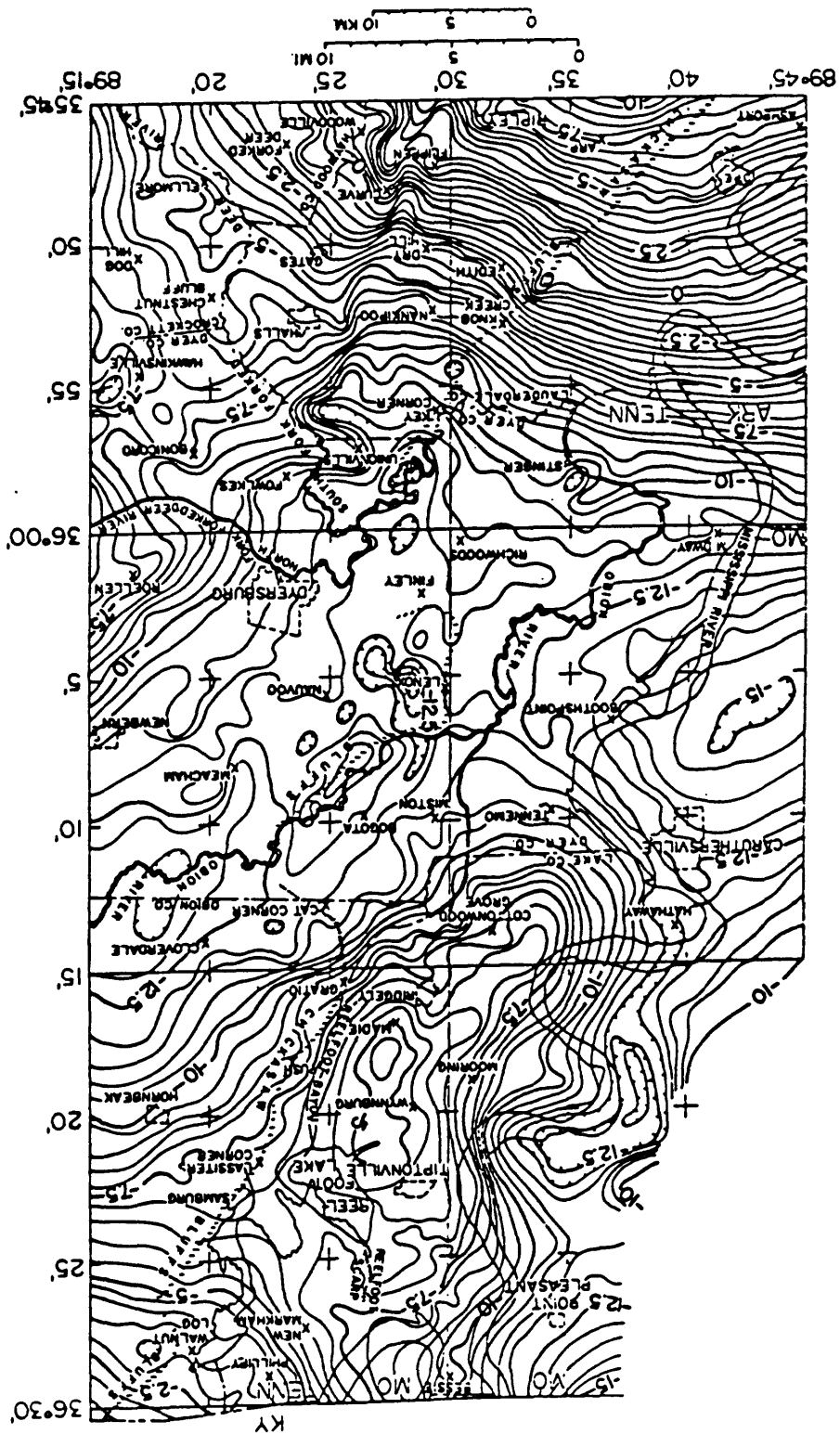


Figure 13 - The Bouguer Anomaly Map. This is based on approximately 1200 control stations, generally about one mile apart. From Stearns et al., 1984, Fig. 4.

This anomaly coincides with a positive magnetic anomaly, and may mark a mafic pluton at a depth of a mile or less.

Reelfoot Scarp Area

General

This is the same area where the detailed earth resistivity was done. Faulting and vertical uplift are known here (Fisk, 1944; Stearns, 1979; Russ et al., 1978; and Russ, 1982). Also, many holes have been drilled to 300 feet or more, so gravity modeling can be related to, and accounted for, by known features.

At Reelfoot Scarp (Figure 14), a 3 x 3 mile area has been surveyed with a variable spacing. Within this there are six lines of closer spaced stations, 100-500 feet apart. Here, the high ground west of the scarp (Tiptonville dome) generally has anomaly about 0.5 milligal higher than the low ground east of the scarp (Reelfoot Lake basin). As viewed closely, the middle third of the scarp follows a lesser gravity nose having an amplitude of about 0.2 milligals.

Density Models Based on Drill Hole Lithology and the Gravity

Field at Reelfoot Scarp

The high precision survey data can be compared (Stearns, 1991) with gravity using a model based on real lithology penetrated in shallow drill holes. Densities from Table 2 were used to construct models based on lithology encountered in the shallow drill holes that penetrated both a recent channel and Holocene and Eocene units offset by faults within 300 feet of the land surface. Figure 15 shows the lines in relation to the channel and scarp. Figure 16 shows the density model and calculated anomaly of about 0.1 milligal for the channel alone. Figure 17 shows the density model of the

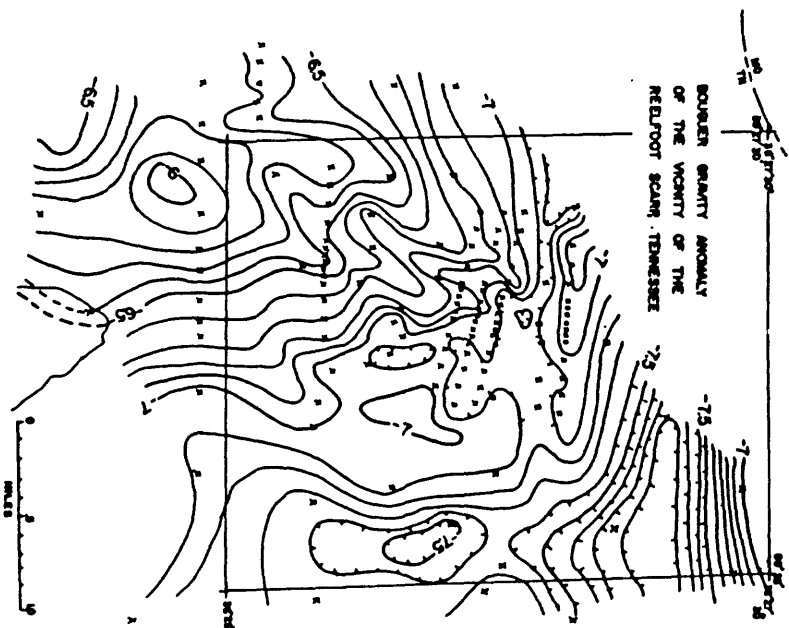
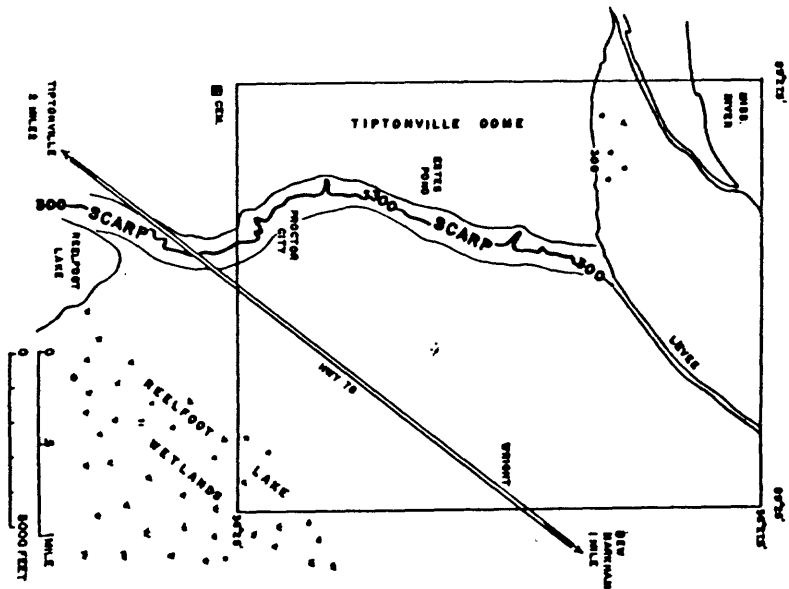
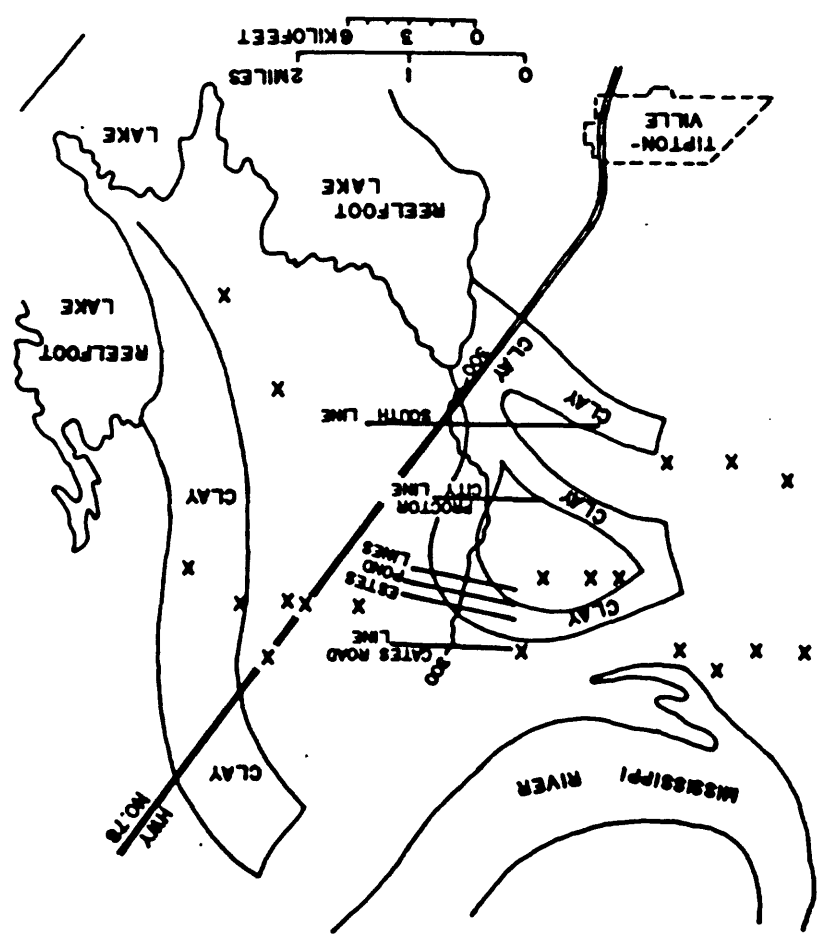


Figure 14 - Gravity anomaly map of the Reelfoot Scarp area. Near Estes Pond the scarp coincides with a minor gravity nose. This nose reflects a graben that will be modeled on Figure 17 using closely spaced stations on the east-west survey lines. From Stearns et al., 1984, Fig. 11.

Figure 15 - The gravity lines in relation to old Mississippi River Channels that are filled with clay (from Saucier, 1964, Reelfoot Lake quadrangle). The 300 foot contour marks Reelfoot Scarp, along which faulting is known.



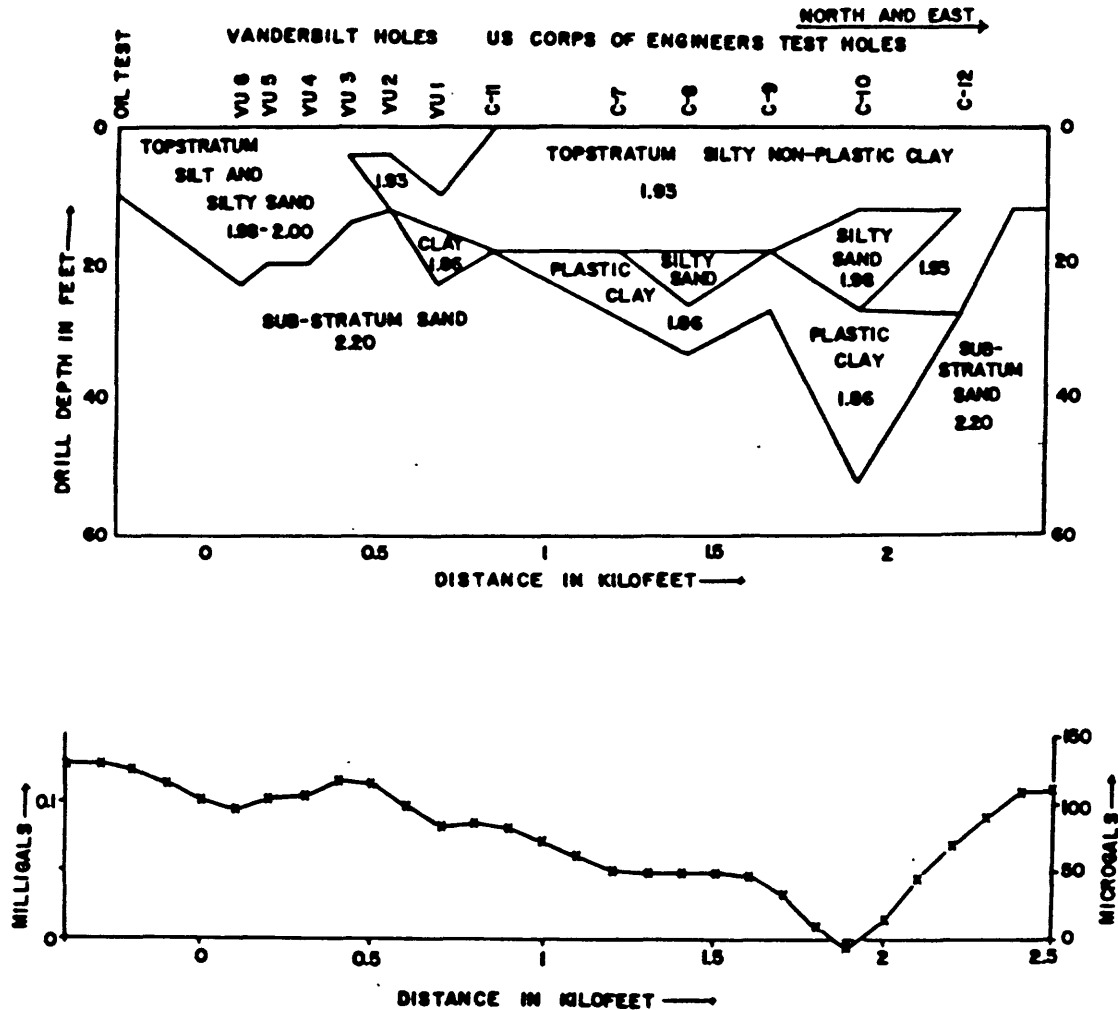


Figure 16 - Gravity anomaly of the Estes Pond Channel: Top - Lithologic and density section based on drill hole lithology and Table 1; Below - Gravity anomaly generated by this section. From Stearns, 1981. Fig. 17.

channel combined with a graben of down-faulted sand underlying the east side of the scarp with the calculated anomaly on top. For comparison, the observed anomaly for the nearby North Estes Pond survey line is shown on the bottom of Figure 17. The calculated anomaly is generally similar, but disagrees in some respects. The similarity is believed to be significant, particularly because the model is not a cut and try version but a single construction from drill data.

This exercise shows that gravity data can be rationalized to a significant degree with details of near-surface geology. It encourages a continued use of gravity as an exploration tool.

EXPLORATION FOR YOUNG FAULTS USING GRAVITY AND EARTH RESISTIVITY

Introduction

Offset in drill holes, earth resistivity abrupt lateral changes, and gravity anomaly lateral changes all relate to faulting. Knowing this, it was decided to exploit these relationships and attempt to explore for faults. Gravity and existing drill hole information should be useful to cover a relatively extensive area. Earth resistivity was to be used as a follow-up means to precisely locate shallow faults in any limited area indicated as likely to be faulted by the gravity or drill hole data. Finally, test drilling was to be used for a verification of the fault location. This project is a test of a combined method to search for faults, and an attempt to apply the method on the Loesscovered upland away from the Mississippi River Alluvial Plain. It turned out that water well data did not lead us to a fault, but gravity followed by earth resistivity did, and test holes verified it.

A northeast trend of gravity anomalies was discovered in 1980 near Ripley in Lauderdale County in the general vicinity (but a bit east) of the rift edge

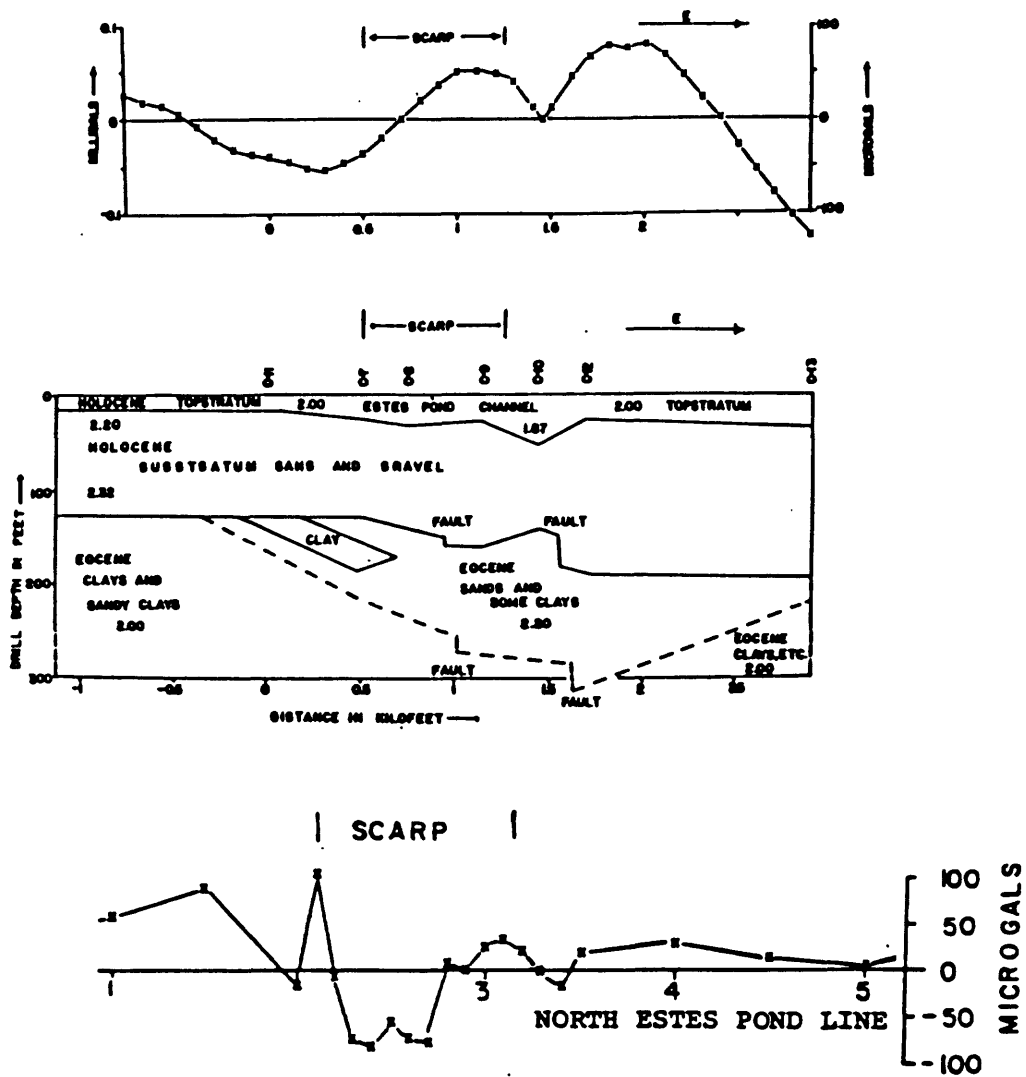


Figure 17 - Calculated anomaly and density model made from drill holes (above). Nearby observed anomaly below. A positive anomaly was observed at the scarp on all six lines. It is due to denser sand downfaulted against lighter clay. From Stearns, 1981, Figs. 20, 21.

inferred by Hildenbrand and others in 1977. Lauderdale County was the center of active exploration for Lignite, and hearsay information was that there is little elevation change of lignite beds near the Mississippi River, but some irregularity (maybe facies change or faulting) complicates correlations in Henning-Ripley area. Accordingly, we extended the survey south of Ripley to include the Henning area in the Ripley South quadrangle.

Gravity Survey and the Fault

General

A fault was discovered east of Henning. It was located by gravity mapping followed by an earth resistivity survey. After the initial discovery, additional gravity stations were set which allowed a comparison of gravity with earth resistivity in detail.

Ripley South Quadrangle

This quadrangle was mapped in somewhat more detail (98 stations) than our usual 60 stations per quadrangle. The anomaly map (Figure 18) is characterized by a strong northeast gradient off the Covington Pluton. A nose east of Henning (at about $35^{\circ}40'N$ and $89^{\circ}47'W$) led to the fault. We manipulated the gravity data to make a second derivative map (Figure 18).

A second derivative map emphasizes smaller features, and the notion was to search for narrow sharp anomalies that could result from faulting at (or above) Paleozoic depth, which here is about half a mile. Maybe faults offsetting Paleozoic extend to the surface, maybe not. The positive between two negatives, in the southeast quadrant of the map where the heavy line is drawn, was an obvious candidate as were anomalies near Ripley at the north center of the map.

The smaller target areas were examined to see where sufficiently long resistivity surveys would be feasible. It turned out that the area of the

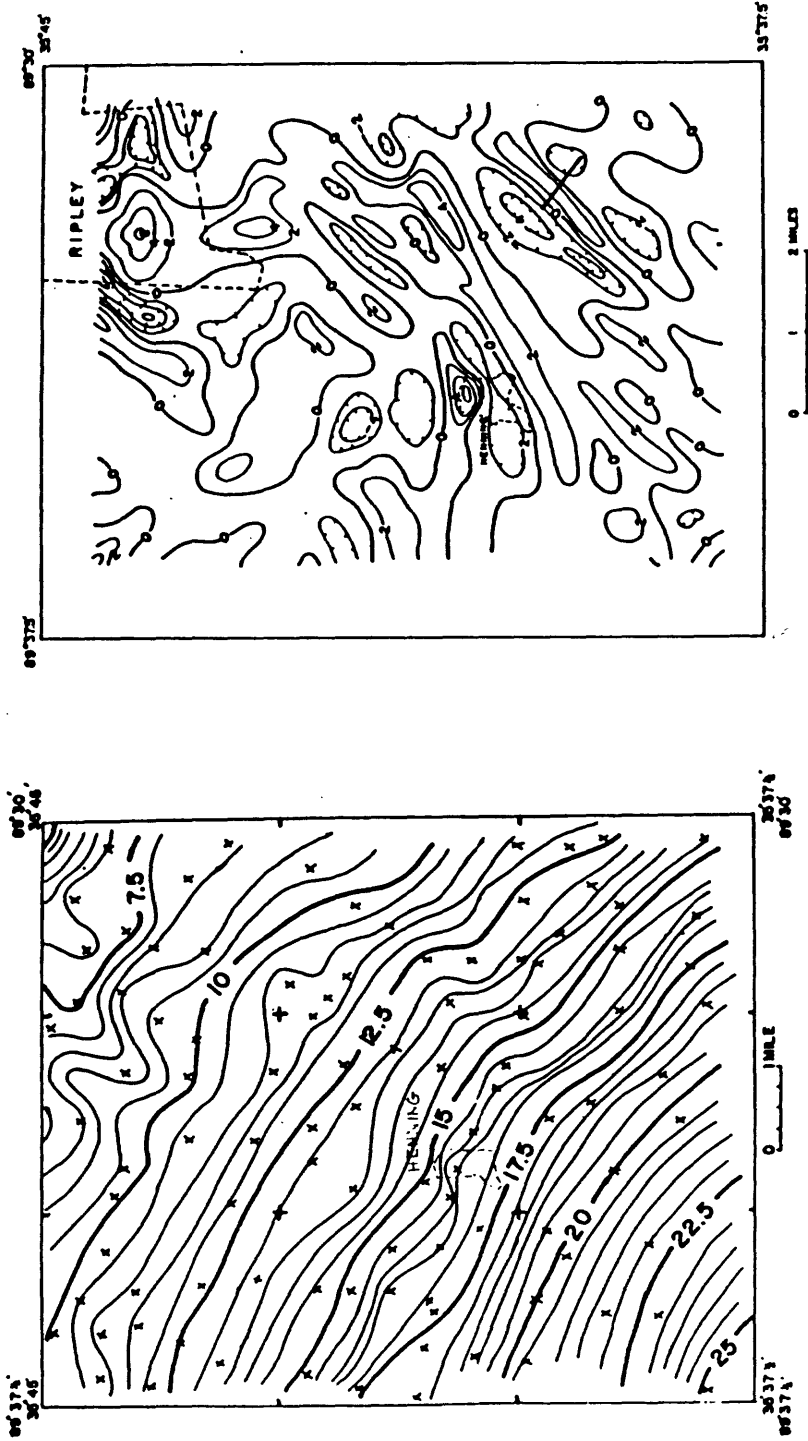


Figure 18 - On the left is the working gravity anomaly map of the Ripley South 7½' quadrangle. The northeast-trending nose east of Henning led to the fault. On the right is a second derivative map based on a 1/2 mile grid. The narrow northeast-trending anomaly 2½ miles east of Henning is the second derivative expression of the gravity nose. The line marks the resistivity survey line.

heavy line (about $35^{\circ}40'N$ and $89^{\circ}47'W$) was the most convenient area. Here a single farm field extended for nearly a mile. Elsewhere, small lots, the likelihood of buried utilities, and thick woods made earth resistivity surveying difficult. This "path of least resistance" is the heavy line on Figure 18 where a fault was discovered.

Earth Resistivity

Because earth resistivity closely located the fault at Reelfoot Scarp, it was hoped that here too this technique might pinpoint a fault, if present. It was hoped that clays, sands and silts known to be present would provide the contrast, and that a fault, if present, would offset sufficiently thick layers far enough to provide lateral contrasts. The Wenner array that worked best at Reelfoot Scarp was employed to get information for a Barnes Layer Profile (for a preliminary cross section) and for Wenner curves (to estimate electrical depths more reliably).

Figure 19 summarizes the results. On the top panel, the Barnes Layer section suggests even layering for the top 100 feet or more from stations 1 to 6, but a near surface offset between 6 and 7. The Wenner soundings, shown in the middle panel, are consistent with this (as is to be expected in view of the fact that they use the same data). A fault was interpreted between stations 6 and 7. The bottom panel is an estimated lithologic section, made before drilling, interpreting the apparent electrical layers in terms of the lithology to be expected from our earlier experience. The middle panel is used as the ruling interpretation of layer depths, to predict throw (estimated to be anywhere from 75 to more than 100 feet).

Interestingly, the resistivity line completely crossed both flanks of the second derivative gravity "ridge" (Fig. 19); on the west side faulting within 100 feet of the surface is indicated by resistivity; on the east side it was

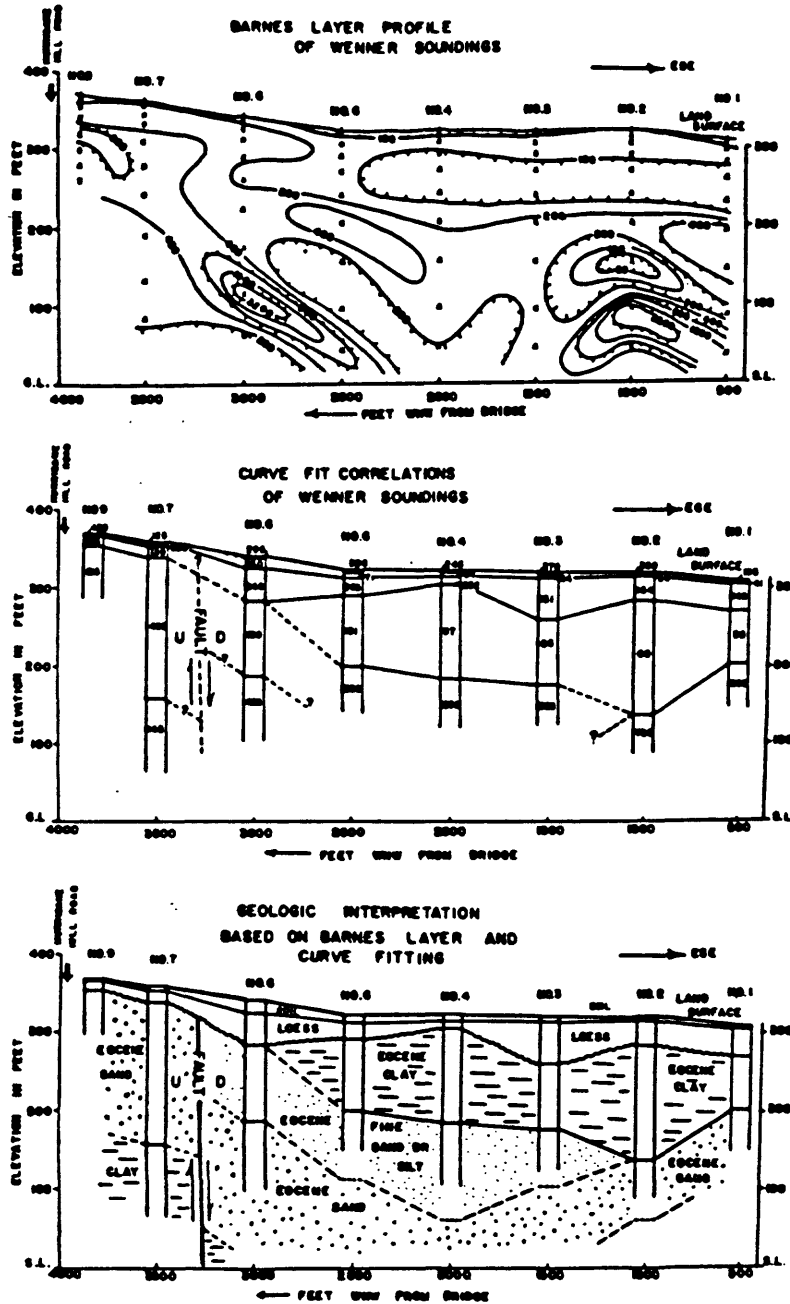


Figure 19 - Results of the earth resistivity survey. The top panel is designed to show lateral changes, but depths are uncertain. The center panel theoretically gives reliable depth estimates. The bottom panel is a geologic interpretation. From Stearns et al., 1984, Fig. 20.

not. However, faulting between stations 2 and 3 at a depth of 200 feet or more looks possible. So far, the exploration process was a success; gravity located several possibilities: of two tested by earth resistivity (each side of the gravity ridge), one appeared to be faulted within 100 feet or so of the land surface.

Drilling The Fault

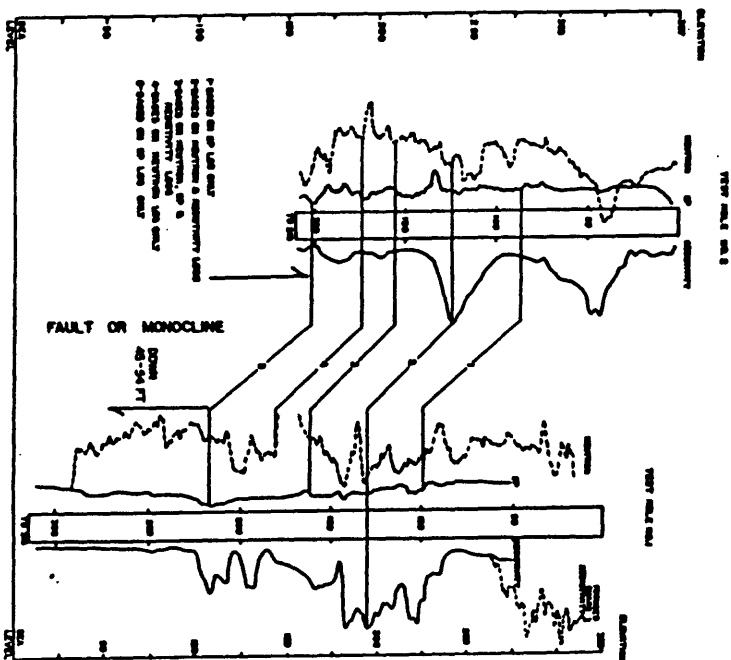
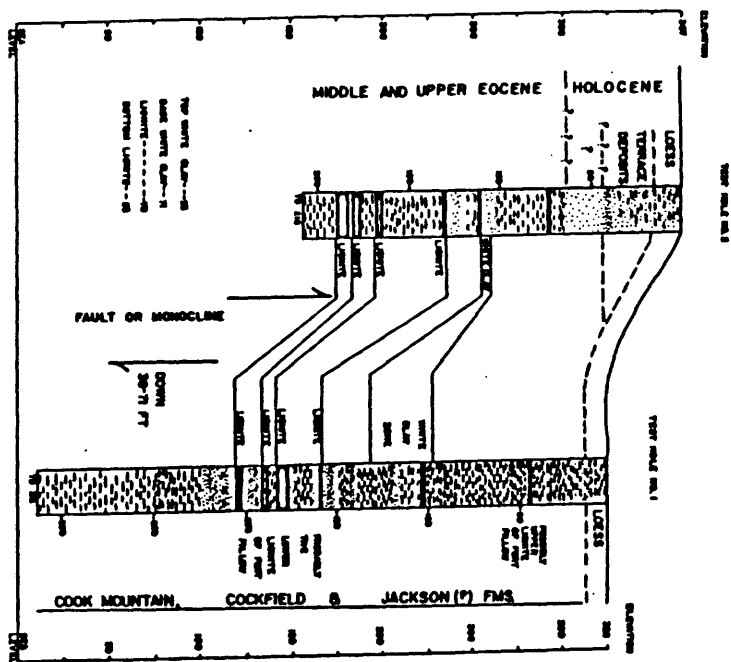
Two drill holes were placed on either side of the inferred fault--one at resistivity station 5, the other close to resistivity station 9. These sites were selected some distance apart for access with a minimum of damage in a field where crops were planted. The results prove the offset. Actually, it is possible that a monocline is present, rather than a fault, but the offset sense is identical to that of an actual fault.

Figure 20 shows the two drill holes with lithology and down hole electric logs. The eastern (right) hole is down, but the exact offset is subject to interpretation (36-71 feet) and may be greater for deeper layers than for shallow layers.

Relation to Gravity

Additional gravity stations were set parallel to the line of earth resistivity stations to see whether a detailed correspondence exists. Figure 21 shows the results. Anomaly increases on the down side of the fault. This may be due to clay (less dense) being closer to the land surface on the up side of the fault. Such clay was encountered below the lignite section in both of the holes.

This gravity section is significant for two reasons. First, it indicates a detailed correspondence here between gravity and near surface structure. Second, it shows that the fault has a 0.5 milligal anomaly, big enough to overcome survey problems relating to a loose meter dial.



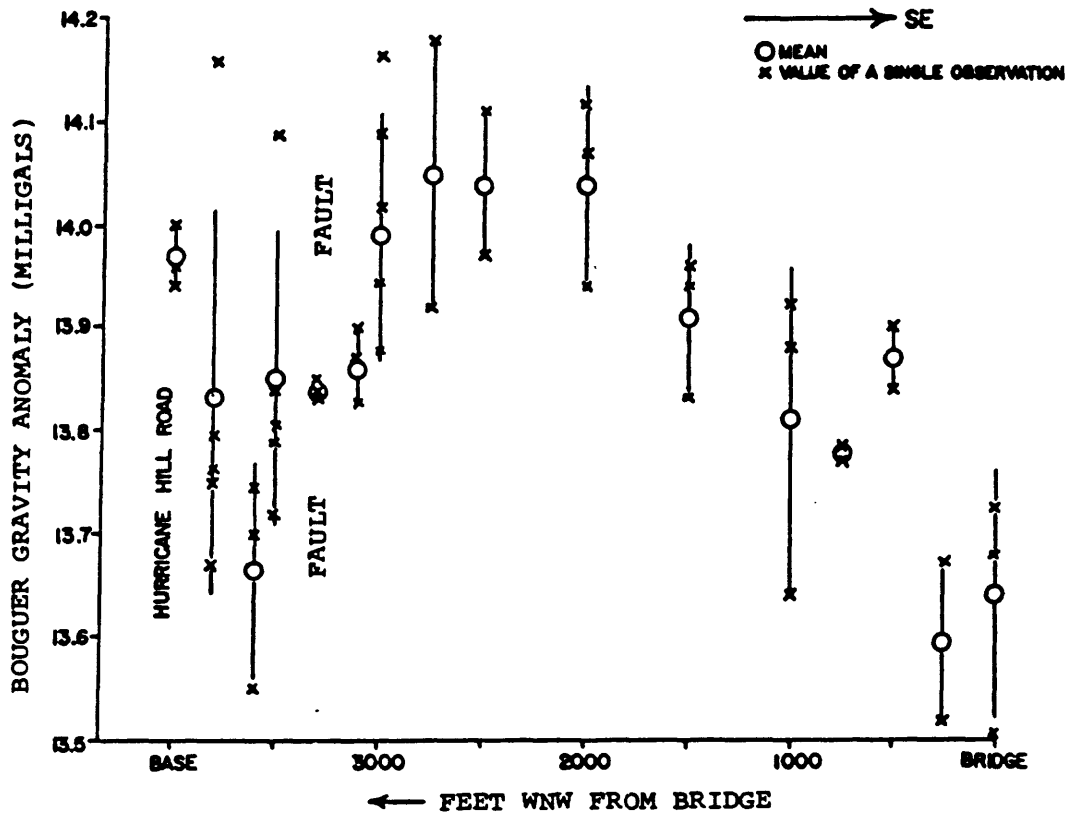


Figure 21 - Gravity profile along Durhamville Road across the fault. The vertical lines are error bars marking \pm standard deviation from the mean (circles). Relatively large uncertainties are due to backlash in the meter dial. Stations with small error bars were occupied last after we recognized the mechanical problem.

SUMMARY AND CONCLUSIONS

Earth Resistivity

Surface earth resistivity was successful in probing to a shallow (plow layer to 100 feet or so) depth in Mississippi River alluvium; and somewhat deeper (to about 30.0 feet) in Loess and Eocene of the upland. Profiling, Barnes Layer sections, Wenner soundings, and circle soundings proved useful. Wenner soundings are preferred, because data can be used for Barnes Layer profiles.

Features of abandoned river channels (a central low resistivity clay 'plug' and lateral high resistivity, sandy natural levees) were readily located and mapped by profiling. Faults were located by combinations of techniques including profiling, Barnes Layer profiling and circle soundings. Faults were closely located within 10 feet or less by circle soundings.

Resistivity columns were made by measuring the resistivity of samples from small diameter auger holes. At the sites of these measured columns, surface soundings gave layer thickness estimates within 25 to 30% of measured thickness.

Gravity

Owing to a strong density contrast between the 2000-foot deep boundary between dense Paleozoic rock and light younger unconsolidated material, many details of the larger gravity field originate from that depth. Also, many relate to near surface structure, because Paleozoic depth structures extend to a shallow depth. For example, Mississippi River bends north of 36°05' relate closely to gravity anomaly, likely due to faults cutting the Paleozoic surface and extending into younger materials, maybe to the land surface.

The relationship of gravity anomaly and geology within 300 feet of the land surface was demonstrated at Reelfoot Scarp by correspondence between

observed anomaly and anomaly calculated by density models using observed drill hole lithology as a density basis (clay of about 1.9 gm/cm³ contrasted with sand of about 2.2 gm/cm³). The density models included faulted Eocene and a clay-filled channel of an abandoned course of Mississippi River.

Gravity Plus Resistivity and Discovery of a Fault

A search for faults was made using gravity as a preliminary technique to cover an entire 7-1/2 quadrangle search area, followed by a Barnes Layer resistivity profile, which pinpointed a fault across a narrow elongated second derivative gravity anomaly. A line of Wenner Soundings correctly predicted the sense of offset of the fault (down to the east), and approximately predicted the throw (36-71 feet measured by drilling vs. 75-100 feet plus estimated from earth resistivity).

The fault was discovered on loess-covered upland near the east edge of Reelfoot Rift, whereas earlier tests were made on the Mississippi River alluvial plain. Most of the New Madrid region is underlain by these materials. The position of the fault near the east edge of the buried Reelfoot Rift may open the possibility that the entire width of the rift could have been reactivated after Upper Eocene time.

REFERENCES CITED

- Barnes, H. E., 1954, Electrical subsurface exploration simplified: Roads and Streets, v. 97, p. 81-84.
- Fisk, Harold N., 1944, Geologic investigation of the alluvial valley of the lower Mississippi River: U. S. Army Corps of Engineers, Vicksburg, Miss., 78 p.
- Orellana, E. and Mooney, H. J., 1966, Master tables and curves for vertical electrical soundings over layered structures: Madrid Interiencia, 150 p., 66 tables.
- Russ, D. P., Stearns, R. G., and Herd, D. G., 1978, Map of exploratory trench across Reelfoot Scarp, northwestern Tennessee, U. S. Geol. Survey, Misc. Field Studies Map MF-985.

- Russ, D. P., 1982, Style and significance of surface deformation in the vicinity of New Madrid, Missouri, U. S. Geol. Survey Prof. Pap. 1236 F, p 94-114.
- Saucier, R. T., 1964, Geologic investigation of the St. Francis Basin: Vicksburg, Mississippi, U. S. Army Corps of Engineers Waterways Experiment Station, Technical Report 3-659, 59 p.
- Stearns, Richard G., 1979, Recent vertical movement of the land surface in the Lake County Uplift and Reelfoot Lake Basin areas, Tennessee, Missouri and Kentucky, U. S. Nuclear Regulatory Commission, Document, NUREG/CR-0874.
- Stearns, Richard G., 1980, Monoclinial structure and shallow faulting of the Reelfoot Scarp as estimated from drill holes with variable spacings, U. S. Nuclear Regulatory Commission, NUREG/CR-1501, 37 p.
- Stearns, R. G., 1981, Influence of shallow structure, and a clay-filled Mississippi River channel on details of the gravity field at the Reelfoot Scarp, Lake County, Tennessee, U. S. Regulatory Commission, NUREG/CR-2130 61 p.
- Stearns, R. G., Haselton, T. M., and Tsau, Jau Ping, 1982, Earth resistivity as a tool for shallow exploration in the Reelfoot Lake Area, Tennessee, U. S. Nuclear Regulatory Commission, NUREG/CR-2653, 117 p.
- Stearns, R. G., Towe, S. K., Hagee, V. L., Nava, S. J., and Wilson, S. L., 1984, Description and significance of the gravity field in the Reelfoot Lake region of northwest Tennessee, U. S. Nuclear Regulatory Commission, NUREG/CR-3769, 39 p.
- Zohdy, A. A. R., 1970, Variable Azimuth Schlumberger Sounding and Profiling near a Vertical Boundary. U. S. Geol. Survey Bull. 1313-B, 22 p.
- Zohdy, A. A. R.; Eaton, G. P.; and Mabey, D. R., 1974, Techniques of water research investigations of the United States Geological Survey, Chapter D-1, Application of surface geophysics to ground water investigations: U. S. Government Printing Office, Washington, D. C., 116 p.
- Zohdy, A. A. R., 1974, Use of Dar Zarrouk Curves in the Interpretation of Vertical Electrical Sounding Data, U. S. Geol. Survey Bull. 1313-D, 41 p.

ACKNOWLEDGMENTS

The dedicated work of Vanderbilt students, despite extreme heat of summer, bitter cold of winter, and long hours made this report possible. Special thanks are due to Thomas M. Haselton, Jau-Ping Tsau, Susan K. Towe, Parrish N. Erwin, Jr., Michael Shea, Robert G. Perry, Susan Nava, and Sharon L. Wilson.

Thomas M. Haselton had a leading role in preliminary test of resistivity profiling and soundings, as did Jau-Ping Tsau for circle soundings and sample resistivity. Susan Towe made the first gravity models of Reelfoot Scarp. All had a hand in the gravity surveys. Parrish Erwin, among other things, supervised and did detailed gravity surveying at Reelfoot Scarp. Susan Nava and Sharon Wilson helped explore for and discover the Henning fault.

The hospitality and patience of owners and farm operators is gratefully acknowledged. Among others, Howard Vaughn, L. D. Cook, Terry Jameson, and Jack Lorraine permitted repeated access to their fields at Reelfoot Scarp over a period of more than 2 years. C. S. Carney and Doo Daniels allowed use of their property near Henning.

Gravimeters were loaned by Tennessee Division of Geology and Tennessee Valley Authority. Electric logs of test wells were run by U. S. Geological Survey.

The beginning of this study in 1976 was funded by National Science Foundation (Grant EAR-75-17383). Most was funded by U. S. Nuclear Regulatory Commission in Contract NRC-04-81-195-02.

SEISMIC-REFRACTION STUDIES OF THE MISSISSIPPI EMBAYMENT:

AN OVERVIEW

by

Walter D. Mooney

and

Mary C. Andrews

U.S. Geological Survey

345 Middlefield Road, MS 977

Menlo Park, CA 94025

INTRODUCTION

In September 1980 the United States Geological Survey conducted a seismic refraction investigation of the northern Mississippi Embayment. Thirty-four shots from nine shot points were recorded along a series of profiles oriented parallel to and across a Precambrian rift which has been inferred from gravity and magnetic data. This study provided the highest resolution to date of crustal structure in this area by virtue of the number of crossing profiles and the relatively close station spacing along the profiles.

The major results of the seismic refraction study have been reported by Ginzburg and others (1983) and Mooney and others (1983). Our purpose is to

critically review these results, emphasizing the remaining uncertainties and distinguishing those aspects of the interpretation which are required by the data from those that are merely consistent with it. Our intent is to clarify the constraints that seismic refraction studies provide on the structure, composition and evolution of the embayment.

In describing details of the crustal structure we note that there are uncertainties in the interpretation of seismic refraction data which arise from several sources. First, although traveltimes and amplitude anomalies observed in refraction data often provide evidence for more subtle structures, all of the published seismic interpretations in the area describe the crust in terms of discrete layers separated by abrupt velocity discontinuities. While this is a useful description of the gross structure, it only approximates the actual structure of the earth where uneven and transitional boundaries are common. Secondly, the quality of seismic refraction data is strongly dependant on the ambient noise level, shot point efficiency, recovery rate of records, and other factors. The Mississippi embayment has long been known as a 'poor data' area due to the high noise levels in this broad sedimentary trough. Finally, due to the limited lengths of the profiles in the recent studies, the deeper layers are mainly evidenced by secondary arrivals (wide-angle reflections) which vary in quality. Subjective judgements are therefore sometimes required for the interpretation of the arrivals from these layers. Fortunately, these judgements are strongly constrained by comparing the interpreted structure along profiles where they cross and requiring that the depths and velocities agree at these points. Assuming in the present case

that the seismic method is accurate to 10%, there will be errors as large as 3 km at a depth of 30 km. Detailed discussions of the subjective aspects of the interpretation of seismic refraction data are presented by Ansorge and others, 1982 and Mooney and Prodehl, 1984.

In the discussion below we will refer repeatedly to specific seismic refraction profiles from the recent work. The nomenclature for referring to individual profiles is by the terminal and central shot point (SP) numbers, e.g., profile 2-3-4, where the first mentioned shot point is at the origin. The northeast-southwest trending profile 1-3-5-6 is referred to as the axial profile, profile 8-2 as the west flank profile and all others are considered cross profiles (figure 1). We begin by summarizing the available seismological data and then discuss the overall structure beginning at the surface and proceeding with depth to the upper mantle.

PREVIOUS STUDIES OF THE CRUST AND UPPER MANTLE OF THE CENTRAL US

The earliest seismic refraction studies of the crustal structure of the central US were reported by McCamy and Meyer (1966), Stewart (1968), and Warren (1968) (fig. 2). Together, these studies indicate a difference in crustal structure within and outside of the embayment. Outside of the Mississippi embayment, in central Missouri and central Tennessee, Stewart (1968) and Warren (1968) report crustal velocities that are "normal" for a stable continental area, i.e., a 22 km thick upper crust with a velocity of

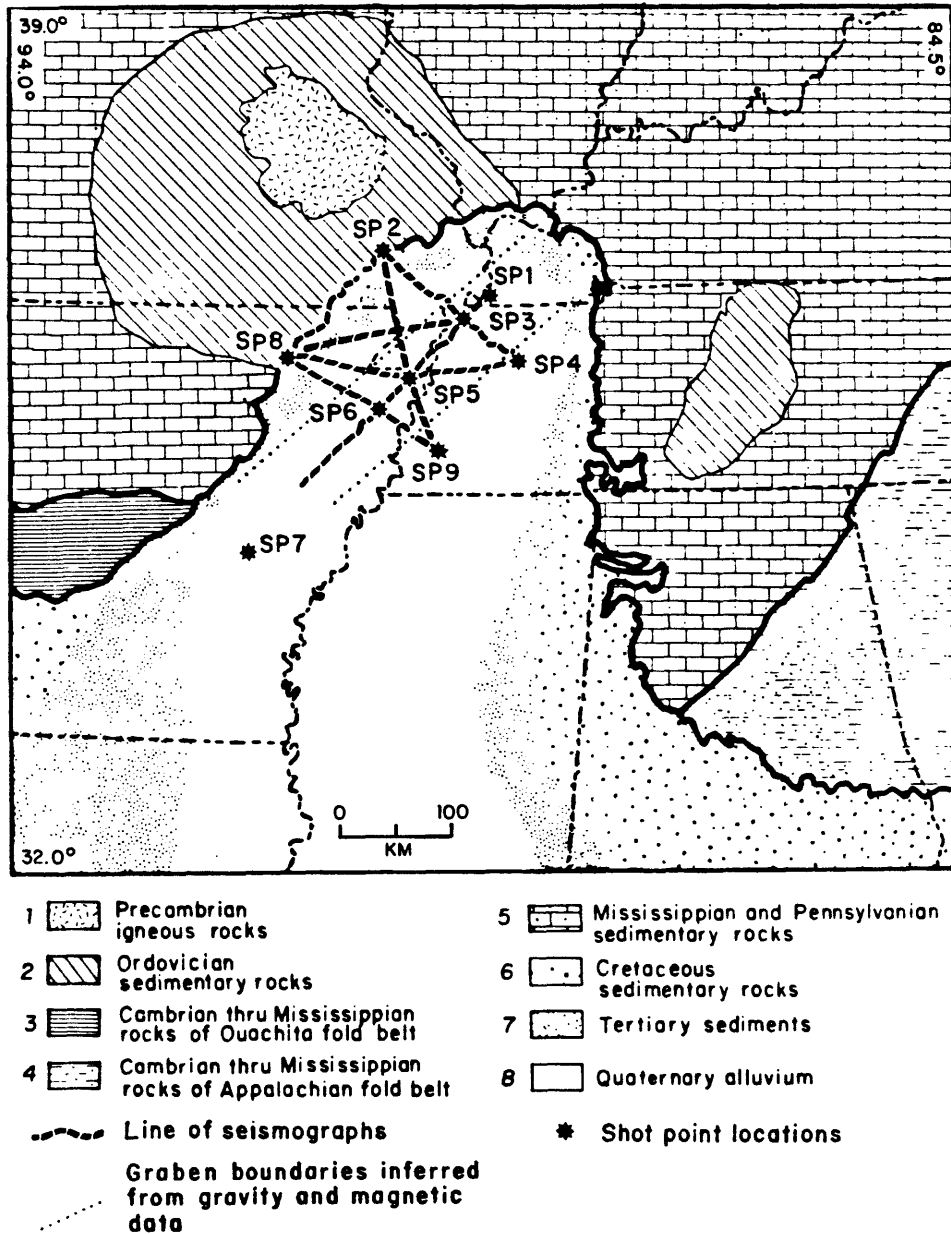


Figure 1. Generalized geologic map of the Mississippi embayment with the locations of the shot points and seismic refraction profiles reported by Ginzburg and others (1983) and Mooney and others (1983).

Seismic Refraction Profiles in the Area of the Mississippi Embayment

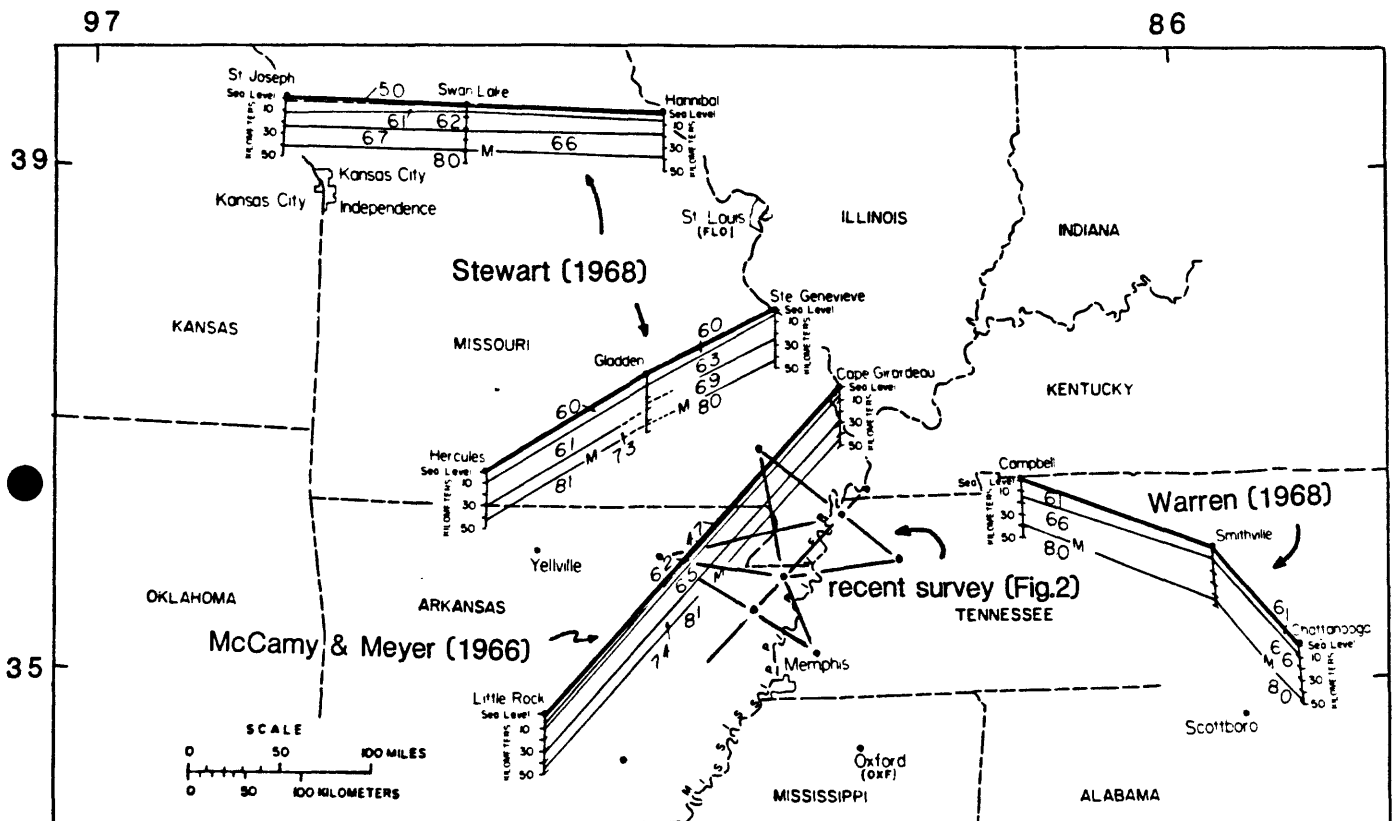


Figure 2. Seismic refraction profiles within and near the Mississippi embayment. The shot point numbers and profile lines for the recent seismic survey is shown in figure 1.

6.1 km/s overlying a 18 km thick lower crust with a velocity of 6.6 km/s (fig. 2). The profile of McCamy and Meyer (1966) was recorded on the west flank of the embayment and indicated, in addition to layers with velocities of 6.1 and 6.6 km/s, high-velocity 7.3 km/s layer at the base of the crust. Stewart (1968) also interpreted a lower crustal 7.3 km/s layer in southern Missouri on a profile 200 km northwest of the profile of McCamy and Meyer (1966). The presence of this layer was confirmed by more recent seismic measurements obtained from the interpretation of local earthquake traveltimes (Mitchell and Hashim, 1977), from the dispersion of Rayleigh waves (Austin and Keller, 1982), and from the more recent seismic refraction data which we review here (fig. 1).

The basal crustal layer identified by McCamy and Meyer (1966) was cited as evidence for the origin of the embayment as a rift by Ervin and McGinnis (1975). They modelled the regional gravity data by thickening this layer beneath the embayment, thereby forming a "fossil rift cushion". The hypothesis of a rift origin of the embayment was strongly supported by the identification, in an analysis of aeromagnetic data by Hildenbrand and others (1977), of an upper crustal graben. The interpretation of the embayment as a late-Precambrian rift has been thoroughly discussed (e.g., Ervin and McGinnis, 1975; Kane and others, 1981; McKeown, this volume) and is not reviewed here. In the present paper we refer to the embayment rift when we mean the entire crustal section, and to the embayment graben when we mean the basement structure.

CRUSTAL STRUCTURE

The recent seismic refraction studies of Ginzburg and others (1983) and Mooney and others (1983) show that the crustal structure of the embayment consists of six primary layers. The Cretaceous and Cenozoic deposits are characterized by a compressional wave velocity of 1.8 km/s and overlie Paleozoic carbonate and clastic sedimentary rocks (5.95 km/s) (fig. 3). Along the axis of the embayment graben, Paleozoic rocks are underlain by rocks with a substantially lower velocity (modelled as 4.9 km/s) which are presumed to be clastic sediments filling the graben (fig. 4). Crystalline basement has a velocity of 6.2 km/s and the lower crust a velocity of 6.6 km/s. The basal crustal layer in the embayment has a velocity of 7.3 km/s and the uppermost mantle velocity is 8.0 km/s.

Cretaceous and Cenozoic sediments

The near-surface layer of the embayment consists of Late Cretaceous and Cenozoic unconsolidated and poorly consolidated sediments which are known from geologic mapping and drilling data (Grohskopf, 1955; Schwalb, 1980). Structure within these sediments is best seen in seismic reflection data (Zoback and others, 1980; Hamilton and Zoback, 1982), while the thickness and velocity of these sediments was determined from the seismic refraction data.

Clear arrivals from the unconsolidated sediments, with an average velocity of 1.8 km/s, are present on all profiles except from shot points 8 and 2,

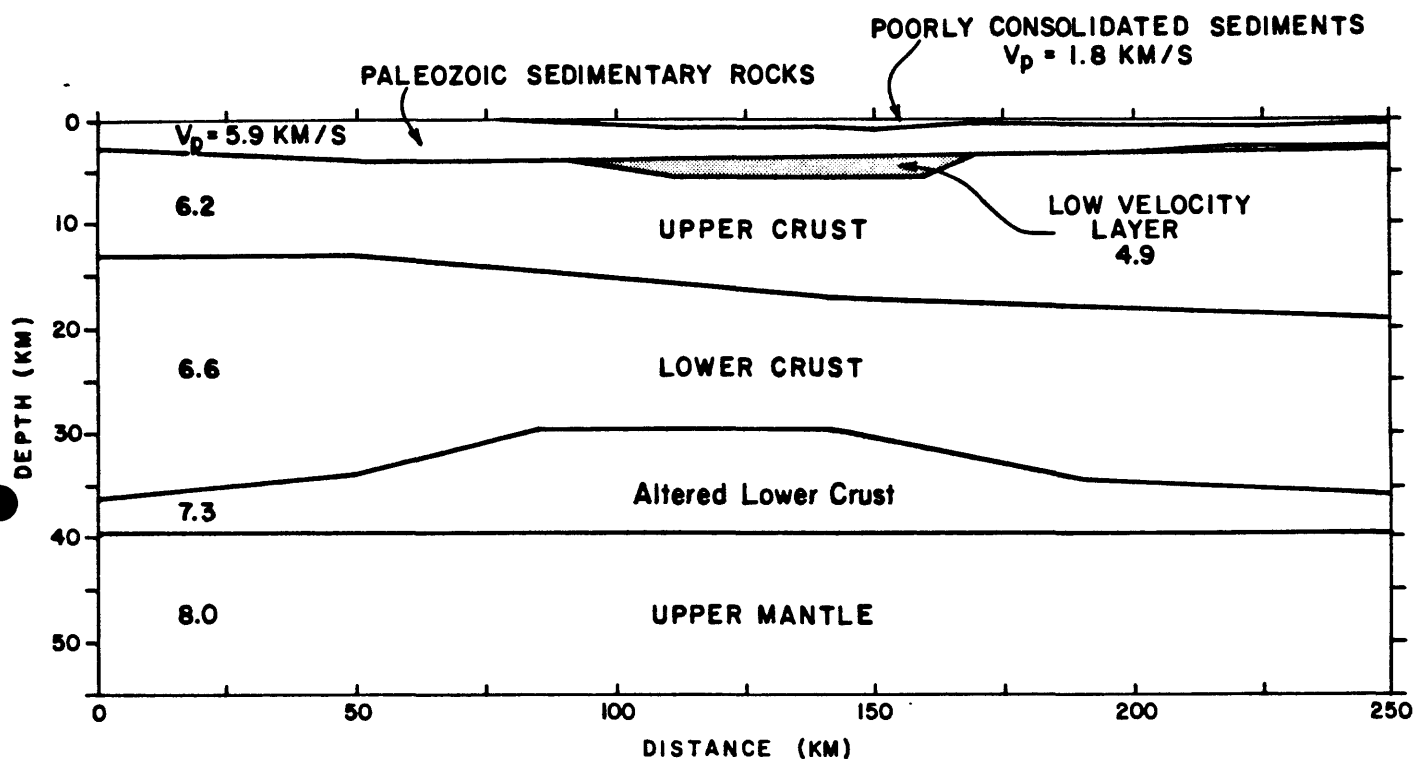


Figure 3. East-west section across the Mississippi embayment showing the six primary crustal layers and their velocities. The crustal thickness, 40 km, corresponds to the latitude of shot point 6 (fig. 6).

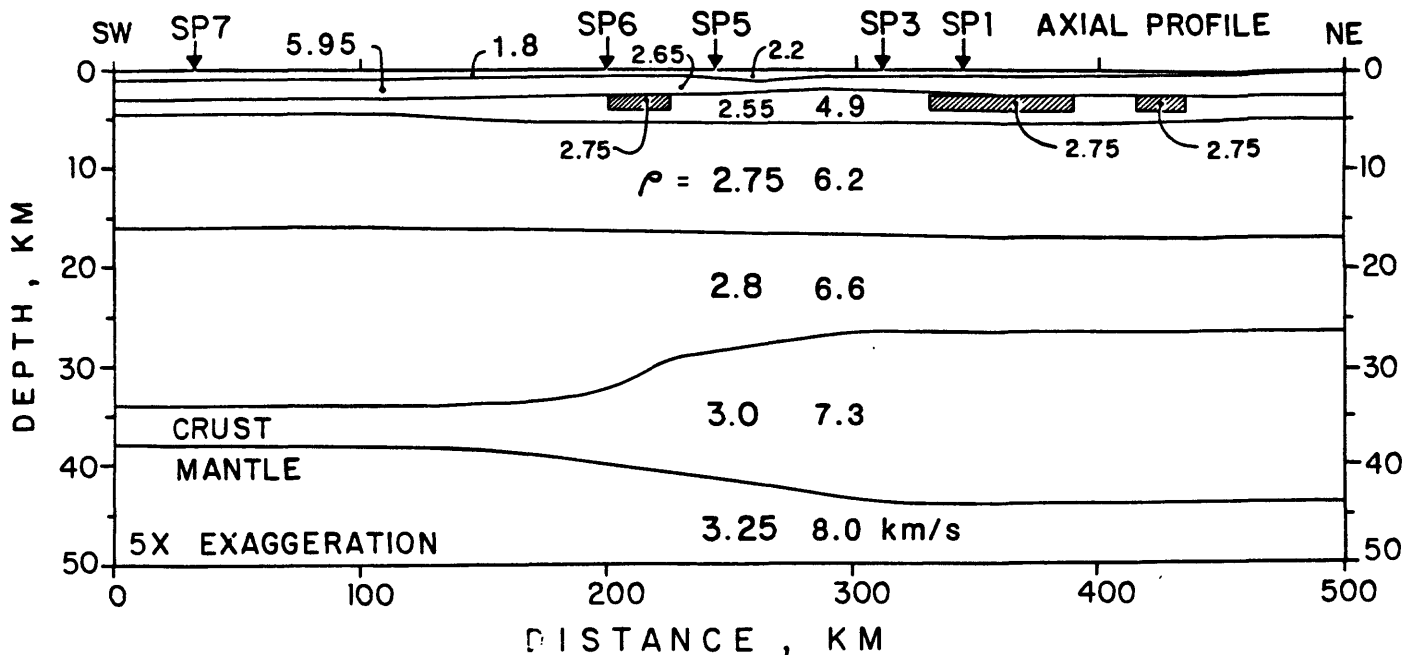


Figure 4. Northeast-southwest crustal section along the axial profile of the recent seismic refraction survey. Both layer densities and seismic velocities are indicated. Shaded boxes represent plutonic rocks which are identified either in the regional gravity data or seismic refraction data, or both. The 7.3 km/s basal crustal layer (density 3.0 g/cc) thickens to the northeast and the depth to the mantle increases.

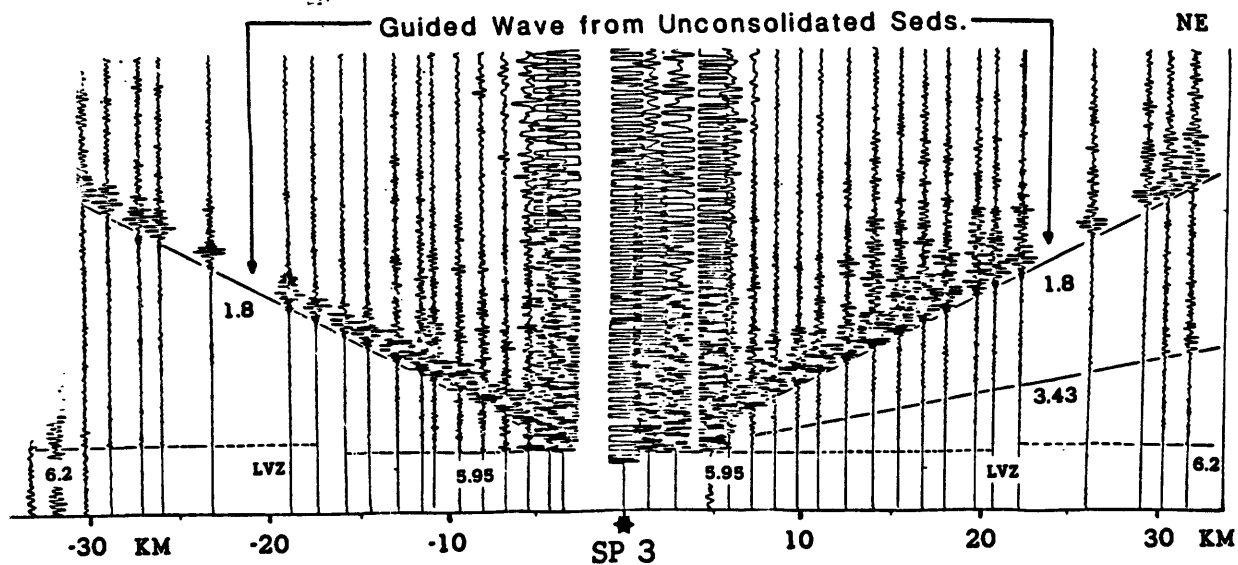
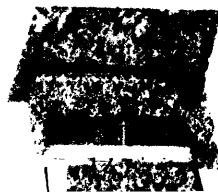


Figure 5. Seismic record section for the axial profile, shot point 3. The most prominent phase on the record section is the guided wave propagating within the unconsolidated sediments.

where the sediment cover is thin or absent. Since the arrivals from this layer are first arrivals only within 1 or 2 km of the shot point, we can directly determine the sediment thickness only in the vicinity of each shot. Changes in the thickness between shot points have been inferred from the relative advances and delays of arrivals from deeper horizons. Along the axial profile these sediments range in thickness from 0.7 to 1.1 km, with the greatest accumulation at SP 6. To the east, at shot point 4, the sediments are 0.6 km thick, and further south at SP 9 they are 0.9 km thick. The sediments thin and disappear at the flanks of the embayment. At SP 2 there is evidence for only 150-200 m of sediment, and SP 8 is entirely outside the area of sedimentary cover. The arrivals from the unconsolidated sediments are of very high amplitude due to their propagation as a guided wave, consisting of arrivals multiply reflected at the free surface and the lower contact with the Paleozoic sediments (fig. 5). This strong phase is recorded on all profiles with shot points within the unconsolidated sediments. The identification of this phase is important for the evaluation of earthquake hazards because it demonstrates that any earthquake which is large enough to rupture to the surface will generate a likely damaging guided wave that will propagate for large distances within the embayment. The large intensities within the embayment of the earthquake sequence of 1811/1812 was undoubtedly due in part to this phase.

An additional measurement of the properties of these sediments is that of their shear wave velocity. Andrews and others (1984) have determined a velocity of 0.4 km/s on the basis of local earthquake data.



Paleozoic Rocks

Geologic mapping and borehole data (Grohskopf, 1955; Schwalb, 1980) show that the unconsolidated sediments overlies clastic and carbonate rocks of Paleozoic age. Since these rocks are exposed outside of the embayment, their age and composition are well known. Recent seismic reflection studies have identified faults and local areas of uplift (Zoback and others, 1980; Hamilton and Zoback, 1982). These relatively small-scale structures cannot be resolved by the recent seismic refraction data, which is limited to determining its layer velocity and thickness. Arrivals from the Paleozoic layer are observed in the seismic refraction data for variable distances from the shot points due to differences in the local velocity structure. In general, the traveltimes curves may be divided into two basic types, those for which the arrivals can be traced to distances beyond 25 km and those for which the phase stops at 25 km or less. Where the Paleozoic rocks are underlain by the higher velocity crystalline basement, the traveltimes curve is continuous, and where they are underlain by the lower velocity rocks filling the basement graben, a shadow zone occurs. The upper crustal low-velocity zone is discussed in the next section.

Continuous traveltimes curves are observed in all directions from shot points 2, 8, and 9, and discontinuous curves from shot points 1, 3, 4, 5, and 6. The latter shot points are located within or on a flank of the graben.

The thickness of the Paleozoic layer in the vicinity of a shot point can



be well determined for those profiles with discontinuous traveltime curves. The top of the layer is determined from the change in apparent velocity from 1.8 km/s to 5.95 km/s, and the bottom is determined from the distance to the shadow zone. An average thickness of 1.7-2.0 km has been determined along the axial profile, and near shot point 4.

It is more difficult to determine the thickness where the layer overlies crystalline basement. In these areas the refracted arrival from the Paleozoic layer merges smoothly into the refraction from the basement, making difficult the identification of the cross-over distance (e.g., fig. 6). The depth to basement in these areas has been more reliably determined from the analysis of aeromagnetic data (Hildenbrand and others, 1982). Combining the seismic and aeromagnetic determinations we can say that the thickness of the Paleozoic rocks appears to be thinnest along the axis of the graben (1.7-2.0 km) relation to the flanks (3 km).

An additional observation of the refraction data on the flanks of the embayment is the shear wave velocity of the Paleozoic rocks (3.43 km/s), which indicates a normal Poisson's ratio of 0.25 (Andrews and others, 1984).

Upper Crustal Low Velocity Layer

The identification of a clear cut-off of the refracted arrival from the 5.95 km/s layer (Paleozoic rocks) was one of the most significant observations of the recent seismic refraction study. This observation, which is unambiguous (fig. 7 and 8), is due to the presence of a layer with



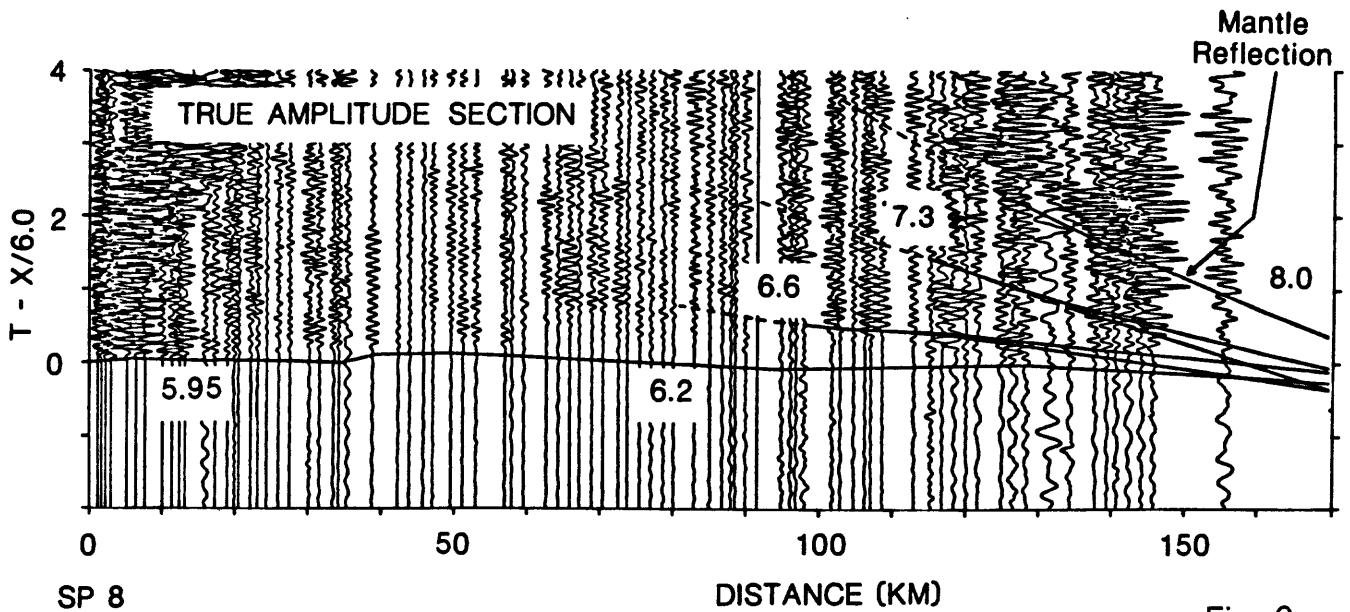


Fig. 6

Figure 6. Seismic record section for the profile 8-3. There are no sedimentary cover rocks, as is evidenced by the near-zero intercept time on the 5.95 km/s refraction. This refraction merges smoothly into the 6.2 km/s refraction, without a shadow zone (c.f., figure 7). Reflected phases from the 6.6 (lower crust) and 8.0 km/s layers (mantle) are clear; that from the 7.3 km/s layer is less clear.

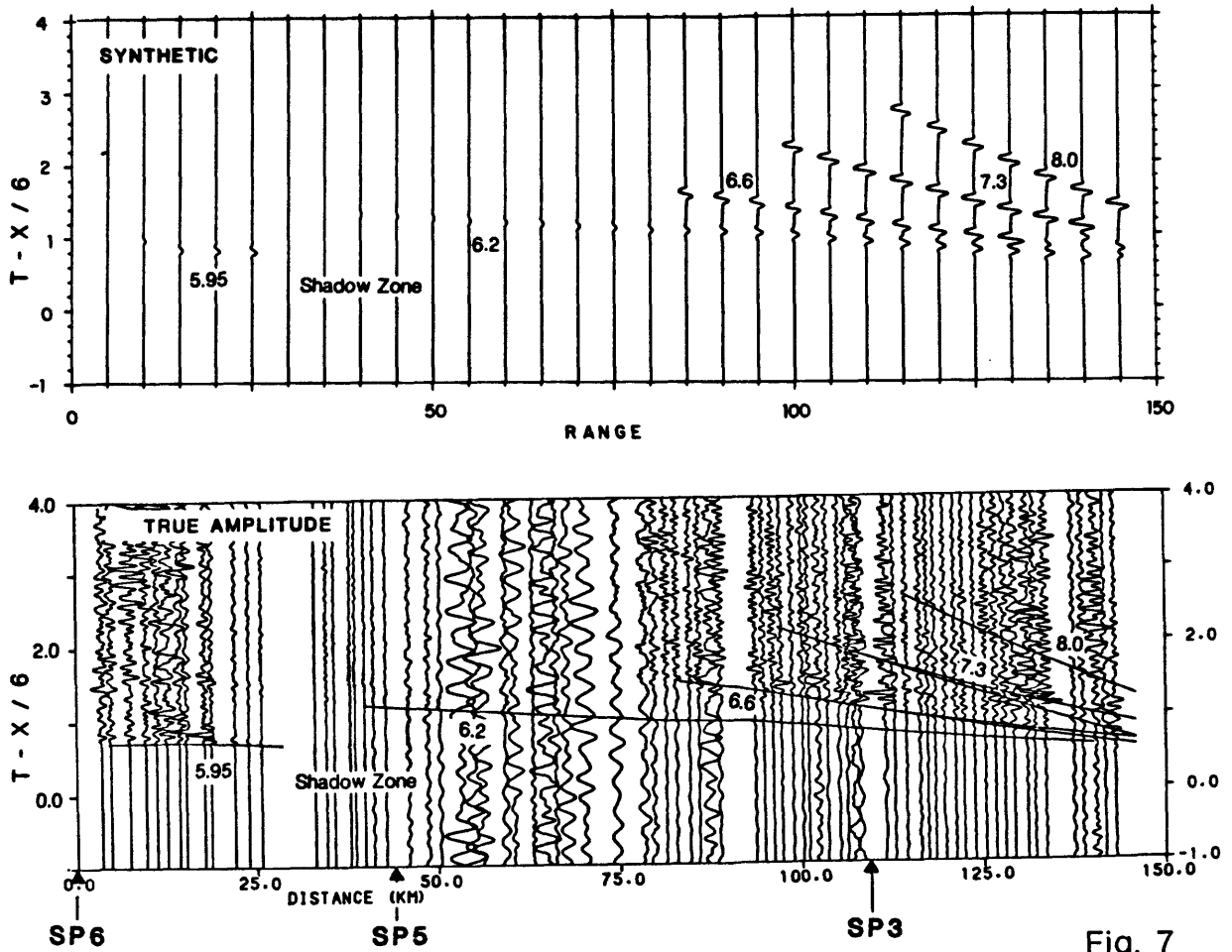


Figure 7. Synthetic and observed record sections for shot point 6 northeast. The presence of a low-velocity layer is clearly indicated by the cut-off of the 5.95 km/s refractor (labelled shadow zone) and the delay on the 6.2 km/s basement refractor. The reflection from the 6.6 km/s layer is clear, whereas the 7.3 and 8.0 km/s reflections are weak. The synthetic record section matches many of the traveltime and amplitude features of the observed section.

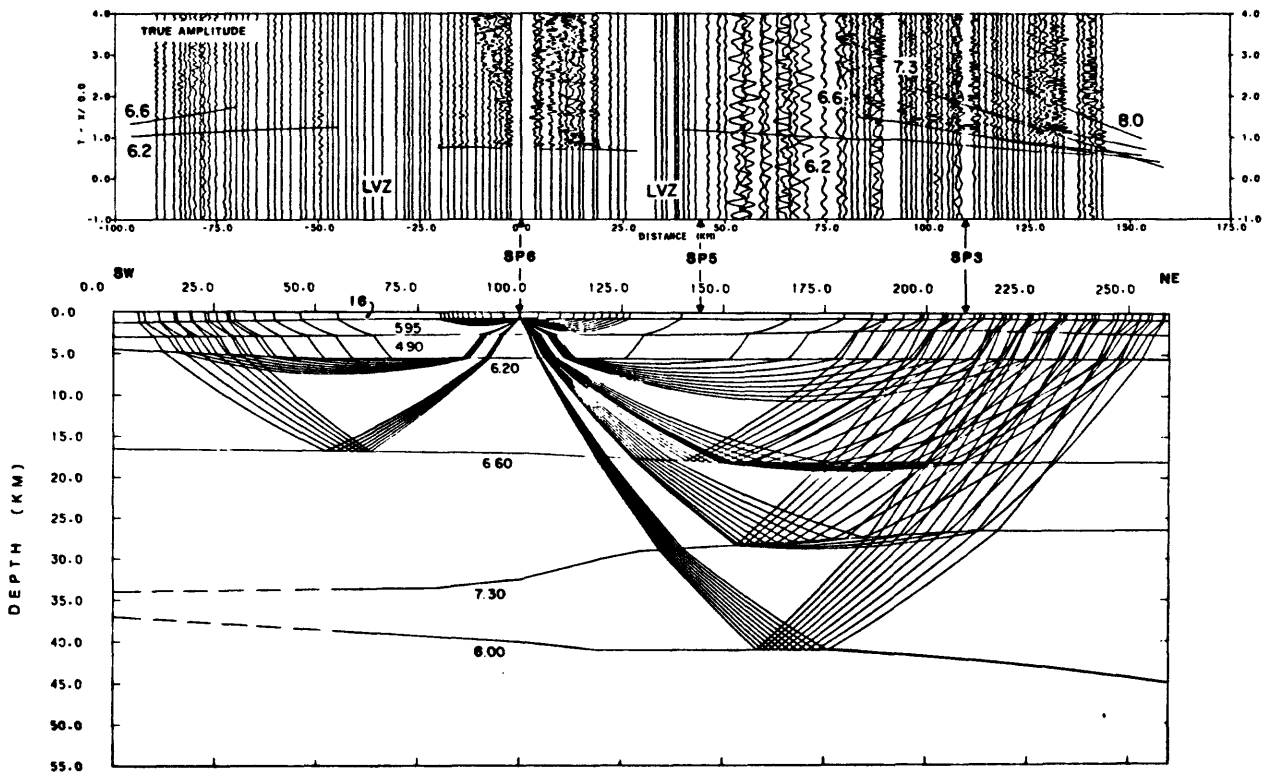


Figure 8. Seismic record section and ray diagram for shot point 6 of the axial profile. The data northeast of the shot point are reproduced at a larger scale in figure 9. The ray diagram for the traveltime curves that appear as solid lines superimposed on the record section. The bottoming points for the rays indicates the area of subsurface coverage.

substantially lower seismic velocity beneath the Paleozoic rocks. The sharpness of the energy cut-off is indicative of a large velocity decrease, and a velocity of 4.9 km/s was used on the basis of unpublished well log data. The depth of the low velocity zone is shallow, as is evidenced by the fact that the refracted arrivals are cut-off only 25 km or so from the shot point. Beyond 40 km the refracted arrivals from the underlying crystalline basement are observed with a delay of approximately 0.3 sec relative to an extrapolation of the 5.95 km/s arrival. The magnitude of this shadow zone (in distance and time) indicates that the low-velocity zone has a thickness of about 3 km. Within the resolution of the data, the zone appears to be relatively uniform in depth and thickness along the axis of the graben, while the west flank and cross profiles demonstrate that the zone is absent outside of the graben boundaries, as defined by gravity and aeromagnetic data (Hildenbrand and others, 1977; Kane and others, 1981; Hildenbrand and others, 1982). The precise lateral extent of the low velocity zone is difficult to determine from the recent seismic refraction data. For this reason, the evidence for the position of the graben boundaries, as defined by the aeromagnetic data, was used in constructing the seismic models of Ginzburg and others (1983) and Mooney and others (1983).

The lithology of the graben fill is probably known within the exploration industry on the basis of drill hole data. Lacking access to this data, we infer from the velocity (e.g., our estimate of 4.9 km/s) that it consists of clastic sedimentary rocks associated with the late Precambrian/early Paleozoic rifting of the embayment. This inference is in part based on the known

composition of the sedimentary rocks in the Rough Creek graben to the northeast (Schwalb, 1980).

An important unresolved question is the extent of the low velocity zone to the north and south of the area of the present seismic refraction coverage. In fact, since the zone shows up so clearly on the refraction data, there is an excellent opportunity to trace the embayment graben into southern Arkansas and to the northeast in Indiana and Kentucky where it may join other rifts (c.f., Braile and others, 1982).

Crystalline Basement

We refer to that layer with a velocity of 6.2 km/s as the upper crustal layer. Refractions from this layer are recorded with variable clarity in the recent refraction data. Along the axial profile, the delay due to the low velocity zone causes the 6.2 km/s refractor to be well separated in time from the 5.95 km/s refraction, making its identification easier [(e.g., profiles 3-5-6, 5-3, 5-6, and 3-8)]. For shot points outside the embayment graben, the low velocity zone is absent and the 5.95 km/s and 6.2 km/s refractors merge together. Examples of this are on profiles 8-3, 8-5-4, 2-5-9, 9-6-8, and 9-5-2 (e.g., fig. 6). We note that profiles with common shot points do not always have equally clear 6.2 km/s refractors. For example, the refractor is weak on profiles 8-2 and 8-6-9, but quite clear on profiles 8-3 and 8-5-4. Since this shot point was a water shot (in a flooded quarry), the differences are not due to coupling of energy at the shot point. A major factor is likely to be the heterogeneity of the crust along the profile. Features such as

shallow plutons might be expected to cause scattering of the seismic waves. Profile 8-6-9, for example, traverses the Jonesboro pluton (Hildenbrand and others, 1977).

The depth to the top of the crystalline upper crust varies systematically in the embayment. Within the graben, it lies at a depth of approximately 5 km, while outside the graben it is only 2-3 km deep. As noted above, the 6.2 km/s refractor is isolated in time and distance from the 5.95 km/s refractor on the profiles with shot points within the graben, making the depth calculation more reliable. Outside the graben, the 5.95 km/s and the 6.2 km/s refractors merge into one another, making it difficult to accurately determine depths. Despite these difficulties, the regional depths to the upper crust are in good agreement with the depths calculated from aeromagnetic data (Hildenbrand and others, 1982; their figure 5). However, the aeromagnetic data also resolves the flanks of the graben, whereas the seismic refraction data is too sparse to identify these. As previously stated, the locations of the graben flanks shown in the seismic cross sections, of Ginzburg and others (1983) and Mooney and others (1983), were taken from the aeromagnetic results.

We were unable to resolve any velocity variations in the upper crustal layer, despite the evidence in the aeromagnetic data of a change in the crustal composition from east to west across the embayment (Hildenbrand and others, 1982).

Lower crust

All deep crustal structure studies of the central U.S. show that the upper crust is underlain by a higher velocity lower crust. The boundary between the upper and lower crust has traditionally been referred to as the Conrad discontinuity, a term which is no longer widely used because the boundary is often more variable and difficult to detect than, for example, the ubiquitous M-discontinuity.

We have modeled the Conrad discontinuity in the Mississippi embayment mainly on the basis of wide-angle reflections. The reflections, which occur as secondary arrivals at distances greater than 50 km are more pronounced and therefore easier to identify than the corresponding, relatively weak refractions from the lower crust. Particularly clear reflections are recorded on the axial profile 6-5-3, the west flank profile 8-2 (fig. 9) and on the cross profiles (fig. 6). These data provide strong evidence that the lower crust has a velocity of 6.6 km/s and a depth which varies from 15 km along the western flank of the rift, to 17 km along the axis. We are less confident of the depths determined along profiles 2-3-4 and 8-6-9 (fig. 10 and 11) because the reflections observed on these profiles are generally weak and incoherent.

The quality of the reflected arrivals provides some information on the nature of the boundary between the upper and lower crust. The clear high-amplitude arrivals observed locally along the axial and western flank profiles indicate that in these areas the boundary is abrupt and well-defined. The weaker arrivals observed on profile 2-3-4 and 8-6-9 may be interpreted as evidence for a locally transitional boundary between the upper and lower crust.

MISSISSIPPI EMBAYMENT WEST FLANK PROFILE SP8 AND SP2

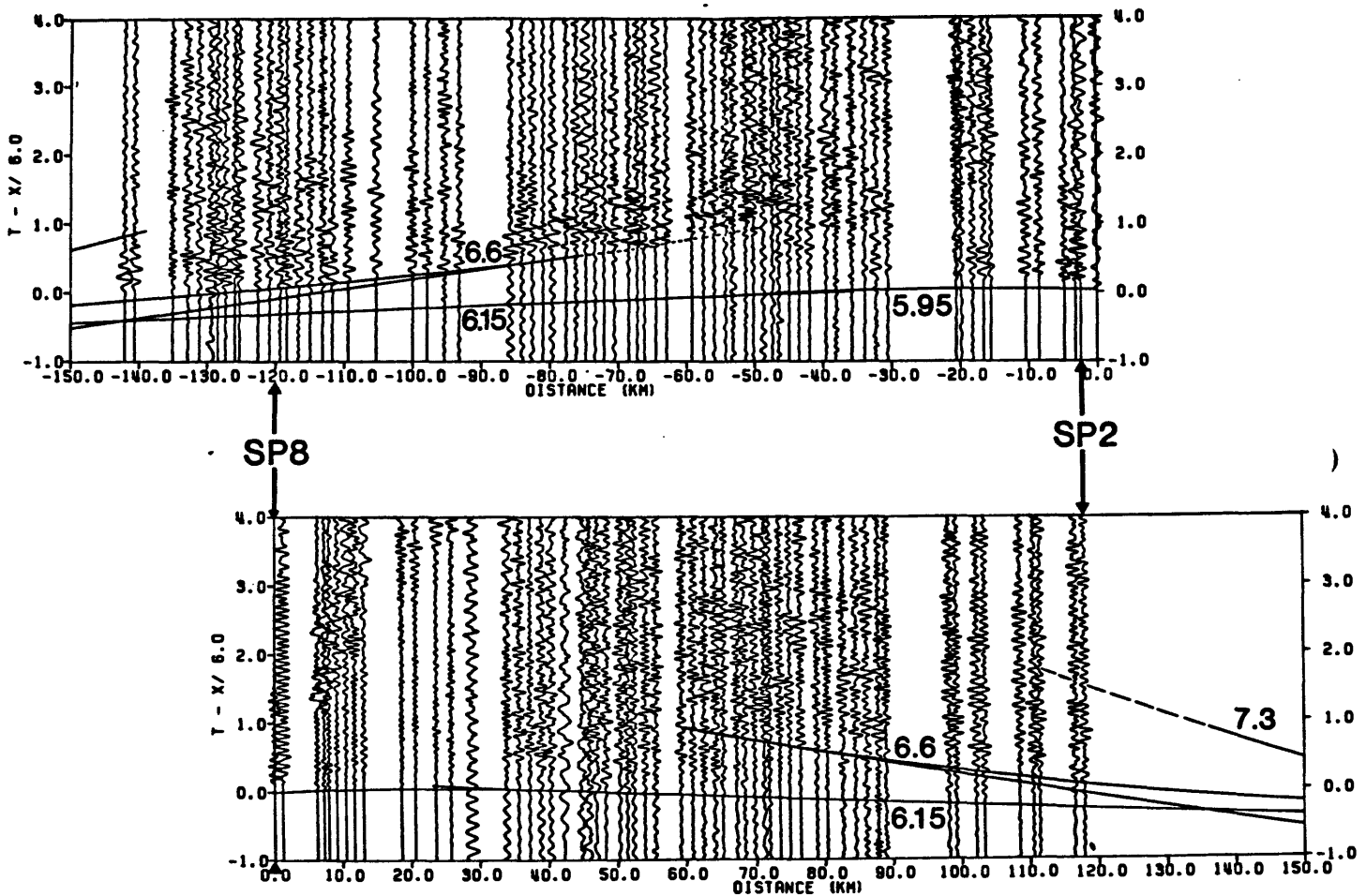


Figure 9. Reversed profile on the west flank of the embayment from shot point 8 to 2. The 5.95 and 6.15 km/s refractors merge smoothly together, indicating that the Paleozoic rocks directly overlie crystalline basement. The reflection from the lower crust (6.6 km/s) is very clear on the profile from shot point 2, but is significantly less clear on the reversing shot.

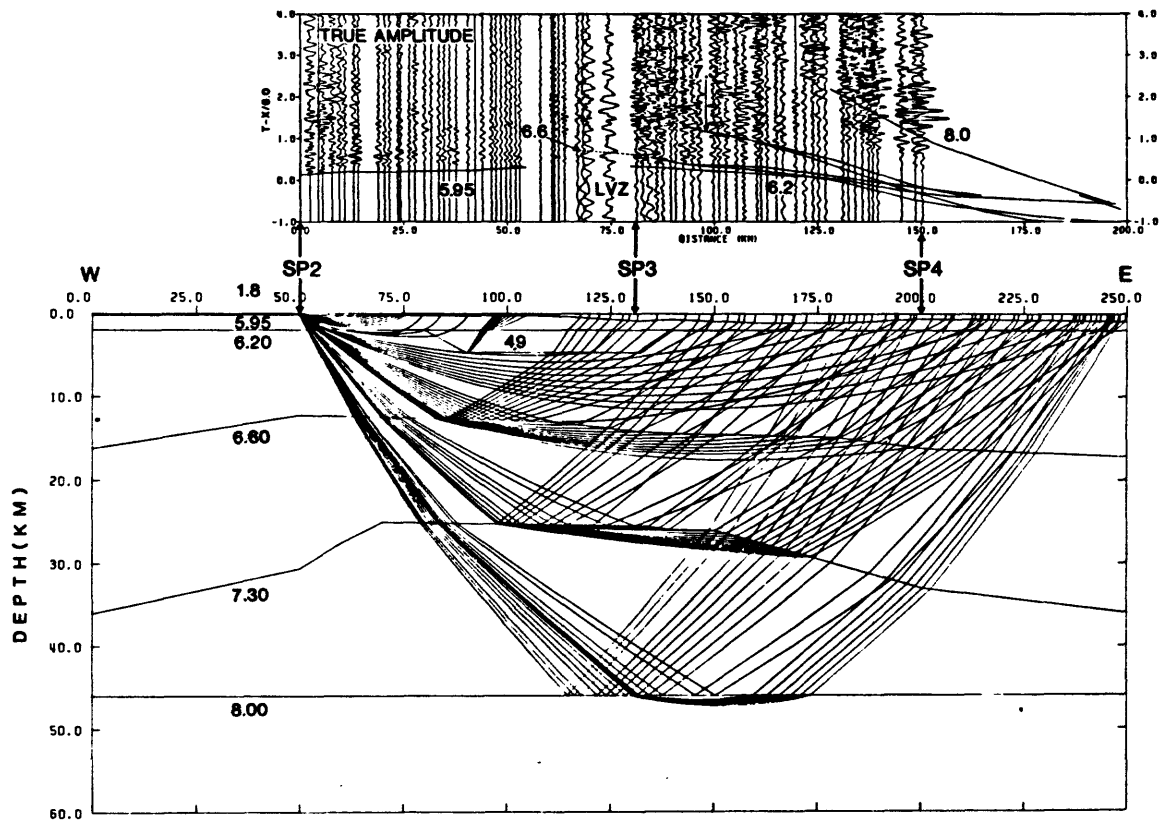


Figure 10. Record section and ray diagram for the profile 2-3-4 in the northern embayment. The basal crustal layer (7.3 km/s) is interpreted to be thickest, and the depth to mantle deepest at this latitude. Bottoming points on ray paths indicate areas of subsurface coverage.

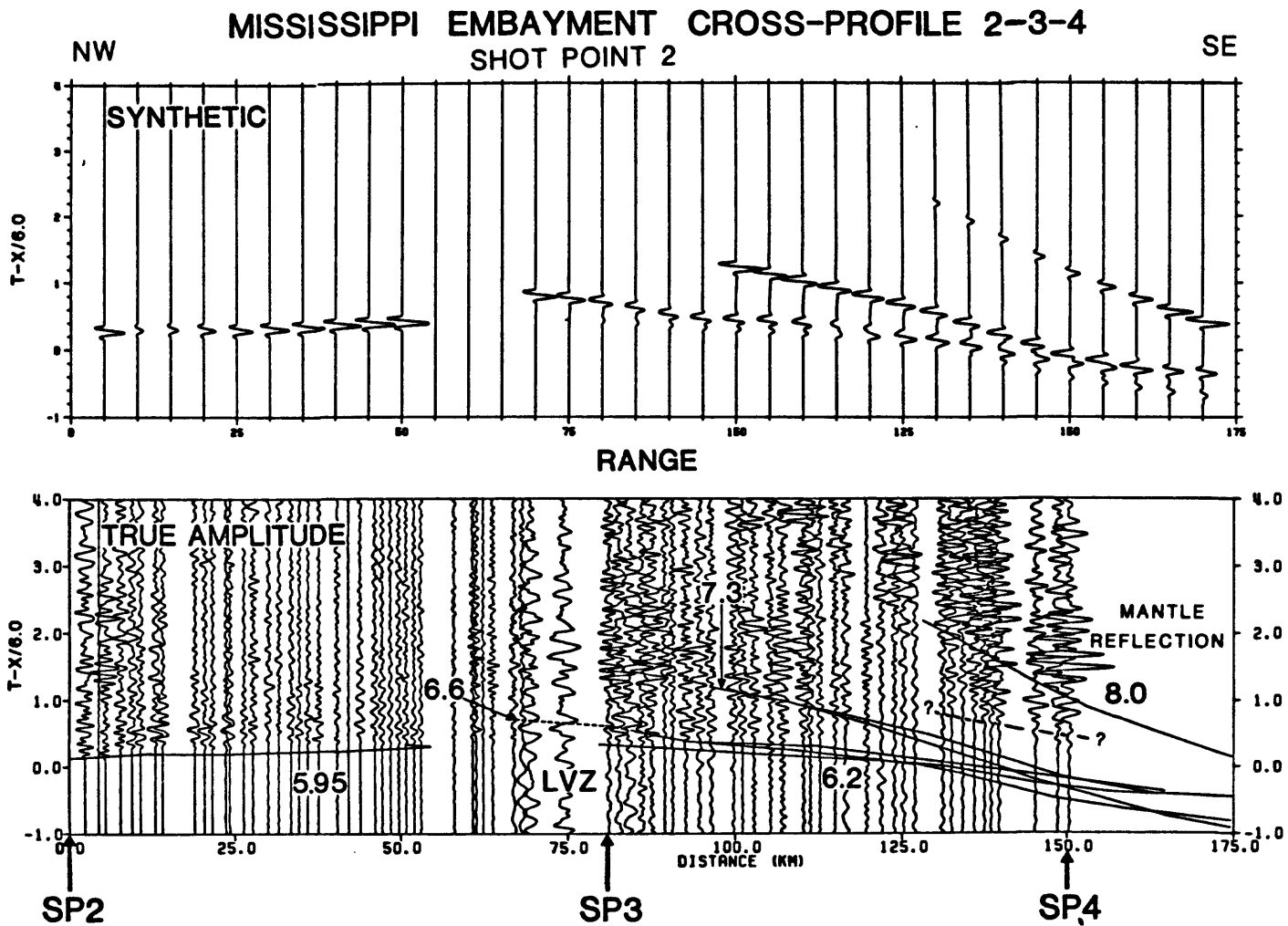


Figure 11. Synthetic and observed record section for profile 2-3-4. The mantle reflection is particularly clear on this profile.

Our models of the Conrad discontinuity on all of the profiles show that it is a planar boundary with a gentle eastward dip. The dip is not particularly well-constrained, and we have included it in the models only to satisfy the different depths inferred from the west flank and axial profiles. The overall consistency of apparent velocities and intercept times makes it quite clear, however, that the boundary is essentially planar. At first, this result is surprising in the light of the rift related structures observed in the adjacent layers, and in this regard the geometry of this layer is quite unlike that predicted by Ervin and McGinnis (1975) based on their modelling of gravity data. Perhaps the boundary did suffer some changes in the Precambrian and has since readjusted, as one might expect if the boundary were dominantly a metamorphic boundary rather than a compositional boundary.

McCamy and Meyer (1966) report a depth to the Conrad discontinuity of only 6-10 km on a profile 10 km east of our west flank line. In view of the reliable depth determination of 15 km from our profile 8-2 (fig. 9), we have re-examined their data and find that we can fit their traveltimes curves with an alternate model that is consistent with our profiles. Specifically, we have increased the velocity of the lower crustal refractor from 6.4 to 6.6 km/s. The resulting change in intercept time accounts for the increase in calculated depth to the lower crust to 16 km.

Basal crustal layer

As previously mentioned, a 7.3 km/s layer at the base of the crust on the west flank of the enbayment was first identified by McCamy and Meyer (1966),

and has since been confirmed by later seismic studies in the embayment. The recent seismic refraction data has provided additional information about the three-dimensional structure of this layer.

Based on the relatively clear arrivals observed on the axial profile and two of the cross profiles, we have modeled the top of this layer with significant relief. The northernmost cross profile, 2-3-4, indicates a depth of 26 km (fig. 10), whereas the southernmost cross profile, 8-6-9, indicates a depth of 30 km. The deepening to the southwest is confirmed by the traveltime delays and high apparent velocity of arrivals from this layer observed on the SP 6 southwest profile. While the precise amount of topography on the top of the basal crustal layer is beyond the resolution of the data, the evidence is rather clear for a southwest deepening from a relative high beneath SP 3 in the northernmost embayment.

The seismic refraction profiles do not provide sufficient coverage to determine the configuration of the 7.3 km/s layer in an east-west direction. The arrivals observed along the cross profiles bottom along the axis of the embayment, and we could not identify arrivals from this layer on the west flank profile. However, several lines of evidence suggest that it does deepen on the flanks of the embayment. McCamy and Meyer (1966) report a depth of 30 km on the west flank, Warren (1968) reports no 7.3 km/s layer in central Tennessee, and Schlittenhardt and Prodehl (1984) reinterpret Warren's data to show a 7.3 km/s layer at a depth of 40 km. All of these estimates are deeper than the reliable estimate of 26 km beneath SP 3. In addition, modelling of

gravity data reveals that, despite the thick accumulation of unconsolidated sedimentary rocks, a general gravity high is observed across the embayment. The lower Bouguer gravity on the flanks of the rift are attributed to the deepening of the 7.3 km/s layer.

The 7.3 km/s layer probably consists of a mixture of lower crustal and mafic intrusive rocks derived from the mantle. The velocity is too high for most high-grade metamorphic rocks, but agrees well with igneous rocks of a basaltic composition (Birch, 1961; Kirn and Richter, 1980).

Mantle

The most direct information on the velocity and depth of the uppermost mantle in the Mississippi embayment comes from the mantle refractions (Pn) recorded on the reversed long range refraction profile of McCamy and Meyer (1966). Their data indicates a mantle velocity of 8.0 ± 0.1 km/s and a total crustal thickness of 45 km. The recent refraction studies in the embayment were not designed to record to Pn range, so we cannot determine the mantle velocity. However, some of the profiles do include clear pre-critical and near-critical reflected phases (PmP) from the crust-mantle boundary which may be used to calculate total crustal thickness, assuming that the velocity structure of the crust has been correctly modeled. The clearest PmP phases were recorded on profiles 8-3 (fig. 6) and 2-3-4 (fig. 11). These are interpreted to indicate a crustal thickness of 45 km at the northern end of embayment. To the south, the PmP phase is less clear and we have interpreted

a crustal thickness of about 40 km from profile 8-6-9 (fig. 1). These results indicate that the depth to the mantle increases as the thickness of the 7.3 km/s layer increases, as is expected from isostasy (fig. 4). The depths are generally consistent with the results of McCamy and Meyer (1966) and are somewhat smaller than the "47 km minimum thickness" determined by Austin and Keller (1982) for a Rayleigh wave great circle path that passes through the northeastern portion of the embayment.

It is not clear why the PmP phase is clearly recorded on some profiles and is totally absent on others. The variability of the reflector may be attributed to one or more properties of the lower crust and upper mantle. First, the crust-mantle boundary may locally be transitional rather than abrupt. A gradual transition for the lower crust to the upper mantle is not unexpected in a region where mantle derived intrusions have altered the lower crust. Secondly, the presence of the thick 7.3 km/s layer reduces the velocity contrast at the crust-mantle boundary to 0.7 km/s, yielding lower amplitude reflected arrivals. If anisotropy is present in the mantle, this velocity contrast could be even lower along certain azimuths. Another possibility is that there is relief on the crust-mantle boundary and the resultant dips causes the reflected phases to return to the surface off the end of the recording array for some profiles (i.e., as would occur when shooting down-dip on a boundary).

A topic of much interest is the geometry of the crust-mantle boundary in an east-west direction across the embayment. One concept (e.g., as indicated in the gravity model of Ervin and McGinnis, 1975) is that the crust thickens

beneath the embayment due to the presence of the "fossil rift cushion". A thickening of the crust is also supported by the surface wave results of Austin and Keller (1982) who find that their data could support a crustal thickness of as much as 55 km in the northern embayment.

Contradicting this viewpoint is a gravity model (Mooney and others, 1983) which fits the recent seismic data and which does not show a thickening of the crust beneath the embayment. In this model the regional gravity high over the embayment was matched by the relief on the top of the 7.3 km/s layer. We have already emphasized that the relief on the 7.3 km/s layer is poorly constrained on the flanks of the embayment, however, the possible relief is sufficient to account for the observed gravity anomalies. While it appears that there is little or no crustal thickening between the west flank line of McCamy and Meyer and the seismic control in the north-central embayment (i.e. profile 2-3-4), additional seismic control is needed to settle the question of the relief on the crust-mantle boundary.

DISCUSSION

The prevailing tectonic model for the evolution of the Mississippi embayment has changed little in the past decade from the rift hypothesis of Ervin and McGinnis (1975). The recent geophysical investigations have supported and added details to this model, such as the identification of the basement graben using aeromagnetic data (Hildenbrand and others, 1977; 1982). The recent seismic refraction data has confirmed the presence of the graben,

and has provided three-dimensional control on the basal crustal layer. The apparent thickening of the basal layer in the northernmost embayment could be evidence of a Precambrian mantle plume in that area, and the embayment may be viewed as an arm of a triple junction, the other arms extending into Kentucky and Illinois. It should be possible to test this hypothesis by tracing the upper crustal low-velocity layer to the north using seismic refraction and aeromagnetic data, assuming that the other arms of the triple junction have basement grabens above them.

The thickening of the basal crustal layer in the northernmost embayment corresponds to the area of greatest seismic activity. Andrews and others (1984) have recently relocated earthquakes in the embayment using the new crustal velocity models and a knowledge of S-to-P converted phases derived from three-component data. The seismicity is concentrated above 14 km depth, placing most events in the upper crustal layer. It therefore appears that faulting and weakening of the upper crust has been most pronounced in the area above the largest amount of lower crustal alteration. Interestingly, there are very few earthquakes below the Conrad discontinuity. This may be indicative of rocks with different rheological properties below that boundary.

The overall program of study of the Mississippi embayment has been an interdisciplinary one. Seismic refraction measurements have provided the general framework of the crustal structure within which these other studies may be placed. Continued broadly based studies are the most likely to yield new insights into the embayment.



REFERENCES

- Andrews, M. C., Mooney, W. D., and Meyer, R. P., 1984, The relocation of microearthquakes in the northern Mississippi Embayment, J.G.R., in press.
- Anson, J., Prodehl, C., and Banford, D., 1982, Comparative interpretation of seismic refraction data, *Journal of Geophysics*, 51, p. 69-84.
- Austin, C. B. and Keller, G. R., 1982, A crustal structure study of the northern Mississippi Embayment, U.S. Geol. Surv., Prof. Pap., 1236, in press.
- Birch, F., 1961, The velocity of compressional waves in rocks to 10 kilobars, *J. Geophys. Res.*, 66: 2199-2224.
- Braile, L. W., Keller, G. R., Hinze, W. J., and Lidiak, E. G., 1982, An ancient rift complex and its relation to contemporary seismicity in the New Madrid Seismic Zone, *Tectonics*, 1(2): 225-237.
- Ervin, C. P. and McGinnis, L. D., 1975, Reelfoot rift: reactivated precursor to the Mississippi Embayment, *Geol. Soc. Am. Bull.*, 896: 1287-1295.
- Ginzburg, A., Mooney, W. D., Walter, A. D., Lutter, W. J. and Healy, J. H., 1983, Deep Structure of the Northern Mississippi Embayment, *Am. Assoc. Pet. Geol.*, 67, pp. 2031-2046.
- Grohskopf, J. G., 1955, Subsurface geology of the Mississippi Embayment of southeast Missouri: Missouri Geological Survey and Water Resources, v. 37, series , 133p.
- Hamilton, R. M. and Zoback, M. D., 1982, Tectonic features of the New Madrid seismic zone from seismic reflection profiles, U.S. Geol. Survey Prof. Paper 1236, p. 55-82.
- Hildenbrand, T. G., Kane, M. F. and Stauder, S. J., 1977, Magnetic and gravity anomalies in the northern Mississippi Embayment and their spatial relation to seismicity, U. S. Geol. Surv., Misc. Field Stud. Map MF-914.
- Hildenbrand, T. G., Kane, M. F., and Hendricks, J. D., 1982, Magnetic basement in the upper Mississippi embayment - A preliminary report, U.S. Geol. Survey Prof. Paper 1236, p. 39-53.
- Kane, M. F., Hildenbrand, T. G. and Hendricks, J. D., 1981, A model for the tectonic evolution of the Mississippi Embayment and its contemporary seismicity, *Geology*, 9: 563-567.
- Keller, G. R., Braile, L. W. and Schlue, J. W., 1979, Regional crustal structure of the Rio Grande Rift from surface wave dispersion measurements, In: R. E. Riecker (Editor), *Rio Grande Rift: Tectonics and Magmatism*, American Geophysical Union, Washington, D.C., pp. 115-126.

- Kirn, H., and Richter, A., 1981, Temperature derivatives of compressional and shear wave velocities in crustal and mantle rocks at 6 kbar confining pressure, *J. Geophys.* 49, 47-56.
- McCamy, K. and Meyer, R. P., 1966, Crustal results of fixed multiple shots in the Mississippi Embayment, In: J. S. Steinhart and T. J. Smith (Editors), *The Earth Beneath the Continents*, Geophys. Monogr., Am. Geophys. Union, 10: 370-381.
- McKeown, F. A., 1978, Hypothesis: many earthquakes in the central and southeastern United States are casually related to mafic intrusive bodies, *J. Res., U.S. Geol. Survey*, 6(1): 41-50.
- McMechan, G. A. and Mooney, W. D., 1980, Asymptotic ray theory and synthetic seismograms for laterally varying structures: theory and application to the Imperial Valley, California, *Seismol. Soc. Am. Bull.*, 70: 2021-2035.
- Mitchell, B. J. and Hashim, B. M., 1977, Seismic velocity determination in the New Madrid Seismic Zone: a new method using local earthquakes, *Seismol. Soc. Am. Bull.*, 67: 413-424.
- Mooney, W. D., Andrews, M. C., Ginzburg, A., Peters, D. A., and Hamilton, R. M., 1983, Crustal structure of the northern Mississippi embayment and a comparison with other continental rift zones, *Tectonophysics*, 94, 327-348.
- Mooney, W. D. and Prodehl, C., Proceedings of the Workshop on seismic refraction interpretation of the USGS/DGMR Saudi Arabia profile, U.S.G.S. Circular (in press, 1984).
- Schlittenhardt, J. and Prodehl, C., Crustal structure of the Appalachian Highlands in Tennessee from stacked seismic data, *Bull. Seis. Soc. Am.*, in press, 1984.
- Schwalb, H. R., 1980, Paleozoic geology of the New Madrid area, Nuclear Reg. Comm. Rep. CR 2129, Washington, D.C., pp. 183-200.
- Stauder, W., Kramer, M., Fischer, G., Schaefer, S. and Morrissey, S. T., 1976, Seismic characteristics of southeast Missouri as indicated by a regional telemetered microearthquake array, *Seismol. Soc. Am. Bull.*, 66: 1953-1964.
- Stewart, S. W., 1968, Crustal structure in Missouri by seismic refraction methods, *Seismol. Soc. Am. Bull.*, 58: 291-323.
- Zoback, M. D., Hamilton, R. M., Crone, A. J., Russ, D. P., McKeown, F. A. and Brockman, S. R., 1980. Recurrent intraplate tectonism in the New Madrid seismic zone, *Science*, 209: 971-976.

**RIFT STRUCTURE OF THE NORTHERN MISSISSIPPI
EMBAYMENT FROM THE ANALYSIS OF GRAVITY AND MAGNETIC DATA**

by

**Thomas G. Hildenbrand
U.S. Geological Survey
Denver, Colorado 80225**

ABSTRACT

Gravity and magnetic data have been simultaneously inverted to derive a crustal model of the northern Mississippi Embayment which is compatible with geologic and seismic refraction data. The results indicate that this region is a site of an ancient rift system. An anomalous crustal layer is present at the base of the crust and thickens beneath a broad northeast-trending graben that developed on the Precambrian surface. The thickest part of anomalous crust occurs beneath the region of greatest seismic activity, which lies within the geographic limits of the graben. This strong correlation suggests that strain accumulates within the anomalous crust layer, which acts as an inhomogeneity in a relatively homogeneous lithosphere.

Anomalous crust also thickens under the northwest margin of the graben and may explain why more plutons were emplaced there than along the southeast margin. The boundary between upper and lower crust is relatively flat. Because there is evidence that the crust isostatically sagged into the mantle, the once dipping mid-crustal boundary may have become planar due to subsequent metamorphism and pressure changes with depth.

The upper Mississippi Embayment region experienced many periods of extension, manifested by graben faulting and by igneous dike intrusion

throughout the crust. Based on the consideration of anomalous volumes inferred from the derived crustal model, total extension associated with and subsequent to the development of the rift is about 22 km.

Based on the results of this study and previous geophysical studies, the complex tectonic evolution of the upper Mississippi Embayment since Late Precambrian is: rift formation along a pre-existing shear zone, graben development in Cambrian time, reactivations in Permian and Cretaceous time, and subsequent development of the present Mississippi Embayment and fault zones with large influences from rift structures.

INTRODUCTION

Gravity and magnetic studies have provided significant information on structures of the northern Mississippi Embayment. Major features identifiable on gravity anomaly maps include a graben (filled with low-density clastics), dense igneous intrusions, and anomalous high-density lower crust. The magnetic method has been particularly useful in Mississippi Embayment studies because it permits the mapping of crystalline basement beneath nonmagnetic sedimentary rocks. One of the most important contributions from the interpretation of magnetic and gravity data has been the delineation of an ancient rift system that seems to be intimately related to the cause of present-day earthquakes.

Although rifting in the area was suggested by Hely (1967) based on discussions with H. R. Joesting (U. S. Geological Survey), Burke and Dewey (1973) suggested a Mesozoic failed arm rift origin for the Mississippi Embayment. Ervin and McGinnis (1975) synthesized gravity with seismic, stratigraphic and petrologic data and suggested that the rift, which they called the Reelfoot rift, developed in Late Precambrian or Early Paleozoic and was reactivated in Cretaceous time. Of major importance were gravity

interpretations (Ervin and McGinnis, 1975; Cordell, 1977) indicating a "fossil rift cushion" at the base of the crust. The presence of an anomalously-dense, lower-crustal layer is compatible with later interpretations based on the correlation of seismic refraction and gravity data by Mooney and others (1982) and on the analysis of Rayleigh wave dispersion data by Austin and Keller (1982).

In 1974, detailed aeromagnetic and gravity surveys were initiated by the U.S. Geological Survey to delineate structures that may be responsible for the generation or control of seismic energy. The resulting data (Hildenbrand and others, 1977, 1980; Kane and others, 1979) revealed a northeast-trending 70-km-wide graben in the Precambrian surface which a structural relief of about 2 km (Figure 2). The very straight boundaries and intervening magnetically quiet area, implying abruptly greater depth to magnetic basement, provided an empirical demonstration of a graben beneath the embayment and provided the impetus for intensive study during the last several years. The graben, renamed the Mississippi Valley graben by Kane and others (1979), probably developed in association with rifting in late Precambrian or Cambrian. Dense and highly magnetic plutons (Jespersen, 1964; Phelan, 1969; Ervin and McGinnis, 1975; and Hildenbrand and others, 1977) intruded both rift-border and rift-axial faults. However, this magmatism occurred hundreds of millions years after formation of the structural graben (Ervin and McGinnis, 1975; Hildenbrand, 1978). Today the graben contains the area of principal seismic activity, and a linear zone of seismicity (Figure 1) coincides with the axis of the graben (Hildenbrand and others, 1977, 1982).

Clearer definition of upper Mississippi Embayment structures have evolved from recent analyses of gravity and magnetic data. Models derived from the interpretation of truck-borne magnetometer data suggest that the margin of the

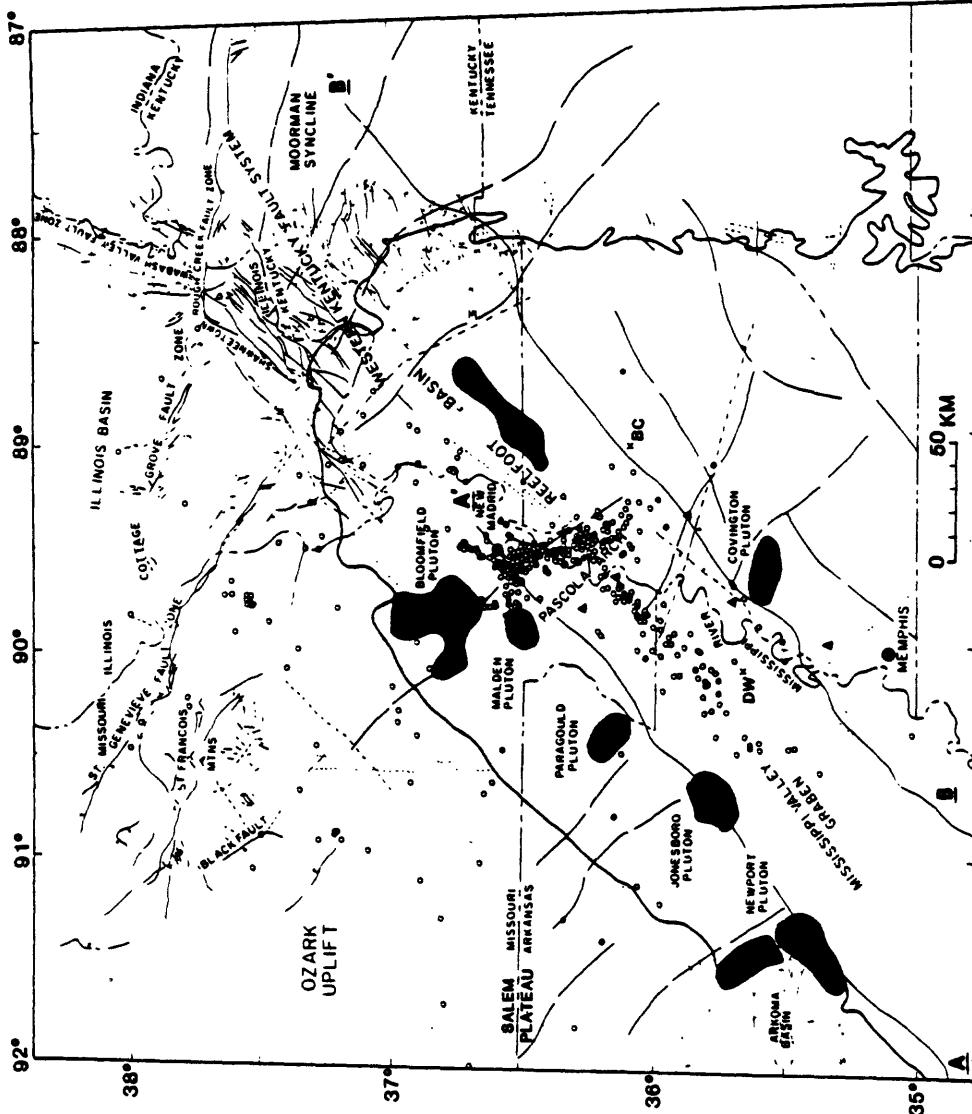


Figure 1.--Reference map modified from the "Tectonic Map of the United States" (Cohes and others, 1962) and the seismotectonic map of the Mississippi Valley (Heyl and McKeown, 1978), with epicenters of earthquakes detected by the southeast Missouri regional seismic network from July 1974 to June 1977 (W. Stauder, R. Herrmann, R. Perry, S. Singh, M. Woods, and S. Morrissey, written commun., 1974-1977) and major structures indicated in the magnetic field added. (After Hildenbrand and others, 1982).

EXPLANATION

Northern limit of coastal-plain material of the Mississippi Embayment

Mafic or ultramafic intrusion within the Mississippi Embayment - Identified in a drill-hole core

Mafic or ultramafic intrusion within the Mississippi Embayment interpreted from the magnetic field - Approximate boundary of intrusion determined from zero contour of associated anomaly on the second vertical derivative magnetic map

Principal magnetic lineaments reflecting faulting and lithologic contrasts in magnetic basement

Fault - Bar and ball on downthrown side. Dashed where inferred

Possible or hypothetical fault - Based upon subsurface data or exceptionally strong lineaments from aerial photos

Approximate margins of the Mississippi Valley Graben - Shown by sections A-A' and B-B'

Earthquake epicenter

xBC or DW Location of the Big Chief Drill Company Well, Gibson County, Tennessee, and the Dow Chemical Lee Wilson and Company No. 1, Mississippi County, Arkansas, respectively.

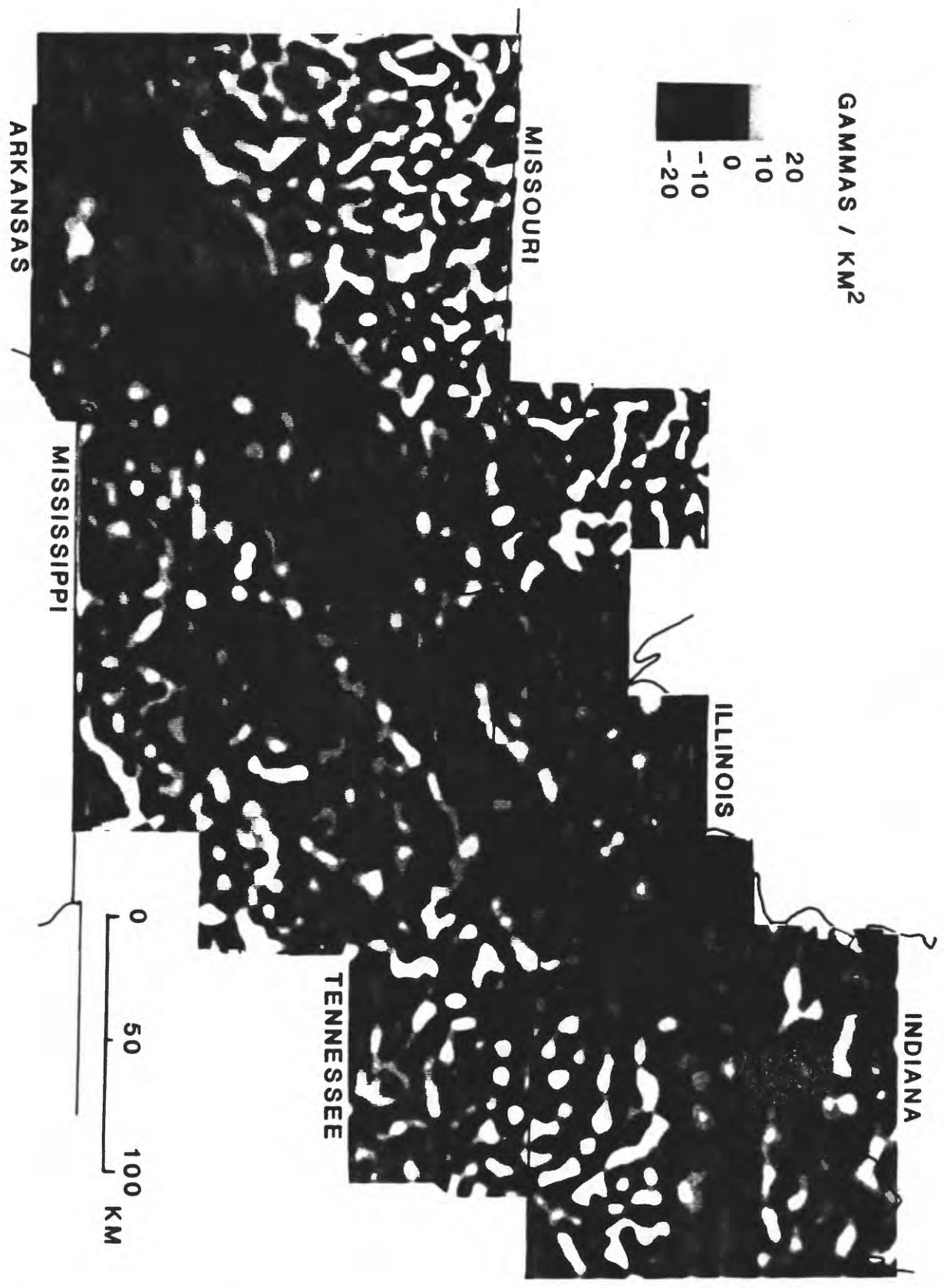


Figure 2.--Gray-shaded map of the second vertical derivative of the residual total magnetic field reduced to the North Pole.

.10/1.60

graben near Memphis, Tennessee, is characterized by a 5.5-km-wide fault zone in which magnetic basement has an average dip of 20° (we suppose the dip of individual faults is steeper) into the graben (Hildenbrand, 1982). Kane and others (1981) suggested that structures in the upper Mississippi Embayment developed from a rotating horizontal stress field on a crustal flaw of Precambrian age. Braile and others (1982 a,b) indicated that the Reelfoot rift at its northern terminus branches into three distinct arms. A general study of magnetic features and their relation to the development of the upper Mississippi Embayment was given by Hildenbrand and others (1982). In this study, the rift is thought to have developed along a structure that separates contrasting magnetic terranes.

These gravity and magnetic studies resolved many questions concerning the tectonic development of the northern Mississippi Embayment but have raised other questions. For example, was there uplift during the initial phases of rifting? Why was more igneous material emplaced along the northwestern margin of the graben? Why are the graben's margins exceptionally linear? How much extension has occurred in the upper Mississippi Embayment? Why is this region the site of a continental rift and has this rift any direct relation to the development of the Mississippi Embayment? What is the relation of rift structures to present-day seismicity? This study addresses these questions and others.

The principal means of investigation involves simultaneous inversion of gravity and magnetic data to derive a crustal model of the northern Mississippi Embayment. Upper parts of the model are constrained by geologic and magnetic data. Seismic refraction and gravity data (Mooney and others, 1983) constrain interpretation in parts of the middle and lower crust. The resulting crustal model is thus compatible with gravity, magnetic, seismic

refraction, and geologic data. Cross section's, each about 500 km long, were determined for 4 profiles: 3 normal to the graben and 1 along the graben's axis.

GEOLOGIC HISTORY

Because of the thick sedimentary strata in the northern Mississippi Embayment, structure and geology of Precambrian basement are inferred from the effects of Precambrian structures on younger rocks, from drill records, and from geophysical surveys. In general, the Precambrian surface rises and outcrops on the west in the San Francois Mountains toward the crest of the Ozark Uplift and descends deeply to the north and south beneath the Illinois Basin and Mississippi Embayment, respectively. Unmetamorphosed volcanic and related epizonal intrusive rocks about 1,500 m.y. old (Bickford and others, 1981; Kisvarsanyi, 1981) make up the majority of the St. Francois region.

Rifting occurred during Late Precambrian or Early Paleozoic time (Ervin and McGinnis, 1975). The area of the present Mississippi Embayment subsided in early Paleozoic time, a post-rifting event, and the Reelfoot basin (Schwalb, 1978) was formed in western Kentucky and southeastern Missouri. Clastics followed by carbonates were deposited in Cambrian time. From then until Middle Pennsylvanian time, regional deposition and subsidence continued intermittently throughout the northern Mississippi Embayment region (Glick, 1975, 1982). Late Paleozoic and Mesozoic uplift resulted in the formation and later erosion of the NW-SE trending Pascola arch (Figure 1). The rise of the arch created the southern margin of the Illinois Basin and effectively connected the Ozark Uplift and Nashville Dome in south-central Tennessee. Subsidence and accompanying deposition of predominantly marine clastic rocks, attaining a thickness of 1 km west of Memphis, Tennessee, started in late Cretaceous and formed the present Mississippi Embayment (Stearns and Marcher, 1962).

Phanerozoic dikes, diatremes, and plugs intrude Precambrian basement and younger formations possibly along numerous faults within the Mississippi Embayment and surrounding regions. For instance, fracturing associated with the Ste. Genevieve fault (Figure 1) may have accommodated emplacement of intrusions in Early to Middle Devonian time (Zartman and others, 1967). In the Illinois-Kentucky fluorspar district near lat $37^{\circ}30'$ N. and long $88^{\circ}15'$ W., kimberlite dikes and diatremes intruded during Late Pennsylvanian and Permian time are restricted to northwest-trending fractures (Watson, 1967). Lamprophyric dikes have been encountered in drill holes (Figure 1) in rocks of Cambrian and Ordovician age on the Pascola arch (Kidwell, 1951; Grohskopf, 1955), a structure of major folding and faulting. Late Cretaceous lamprophyres, syenites, and nepheline syenites (Moody, 1949; Kidwell, 1951) have been detected in wells in southwest Tennessee. Bond and others (1971) suggested that these intrusions were emplaced along faults over a large area paralleling the Mississippi River in southwest Tennessee. In central Arkansas, the Magnet Cove ring-dike complex (Erickson and Blade, 1963) and the syenite bodies near Little Rock (Gordon and others, 1958) may be aligned along a zone of weakness associated with the Ouachita orogeny.

MAGNETIC AND GRAVITY FEATURES

Figure 3 is an aeromagnetic anomaly map of the northern Mississippi Embayment and surrounding region. The northeast-trending zone of subdued magnetic expression has been interpreted by Hildenbrand and others (1977) and Kane and others (1979) as an expression of a graben that developed in association with rifting in late Precambrian or early Paleozoic time. A distinction between the Mississippi Valley graben and the Reelfoot rift needs to be made. The rift is defined here as a large tectonic system with many related structures, many extensional, at depth as well as in the near-surface

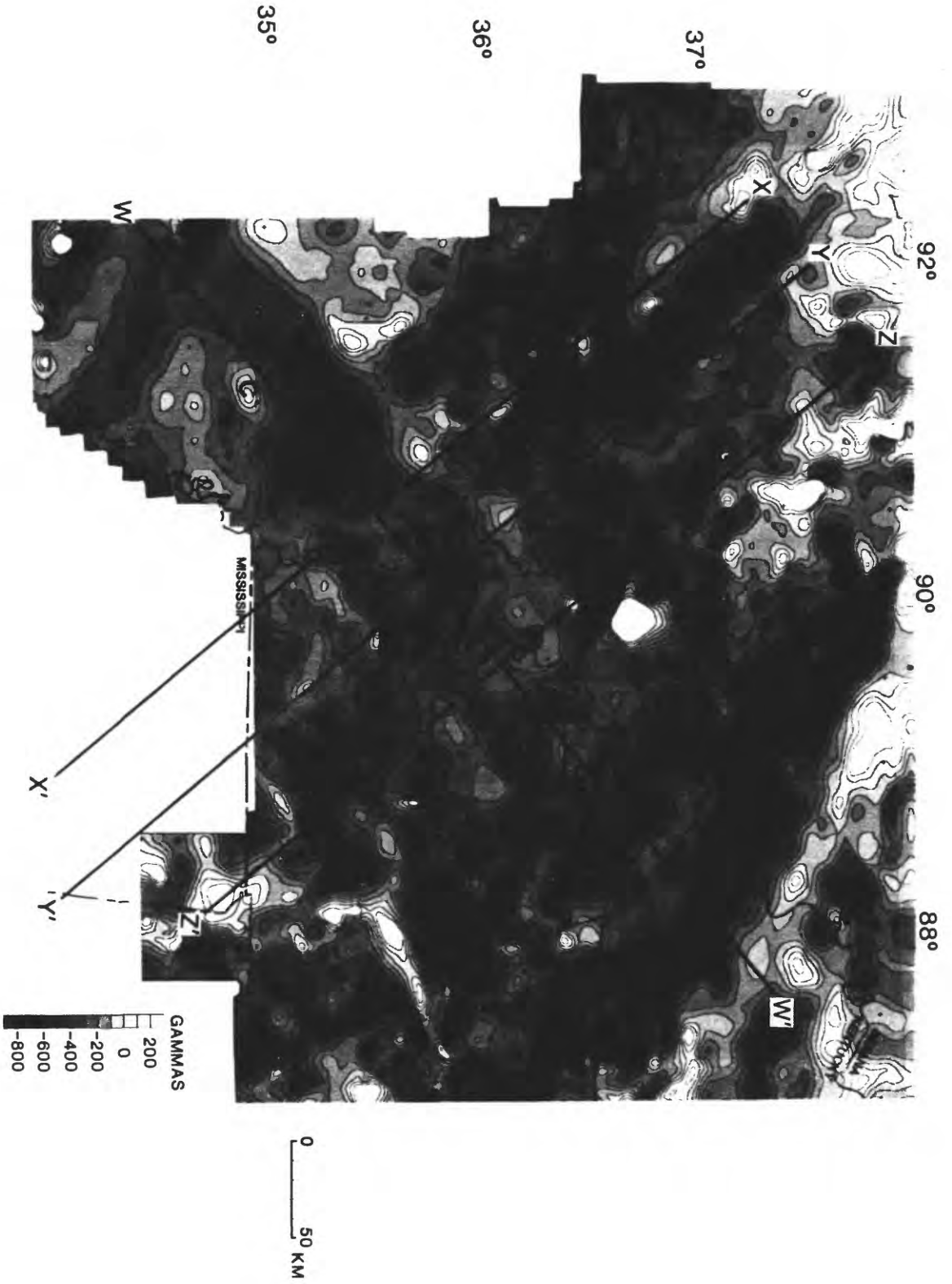


Figure 3.--Gray-shaded residual aeromagnetic map. Upper case letters (A, B, C, and D) denote locations of magnetic anomalies associated with igneous bodies within the graben. Profiles X-X', Y-Y', Z-Z', and W-W' are shown in Figure 5.

and having horizontal dimensions of several 100's of kilometers in all directions (see also Cordell, 1979). The graben is a near-surface manifestation of the rift and is a 70-km wide feature with secondary faulting along its axis. A depth-to-magnetic-basement map (Hildenbrand and others, 1979) depicts the pronounced depression (about 2 km) of basement within the graben.

The margins of the graben are characterized by a series of magnetic highs, caused by shallow mafic or ultramafic igneous bodies. The prominent long-wavelength anomalies probably reflect large plutonic masses (Figure 1) while the shorter-wavelength, lower-intensity intervening magnetic highs may delineate plugs, dikes and sills. Drill-hole information (Caplan, 1954; Glick, 1982) and magnetic interpretations (Hildenbrand, 1978; Hildenbrand and others, 1982) suggest that the large plutons were emplaced along the graben's border faults subsequent to Early Mesozoic time, probably during Late Cretaceous. This igneous period represented reactivation of the rift, in the sense that the graben's border faults provided channelways for the magma.

Sparse distribution of similar mafic bodies within the graben may account for part of the observed contrast in magnetic signatures (Figures 2 and 3). Four isolated regions in the graben, however, may be intruded by mafic intrusions (Hildenbrand and others, 1982). Two of these are represented as large circular magnetic anomalies (A and B, Figure 3). Drill-holes within the areal extent of anomaly A have encountered mica peridotite sills dated at 267 m.y. (Permian) by the K-Ar method (Zartman, 1977). Inferred mafic intrusions represented by magnetic highs C and D on Figure 3 were emplaced near the center of the graben floor, suggesting that faults along the graben's axis provided channelways for ascending magma. The sparsity of igneous bodies lying within the graben and the lack of evidence for major volcanism in the

embayment indicate that the raising mantle and associated partial melting of the crust did not provide a source of plutonism or volcanism within the shallow regions of the crust during the initial phases of rifting (Hildenbrand and others, 1982).

On the basis of magnetic trends (Figures 1-3) and drill-hole information, Hildenbrand and others (1982) proposed that magnetic basements flanking the graben are different in lithology and age from one another. The graben, therefore, may have developed along (or subsequently become) a boundary separating different basement rock types.

Figure 4 is a complete Bouguer gravity anomaly map of the northern Mississippi Embayment and surrounding region. A zone of low-amplitude gravity anomalies, reflecting low-density graben fill, coincides with the northeast-trending zone of subdued magnetic expression. Many of the igneous intrusions along the graben's axial and border faults are expressed as prominent gravity highs.

CRUSTAL MODELING

Gravity and magnetic anomaly data along 4 individual profiles shown in Figures 3 and 4 were simultaneously inverted to derive crustal models of the northern Mississippi Embayment. The 2 1/2-dimensional modeling program by M. W. Webring (U.S. Geological Survey, written commun., 1984) is based on generalized inverse theory. The program requires an initial guess for the model parameters (depth, shape, density, and susceptibility of sources) and then varies selected parameters in an attempt to reduce the weighted root-mean-square error between the observed and calculated gravity and magnetic fields. Induced magnetization was assumed (inclination = 67°N and declination = 5°W). Where the axial profile W-W' intersects the profiles oriented normal to the graben, the results are compatible.

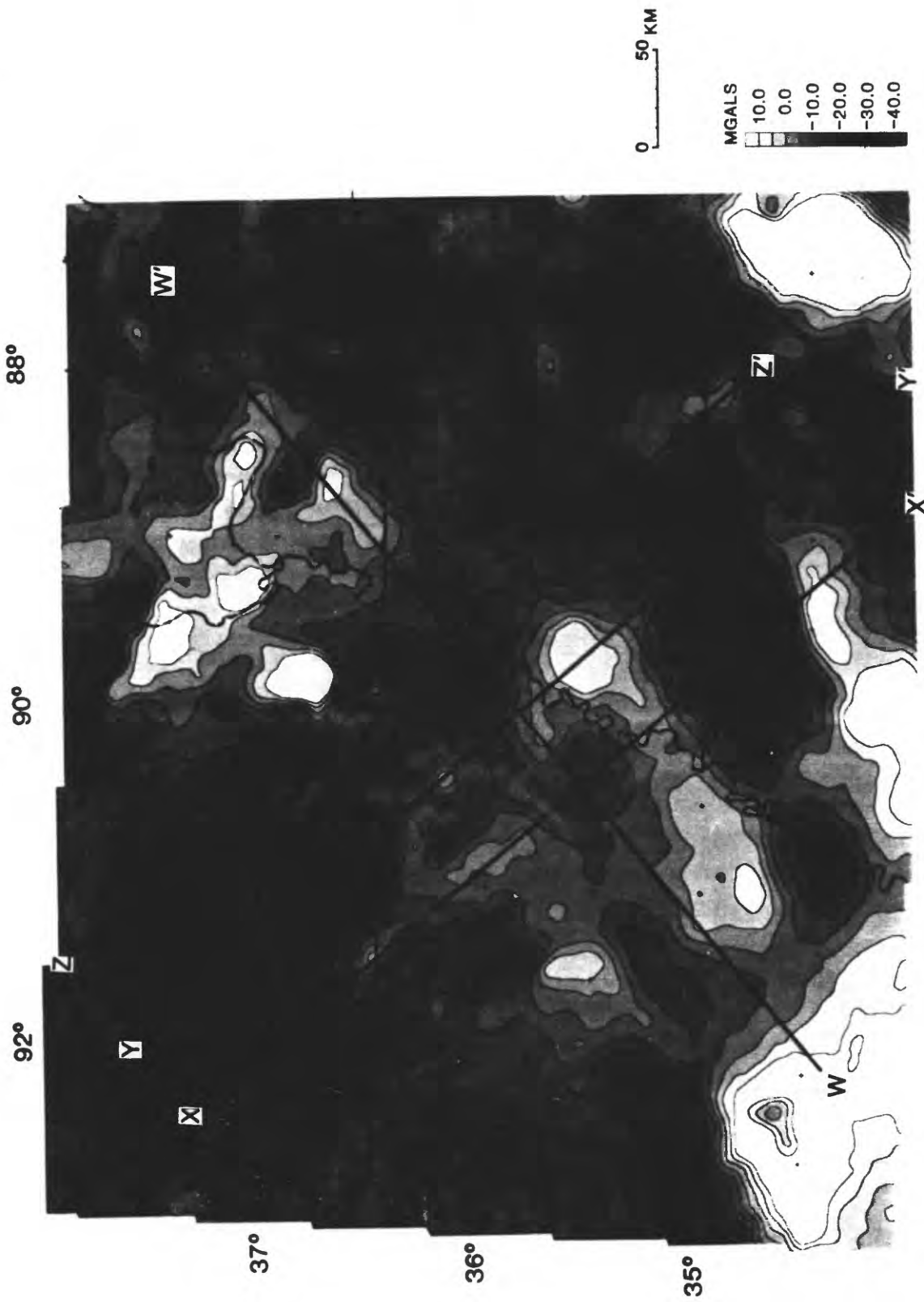


Figure 4. Gray-shaded complete Bouguer anomaly map (reduction density = 2.67 g/cm^3). Profiles X-X', Y-Y', Z-Z', and W-W' are shown in Figure 5.

.12/1.60

A priori knowledge of several parameters facilitated the selection of the initial guess for the crustal model. Drill-hole data supplied by Stearns and Marcher (1962) and E. E. Glick (U.S. Geological Survey, oral commun., 1984) provided information on the depth and extent of the Cenozoic clastic sediments and the Paleozoic carbonate section, respectively. Seismic refraction studies (Mooney and others, 1983) suggest that the graben fill is a low-velocity layer of clastics, possibly arkose (Denison, 1984). Previous studies of magnetic basement (Hildenbrand and others, 1979) provided estimates of depths to Precambrian basement and igneous intrusions. Segments of the lower crustal layers were restricted by seismic refraction results (Mooney and others, 1983).

Values for densities and susceptibilities were obtained from a variety of sources. Densities cited by Cordell (1977) for the Cenozoic (2.2 g/cm^3) and Paleozoic (2.65 g/cm^3) sediments were used. The velocity-density relationship of Birch (1961) and velocities cited by Mooney and others (1983) were used to select representative densities for the upper crust (2.75 g/cm^3), lower crust (2.9 g/cm^3), anomalous crust (3.1 g/cm^3), and mantle (3.25 g/cm^3). The Dow Chemical #1 Wilson well (Figure 1) penetrated several hundred feet of Precambrian granitic gneiss (upper crust) with densities generally above 2.7 g/cm^3 (Denison, 1984). Upper and lower crustal magnetic susceptibilities, respectively 0.5 and 3.5×10^{-3} cgs, were selected on the basis of modeling results by Hildenbrand (1982) and Schnetzler and Allenby (1983). Both densities and susceptibilities of the near-surface igneous bodies were allowed to vary and are listed in Appendix A.

The interpretation of potential-field data yields nonunique solutions because numerous geometrical models will have an associated field that closely matches the measured field. Available drill-hole information, simultaneous

inversion of gravity and magnetic data, seismic refraction information, and geological reasoning have presumably aided in deriving a suitable geophysical model to represent the geologic situation in the northern Mississippi Embayment. The attempt here to model the entire crust required consideration of very simple geometrical sources, particularly in the lower and middle crustal regions. Moreover, to adequately sample the long-wavelength field components associated with lower crustal sources, lengths of the selected profiles had to be exceptionally long. The NW-SE profiles extend from the St. Francois Mountains to the East Continental Rift System (Keller and others, 1983), both structures that are not of primary interest in this paper and thus have been modeled with very simple source configurations. Profile W-W' begins near the Ouachita foldbelt where it bends beneath the embayment. In this region low-density shales (about 2.5 g/cm^3) overlay thick Paleozoic carbonates (density = 2.65 g/cm^3) but have not been included in the model.

In addition to the ambiguity in the proper selection of the interpretational model, several geometrical configurations of the chosen model can yield results that are nearly identical. For example, increasing the density and decreasing the depth to the bottom of an intrusion will generally not produce an appreciable change in the computed fields. Although these uncertainties in a suitable model and its configuration exist, the interpreted crustal models shown in Figure 5 are considered valid but very simple geologic representations of the northern Mississippi Embayment. These models are consistent with the magnetic, gravity, and seismic refraction data and should be considered interpretative geologic cross-sections.

Profile X-X'

Of the 3 profiles oriented normal to the graben, profile X-X' (Figure 5a) best depicts the graben and other major structures in the upper embayment.

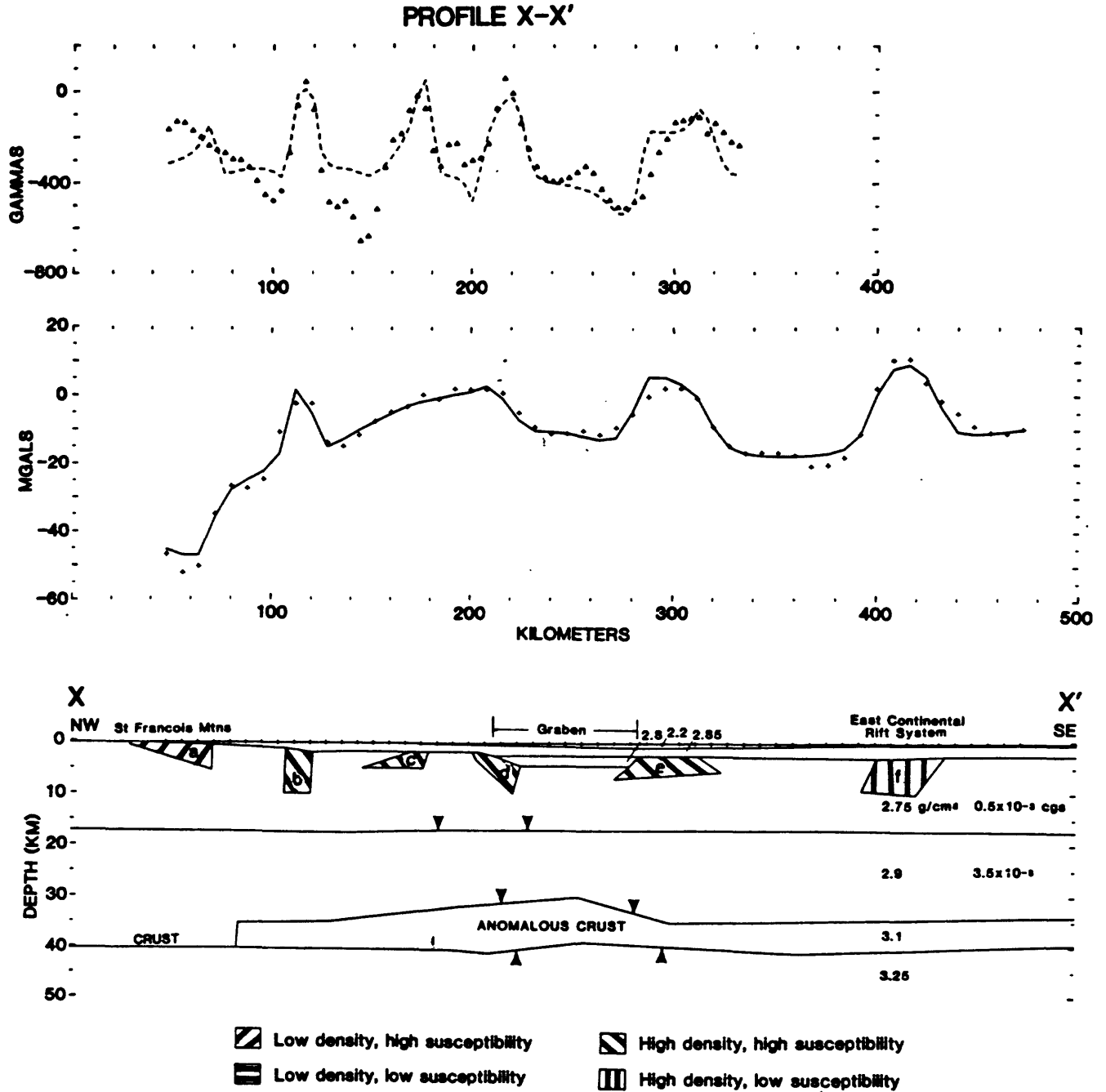


Figure 5.--Profiles (a) X-X', (b) Y-Y', (c) Z-Z', and (d) W-W' (shown in Figures 3 and 4) and derived structural models. In the upper figure, the dashed line represents the computed magnetic effect and the triangles represent the actual magnetic profile. In the center figure, the solid line represents the computed gravity effect and the crosses denote the actual gravity profile. Vertical exaggeration on the lower figure, the structural model, is 2 1/2 X. Numbers denote layer densities or susceptibilities. Near-surface igneous bodies are labeled with lower-case letters and their densities and susceptibilities are listed in Appendix A. Depths to boundary segments indicated by arrows are restrained by seismic refraction data (Mooney and others, 1983).

PROFILE W-W'

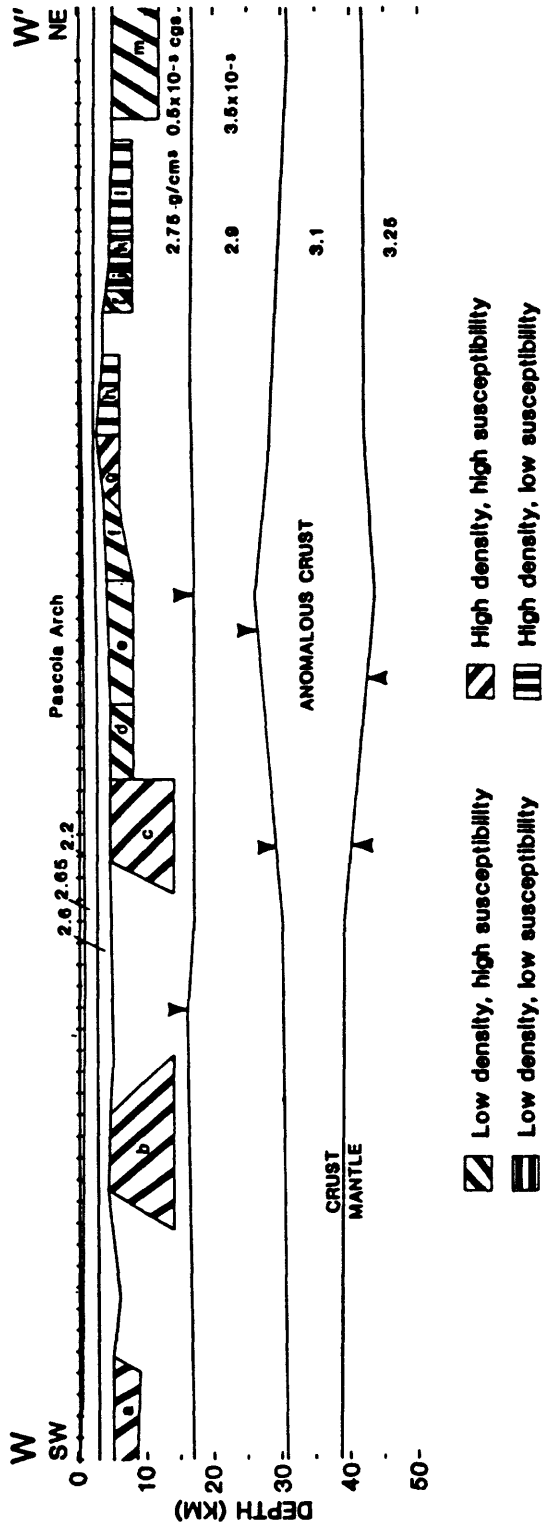
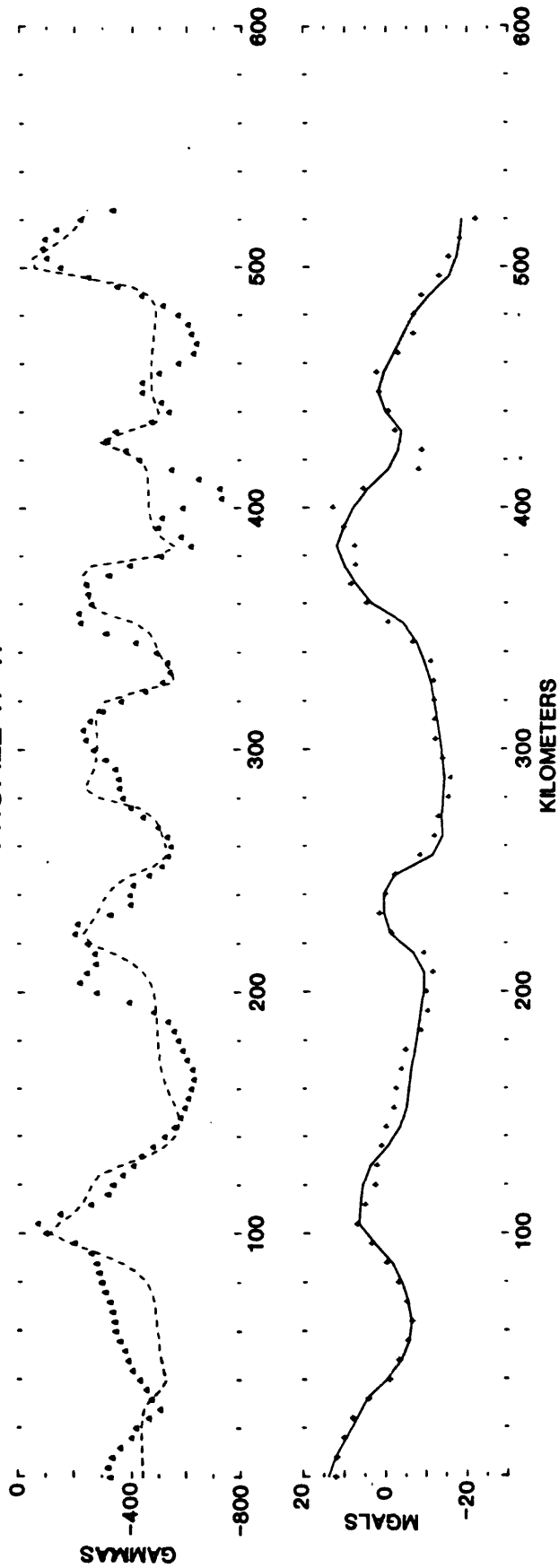


Figure 5d.

PROFILE Z-Z'

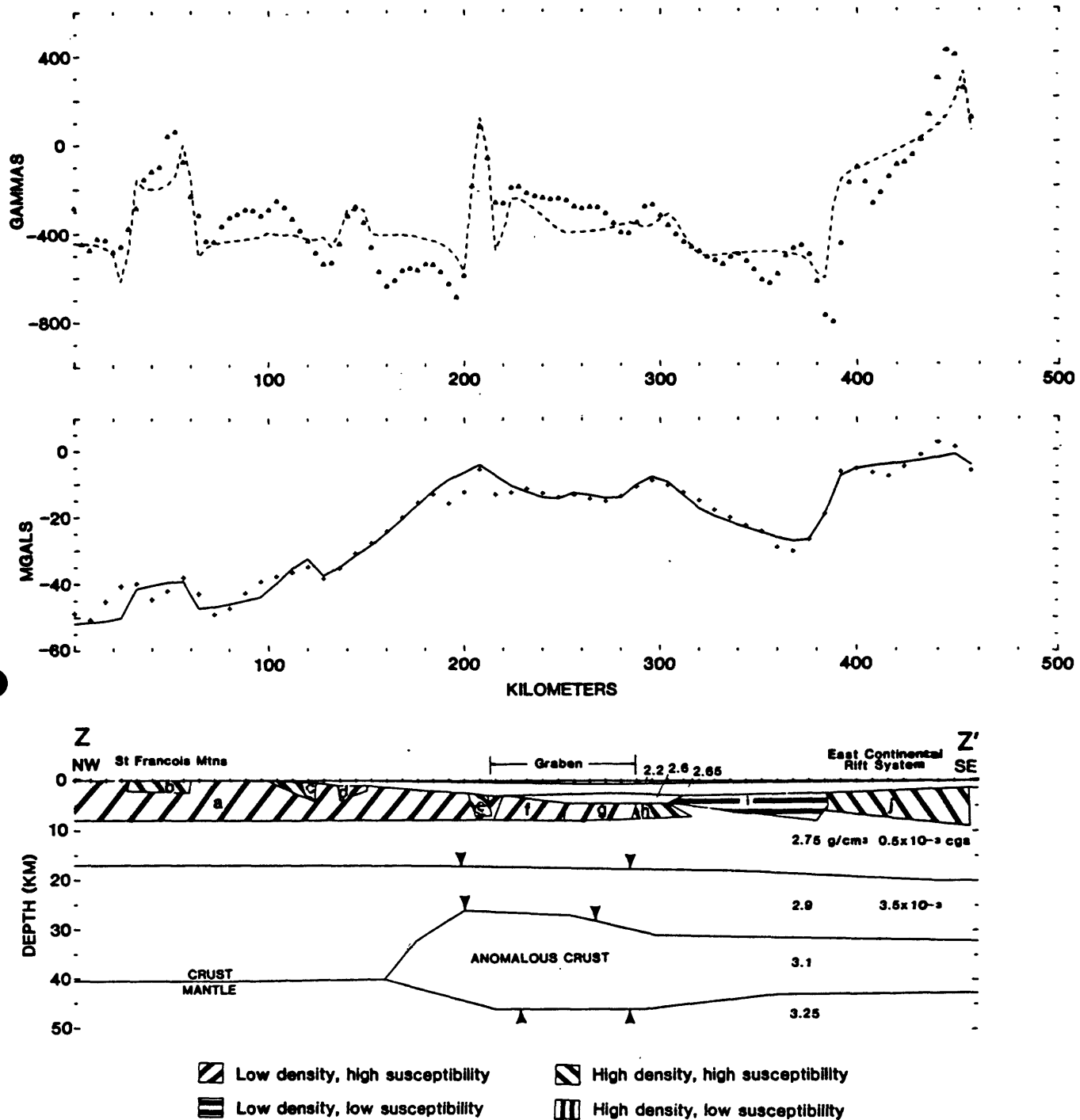


Figure 5c.

PROFILE Y-Y'

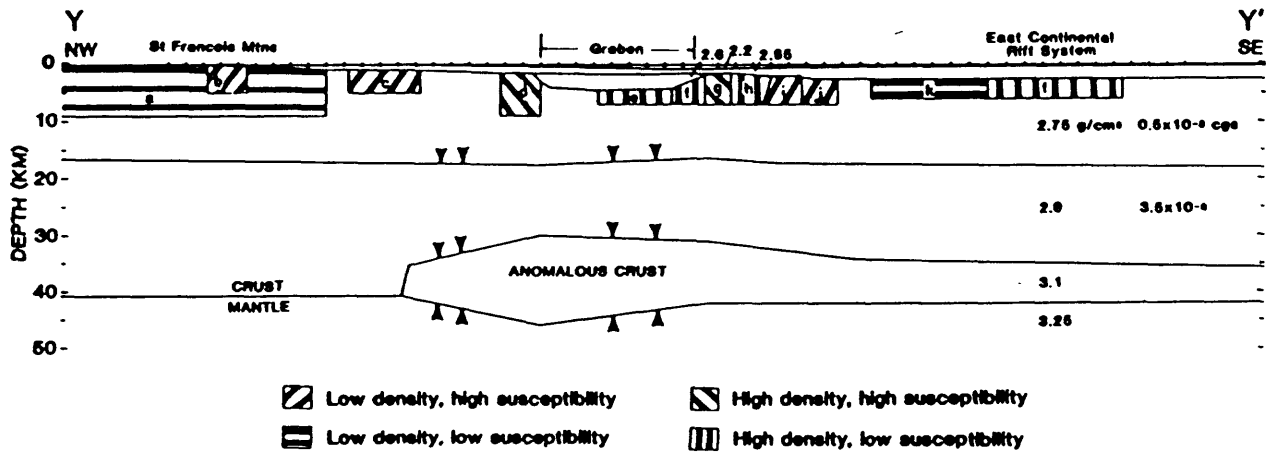
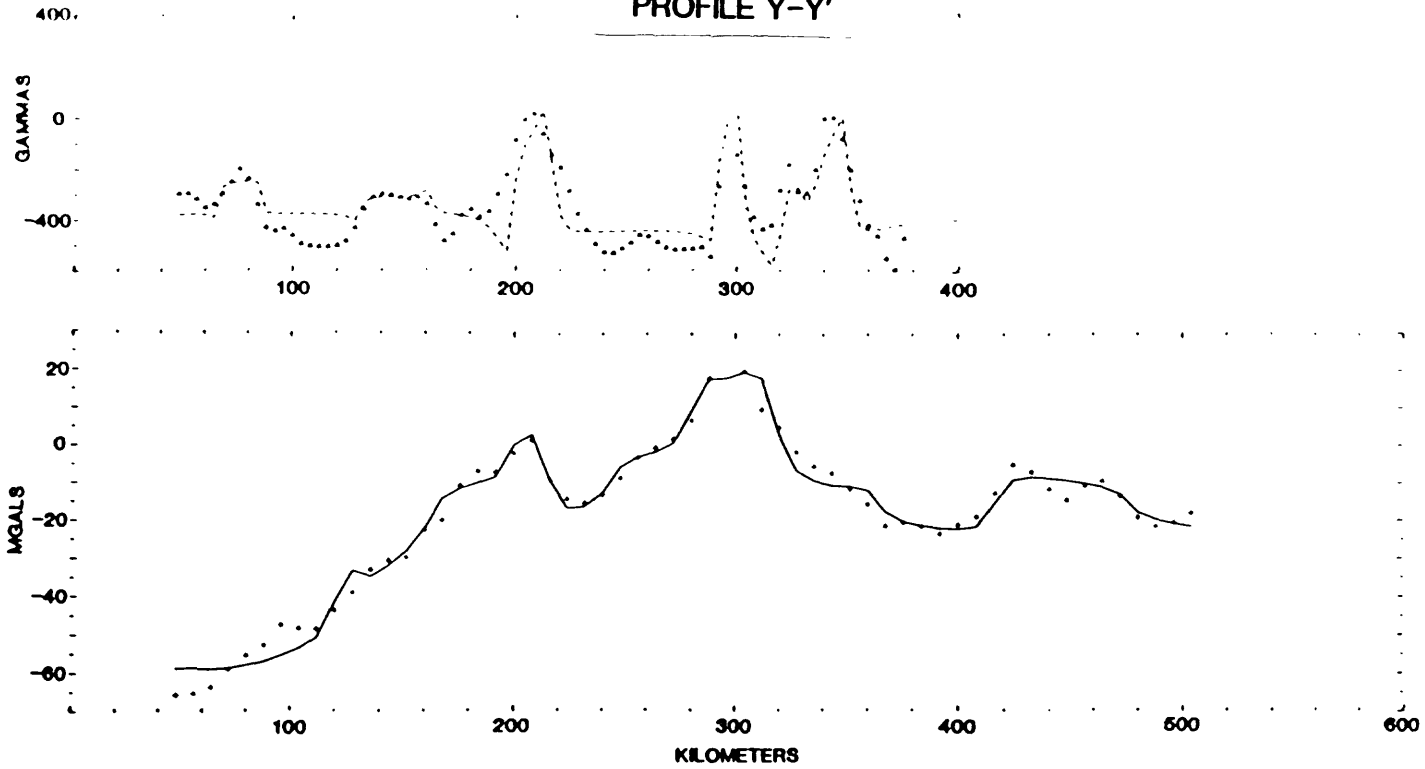


Figure 5b.

The graben contains approximately 2 km of low-density fill and is flanked by dense and highly magnetic bodies (e.g. d and e in Figure 5a). Basement within the graben descends to a maximum depth of about 5 km. To the northwest, two intense magnetic highs suggest the presence of underlying mafic intrusions (b and c). Associated gravity highs support this interpretation. Farther northwest, a near-surface body (a) in the St. Francois Mountains may represent the relatively low-density, unmetamorphosed volcanic and related epizonal intrusive rock of late Precambrian age (Kisvarsanyi, 1981). Near the southeast end of profile X-X', a prominent gravity high probably reflects an igneous body (f) associated with the East Continental Rift System delineated by Keller and others (1982).

The boundary between the upper crust and lower crust is essentially horizontal which supports earlier interpretations made by Mooney and others (1983). As in their model, an anomalous crustal layer is present at the base of the crust and represents mantle material (a fossil rift cushion) emplaced during the initial phases of rifting and during subsequent reactivations. This layer both shallows and thickens beneath the graben. It extends eastward beneath and possibly beyond the East Continental Rift System. Although it may be possible to thin or remove anomalous crust east of the graben, the anomalous crustal layer was inserted into the model there because seismic refraction studies by Schlittenhardt and Prodehl (1984) indicate its presence in central Tennessee.

Anomalous crust is absent beneath the St. Francois Mountains. The broad gravity low over these mountains may reflect the low-density batholithic rocks in the near surface as well as at depth.

Profile Y-Y'

Modeling results of profile Y-Y' (Figure 5b), although similar to those of profile X-X', do indicate the presence of more complex features. For

example, the profile crosses an interpreted ring-dike complex (e) (Hildenbrand and others, 1982; Figure 3) near the axis of the graben west of the Covington pluton (f-h). The Covington pluton may be laterally differentiated because it is characterized by a dense and highly magnetic central core (g) and a dense but low-susceptibility outer ring (f and h). Profile Y-Y' crosses a larger part of the St. Francois Mountains than that along profile X-X'.

Consequently, the resulting model along profile Y-Y' depicts a larger zone (a) of the low-density (about 2.68 g/cm^3), near-surface granite-rhyolite terrane and underlying batholith of southeastern Missouri. A low-density layer (k) at a depth of about 3 km is also present in a region southeast of the graben.

The lower boundary of the anomalous crustal layer noticeably sags into the mantle. This thickening of the anomalous crust occurs beneath the graben.

Profile Z-Z'

The low-density layer associated with the St. Francois batholithic rocks appears to extend southeastward beneath the graben and beyond (Figure 5c). These rocks may be more magnetic than those of the same low-density layer observed on the other two profiles. The margins of the graben are not clearly defined along profile Z-Z'.

At depth, however, structures are similar to those interpreted along the previous profiles, except that the anomalous crustal layer is exceptionally thick beneath the graben.

Profile W-W'

The axial profile extends from eastern Arkansas to western Kentucky, the interpreted extent of the graben. To the southwest the anomaly associated with the graben (Figures 3 and 4) is terminated abruptly by a northwest-trending feature (related to the Ouachita trend) in eastern Arkansas. Intense magnetic and gravity highs (Hildenbrand and others, 1982; Hildenbrand, 1984)

bounded on the north by this gradient reflect mafic or ultramafic igneous bodies, probably like the exposed Cretaceous Magnet Cove complex, a ring-dike complex (Erickson and Blade, 1963). This northwest-trending zone of igneous intrusions, marking the southwest terminus of the graben, are shown in the model of profile W-W' (a in Figure 5d).

To the northeast a trapezoidal body (b) probably represents a dense and highly magnetic pluton probably emplaced along the graben's axial faults (Hildenbrand and others, 1982; Hamilton and Zoback, 1982). Farther northeast the ring-dike complex (c) west of the Covington pluton and the low-density zone (d-f) extending southeast from the St. Francois Mountains are shown. Flanking the low-density zone on the northeast are several dense (some highly magnetic) igneous intrusions (g, h, and j-l) that probably intruded the graben's axial faults. The prominent magnetic high at the northeastern end of the profile may reflect Paleozoic igneous bodies (m) and is associated with the south central magnetic lineament, a continental-scale feature extending from eastern Tennessee to southeastern Nebraska (Hildenbrand, 1984). In this region, the Mississippi Valley graben may terminate at its intersection with the east-west trending Rough Creek graben (Moorman Syncline, Figure 1), also thought to have developed in association with rifting in early Paleozoic (Soderberg and Keller, 1981).

The boundary between upper and lower crust is relatively flat along the graben's axis. Anomalous crust is, however, thickest beneath the low-density layer extending from the St. Francois Mountains and is thinner to the southwest than to the northeast.

DISCUSSION

The modeling results elaborate from a premise that the northern Mississippi Embayment region is a site of an ancient rift system. The clearly

defined graben, probably formed during the initial phases of rifting, contains about 2 km of low-density fill and is flanked by dense and highly magnetic plutons. At depth the boundary between upper and lower crust is relatively flat.

Anomalous crust thickens and lies at shallow depths beneath the graben as shown in Figures 6 and 7. As expected, depth to anomalous crust (or thickness of normal crust) decreases under the graben (i.e. the region where extension was greatest during rifting). A corresponding thickening of a anomalous crust occurs beneath the northeast-trending graben as well as along a NW-SE trend that coincides with the Pascola arch (Figure 7). The thickest parts of anomalous crust occur under the crest of the arch and also along the northwest margin of the graben. The latter thickening may have occurred in post-early Mesozoic time during emplacement of the large plutons along this margin. The anomalous crust is much thinner along the southeast margin of the graben. This apparent asymmetry in volume of anomalous crust under the margins of the graben may explain the asymmetry in the number of plutons emplaced along the margins. In other words, faults along the graben's northwest margin in post-early Mesozoic time possibly allowed larger volumes of mantle material to ascend into both lower crust and near-surface regions.

The NW-SE trend in the distribution of anomalous crust may be intimately related to the overlying Pascola arch and a low-density zone (LDZ, Figure 6), extending southeastward from the St. Francois Mountains. Limited drill-hole data support the presence of a LDZ. Near the southwest edge of this zone, the Dow Chemical #1 Wilson Well (Figure 1), penetrated about 537 feet of Precambrian granitic gneisses (Denison, 1984) with densities greater than 2.7 g/cm³. To the northeast within the horizontal extent of the LDZ, feldspar-bearing basement rocks in the Big Chief Well (Figure 1) have densities

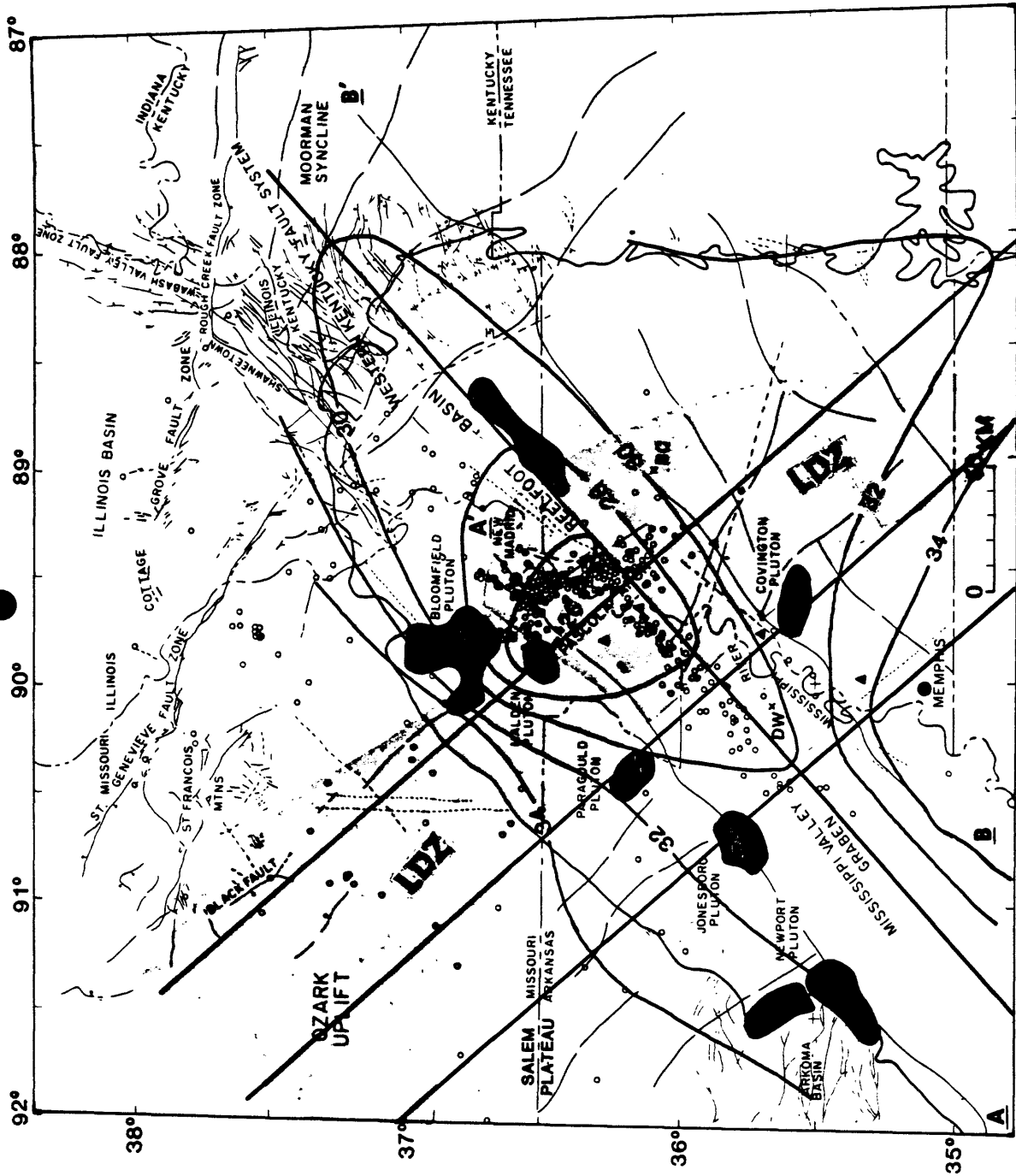


Figure 6.--Contours of depth to anomalous crust superimposed on the seismotectonic map shown in Figure 1. Gray-shaded zone denotes the inferred low-density zone (LDZ) extending southeastward from the St. Francois Mountains. Open circles represent earthquakes detected by the southeast Missouri regional seismic network from July 1974 to June 1977. Heavy lines are the profiles X-X', Y-Y', Z-Z', and W-W' shown in Figures 3 and 4. Contour interval is 2 km.

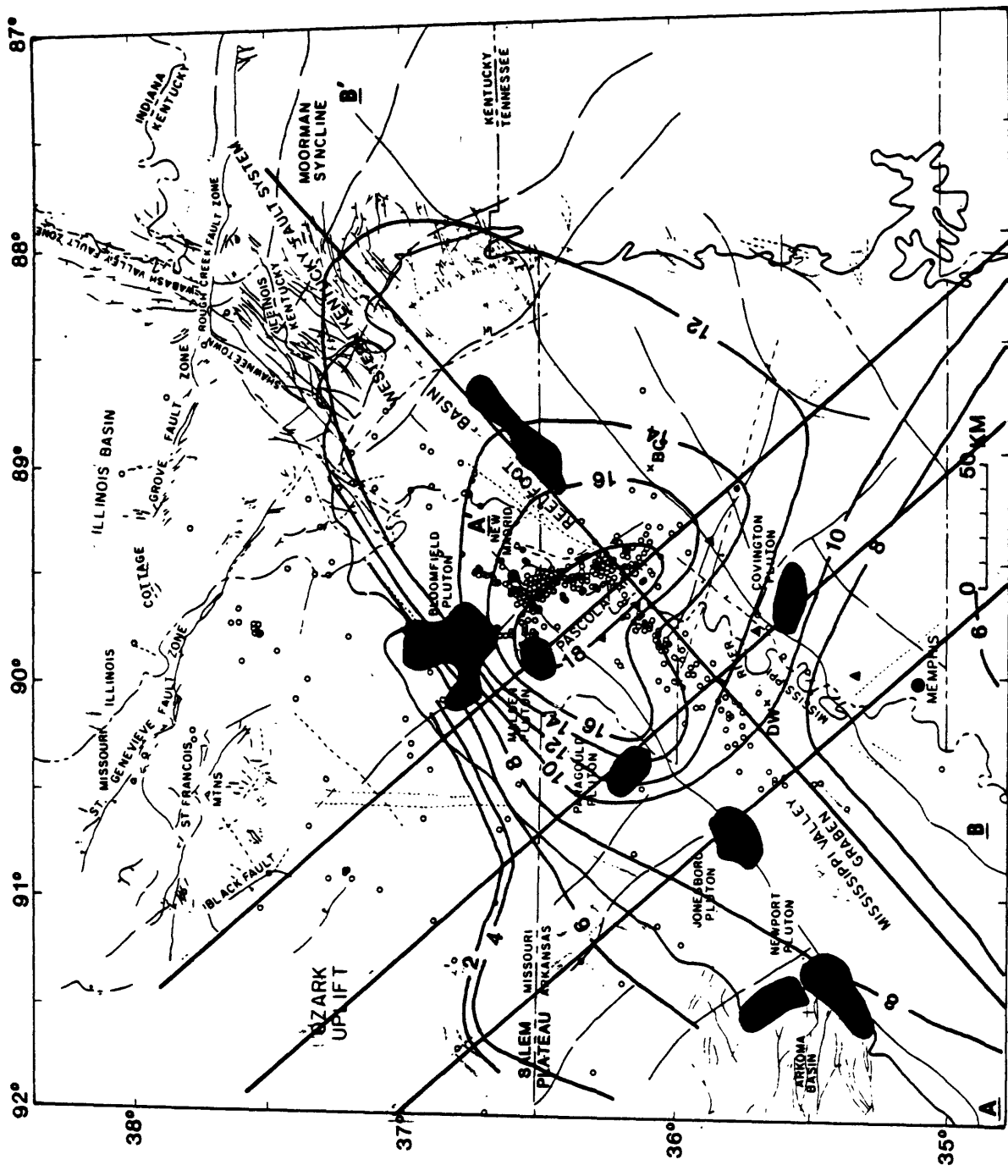


Figure 7.--Contours of thickness of anomalous crust superimposed on the seismotectonic map shown in Figure 1. Open circles represent earthquakes detected by the southeast Missouri regional seismic network from July 1974 to June 1977. Heavy lines are the profiles X-X', Y-Y', Z-Z', and W-W' shown in Figures 3 and 4. Contour interval is 2 km.

generally ranging between 2.65 and 2.68 g/cm³. Further support for the existence of the LDZ is based on the interpretation of the Missouri gravity low by Guinness and others (1982). They suggested that a gravity low, extending from the midcontinent gravity high in southeastern Nebraska to the northwest margin of the Mississippi Valley graben, represents a rifting event that preceded the formation of the granite-rhyolite terrane of the St. Francois Mountains. More detailed modeling here indicates that the LDZ associated with the Missouri gravity low in the embayment lies in shallow crustal regions and extends eastward beneath the graben to western Tennessee. Because the LDZ is linear and fairly uniform in width over a large distance, its development may be structurally controlled.

Subsequent to the formation of the LDZ and the graben, Late Paleozoic orogenic activity along the southern margin of North America formed the Ouachita foldbelt and thrust it onto the craton (Walper, 1977). The Pascola arch emerged during this period, possibly along structures that formed the LDZ. In the region where anomalous crust is thickest and is coincident with the crest of the arch, mica peridotite sills encountered in drill-holes in northwestern Tennessee (triangles in Figure 1) have been dated at 267 m.y. (Permian) by the K-Ar method (Zartman, 1977). During emergence of the NW-SE trending Pascola arch, magma may have been emplaced under the arch at the base of the crust (as suggested by the configuration of anomalous crust) and near the arch's crest (as indicated by drill-hole data).

Seismicity

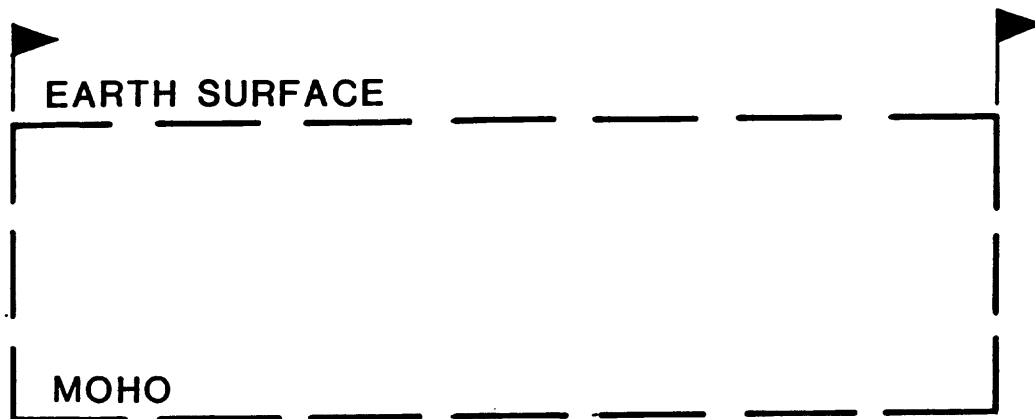
The present-day seismicity pattern (Figure 7; Andrews and others, 1984) suggests linear active zones (Stauder, 1982). The graben structure noticeably contains the area of principal seismicity in the upper Mississippi Embayment and, in particular, the epicentral line of the devastating 1811-1812 New

Madrid earthquake series (Fuller, 1912; Nuttli, 1982). Focal mechanism studies (Herrmann and Canas, 1978; Stauder, 1982) indicate significant components of right-lateral motion occurring along the northeast-trending zone of seismicity. Hildenbrand and others (1977, 1982), Kane and others (1981), and Braile and others (1982 a,b) suggested that graben structures represent zones of crustal weakness along which strain, produced by tectonic forces different from that which formed the graben, is being relieved. Subsurface faults along the linear active zones have been delineated from seismic reflection studies (Hamilton and Zoback, 1982).

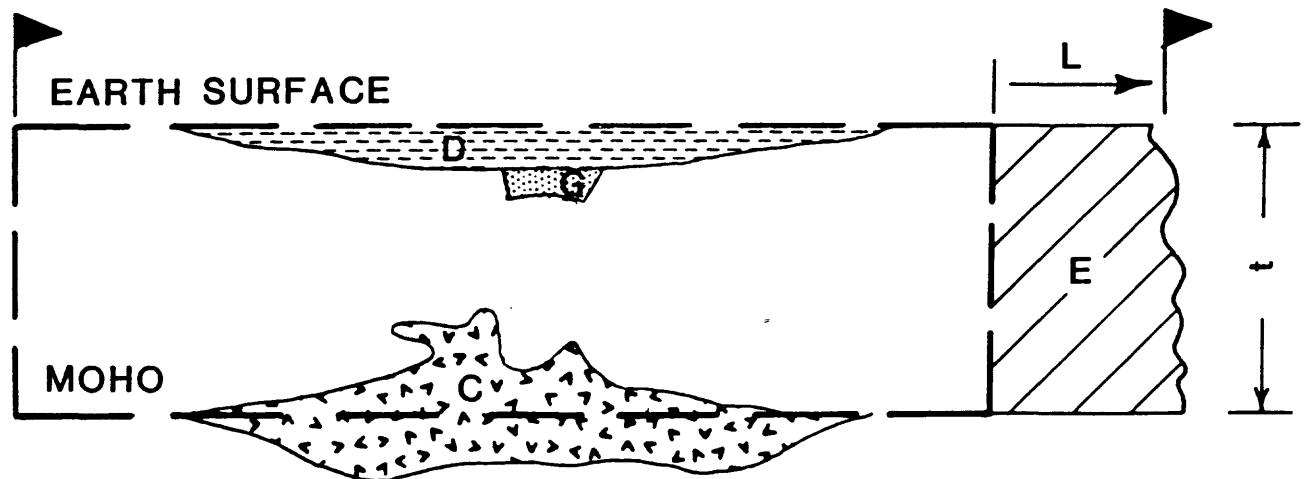
Seismicity trends change abruptly from northeast to slightly west of north at the intersection of the graben with the Pascola arch. The greatest concentration of earthquakes also occurs in this region and correlates very well with the region of thickest anomalous crust (Figure 7). This strong correlation may explain the reason for earthquake concentrations in the northern Mississippi Embayment and for the abrupt change in trend of seismicity. Stresses may concentrate within anomalous crust in much the same manner as stress concentrations occur within knots in boards under stress (Campbell, 1978). In other words, the E-W regional stress field, possibly due to lithospheric drag (Zoback and Zoback, 1980), would accumulate strain within the thickest part of the anomalous crust, which acts as a heterogeneity in a relatively homogeneous lithosphere. Focal depths generally range from 3-14 km (Andrews and others, 1984). Seismic slip at these shallow depths would be a result of aseismic slip at greater depths near the anomalous crust.

Extension

The northern Mississippi Embayment region has apparently experienced several periods of extension, but the one in Cambrian time would appear to be the major extensional event. Extension is manifested by graben faulting and



a) PRE-RIFTING



b) PRESENT DAY

Figure 8.--(a) Initial state showing assumed horizontal layer boundaries before rifting. Control area of the crust shown by heavy dashed line.
 (b) Present-day crustal model following several periods of extension. Frame of reference fixed with respect to left edge of figure. Upper case letters D, G, and C represent volumes per unit length of the surface trough, graben, and anomalous crust within the control area, respectively. L is linear measure of mean crustal extension; E is volume per unit length element associated with extension in the crust; t is crustal thickness.

by igneous dike intrusion throughout the crust (McKenzie, 1978). How much total extension has occurred? Cordell (1982) developed an innovative technique to answer this question and applied it to the Rio Grande rift. His theory, based on the consideration of anomalous volumes inferred from gravity data, is applied here to calculate total extension associated with and subsequent to the development of the Reelfoot rift. The Reelfoot rift actually allows a somewhat simpler formulation of the problem because topographic and gravity effects of the low-velocity, upper mantle have long since died away.

Figure 8a shows a sketch of the frame of reference with assumed horizontal layer boundaries prior to rifting. Present-day major crustal features as determined from modeling are shown in Figure 8b. The left edge of Figures 8a and 8b is fixed, and the control area is shown by the heavy dashed lines. A budget-type calculation of volumes that have entered and left the control area permits analysis of extension related volume components.

During rifting and subsequent igneous events, uplift (?) and lithospheric thinning may have resulted in the emplacement of new material at the base of the crust. This material cooled and isostatically sagged back into the mantle leaving a certain volume (C in Figure 8b) in the control area and producing a trough of volume D at the surface. Sediment loading assisted in forming the near-surface trough. Extension formed a graben of volume G during the initial phases of rifting. Considering the left edge of Figure 8b fixed, the total horizontal extension related component of displacement (E) is symbolically represented by the extra material on the right side of Figure 8b. The total flux of material into the control area from below and above is equal to the total flux of material out of the control area:

$$E = D + G + C .$$

The linear measure of mean crustal extension (L) is determined by dividing E by the present-day thickness of the crust, about 40 km:

$$L = E/40 .$$

Crustal thicknesses before and after periods of extension are assumed to be approximately equal to the present crustal thickness.

Calculating relevant volumes from the modeling results (Figure 5) led to total mean crustal extensions of 18.7, 21.8, and 25.0 km for profiles X-X', Y-Y', and Z-Z', respectively. The calculated values are remarkably consistent considering that the technique is inherently poorly constrained. Extension increases northward and is maximum in the region of thickest anomalous crust and greatest seismic activity (Figure 7).

REFERENCES

- Andrews, M. C., Mooney, W. D., and Meyer, R. P., 1984, The relocation of microearthquakes from the northern Mississippi Embayment: J. Geophys. Res. (in press).
- Austin, C. B., and Keller, G. R., 1982, A crustal structure study of the northern Mississippi Embayment, in Pakiser, L. C., and McKeown, F. A., eds., Investigations of the New Madrid, Missouri, earthquake region: U.S. Geological Survey Professional Paper 1236-G, p. 83-93.
- Ben-Auraham, Zui, 1984, Structural framework of the Gulf of Elat (AQBA)-- northern Red Sea: J. Geophys. Res. (in press).
- Bickford, M. E., Harrower, K. L., Hoppe, W. J., Nelson, B. K., Nusbaum, R. L., and Thomas, J. J., 1981, Rb-Sr and U-Pb geochronology and distribution of rock types in the Precambrian basement of Missouri and Kansas: Geol. Soc. Am. Bull, v. 92, p. 323-341.
- Birch, F. 1961, The velocity of compressional waves in rocks to 10 kilometers: J. Geophys. Res., v. 66, p. 2199-2224.
- Bond, D. C., and others, 1971, Possible future petroleum potential of region 9-Illinois Basin, Cincinnati arch, and northern Mississippi embayment: American Association of Petroleum Geologists Memoir 15, v. 2, p. 1165-1218.
- Braile, L. W., Hinze, W. J., Keller, G. R., and Lidiak, E. G., 1982a, The northeastern extension of the New Madrid seismic zone, in Pakiser, L. C., and McKeown, F. A., eds., Investigations of the New Madrid, Missouri, Earthquake Region: U.S. Geological Survey Professional Paper 1236-L, p. 175-184.

- Braile, L. W., Keller, G. R., Hinze, W. J., and Lidiak, E. G., 1982b, An ancient rift complex and its relation to contemporary seismicity in the New Madrid seismic zone: *Tectonics*, v. 1, n. 2, p. 225-237.
- Burke, K., and Dewey, J. F., 1973, Plume-generated triple junctions--key indicators in applying tectonics to old rocks: *Jour. Geology*, v. 81, p. 406-433.
- Campbell, D. L., 1976, Investigations of the stress-concentration mechanism for intraplate earthquakes: *Geophys. Res. Letters*, v. 5, n. 6, p. 477-479.
- Caplan, W. M., 1954, Subsurface geology and related oil and gas possibilities of northeastern Arkansas: Arkansas Resources Development Commission, Division of Geology Bulletin 20, 124 p.
- Chapin, C. E., and Cather, S. M., 1981, Eocene tectonics and sedimentation in the Colorado Plateau - Rocky Mountains area, in *Relations of Tectonics to Ore Deposits in the southern Cordillera*: Arizona Geological Society Digest, v. 14, p. 173-198.
- Cohee, G. V., and others, 1962, Tectonic map of the United States: U.S. Geological Survey and American Assoc. of Petroleum Geologists, scale 1:2,500,000.
- Cordell, Lindrith, 1977, Regional positive gravity anomaly over the Mississippi Embayment: *Geophysical Research Letters*, v. 4, n. 7, p. 285-287.
- _____, 1982, Extension of the Rio Grande rift: *Journal of Geophysical Research*, v. 87, n. 87, p. 8561-8569.
- Denison, R. E., 1984, Basement rocks in northern Arkansas: Arkansas Geological Commission (in press).
- Erickson, R. L., and Blade, L. V., 1963, Geochemistry and petrology of the Alkalic igneous complex at Magnet Cove, Arkansas: U.S. Geological Survey Professional Paper 425, 95 p.
- Ervin, C. P., and McGinnis, L. D., 1975, Reelfoot rift - Reactivated precursor to the Mississippi Embayment: *Geological Society of America Bulletin*, v. 86, p. 1287-1295.
- Freund, Raphael, 1982, The role of shear in rifting, *in* Palmason, Gudmundur, ed., *Continental and Ocean Rifts*: Amer. Geophys. Union, Geodynamics Series, v. 8, p. 31-40.
- Fuller, M. L., 1912, The New Madrid Earthquake: U.S. Geological Survey Bulletin 494, 119 p.
- Glick, E. E., 1975, Arkansas and northern Louisiana, in *Paleotectonic Investigations of the Pennsylvanian System in the United States - Part I - Introduction and Regional Analyses of the Pennsylvanian System*: U.S. Geological Survey Professional Paper 853-I, p. 157-175.

- _____ 1982, Stratigraphy and structure of sediments above the Newport pluton of northeastern Arkansas, in Pakiser, L. C., and McKeown, F. A., eds., Investigations of the New Madrid, Mo., Earthquake Region: U.S. Geological Survey Professional Paper 1236, p. 151-174.
- Gordon, M., Jr., Tracey, J. I., Jr., and Ellis, M. W., 1958, Geology of the Arkansas bauxite region: U.S. Geological Survey Professional Paper 229, 268 p.
- Grohskopf, J. G., 1955, Subsurface geology of the Mississippi Embayment of southeast Missouri: Missouri Division of Geological Survey and Water Resources, v. 37, 2nd ser., 133 p.
- Guinness, E. A., Arvidson, R. E., Strebeck, J. W., Schulz, K. J., Davies, G. F., and Leff, C. E., 1982, Identification of a Precambrian rift through Missouri by digital image processing of geophysical and geological data: J. Geophys. Res., v. 87, n. B10, p. 8529-8545.
- Hamilton, R. M., and Zoback, M. D., 1982, Tectonic features of the New Madrid seismic zone from seismic-reflection profiles, in McKeown, F. A., and Pakiser, L. D., eds., 1982, Investigations of the New Madrid, Missouri, earthquake region: U.S. Geological Survey Professional Paper 1236, p. 55-82.
- Herrmann, R. B., and Canas, J., 1978, Focal mechanism studies in the New Madrid seismic zone: Seismological Society of America Bulletin, v. 68, p. 1095-1102.
- Heyl, A. V., and McKeown, F. A., 1978, Preliminary seismotectonic map of central Mississippi valley and environs: U.S. Geological Survey Miscellaneous Field Studies Map MF-1011.
- Hildenbrand, T. G., 1978, Approximate ages of igneous intrusions in the upper Mississippi Embayment utilizing the total magnetic field anomalies: American Geophysical Union 1978 Midwest Meeting, Abstracts, p. 6.
- _____ 1982, Model of southeastern margin of the Mississippi Valley graben near Memphis, Tennessee, from interpretation of truck-magnetometer data: Geology, v. 10, p. 467-480.
- _____ 1984, Magnetic terrane in central USA from the interpretation of digital data: Geophysics (in press).
- Hildenbrand, T. G., Kane, M. F., and Hendricks, J. D., 1982, Magnetic basement in the upper Mississippi Embayment region--a preliminary report, in McKeown, F. A., and Pakiser, L. C., eds., Investigations of the New Madrid, Missouri, earthquake region: U.S. Geological Survey Professional Paper, 1236, p. 39-53.
- Hildenbrand, T. G., Kane, M. F., and Stauder, William, 1977, Magnetic and gravity anomalies in the northern Mississippi Embayment and their spatial relation to seismicity: U.S. Geological Survey Miscellaneous Field Studies Map MF-914.

Hildenbrand, T. G., Kucks, R. P., Kane, M. F., and Hendricks, J. D., 1979, Aeromagnetic map and associated depth map of the upper Mississippi Embayment region: U.S. Geological Survey Miscellaneous Field Studies Map MF-1158, scale 1:1,000,000.

Hinze, W. J., Braile, L. W., Keller, G. R., and Lidiak, E. G., 1980, Models for midcontinent tectonism, in Continental Tectonics: National Academy of Sciences, Studies in Geophysics, p. 73-83.

Illies, J. H., 1977, Ancient and recent rifting in the Rhinegraben: Geologie en Mijnbouw, v. 56, n. 4, p. 329-350.

_____ 1982, Der hohenzollerngraben und intraplatten-seismizitat infolge vergitterung lamellarer scherung mit einer riftstruktur: Obernhhein. Geol. Abh., v. 31, p. 47-78.

Jespersen, Anna, 1964, Aeromagnetic prospecting for bauxite deposits in the Mississippi Embayment, Arkansas and Missouri: U.S. Geological Survey Geophys. Invest. Map GP-370, scale 1:925,000.

Kane, M. F., Hildenbrand, T. G., and Hendricks, J. D., 1979, The Mississippi Valley graben, a hidden rift (abs.): EOS (American Geophysical Union Transactions), v. 60, p. 954.

_____ 1981, A model for the tectonic evolution of the Mississippi Embayment and its contemporary seismicity: Geology, v. 9, p. 563-567.

Keller, G. R., Lidiak, E. G., Hinze, W. J., and Braile, L. W., 1983, The role of rifting in the tectonic development of the midcontinent, U.S.A.: Tectonophysics, v. 94, p. 391-412.

Kidwell, A. L., 1951, Mesozoic igneous activity in the northern Gulf Coast Plain: Gulf Coast Association of Geological Societies, 1st Annual Meeting, Transactions, P. 182-199.

Kisvarsanyi, E. B. 1974, Operation basement--Buried Precambrian rocks of Missouri--Their petrography and structure: American Association of Petroleum Geologists Bulletin, v. 58, no. 4, p. 674-684.

_____ 1981, Geology of the Precambrian St. Francois terrane, southeastern Missouri: Missouri Department of Natural Resources, Contributions to Precambrian Geology, no. 8, 58 p.

Kumarapeli, P. S., and Saull, V. A., 1966, The St. Lawrence valley system--A North American equivalent of the East African rift system: Canadian Journal of Earth Science, v. 3, p. 639-658.

McKenzie, Dan, Some remarks on the development of sedimentary basins: Earth Planet. Sci. Lett., 40, p. 25-32.

McKeown, F. A., 1982, Overview and discussion, in Paksier, L. C., and McKeown, F. A., eds., Investigations of the New Madrid, Missouri, Earthquake Region: U.S. Geological Survey Professional Paper 1236-A, p. 1-14.

- _____. 1984, New Madrid seismic zone, Part I--Historical review of studies and Part II--Contemporary studies by the U.S. Geological Survey: U.S. Geological Survey Open-File Report (in press).
- Moody, C. L., 1949, Mesozoic igneous rocks of the northern Gulf Coastal Plain: American Association of Petroleum Geologists Bulletin, v. 33, p. 1410-1428.
- Mooney, W. D., Andrews, M. C., Ginzburg, A., Peters, D. A., and Hamilton, R. M., 1983, Crustal structure of the northern Mississippi Embayment and a comparison with other continental rift zones: Tectonophysics, v. 94, p. 327-348.
- Nuttli, O. W., 1982, Damaging earthquakes of the central Mississippi valley, in Pakiser, L. C., and McKeown, F. A., eds., Investigations of the New Madrid, Missouri, Earthquake Region: U.S. Geological Survey Professional Paper 1236-B, p. 15-20.
- Phelan, M., 1969, Crustal structure in the central Mississippi Valley (Ph.D. dissert.): St. Louis, Washington, University, 166 p.
- Salveson, J. O., 1978, Variations in the geology of rift basins--A tectonic model: International Symposium on the Rio Grande rift, Sante Fe, New Mexico, 1978, p. 82.
- Schlittenhardt, J., and Prodehl, 1984, Crustal structure of the Appalachian highlands in Tennessee from stacked seismic data: Bull. Seism. Soc. Amer. (in press).
- Schnetzler, C. C., and Allenby, R. J., 1983, Estimation of lower crust magnetization from satellite-derived magnetic field: Tectonophysics, v. 93, p. 33-?
- Schwalb, H. R., 1978, Paleozoic geology of the New Madrid area, Annual progress report-fiscal year 1978, contract no. NRC-04-76-321, in T. C. Buschbach, New Madrid seismotectonic study--Activities during fiscal year 1978: Illinois State Geological Survey, prepared for the Division of Reactor Safety Research Office of Nuclear Regulatory Research, U.S. Nuclear Regulatory Commission, contract no. NRC 04-76-204.
- Soderberg, R. K., and Keller, G. R., 1981, Geophysical evidence for deep basin in western Kentucky: Am. Assoc. Pet. Geol. Bull., v. 65, p. 226-234.
- Stearns, R. G., and Marcher, M. V., 1962, Late Cretaceous and subsequent structural development of the northern Mississippi Embayment area: Geological Society of America Bulletin, v. 73, p. 1387-1394.
- Stauder, William, 1982, Present-day seismicity and identification of active faults in the New Madrid seismic zone, in Pakiser, L. C., and McKeown, F. A., eds., Investigations of the New Madrid, Missouri, Earthquake Region: U.S. Geological Survey Professional Paper 1236-C, p. 21-30.
- Walper, J. L., 1977, Paleozoic tectonics of the southern margin of North America: Gulf Coast Assoc. Geol. Soc. Trans., v. 27, p. 230-241.

Watson, K. D., 1967, Kimberlites of eastern North America, in Wyllie, P. J., ed., Ultramafic and related rocks: New York, John Wiley and Sons, Inc., p. 312-323.

White, P. E., 1967, Outline of thermal and mineral waters as related to origin of Mississippi Valley ore deposits, with discussions, in Brown, J. S., ed., Genesis of stratiform lead-zinc-barite-fluorite deposits - A symposium, New York, 1966: Economic Geology Monograph 3, p. 382.

Zartman, R. E., 1977, Geochronology of some alkalic rock provinces in eastern and central United States: Earth and Planetary Science Letters Annual Review, v. 5, p. 257-286.

Zartman, R. E., Brock, M. R., Heyl, A. V., and Thomas, H. H., 1967, K-Ar and Rb-Sr ages of some alkalic intrusive rocks from the central and eastern United States: American Journal of Science, v. 165, p. 848-870.

Zoback, M. L., and Zoback, M. D., 1980, State of stress in the conterminous United States: Journal of Geophysical Research, v. 85, p. 6113-6156.

APPENDIX A

The models shown in Figures 5a-5d include near-surface igneous bodies denoted by lower-case letters. Their densities and susceptibilities varied and are given in the following tables.

Profile X-X':

| <u>Body</u> | <u>Density (g/cm³)</u> | <u>Susceptibility (10⁻³cgs)</u> |
|-------------|-----------------------------------|--|
| a | 2.64 | 2.0 |
| b | 2.95 | 2.5 |
| c | 2.76 | 4.5 |
| d | 2.81 | 4.2 |
| e | 2.90 | 4.9 |
| f | 2.88 | 0.5 |

Profile Y-Y':

| <u>Body</u> | <u>Density (g/cm³)</u> | <u>Susceptibility (10⁻³cgs)</u> |
|-------------|-----------------------------------|--|
| a | 2.68 | 0.5 |
| b | 2.69 | 1.1 |
| c | 2.70 | 1.1 |
| d | 2.84 | 2.9 |
| e | 2.94 | 0.5 |
| f | 2.97 | 0.5 |
| g | 2.98 | 4.0 |
| h | 2.91 | 0.5 |
| i | 2.75 | 3.3 |
| j | 2.75 | 5.0 |
| k | 2.67 | 0.5 |
| l | 2.81 | 0.5 |

Profile Z-Z':

| <u>Body</u> | <u>Density (g/cm³)</u> | <u>Susceptibility (10⁻³ cgs)</u> |
|-------------|-----------------------------------|---|
| a | 2.69 | 1.5 |
| b | 2.80 | 6.3 |
| c | 2.77 | 1.2 |
| d | 2.71 | 3.2 |
| e | 2.80 | 10.0 |
| f | 2.65 | 6.0 |
| g | 2.73 | 6.6 |
| h | 2.86 | 5.6 |
| i | 2.63 | 0.5 |
| j | 2.82 | 5.3 |

Profile W-W':

| <u>Body</u> | <u>Density (g/cm³)</u> | <u>Susceptibility (10⁻³ cgs)</u> |
|-------------|-----------------------------------|---|
| a | 2.83 | 2.0 |
| b | 2.93 | 3.6 |
| c | 2.91 | 2.5 |
| d | 2.68 | 1.3 |
| e | 2.65 | 5.0 |
| f | 2.65 | 1.2 |
| g | 2.86 | 4.4 |
| h | 2.89 | 0.5 |
| i | 2.75 | 2.9 |
| j | 2.86 | 0.5 |
| k | 2.92 | 0.5 |
| l | 2.89 | 0.5 |
| m | 2.75 | 5.7 |

TECTONIC DEVELOPMENT OF THE
NEW MADRID SEISMIC ZONE

by

Lawrence W. Braile, William J. Hinze, John L. Sexton¹
Department of Geosciences
Purdue University
West Lafayette, IN 47907

G. Randy Keller
Department of Geological Sciences
University of Texas at El Paso
El Paso, TX 79968

and

Edward G. Lidiak
Department of Geology and Planetary Sciences
University of Pittsburgh
Pittsburgh, PA 15260

ABSTRACT

Geological and geophysical studies of the New Madrid Seismic Zone have revealed a buried late Precambrian rift beneath the upper Mississippi Embayment area. The rift has influenced the tectonics and geologic history of the area since late Precambrian time and is presently associated with the contemporary earthquake activity of the New Madrid Seismic Zone. The rift formed during late Precambrian to earliest Cambrian time as a result of continental breakup and has been reactivated by compressional or tensional stresses related to plate tectonic interactions. The configuration of the buried rift is interpreted from gravity, magnetic, seismic refraction, seismic reflection and stratigraphic studies. The increased mass of the crust

1) Now at: Arco DST 12104, PO Box 2819, 400 N. Olive, Skyway Tower,
Dallas, TX 75201

in the rift zone, which is reflected by regional positive gravity anomalies over the upper Mississippi Embayment area, has resulted in periodic subsidence and control of sedimentation and river drainage in this cratonic region since formation of the rift complex. The correlation of the buried rift with contemporary earthquake activity suggests that the earthquakes result from slippage along zones of weakness associated with the ancient rift structures. The slippage is due to reactivation of the structure by the contemporary, nearly east-west regional compressive stress which is the result of plate motions.

INTRODUCTION

The New Madrid Seismic Zone has been the subject of increasing interest and a large number of geological and geophysical studies in the past several years. This interest has followed the recognition of the earthquake hazard in the New Madrid area as evidenced by the 1811-1812 series of earthquakes near New Madrid, Missouri (Nuttli, 1973; 1982) and of the significance of the New Madrid area as an example of intraplate seismicity. As the geological and geophysical data base in the New Madrid Seismic Zone has improved, more detailed interpretations of the subsurface structure and geologic history of the area have become possible. In this paper, we review the tectonic development of the New Madrid Seismic Zone since its earliest known history in late Precambrian time. The interpretations of the geologic evolution of this area are based on geological data and geophysical models of the Phanerozoic sedimentary rocks and underlying structure of the crust, as well as related plate tectonic activities of the eastern North American craton.

Interpretation of the Reelfoot Rift beneath the upper Mississippi Embayment by Ervin and McGinnis (1975) was the first suggestion of a

recognizable upper crustal feature which is correlative with the contemporary earthquake activity of the New Madrid Seismic Zone. Subsequently, Hildenbrand et al. (1977, 1982) and Kane et al. (1981) utilized gravity and magnetic data to better delineate the location of the buried Reelfoot Rift and infer a thick section of sedimentary rocks filling the graben associated with the rift. In addition, they noted that the New Madrid Seismic Zone was located near the center of the buried Reelfoot Rift. Braile et al. (1982a,b) utilized local gravity and magnetic maps to infer extensions of the Reelfoot Rift to the northwest and northeast. Soderberg and Keller (1981) described the subsurface structure of the Rough Creek Graben in western Kentucky adjacent to the northern end of the Reelfoot Rift. An integrated interpretation of these studies (Braile et al., 1982b) indicates that a failed rift system exists beneath the upper Mississippi Embayment which these authors termed the 'New Madrid Rift Complex' (Figure 1). The rift complex was delineated primarily on the basis of short-wavelength gravity and magnetic anomalies which are associated with the edges of the rift. However, the regional gravity data of Cordell (1977), illustrated in Figure 1, also show a clear correlation with the rift complex.

The historical seismicity of the New Madrid Seismic Zone was described by Nuttli (1973, 1979, 1982) and microearthquake activity since 1974 has been reported by Stauder et al. (1977) and Stauder (1982). Earthquake activity within the New Madrid Seismic Zone and adjacent area is generally correlative with the configuration of the New Madrid Rift Complex (Braile et al., 1982b,c) as illustrated in Figure 1. Additional important information from earthquake studies have been provided by Herrmann and Canas (1978) who have shown that focal

mechanisms of earthquakes within the New Madrid Seismic Zone are consistent with right lateral strike-slip faulting along the primarily northeasterly trend of the microearthquake seismicity southwest of the town of New Madrid (Figure 1).

A variety of models have been proposed to explain the occurrence of earthquake activity in the intraplate region of midcontinent North America. Hinze et al. (1980) reviewed the various models and grouped them into five different types. More recently, these authors (Hinze et al., 1984) have suggested that only two of these mechanisms provide viable models for explaining the intraplate earthquakes in midcontinent North America. These models are termed the 'zone of weakness model' and the 'local basement inhomogeneity model'. The zone of weakness model was proposed by Sbar and Sykes (1973) and Sykes (1978) and was suggested by Zoback and Zoback (1981) and Braile et al. (1982b,c) to be the cause of earthquake activity in the New Madrid region. According to this model, contemporary earthquake activity is due to a reactivation of ancient faults within the crystalline crust which are presently subjected to an appropriately oriented regional stress field. The orientation of the New Madrid Seismic Zone, the earthquake focal mechanisms, the correlation of the trend of seismicity with the buried Reelfoot Rift, and the nearly east-west compressive stress field of the New Madrid region are consistent with this hypothesis as an explanation for the earthquake activity in the New Madrid Seismic Zone. The local basement inhomogeneity model appears to best explain some small zones of earthquake activity which can be shown to be associated with local crustal inhomogeneities evidenced by pronounced gravity and magnetic anomalies (Hinze et al., 1984). This model, originally suggested by Long (1976); Kane (1977); and McKeown (1978), may be the mechanism for a

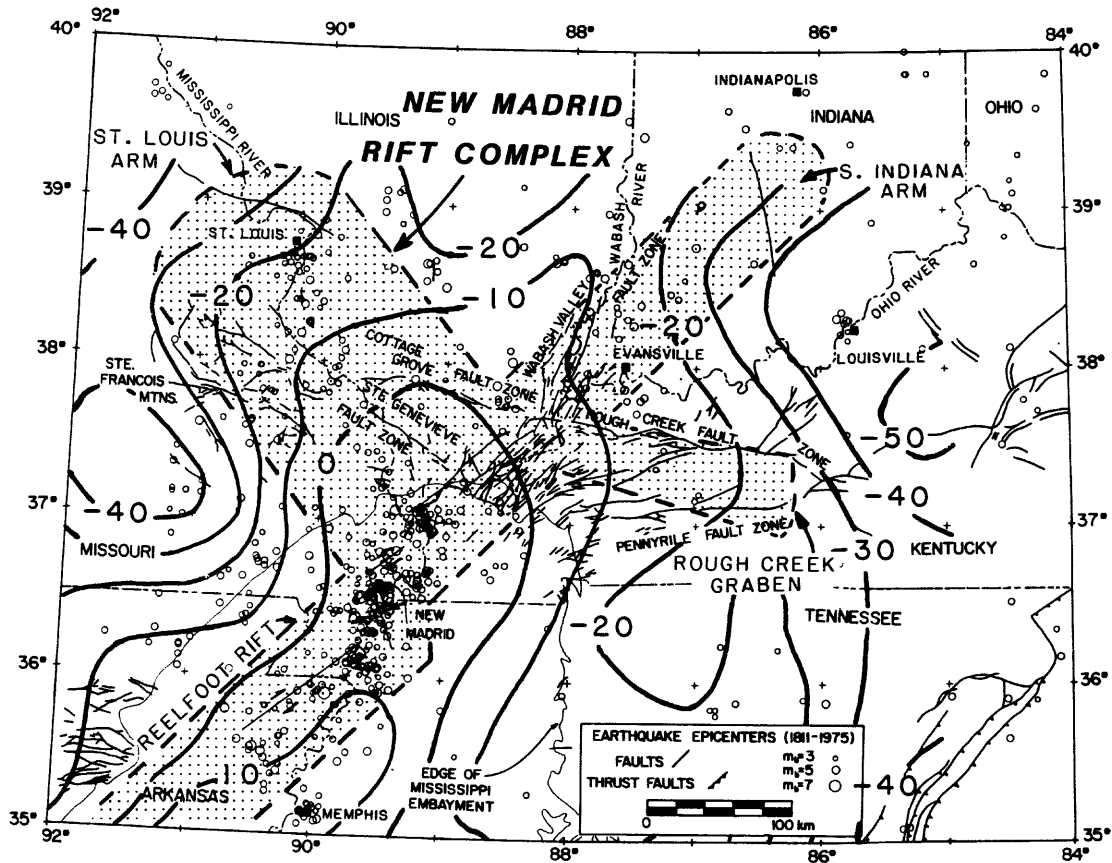


Figure 1. Index map of the New Madrid Seismic Zone and surrounding regions. The outline of the New Madrid Rift Complex is from Braille *et al.* (1982b). Major faults (Pre-Cenozoic) are shown from the work of Heyl (1972); Heyl and McKeown (1978); Bristol and Treworgy (1979); and Ault *et al.* (1980). Circles are earthquake epicenters from the data file provided by Otto W. Nuttli. Locations of epicenters have been "randomized" by adding a random number uniformly distributed between $\pm 0.2^\circ$ to the latitude and longitude. This randomization prevents an artificial alignment of epicenters along even lines of latitude and longitude caused by round-off of the original epicenter locations to the nearest 0.1° . The solid line in the vicinity of New Madrid indicates the location of the linear trend of microearthquake epicenters reported by Stauder *et al.* (1977) and Stauder (1982). The arrows indicating strike-slip and thrust fault mechanisms along these linear trends of epicenters are inferred from the focal mechanisms of Herrmann and Canas (1978). The contours shows the Bouguer gravity anomaly (in mGal) from the geologic corrected regional gravity map presented by Cordell (1977).

small percentage of intraplate earthquakes in midcontinent North America which appear not to be related to major buried structures.

IDENTIFICATION OF THE NEW MADRID RIFT COMPLEX

The New Madrid Rift Complex can be broadly correlated with a linear positive gravity anomaly (Figure 1) trending roughly northeastward along the axis of the upper Mississippi Embayment. The anomaly extends north of the Embayment and broadens near the junction of the arms of the New Madrid Rift Complex. Ervin and McGinnis (1975) and Cordell (1977) interpreted this anomaly to be due to a mass excess in the lower crust caused by intrusion associated with late Precambrian rifting during the formation of the Reelfoot Rift. From Figure 1, it can be seen that near the northern end of the linear gravity anomaly, the anomaly splits into lobes approximately following the outline of the inferred rift complex. More detailed definition of the configuration of the rift complex is provided by detailed gravity and magnetic anomaly maps as presented by Hildenbrand et al. (1977, 1982) and Braile et al. (1982a,b). The characteristic anomalies defining the Rift Complex are correlative positive gravity and magnetic anomalies (many of which are nearly circular) which are approximately coincident with the edges of the rift complex. In some locations, strong linear gradients in the gravity or magnetic field are also related to the edge of the buried rift. Within the rift complex, the gravity and magnetic anomaly expression is generally more subdued reflecting a deeper depth to basement (Hildenbrand et al., 1982). Examples of gravity and magnetic anomalies associated with a portion of the New Madrid Rift Complex are shown in Figures 2 and 3.

The depth to magnetic basement interpretation of Hildenbrand et al.

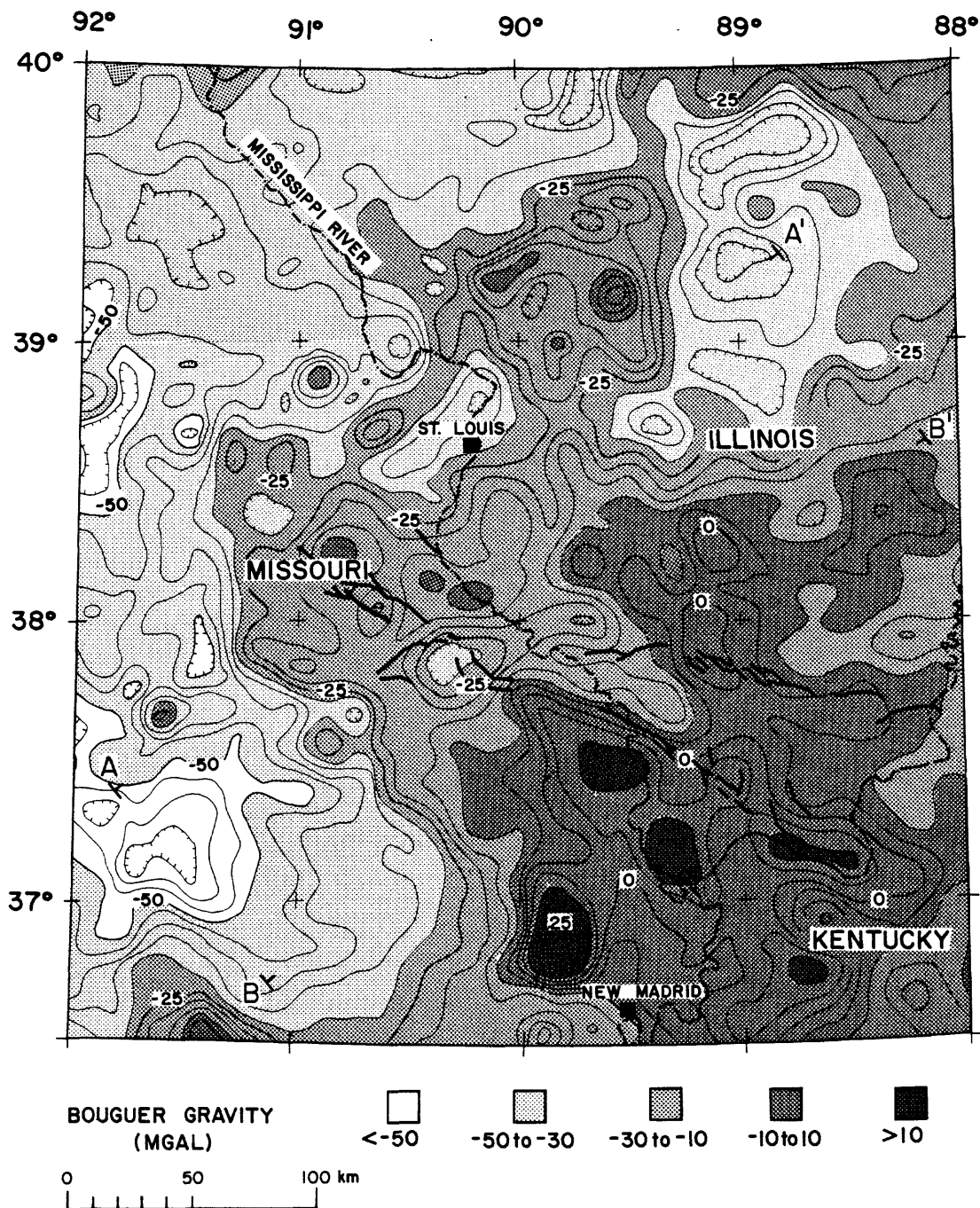


Figure 2. Simple Bouguer gravity anomaly map of the upper Mississippi Embayment area. Contour interval is 5 mGal. Shading interval is 20 mGal. Heavy lines are faults associated with the Cottage Grove and St. Genevieve Fault Zones. Short-wavelength positive anomalies and high gradient zones delineate the approximate edge of the St. Louis Arm of the New Madrid Rift Complex. The gravity data are from Keller *et al.* (1980). Figure from Braile *et al.*, (1982b).

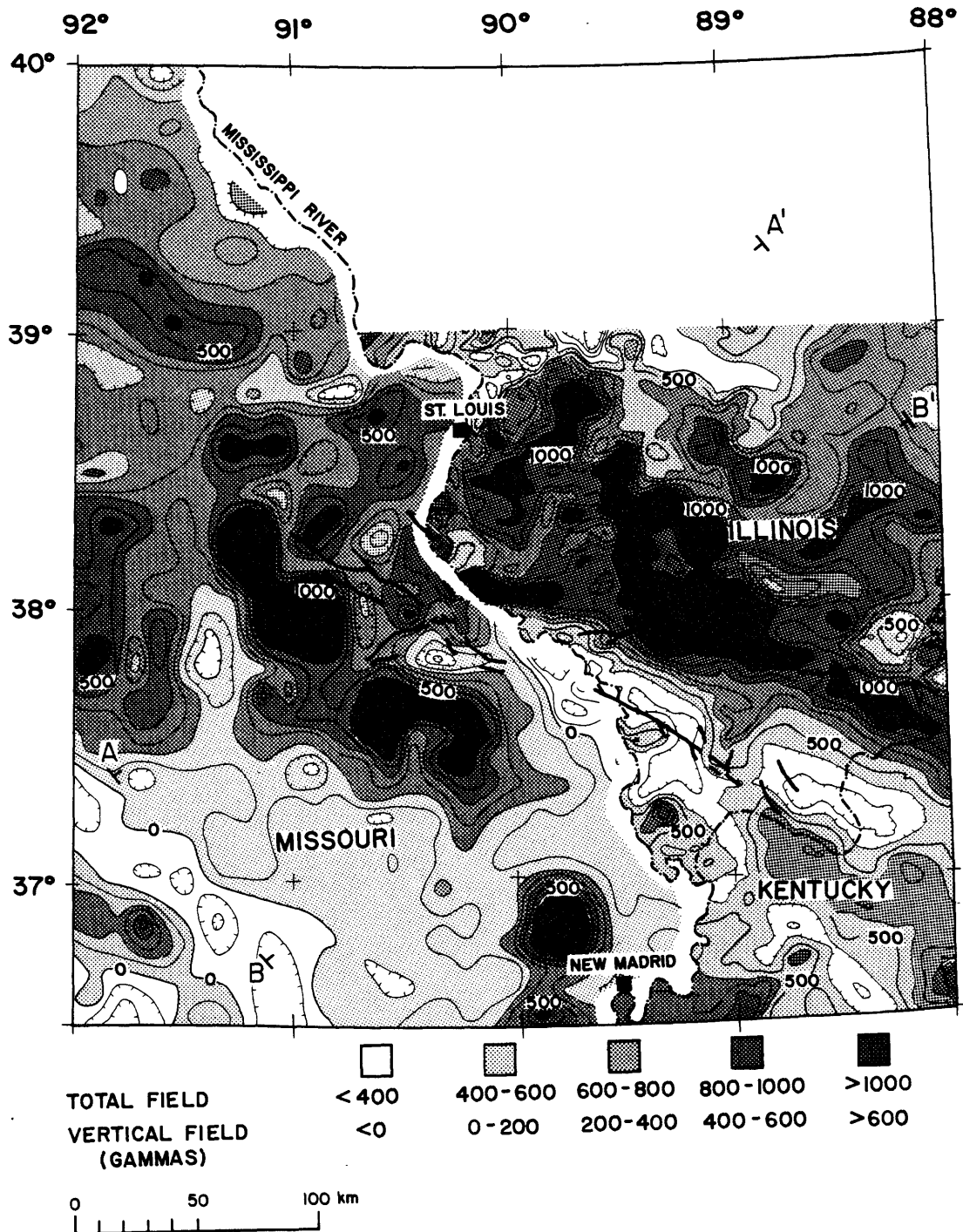


Figure 3. Magnetic anomaly map of the upper Mississippi Embayment area. Data east of the Mississippi River (border between Illinois and Missouri) are total field aeromagnetic values from Johnson *et al.* (1980). Data in Missouri are averaged (over a ten by ten km grid), vertical field, ground magnetic data from Buehler (1941). Contour interval is 100 nT (gammas). Shading interval is 200 nT. Heavy lines are faults associated with the Cottage Grove and St. Genevieve Fault Zones. The prominent short-wavelength anomalies, approximately 100 km on either side of the Mississippi River, mark the approximate edge of the St. Louis Arm of the New Madrid Rift Complex. Figure from Braile *et al.* (1982b).

(1982) suggested the presence of boundary faults associated with the edges of the Reelfoot Rift. Seismic reflection data in the Reelfoot area (Zoback et al., 1980; Hamilton and Zoback, 1982; Sexton et al., 1982) have also been used to identify faults within the rift.

Recently, a seismic reflection profiling experiment conducted in the Wabash River Valley in southern Illinois and southern Indiana near the margin of the inferred southern Indiana arm of the New Madrid Rift Complex (Figure 1) has provided clear evidence for late Precambrian to early Paleozoic faulting associated with the New Madrid Rift Complex. An example of these data is shown in Figure 4 from Sexton et al. (1984) for portions of two seismic reflection record sections centered on the Wabash River (Figure 5). The seismic sections (Figure 4) show good reflections from Paleozoic stratigraphic units and allow identification of the small-offset (20 to 50 meters) Wabash River Valley faults. In addition, the record sections provide evidence for a thick section of pre-Mt. Simon layered rocks existing within a fault-bounded graben beneath the Illinois Basin. A schematic cross section based on the seismic reflection data of Sexton et al. (1984), as well as gravity and magnetic interpretations, across the Southern Indiana Arm of the New Madrid Rift Complex is shown in Figure 6. Two stages of normal fault activity are indicated by these data. Major graben-bounding faults formed in late Precambrian to early Cambrian time. The grabens are filled with pre-Mt. Simon layered rocks. A generally conformable sequence of Paleozoic sedimentary rocks follows with the upper boundary of the sequence being a post-Pennsylvanian unconformity. Relatively minor faulting evidenced by the Wabash Valley Fault System followed. Although we do not have equivalent, detailed seismic reflection data in other areas, the representation of one of the arms of the New Madrid

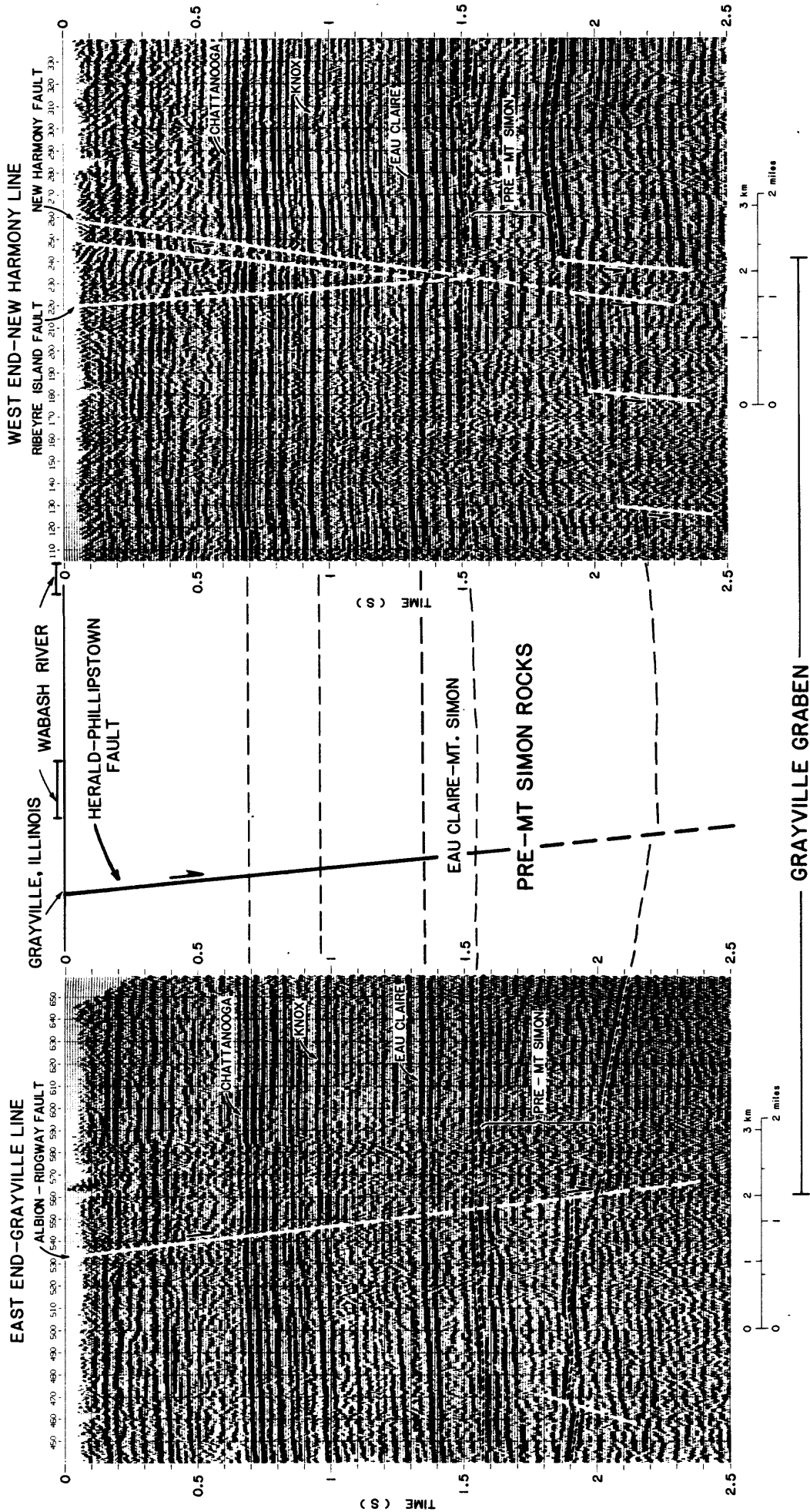


Figure 4. Seismic reflection record section (Sexton *et al.*, 1984) for an east-west line across the Wabash River in southern Illinois and southern Indiana. The surface location of the Wabash Valley Faults (Albion-Ridgway, Harold-Phillipstown, Ribeyre Island, and New Harmony Faults) is from Bristol and Treworgy (1979) and Ault *et al.* (1980). The depth to the Eau Claire reflector is approximately 3.6 km below sea level and to the prominent faulted reflector below the pre-Mt. Simon layered rocks approximately 5.2 to 6.2 km. Vertical exaggeration varies, but is approximately 1.2.

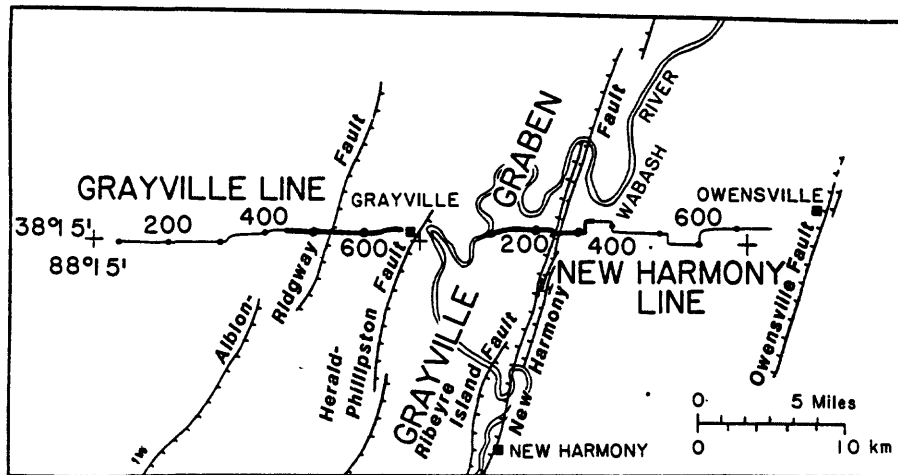


Figure 5. Index map of the southern Illinois and southern Indiana area surrounding the Wabash River for the seismic reflection record sections illustrated in Figure 4. The seismic reflection lines are shown by the solid lines with small dots every 100 source point locations. The heavy lines indicate the locations of the sections which are shown in Figure 4.

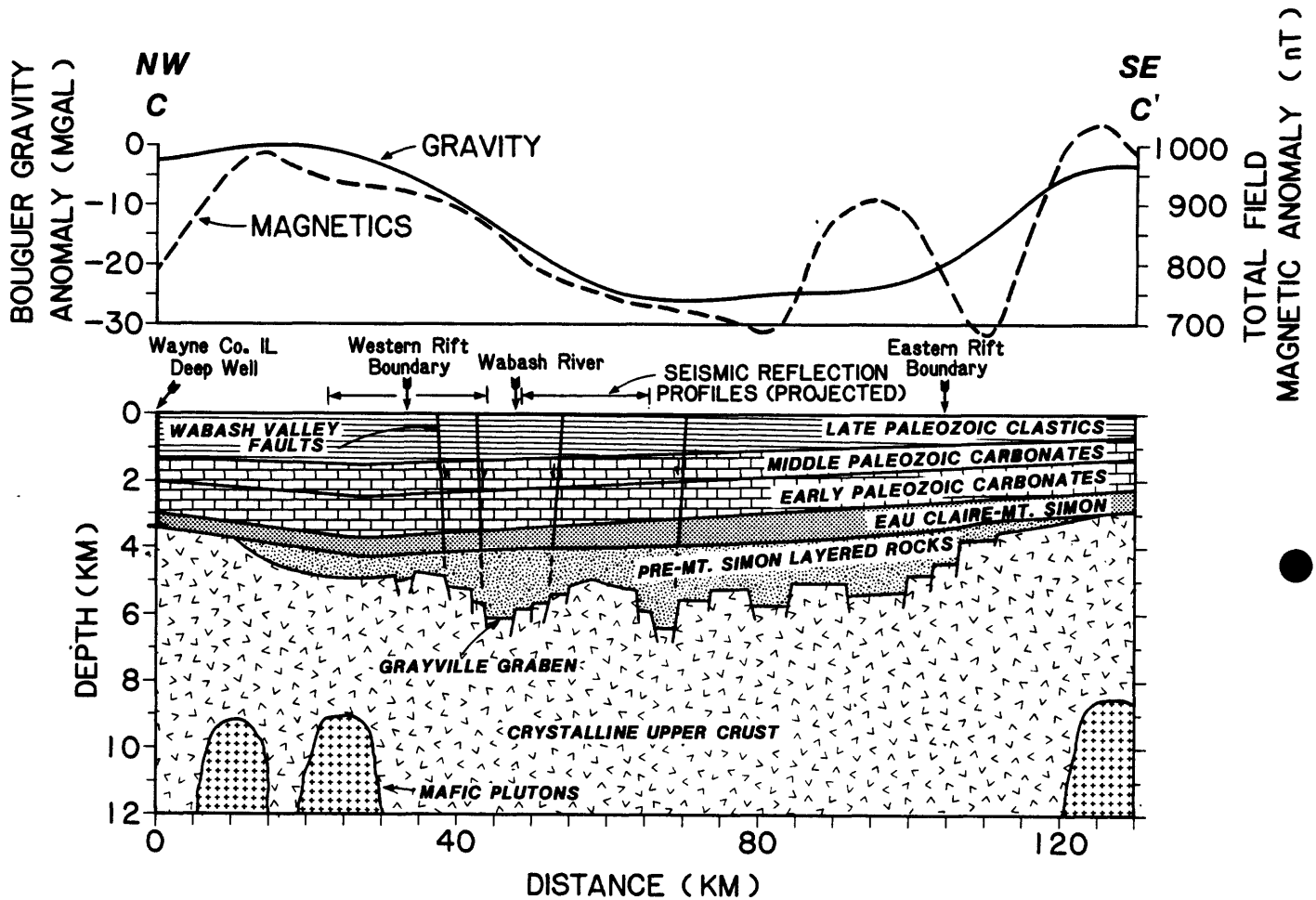


Figure 6. Schematic diagram illustrating the geologically and geophysically determined configuration of Phanerozoic sedimentary rocks and crystalline basement beneath the Southern Indiana Arm of the New Madrid Rift Complex (Sexton *et al.*, 1984). The cross section is along a northwest to southeast profile through the area shown on Figure 5.

Rift Complex, as illustrated in Figure 6, is consistent with the interpretations in the Reelfoot area and we expect that other sections of the rift complex will have a similar configuration.

Seismic refraction data are also available which support the interpretation of a buried rift complex beneath the northern Mississippi Embayment area. McCamy and Meyer (1966) discovered that an anomalous, basal high-velocity layer existed in the crust beneath the upper Mississippi Embayment. Recent refraction (Mooney *et al.*, 1983) and surface wave (Austin and Keller, 1982) studies have better defined the extent of this high-velocity layer and correlated it with the excess mass in the crust required to explain the gravity data. Mooney *et al.* (1983) also have interpreted a low-velocity layer beneath the Paleozoic carbonates in the Reelfoot Rift area which they suggest is due to late Precambrian to early Paleozoic graben-filling sedimentary rocks. Baldwin (1980) utilized refraction data in southern Indiana to suggest a similar increased thickness of sedimentary rocks in the southern Indiana Arm of the rift complex. He also found that the basement beneath one of the rift margin gravity and magnetic anomalies exhibited an anomalously high seismic velocity.

TECTONIC EVOLUTION OF THE NEW MADRID SEISMIC ZONE

Hinze *et al.* (1980) and Braile *et al.* (1982b) argued that the New Madrid Seismic Zone is related to a late Precambrian rift and that the origin of this rift and its subsequent tectonic evolution has been intimately related to the plate tectonic activity of the North American continent. This view has provided a plate tectonics framework for the contemporary intraplate seismicity of the New Madrid Seismic Zone, as well as the basis for understanding the geologic history of the region.

Although the basic conclusions of these studies are not changed here, much additional evidence for this tectonic evolution has been gathered in the past few years and a more detailed picture of the geological history of the midcontinent region of the North American craton and its relationship to plate interactions along the eastern and southern margins of the continent are now available. The data indicate a causal relationship between plate tectonic activities of the North American craton and tectonism and sedimentation in the New Madrid area at the interior of the craton. The New Madrid Rift Complex, a failed rift or aulacogen, influenced the geologic history of this region since late Precambrian time. It has controlled sedimentation, drainage of major river systems, and contemporary earthquake activity, as well as possibly localizing ore deposits. This control appears to have been exercised by two properties of the rift complex which were produced at its formation. Firstly, a mass excess, probably due to intrusion of mafic rocks, exists within the crust along the rift zone. This mass excess is clearly reflected in the linear positive gravity anomalies (Figure 1). Under appropriate thermal and stress conditions, this mass excess has resulted in periodic subsidence of the craton in the New Madrid region, thus influencing sedimentation and the drainage of major river systems. Secondly, the deep-seated normal faults associated with the initial rifting of the New Madrid Rift Complex have served as zones of weakness and have localized intrusive activity in late Paleozoic and Mesozoic time. Heyl (1972) showed that intrusives and ore bodies in the midcontinent area are related with structures which we now associate with the buried rifts. Faults within the rift provided a means for reactivation in later phases of faulting, such as in the Wabash Valley Fault System in post-Pennsylvanian time. They may also be the fault

planes related to the contemporary earthquake activity in the New Madrid Seismic Zone.

The stratigraphy of Paleozoic rocks in the Illinois basin and interpretation of deep seismic reflection results (such as those shown in Figure 4) indicate that the rifting of the New Madrid Rift Complex occurred prior to deposition of the basal clastic sedimentary rock that is characteristic of midcontinent North America known as the Mt. Simon formation of late Cambrian time. Thus, the initial rifting event was either latest Precambrian or earliest Paleozoic. Pre-Mt. Simon rocks are largely confined to the area within or immediately adjacent to the rift complex and are interpreted to be contemporaneous with rifting of the New Madrid Rift Complex. Adjacent areas were largely topographic highs as evidenced by the fact that Mt. Simon sedimentary rocks typically rest on crystalline basement (Schwalb, 1982). Subsequently, the mass excess in the crust beneath the New Madrid Rift Complex caused subsidence during Paleozoic time resulting in sedimentary basins above the rift complex. Figure 7 shows isopach data for early Paleozoic sedimentary units which indicate a significant thickening of the formations approximately coincident with sections of the New Madrid Rift Complex. Subsidence of the area generally persisted throughout Paleozoic time with thickened sedimentary units in the Illinois basin and the Reelfoot Basin - a trough between the Arcoma and Black Warrior basins underlying what is presently the Mississippi Embayment (Figure 8).

After a period of uplift and erosion in Mesozoic time, subsidence of the southern part of the New Madrid Rift Complex has continued adjacent to the downwarping coastal plain causing the Mississippi Embayment (Figure 8). The subsidence and structural control of the underlying

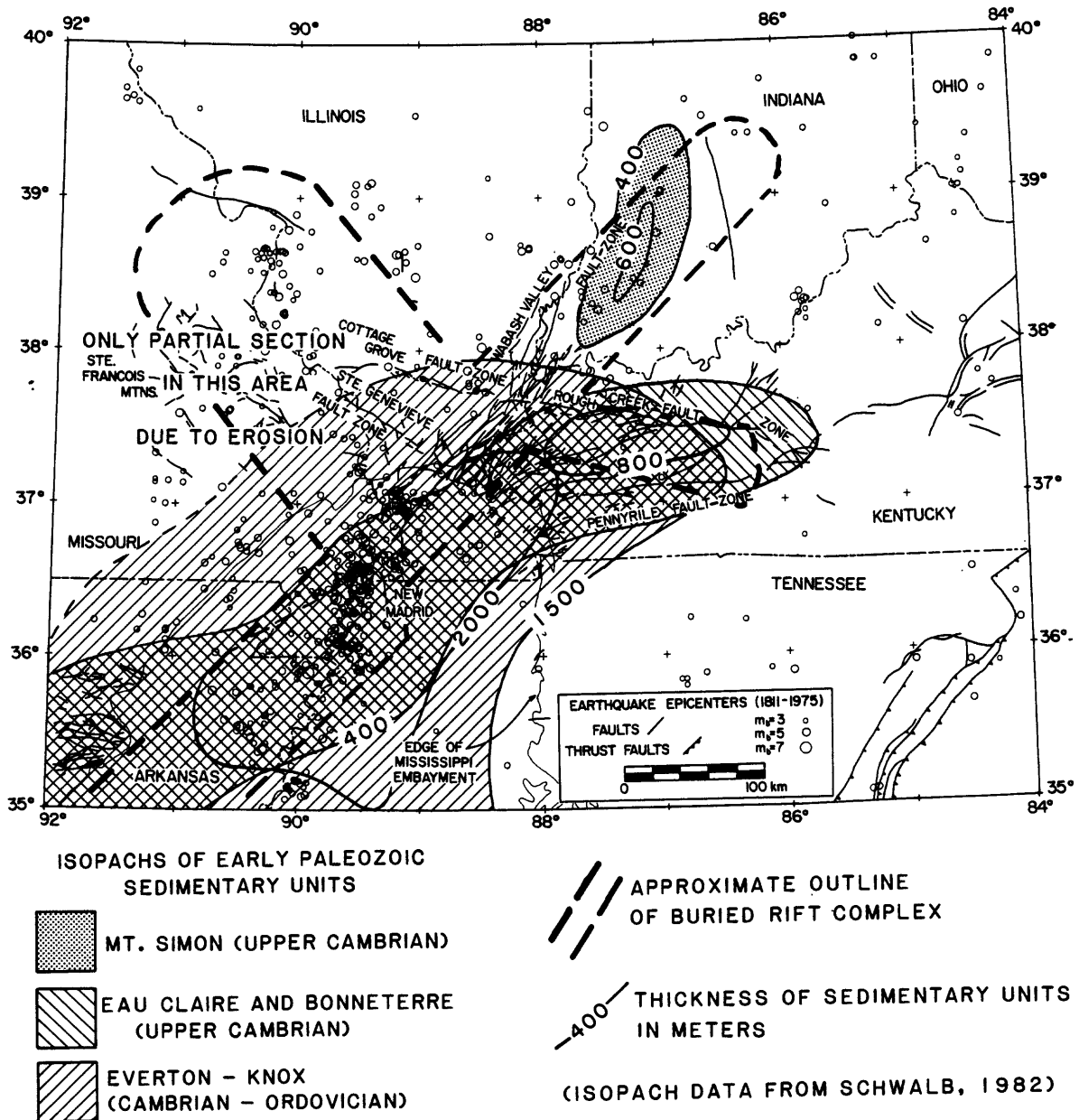


Figure 7. Index map of the New Madrid area showing isopachs of early Paleozoic sedimentary rocks after Schwalb (1982). Additional features are as described in Figure 1.

SEDIMENTARY BASINS, MAJOR RIVER SYSTEMS, REGIONAL POSITIVE GRAVITY ANOMALY AND THE NEW MADRID RIFT COMPLEX

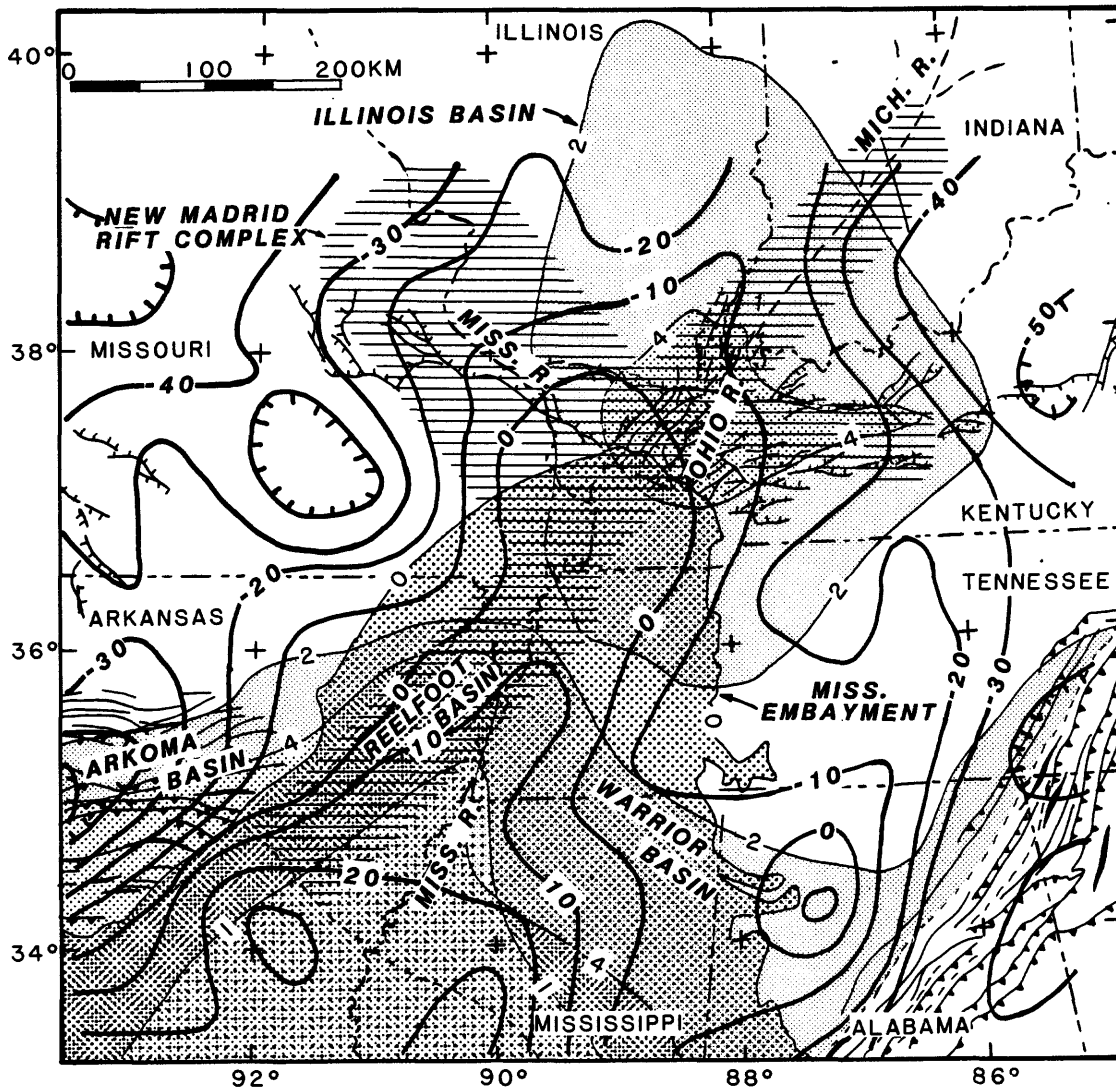


Figure 8. Map of the upper Mississippi Embayment area showing Paleozoic sedimentary basins (contours are depth to basement in km for the Paleozoic sedimentary rocks and depth to base of the Cretaceous sediments for the Mississippi Embayment; the zero contour marks the edge of the embayment), the geologic corrected Bouguer gravity anomaly data of Cordell (1977), the locations of major river systems which have been structurally controlled and the approximate outline of the New Madrid Rift Complex. The sedimentary basins containing Paleozoic rocks are shown with the small dot pattern. Cretaceous to present sedimentary rocks in the Mississippi Embayment are shown with the large dot pattern. Stratigraphic data are from Schwalb (1982) and Buschbach (1983).

faults within the rift complex have also served to control the drainage of major river systems for tens to hundreds of millions of years. As illustrated in Figure 8 and demonstrated by Potter (1978), the lower Mississippi River has been nearly in its present position approximately coincident with the Reelfoot section of the New Madrid Rift Complex since early Mesozoic time. Potter also showed that the predecessor to the Ohio River, which he called the Michigan River System flowed southwestward approximately down the center of the inferred Southern Indiana Arm of the New Madrid Rift Complex (Figure 8). The lower part of the Ohio River was part of this river system, which like the lower Mississippi, has followed approximately its present course for the last 250 million years. The locations of the present upper Ohio and Wabash Rivers are due to disruption by Pleistocene glaciation. The upper Mississippi River, which flows down the center of the St. Louis Arm of the New Madrid Rift Complex, has been interpreted by Flint (1941) to be structurally controlled and approximately in the same position since at least mid-Tertiary time.

The tectonic evolution of the New Madrid Rift Complex and its relationship to adjacent plate tectonic activity since the late Precambrian are illustrated in Figures 9 and 10. Plate reconstructions of a portion of the North American craton and adjacent plates which have influenced its history are shown in Figure 9. Schematic cross sections (Figure 10) through the New Madrid Rift Complex (approximately northwest-southeast) illustrate the geologic activity of the rift complex related to plate interactions of the North American craton. The configuration of the New Madrid Rift Complex through time and the plate reconstructions (Figure 9) are modified and updated from the presentations of Hinze et al. (1980) and Keller et al. (1983). The

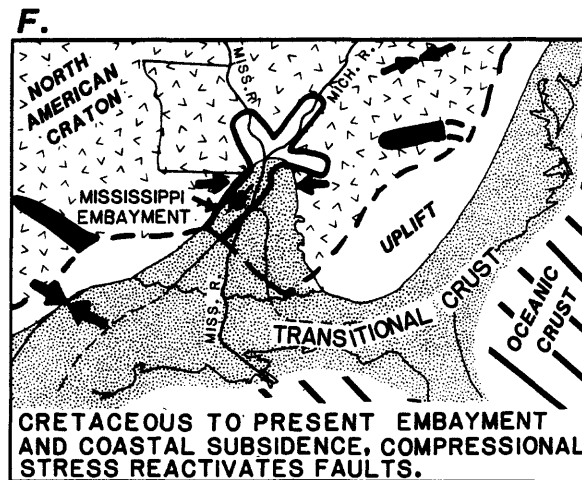
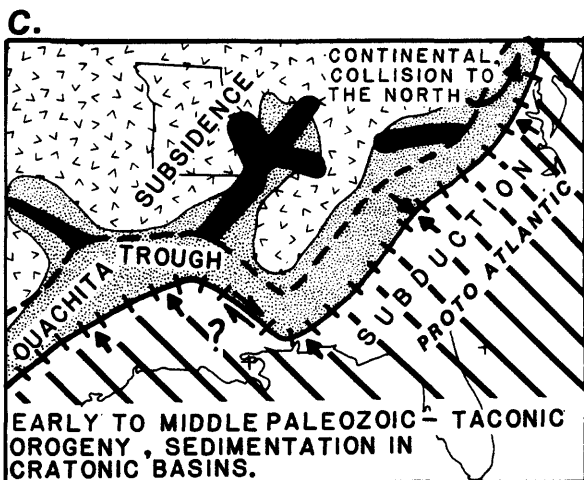
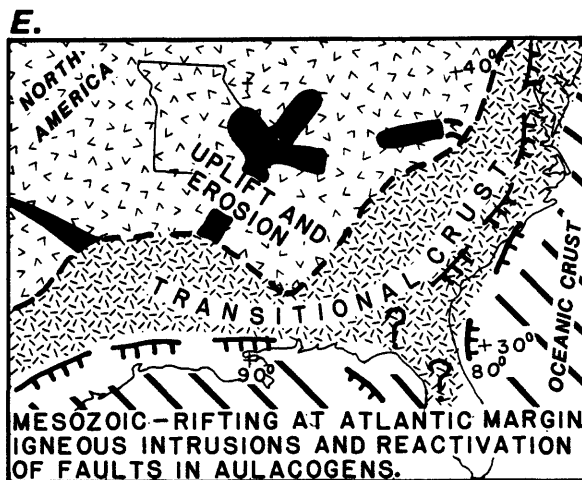
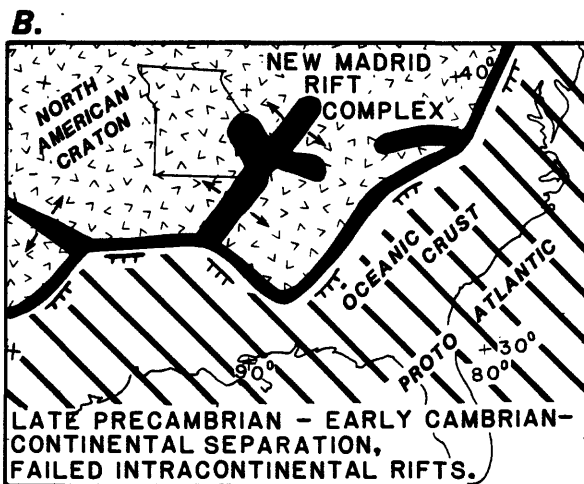
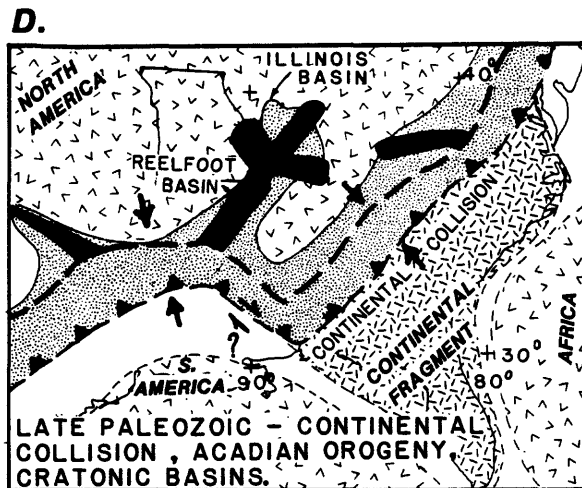
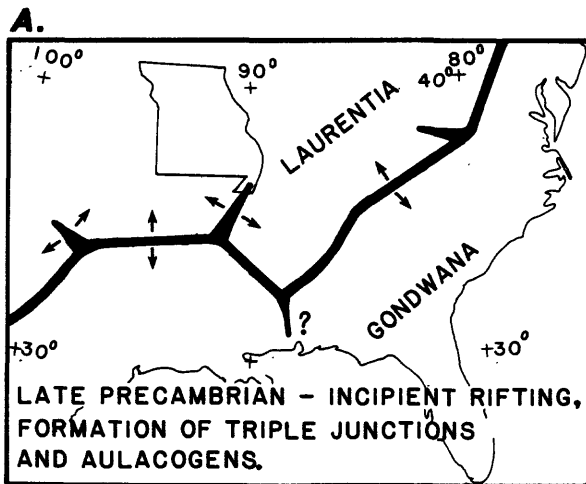


Figure 9. Schematic diagrams illustrating the plate reconstruction of the North American craton and interactions with adjacent plates and geologic activity of the New Madrid Rift Complex during the last 600 million years. The outline of the State of Missouri is shown for location and approximate scale.

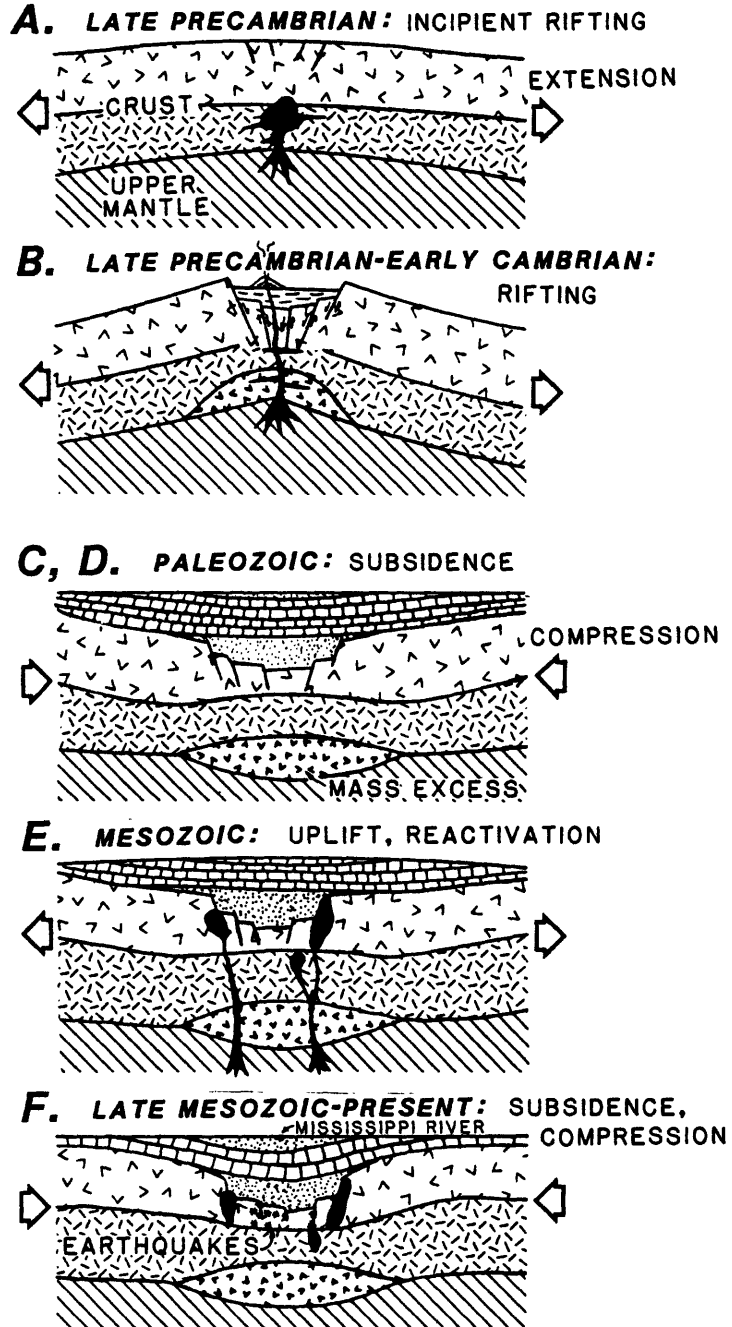


Figure 10. Schematic cross sections for a northwest-southeast profile through the New Madrid Rift Complex illustrating the evolution of the rift complex and associated cratonic basins through time. Stages of development shown in parts A through F are related approximately to the map views illustrated in the corresponding diagrams in Figure 9.

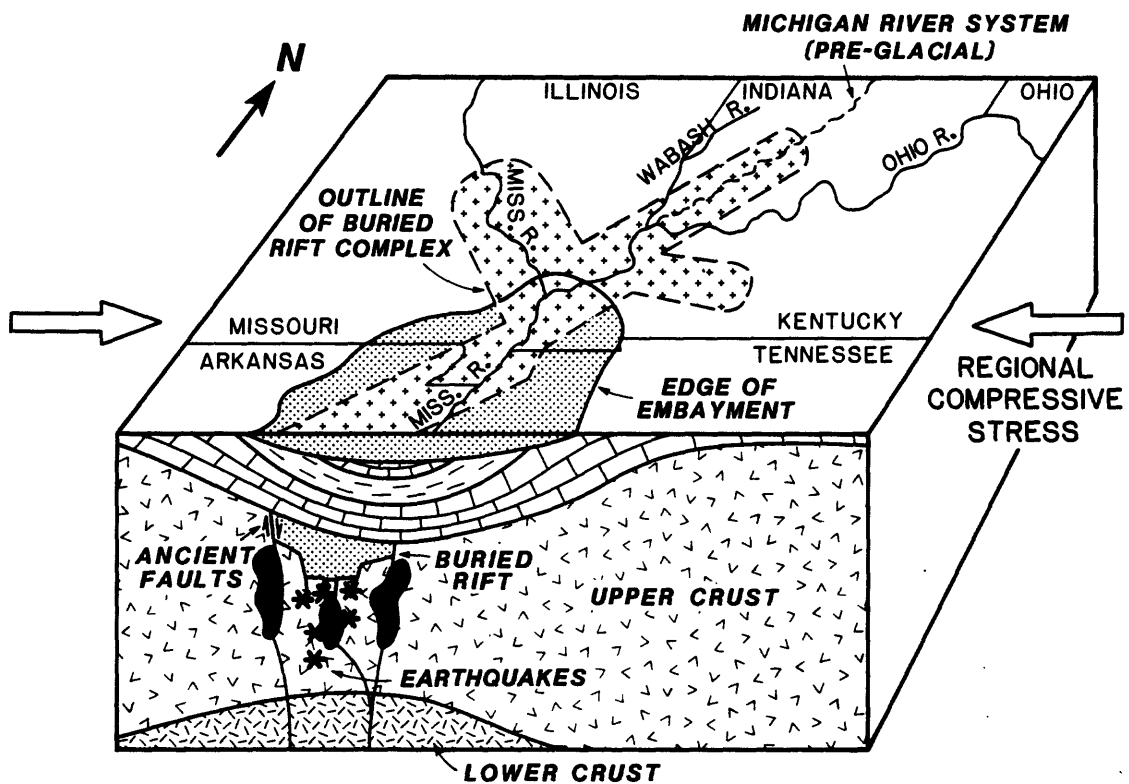


Figure 11. Block diagram illustrating the present configuration of the buried New Madrid Rift Complex. The structurally controlled rivers, Paleozoic rocks in cratonic sedimentary basins, and the Mississippi Embayment, all associated with the buried rift complex, are also shown. Dark areas indicate intrusions near the edge of the buried rift. An uplifted and possibly anomalously dense lower crust is suggested as the cause of the linear positive gravity anomaly associated with the upper Mississippi Embayment.

local geology and structural evolution of the area surrounding the New Madrid Rift Complex are based primarily on stratigraphic data (Schwalb, 1982) and the interpretation of the rift complex determined from geophysical data as described previously. The plate reconstructions are based primarily on paleomagnetic (LeFort and Van der Voo, 1981; Van der Voo, 1982) and geological and geophysical (Keller and Cebull, 1973; Morris, 1974; Cook et al., 1980; Burke, 1980; Lillie et al., 1983) data related to the plate interactions of the North American craton during the past 600 million years.

The tectonic development of the New Madrid Rift Complex (Figures 9 and 10) indicates the important control of the rift complex on the geologic history of this portion of the North American craton, as well as the connection between cratonic tectonism and plate margin interaction through time. After formation of the rift during continental breakup (Figures 9A and B, and 10A and B), the increased mass of the crust beneath the rift complex caused subsidence during times of compression associated with either continent-ocean subduction or continent-continent collision along the eastern and southern margins of the North American craton. During early Mesozoic rifting of the continents (Figures 9E and 10E), the craton was undergoing uplift and erosion resulting in the broad unconformity which is observed in the cratonic basins of North America and erosion of considerable thicknesses of sedimentary rocks over intracontinental arches such as the Pascola Arch centered near southeastern Missouri. Reactivation of faults associated with the New Madrid Rift Complex caused structural uplifts and intrusion of plutons near the margins of the rift complex. Since Cretaceous time (Figures 9F and 10F), the eastern margin of the North American craton has been the trailing edge of a rifted continental

margin and the continent has been under a regional compressive stress. The New Madrid Rift Complex has continued to exert control on depositional patterns as evidenced by the subsidence of the Mississippi Embayment and the location of the drainage of major river systems. The correlation of earthquake epicenters with the location of the buried rift complex suggests that the earthquakes in the New Madrid Seismic Zone are the result of slippage along pre-existing zones of weakness inherited from the late Precambrian rift. The fault planes are reactivated by the contemporary stress field which is approximately east-west compression in the New Madrid area (Haimson, 1976; Zoback and Zoback; 1980, 1981).

The correlation of cratonic basin subsidence with compression of the continental crust caused by continental margin subduction and of cratonic uplift with extension in the crust (Figures 9 and 10) is consistent with a model for cratonic basin subsidence suggested by DeRito et al. (1983). These authors show that many cratonic basins occur over ancient rift zones and that these rift zones are recognizable by a positive linear gravity anomaly. DeRito et al. (1983) suggest that the driving force for subsidence of these basins is the isostatically uncompensated ancient mass excess. Their numerical modeling of lithospheric flexure for a crust containing a mass excess indicates that periods of subsidence due to the mass excess will be correlated with periods of horizontal compressional stress in the lithosphere and that relaxation of the compressional stress, such as during a period of rifting along a continental margin adjacent to the craton, may allow the cratonic region to rebound producing uplift and erosion. Their model appears to qualitatively fit the observations for the New Madrid area and helps explain the continued influence of the rift complex

through time.

Although not all ancient intracontinental rifts are reactivated as contemporary seismic zones, cratonic basins are commonly underlain by rifts (DeRito et al., 1983). Other Precambrian rifts beneath cratonic basins have been identified in southern Alberta (Kanasewich, 1968), the Michigan Basin (Hinze et al., 1975; Brown et al., 1982), the Rome trough (Ammerman and Keller, 1979), the southern Oklahoma aulacogen (Burke and Dewey, 1973; Brewer et al., 1983), and the Lake Superior basin and midcontinent geophysical anomaly (King and Zietz, 1971; Ocola and Meyer, 1973; Wold and Hinze, 1982). These rifts may have had a similar tectonic history to that displayed in the New Madrid Rift Complex. Each has certainly had a continued influence on the geological evolution of the associated cratonic basin.

CONCLUSIONS

The New Madrid Rift Complex has had a significant and consistent influence on tectonism of the North American craton since its formation in late Precambrian time. It has controlled sedimentation by causing subsidence in cratonic basins, influenced the location of major river systems, localized intrusive activity during reactivation of rift structures, and is probably the cause of contemporary earthquake activity. The geologic and tectonic activity of this intracratonic region are also correlated with plate interaction events of the North American plate. The history of the New Madrid Rift Complex through time provides a plate tectonic framework for understanding the formation of cratonic basins associated with the rift complex and intraplate seismicity of the New Madrid Seismic Zone. Thus, the New Madrid Rift Complex, formed by plate tectonic interactions about 600 million years

ago, has influenced the geologic activity of the midcontinent in response to plate interactions at the margin of the North American plate. And, it is plate motions which are presently producing the compressive stress within the North American craton (Zoback and Zoback, 1980) which probably cause the reactivation of faults within the New Madrid Seismic Zone.

ACKNOWLEDGEMENTS

This research was supported by the U.S. Nuclear Regulatory Commission under Contracts No. NRC-04-81-195-01 and NRC-04-80-224. We are grateful to many graduate students who have assisted in the collection, compilation and processing of data upon which many of the interpretations contained in this paper are based. We thank Paul Morgan for a number of helpful comments. We greatly appreciate the many useful discussions with colleagues of the 'New Madrid Study Group' concerning the seismotectonics of the New Madrid area.

REFERENCES

- Ammerman, M.L. and G.R. Keller, Delineation of Rome trough in eastern Kentucky with gravity and deep drilling data, Am. Assoc. Pet. Geol. Bull., 63, 341-353, 1979.
- Ault, C.H., D.M. Sullivan and G.T. Tanner, Faulting and Posey and Gibson Counties, Indiana, Proc. Indiana Acad. of Sci., 89, 275-289, 1980.
- Austin, C.B. and G.R. Keller, A crustal structure study of the Northern Mississippi embayment, in Investigations of the New Madrid, Missouri, Earthquake Region, F.A. McKeown and L.C. Pakiser (eds.), Geological Survey Professional Paper 1236, 83-93, 1982.
- Baldwin, James L., A crustal seismic refraction study in southwestern Indiana and southern Illinois, M.S. Thesis, West Lafayette, IN, Purdue University, 1980.
- Braile, L.W., W.J. Hinze, G.R. Keller and E.G. Lidiak, The north-eastern extension of the New Madrid Seismic Zone, in Investigations of the New Madrid, Missouri, Earthquake Region, F.A. McKeown and L.C. Pakiser (eds.), Geological Survey Professional Paper 1236, 175-184, 1982a.
- Braile, L.W., G.R. Keller, W.J. Hinze and E.G. Lidiak, An ancient rift complex and its relation to contemporary seismicity in the New Madrid Seismic Zone, Tectonics, 1, 225-237, 1982b.
- Braile, L.W., W.J. Hinze, J.L. Sexton, G.R. Keller and E.G. Lidiak, Seismicity and tectonics of the midcontinent United States, Proceedings Third International Earthquake Microzonation Conference, Seattle, Washington, June 28-July 1, 25-38, 1982c.
- Brewer, J.A., R. Good, J.E. Oliver, L.D. Brown and S. Kaufman, COCORP profiling across the Southern Oklahoma aulacogen: Overthrusting of the Wichita Mountains and compression within the Anadarko Basin, Geology, 11, 109-114, 1983.
- Bristol, H.M. and J.D. Treworgy, The Wabash Valley Fault System in Southeastern Illinois, Circ. Ill. State Geol. Surv., 509, 1979.
- Brown, L., L. Jensen, J. Oliver, S. Kaufman and D. Steiner, Rift structure beneath the Michigan Basin from COCORP profiling, Geology, 10, 645-649, 1982.
- Buehler, H.A., Magnetic map of Missouri, Scale 1:500,000, Mo. Geol. Surv. and Water Resources, Rolla, Mo., 1943.
- Burke, K., Intracontinental rifts and aulacogens, in Continental Tectonics, National Academy of Sciences, Washington, DC, 42-49, 1980.

- Burke, K. and J.F. Dewey, Plume-generated triple junctions: Key indicators in applying plate tectonics to old rocks, J. Geol., 81, 406-433, 1973.
- Buschbach, T.C., New Madrid seismotectonic study, U.S. Nuclear Regulatory Commission Report, NUREG/CR-3173, 1983.
- Cook, F.A., L.D. Brown and J.E. Oliver, The Southern Appalachians and the growth of continents, Sci. Am., 243, 156-168, 1980.
- Cordell, L., Regional positive gravity anomaly over the Mississippi embayment, Geophys. Res. Lett., 4, 285-287, 1977.
- DeRito, R.F., F.A. Cozzarelli and D.S. Hodge, Mechanisms of subsidence of ancient cratonic rift basins, Tectonophysics, 94, 141-168, 1983.
- Ervin, C.P. and L.D. McGinnis, Reelfoot rift: Reactivated precursor to the Mississippi embayment, Geol. Soc. Am. Bull., 86, 1287-1295, 1975.
- Flint, R.F., Ozark segment of Mississippi River, J. Geol., 49, 626-640, 1941.
- Haimson, B.C., Crustal stress in the continental United States as derived from hydrofracturing tests, in The Earth's Crust, J.G. Heacock (ed.), Am. Geophys. Union Geophys. Monogr. Ser. vol. 20, 576-592, 1976.
- Hamilton, R.M. and D. Zoback, Tectonic features of the New Madrid seismic zone from seismic reflection profiles, in Investigations of the New Madrid, Missouri, Earthquake Region, F.A. McKeown and L.C. Pakiser (eds.), Geological Survey Professional Paper 1236, 55-82, 1982.
- Herrmann, R.B. and J.A. Canas, Focal mechanisms studies in the New Madrid seismic zone, Bull. Seismol. Soc. Am., 68, 1095-1102, 1978.
- Heyl, A.V., The 38th parallel lineament and its relationship to ore deposits, Econ. Geol., 67, 879-894, 1972.
- Heyl, A.V. and F.A. McKeown, Preliminary seismotectonic map of central Mississippi valley and environs, Miscellaneous Field Studies, Map MF-1011, U.S. Geol. Surv., Reston, VA, 1978.
- Hildenbrand, T.G., M.F. Kane and W. Stauder, Magnetic and gravity anomalies in the northern Mississippi embayment and their spatial relation to seismicity, Map MF-914, U.S. Geol. Surv., Reston, VA, 1977.

- Hildenbrand, T.G., M.F. Kane and J.D. Hendricks, Magnetic basement in the upper Mississippi embayment region - A preliminary report, in Investigations of the New Madrid, Missouri, Earthquake Region, F.A. McKeown and L.C. Pakiser (eds.), Geological Survey Professional Paper 1236, 39-54, 1982.
- Hinze, W.J., R.L. Kellogg and N.W. O'Hara, Geophysical studies of basement geology of Southern Peninsula of Michigan, Am. Assoc. Petrol. Geol. Bull., 59, 1562-1584, 1975.
- Hinze, W.J., L.W. Braile, G.R. Keller and E.G. Lidiak, Models for mid-continent tectonism, in Continental Tectonics, National Academy of Sciences, Washington, DC, 73-83, 1980.
- Hinze, W.J., L.W. Braile, G.R. Keller and E.G. Lidiak, Models for mid-continent tectonism: An update, (in preparation), 1984.
- Johnson, R.W., Jr., C. Haygood, T.G. Hildenbrand, W.J. Hinze and P.M. Kunselman, Aeromagnetic map of the east-central midcontinent of the United States, U.S. Nuclear Regulatory Commission Report, NUREG/CR-1662, 1980.
- Kanasewich, E.R., Precambrian rift: Genesis of strata-bound ore deposits, Science, 161, 1002-1005, 1968.
- Kane, M.F., T.G. Hildenbrand and J.D. Hendricks, A model for the tectonic evolution of the Mississippi Embayment and its contemporary seismicity, Geology, 9, 563-567, 1981.
- Keller, G.R., D.R. Russell, W.J. Hinze, J.E. Reed and P.J. Geraci, Bouguer gravity anomaly map of the east-central Midcontinent of the United States, U.S. Nuclear Regulatory Commission Report, NUREG/CR-1663, 1980.
- Keller, G.R. and S.E. Cebull, Plate tectonics and the Ouachita System in Texas, Oklahoma and Arkansas, Geol. Soc. Am. Bull., 83, 1659-1666, 1973.
- Keller, G.R., E.G. Lidiak, W.J. Hinze and L.W. Braile, The role of rifting in the tectonic development of the midcontinent, U.S.A., Tectonophysics, 94, 391-412, 1983.
- King, E.R. and I. Zietz, Aeromagnetic study of the midcontinent gravity high of central United States, Geol. Soc. Am. Bull., 82, 2187-2208, 1971.
- LeFort, J-P. and R. Van der Voo, A kinematic model for the collision and complete suturing between Gondwanaland and Laurussia in the carboniferous, J. Geol., 89, 537-550, 1981.

- Lillie, R.J., K.D. Nelson, B. De Voogd, J.A. Brewer, J.E. Oliver, L.D. Brown, S. Kaufman and G.W. Viele, Crustal structure of Ouachita Mountains, Arkansas: A model based on integration of COCORP reflection profiles and regional geophysical data, Am. Assoc. Pet. Geol. Bull., 67, 907-931, 1983.
- McCamy, K. and R.P. Meyer, Crustal results of fixed multiple shots in the Mississippi Embayment, in The Earth Beneath the Continents, J.S. Steinhardt and T.J. Smith (eds.), Am. Geophys. Union Monogr. Ser. vol. 10, 370-381, 1966.
- McKeown, F.A., Hypothesis: many earthquakes in the central and south-eastern United States are causally related to mafic intrusive bodies, J. Res. U.S. Geol. Surv. 6, 41-50, 1978.
- Mooney, W.D., M.C. Andrews, A. Ginzburg, D.A. Peters and R.M. Hamilton, Crustal structure of the Northern Mississippi Embayment and a comparison with other continental rift zones, Tectonophysics, 94, 327-348, 1983.
- Morris, R.C., Sedimentary and tectonic history of the Ouachita Mountains, in Tectonics and Sedimentation, W.R. Dickinson (ed.), Soc. of Econ. Paleontologists and Mineralogists Special Publication No. 22, 120-142, 1974.
- Nuttli, O.W., The Mississippi valley earthquakes of 1811 and 1812, intensities, ground motion, and magnitudes, Bull. Seismol. Soc. Am., 63, 227-248, 1973.
- Nuttli, O.W., Seismicity in the central United States, Geol. Soc. Am. Rev. Eng. Geol., 4, 67-93, 1979.
- Nuttli, O.W., Damaging earthquakes of the central Mississippi valley, in Investigations of the New Madrid, Missouri, Earthquake Region, F.A. McKeown and L.C. Pakiser (eds.), U.S. Geological Survey Professional Paper 1236, 15-20, 1982.
- Ocola, L.D. and R.P. Meyer, Central North American rift system: 1. Structure of the axial zone from seismic and gravimetric data, J. Geophys. Res., 78, 5173-5194, 1973.
- Potter, P.E., Significance and origin of Big Rivers, J. Geol., 86, 13-33, 1978.
- Rankin, D.W., Appalachian salients and recesses: late Precambrian continental breakup and the opening of the Iapetus Ocean, J. Geophys. Res., 81, 5605-5619, 1976.
- Sbar, M.L. and L.R. Sykes, Contemporary compressive stress and seismicity in eastern North America: An example of intraplate tectonics, Geol. Soc. Am. Bull., 84, 1861-1882, 1973.
- Schwalb, H.R., Paleozoic geology of the New Madrid area, U.S. Nuclear Regulatory Commission Report, NUREG/CR-2909, 1982.

- Sexton, J.L., E.P. Frey and D. Malicki, High-resolution seismic-reflection surveying on Reelfoot scarp, northwestern Tennessee, in Investigations of the New Madrid, Missouri, Earthquake Region, F.A. McKeown and L.C. Pakiser (eds.), U.S. Geological Survey Professional Paper 1236, 137-150, 1982.
- Sexton, J.L., L.W. Braile, W.J. Hinze and M.J. Campbell, Evidence for a buried Precambrian rift beneath the Wabash Valley Fault Zone from seismic reflection profiling, submitted to Geophysics, 1984.
- Soderberg, R.K. and G.R. Keller, Geophysical evidence for deep basin in Western Kentucky, Am. Assoc. Pet. Geol. Bull., 65, 226-234, 1981.
- Stauder, W., M. Kramer, G. Fischer, S. Schaefer and S. Morrissey, Seismic characteristics of southeast Missouri as indicated by a regional telemetered microearthquake array, Bull. Seismol. Soc. Am., 66, 1953-1964, 1977.
- Stauder, W., Present-day seismicity and identification of active faults in the New Madrid seismic zone, in Investigations of the New Madrid, Missouri, Earthquake Region, F.A. McKeown and L.C. Pakiser (eds.), U.S. Geological Survey Professional Paper 1236, 21-30, 1982.
- Sykes, L.R., Intraplate seismicity, reactivation of pre-existing zones of weakness, alkaline magmatism, and other tectonism postdating continental fragmentation, Rev. Geophys. Space Phys., 16, 621-688, 1978.
- Van der Voo, R., Pre-Mesozoic paleomagnetism and plate tectonics, Ann. Rev. Earth Planet. Sci., 10, 191-220, 1982.
- Wold, R.J. and W.J. Hinze, (eds.), Geology and Tectonics of the Lake Superior Basin, Geol. Soc. of Am. Memoir 156, 1982.
- Zoback, M.D., R.M. Hamilton, A.J. Crone, D.P. Russ, F.A. McKeown and S.R. Brockman, Recurrent intraplate tectonism in the New Madrid seismic zone, Science, 209, 971-976, 1980.
- Zoback, M.D. and M.L. Zoback, State of stress and intraplate earthquakes in the United States, Science, 213, 96-104, 1981.
- Zoback, M.L. and M.D. Zoback, State of stress in the conterminous United States, J. Geophys. Res., 85, 6113-6156, 1980.

ANOMALOUS CRUST AND UPPER MANTLE PROPERTIES
IN THE NEW MADRID AREA

by

Brian J. Mitchell

Department of Earth and Atmospheric Sciences

Saint Louis University

St. Louis, MO 63156

James Kohsmann

Texaco Bellaire Research Laboratories

Bellaire, TX 77041

and

Haydar Al-Shukri

Department of Earth and Atmospheric Sciences

Saint Louis University

St. Louis, MO 63156

ABSTRACT

New teleseismic P-wave data recorded over a broad region including the New Madrid seismic zone are consistent with data obtained in an earlier study, and in addition, provide more detailed data pertaining to a much larger region. As found in the earlier work, lateral variations in velocity occur in both the crust and upper mantle, with lower than average values occurring beneath the most active portion of the seismic zone. In the broader area of the present study, however, other regions with equally low velocities are found which lie at some distance from the seismically active region. A band of low velocities in the crust passes through the most seismically active region in a NE-SW direction.

Average velocities in both the lower crust and upper mantle beneath the Ozark uplift are slightly faster than those beneath the central portion of the Mississippi Embayment at the same depths. This suggests that broad-scale variations in gravity correlate negatively with broad-scale variations in velocity in either the crust or upper mantle in this region.

Theoretical heat flow values were calculated for finite cylindrical intrusions with realistic material properties. We find that the emplacement of mafic intrusions with radial dimensions of a few tens of km and mid-Eocene age is one mechanism that can produce the anomalous heat flow patterns observed in the New Madrid region. Thermal shearing stresses produced by such hypothetical intrusions are also computed, assuming purely elastic behavior of the crust. They are predicted to be in the range of hundreds of bars 10 million years after the time of intrusion and in the range of several tens of bars 40 million years after that time for a 20-km deep intrusion of 20 km radius. These values are expected to be reduced if viscoelastic flow or inelastic behavior occurs in the crust or upper mantle. The maximum principle stresses for this model are predicted to be oriented in a radial direction from the intrusion axis at small distances and in a circumferential direction at larger distances.

INTRODUCTION

In a study of teleseismic P-wave residuals using stations of the Saint Louis University network, Mitchell et al. (1977) showed that compressional-wave velocities in the crust and mantle in the region sur-

rounding the New Madrid seismic zone can vary by as much as 5%. The lowest values were found to occur beneath the most seismically active portion of that region and to extend to depths of 100 km or more into the upper mantle. That study was limited by the relatively small spatial extent and large station spacing of the seismic network in operation at that time.

One purpose of the present study is to update results of that earlier work using additional stations which have recently begun operation. The new stations allow us to study crust and upper mantle velocities over a much larger area than before and to achieve a greater resolving power than had been previously possible. In addition, new compilations of gravity data for the New Madrid region have become available and it is now possible to compare lateral variations of our velocity models with the most recent Bouguer gravity maps.

In a more speculative aspect of this work, we will attempt to predict anomalous stresses in the crust of the New Madrid region, assuming that the low-velocity material in the crust and upper mantle beneath the seismic zone corresponds to a region which is occupied by a mafic igneous intrusion which was once molten. New methods (Kohsmann, 1983; Kohsmann and Mitchell, in preparation) now permit us to compute the temperature distribution and surface heat flow produced by a finite cylindrical intrusion embedded in an elastic medium. These calculations will yield stress as a function of time following the intrusion. If the crust and upper mantle behave viscoelastically over long intervals of time, or if the stresses have been partially relieved by inelastic processes, then real stresses may be much smaller than these calculated stresses.

THREE-DIMENSIONAL VELOCITY STRUCTURE

Most traditional studies of velocity structure yield plane-layered models in which the velocity of each layer is assumed to be uniform. Such studies have provided much of our knowledge of the seismic structure of the crust and upper mantle. The models obtained, however, are known to be only first-order approximations to true structure because the methods preclude the possibility of detecting lateral variations in velocity.

Aki et al. (1977) introduced a method, employing modern inversion theory and using residuals of teleseismic P-wave observations, to infer three-dimensional structure of the lithosphere. Mitchell et al. (1977) applied the method to the New Madrid region. The method begins with a plane-layered structure, based upon results from refraction studies, but allows each layer to be divided into a number of rectangular blocks, in each of which velocity can vary from the mean value in the layer. Ray paths from teleseismic events are traced through the model and velocities in the three-dimensional structure are obtained from a formal inversion of the observed P-wave residuals. Mitchell et al. (1977) obtained two three-dimensional models using blocks of a different size in each case. First, they used blocks which were 50-km square in horizontal cross section and which covered a region between latitudes of about 35.1°N and 38.2°N and between longitudes of about 88.3°W and 99.7°W . In a second inversion they used 30-km square blocks covering a region between latitudes of about 35.5°N and 37.7°N and between longi-

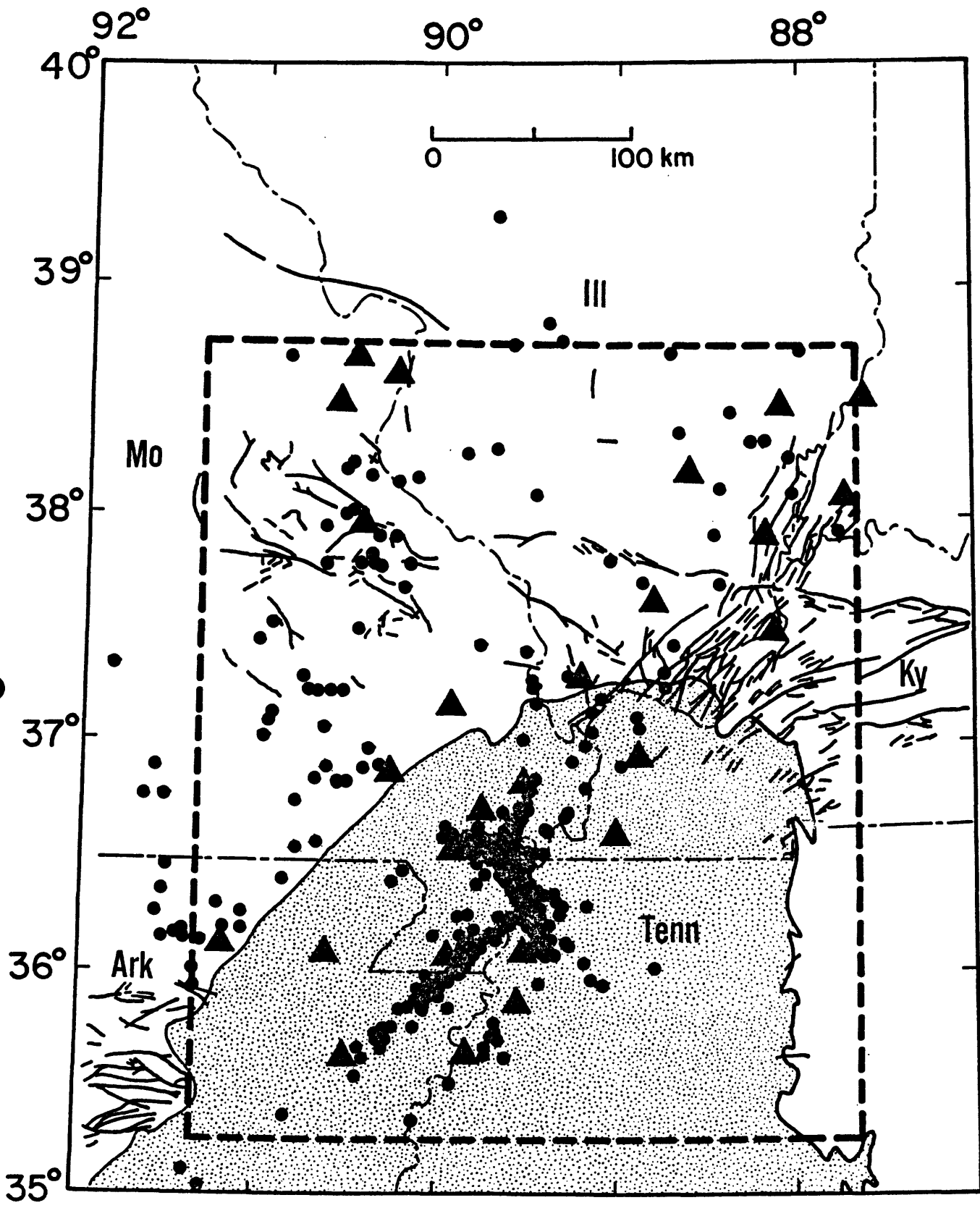


Figure 1. Map of the northern Mississippi embayment (shaded) and surrounding tectonic features (modified from Heyl and McKeown, 1978). Circles denote earthquakes located by the Saint Louis University seismic network for the period January 1, 1980 - September 30, 1983. The dashed rectangle delineates the area beneath which a three-dimensional velocity model has been determined in Figures 3a-3d.

tudes of 88.8°W and 90.6°W . The former configuration was relatively large, but the large block size prevented a detailed determination of velocity variations. The latter configuration permitted greater detail where station coverage was adequate, but covered a much smaller area. The most conspicuous feature of both models was a region of low velocities which was situated in both the crust and upper mantle beneath the area of greatest seismic activity.

Since the time of that study, several stations have been added to the network. These stations allow us to use 30-km square blocks to study an area which is larger than that formerly studied with 50-km square blocks. The area beneath which the model is obtained is delineated in Figure 1. It covers much of the northern Mississippi Embayment, the Ozark uplift, and the areas to the north and east of the embayment. Because of the sparse station coverage in some regions, especially those at large distances from the seismically active zone, ray paths did not traverse some blocks and velocities in those blocks could not be determined.

Mitchell et al. (1977) used deconvoluted readings of teleseismic P-waves and measured arrival times visually from enlargements of the film. In the present work we use digitally recorded data and cross-correlate the wave form at each station with a reference trace using a method described by Herrmann (1982). The maximum correlation between wave forms is assumed to occur at the time shift which gives the travel-time residual of each station with respect to the reference station.

Wave forms were recorded from 95 teleseisms for the period 1 March

1980 through 31 December 1983. The locations of those events are shown in Figure 2. The greatest concentrations of events lie to the northwest, in a zone between the Kurile Islands and Alaska, and to the south-southeast in western South America and Central America.

In order to insure that errors in origin time and errors due to source effects are minimized, the average network residual of each event is removed from the residual at each station. The residuals vary between about -1.0 and +1.5 seconds, a range of about 2.5 seconds. Those times were corrected for variations in elevation and sediment thickness beneath each station. The maximum variation produced by these effects is about 0.45 sec.

The inversion procedure used to obtain three-dimensional velocity models from teleseismic P-wave residuals has been thoroughly discussed by Aki *et al.* (1977) and will not be repeated here. The method allows the determination of velocity perturbations within individual layers, but not the determination of absolute velocity values. Table 1 shows the starting model used for the inversion. The crustal model and uppermost mantle velocity are taken from a simplification of a model of the New Madrid seismic zone obtained by Mitchell and Hashim (1977), whereas the velocity value for the deeper portion of the mantle is taken from Nuttli *et al.* (1969). Mitchell *et al.* (1977) had earlier found that a four-layer model was optimum for this type of study in the New Madrid region. Velocities are assumed to be laterally uniform at depths beneath the fourth layer.

The model obtained in the present study appears in Figure 3a-3d. Since the area covered is large and the station coverage is not optimum,

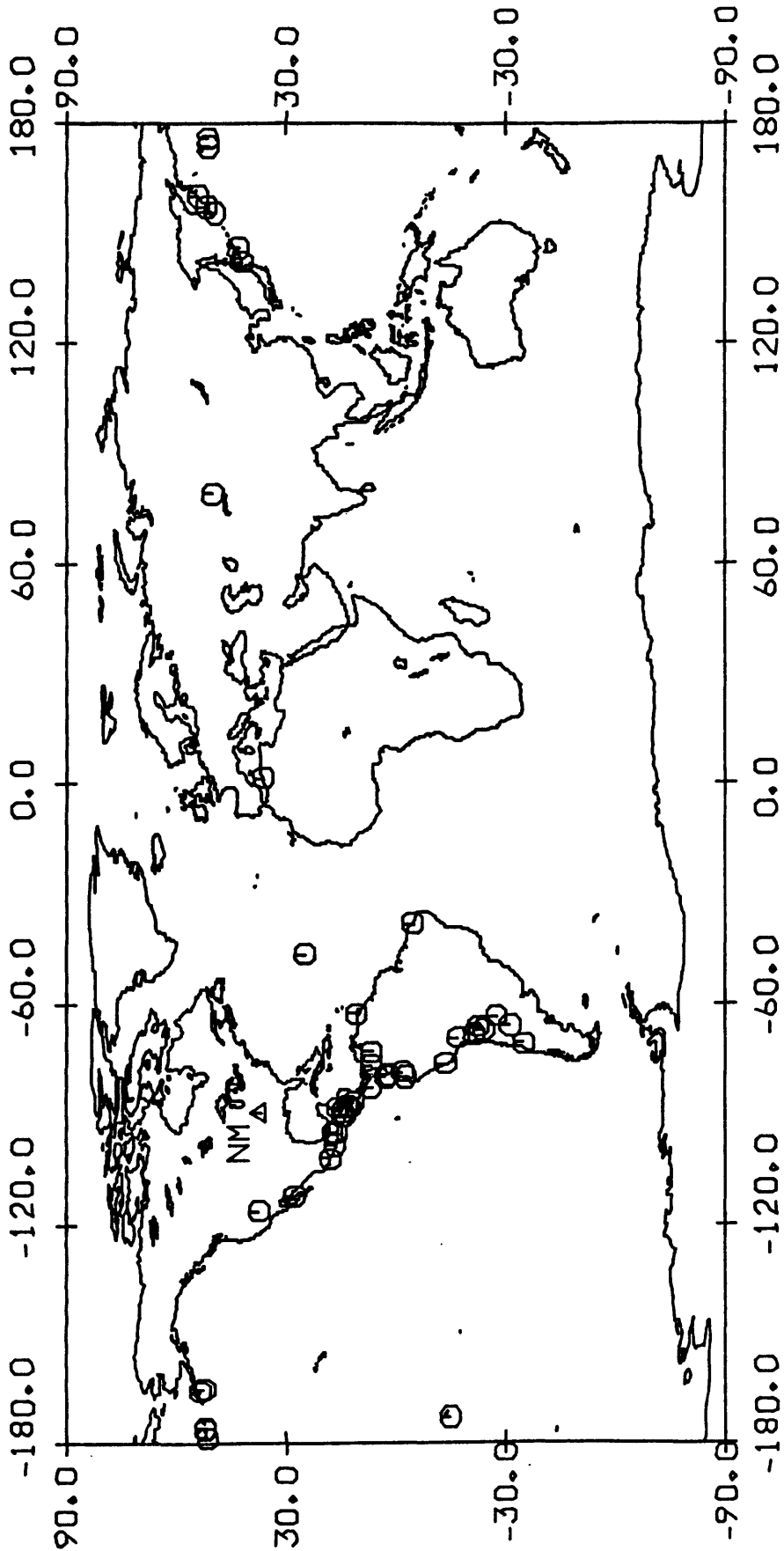


Figure 2. Teleseisms recorded by the Saint Louis University network for the period March 1, 1980 - December 31, 1983 and used to invert for velocity structure.

| | | | | | | | | | |
|-------|------|-------|-------|-------|-------|-------|-------|-------|------|
| - | - | 0.98 | 1.69 | - | - | - | - | 2.56 | 1.94 |
| - | - | -2.43 | - | - | - | 1.43 | -1.31 | 1.27 | 1.35 |
| - | - | 0.92 | - | - | - | 1.77 | -2.05 | 1.41 | 0.99 |
| - | - | 0.19 | - | - | - | - | - | 0.50 | - |
| - | - | - | - | - | - | 1.92 | - | -0.62 | - |
| - | - | - | -0.16 | -1.69 | - | 0.41 | - | - | - |
| - | - | -0.35 | -0.25 | 1.48 | - | 0.44 | - | - | - |
| - | - | -0.28 | 0.36 | 1.95 | 1.14 | -0.72 | -0.09 | - | - |
| - | - | - | - | -0.06 | 0.23 | -1.83 | -1.08 | - | - |
| -0.04 | 0.53 | - | - | 0.25 | 0.02 | - | - | - | - |
| - | 0.59 | -0.81 | - | 0.52 | 1.54 | - | - | - | - |
| - | - | 1.14 | - | -0.51 | -0.42 | - | - | - | - |

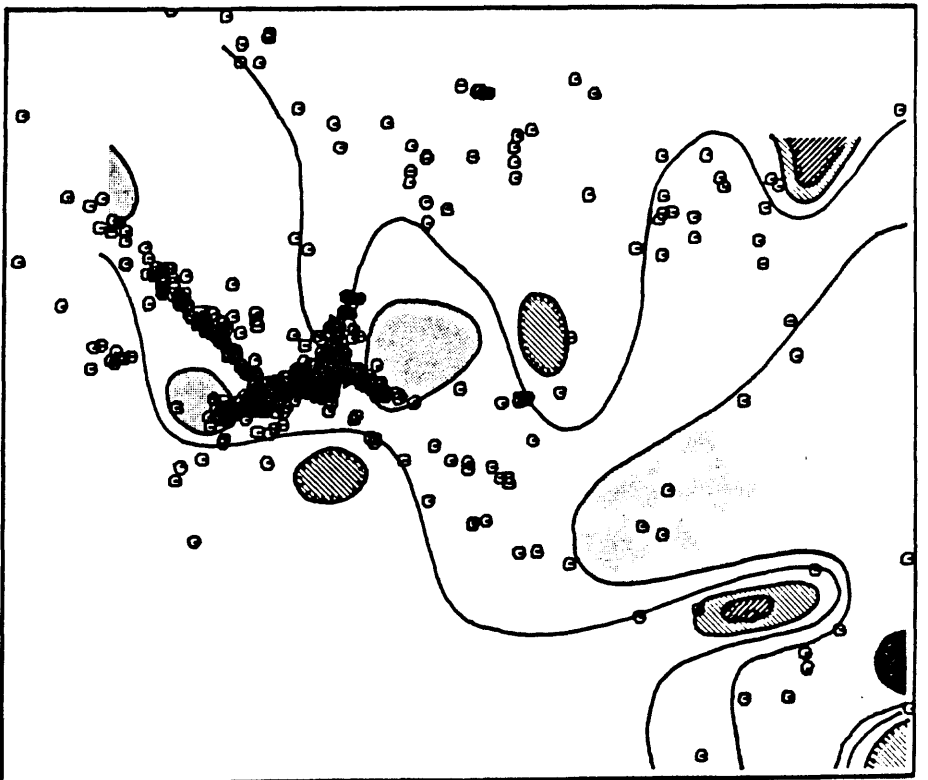


Figure 3a. Preliminary model for layer 1 (the upper 24 km of the crust) derived from the inversion of teleseismic P-wave residuals. (Left) Numbers denote percentage velocity perturbations from the average layer velocity, positive numbers indicating higher than average velocities and negative numbers indicating lower than average velocities. Dashes indicate blocks for which no data could be obtained. (Right) Velocity perturbations contoured at 1% intervals.

| | | | | | | | | | | |
|-------|-------|-------|-------|-------|-------|-------|-------|-------|-------|-------|
| - | 0.71 | 0.04 | -0.27 | - | - | - | - | 0.25 | 0.64 | 0.72 |
| - | -0.41 | -0.88 | 1.07 | - | - | - | -0.07 | 0.06 | -0.25 | 1.02 |
| - | -0.11 | -1.03 | 1.64 | - | - | - | 1.69 | -1.04 | 0.15 | -0.81 |
| - | -0.51 | -0.25 | 0.91 | - | - | -0.34 | -0.63 | 1.32 | -0.52 | 1.60 |
| - | - | - | - | - | -0.16 | 1.23 | 1.37 | 0.20 | 0.51 | - |
| - | - | - | -0.87 | 0.06 | -1.07 | 0.32 | - | - | -0.98 | - |
| - | - | -1.26 | -1.01 | 1.26 | -0.51 | -0.28 | 0.15 | - | - | - |
| - | - | -0.71 | -0.11 | -1.19 | 0.25 | -0.47 | 0.15 | - | - | - |
| - | - | - | - | 1.06 | 1.03 | -1.52 | -0.64 | - | - | - |
| -1.59 | 0.65 | - | 0.53 | 0.15 | 1.39 | 0.32 | - | - | - | - |
| 1.23 | 0.50 | -0.66 | -0.47 | 0.20 | -0.12 | - | - | - | - | - |
| - | - | -0.04 | - | -0.48 | -0.03 | - | - | - | - | - |
| - | - | 0.81 | - | 0.08 | - | - | - | - | - | - |

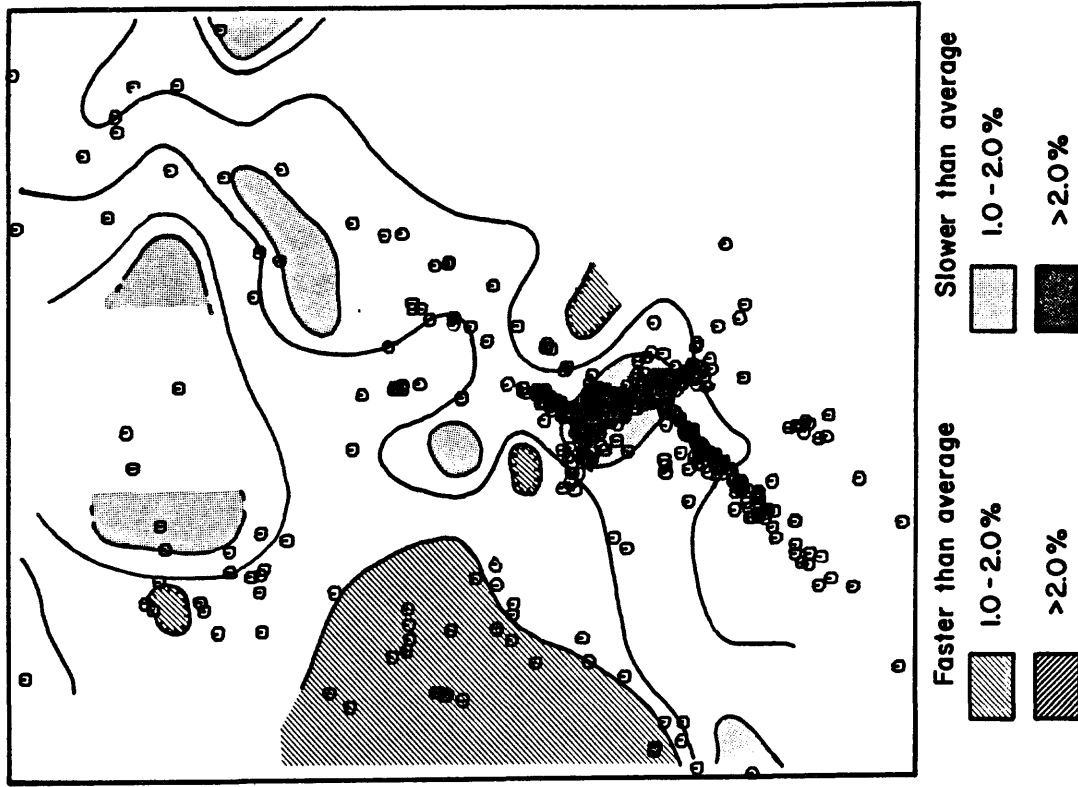


Figure 3b. Preliminary model for layer 2 (the lower 18 km of the crust) derived from the inversion of teleseismic P-wave residuals. See caption for Figure 3a.

| | | | | | | | | | | |
|---|-------|-------|-------|-------|-------|-------|-------|-------|-------|-------|
| - | 0.83 | -1.5 | 2.81 | 0.80 | - | - | 2.02 | 0.91 | -0.13 | 2.11 |
| - | -0.22 | -0.94 | -1.14 | - | - | - | -0.27 | 0.17 | 1.37 | 0.29 |
| - | -0.35 | -0.63 | -0.37 | 0.68 | 0.38 | - | 2.44 | 0.08 | 1.52 | 1.32 |
| - | -1.62 | 2.48 | 0.12 | 3.33 | 0.57 | 0.82 | -0.60 | 1.41 | -0.64 | 0.74 |
| - | - | -0.52 | -2.45 | -0.08 | -1.08 | 0.09 | 0.60 | -1.50 | 2.44 | -0.28 |
| - | - | - | -2.08 | -1.11 | 0.63 | -0.84 | 0.86 | -1.40 | -0.57 | 1.34 |
| - | -0.36 | -0.42 | -1.19 | -1.50 | -0.23 | 2.21 | -0.79 | 0.64 | -0.18 | -2.74 |
| - | - | -0.65 | -1.27 | -0.91 | 1.88 | -1.49 | -0.02 | -0.45 | -0.33 | - |
| - | -4.96 | - | -0.74 | -0.97 | 1.72 | 1.65 | -0.34 | 0.77 | -0.65 | - |
| - | -1.97 | 1.18 | -0.36 | -0.13 | 1.62 | 2.35 | 0.64 | -1.66 | - | - |
| - | 1.68 | 1.27 | 1.75 | 0.58 | 1.52 | 1.80 | -1.95 | -0.48 | - | - |
| - | 0.18 | 0.15 | 3.04 | -2.35 | -0.14 | -2.48 | -0.49 | - | - | - |
| - | 0.08 | 2.25 | - | -1.53 | -1.32 | -0.12 | - | - | - | - |



Figure 3c. Preliminary model for layer 3 (the upper mantle at depths between 42 and 99 km) derived from the inversion of teleseismic P-wave residuals. See caption for Figure 3a.

| | | | | | | | | | | |
|-------|-------|-------|-------|-------|-------|-------|-------|-------|-------|-------|
| 1.63 | -0.60 | -1.32 | - | 3.20 | 2.52 | 1.31 | 0.62 | 0.65 | 0.94 | 2.51 |
| -0.05 | -2.20 | 0.48 | 0.26 | 2.32 | -0.82 | 0.24 | 0.95 | -0.15 | 0.30 | 2.64 |
| -1.17 | - | 0.30 | -0.46 | -0.83 | -1.31 | -1.55 | -0.25 | - | -1.06 | -2.52 |
| -0.35 | 0.57 | -2.86 | 1.77 | -0.95 | 0.02 | - | - | -1.91 | 1.06 | -2.73 |
| -2.19 | 3.48 | -0.45 | -1.11 | 0.13 | 0.69 | -0.18 | 1.15 | 0.59 | -0.07 | -3.00 |
| -1.05 | -1.48 | -0.22 | 2.44 | 2.05 | 0.78 | 1.87 | 0.32 | -0.36 | 0.78 | -1.90 |
| -1.24 | -0.28 | -1.83 | 0.21 | 0.97 | 0.41 | -2.22 | 0.93 | 0.30 | 0.42 | -0.05 |
| -2.39 | -0.53 | 0.47 | 0.09 | 1.38 | 0.42 | -3.24 | -1.03 | -0.81 | 1.03 | 0.16 |
| -2.87 | 0.18 | -1.45 | 0.95 | 1.96 | -0.30 | 1.67 | -1.44 | -1.35 | -4.15 | - |
| -1.78 | -0.55 | -0.82 | 3.07 | 0.69 | 2.69 | 2.52 | -0.61 | -0.30 | -1.18 | - |
| -1.17 | 0.55 | 0.70 | -0.24 | 1.20 | 1.81 | 0.88 | -0.74 | -0.48 | - | - |
| 0.08 | 1.56 | -2.36 | 0.23 | 0.34 | 1.24 | 0.65 | -0.10 | -0.38 | - | - |
| -2.42 | -0.10 | 1.06 | -2.32 | -0.33 | 0.34 | 1.66 | -1.65 | -0.50 | - | - |

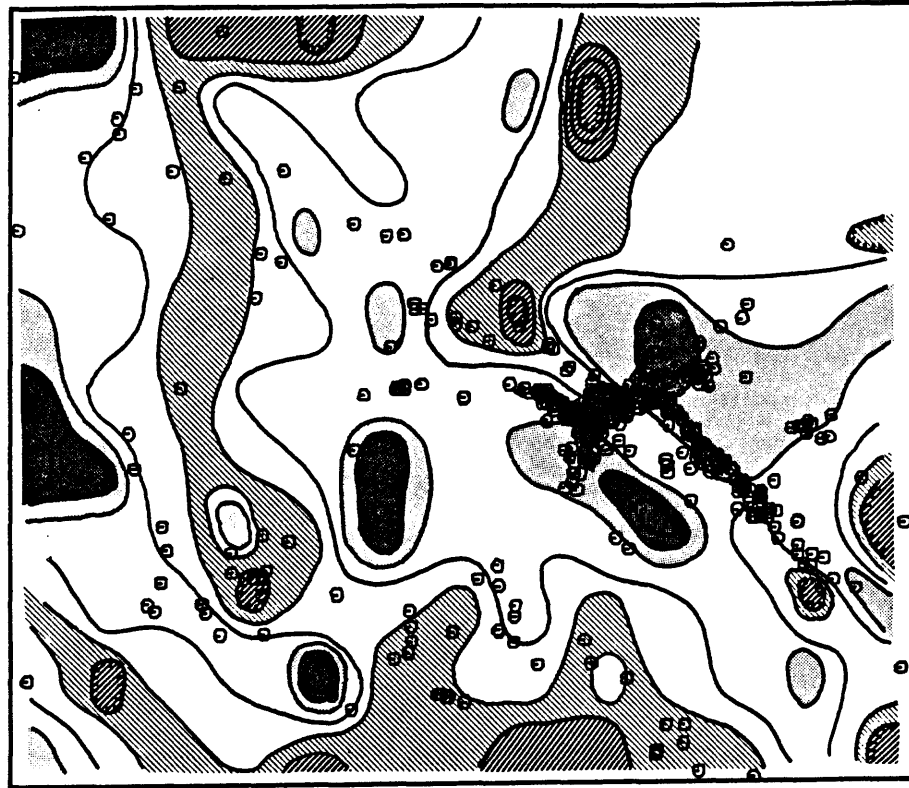


Figure 3d. Preliminary model for layer 3 (the upper mantle at depths between 99 and 156 km) derived from the inversion of teleseismic P-wave residuals. See caption for Figure 3a.

there are several blocks, especially in the two crustal layers, which have not been sampled by even a single ray. Some blocks were sampled by only a few rays. The resolution of velocities in those blocks sampled by a small number of rays is, of course, much smaller than that for blocks sampled by many rays. A detailed discussion of the resolving power and standard deviations corresponding to these velocity determinations will be presented in another paper (Al-Shukri and Mitchell, in preparation). In general, the upper mantle velocities and crustal velocities in the central portion of the model are well resolved, but those on the periphery of the crustal layers are not.

Velocity perturbations in the uppermost layer, corresponding to a depth interval of 0-24 km appear in Figure 3a. A sinuous zone of low velocities runs in a NE-SW direction across the figure. This feature approximately follows a basement rift mapped by Hildenbrand et al. (1977) and it is interesting to speculate that these low velocities are related to the processes which produced rifting. Two localized velocity lows occur near the northern and southern extremes of the NNW-SSE trending zone of greatest earthquake activity.

Figure 3b presents velocity perturbations in the lower crust, at depths between 24 and 42 km. Note that the NE-SW trending zone of low velocities is still present and that a localized zone of low velocities with a diameter of 50-60 km lies directly beneath the zone of most active seismicity.

Upper mantle velocity perturbations in the depth range of 42-99 km appear in Figure 3c. There may be an indication of a NE-SW trending zone of low velocities, but the pattern is more complex than the

patterns in the crust. Velocity perturbations also deviate much more from the mean (-4.9% to +3.3%) than do the perturbations in the crust (-1.8% to +2.0%). The same complexity extends down through layer 4 at depths between 99 and 156 km in the mantle (Figure 3d). It is possible that a portion of these perturbations in layer 4 are produced by anomalies at greater depths and our assumption of uniformity there produces slightly larger perturbations than those which really occur. Low velocities occur beneath the seismically active zone as well as in other regions of the mantle well removed from that zone.

CORRELATION OF VELOCITY AND DENSITY

Braille *et al.* (1982) have compiled a Bouguer gravity map of the New Madrid seismic zone and surrounding area using data reported by McGinnis *et al.* (1976), Hildenbrand *et al.* (1977), Keller *et al.* (1978), and the National Geophysical and Solar-Terrestrial Data Center. A portion of that map corresponding to our area of study is reproduced in Figure 4. It is interesting to compare that map with the velocity model of Figures 3a-3d to see if any correlation occurs between velocity and gravity anomalies. The surface projection of the region of low velocities in the upper crust at the northern end of the most seismically active area (Figure 3a) overlaps the circular gravity high produced by the Bloomfield pluton. The velocity low at the southern end of the zone lies somewhat to the north of the gravity anomaly caused by the Covington pluton. Since those plutons are thought to be mafic or ultramafic (Hildenbrand, 1978), we would expect that they would be faster than surrounding rock in the upper crust. Therefore the possible correlation of low velocities with those plutons may be illusory, and is

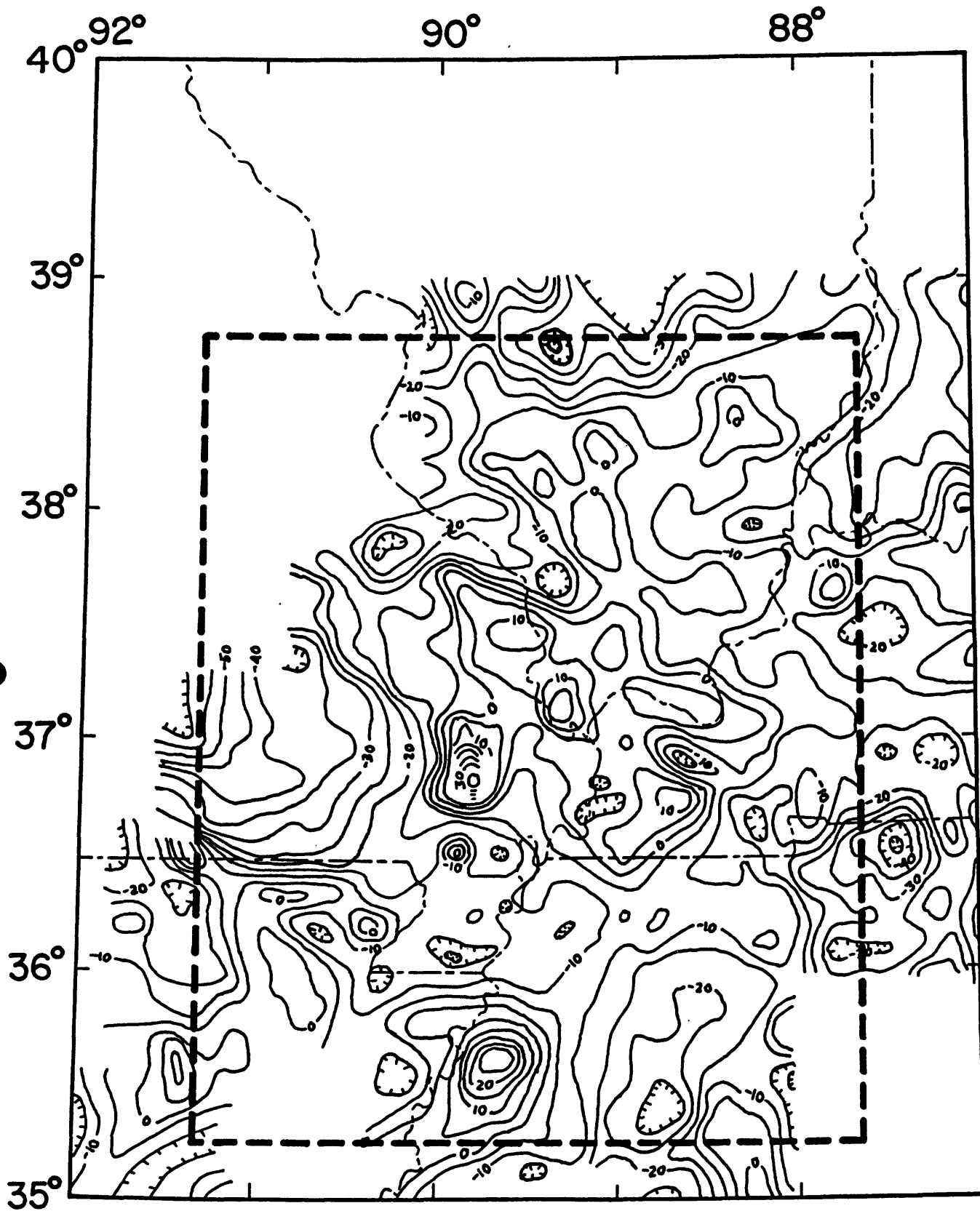


Figure 4. Preliminary Bouguer gravity map of the region of study (adapted from Braille *et al.*, 1982). Contour interval is 5 mgal. The dashed rectangle delineates the area beneath which a three-dimensional velocity model has been determined.

due only to the limited spatial resolution inherent in the inversion method.

If we consider broader scale features, some interesting correlations appear. The high lower crust and upper mantle velocities (Figures 3b and 3c) in the western portion of the model correlate with a broad low on the Bouguer gravity map. These features correspond approximately to the eastern portion of the Ozark uplift. This negative correlation is not to be expected from empirical velocity-density relationships and precludes the possibility that both the velocity and density anomalies are due solely to temperature effects. This correlation is currently being studied further (Al-Shukri and Mitchell, in preparation) using correlation analysis methods; however, our present data and results permit us to speculate on the reason for this negative correlation.

The fact that a broad gravity low correlates with a broad velocity high suggests that a region of higher-than-average velocity in either the crust or upper mantle, or both, in our area of study is associated with lower-than-average densities. The same type of correlation was found by Dziewonski *et al.* (1977) in the mantle at depths greater than 1100 km. They discussed two principal causes of that negative correlation between gravity and density anomalies - compositional inhomogeneities and mantle convection.

Since we are dealing with the lithosphere in the present study, we can neglect causes related to mantle convection and consider only the sorts of compositional factors which might produce the observed correlation between gravity and velocity anomalies. Dziewonski *et al.* (1977) discussed densities and velocities obtained for peridotite (Christensen,

1966) and eclogite (Birch, 1960) at 10 kbars pressure. Peridotite samples have higher velocities and lower densities than eclogite samples collected at various sites around the world. All possible combinations of different samples of these would yield a negative correlation between velocity and gravity in the upper mantle. It is therefore possible that our results can be explained by lateral variations in the composition of the upper mantle. Regions of positive gravity anomalies and negative upper mantle velocity anomalies might correspond to regions where the upper mantle contains more eclogite and less peridotite than other regions.

Another possibility for that correlation discussed by Dziewonski et al. (1977) is variations in the components of the system $\text{SiO}_2\text{-MgO-FeO}$. Substitution of either MgO or FeO for SiO_2 will tend to produce a negative correlation between velocity and gravity anomalies.

TEMPERATURE AND HEAT FLOW

Swanberg et al. (1982) made four determinations of heat flow in the region of the upper Mississippi Embayment and presented results of an analysis of several hundred bottom-hole temperature measurements there. All of those data indicated a small, but well-defined, thermal anomaly associated with the New Madrid seismic zone. The areal extent of that anomaly is roughly between 50 and 100 km in diameter. The authors suggested three possible mechanisms for the thermal anomaly, (1) a mantle source corresponding to the region of low velocities found by Mitchell et al. (1977), (2) heat production due to the release of elastic strain or frictional heating during earthquakes, and (3) a convec-

tive component due to ground water ascending along active faults. The possibility of a mantle source was rejected because a mantle source would produce a broader thermal anomaly at the surface than that which is observed. The possibility that the anomaly is associated with earthquake processes was also thought to be unlikely because of the small magnitudes and low energy release of most New Madrid earthquakes. The enhancement of heat flow due to a convective component was therefore the mechanism favored by Swanberg et al. (1982).

In the present work we investigate a fourth possibility, that of heat produced by an igneous intrusion emplaced at mid-crustal depths. There is ample evidence that intrusive activity occurred in the past in the New Madrid region. In this study we compute the temperature field and heat flow produced by intrusions of mid-Eocene age (Hamilton and Zoback, 1982) and mid-Mesozoic age (Hildenbrand et al., 1982) to see if thermal effects of igneous intrusions emplaced at those times might still be seen in the region of the upper Mississippi Embayment. The method of calculation is discussed by Kohsmann (1983) and Kohsmann and Mitchell (in preparation). The method assumes (1) that the intrusion is a finite right-circular cylinder, (2) that the intrusion has been emplaced instantaneously, (3) that the intrusion was intruded isothermally and the temperature of the intrusive is the pre-intrusive temperature at the base of the cylindrical source region, (4) that the basal temperature of the source region and the temperature of the plane containing the base of the source remain constant in time, (5) that the half-space into which the intrusion was emplaced has thermophysical properties which are identical to those of the source and that those properties are homogeneous, isotropic, and temperature invariant, (6) that

heat conduction is the only process responsible for influencing the cooling history of the intrusion and its surroundings, (7) that the equations of conduction within the half-space are not coupled with the thermoelastic displacements associated with the temperature anomaly, and (8) that a depth-dependent, linear temperature distribution existed prior to the intrusion and will occur after the effects of the intrusion have abated. Although several assumptions have been made, mostly for the sake of mathematical simplicity, we feel that they are reasonable and allow us to model the effects of a realistic intrusion in the crust.

The temperature distribution produced by a cylindrical intrusion with a radius of 30 km and a depth of burial of 20 km is shown for three post-intrusion times in Figure 5. For those calculations, we assumed that the intrusion had an initial temperature of 1200°C (a typical temperature for molten basic rock observed at the surface) and that it was emplaced in a region where the thermal gradient was originally 12°C/km. The thermal diffusivity and thermal conductivity values for the region are taken to be 0.0068 cm²/sec and 0.01 cal/cm-sec-°C, respectively, values typical for granites. Those calculations show that temperatures at shallow depths are perturbed only slightly at a post-intrusion time of 1 million years. This result illustrates the slowness of conductive thermal processes acting in the Earth. After 10 million years the temperatures are perturbed much more, and after 50 million years the temperature effects are still felt, but are levelling off.

Figure 6 presents heat flow values expected at the surface for post-intrusion times of 40 million years and 100 million years. These are taken to represent times of post mid-Eocene and post early-Mesozoic

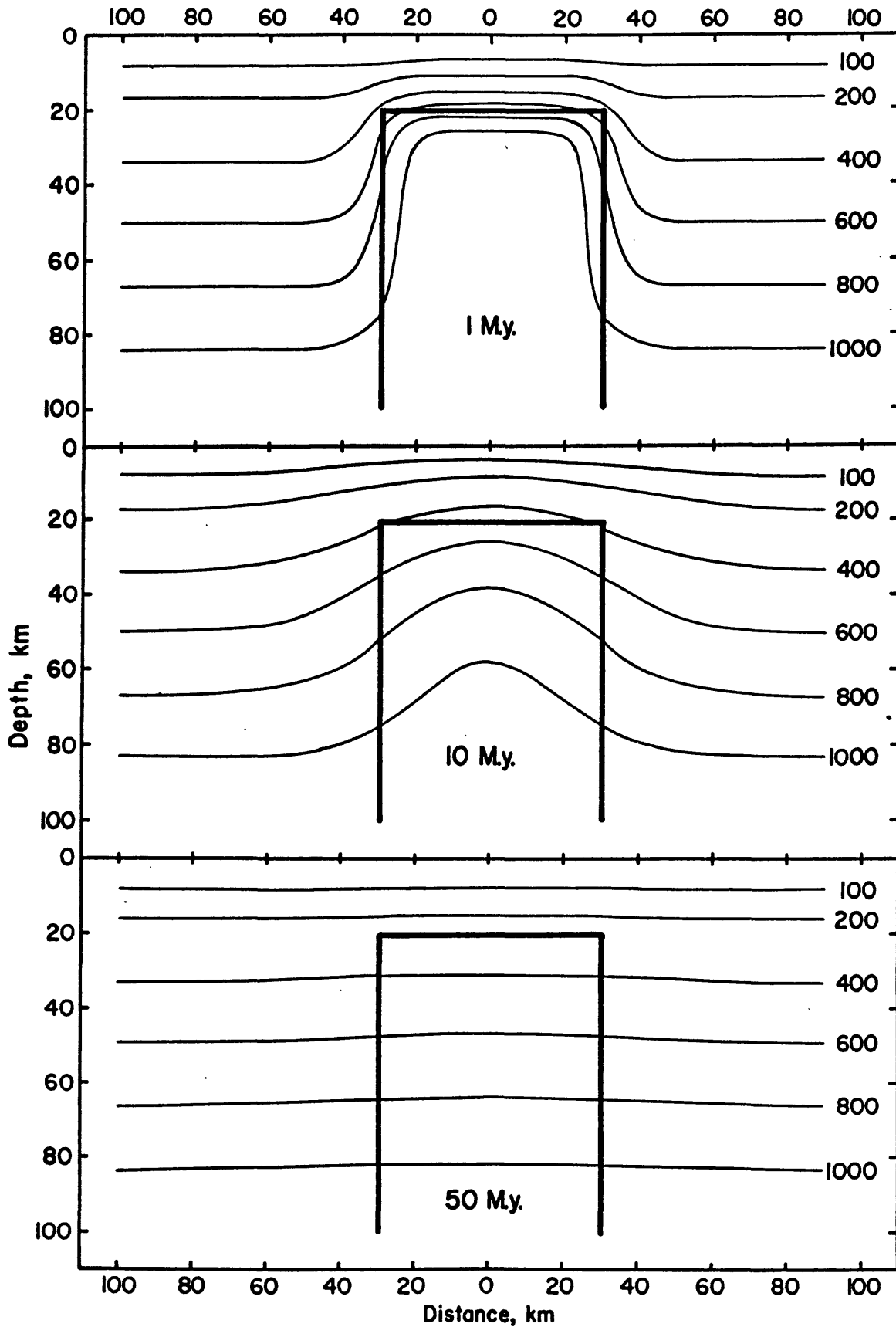


Figure 5. Contoured temperatures (in degrees Celsius) about a cylindrical intrusion of 30 km radius buried at a depth of 20 km (heavy lines) for three post-emplacement times.

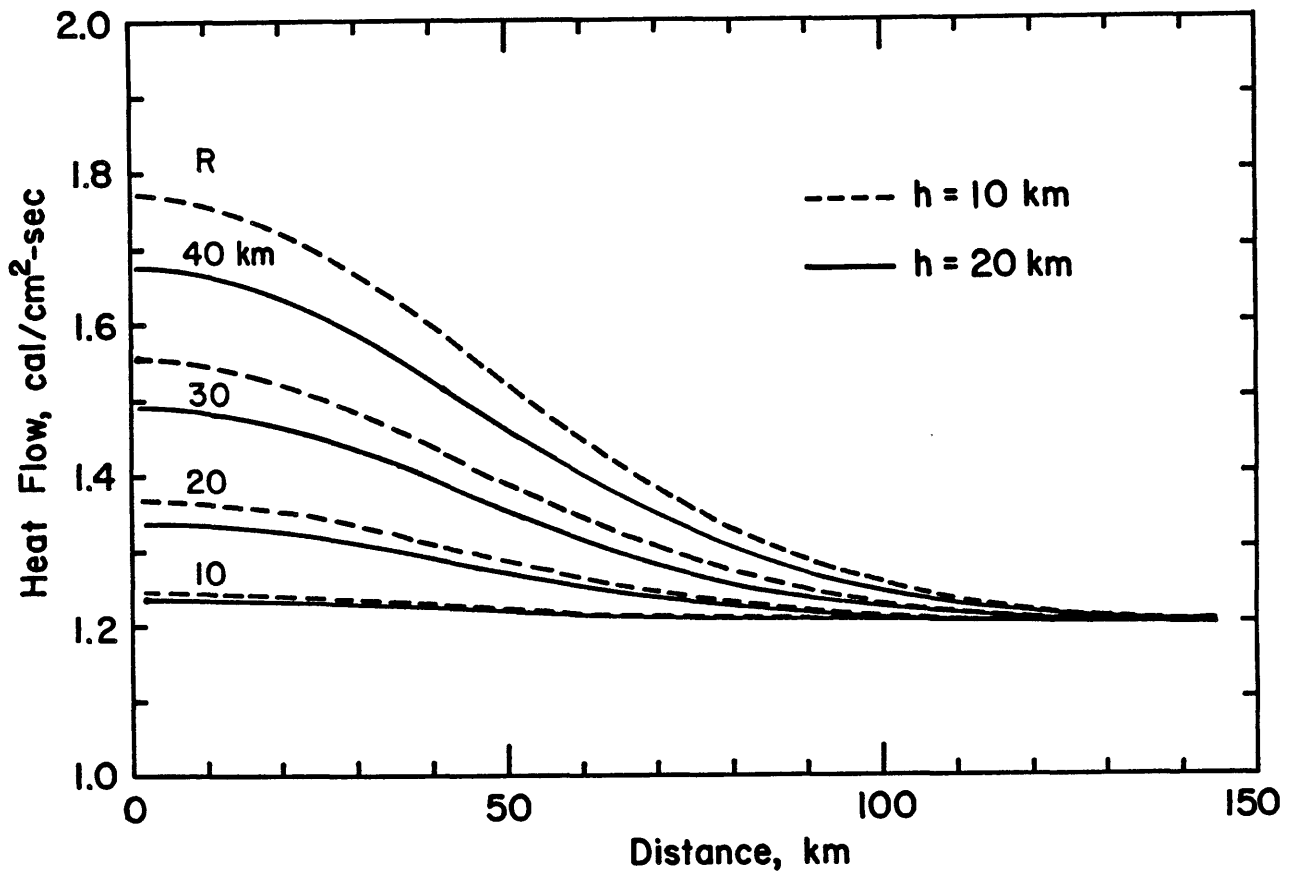


Figure 6. Surface heat flow values and variation with distance from cylindrical intrusions of various radius values (R) and at three post-emplacment times and two depths of burial (h).

intrusive activity which is known to have occurred in the New Madrid region. Calculations were performed for intrusions of various radial dimensions and depths of burial.

Heat flow values determined by Swanberg et al. (1982) in the active portion of the New Madrid region were between 55.2 w/m-sec^2 (1.32 hfu) and 65.2 w/m-sec^2 (1.56 hfu). These values are higher than the mean mid-continent value of 50.2 w/m-sec^2 (1.2 hfu). The high-temperature region delineated by observations of bottom-hole measurements is between 30 and 50 km in radius. Note that the temperature distribution produced by post middle-Eocene intrusions (40 million year age) with radial dimensions between 20 km and 30-35 km can easily explain the heat flow levels and spatial pattern of high temperatures. The depths of burial of these particular intrusions have a minor effect, deeper intrusions causing somewhat lower heat flow values. Post early-Mesozoic intrusions (100 millions years ago) can explain the heat flow anomaly if they are large enough, but the computed heat flow anomaly is much broader than that observed in the New Madrid region.

The results of these calculations indicate that the present heat flow anomaly in the New Madrid region could be due to a buried intrusion of approximately mid-Eocene age. It must be emphasized that this explanation for the heat flow anomaly is only one viable possibility. Another is that the anomaly is the result of a convective component of heat flow due to the upward migration of ground water in a region of active faulting. It is also possible that both mechanisms combine to produce the observed anomaly.

THERMAL STRESSES

The anomalous temperature distributions described and modelled in the previous section will produce deviatoric stresses in the crust, the level of the stresses being dependent upon the severity of the temperature changes in space and time and upon the properties of the crust. Following the methods of Kohsmann (1983) and Kohsmann and Mitchell (in preparation), we have computed the theoretical stress field produced by several idealized igneous intrusions as a function of time since emplacement. The thermophysical constants of the intrusions and their surroundings, as well as the ambient geothermal gradient and initial temperature of the intrusion, are set at the values used in the heat flow calculations described earlier.

All of the assumptions made for the thermal calculations in the preceding section are also made for the calculation of thermal stresses. In addition, we assume that the Earth's surface is free of vertical tractions. This allows the surface to deviate from plane geometry, but it is assumed that the deviation is small enough to allow the decoupling of the thermoelastic equations from the motion of the free surface. In addition, we assume that accelerations due to thermal stresses are small.

We start with the Duhamel-Neuman relation (e.g. Nowacki, 1962) and determine thermoelastic stresses assuming a perfectly elastic medium. A major unknown in our calculations is the extent to which viscoelastic or plastic behavior occurs in the crust and upper mantle in the central United States. Since these calculations assume perfect elasticity, the true stress may be smaller because of partial relief by viscoelastic

flow. If viscoelastic flow occurs, we would expect its effect would be greatest at large times and that our results would be better approximations at early times than at late times following emplacement.

The results of our computations are shown in Figures 7a and 7b for an intrusion buried at a depth of 20 km and having a radial dimension of 20 km. The stress values can be quite high, especially at post-intrusion times which are not very large. At a post-intrusion time of 10 million years, all stress components have maximum values of several hundred bars. The stresses become smaller with time, being several tens of bars for most components at a post-intrusion time of 40 million years. The magnitudes of σ_{rr} and the magnitudes of $\sigma_{\theta\theta}$ are larger and σ_{zz} and σ_{rz} are smaller at a depth of 5 km than at a depth of 10 km. The net result of these changes with depth is that shearing stresses are greater at 5 km than they are at 10 km for these post-intrusion times.

The maximum (σ_{\max}) and minimum (σ_{\min}) principal stresses were calculated and the shearing stresses were obtained from $(\sigma_{\max} - \sigma_{\min})/2$. This quantity is often taken as a measure of the stress required to achieve fracture. Values of shearing stress at a depth of 5 km for an intrusion buried at a depth of 20 km and having a radius of 20 km are plotted along with predicted focal mechanisms in Figure 8. At times shortly after emplacement, those values can be quite high, well above the stress level needed to fracture granite (Kohsmann and Mitchell, in preparation). At a time of 10 million years the values are in the range of several hundred bars and at a time of 40 million years they are still in the range of several tens of bars. At a depth of 10 km the shearing stresses produced by the same intrusion are reduced by about 30% near

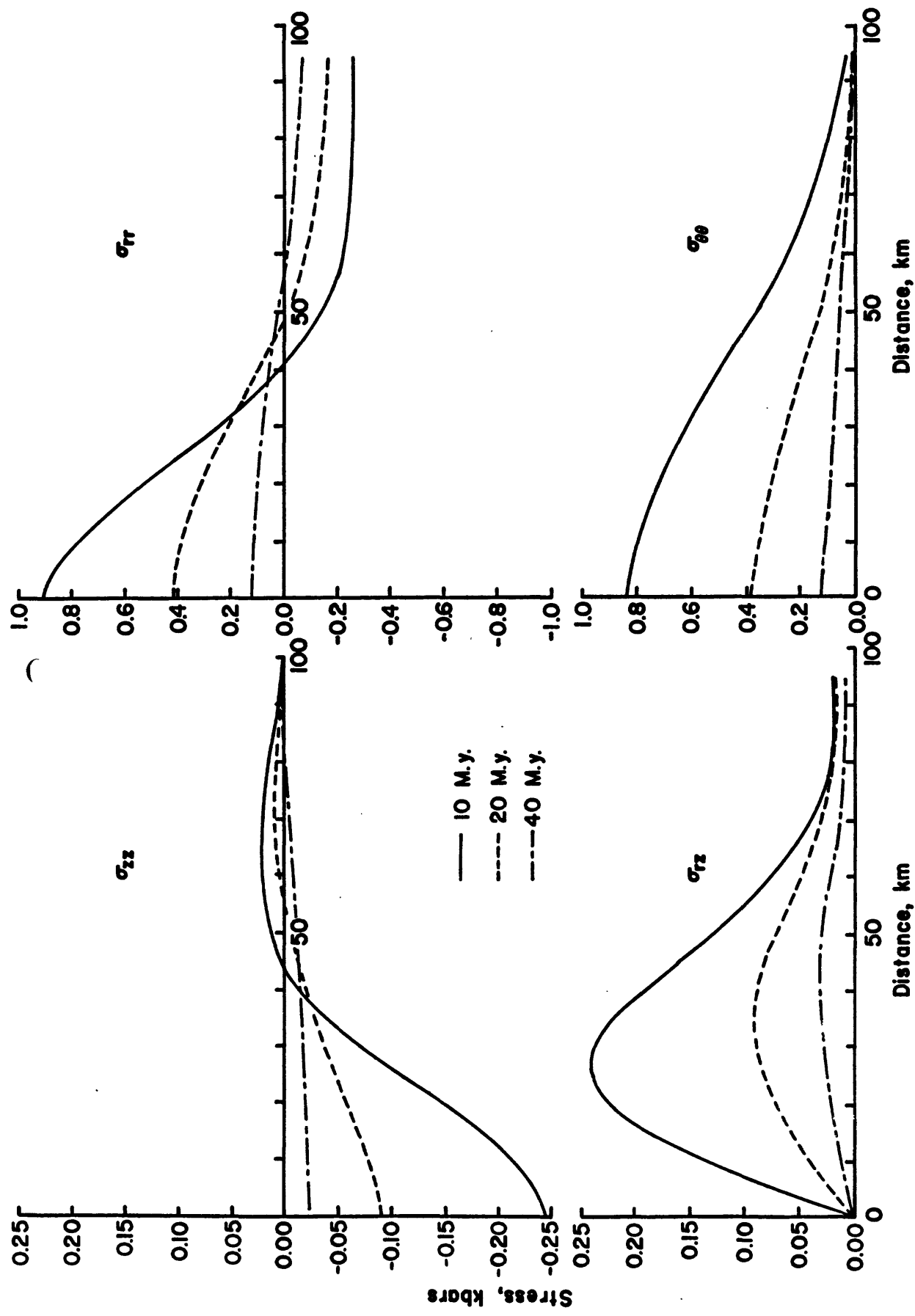


Figure 7a. Vertical stress (σ_{zz}), radial stress (σ_{rr}), vertical-radial shear (σ_{rz}), and circumferential stress ($\sigma_{\theta\theta}$) versus distance from the axis of a cylindrical intrusion which is 20 km deep and has a radial dimension of 20 km. The observation depth is 5 km and stresses are plotted for 3 times as indicated.

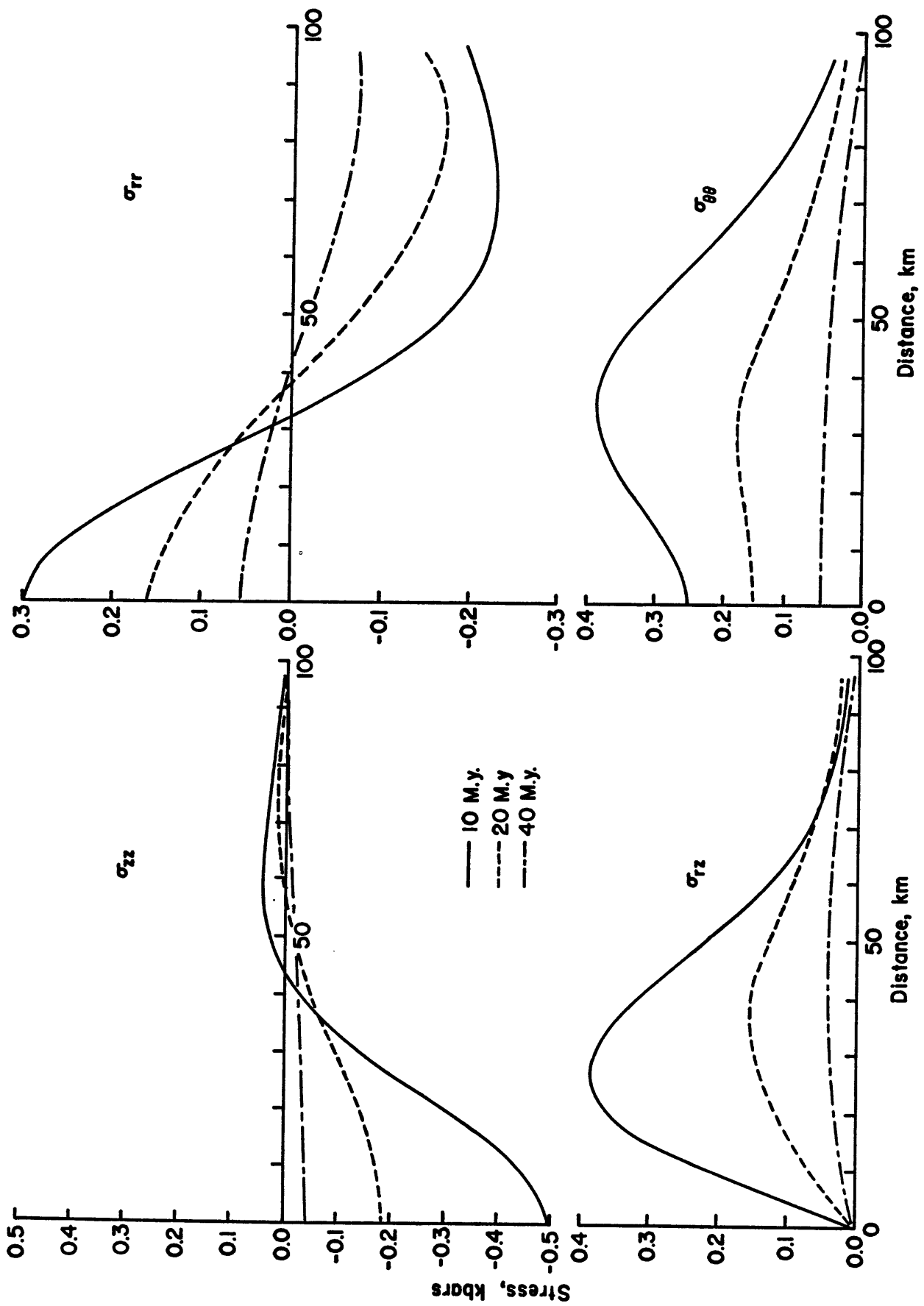


Figure 7b. Stresses produced by the same model as that in Figure 7a, but at an observation depth of 10 km.

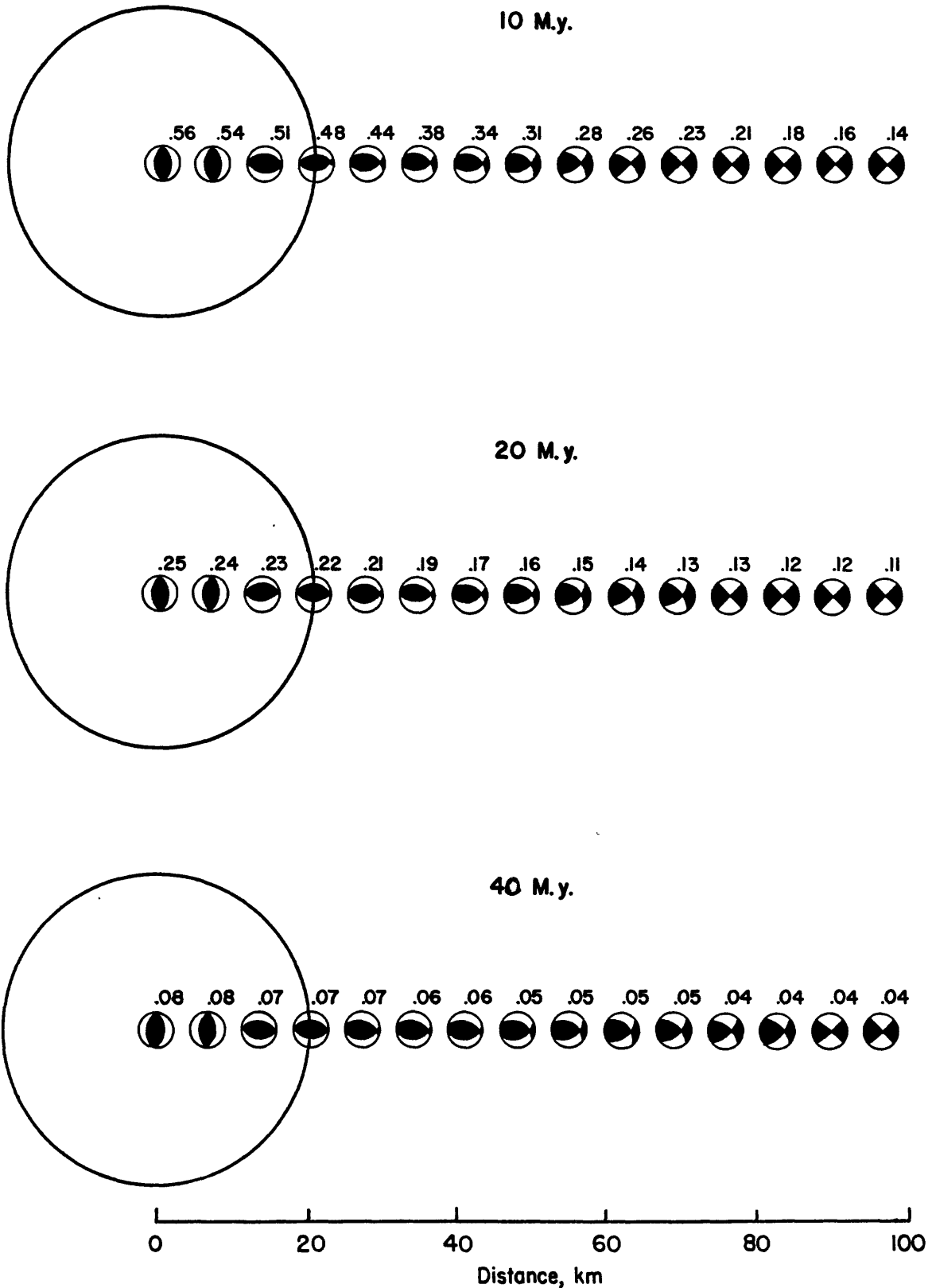


Figure 8. Hypothetical focal mechanisms and shearing stresses $(\sigma_{\max} - \sigma_{\min})/2$ at a depth of 5 km produced by a cylindrical intrusion which is 20 km deep and has a radial dimension of 20 km.

the axis of the intrusion and by about 10% at a distance of 100 km from the axis. In general, for this range of times and this particular model, shearing stresses decrease with increasing depth of observation and increase for intrusions of greater radial dimensions. Those values can be compared with stress drops reported for New Madrid earthquakes (Street et al., 1975) which are 10 bars or less. Shearing stresses produced by a large cylindrical intrusion in an elastic medium are high enough to cause fracture in granite shortly after emplacement and after 40 million years can be much larger than stress drops observed for New Madrid earthquakes. If the crust in that region behaves elastically, therefore, stresses produced by a mid-Eocene intrusion might still be relatively large. As stated earlier, however, if non-elastic processes have occurred, they will have partially relieved accumulated stress to an extent not known at the present time.

Our computed directions of the maximum principal stress are approximately horizontal at most distances from the intrusion. Reverse faulting is predicted to occur above and near the intrusion and strike-slip faulting is predicted to occur at greater distances. This type of faulting pattern is observed along the New Madrid seismic zone at the present time (Herrmann and Canas, 1978). The observed direction of the maximum principle stress axis is, however, oriented at a direction which is radial to the hypothetical intrusion, rather than circumferential, as our calculations would predict. This partial disagreement of theoretically predicted stress patterns with those observed may indicate that anomalous stresses are produced by factors other than those discussed here or that motion along pre-existing faults may occur which is not consistent with the stress field produced in an unfaulted medium.

CONCLUSIONS

Teleseismic P-wave residuals observed by the Saint Louis University network indicate both localized and broad-scale anomalies in seismic velocities in the crust and upper mantle beneath the New Madrid region. A region of slightly lower than average velocity in the crust follows a NE-SW trend through the zone of greatest seismic activity. This may be a deep-seated manifestation of the basement rift found earlier from magnetic and gravity interpretations (e.g. Hildenbrand *et al.*, 1977). Localized regions of low velocity occur beneath the zone of most active seismic activity as well as at points well removed from that zone.

On a broader scale, surface projections of regions of higher than average lower crustal and upper mantle velocities correlate with regions of low Bouguer gravity values. This negative correlation may be caused by laterally varying composition of the crust or upper mantle. Two possibilities which might produce that correlation are variations in the content of eclogite relative to peridotite in the upper mantle and variations in the components of the system $\text{SiO}_2\text{-MgO-FeO}$.

A basic igneous intrusion buried at mid-crustal depths and having a radial dimension between 20 and 35 km could produce the heat flow anomaly observed at the New Madrid seismic zone if the intrusion is of post middle-Eocene age.

Thermal stresses produced by a large basic igneous intrusion at mid-crustal depths are sufficiently large to produce shearing stresses of several hundred bars 10 million years after emplacement and several tens of bars or more 40 million years after emplacement if the crust and

mantle behave elastically over long time intervals. These stresses are large enough to explain stress drops observed for New Madrid earthquakes. The maximum principal stress axis at large distances from the intrusion is predicted to be oriented circumferentially to the intrusion rather than radially to it as observed from focal mechanism studies.

Acknowledgement

We thank Robert B. Herrmann for writing the cross-correlation program used in the determination of travel-time anomalies, K. Aki for providing us with his three-dimensional velocity inversion program, and C.C. Cheng for writing modifications to that program which were useful in the present research. We also express our appreciation to Bellaire Research Laboratory of Texaco Inc. for providing facilities used in a portion of this work. This research was partly supported by the Division of Earth Science, National Science Foundation, under grant EAR-8110868 and by the U.S. Geological Survey under contract 14-08-0001-2188.

REFERENCES

- Aki, K., A. Christofferson, and E.S. Husebye, 1977, Determination of the three-dimensional seismic structure of the lithosphere, J. Geophys. Res., 82, 277-296.
- Birch, F., 1960, The velocity of compressional waves in rocks to 10 kilobars, 1, J. Geophys. Res., 65, 1083-1102.
- Braille, L.W., W.J. Hinze, G.R. Keller, and E.G. Lidiak, 1982, The northeastern extension of the New Madrid seismic zone, in Geol. Survey Prof. Paper 1236-L, Investigations of the New Madrid, Missouri, Earthquake Region, edited by F.A. McKeown and L.C. Pakiser, 175-184.
- Christensen, N.I., 1966, Elasticity of ultrabasic rocks, J. Geophys. Res., 71, 5921-5931.
- Dziewonski, A.M., B.H. Hager, and R.J. O'Connell, 1977, Large-scale heterogeneities in the lower mantle, J. Geophys. Res., 82, 239-255.
- Hamilton, R.M., and M.D. Zoback, 1982, tectonic features of the New Madrid seismic zone from seismic-reflection profiles, in Geol. Survey Prof. Paper 1236-L, Investigations of the New Madrid, Missouri Earthquake Region, edited by F.A. McKeown and L.C. Pakiser, 55-82.
- Herrmann, R.B., 1982, Digital processing of regional network data, Bull. Seism. Soc. Am., 72, 5261-5276.
- Herrmann, R.B., and J.A. Canas, 1978, Focal mechanism studies in the New Madrid seismic zone, Bull. Seism. Soc. Am., 68, 1095-1102.
- Hildenbrand, T.G., M.F. Kane, and W. Stauder, 1977, Magnetic and gravity anomalies in the northern Mississippi Embayment and their spatial relation to seismicity, U.S. Geol. Survey Miscellaneous Field Studies Map MF-914.
- Hildenbrand, T.G., 1978, Approximate ages of igneous intrusions in the upper Mississippi Embayment utilizing the total magnetic field anomalies, Am. Geophys. Union 1978 Midwest Mtg., Abstracts, p. 6.
- Hildenbrand, T.G., M.F. Kane, and J.D. Hendricks, 1982, Magnetic basement in the upper Mississippi Embayment region --- a preliminary report, in Geol. Survey Prof. Paper 1236-L, Investigations of the New Madrid, Missouri, Earthquake Region, edited by F.A. McKeown and L.C. Pakiser, 39-53.
- Keller, G.R., R.K. Solderberg, G.M. Graham, M.L. Dusing, and C.B. Austin, 1978, Bouguer gravity map of Kentucky, Western sheet, Kentucky Geological Survey Map.
- Kohsmann, J., 1983. A Computational Study of Two Possible Intraplate Earthquake Triggering Mechanisms, Ph.D. Dissertation, Saint Louis University, 331 pp.

- McGinnis, L.D., P.C. Heigold, C.P. Ervin, and M. Heidari, 1976, The gravity field and tectonics of Illinois, Ill. State Geol. Survey Circular 494, 24 p.
- Mitchell, B.J., and B.M. Hashim, 1977, Seismic velocity determinations in the New Madrid seismic zone: A new method using local earthquakes, Bull. Seism. Soc. Am., 67, 413-424.
- Mitchell, B.J., C.C. Cheng, and W. Stauder, 1977, A three-dimensional velocity model of the lithosphere beneath the New Madrid seismic zone, Bull. Seism. Soc. Am., 67, 1061-1074.
- Nowacki, W., 1962. Thermoelasticity, Addison-Wesley, New York, 628 pp.
- Nuttli, O.W., W. Stauder, and C. Kisslinger, 1969, Travel-time tables for earthquakes in the central United States, Seism. Soc. Am., Earthquake Notes, 40, 19-28.
- Street, R.L., R.B. Herrmann, and O.W. Nuttli, 1975, Spectral characteristics of the Lg wave generated by central United States earthquakes, Geophys. J. Roy. Ast. Soc., 41, 51-63.
- Swanberg, C.A., B.J. Mitchell, R.L. Lohse, and D.P. Blackwell, 1982, Heat flow in the upper Mississippi Embayment, in Geol. Survey Prof. Paper 1236-L, Investigations of the New Madrid, Missouri, Earthquake Region, edited by F.A. McKeown and L.C. Pakiser, 185-189.

Table 1. Initial model parameters for the crust and upper mantle beneath the New Madrid seismic zone.

| Layer | Thickness km | P-wave Velocity km/sec |
|-------|-----------------|---------------------------|
| 1 | 24 | 6.32 |
| 2 | 18 | 7.17 |
| 3 | 57 | 8.10 |
| 4 | 57 | 8.37 |

THE SEISMICITY OF THE NEW MADRID SEISMIC ZONE

by

Robert B. Herrmann

Professor of Geophysics

Department of Earth and Atmospheric Sciences

Saint Louis University

P. O. Box 8099 Laclede Station

St. Louis, MO 63156

INTRODUCTION

Prior to the disastrous 1906 California earthquake, which focused attention to earthquakes in the western United States, the New Madrid earthquakes of 1811-1812 were always prominently mentioned in any discussion of earthquakes (Blake, 1926). Modern interest in U. S. earthquakes can be traced to studies of the 1886 Charleston, South Carolina, earthquake which were performed by the relatively new U. S. Geological Survey. This interest in earthquakes lagged subsequently but was rekindled by the the occurrence of the 1906 California earthquake. This earthquake renewed interest in other earthquakes, including the New Madrid earthquakes of 1811-1812. Fuller (1912) provided a detailed description of the effects of the earthquakes, both as reported by observers at the time and as seen in the landforms in the early 1900's. Nuttli (1973) studied the historical accounts in order to quantify the earthquake effects and to estimate magnitudes for the three largest earthquakes of the sequence. Penick (1976) provided a detailed historical account of the region and the earthquakes.

Much can be learned from the pattern of historical earthquake locations. Figure 1 presents the locations of earthquakes which occurred between 1800 and 1975 in the region about New Madrid. These locations are taken from a catalog compiled by Nuttli and Brill (1980). It is obvious from this figure that the region has been exposed to considerable seismic activity during the past two centuries. Most earthquakes occurred in the immediate vicinity of the New Madrid Seismic Zone which includes northeastern Arkansas, the Missouri Bootheel and adjacent portions of Tennessee and Kentucky. Other significant seismic activity has occurred along a line connecting St. Louis to Little Rock. A third pattern follows the Mississippi River from St. Louis, Missouri to Cairo, Illinois. Another pattern, not as distinct, can be placed in the Wabash River Valley.

The catalog of historical earthquakes has been very valuable for a number of studies. Using modern instrumental data together with corresponding isoseismal data, Nuttli (1976) developed a method for assigning a magnitude to the preinstrumental earthquakes. Once magnitudes were assigned systematically to the earthquake catalog, the recurrence relations of the earthquakes could be defined (Nuttli, 1974).

RECENT INVESTIGATIONS

The improvement in our knowledge of earthquakes near New Madrid is traced to the installation of a dense modern network of seismograph stations in the region since 1974. Within a few months of the installation of the network, a substantially clearer picture of the spatial pattern of earthquake occurrence emerged (Stauder et al, 1976). The initial network of 16 stations has almost quadrupled. Figure 2 presents the

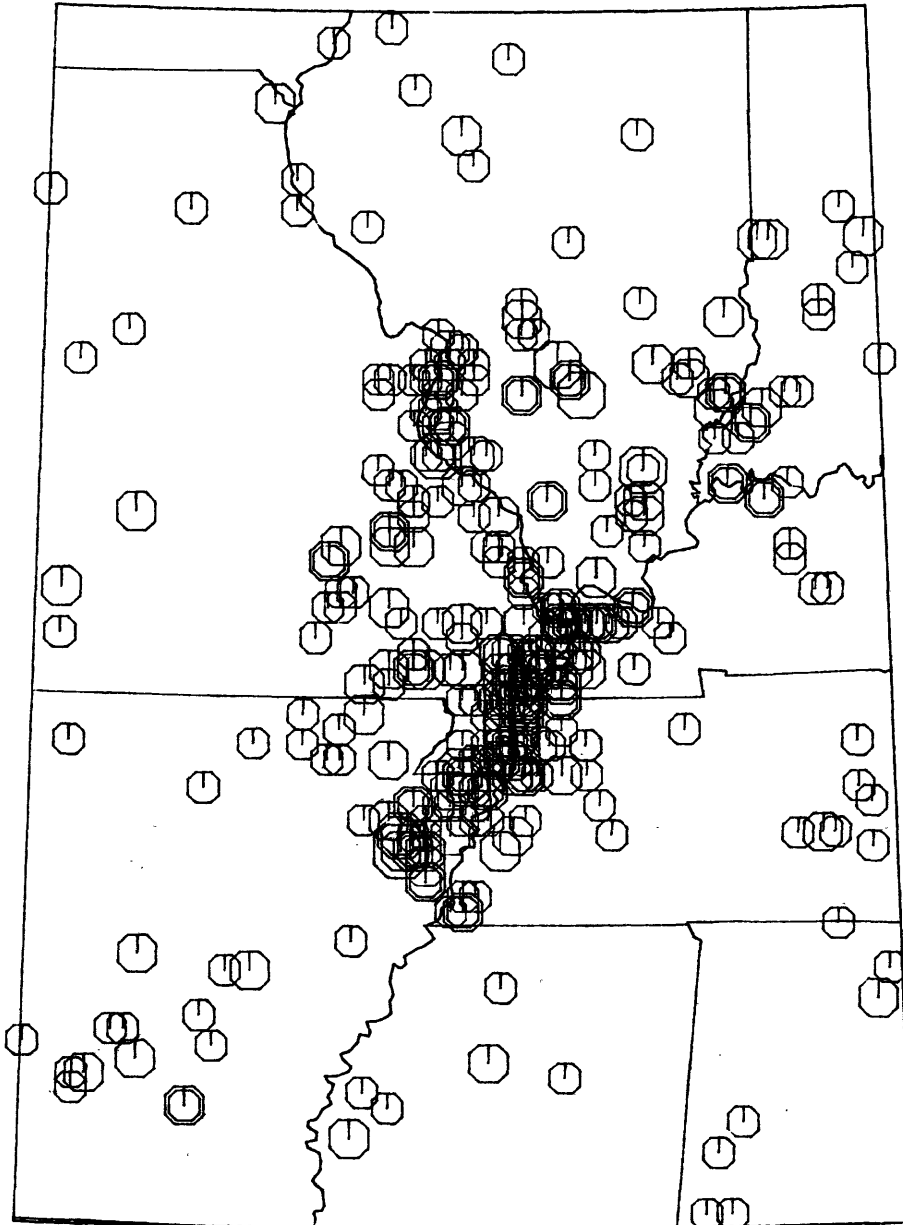


Fig. 1. Location of all known historical earthquakes from 1800 - 1975 which occurred in the central Mississippi Valley. The size of the symbols is indicative of the earthquake magnitude. This figure is based on the catalog of Nuttli and Brill (1980).

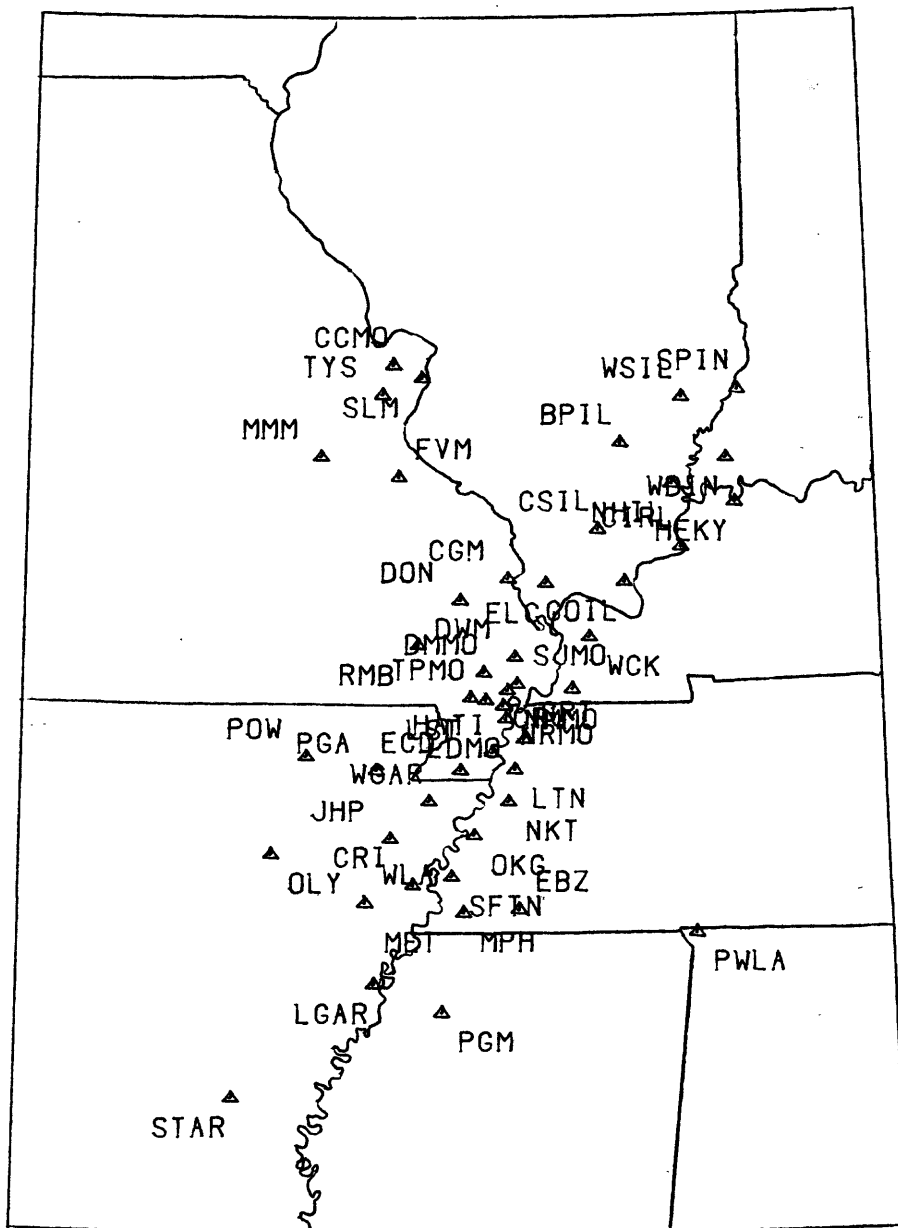


Fig. 2. Locations of active seismograph stations. Each station location is indicated by the center of the triangle. Adjacent to each station is a three or four letter unique station code. The data from most of the stations is telemetered directly to Saint Louis University for recording and analysis.

locations of most of the seismograph stations in the region. These stations are operated by the Tennessee Earthquake Information Center, the University of Kentucky, Indiana University, University of Michigan and Saint Louis University. Operational support is provided by the U. S. Geological Survey, the U. S. Nuclear Regulatory Commission, and the States of Tennessee, Kentucky and Indiana.

Figure 3 presents the locations of earthquakes that occurred since 1976. This figure is presented at the same scale as Figure 1. The pattern of seismicity is remarkably clearer in the immediate vicinity of New Madrid. Pronounced linear features are seen. In addition other patterns are prominent: a pattern from St. Louis southeastward along the Mississippi River, a more diffuse pattern southwestward from St. Louis, and an almost north-south pattern just west of the Wabash River in southeastern Illinois. Given the resolution of these patterns in Figure 3, the same patterns can be discerned in Figure 1.

Figure 4 presents a closeup of the modern earthquake locations in the vicinity of New Madrid. The region outlined in Figure 4 will be called the New Madrid Seismic Zone, while the extended region of Figures 1 and 3 will be called the Central Mississippi Valley Earthquake Zone. The remarkable features of the earthquake locations in Figure 4 are the lengthy linear segments. A 120 km long trend extends from Marked Tree, Arkansas, at the lower left hand corner of the Figure northeastward to Caruthersville, Missouri, where it terminates at the Mississippi River. Another 60 km long trend extends northwestward from Obion County, Tennessee, across the Mississippi River to New Madrid, Missouri. At New Madrid, shorter linear patterns to the northeast and west can be seen.

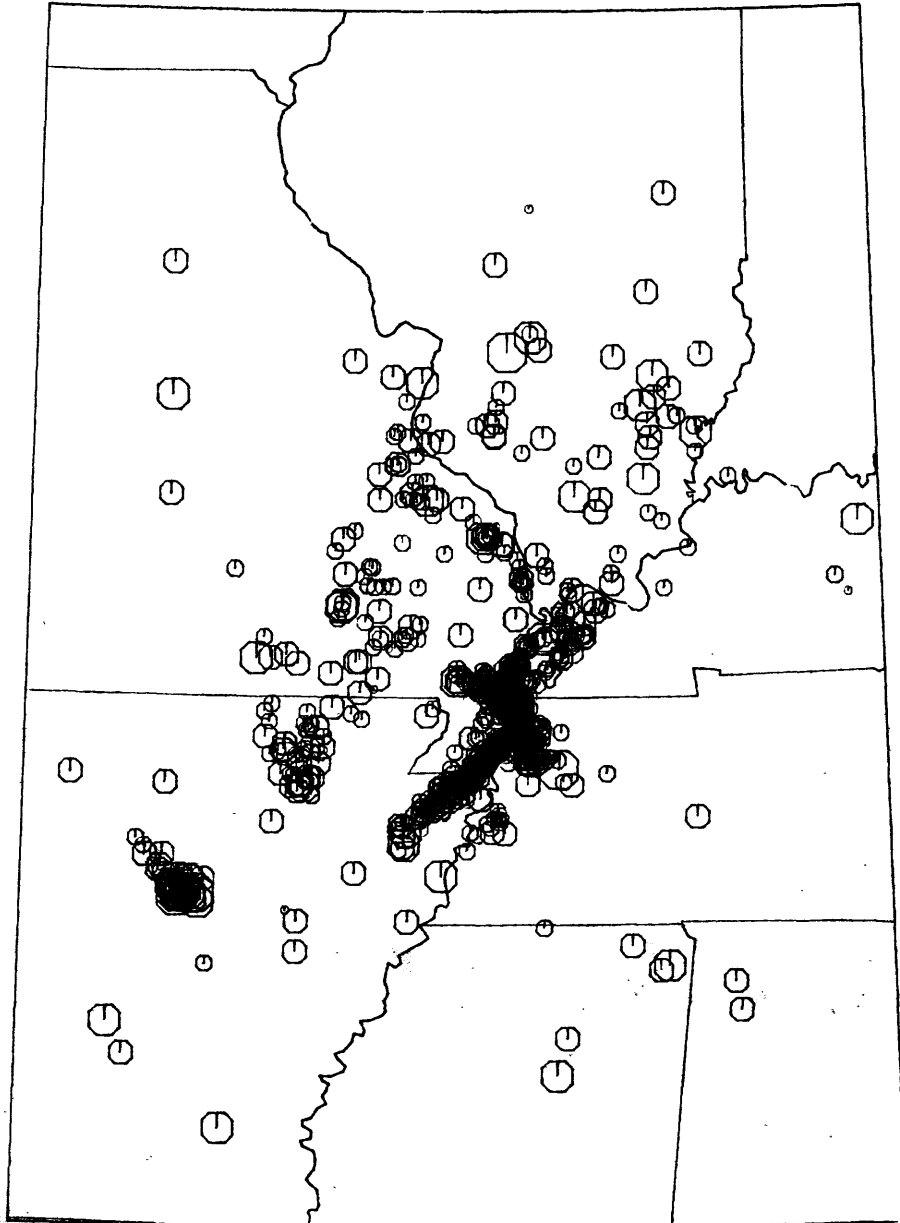


Fig. 3. Location of earthquakes detected and located using the dense regional network for the reporting period 1976 - 1982.

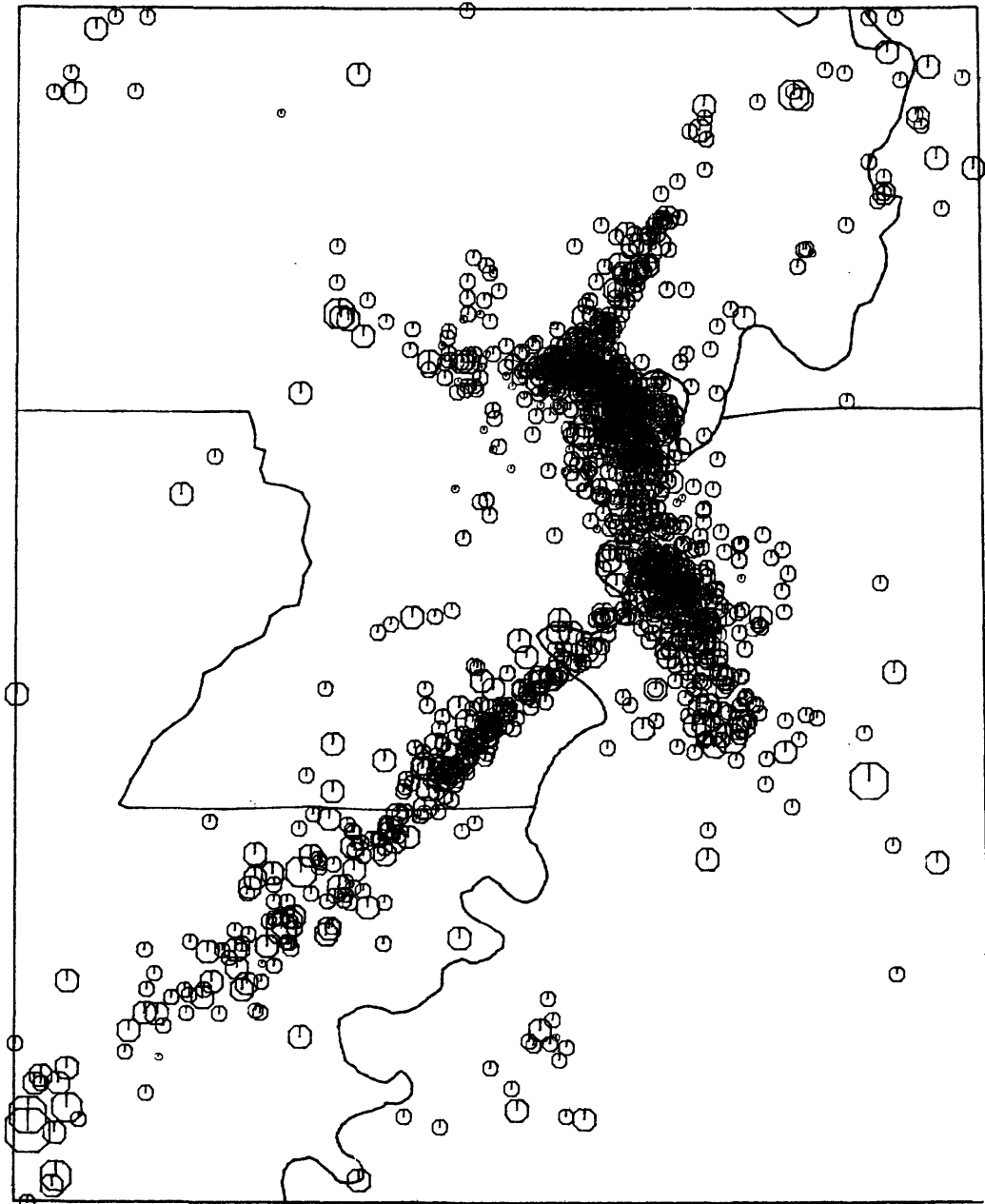


Fig. 4. Location of earthquakes detected and located using the dense regional network for the reporting period 1976 - 1982 in the immediate vicinity of New Madrid, Missouri.

The lengths of the trends are very important. The seismicity pattern indicates that the earthquakes are occurring on a few long faults or on a number of shorter segments which are not offset much. Given earthquake experience elsewhere, this means that there is the potential for large earthquakes along these long, linear trends.

Focal mechanism studies by Herrmann and Canas (1978) used body- and surface-wave data from larger earthquakes in the area together with P-wave first motion data from earthquakes detected by the seismic networks. They concluded that the motion along the 120 km Arkansas seismicity trend was characterized by predominantly right lateral strike slip motion. They were not able to obtain a clear picture of the nature of faulting along the left stepping seismicity trend between Ridgely, Tennessee, and New Madrid, Missouri. They were able to conclude that motion associated with the earthquakes is compatible with a horizontal compressive stress field trending approximately east-west.

Extensive studies are being conducted to relocate the earthquakes of Figure 4 using recent models of earth structure in the zone. L. Himes (personal communication) has investigated earthquakes on each linear trend and has obtained a much improved picture of the distribution of these earthquakes with depth.

Perry (1981) studied the recurrence of earthquakes in the region. In particular he compared the recurrence estimated from the historical earthquake data set and that estimated by more recent microearthquake network data. This comparison is important because it tells us whether or not present day activity is at the same level as the historical pattern. The seismicity data are grouped according to magnitude, m , and fit

to a mathematical model

$$\log_{10} N_c = a - bm$$

where N_c is the mean annual number of earthquakes greater than magnitude m . Perry (1981) found that the historical data set had enough resolution to permit a consideration of the entire New Madrid Seismic Zone of Figure 4 and also the Arkansas trend by itself. The results of his study are summarized in the following table.

| Source Zone | a | b |
|-----------------------|-------|-------|
| New Madrid-Historical | 3.741 | 1.000 |
| New Madrid-Network | 3.407 | 1.009 |
| Arkansas-Historical | 2.725 | 0.906 |
| Arkansas-Network | 2.740 | 0.899 |

The agreement is quite remarkable considering the fact that the magnitudes assigned to the individual earthquakes in the two data sets were estimated differently and that the microearthquake networks had been operating only 6 years, so that the two catalogs overlapped only in the magnitude range of 3 - 4, where both suffered from incomplete data sets. Using these numbers, we can compute that the mean annual number of earthquakes greater than or equal to a magnitude 5 is on the order of 0.023 to 0.055. If these numbers are inverted, we can say that an earthquake with magnitude greater than or equal to 5 will recur every 18 to 43 years, on the average. Note that this just applies to the New Madrid Seismic zone of Figure 4. There is also the possibility that earth-

quakes this large can occur elsewhere in the extended region of Figure 3. A conclusion of the Perry (1981) study is that the rate of earthquake occurrence since 1974 is comparable with the rate estimated from the historical record since the 1830's.

DISCUSSION

This brief paper focused on the current state of knowledge of earthquakes in the New Madrid Seismic Zone. Present and future efforts will be directed toward continued monitoring of the earthquake activity in the area and toward understanding the mechanics of present day faulting. Because of the high level of seismic activity relative to the rest of eastern North America, this region must continue to serve as a field laboratory for earthquake studies. Thus, significant results on the excitation and attenuation of strong ground motion as well as theoretical estimates of strong ground motion are expected in the future.

ACKNOWLEDGMENTS

The research reported on has been supported through contracts from the U. S. Geological Survey and the U. S. Nuclear Regulatory Commission.

REFERENCES

- Blake, J. L. (1826). A Geographical, Chronological, and Historical ATLAS, on a new and improved plan; or, A View of the Present State of all the Empires, Kingdoms, States and Colonies in the Known World, Cooke and Co., New York, pp 51-54.
- Fuller, M. L. (1912). The New Madrid Earthquake, U. S. Geol. Surv. Bull. 394, Washington, D. C.
- Herrmann, R. B. and J. A. Canas (1978). Focal mechanism studies in the New Madrid Seismic zone, Bull. Seism. Soc. Am. 68, 1095-1102.
- Nuttli, O. W. (1973). The Mississippi Valley earthquakes of 1811 and 1812: Intensities, ground motion and magnitudes, Bull. Seism. Soc. Am. 63, 227-248.
- Nuttli, O. W. (1974). Magnitude-recurrence relation for central Mississippi Valley earthquakes, Bull. Seism. Soc. Am. 64, 1189-1207.
- Nuttli, O. W. (1976). Comments on "Seismic intensities, 'size' of earthquakes and related parameters" by Jack F. Evernden, Bull. Seism. Soc. Am. 66, 331-338.
- Nuttli, O. W. and K. G. Brill (1980). Earthquake source zones in the Central United States determined from historical seismicity, in A Seismic Zoning Map for Siting Nuclear power Generating Facilities in the Eastern United States, Final Report, September 28, 1978 - September 28, 1980, Roundout Associates, Inc., Prepared for U. S. Nuclear Commission under Contract No. NRC-03-78-154, NUREG/CR-1577.

Penick, J., Jr. (1976). The New Madrid Earthquakes of 1811-1812,
University of Missouri Press, Columbia of Missouri.

Perry, R. G. (1981). Seismic Hazard Analysis for the Central United
States, Masters Thesis, Saint Louis University, St. Louis, Mis-
souri, 175pp.

Stauder, W., M. Kramer, G. Fischer, S. Schaefer and S. T. Morrisey
(1976). Seismic characteristics of southeast Missouri as indicated
by a regional telemetered microearthquake array, Bull. Seism. Soc.
Am. 66, 1953-1964.

RECURRENCE RATES AND PROBABILITY ESTIMATES FOR THE NEW MADRID SEISMIC ZONE

by

Arch Johnston and Susan J. Nava

Tennessee Earthquake Information Center

Memphis State University, Memphis, Tennessee

ABSTRACT

An updated frequency-magnitude relation for the New Madrid seismic zone is used to derive conditional probabilities for future, large New Madrid earthquakes. We estimate that there is a probability of a m_b 6.0 (M_s 6.3) event occurring by the year 2000 and a 86-97% probability by the year 2035. The estimates for a great 1812-type event are less than 1% probability by 2000 A.D. and less than 4% by 2035 A.D. These probabilities are contingent on many factors, a number of which remain assumptions because the lack of a geological or paleoseismological chronology of past New Madrid activity. A conditional probability requires knowledge of a mean recurrence time, the type of distribution, and the standard deviation of actual repeat times about this mean. Four assumed distribution functions--Gaussian, log-normal, Weibull and Poisson--were fit to recurrence estimates based on a combination of historical and instrumental seismicity data. Standard deviation was allowed to vary between one-third and one-half of the mean recurrence time, and a range of conditional probabilities were generated for time intervals of 15 and 50 years from the year 1985. The largest uncertainty in this procedure was the size of the seismicity source area to use for recurrence estimation. Calculations were done for both a large and a small source zone which led to variation in estimated recurrence intervals of a factor of two. The large source zone was favored for the final probability estimates because of the large crustal volume required to elastically store strain energy for great New Madrid earthquakes.

INTRODUCTION

Over the past decade remarkable progress has been made in our understanding of the geological, geophysical and tectonic framework of the New Madrid seismic zone. Many aspects of the seismicity, such as spatial dimensions of the active portions of the rift, type and depth of faulting and estimates of source parameters and ground motion are today subject to fairly well defined constraints compared to ten years ago. Such progress has not been matched, however, in the important question of providing accurate estimates of the recurrence times and associated probabilities of large New Madrid earthquakes. In this paper we will review and update the past work on this topic. In addition we will use the derived recurrence rates in combination with some assumed properties of the seismicity to generate probabilistic estimates of future large New Madrid events.

Input data for estimating recurrence intervals are available from three sources: (1) instrumental monitoring; (2) historical seismicity listings; (3) geological and/or tectonic evidence. The applicable time frame for these sources is decades, centuries and the Quaternary Period respectively. Instrumental seismicity is generally the most complete and homogeneous data set, but it suffers the rather severe limitation of sampling only a small fraction of the repeat time of large events. Historical seismicity may span one or more recurrence intervals of major quakes (in some cases) but is usually a more suspect data set because of lack of completeness and rather large uncertainties in magnitude assignment and epicentral location. Where recoverable, slip rates on Quaternary faults have been incorporated into seismic hazard analysis to good effect, e.g., the Wasatch Front (Ryall and Smith, and following papers, 1980) and intraplate Japan (Wesnousky et al., 1982; 1983). The ratio of seismic to aseismic movement for these faults is generally unk-

nown and this introduces an uncertainty in this technique.

More recent geological information may be gained by analyzing deformation preserved in sediments over and along fault zones as has been done in southern California (Sieh, 1978; Raleigh et al., 1982) and New Madrid (Russ, 1979). Such estimates are subject to their own set of uncertainties such as the difficulty of establishing reliable dates of the deformational episodes and of determining magnitudes of the causative events.

No first-hand fault slip information is available for the New Madrid seismic zone because of the thick cover of alluvium. Moreover, no chronology of past large slip events exists, although the conclusion of Russ (1979) that three such events occurred in a maximum interval of 2,250 years provides a general and important constraint. Therefore in this paper we must rely solely on instrumental and historical seismicity data for the estimation of New Madrid recurrence intervals. As will be shown in a later section, such information is not adequate to confidently assign probabilities to these recurrence values. In the absence of measured values of such necessary quantities as strain rate or the distribution of actual recurrence times about the estimated mean return periods, plausible values are taken from theoretical studies or from literature on other fault zones and used to construct rough estimates of the conditional probability of large New Madrid earthquakes. These are the first published conditional probabilities for the New Madrid zone. We hope they will serve as a reference frame that can be refined and improved as additional data become available.

FREQUENCY-MAGNITUDE RELATION

The magnitude distribution of earthquake occurrences is generally

observed to follow the Gutenberg-Richter relationship

$$\log(N_c) = a - bM \quad (1)$$

where N_c is the number of events greater than or equal to magnitude M , and a and b are constants. Applied over a given time period, the number of earthquakes in a given magnitude range is obtained, yielding a characteristic recurrence time for that magnitude, based on the assumption that the process is stochastic (i.e., that the occurrence rate is not a function of time). The constant a , the activity parameter, provides a measure of the overall occurrence rate of earthquakes in the zone considered and is the zero magnitude intercept on a semilog plot. The constant b , or b -value, is controlled by the distribution of events between the higher and lower magnitude ranges. Both constants influence derived recurrence times; therefore it is essential that the values and the variance of these constants be determined as accurately as possible.

PREVIOUS STUDIES

Early efforts at obtaining a recurrence relation for the New Madrid region used historical compilations and Modified Mercalli intensities rather than magnitudes (McClain and Myers, 1970; Algermissen, 1972; Mann et al., 1974). The average return periods for large earthquakes ($MMI_0 \geq X$) as determined by these studies varied between 175 and 700 years (Nuttli, 1974).

Table 1 provides a summary of previous New Madrid recurrence formulas based on magnitude. These results are not directly comparable because of differences in magnitude, area normalization, cumulative versus non-cumulative number of events and varying time windows. They do, however, provide an indi-

TABLE 1

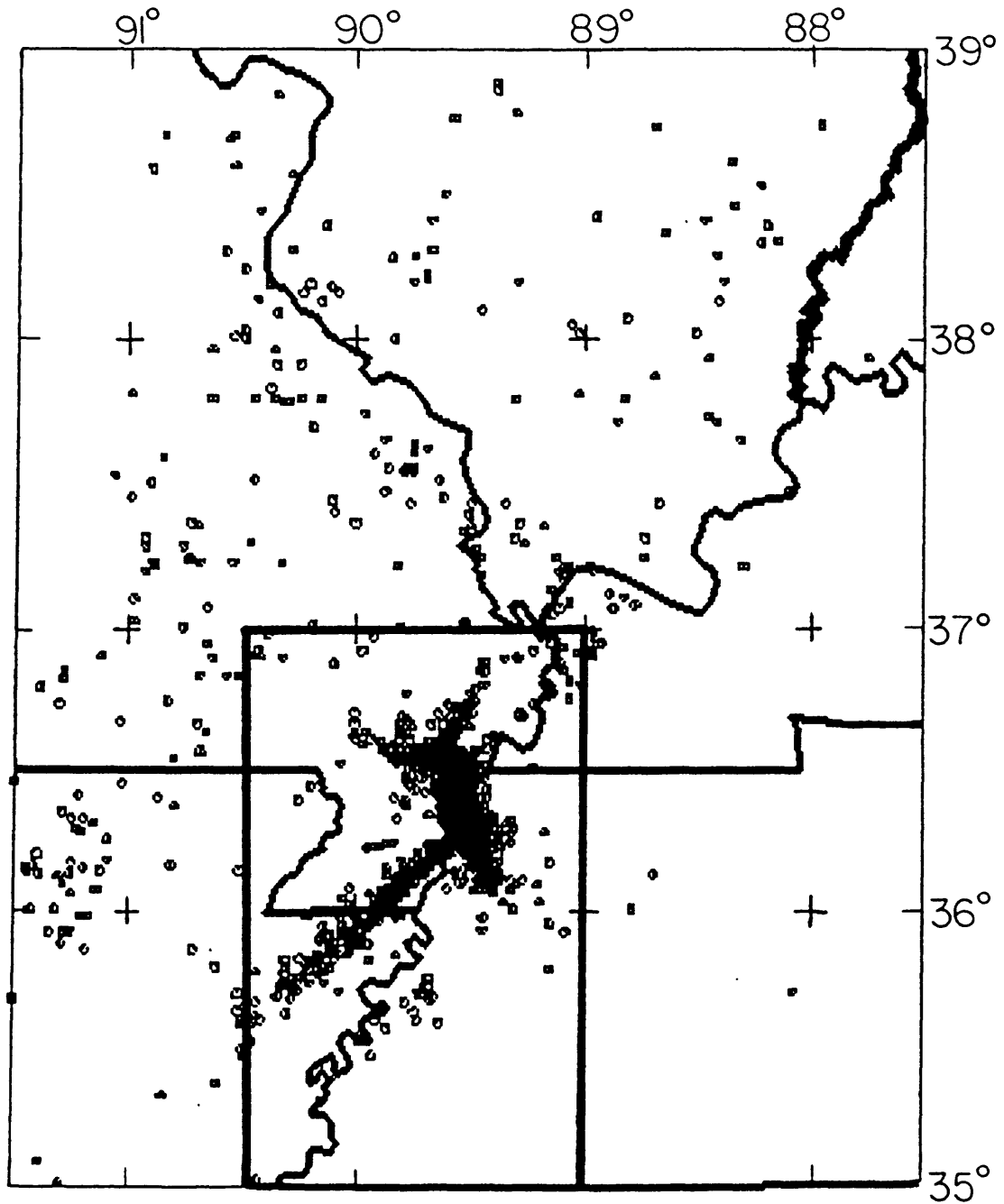
PREVIOUS NEW MADRID FREQUENCY-MAGNITUDE FORMULA

| Authors | Data Base/ Time Period | Region | Magnitude Range | Analysis Method | Av. Recurrence Time (yrs) | |
|------------------------------|---|---|------------------------------------|--|--|--|
| | | | | | log(N ₀)=a-bM or log(N) =a-bM | Mb6.0 Mb7.0 Mb7.3 (Ms6.3) (Ms6.3) (Ms8.8) |
| Nuttli (1974) | Historical, 1833-1972 (140 years) | Cent. MS Valley -250,000 km ² | 3.0 < mb < 6.2 | Max. Likelihood (non-cumulative) Max Likelihood | log(N)=3.55-0.87mb log(N)=3.76-0.92mb | 47 347 773 58 497 1,117 |
| Stauder and others (1976) | Instrumental, 7/74 - 12/85 (1.5 yrs) | NMSZ, 1.5 ⁰ X 1.5 ⁰ -22,800 km ² | -1.2 < mb < 4.3 | Visual line fit | log(N ₀)=3.20-0.75mb | 30 169 224 |
| Nuttli & Herrmann (1978) | Historical, 1811-1975 233 events/164 yrs Historical, 1811-1975 303 events | NMSZ (A) 22,506 km ² NMSZ (A+B) 50,012 km ² | 3.7 < mb < 7.4 3.2 < mb < 7.4 | -Area normalized to 100,000 km ² -b restricted to 0.92 -weighted least squares | log(N ₀)=3.90-0.92mb log(N ₀)=3.95-0.92mb | 42 347 810 37 309 721 |
| Nuttli (1979) | Historical plus Instrumental 1811-1975, 165 yrs | NMSZ | -1.0 < mb < 7.4 | -line fit: not available -area normalized to 15,000 km ² | log(N ₀)=3.31-0.77mb | 21 120 240 |
| Howell (1980) | Nuttli (1974) Hist. List | Cent. MS Valley -250,000 km ² | 3.0 < mb < 6.2 | Converts to cumulative; applies Gumbel extreme Value theory (Type 1) | log(N ₀)=3.63-0.87mb log(N ₀)=3.82-0.92mb | 69 510 1,100 |
| Johnston (1981) | Hist.(Nuttli & Brill, 1982) plus Instr. (Stauder, et.al., 1974-1980) 1816-1980/167 yrs. | NMSZ -37,500 km ² (hist) -14,400 km ² (instr) | 1.7 < mb < 6.2 | -Avg. of least squares & max likelihood -normalized time periods | log(N ₀)=3.27-0.89mb | 118 912 1,687 |
| Perry (1981) | Hist.(Nuttli & Brill, 1982). Instr. (1974- 1980) | Nuttli & Brill config. 25,891 km ² Russ (1980) config. 32,635 km ² | -1.7 < mb < 6.2 -1.7 < mb < 6.2 | max likelihood max likelihood | log(N ₀)=3.132-0.873mb log(N ₀)=3.123-0.895mb | 127 953 1,741 176 1,387 2,573 |
| Nuttli (1981) | Historical plus instrumental | NMSZ | 1.7 < mb < 7.2 | Not available | log(N ₀)=3.33-0.87mb | 78 525 1,050 |
| Stauder (1982) | Instrumental | NMSZ, 1.5 X 1.5 -22,800 km ² | 1.0 < mb < 3.5 | least squares | log(N ₀)=3.437-0.783mb | not applicable to large events |

cation of general recurrence ranges developed by a variety of workers using a variety of approaches and boundary conditions. These data imply that a destructive New Madrid earthquake ($m_b 6.0$) can be expected on the order of every 50-100 years, a great earthquake ($m_b 7.0/M_s 8.3$) every 300-1000 years and a maximum magnitude event ($m_b 7.3/M_s 8.8$) every 500-1500 years. This assumes that New Madrid behaves in a time-predictable manner as has been demonstrated for both interplate (Bufe et al., 1977) and intraplate (Shimazaki and Nakata, 1980) fault zones. Since a prehistoric chronology is not available for New Madrid we cannot verify such behavior; it remains the fundamental assumption of this paper.

A CURRENT FREQUENCY MAGNITUDE RELATION FOR NEW MADRID

Data Base. The historical seismicity listing compiled by Nuttli and Brill (1981) was combined with the instrumental record of the St. Louis University seismic network (Stauder and others, 1974-1983) to estimate mean recurrence rates for the New Madrid seismic zone. Two different source zones were used in this study (Figure 1), an approach taken in response to the work of Wesnousky and Scholz (1983). Based on Quaternary fault slip rates in intraplate Japan, they suggested that the observed logarithmic distribution of earthquake magnitude is a consequence of a logarithmic distribution of individual fault dimensions rather than a distribution of earthquake size on a single fault. Thus, it is not critical (or even advisable) to restrict the source zone to only the most active portion of New Madrid, even though it is probable that major earthquakes could only occur there. The smaller source zone is about one-fifth the size of the larger zone, yet contains 60% of the



1974 - 1983

Figure 1. Map of the Central United States with the 1974-1983 instrumental seismicity data set (Stauder and others, 1974-1983). The boundaries of the two source zones used for frequency-magnitude determination are: large zone, 35.0° - 39.0° N/ 87.7° - 91.5° W; small zone, 35.0° - 37.0° N/ 89.0° - 91.5° W.

historical data and 76% of the instrumental data. It is represented by the small rectangle of Figure 1. Table 2 lists the parameters for each source zone. Arguments favoring selection of the larger source zone for New Madrid recurrence rates are presented in the final section.

A cumulative frequency-magnitude plot of the combined historical and instrumental data sets for both source zones is shown in Figure 2; it was generated following the technique outlined in Johnston (1981). From the instrumental data set, nine years of data were available, ranging from a completeness threshold magnitude of 1.7 to a maximum of 5.0. This was combined with the historical listing, 158 years of data, ranging from a threshold magnitude of 3.6 to a maximum of 6.2. In order to combine the data sets, each set was normalized to cumulative events per year.

The transition from instrumental to historical data was made between magnitude 3.5 and 3.6. This assured a near completeness of both data sets, as reporting of low magnitude in Nuttli and Brill is complete to M3.6 (Johnston, 1981), and magnitudes above 3.5 for which nine years may not be an adequate sampling time are excluded from the instrumental portion of the plot.

Methodology. Both linear regression and maximum likelihood techniques were used to determine the Gutenberg-Richter constants a and b for the "best-fit" line through the data. Each technique has advantages and disadvantages that have been extensively discussed in the literature (e.g., Weichert, 1980; Bender, 1983). As pointed out by Weichert, conventional least squares (LS) is the maximum likelihood method for independent data with a Gaussian error distribution. For cumulative frequency-magnitude plots as used in this study, these conditions are obviously violated.

Conceptually maximum likelihood (ML) is the superior estimation technique; in practice, however, ML accords so little weight to the upper

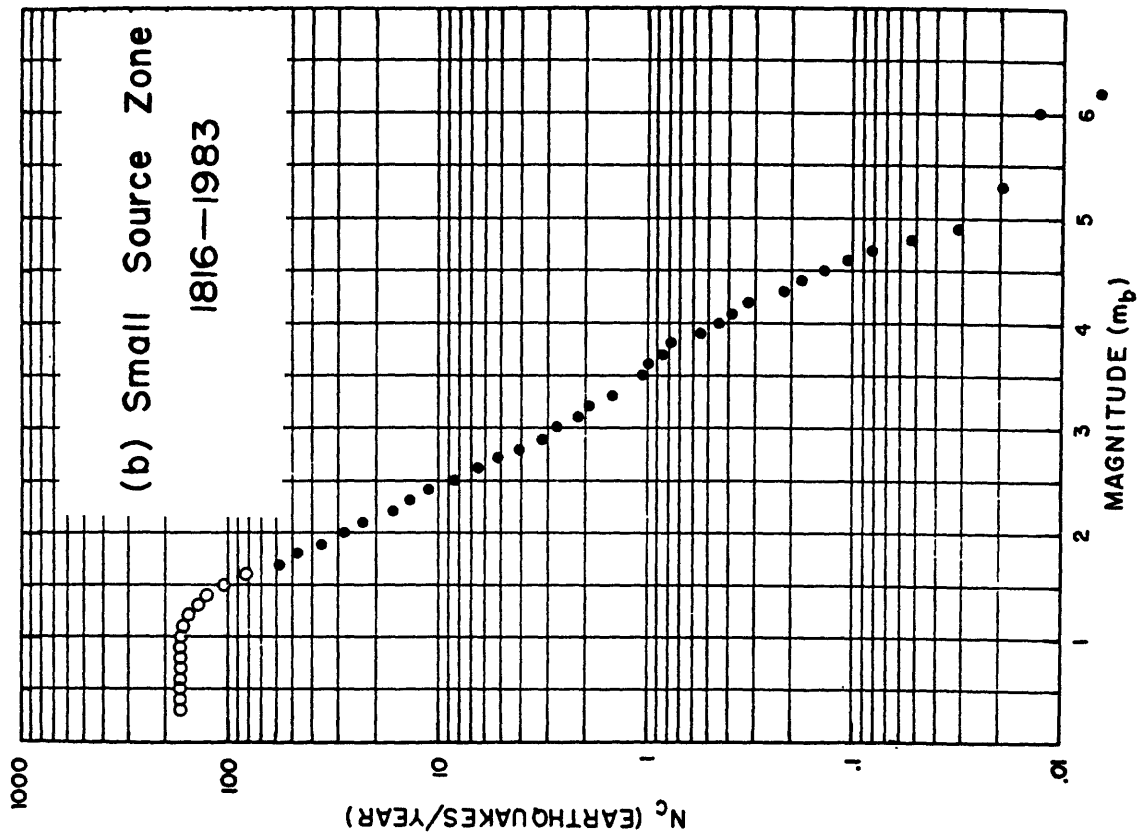
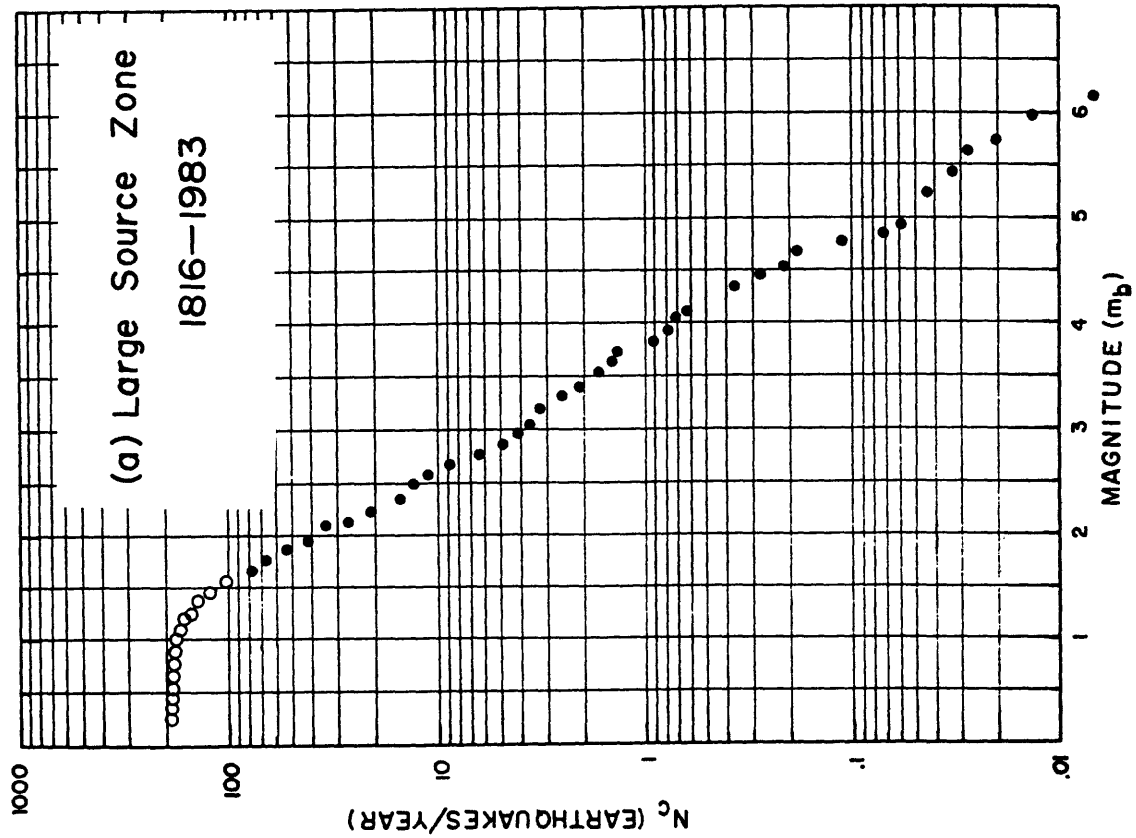


Figure 2. Cumulative frequency-magnitude data base for determining the Gutenberg-Richter constants, a and b. Instrumental data from 1974-1983 was used for $m \leq 3.5$; historical data for $m > 3.6$. Open symbols denote data points not used in computation. (a) Data base from large source zone of Fig. 1. (b) Data base from small source zone. See Table 2 for computed recurrence formula from these data.

TABLE 2

NEW MADRID FREQUENCY-MAGNITUDE PARAMETERS

| Data Set/Method | Increment | a | σ_a | b | σ_b (Bolt, 1982) | T_r (years) (M26.0) | T_r (years) (M27.0) |
|---|---------------|-------|----------------|-------|----------------------------|--------------------------|--------------------------|
| <u>Large Source Zone</u> | | | | | | | |
| 157,700 km ² (Fig.1) | . | . | . | . | . | . | . |
| 956 events; 1816-1983 | . | . | . | . | . | . | . |
| Magnitude: 1.7-6.2 | . | . | . | . | . | . | . |
| Least Squares | $\Delta M=.1$ | 3.346 | ($\pm .037$) | .882 | ($\pm .028$) | 88 | 673 |
| | $\Delta M=.5$ | 3.550 | ($\pm .070$) | .882 | ($\pm .030$) | 55 | 420 |
| | | | | | | 70 | 550 |
| <u>Small Source Zone</u> | | | | | | | |
| 29,959 km ² (Fig.1) | . | . | . | . | . | . | . |
| 685 events; 1816-1983 | . | . | . | . | . | . | . |
| Magnitude: 1.7-6.2 | . | . | . | . | . | . | . |
| Least Squares | $\Delta M=.1$ | 3.187 | ($\pm .055$) | .896 | ($\pm .046$) | 155 | 1,216 |
| | $\Delta M=.5$ | 3.488 | ($\pm .095$) | .930 | ($\pm .043$) | 124 | 1,052 |
| | | | | | | 140 | 1,100 |
| <u>Maximum Likelihood</u> | | | | | | | |
| (Bender, 1983) | $\Delta M=.1$ | 3.899 | --- | 1.019 | ($\pm .053$) | 164 | 1,714 |
| | $\Delta M=.5$ | 3.851 | --- | 1.001 | ($\pm .050$) | 143 | 1,432 |
| * Included for comparison only -- see text. | | | | | | | |
| * Maximum Likelihood (Bender, 1983) | | | | | | | |
| * Maximum Likelihood (Bender, 1983) | | | | | | | |

magnitude points, that it is less suitable than least squares for estimating the recurrence intervals of high magnitude, infrequent earthquakes (See Shi and Bolt [1982] for a discussion.) This is especially true for large data sets such as used in this study. For large, well defined data sets, then, cumulative least squares provides a reliable estimation of the data (c.f., Weichert, 1980).

Because of the arguments of the foregoing paragraph and because of the rather ad hoc manner in which the constant a is determined by ML (most authors constrain the line slope b through either the minimum or the average magnitude data point), we chose to base our derived frequency-magnitude formula on least-squares regression. Table 2 contains the constants a and b of equation (1) and their uncertainties computed by both LS and ML for magnitude increments of 0.1 and 0.5 for both the large and small source zone.

Statistical uncertainties were computed as follows. For a, with n magnitude intervals, x_i =ith magnitude interval and $y_i=(\log N_i)$,

$$\sigma_a = \frac{\sqrt{\sum_{i=1}^n [y_i - (a - bx_i)]^2 / n - 2}}{\sqrt{\sum_{i=1}^n x_i^2 - \frac{(\sum_{i=1}^n x_i)^2}{n}}} \cdot \sqrt{\frac{\sum_{i=1}^n x_i^2}{n}} \quad (2)$$

(e.g., Miller, 1982). For b, the standard error of b for a large number of events from Shi and Bolt (1982) is used:

$$\sigma_b = 2.30 b^2 \sqrt{\frac{\sum_{i=1}^n (M_i - \bar{M})^2}{n(n-1)}} \quad (3)$$

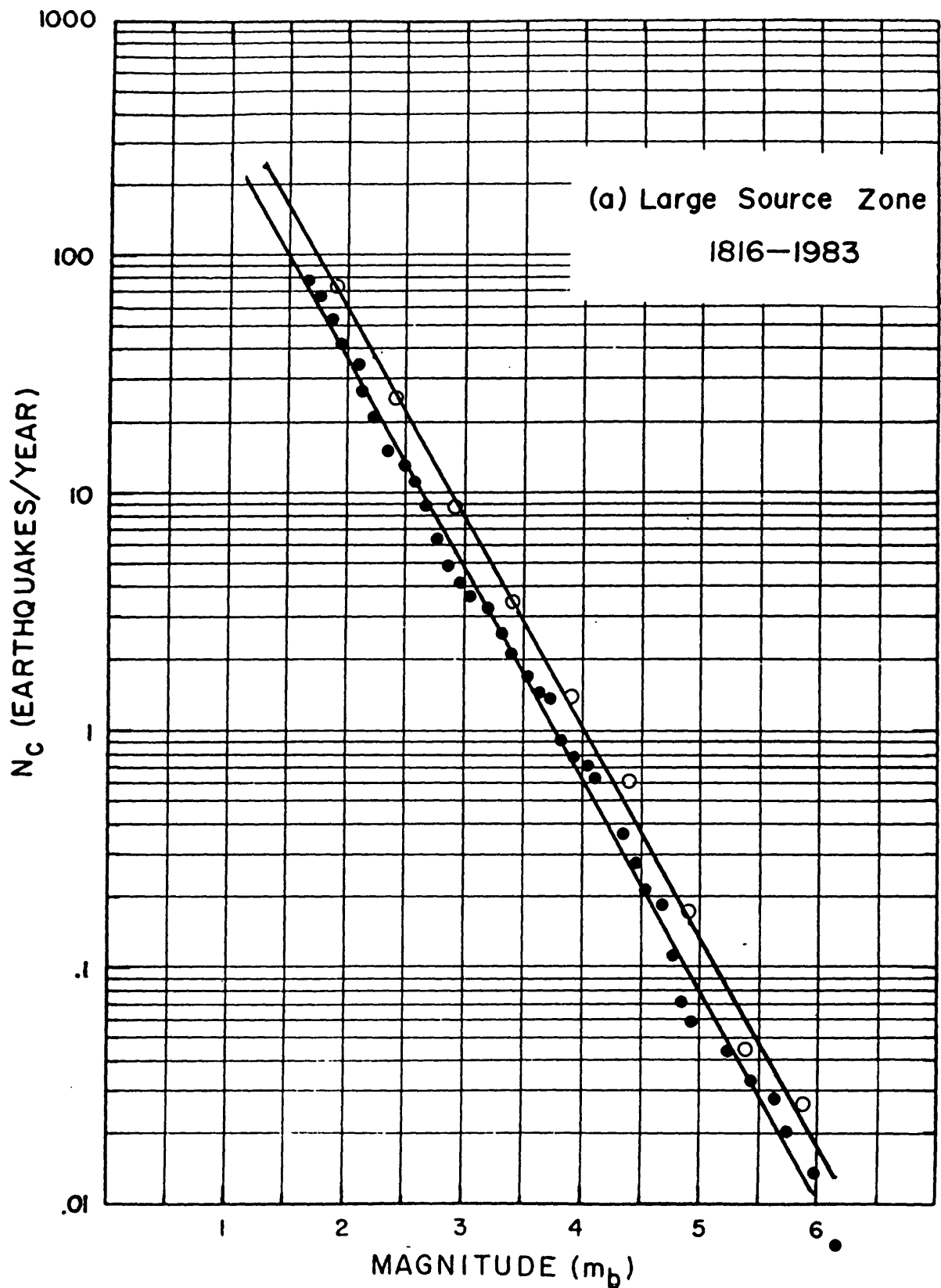


Figure 3. Illustration of the effect of varying Δm , the magnitude increment. Magnitude increments of 0.1 and 0.5 are shown.

where \bar{M} is the mean magnitude corrected for grouped magnitudes following Bender (1983).

Also included in Table 2 are mean recurrence intervals T_r of 70 and 140 years for $m_b \geq 6.0$, and 550 and 1,100 years for $m_b \geq 7.0$. These are the values of T_r to be used in the subsequent probability analysis, and are intermediate to values determined by LS for $\Delta M = 0.1$ and 0.5. ML recurrence values are included in Table 2 for reference but are not used for probability estimation.

A frequency-magnitude relation for New Madrid derived from the least-squares analysis and from the intermediate recurrence times of Table 2 is:

$$\log(N_c) = 3.43 - 0.88 (m_b) \quad [\text{Large source zone}] \quad (4a)$$

$$\log(N_c) = 3.32 - 0.91 (m_b) \quad [\text{small source zone}] \quad (4b)$$

with $\sigma_a = 0.070$ and $\sigma_b = 0.040$.

PROBABILITY ESTIMATES

A problem of increasing concern in the Central United States is the likelihood of occurrence of the next large New Madrid earthquake. (This is a separate and simpler question than that of finding the total seismic hazard which entails estimating the level of ground motion generated by multiple source zones and the chance of exceeding it at a given location.) In this section we will examine how well probabilities of occurrence can be estimated for the New Madrid seismic zone.

The average return period or recurrence interval, as previously derived, does not in and of itself supply sufficient information to determine probability of occurrence. It is also necessary to know the frequency distribution of recurrence intervals for a given magnitude or magnitude range. That is, for a time span much greater than the estimated recurrence time, what is the distribution of actual repeat times about the estimated mean? Given the mean, the type of distribution and the standard deviation of the observations, either cumulative probability, (the probability that an earthquake would already have happened) or future (conditional) probability may be ascertained.

For the New Madrid seismic zone, neither the type of distribution of recurrence intervals, nor their standard deviation from the mean is known. Because of this lack of necessary information we can only proceed by assuming New Madrid behaves in certain ways. Our approach is to take a range of assumed distributions and standard deviations and examine the effect of these assumptions on probabilistic estimates. If the final estimates do not diverge too much, we can have confidence that the determined probabilities are fairly stable or robust, i.e., insensitive to the statistical assumptions. This presumes, of course, that our assumptions are comprehensive enough to encom-

pass the actual behavior of the New Madrid seismic zone.

Terminology and Definitions

Before examining individual cases we define some frequently used terms and concepts.

(1) The statement "x has the probability $P(x)$ " means that if an operation (read 'earthquake occurrence') is repeated a great number of times, it is practically certain that the relative frequency of x is equal to $P(x)$. Here relative frequency is just the number (range) of actual outcomes divided by the number (range) of possible outcomes.

(2) Cumulative Probability Distribution. If X is a random continuous variable that is a property of events of a population, then for any real number x the distribution of X, denoted $F(x)$, is defined as the number (range) of all events with $X \leq x$ divided by the total number (range) of events. Therefore $F(x)$ also gives the probability of choosing at random an event with $X \leq x$. Thus

$$F(x) = P(X \leq x).$$

$F(x)$ is the cumulative probability distribution (or distribution function) for an arbitrary distribution F and arbitrary variable x. In this study we are interested in variations with time t and assign specific cumulative distributions as follows: Gaussian (or normal), $G(t)$; log-normal, $L(t)$; Weibull, $W(t)$; Poisson, $S(t)$, (to avoid confusion with cumulative probability, $P(t)$).

(3) Probability density. If x is a continuous variable then there exists a function f such that

$$F(x) = \int_{-\infty}^{\infty} f(x) dx \quad . \quad (5)$$

$f(x)$ is called the probability density; it is just the derivative of the cumulative distribution function, i.e.,

$$F'(x) = f(x) \quad . \quad (6)$$

Note that since $F(x)=P(X \leq x)$, if events in the sample space are mutually exclusive and collectively exhaustive, it follows that

$$P(x) = \int_{-\infty}^{+\infty} f(x)dx = 1$$

$$P(a \leq x \leq b) = F(b) - F(a) = \int_a^b f(x)dx \quad . \quad (7)$$

and

Specific probability densities in this paper are denoted as follows: Gaussian, $g(t)$; log-normal, $l(t)$; Weibull, $w(t)$; Poisson, $s(t)$.

(4) Conditional probability. Let A and B be two events (or two sets of outcomes) in a sample space. Conditional probability is defined as the probability of event B occurring given that event A has already occurred. It is denoted by $P_c = P(B|A)$. Thus P_c is just the ratio

$$P_c = P(B|A) = \frac{P(A \cap B)}{P(A)} \quad ,$$

where $P(A \cap B)$ is the intersection of A and B, that is, a subset of sample space consisting of all possible outcomes contained in both A and B. In the context of earthquake recurrence, A and B are events in the same magnitude range and

$$P_c = \text{Prob.} \left[\text{Next event (B) within } (t, t+\Delta t) \mid \text{Preceding event (A) at } t_0 \right] \quad .$$

A useful formulation of conditional probability is in terms of cumulative probability or area beneath the curve of a probability density function. This is illustrated in Figure 4 for an arbitrary distribution $F(t)$. P_c is the ratio of two areas: one area beneath $f(t)$ between t and $t+\Delta t$ representing the probability of occurrence during this time interval; the other is the area beneath $f(t)$ from t to $+\infty$ representing the probability that the event will eventually occur given that at time t it has not yet happened. Thus

$$P_c = \frac{\int_t^{t+\Delta t} f(\tau) d\tau}{\int_t^{\infty} f(\tau) d\tau} \quad , \quad (8)$$

or from equations (5) and (7)

$$P_c = \frac{F(t+\Delta t) - F(t)}{1 - F(t)} = \frac{\Delta F}{1 - F(t)} \quad . \quad (9)$$

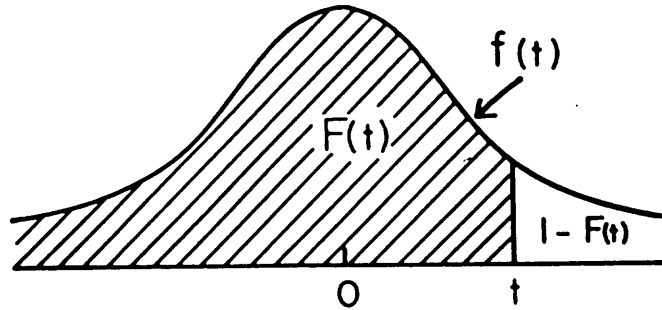
Frequently the computation of P_c is simplified by using $F'(x) = f(x)$ (from equation 6) and expanding $F(x)$ in an incremental Taylor series:

$$\Delta F = F(x+\Delta x) - F(x) = \Delta x F'(x) + \frac{\Delta x^2}{2!} f''(x) + \dots \quad (10)$$

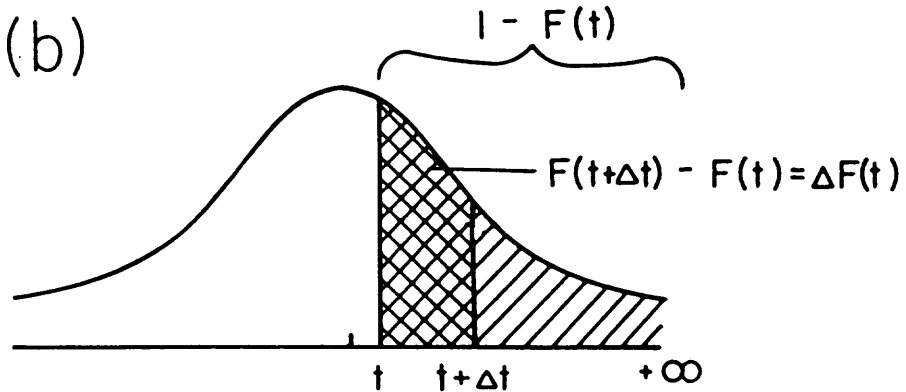
Thus, for example, for a Gaussian conditional probability, a first-order approximation is

$$P_c = \frac{\Delta G}{1 - G(t)} \approx \frac{\Delta t g(t)}{1 - G(t)} \quad . \quad (11)$$

(a)



(b)



$$P_c = \frac{\Delta F(t)}{1 - F(t)}$$

Figure 4. (a) An arbitrary distribution function illustrating the concept of $f(t)$, the probability density function and $F(t)$, the cumulative probability function. Note that for normalized or standard distributions the total area between $f(t)$ and the abscissa is 1. (b) Formulation of conditional probability P_c in terms of the ratio of two areas beneath a standardized probability density function.

Care must be taken, however, to apply this approximation only for $\Delta t \ll t$; otherwise unreasonably large conditional probabilities will be obtained (in extreme cases P_c will exceed 1). Figure 5 illustrates the difference between computing an approximate P_c from equation (11) and an exact P_c from equation (9).

Specific Probability Distributions

Four possible probability distributions were considered as representations of the actual recurrence interval distribution of New Madrid earthquakes for a given magnitude range. Each distribution has seen previous use in seismic hazard analysis. In the absence of an actual New Madrid chronology, we feel that this approach has a high likelihood of bracketing the actual behavior of the New Madrid seismic zone.

Poisson

The discrete Poisson distribution has the property that the probability of occurrence of an event is exactly the same for a given time interval anywhere along the time axis. This time-stationarity property is usually expressed in a distribution function for the number of events per unit time. More useful for our purposes is the distribution of interevent times which may be shown to follow a negative exponential distribution for a Poisson process (Lomnitz, 1974):

$$s(t) = \frac{1}{T_i} e^{-t/T_i} \quad , \quad (12)$$

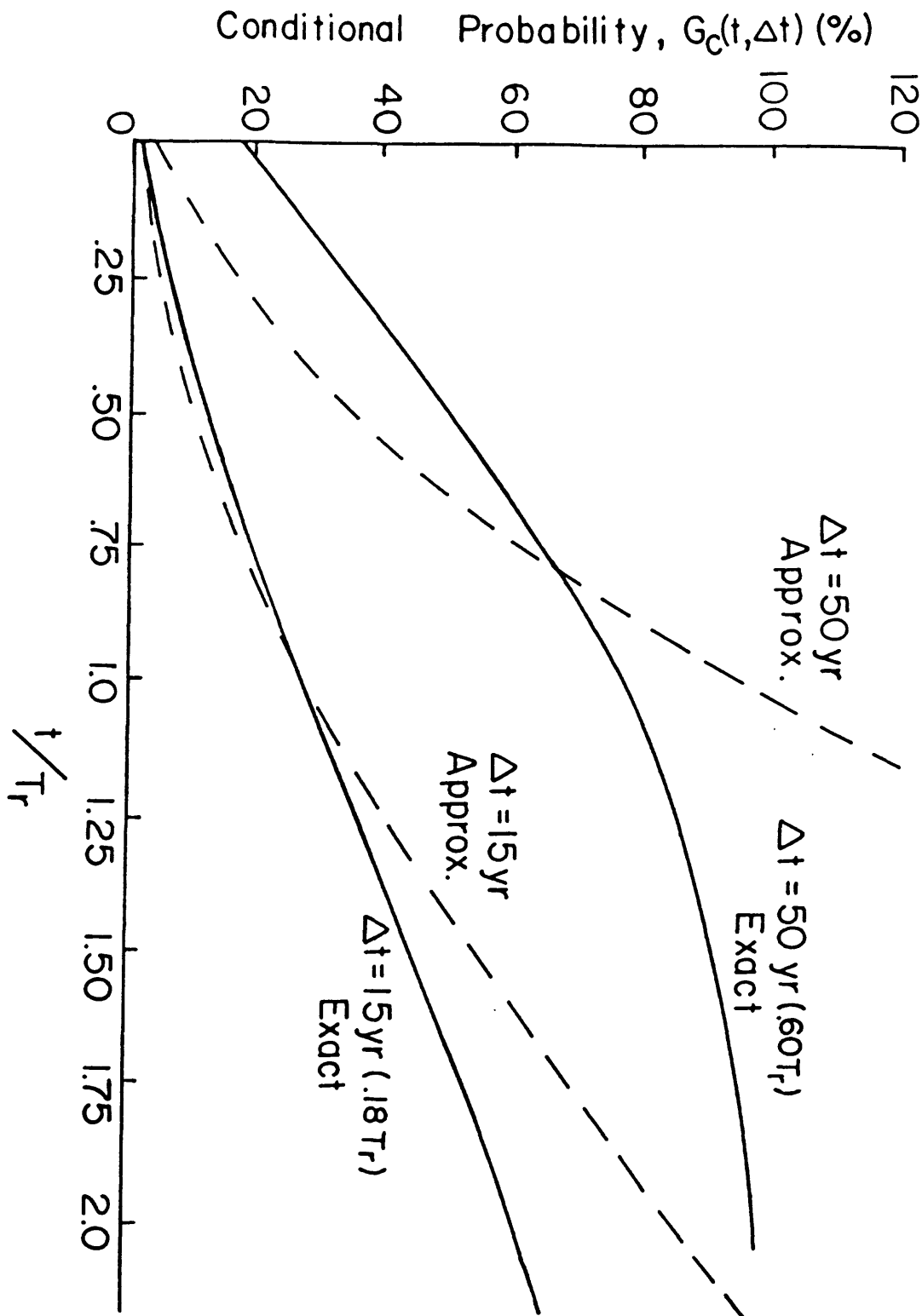


Figure 5. Conditional probability by approximate and exact methods. The Gaussian distribution for an quake is chosen for this illustration. The approximation method is the first-order Taylor expansion of the cumulative probability (equations 10 and 11); the exact method is the ratio of areas (equations 8 and 9). Note that the first-order approximation is a good representation of conditional probability only for small Δt and for elapsed times t less than T_r , the average repeat time.

where T_i is the average interevent time. Figure 6 shows the distribution of instrumental New Madrid seismicity and the Poisson probability density function for $T_i = 2.04$ days.

Poisson statistics have been used extensively to represent time sequences of earthquakes. In many cases seismic zones seem to closely emulate a Poisson process (e.g., Fig. 6). However, this is a different property from the one of interest here, which is the distribution of occurrence times about an average recurrence time for a given magnitude range. For this, Poisson probabilities are not an adequate representation because the independence of Poisson events results in a constant conditional probability rather than one increasing in time since the last event as required by the time-predictable model assumed for New Madrid.

Even though Poisson probabilities are not appropriate for this study, their extensive use in the seismic hazard literature make them useful as a reference level when time-dependent conditional probability is discussed.

The cumulative Poisson probability when T_r is the average recurrence time is:

$$S(T \leq t) = \int_0^t s(\tau) d\tau = 1 - e^{-t/T_r} \quad . \quad (13)$$

Substitution in equation (9) yields a conditional probability:

$$S_c(t, \Delta t) = 1 - e^{-\Delta t/T_r} \quad , \quad (14)$$

where Δt is the interval under consideration for an earthquake reoccurrence.

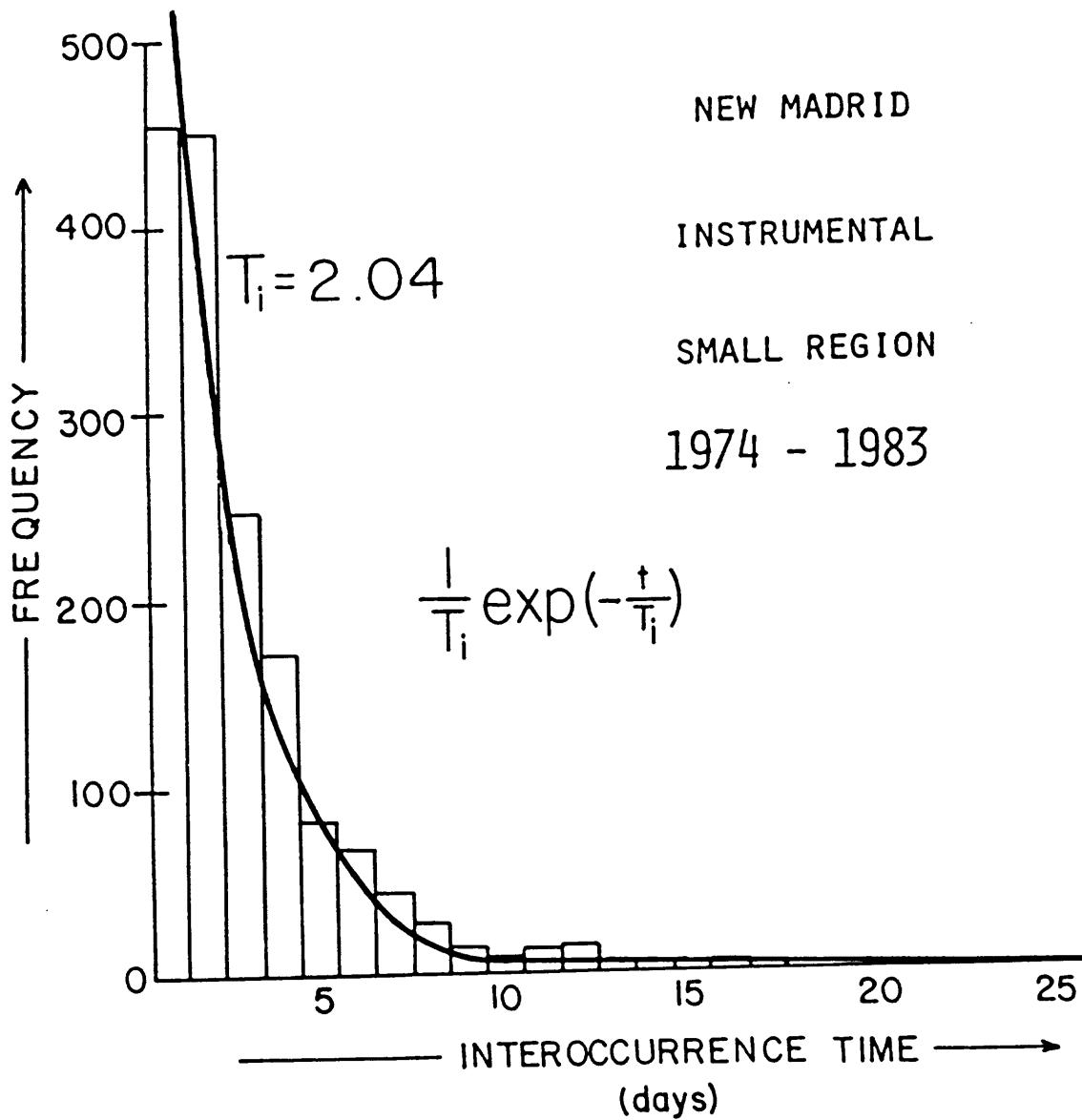


Figure 6. Observed interoccurrence times of the instrumental New Madrid data set. A Poisson distribution function in terms of interevent times (equation 12) is shown for comparison.

Note that for a given Δt , S_c is constant and does not depend on t , the elapsed time since the last event.

Gaussian

The Gaussian (or normal) probability density function is given by

$$g(t) = \frac{1}{\sigma\sqrt{2\pi}} \exp \left[-\frac{1}{2} \left(\frac{t-T_r}{\sigma} \right)^2 \right] , \quad (15)$$

where σ is the standard deviation and T_r is the mean repeat or recurrence time. The cumulative probability is

$$G(T \leq t) = \int_{-\infty}^t g(\tau) d\tau . \quad (16)$$

This integral cannot be evaluated by standard techniques, but extensive tables of values are available when $G(T \leq t)$ is transformed into a standardized normal distribution using

$$z = \frac{t-T_r}{\sigma} . \quad (17)$$

From equations (9) and (26) the Gaussian conditional probability is

$$G_c(t, \Delta t) \rightarrow G_c(z, \Delta z) = \frac{G(z+\Delta z) - G(z)}{1 - G(z)} . \quad (18)$$

Values for $G(z+\Delta z)$ and $G(z)$ were taken from Tables of Normal Probability Functions (National Bureau of Standards, 1953) for this report.

The Gaussian distribution has recently been used by a number of authors to estimate conditional probabilities of seismic zones in Japan and the United States (Wesnousky et al., 1984; Sykes and Nishenko, 1984; Jacob, 1984). In these studies either long historical chronologies, geological slip rates or paleoseismic data were available to place constraints on either the estimates of mean recurrence time or the appropriate distribution to apply. Gaussian conditional probabilities will be an important component of this paper, but we emphasize that no independent evidence exists that favors its use for New Madrid.

Log-Normal

The log-normal distribution has found frequent application in the earth sciences (e.g., Till, 1974) and in at least one case has been applied to earthquake recurrence times. Jacob (1984) compared the fit of the interoccurrence intervals of large ($M_s \geq 7.8$) Aleutian earthquakes to both Gaussian and log-normal distributions and considered the log-normal to be the more appropriate representation. It is included in this study as a potentially valid distribution for New Madrid recurrence times.

The log-normal distribution can be generated from the Gaussian (or vice-versa) by the variable transform $t = \ln(t)$, where \ln is the natural (base e) logarithm. A log-normal density function $l(z)$ is obtained from the standardized normal distribution using the following relations:

$$Z = \frac{\ln(t) - T_r^*}{\sigma^*} \quad ; \quad \sigma^* = \sqrt{\ln\left(\frac{\sigma^2 + T_r^2}{T_r^2}\right)} \quad (19)$$

$$T_r^* = \ln(T_r) - \frac{\sigma^{*2}}{2}$$

where T_r^* and σ^* are the mean and standard deviation of the log-normal distribution.

Weibull

The Weibull distribution was originally developed by Weibull (1951) on a purely empirical basis for application to instances of failure of individual components of large systems. Hagiwara (1974) and Rikitake (1975) applied this distribution to data on crustal strain preceding large earthquakes. If the strain rate is approximately constant (as required by the time-predictable model) a Weibull distribution of "ultimate strain" will allow estimates of probability of occurrence. Since this Japanese work, Weibull statistics have been increasingly applied in seismic hazard research (e.g., Brillinger, 1982; Kiremidjian and Anagnos, 1984; Nishenko, 1984).

The Weibull probability density function is given by

$$w(t) = \lambda v t^{v-1} e^{-\lambda t^v} \quad , \quad (20)$$

where λ and v are constants that are related to T_r , the mean time to failure and to σ , the standard deviation, as follows (Hagiwara, 1974):

$$T_r = \int_0^{\infty} t w(t) dt = \lambda^{-1/v} \Gamma\left(\frac{v+1}{v}\right) \quad (21)$$

$$\frac{\sigma}{T_r} = \sqrt{\Gamma\left(\frac{v+2}{v}\right) - \Gamma^2\left(\frac{v+1}{v}\right)} / \Gamma\left(\frac{v+1}{v}\right) \quad , \quad (22)$$

where Γ is the gamma function. ν is often referred to as the shape parameter and increases as σ decreases. λ is exponentially related to the mean rate of failure and increases as T_r decreases. Table 3 lists the Weibull parameters computed for this study from equations (21) and (22) as well as some found in the literature.

Equation (20) may be directly integrated to obtain the cumulative Weibull probability:

$$W(T \leq t) = \int_0^t w(\tau) d\tau = 1 - e^{-\lambda t^\nu}, \quad (23)$$

which yields a conditional Weibull probability of

$$W_c(t, \Delta t) = \frac{\exp[-\lambda t^\nu] - \exp[-\lambda(t+\Delta t)^\nu]}{\exp[-\lambda t^\nu]} \quad (24)$$

We note that the Weibull hazard rate, defined as $dW(t)/dt = \lambda \nu t^{\nu-1}$ is often used as a conditional probability (e.g., Kiremidjian and Anagnos, 1984; Hagiwara, 1974). This expression is just a first-order Taylor expansion and can lead to significant overestimates of $W_c(t, \Delta t)$ in the same manner as shown for the Gaussian distribution (Fig. 5).

Cumulative and Conditional Probabilities for New Madrid

In this section we present probability estimates for large ($m_b \geq 6.0$) and great ($m_b \geq 7.0/M_s \geq 8.3$) New Madrid earthquakes based on the information presented in the preceding sections.

Cumulative and conditional probability estimates require choice of a pro-

TABLE 3

WEIBULL CONSTANTS

| Aver. Recurrence Interval T_r (years) | Standard Deviation σ (% of T_r) | λ (rate parameter) | ν (shape parameter) | References |
|--|--|-------------------------------|----------------------------|---------------------------------|
| 35 | 24 yr (69%) | .0061 | 1.41 | Kiremidjian & Anagnos (1984) |
| 87 | 34 yr (39%) | 3.52×10^{-6} | 2.70 | Hagiwara (1974) |
| 70 | 33% | 5.69×10^{-7} | 3.30 | This study |
| 70 | 50% | 1.03×10^{-4} | 2.10 | This study |
| 140 | 33% | 5.78×10^{-8} | 3.30 | This study |
| 140 | 50% | 2.41×10^{-5} | 2.10 | This study |
| 550 | 33% | 6.32×10^{-10} | 3.30 | This study |
| 550 | 50% | 1.36×10^{-6} | 2.10 | This study |
| 1100 | 33% | 6.42×10^{-11} | 3.30 | This study |
| 1100 | 50% | 3.18×10^{-7} | 2.10 | This study |

bability distribution, specification of the distribution mean, and specification of the standard deviation of observations about the mean. Conditional probabilities also require the length of the future time interval, Δt . Figure 7 is a parameter tree depiction of the various parameter combinations that were chosen for analysis and illustration. The choices were dictated by a variety of factors as discussed below.

Magnitude. We restrict our data presentation to two magnitudes: an $m_b 6.0(M_s 6.3)$ event which could be locally destructive over one or more counties and $m_b 7.0(M_s 8.3)$ which we take as a great 1812 - type New Madrid event. A maximum magnitude quake ($m_b 7.3/M_s \sim 8.9$ [Nuttli, 1983]) has such low cumulative and conditional probabilities as to be of little interest for this paper.

Average Recurrence Interval. In the absence of any geological or paleoseismological information, this parameter is taken directly from the frequency-magnitude analysis of the first part of this paper. As is evident from Table 2 recurrence estimates for a given magnitude range have a large range. Dimensions of the source area and the line-fitting technique are the two principal sources of this variability. Differences in the size of the chosen source zone cause differences of roughly 100% in the estimates of mean recurrence times, and different line-fitting methods yield variations on the order of 50%.

Such a large range of estimated repeat times must be considered in any realistic probabilistic analysis. Our approach was to take a value from the low and from the high end of the range of estimates of T_r for use in the probability analysis, and thereby bracket the actual behavior of New Madrid. Extreme points were not selected because this would smear the results beyond usefulness and because extremes are accounted for to a degree by selecting a

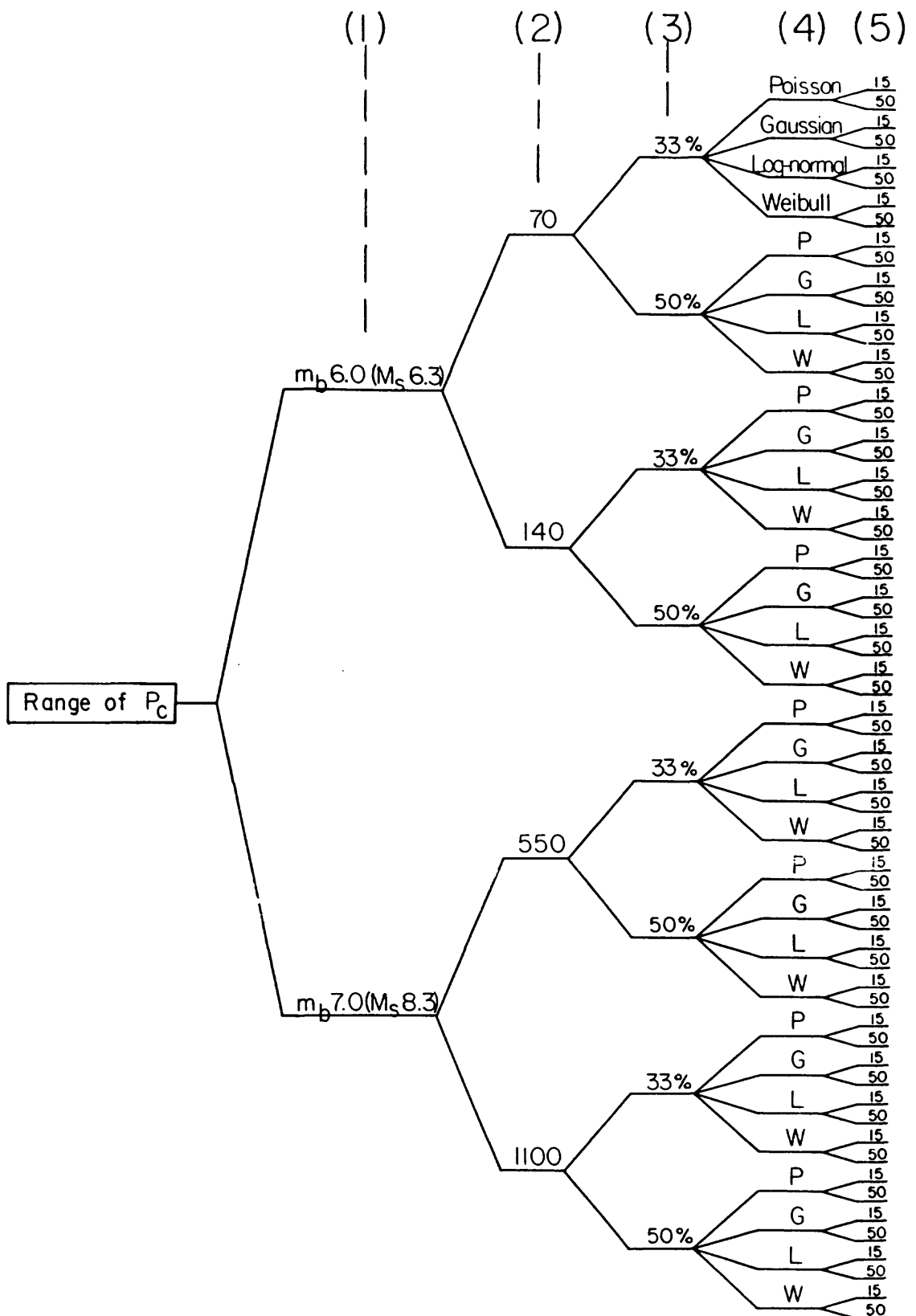


Figure 7. Logic tree of the five parameters which are allowed to vary to obtain an estimates of conditional probability P_c . The branches are labeled as follows: (1) is for a magnitude range m_b 6.0-7.0 (M_s 6.3-8.3); (2) average recurrence interval (yrs); (3) standard deviation as a percentage of the average recurrence interval; (4) the assumed probability distribution; (5) time increment in years over which conditional probabilities apply.

range of standard deviations about the estimated mean (see next section). Thus in Figure 7, a range of 70-140 years is used for T_R ($m_b 6.0$) and 550-1,100 years for T_R ($m_b 7.0$).

Standard Deviation. Frequency-magnitude analysis yields an estimated recurrence time T_R but no estimate of the variation of T_R as the seismic zone proceeds through many seismicity cycles. This variability is physically real (as opposed to the variability induced by methodology as discussed in the last section) and is exhibited by virtually all seismic zones that have been identified as behaving in a cyclic manner. Table 4 presents a representative (but not exhaustive) listing of repeat times and standard deviations that have been reported in the literature for various seismic zones worldwide.

Information such as that in Table 4 is not available for New Madrid; therefore standard deviation must be an assumed parameter. Using Table 4 as a guide, the standard deviation σ is allowed to vary from one-third (33%) to two-thirds (67%) of T_R (Fig. 7). For σ in excess of $.5T_R$ the very concept of the time-predictable seismicity model loses its usefulness. The observed variability of the repeat times of magnitude 5 and 6 quakes in the historical record suggests σ should not be smaller than one-third of T_R .

Type of Distribution. Type of distribution is another assumed parameter for New Madrid. As previously discussed we selected four commonly used distributions for analysis. One of them, the Poisson, is included only for reference as it is not applicable to a time-predictable model.

For New Madrid earthquakes of body-wave magnitude 6.0 and above, the elapsed time since the last event(s) is still less than the estimated repeat time (with the exception of $T_R = 70$ years). The analysis of this section will show that for such a time frame, choice of probability distribution makes little difference in computed probabilities. Sykes and Nishenko (1984) reach a

TABLE 4

WORLDWIDE MEAN RECURRENCE TIMES AND STANDARD DEVIATIONS

| <u>LOCATION (Reference)</u> | <u>Mean Recurrence Interval T_r (years)</u> | <u>Standard Deviation years</u> | <u>Standard Deviation (% of T_r)</u> |
|--|---|-------------------------------------|--|
| <u>Southern San Andreas fault, USA</u> 9 events (Sieh, 1978) | 164 | ± 76 | 46% |
| <u>Southern California, USA</u> (Sykes and Nishenko, 1984) | | | |
| Parkfield | 22 | ± 7 | 32% |
| Pallet Creek (12 events) | 145 | ± 61-73 | 42-44% |
| Imperial fault | 32 | ± 10 | 32% |
| <u>Aleutian Arc, Alaska, USA</u> 28 events (Jacob, 1984) | 73 | ± 32 | 44% |
| <u>Oaxaca, Mexico</u> (McNally and Minister, 1981) | 35 | ± 24 | 69% |
| <u>From (Rikitake, 1977)</u> | | | |
| Nankai - Tokai, Japan | 170 | ± 68.9 | 41% |
| Hokkaido - Kuriles Arc | 85.3 | ± 24.6 | 29% |
| Northern South America | 46.3 | ± 30 | 65% |
| Southern South America | 100 | ± 22.5 | 23% |
| <u>South Kanto, Japan</u> (Hagiwara, 1974) | 87 | ± 34 | 39% |

similar conclusion for several California fault systems.

Time Interval, Δt . The choice of a time interval for computing conditional probabilities is completely arbitrary since the exact form (equation 9) of P_c rather than the first-order Taylor series approximation (equation 11) is employed in this study. We selected a Δt of 15 years to coincide with a probability of occurrence by the turn of the century and a Δt of 50 years as representative of the probability of occurrence during a lifetime.

Cumulative Probability

It is of greater interest to know the probability of a large earthquake happening during some future time interval than to know the probability that it would have already happened by now (the present). For this reason we emphasize conditional rather than cumulative probabilities. We do include, however, the general behavior patterns of cumulative probability for the four distributions considered in this study. These are illustrated in Figure 8 and summarized in Table 5.

In Figure 8(a) cumulative probabilities are shown for an $m_b \geq 6.0$ quake with a mean recurrence interval from the extreme upper-end of its range ($T_r = 140$ yrs). Gaussian and Weibull values are within 1% and vary from the log-normal by a maximum of 5%. Poisson values are significantly higher than the other distributions for $t < T_r$ and lower for $t > T_r$. This behavior holds for all choices of T_r and σ and carries over into the conditional probability estimates.

Figure 8(b) illustrates the dependence of cumulative probability on T_r and σ for an $m_b \geq 7.0$ earthquake. For the range of recurrence intervals and standard deviation considered in this study, cumulative probability can vary up to $\sim 60\%$ with T_r and $\sim 10\%$ with σ . Only the Gaussian and Poisson cases are

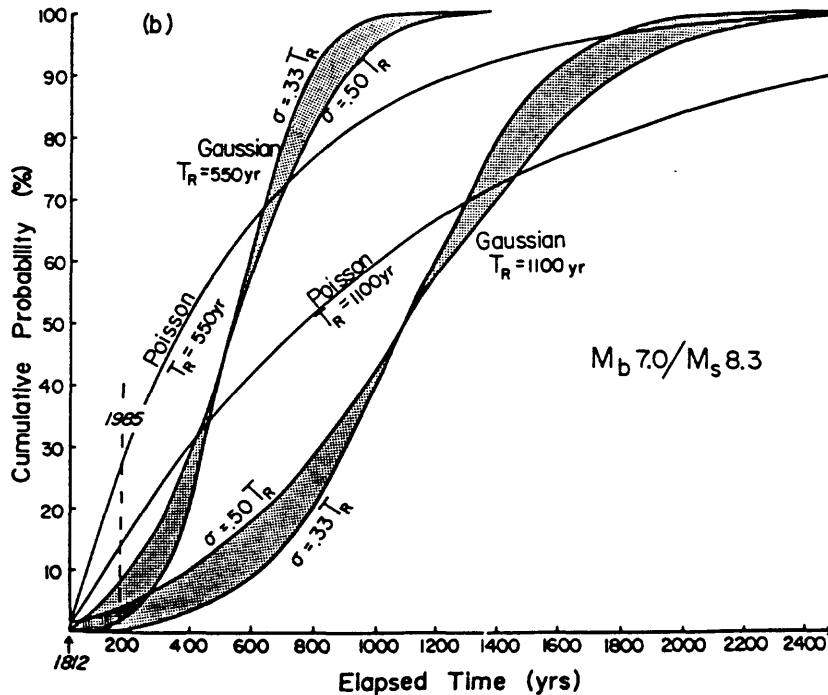
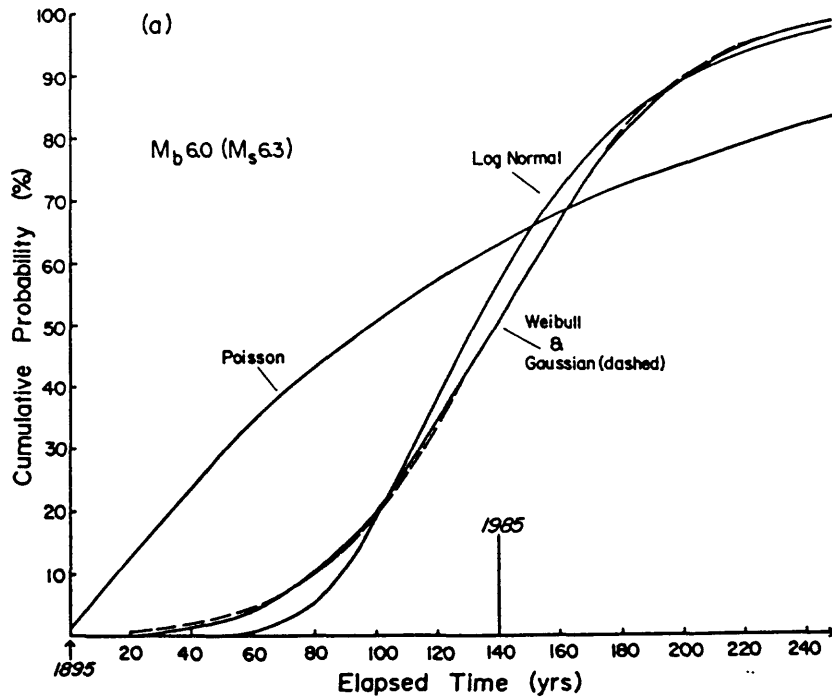


Figure 8. (a) Cumulative probabilities for the four distributions considered in this study for the representative case of a quake m_b 6.0, mean recurrence time T_r of 140 years, standard deviation of $T_r/3$. The Gaussian and Weibull distributions are nearly identical in this case. (b) Illustration of the variation of cumulative probabilities with T_r and σ for a quake m_b 7.0 for the Poisson and Gaussian distributions. The Weibull and log-normal distributions would vary a relatively minor amount from the Gaussian.

TABLE 5

SUMMARY OF CUMULATIVE PROBABILITIES: 1985

| Δt (years) | $T_r(\sigma=.33T$ to $.50T_r)$ (years) | $G_c(t=1985)$ (Gaussian) | $L_c(t=1985)$ (Log-normal) | $W_c(t=1985)$ (Weibull) | $P_c(t=1985)$ (extreme range) | $S_c(t=1985)$ (Poisson) |
|-----------------------------|---|-----------------------------|-------------------------------|----------------------------|----------------------------------|----------------------------|
| | | $mb \geq 6.0$ (Ms6.3) | | | | |
| 1895 [$t-t_0 = 90yr$] | $70 \pm (\sigma=23-35)yr$ | 80-72% | 83-78% | 81-73% | 11-83% | 72% |
| | $140 \pm (\sigma=47-70)yr$ | 14.2-23.8% | 11.5-24.2% | 15.0-26.4% | | 47% |
| | | $mb \geq 7.0$ (Ms8.3) | | | | |
| 1812 [$t-t_0 = 173yr$] | $550 \pm (\sigma=183-275)yr$ | 2.0-8.5% | 0.3-1.3% | 1.5-6.6 | <<1.0-8.5% | 27% |
| | $1,100 \pm (\sigma=367-550)yr$ | 0.6-4.6% | <<1.0-.011% | 0.16-1.6% | | 15% |

shown since Weibull and log-normal differences from Gaussian are <10% (Poisson is shown for reference only). Thus the estimate of T_R has much the greater effect on calculated cumulative (and conditional) probability; choice of σ and choice of distribution provide a modulation of only about 10%.

Table 5 summarizes cumulative probabilities for New Madrid for the year 1985. For the large source area of Figure 1 ($T_R=70$ and 550 yr) the probability that an $m_b \geq 6.0$ quake would have occurred between 1895 (the last $m_b > 6.0$ event, Charleston, MO) and 1985 has reached 72-83%. Similarly for $m_b \geq 7.0$ since 1812, $P(t=1985)$ is only 0.3-8.5%. If recurrence intervals derived for the small source zone are considered ($T_R=140$ and 1100 yr), the computed values fall to 11.5-26.4% and <<1.0-4.6%. In all but the case for $T_R=70$ yr and the elapsed time $t=90$ yr, Poisson statistics significantly overestimate the likelihood of occurrence.

Conditional Probability

Conditional probabilities for large New Madrid earthquakes for the next 15 and the next 50 years are presented in this section. Choice of values for the parameters which affect the calculations -- type of distribution, mean recurrence time and standard deviation -- have been previously discussed and are summarized in Figure 7.

The data are presented in a series of four figures (Fig. 9 a,b,c,d) each depicting conditional probabilities (P_C) for Gaussian, Weibull, log-normal and Poisson (reference only) distributions. Figure 9(a) and (b) are for an $m_b \geq 6.0$ earthquake with T_R ranging from 70 to 140 yrs; Fig. 9(c) and (d) are for an $m_b \geq 7.0$ event with T_R equal to 550 or 1,100 years. The plots have been carried out to elapsed time roughly twice T_R so that the asymptotic behavior of P_C at large t would be shown. Three reference times, t_0 , T_R , and $t=1985$, are shown

$M_b 6.0/M_s 6.3$

$T_R = 70$ years

Last Occurrence: 1895

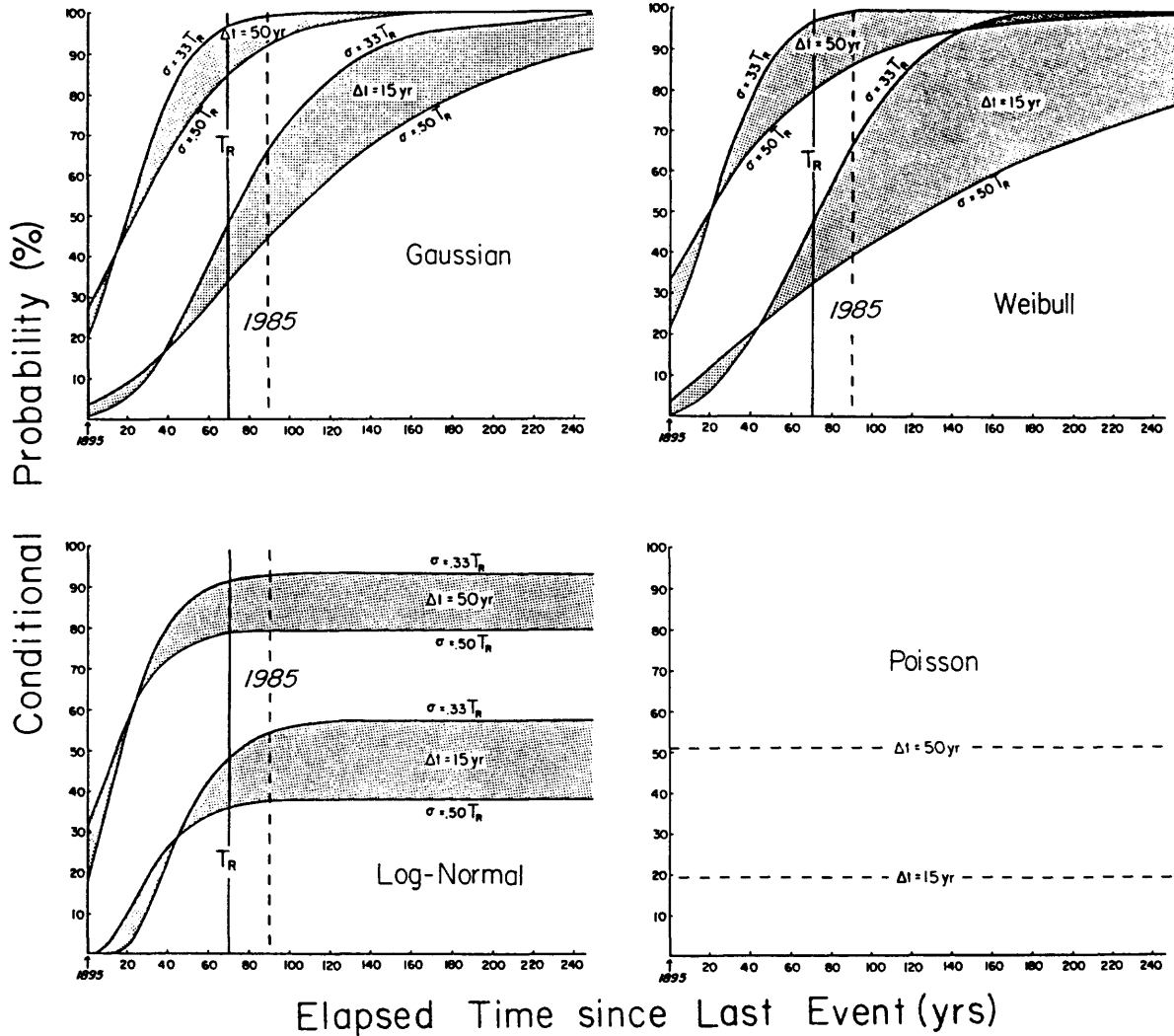


Figure 9a. $T_R = 70$ years

Figure 9. Computed conditional probabilities for the various parameters shown in the parameter tree of Figure 7. (a) Mean recurrence interval, $T_R = 70$ years; (b) $T_R = 140$ years; (c) $T_R = 550$ years; (d) $T_R = 1,100$ years. Poisson conditional probabilities are shown for reference only. See text for discussion.

$M_b 6.0/M_s 6.3$

$T_R = 140 \text{ years}$

Last Occurrence: 1895

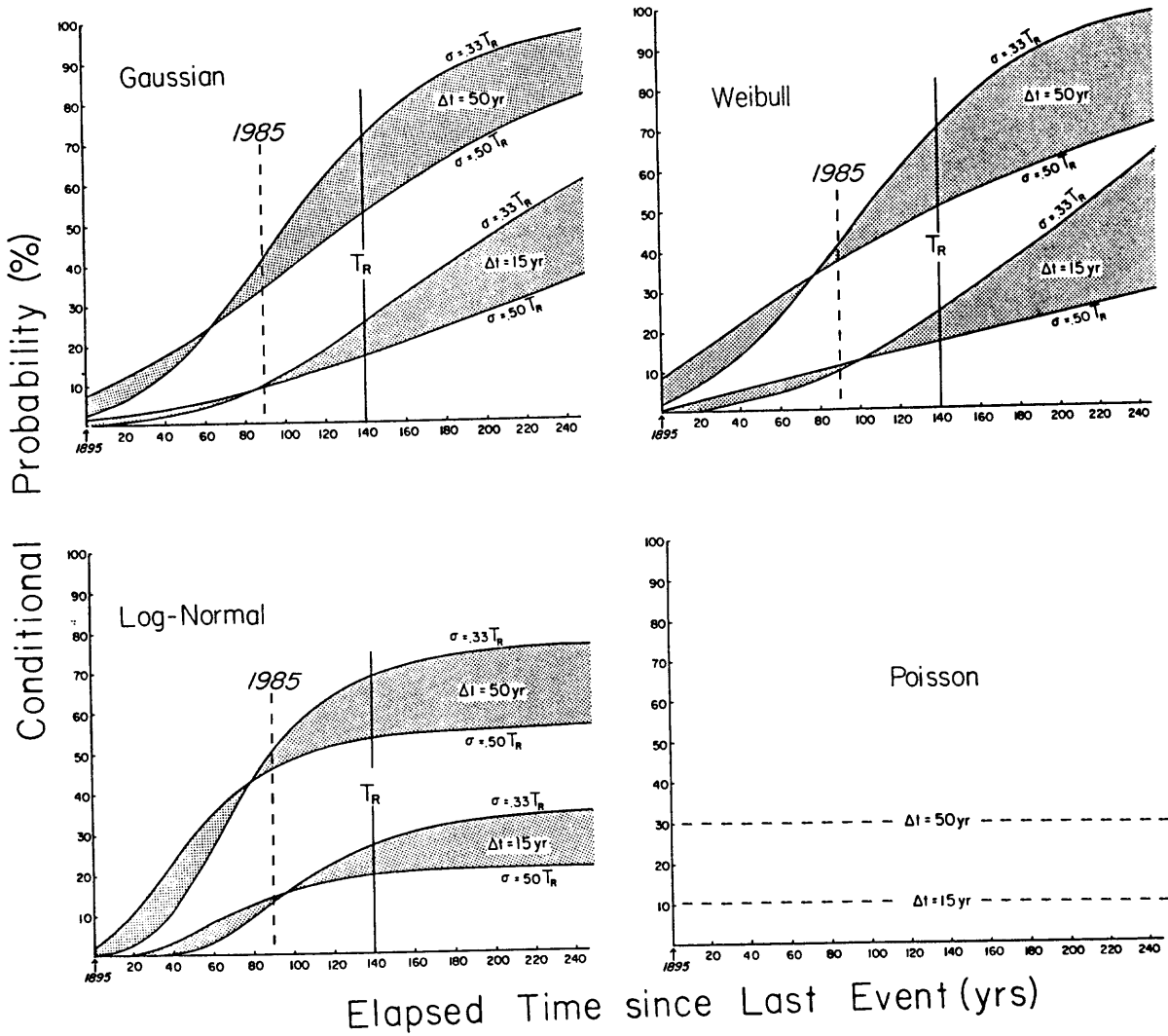


Figure 9b. $T_R = 140 \text{ years}$

$M_b 7.0/M_s 8.3$

$T_R = 550 \text{ years}$

Last Occurrence: 1812

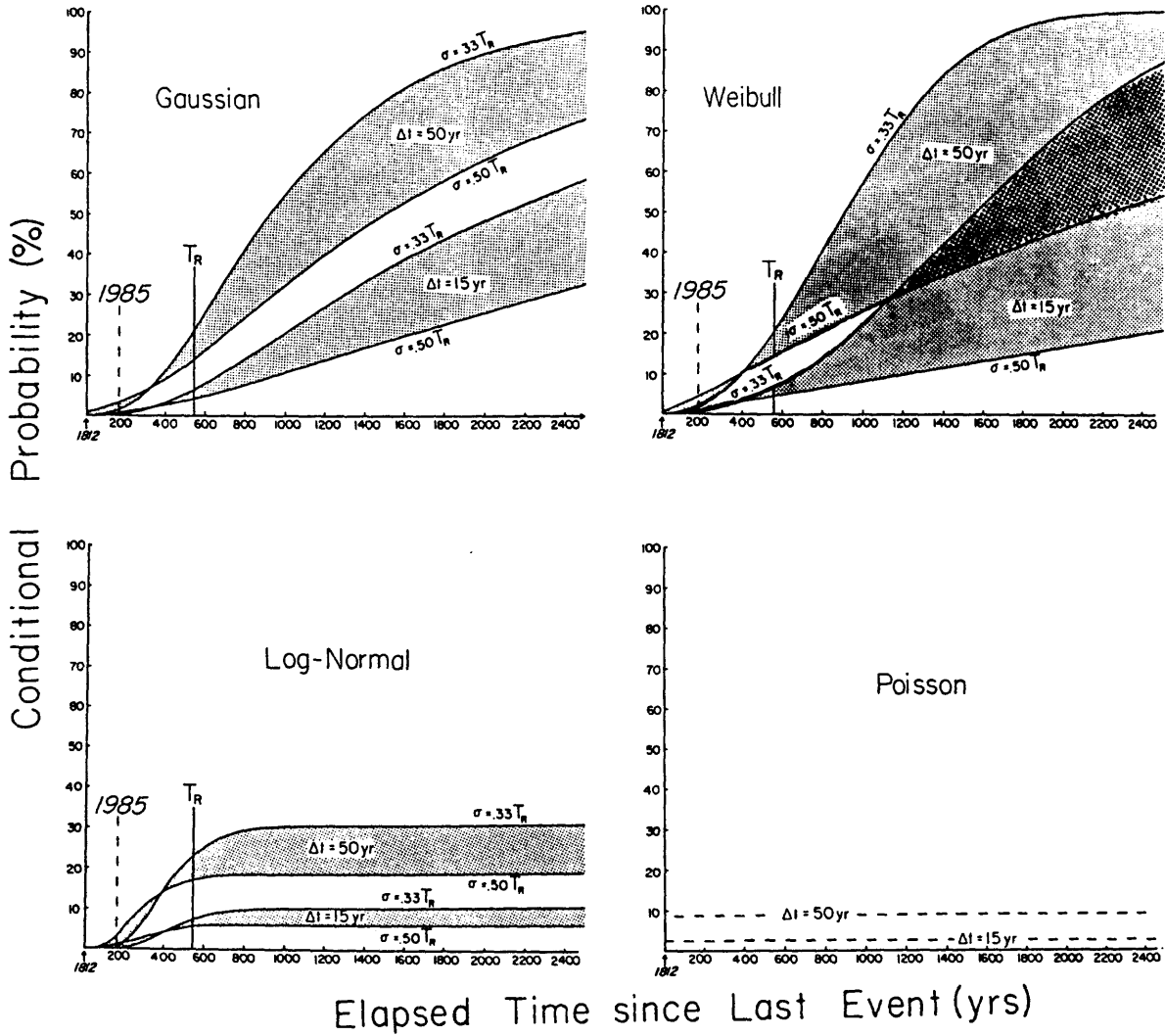


Figure 9c. $T_r = 550$ years

$M_b 7.0 / M_s 8.3$

$T_R = 1,100$ years

Last Occurrence: 1812

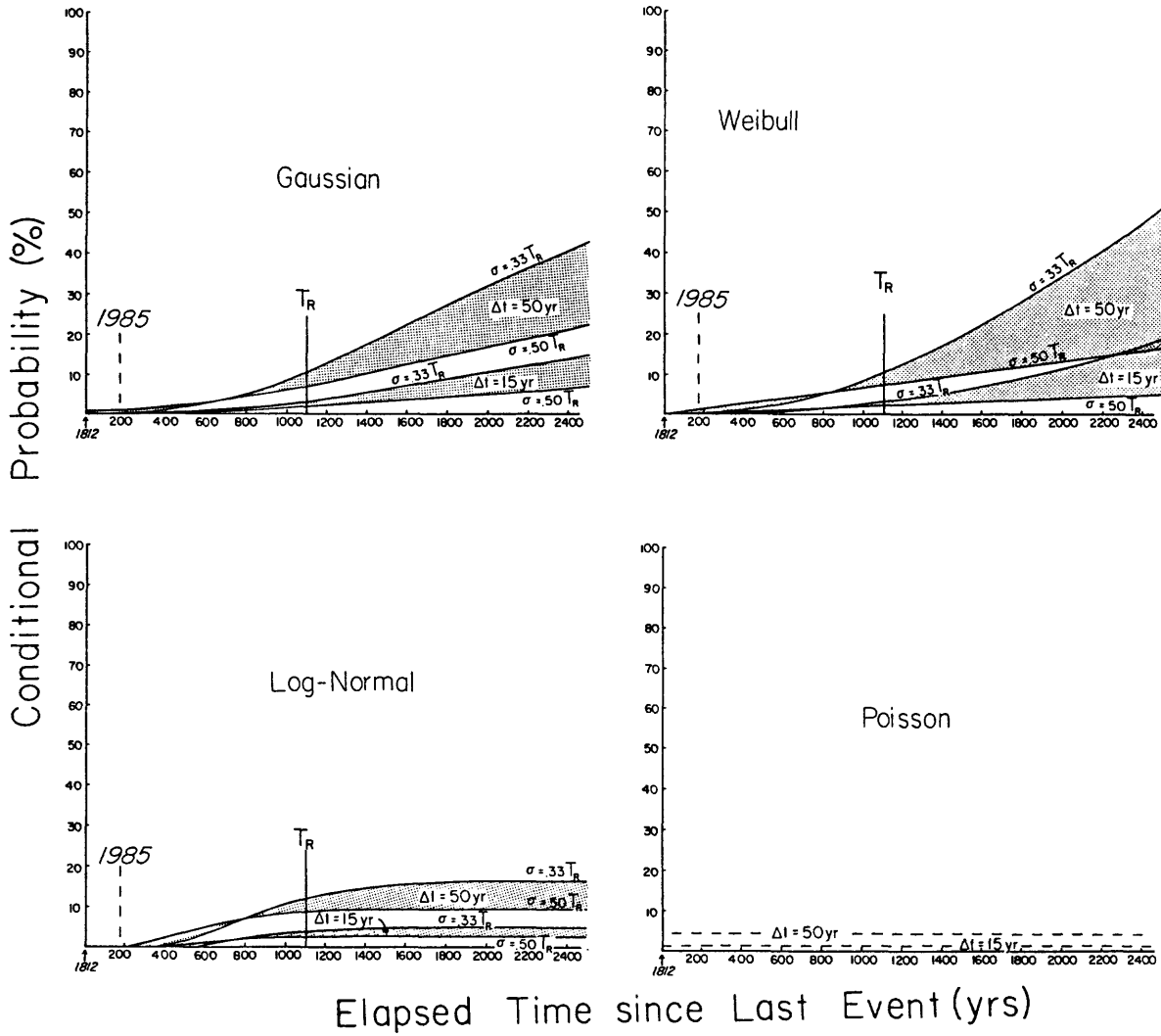


Figure 9d. $T_R = 1,100$ years

on each graph. Shaded regions indicate the range of P_C for a given Δt as the standard deviation varies from one-third to one-half of T_R .

There are several important features in Figure 9 to which we call attention.

(1) In all cases the present (year 1985) is less than $1.5T_R$. In this time range, the choice of probability distribution makes little difference in P_C . This is particularly true for the Weibull and Gaussian cases; log-normal yields the lowest P_C for times close to Δt and rises most steeply as t approaches T_R .

(2) Allowing σ to range from $.33T_R$ to $.50T_R$ has a greater effect on conditional than on cumulative probability but only for $t > T_R$, times generally beyond our concern in this study. For times less than roughly one-half T_R an increase in σ increases P_C because area beneath the probability density function is shifted from the distribution mean (T_R) to the tails. However, for $t \geq T_R$, P_C for $\sigma = .50T_R$ is always less than P_C for $\sigma = .33T_R$.

(3) For elapsed time $t \geq 2T_R$ the log-normal distribution yields significantly lower estimates of P_C than either the Weibull or Gaussian. This case appears to apply to the conditional probabilities for some of the Aleutian Arc segments computed by Jacob (1984).

(4) The constant Poisson conditional probabilities will yield estimates that are consistent with the other distributions only over a very restricted range of elapsed times and should not be used for conditional probability estimation for a time-predictable model of seismicity. In contrast, Poisson cumulative probabilities are consistently high for $t < T_R$ and may be used to provide a conservative (i.e., upper bound) estimate of seismic hazard.

Fifteen- and 50-year conditional probability estimates for the year 1985 are compiled in Table 6. The likelihood of a great ($m_b \geq 6.0/M_s \geq 8.3$) New Madrid

earthquake in the next 15 or 50 years is uniformly low, reaching a maximum of 4.7% for a Weibull distribution with $T_R=550$ yr, $\sigma = .5T_R$, $\Delta t=50$ yr. Log-normal estimates are very low, often much less than 1%.

P_C estimates for an $m_b \geq 6.0$ event exhibit a wide variation, ranging from 9 to 67% for $\Delta t=15$ yr and from 34-99% for $\Delta t=50$ yr. About 10% of this variability arises from type of distribution (Poisson excluded), 10-25% from choice of σ , and from 25 to 50% from choice of $T_R=70$ or 140yr. In the 'restricted range' column of Table 6 we give a preferred probability range taken from the low, $T_R=70$ yr recurrence time (the large source area of Figure 1). Arguments supporting this choice are presented in the concluding section.

DISCUSSION AND CONCLUSIONS

The probability estimates of this report rely on the assumption that the New Madrid seismic zone generates major earthquakes in a repeated fashion. It is further assumed that the occurrence of large events is periodic rather than episodic, a distinction we make on the basis of the standard deviation of repeat times about the mean recurrence interval. If σ is greater than 50% of the mean recurrence time, we term the activity episodic and our probability estimates do not apply. If σ is less than 50% the calculated probabilities reported here should be reasonable estimates of the likelihood of future large New Madrid earthquakes.

The 15- and 50-year conditional probabilities listed in Table 6 have a very wide range, e.g., from 9% to 67% for $m_b \geq 6.0$, $\Delta t=15$ yr, and from 34% to 99% for $\Delta t=50$ yr. Most of the variability arises from the choice of source zone boundaries for the seismicity data set. We favor the choice of the

TABLE 6

SUMMARY OF CONDITIONAL PROBABILITIES: 1985

| Δt (years) | T_r ($\sigma=33T$ to $.50T_r$) (years) | $G_C(t, \Delta t)$ (Gaussian) | $L_C(t, \Delta t)$ (Log-normal) | $W_C(t, \Delta t)$ (Weibull) | $P_C(t, \Delta t)$ (extreme range) | $\# P_C(t, \Delta t)$ (restricted range) | $S_C(t, \Delta t)$ (Poisson) |
|-----------------------|---|----------------------------------|------------------------------------|---------------------------------|---------------------------------------|---|---------------------------------|
| | | | | $mb \geq 6.0$ (Ms6.3) | | | |
| 15 | 70±($\sigma=23-35$)yr | 66-44% | 55-38% | 67-39% | 9-67% | 40-63% | 19.3% |
| | 140±($\sigma=47-70$)yr | 9.9-9.3% | 13.5-14.8% | 10.2-11.0% | | | |
| 50 | 70±($\sigma=23-35$)yr | 99-92% | 94-80% | 99-87% | 34-99% | 86-97% | 51.0% |
| | 140±($\sigma=47-70$)yr | 42-34% | 51-46% | 42-37% | | | |
| | | | | $mb \geq 7.0$ (Ms8.3) | | | |
| 15 | 550±($\sigma=183-275$)yr | 0.44-0.97% | 0.05-0.75% | 0.5-1.3% | <<1.0-1.3% | 0.3-1.0% | 2.7% |
| | 1,100±($\sigma=367-550$)yr | 0.07-0.28% | <<1.0-0.01% | 0.05-0.30% | | | |
| 50 | 550±($\sigma=183-275$)yr | 1.8-3.5% | 0.4-3.4% | 2.0-4.7% | <<1.0-4.7% | 2.7-4.0% | 8.7% |
| | 1,100±($\sigma=367-550$)yr | 0.27-1.0% | <<1.0-0.07% | 0.2-1.1% | | | |

* see text

larger source zone (which leads to shorter recurrence times and consequently higher probabilities) and offer the following argument in support of this selection.

The Large Source Zone. According to Nuttli's most recent estimates the three great New Madrid earthquakes of the winter of 1811-12 had surface-wave magnitudes of 8.5, 8.4 and 8.8 (Nuttli, 1983). Even if we neglect the extensive aftershock sequences, these great events represent a strain energy release of $\sim 1.6 \times 10^{25}$ ergs. The question we pose is, what crustal volume is required to store this strain energy as elastic potential energy?

If we consider the simplest case where strain is represented by a single component of shear (ϵ), then strain energy per unit volume (e) is

$$e = \frac{1}{2} \mu \epsilon^2 \quad ,$$

where μ is the rigidity modulus. Taking $\mu = 5 \times 10^{11}$ dyn cm⁻² and using Rikitake's (1981) most recent estimate of ultimate crustal strain, $\epsilon_{\max} = 4.4(\pm 1.7) \times 10^{-5}$, we obtain

$$e = 182-930 \text{ ergs/cm}^3 \quad .$$

That is, typical crustal rock cannot store more than 182 to 930 ergs/cm³ elastically without brittle failure. The 1811-12 events would have required a crustal volume of $1.7-8.8 \times 10^{22}$ cm³ to store the energy released as seismic radiation.

What portion of the crust is elastic? Central U.S. earthquakes occur to depths of 20-25 km. Recently some authors have argued that the crust contains

a ductile shear zone at depths of ~ 20 to ~ 40 km in which ductile deformation (on the order of mm/yr) strains the overlying brittle crust (e.g., Zoback et al., 1984). We take 25 km as a (possibly high) estimate of the thickness of the elastic crust. This yields an area of 680,000 to 3,500,000 km² required for strain energy storage.

The areas of the large and small source zones of Figure 1 are 157,700 km² and 29,960 km² respectively. The required crustal area for strain energy accumulation for great New Madrid quakes far exceeds the small source zone: it is for this reason that we favor the larger zone. Increasing the depth of the ductile-brittle transition to 40 km or assuming values for μ above the already high value taken would not change these conclusions. If an older, higher estimate of ultimate strain is taken, $\epsilon_{\max} \sim 1.5 \times 10^{-4}$ (Tsuboi, 1956), then strain energy density increases to 5,625 ergs/cm³ and the required crustal area to store the prior strain is 138,000 km² (for 25 km depth), still on the order of the dimensions of the large source zone.

By making this order-of-magnitude calculation for the accumulation volume of prior strain, we are not proposing that a great earthquake could occur anywhere in the large source zone of Figure 1. We believe that such an event could only occur in the region within the small source zone. However, the strain storage limitations of the brittle crust require the participation of crustal rock significantly beyond the limits of the small source zone. This would, of necessity, encompass the fault population of the large source zone; hence the large zone is the proper one for recurrence estimation.

Are the mean recurrence times of large events estimated from the large source zone compatible with other lines of evidence? From Table 2, an $m_b \geq 6.0$ event is expected every 55-88 yrs on average (compared to 124-155 yrs for the

smaller zone). Since 1812 two $m_b \geq 6.0$ events have occurred: in 1843 near Marked Tree, AR and in 1895 near Charleston, MO. The average interevent time is 52 yrs; if the dates 1812 and 1895 are used to bracket these events an average recurrence of $58(\pm 30)$ years is obtained. These sparse data are certainly more compatible with the large source zone recurrence estimates than with those of the small zone.

Another order-of-magnitude check can be made from the displacement values that Nuttli (1983) estimates for the great New Madrid quakes. According to Nuttli such events have displacements of 5-8 meters. If a representative source dimension is ~ 100 km, this represents a strain of $5-8 \times 10^{-5}$ which is close to the ultimate strain estimate of Rikitake. A repeat time of 550 yrs requires a strain rate of $\dot{\epsilon} \sim 1-1.5 \times 10^{-7}$ /yr, a high but not unprecedented value. Harada (1978) found for the south Kanto district of intraplate Japan a rate of 1×10^{-7} /yr over a 70-year period. Normal strain rates for active interplate zones are at least an order of magnitude larger.

Our overall conclusion can be stated as follows. Recurrence rates derived from the large source zone of Figure 1 are preferred to those of the small source zone because of the large volume of crustal rock required to store the strain potential energy of great New Madrid earthquakes. The recurrence rates are compatible with the occurrence of $m_b \geq 6.0$ events in the historical record, with displacement estimates for great events, with estimates of ultimate crustal strain, and with intraplate strain rates in Japan. The location of a lower magnitude 6 event would not be restricted to the small source area whereas an $m_b 7-8$ event is considered possible only on the principal fault segments of the New Madrid zone.

Restricted Probability Range. In Table 6 we have included a restricted range of conditional probabilities; these values are based on the arguments

of the previous discussion in favor of large source zone recurrence intervals, i.e., $T_r=70\text{yr}$ for $m_b \geq 6.0$ and $T_r=550\text{yr}$ for $m_b \geq 7.0$. Our restricted range estimates are simply an average of the range of values obtained with the Gaussian, log-normal, and Weibull distributions and are repeated here as one of the main conclusions of this study.

| | <u>Aver. Repeat time</u> | <u>Probability by Year 2000 A.D.</u> | <u>Probability by Year 2035 A.D.</u> |
|-------------------------------|-------------------------------|--------------------------------------|--------------------------------------|
| $m_b \geq 6.0 (M_s \geq 6.3)$ | 70 yr ($\pm 15\text{yr}$) | 40-63% | 86-97% |
| $m_b \geq 7.0 (M_s \geq 8.3)$ | 550 yr ($\pm 125\text{yr}$) | 0.3-1.0% | 2.7-4.0% |

These probability estimates would be much lower if the small source zone were appropriate: for $m_b \geq 6.0$, $\sim 10\%$ by 2000 A.D., and $\sim 39-45\%$ by 2035 A.D.; for $m_b \geq 7.0$, $\ll 1\%$ by 2000 A.D. and 0.2-1.0% by 2035 A.D.

The uncertainties involved in deriving the above estimates of conditional probability rank is as follows:

- (1) Choice of source zone - varies T_r by 100%;
varies P_c by $\sim 50\%$;
- (2) Choice of line-fitting technique - varies T_r by 50-70%; varies P_c by 30-40%;
- (3) Choice of standard deviation - varies P_c by $\sim 10-25\%$;
- (4) Choice of distribution - varies P_c by $\sim 10\%$.

Items (1) and (2) above required a choice be made in order to derive final probability values. Arguments were presented for selecting (1) the large source zone and (2) least-squares regression for the final estimates. The range of the final estimates are due to items (3) and (4).

We have been careful to make clear the number of assumptions necessary to derive the above probability values. The critical data required to reduce or constrain these estimates would be event chronologies based on paleoseismic evidence. Broad zones of the embayment sediments overlying the New Madrid seismic zone have high liquifaction potential. Datable sand blows, slumps or other liquifaction features produced by pre-1811 seismic episodes and preserved in these sediments offer the best hope of obtaining more tightly constrained forecasts of the future seismic behavior of the New Madrid zone.

ACKNOWLEDGMENTS

We wish to acknowledge the Dept. of Earth and Atmospheric Sciences at Saint Louis Univ. and in particular O. Nuttli for the excellent instrumental and historical seismicity data bases used in this study. The paper of Sykes and Nishenko (1984) provided much useful insight into conditional probability formulation. We thank S.T. Algermissen and S.P. Nishenko for helpful discussions and B. Bender for a copy of her computer programs for maximum likelihood estimation of grouped magnitude data. This study benefited considerably from the manuscript preparation of R. Pryor and the patience of an editor. Research support^{was} provided by the Nuclear Regulatory Commission under contract NRC-04-78-200 and by the State of Tennessee.

REFERENCES

- Algermissen, S.T. (1972). The seismic risk map of the United States: development, use, and plans for future refinement, Conf. on Seismic Risk Assessment for Building Standards (March 16, 1972), U.S. Dept. of Housing and Urban Development, Washington, D.C., 11-16.
- Bender, B. (1983). Maximum likelihood estimation of b values for magnitude grouped data, Bull. Seism. Soc. Amer., 73, 831-851.
- Brillinger, D.R. (1982). Seismic risk assessment: Some statistical aspects, Earthquake Predict. Res. 1, 183-195.
- Bufe, C.G., P.W. Harsh, and R.O. Burford (1977). Steady-state seismic slip--a precise recurrence model, Geophys. Res. Lett., 4, 91-94.
- Hagiwara, Y. (1974). Probability of earthquake occurrence as obtained from a Weibull distribution analysis of crustal strain, Tectonophysics, 23, 313-318.
- Harada, T. (1978). Quiet and violence in horizontal movement of the crust, in Earthquake Precursors, C. Kisslinger and Z. Suzuki, eds., Suppl. Issue, J. Phys. Earth, 79-83.
- Howell, B.F. (1980). A comparison of estimates of seismic risk in the Central United States, Earthquake Notes, 51, 13-19.
- Jacob, K.H. (1984). Estimates of long-term probabilities for future great earthquakes in the Aleutians, Geophys. Res. Lett., 11, 295-298.
- Johnston, A.C. (1981). On the use of the frequency-magnitude relation in earthquake risk assessment, Vol. 1, in Earthquakes and Earthquake Engineering-Eastern United States, J.E. Beavers, ed., 161-181, Ann Arbor Science Publishing Co., Ann Arbor, Michigan.
- Kiremidjian, A.S. and T. Anagnos (1984). Stochastic slip-predictable model for earthquake occurrences, Bull. Seism. Soc. Amer., 74, 739-755.
- Lomnitz, C. (1974). Global Tectonics and Earthquake Risk, Elsevier Scientific Publ. Co., Amsterdam, the Netherlands, 320 pp.
- McClain, W.C., O.H. Myers (1970). Seismic history and seismicity of the southeastern region of the United States, Report No. ORNL-4582, Oak Ridge National Lab., Oak Ridge, Tenn.

- McNally, K.C. and J.B. Minister (1981). Nonuniform seismic slip along the middle American Trench, J. Geophys. Res., 86, 4949-4959.
- Mann, O.C., W. Howe, F.H. Kellogg (1974). Regional Earthquake Risk Study, Technical Report, Dept. of Housing and Urban Development, Washington, D.C.
- Miller, A.R. (1982). Fortran Programs for Scientists and Engineers, SYBEX, Berkeley, 280 pp.
- National Bureau of Standards (1953). Tables of Normal Probability Functions, U.S. Dept. of Commerce, N.B.S. Applied Math. Series 23, U.S. Gov't. Printing Office, Washington, D.C., 344 pp.
- Nishenko, S.P (1984). Seismic potential for great interplate earthquakes along the Chilean margin of South America: A quantitative reappraisal, J. Geophys. Res., in press.
- Nuttli, O.W. (1974). Magnitude-recurrence relation for central Mississippi Valley earthquakes, Bull. Seism. Soc. Amer., 64, 1189-1207.
- Nuttli, O.W. (1979). The Seismicity of the Central United States, in Geology in the Siting of Nuclear Power Plants, Geol. Soc. Amer. Bull., 90, Part 1, 1013-1018.
- Nuttli, O.W. (1981). Seismic hazard associated with the New Madrid fault zone, in Evaluation of past studies and identification of needed studies of the effects of major earthquakes occurring in the New Madrid seismic zone, Appendix A, Report submitted to Federal Emergency Management Agency, Kansas City, MO., 15 pp.
- Nuttli, O.W. (1983). Average seismic source - parameter relations for mid-plate earthquakes, Bull. Seism. Soc. Amer., 73, 519-535.
- Nuttli, O.W. and R.B. Herrmann (1978). Credible earthquake for the Central United States; State-of-the-art for assessing earthquake hazards in the United States; Misc. Paper 5-73-1, Report No. 12, U.S. Army Corps of Engineers, Waterways Experiment Station, Vicksburg, MS, 99 pp.
- Nuttli, O.W. and K.G. Brill (1981). Earthquake source zones in the central United States determined from historical seismicity in An Approach to Seismic Zonation for Siting Nuclear Electric Power Generating Facilities in the Eastern United States, NUREG/CR-1577, Nuc. Reg. Comm., Wash. DC, 98-142.

- Perry, R.G. (1981). Seismic hazard analysis for the Central United States, M.S. thesis, Saint Louis Univ., Saint Louis, MO., 175 pp.
- Raleigh, C.B., K. Sieh, L.R. Sykes, and D.L. Anderson (1982). Forecasting Southern California earthquakes, Science, 217, 1097-1104.
- Rikitake, T. (1975). Statistics of ultimate strain of the earth's crust and probability of earthquake occurrence, Tectonophysics, 23, 1-21.
- Rikitake, T. (1977). Possible procedure of earthquake prediction and some problems of earthquake warning, in A Symposium on Earthquake Prediction Research, Z. Suzuki, S. Omote, eds., Seism. Soc. of Japan, Tokyo, 215-224 (in Japanese).
- Rikitake, T., (1981). Practical approach to earthquake prediction and warning, in Current Research in Earthquake Prediction 1, Vol. 2, T. Rikitake, ed., D. Reidel Publ. Co., Dordrecht, 1-52.
- Russ, D.P. (1979). Late Holocene faulting and earthquake recurrence in the Reelfoot Lake area, northwestern Tennessee, Geol. Soc. Amer. Bull., Part 1, 90, 1013-1018.
- Russ, D.P. (1980). Seismic zoning meeting for the Central United States --Final Report, October 21, 1980, Prepared for the U.S. Geological Survey.
- Ryall, A.S. and R.B. Smith (and following papers) (1980). Preface to seismicity of the Wasatch Front and Great Basin-Sierra Nevada boundary, in Special Papers on Seismicity of the Wasatch Front and Great Basin-Sierra Nevada Boundary, Bull. Seism. Soc. Amer., 70, 1429-1594.
- Shi, Y., and B.A. Bolt (1982). The standard error of the magnitude-frequency b value, Bull. Seism. Soc. Amer., 72, 1677-1687.
- Shimazaki, K. and T. Nakata (1980). Time-predictable recurrence model for large earthquakes, Geophys. Res. Lett., 7, 279-282.
- Sieh, K.E. (1978). Prehistoric large earthquakes produced by slip on the San Andreas fault at Pallett Creek, California, J. Geophys. Res., 83, 3907-3939.

- Stauder, W. (1982). Present-day seismicity and identification of active faults in the New Madrid seismic zone, in, Investigations of the New Madrid, Missouri, Earthquake Region, U.S. Geol. Surv. Prof. Paper 1236-C, 21-30.
- Stauder, W. (and others)(1974-1983). Central Mississippi Valley Earthquake Bulletin, No's. 1-36, St. Louis University, St. Louis, Mo.
- Stauder, W., G. Fischer, S. Schaeffer, and S.T. Morrissey (1976). Seismic characteristics of southeast Missouri as indicated by a regional telemetered microearthquake array, Bull. Seism. Soc. Amer., 66, 1953-1964.
- Sykes, L.R. and S.P. Nishenko (1984). Probabilities of occurrence of large plate rupturing earthquakes for the San Andreas, San Jancinto, and Imperial faults, California, 1983-2003, J. Geophys. Res., 89, 5905-5927.
- Till, R. (1974). Statistical Methods for the Earth Scientist, Halstead Press, John Wiley & Sons, Inc., New York, 154 pp.
- Tsuboi, C. (1956). Earthquake energy, earthquake volume, aftershock area, and strength of the earth's crust, J. Phys. Earthq., 4, 63-66.
- Weibull, W. (1951). A statistical distribution function of wide application, J. Appl. Mech., 18, 293-297.
- Weichert, D.H. (1980). Estimation of the earthquake recurrence parameters for unequal observation periods for different magnitudes, Bull. Seism. Soc. Amer., 70, 1337-1346.
- Wesnousky, S.G., C.H. Scholz, and K. Shimazaki (1982). Deformation of an island arc: rates of moment release and crustal shortening in intraplate Japan determined from seismicity and Quaternary fault data, J. Geophys. Res., 87, 6829-6852.
- Wesnousky, S.G., C.H. Scholz, K. Shimazaki, and T. Matsuda (1983). Earthquake frequency distribution and mechanics of faulting, J. Geophys. Res., 88, 9331-9340.
- Wesnousky, S.G., C.H. Scholz, K. Shimazaki, and T. Matsuda (1984). Integration of geological and seismological data for the analysis of seismic hazard: A case study of Japan, Bull. Seism. Soc. Amer., 74, 687-708.
- Zoback, M.D., S.W. Krueger, and W.H. Prescott (1984). Lower crustal strain localization and intaplate seismicity: evidence from the Ramapo fault zone, submitted to Science.

SOURCE CHARACTERISTICS AND STRONG GROUND MOTION OF NEW MADRID EARTHQUAKES

by

Otto W. Nuttli and Robert B. Herrmann

St. Louis University

St. Louis, Missouri

A striking characteristic of the reported effects of the New Madrid earthquakes of 1811 and 1812 was the lack of surface faulting. One exception was the apparent damming of the Mississippi River above and below the town of New Madrid, which best can be explained by fault uplift on the downstream side caused by the great earthquake of February 7, 1812. There were large rifts in the ground caused by soil failure, and uplift and subsidence of as much as 6 meters which must have been associated with faulting. But, considering the fact that there were four earthquakes of M_S larger than 8 (M_S is surface-wave magnitude), the lack of extensive surface rupture is remarkable. An explanation cannot be provided by a failure to survey the area, because it was visited by several competent geologists in the years immediately following the earthquakes. Also, Fuller (1912) could find no evidence of surficial faulting, even though he found ample evidence of sand cratering, fissuring and various other kinds of soil failure caused by the earthquakes. The absence of surface faulting is a general characteristic of earthquakes east of the Rocky Mountains. It serves to place a constraint on the minimum focal depth of the earthquakes. For vertical strike-slip faults, Nuttli and Herrmann (1984) give the relation as

$$\log h_{\min} \text{ (km)} = -1.730 + 0.456 m_b \quad \text{for } m_b \geq 4.5$$

where m_b is body-wave magnitude. If the fault dips at an angle of d with the horizontal, the value of h_{\min} should be multiplied by $\sin d$.

Another notable feature of the 1811-1812 New Madrid earthquakes was their large magnitude, compared to the size of the fault that is capable of

being ruptured. Figure 1 shows the location of recent microearthquakes, which serves to define the horizontal extent of the fault zone. From the figure the southwestern branch can be seen to have a maximum length of 150 km, the central north-northwestwardly striking branch a maximum length of 75 km, and the northeastward branch a maximum length of 100 km. From a description of accounts of the damage effects of the 1811-1812 earthquakes (Nuttli, 1973), the epicenters of the earthquakes of December 16, 1811 at about 2:30 a.m. and 8:15 a.m. (local time) were associated with the southwestern branch of the fault. Nuttli (1973) gave m_b values for these earthquakes of about 7.2 and 7.0, which correspond to M_S values of 8.5 and 8.3, respectively (Nuttli, 1983a). Felt and damage reports of the earthquake of January 23, 1812, of m_b 7.1 and M_S 8.4, indicate that its epicenter lay on the central branch of the fault system (Nuttli, 1973 and 1983a). The largest earthquake, the February 7, 1812 event with an m_b of 7.4 and an M_S of 8.8, occurred on the northeast branch (Nuttli, 1973 and 1983a). If typical relations between fault rupture length and M_S are used (e.g. Kanamori and Anderson, 1975), rupture lengths of approximately 300 to 1000 km are required for earthquakes of M_S 8.0 to 8.8.

Resolution of the two problems, namely the general lack of surface faulting and the large M_S values associated with short fault lengths, was offered by the empirical spectral scaling relations for mid-plate earthquakes (Nuttli, 1983a). Using these spectral relations and equations given by Savage (1972) which relate spectral corner frequencies to fault rupture length and width, he found that typical mid-plate earthquakes of $M_S = 8.3, 8.4, 8.5$ and 8.8 have rupture lengths of 45, 52, 58 and 75 km, respectively, and rupture widths of 29, 33, 36 and 44 km, respectively. These rupture lengths

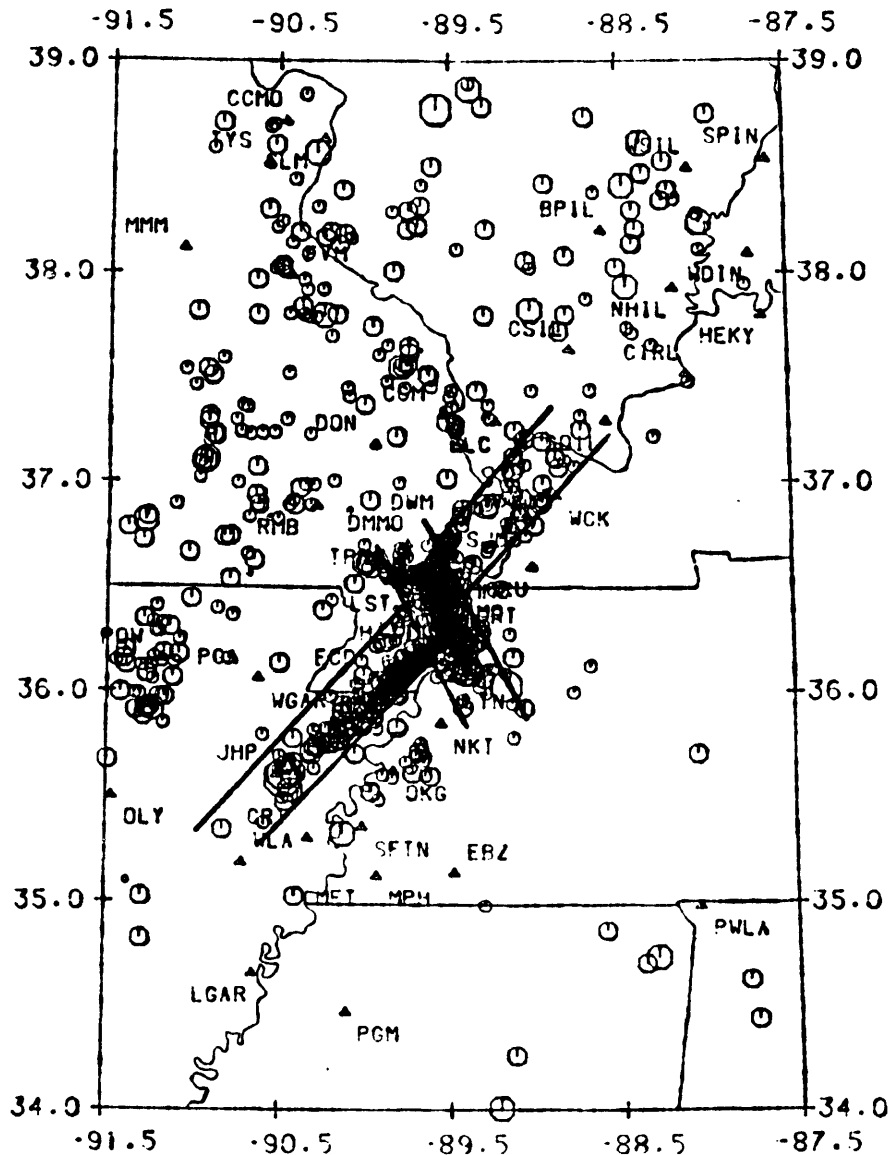


Figure 1. Microearthquakes detected and located in the central Mississippi Valley for the period July 1, 1974 through September 30, 1983. The size of the octagons is proportional to magnitude, with the smallest having m_b values of 0 to 1 and the largest m_b values of 4 to 5. The triangles and 3-letter symbols indicate the location of seismographs of the Saint Louis University and Memphis State University networks. The approximate boundaries of the New Madrid fault zone, as delineated by the epicenters of the microearthquakes, are drawn as straight lines.

can be accommodated by the fault lengths of the three segments of the New Madrid fault system. Herrmann and Canas (1978) found that present-day seismic activity on the southwestern branch is predominantly right-lateral strike slip, with dips of about 70° . Reverse faulting was observed on the central branch and right-lateral strike slip on the northeastward branch, consistent with a regional east-west compressive stress field. For a dip of 70° and a rupture width of 44 km (largest earthquake) the hypocenter would have had to be at a depth of 40 km or greater to not rupture the surface. Because there was suggestion of uplift of the Mississippi river bed by this earthquake, the depth can be assumed to have been about 40 km.

Making use of relations given by Aki (1966) and Geller (1976), the average fault displacements of the earthquakes of $M_S = 8.3, 8.4, 8.5$ and 8.8 are calculated to be 3.7, 4.8, 5.8 and 9.2 meters, respectively, and the static stress drops 80, 90, 100 and 130 bars, respectively (Nuttli, 1983a). The spectral scaling relations are consistent with a rupture velocity of 3.2 km/sec. The rise times of the earthquakes of $M_S = 8.3, 8.4, 8.5$ and 8.8 are 13, 14.5, 16 and 19 sec, respectively. Therefore, the source characteristics of large New Madrid earthquakes can be categorized by relatively short rise times, moderately high static stress drops and small rupture lengths.

Figure 2 shows the empirical spectral scaling relations developed by Nuttli (1983a) for mid-plate earthquakes. Spectral amplitudes at 1 sec, 20 sec and very long periods are assumed to be proportional to m_b , M_S and M_0 (seismic moment), respectively. The spectra were constructed by using observed values of m_b , M_S and M_0 for mid-plate earthquakes and, by a trial-and-error procedure, setting the long-period amplitude level and the corner periods so as to satisfy the data. The corner period T_{02} (period of the in-

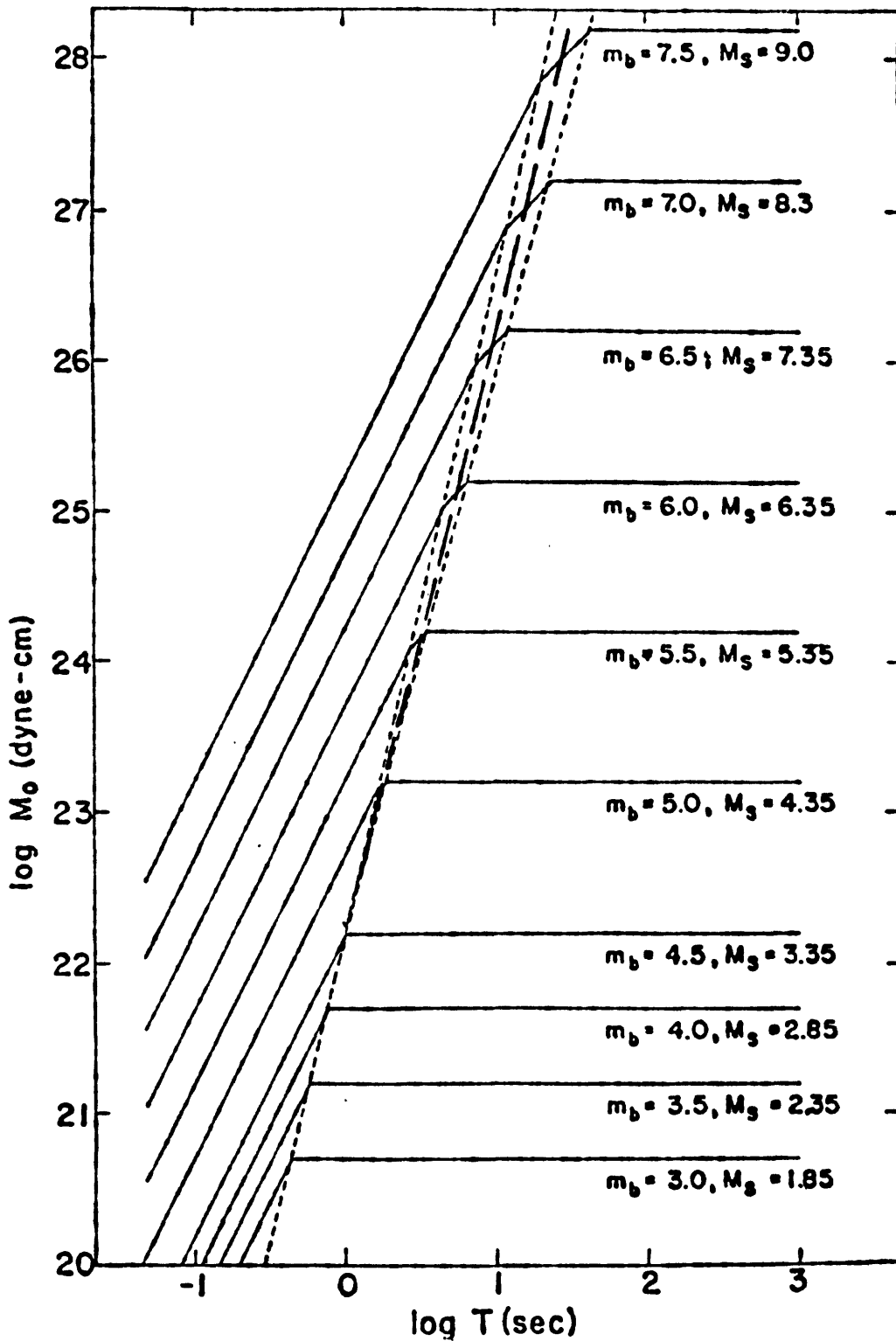


Figure 2. Empirical generalized spectra for mid-plate earthquakes, constructed so as to satisfy observed m_b , M_s and M_0 values (Nuttli, 1983a). The dashed-line curve has a slope of four.

tersection of the portions of the spectrum of slope two and of slope zero) is found to be proportional to $M_0^{\frac{1}{4}}$, i.e. the slope of the curve of $\log M_0$ versus $\log T_{02}$ in Figure 2 is four. If the static stress drop were independent of seismic moment, the slope would be three (Aki, 1967). Such a relation usually is proposed for California earthquakes and plate-margin earthquakes, in general.

Herrmann and Nuttli (1980) considered the consequences of a seismic spectral scaling relation where M_0 is proportional to the fourth power of T_{02} . They concluded that maximum ground acceleration, velocity and displacement then would satisfy the equations

$$\log a_h = A + 0.50 m_b - B \log (R^2 + h^2)^{\frac{1}{2}} - C \log e R$$

$$\log v_h = D + 1.00 m_b - B \log (R^2 + h^2)^{\frac{1}{2}} - E \log e R \quad \text{for } m_b \geq 4.5$$

$$\log d_h = F + 1.50 m_b - B \log (R^2 + h^2)^{\frac{1}{2}} - G \log e R$$

The term $B \log (R^2 + h^2)^{\frac{1}{2}}$ accounts for geometric spreading and dispersion. Observational data suggest that $B = 0.83$, which is consistent with the largest ground motion being produced by an Airy phase of higher-mode surface waves. The quantities C , E and G are numerically equal to the values of the coefficient of anelastic attenuation for the waves that carry the peak ground motion. Because they are frequency dependent, and because the frequency of the maximum ground-motion parameters varies with epicentral distance and magnitude, the terms C , E and G are not strictly constant. However, they shall be treated as constant by assuming that maximum acceleration occurs on average at frequencies of 5 Hz, maximum velocity at 1.5 Hz and maximum displacement at 0.5 Hz. The values of the terms A , D and F

must be obtained from observational strong-motion data for earthquakes of known m_b values. Following more-or-less standard practice, a_h , v_h and d_h are taken to be the arithmetic average of the peak values of acceleration, velocity and displacement, respectively, on the two horizontal components of strong ground motion.

Studies of the attenuation of small- to moderate-sized earthquakes provide values for the coefficient of anelastic attenuation. In particular, Q_0 (1-sec period value of Q) is found to be 1500 and n to be 0.4 (Dwyer et al, 1983), where

$$Q(f) = Q_0 f^n$$

and

$$\gamma(f) = \pi f/V(f) Q(f)$$

The coefficient of anelastic attenuation is γ , and V is the group velocity. These relations lead to values of $C = 0.0016 \text{ km}^{-1}$, $E = 0.00076 \text{ km}^{-1}$ and $G = 0.00040 \text{ km}^{-1}$ for $V = 3.5 \text{ km/sec}$.

Figure 3 shows data for a_h for earthquakes in central and eastern North America (Nuttli and Herrmann, 1984), along with theoretical curves for $m_b = 4.5$ to 7.5. All of the data have been equalized to an $m_b = 5.0$ value. Based on the 35 data points, the standard deviation is 0.24 magnitude units, or a multiplicative factor of 1.74. The data were obtained for a variety of site conditions, but may be considered to be representative of stiff soil site conditions.

Most of the data points of Figure 3 came from earthquakes of m_b between 4.5 and 5.2. Therefore it is especially important to test the curves of larger m_b values, which were developed from theoretical considerations that

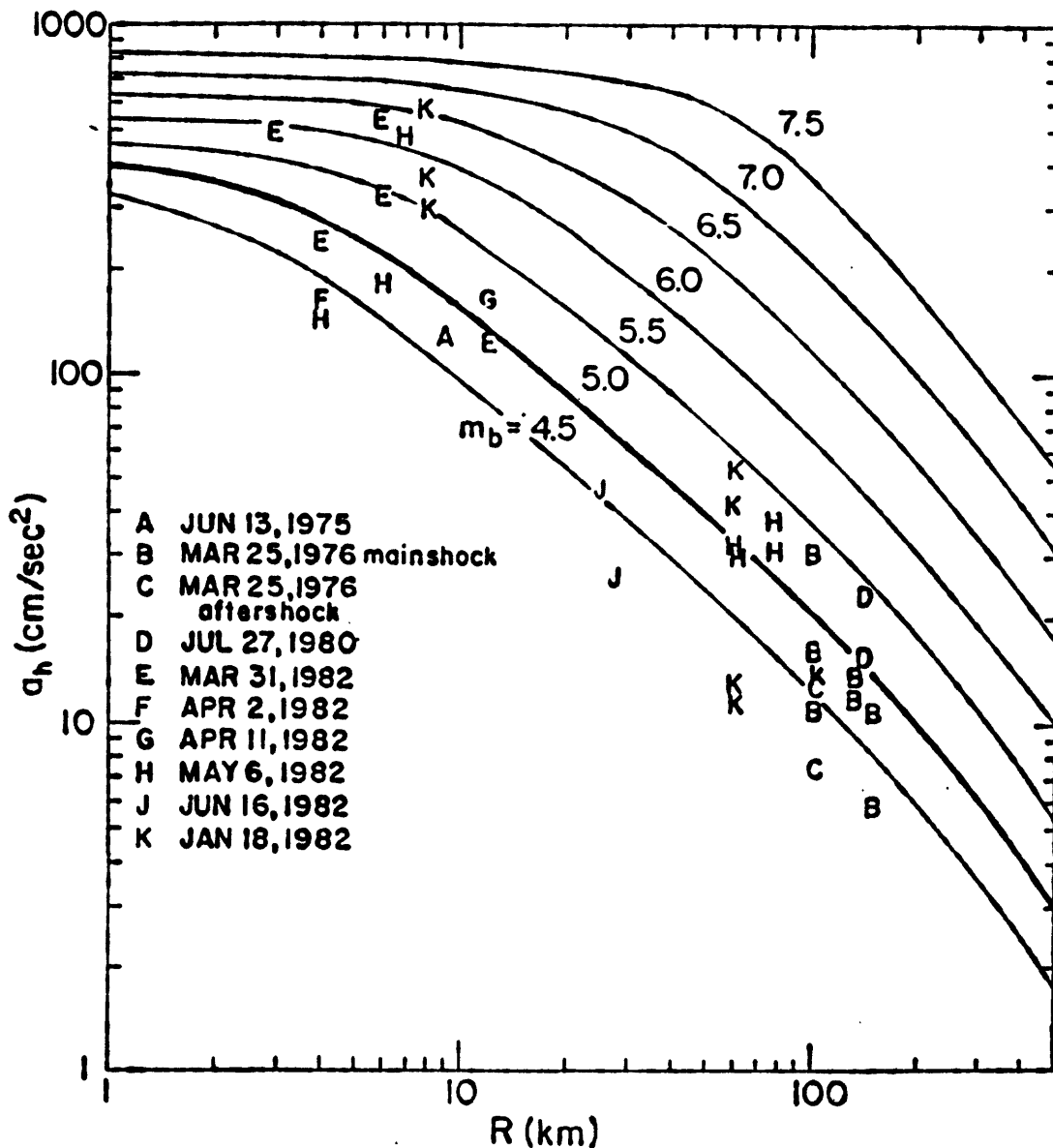


Figure 3. Curves of a_h (arithmetic average of peak acceleration on the two horizontal components) versus epicentral distance, for various body-wave magnitudes (Nuttli and Herrmann, 1984). The data, which have been equalized to $m_b = 5.0$, are taken from: A, B, C (Herrmann, 1977), D (Street, 1982b), E through J (Weichert *et al.*, 1982), K (Chang, 1983). The standard deviation of the log a_h values about the $m_b = 5.0$ curve is 0.24.

made use of the observed relation $M_0/T_{02}^4 = \text{constant}$. Two alternative methods have been used for constructing strong ground-motion curves for central and eastern North America. One method uses intensity attenuation data appropriate to the region and correlations between peak ground-motion values and M.M. intensity, to convert observed intensities to peak ground motion. For a given epicentral intensity, the peak ground-motion values are plotted versus epicentral distance and a best-fitting curve is obtained. A second method is based on the assumption that near-field peak ground motion as a function of m_b does not vary geographically, which was found to be satisfactory for earthquakes of m_b less than approximately 6.5 (Nuttli, 1983a,b). The near-field data then are attenuated by values appropriate to central and eastern North America.

Figure 4 compares a_h values obtained by the intensity-data method (dash-dot curve), the use of near-field western United States data and eastern attenuation (dotted and dashed curves) and the semi-theoretical method described previously (solid-line curves). For distances of 10 to 100 km all the curves for $m_b = 5.0$ are in good agreement. At distances beyond 100 km the curves diverge, reflecting differences in values of the coefficient of anelastic attenuation.

Figure 5 is similar to Figure 4, but for $m_b = 6.5$. Also, more curves are included for comparison purposes. The intensity-data method is represented by the dash-and-two-dot curve and the dash curve, the western United States near-field-data method by the dash-dot, dash-and-three-dot, and dot curves, and the semi-theoretical by the solid-line curve. In order to compare these curves against a typical peak acceleration curve for the western United States, the two-dash-and-dot curve is presented. From Figure 4 it

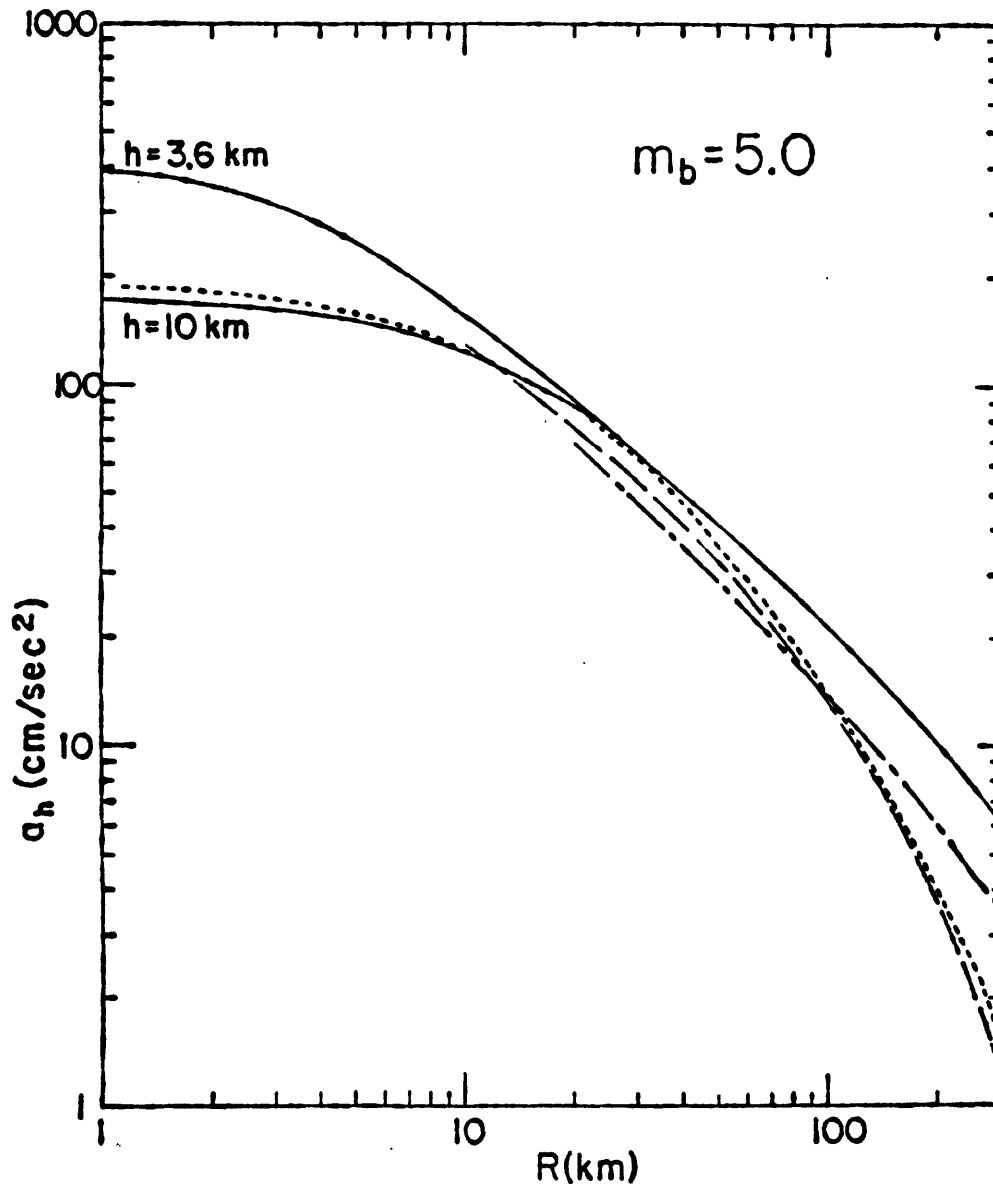


Figure 4. Curves of a_h versus epicentral distance for $m_b = 5.0$, as determined by different methods. The solid-line curves are from Nuttli and Herrmann (1984), the dotted-line curve from Campbell (1981), the dashed-line curve from Nuttli (1979) and the dash-dot curve combines the intensity attenuation relation of Nuttli and Herrmann (1984) and the site intensity versus acceleration relation of Murphy and O'Brien (1977).

can be seen that all of the attenuation curves, with the exception of the dash-dot (western United States) and dash-and-two-dot (intensity attenuation) curves do not differ from each other by more than a factor of two over the distance range of 10 to 500 km. The dash-and-two-dot curve uses a relation of Trifunac and Brady (1975) between intensity and peak acceleration, which does not take account of epicentral distance, and is for the most part based on near-field data where the wave frequencies are high. Thus the acceleration attenuation curve obtained using these data can be expected to be too large, especially at epicentral distances beyond 100 km.

On the basis of Figures 4 and 5 we can conclude that the acceleration attenuation curves of Figure 3 for m_b values of 5.0 to 6.5 are reliable, at least to epicentral distances of 100 km. This magnitude range covers all damaging earthquakes with recurrence periods of 100 years or less. There are no strong-motion data for earthquakes anywhere in the United States to test the validity of extrapolation to $m_b = 7.0$ and 7.5, as given in Figure 3. For the New Madrid seismic zone the average recurrence time of such earthquakes is approximately 350 and 800 years, respectively. Therefore, probably only critical structures will be designed to withstand the motions produced by such large earthquakes.

Figure 6 presents the maximum velocity attenuation curves, along with central and eastern North American data that have been equalized to an $m_b = 5.0$ event. The standard deviation of the 41 points with respect to the $m_b = 5.0$ curve is 0.24 magnitude units, the same as for the maximum acceleration curve. The $m_b = 7.5$ curve is not extended to values greater than 200 cm/sec, as it is doubtful that soil or surficial rock could sustain higher velocities at frequencies of 1 to 2 Hz.

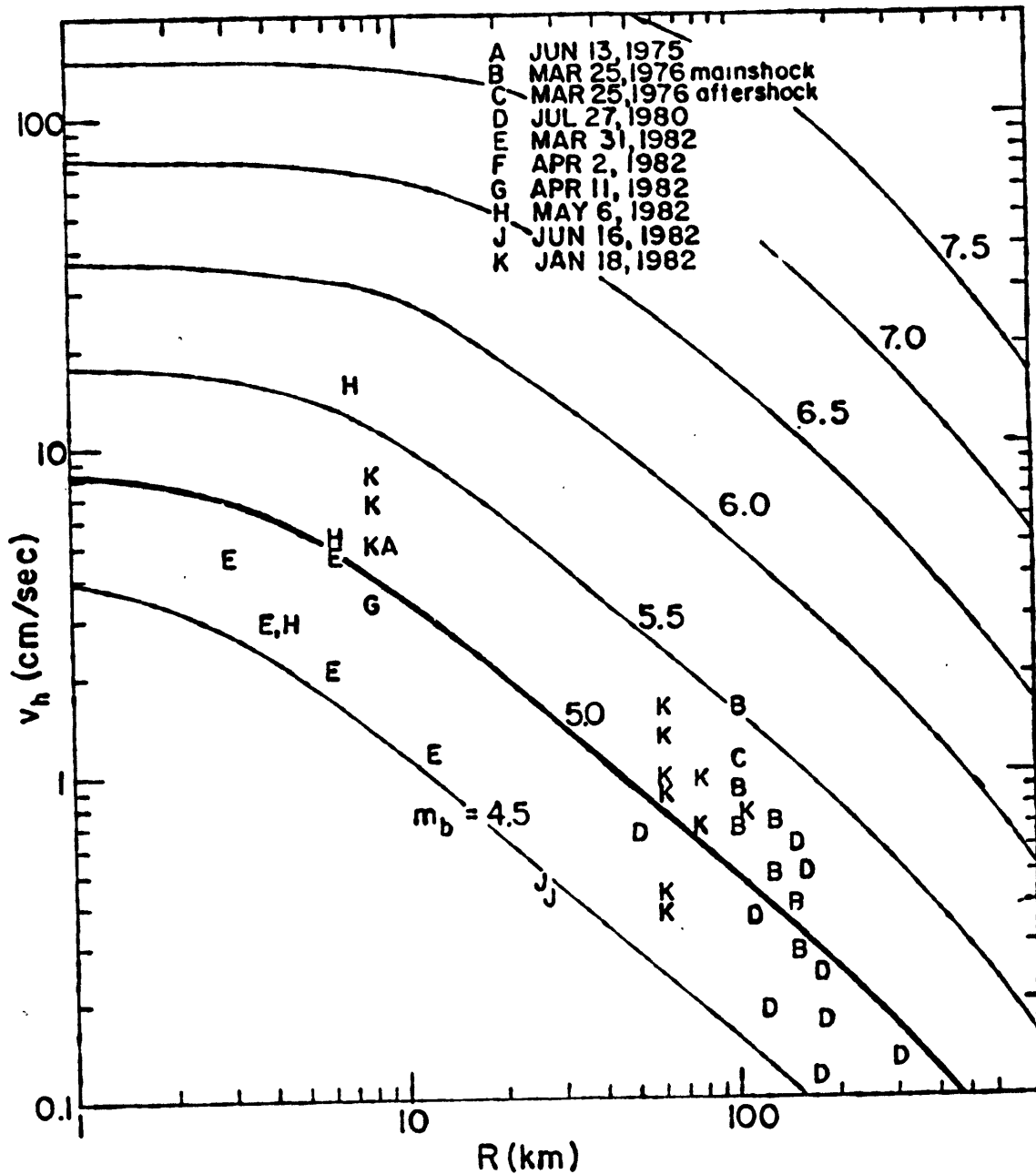


Figure 6. Curves of v_h (arithmetic average of peak velocity on the two horizontal components) versus epicentral distance, for various body-wave magnitudes (Nuttli and Herrmann, 1984). The data, which have been equalized to $m_b = 5.0$, are taken from: A, B, C (Herrmann, 1977), D (Street, 1982b), E through J (Wiechert *et al.*, 1982) K (Chang, 1983). The standard deviation of the log v_h values about the $m_b = 5.0$ curve is 0.24.

Figure 7 compares the $m_b = 5.0$ curve of Figure 6 (solid-line curve) with an intensity-derived peak velocity curve (dashed-line curve) and a curve based on western United States near-field data (dotted line). The intensity-derived velocity values are 5 to 8 times larger than those for the other two curves, most likely because they are based upon near-field observations at higher frequencies. The other two curves do not differ by more than a factor of two from 10 to 300 km. Figure 8 presents curves similar to those of Figure 7, for an $m_b = 6.5$ earthquake. Also included as the dash-dot curve is the Joyner and Boore (1981) relation for the western United States. Beyond 10 km it attenuates much more rapidly than the curves for the central and eastern United States, being ten times smaller at a distance of 200 km.'

Figure 9 shows the maximum ground displacement scaling relations for the central and eastern United States, along with available strong-motion data that have been equalized to an m_b of 5.0. There are 29 data points, and the standard deviation with respect to the $m_b = 5.0$ curve is 0.39, or a multiplicative factor of 2.45. The curves for the larger magnitude earthquakes have not been extended beyond displacements of 100 cm, which is assumed to be the maximum possible displacement of stiff soil at frequencies of 0.5 Hz. The extrapolation of the curves to distances of several thousand kilometers gives displacements which are consistent with those measured by observatory-type seismographs for surface waves of large earthquakes.

Table 1 presents values of maximum horizontal acceleration, velocity and displacement at distances of 25, 100, 300 and 700 km for earthquakes of $M_S = 8.8$, which is representative of the greatest possible earthquake in the New Madrid zone, $M_S = 7.6$, which is the largest potential earthquake at the

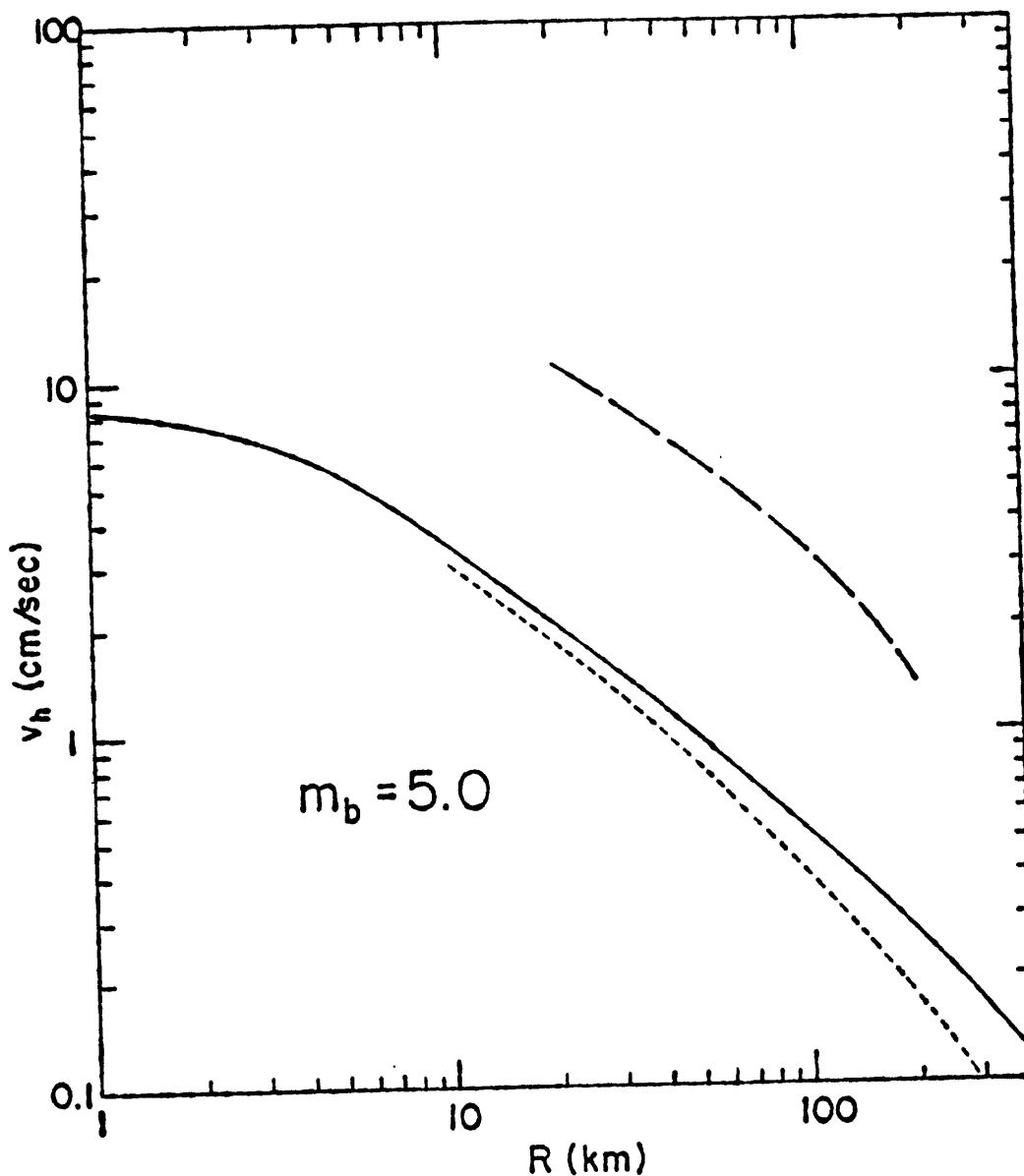


Figure 7. Curves of v_h versus epicentral distance for $m_b = 5.0$, as obtained by different methods. The solid-line curve is from Nuttli and Herrmann (1984), the dotted-line curve from Nuttli (1979) and the dashed-line curve combines the intensity attenuation relation of Nuttli and Herrmann (1984) and the site intensity versus velocity relation of Trifunac and Brady (1975).

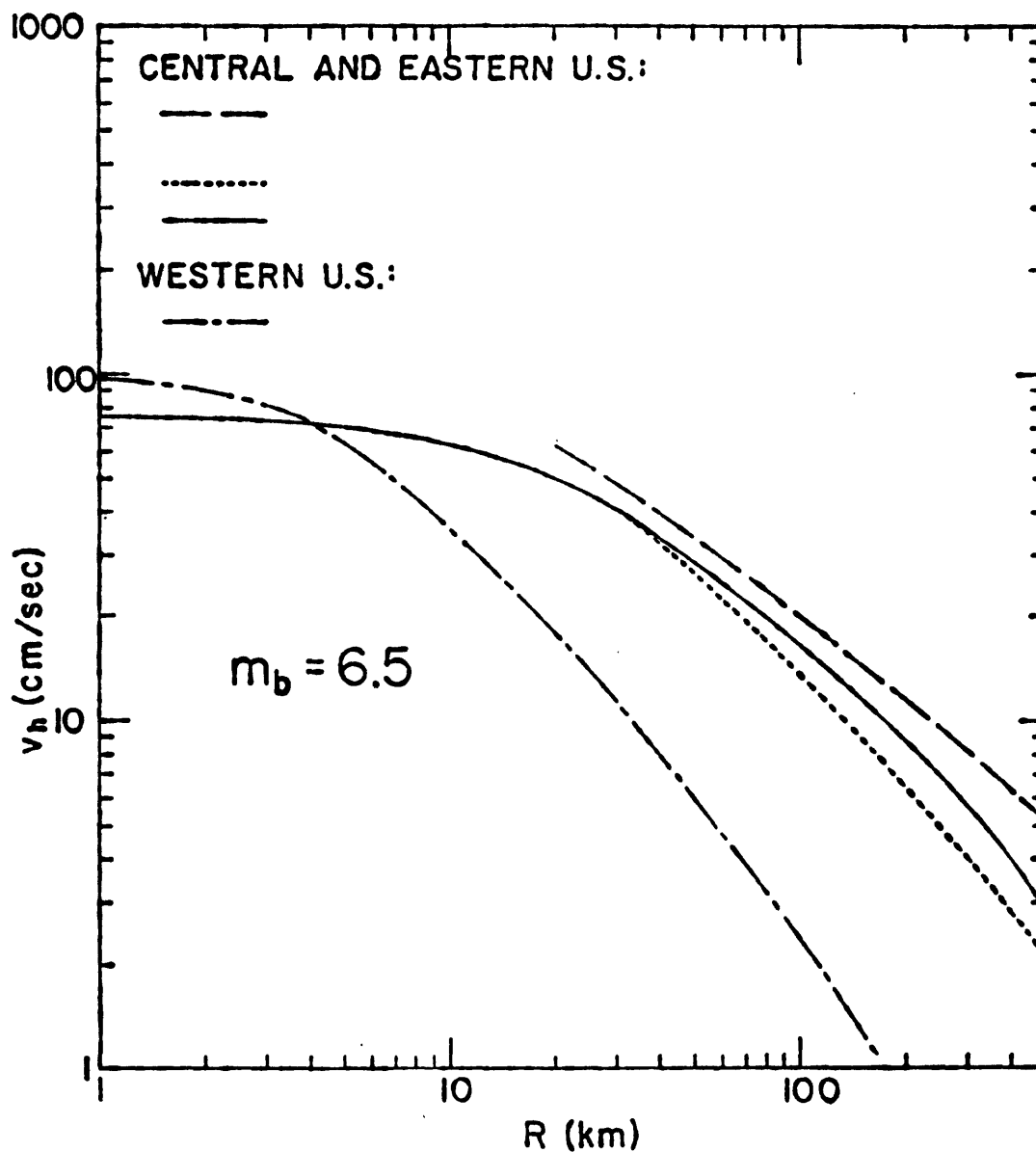


Figure 8. Curves of v_h versus epicentral distance for $m_b = 6.5$, as obtained by different methods. The solid-line curve is from Nuttli and Herrmann (1984), the dotted-line curve from Nuttli (1979) and the dashed-line curve combines the intensity attenuation relation of Nuttli and Herrmann (1984) and the site intensity versus velocity relation of Trifunac and Brady (1975). The dash-dot curve gives the relation of Joyner and Boore (1981) for the western United States.

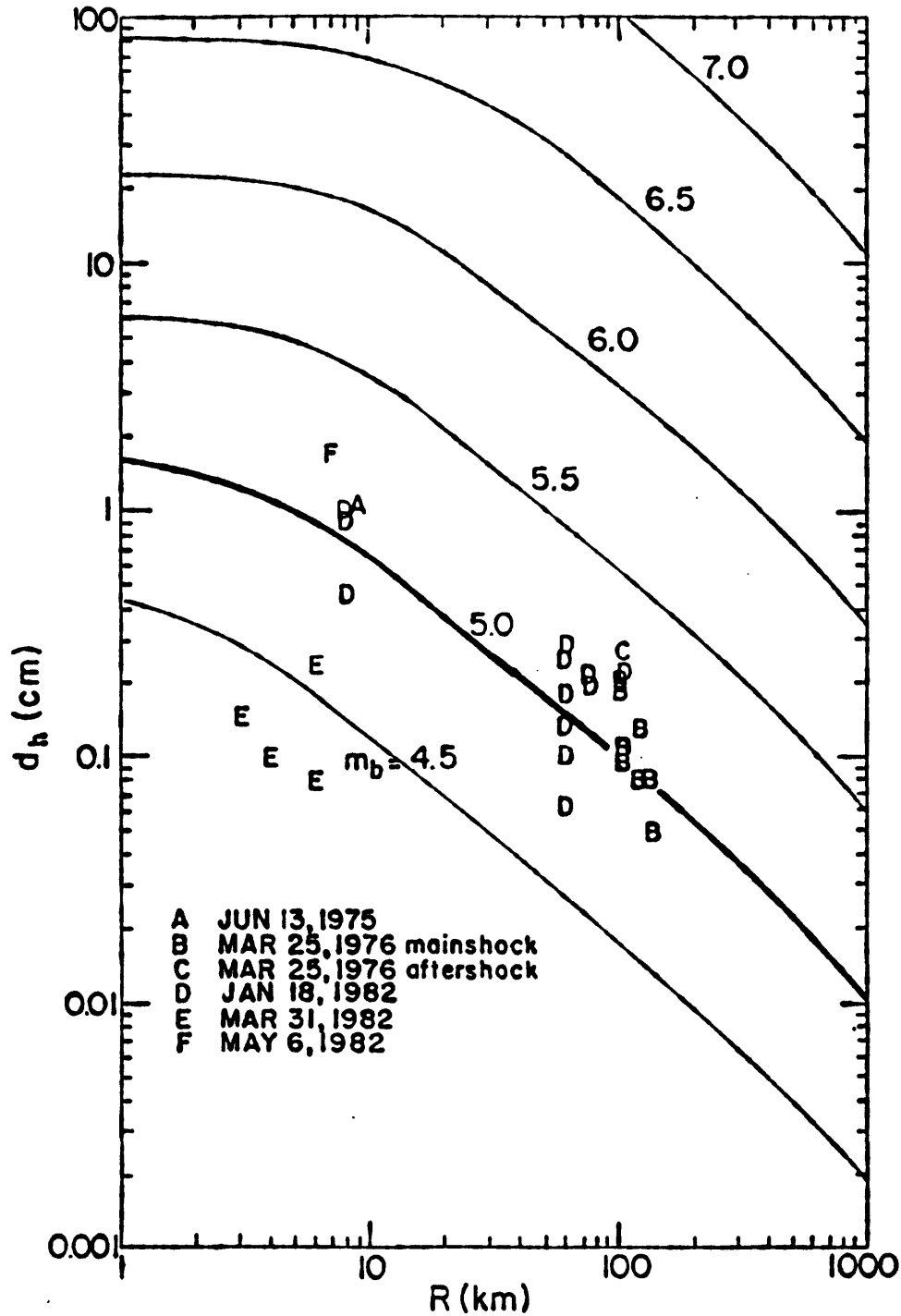


Figure 9. Curves of d_h (arithmetic average of peak displacement on the two horizontal components) versus epicentral distance, for various body-wave magnitudes (Nuttli and Herrmann, 1984). The data, which have been equalized to $m_b = 5.0$, are taken from: A, B, C (Herrmann, 1977), D (Chang, 1983) and E, F (Wiechert et al., 1982). The standard deviation of the log d_h values about the $m_b = 5.0$ curve is 0.39.

TABLE 1

GROUND-MOTION VALUES FOR SELECTED DISTANCES AND MAGNITUDES
FOR STIFF-SOIL SITE CONDITIONS

| M_S | R (km) | a_h (cm/sec ²) | v_h (cm/sec) | d_h (cm) | I (M.M.) |
|-------|--------|------------------------------|----------------|------------|----------|
| 6.5 | 25 | 251 | 19.1 | 13.8 | VIII-IX |
| | 100 | 75.9 | 6.2 | 4.3 | VII |
| | 300 | 21.9 | 2.1 | 1.6 | V |
| | 700 | 5.9 | 0.8 | 0.7 | IV |
| 7.6 | 25 | 417 | 58.9 | 77.6 | IX-X |
| | 100 | 141 | 21.4 | 28.2 | VIII |
| | 300 | 41.7 | 7.4 | 10.7 | VI-VII |
| | 700 | 11.2 | 2.8 | 4.6 | V |
| 8.8 | 25 | 676 | 200* | 100** | XI |
| | 100 | 309 | 107 | 100** | IX-X |
| | 300 | 95.5 | 38.9 | 100** | VIII |
| | 700 | 25.7 | 14.5 | 55.0 | VI-VII |

*Assumed to be maximum velocity that can be sustained by soil or surficial rock.

**Assumed to be maximum displacement that can be sustained by soil or surficial rock.

present time (Nuttli, 1983a) and $M_S = 6.5$, which is an earthquake with an average recurrence period of about 75 years for the New Madrid zone. Cities such as Memphis, Cape Girardeau and Paducah are in the 25 to 100 km distance range, Little Rock and Evansville in the 100 plus km range, St. Louis and Louisville in the 100 to 300 km range, Cincinnati, Kansas City and Jackson, Mississippi in the 300 to 700 km range, and Chicago, Milwaukee, Detroit, Columbus, Atlanta and Dallas are at approximately 700 km distance.

Also included in Table 1 are values of M.M. intensity, obtained by means of the formula (Nuttli and Herrmann, 1984)

$$I(R) = 0.20 + 2.00 m_b - 2.70 \log R - 0.0011 R$$

where R is epicentral distance, in kilometers.

The calculated M.M. intensities for an $M_S = 6.5$ earthquake are very similar to those observed for the 1895 Charleston, Missouri earthquake (Nuttli, 1974; Hopper and Algermissen, 1980). Likewise, the calculated intensities for an $M_S = 8.8$ earthquake are similar to those observed for the largest 1811-1812 New Madrid earthquakes (Nuttli, 1973; Street, 1982). Intensity VIII usually is taken as the lower threshold of structural damage, and intensity VI as the lower threshold of non-structural or architectural damage. However, these intensity values are the ones to be expected for low-rise structures. Response spectra of accelerograms made in Los Angeles buildings for the 1971 San Fernando earthquake show that at selected frequencies the motions of the upper levels of buildings of ten stories and higher often are two or more times larger than the basement motions. This effect can be expected to be more pronounced at larger epicentral distances in the central United States, where dispersion will sort out the surface waves to make the

motion to be near sinusoidal and of longer duration. Therefore the motion of the upper levels of tall buildings may be one or two intensity units higher than those shown in Table 1, particularly at distances exceeding 100 km.

The effects of poor soil conditions, such as are found in river valleys, have not been taken into account in Table 1. Hopper et al (1983) show that these effects can increase site intensity by one to two M.M. units. However, they would not be added to the upper-level shaking effect of tall buildings, because such structures usually are built on bedrock.

Table 1 shows that even an $M_S = 6.5$ earthquake can cause damage over a wide area, particularly in cities or towns built on alluvial sediments and on tall buildings in large metropolitan areas. An $M_S = 7.6$ earthquake would be a major disaster, whose consequences need to be carefully evaluated.

ACKNOWLEDGMENTS

The research reported in this paper was supported by National Science Foundation grant CEE-790975 and by DARPA contract no. F49620-83-C-0015, monitored by the Air Force Office of Scientific Research.

REFERENCES

- Aki, K., 1966, Generation and propagation of G waves from the Niigata earthquake of June 16, 1964: Bulletin of the Earthquake Research Institute, Tokyo University, v. 49, p. 23-88.
- Aki, K., 1967, Scaling law of seismic spectrum: Journal of Geophysical Research, v. 72, p. 1217-1231.
- Algermissen, S. T. and D. M. Perkins, 1976, A probabilistic estimate of maximum acceleration in rock in the contiguous United States: U. S. Geological Survey Open-File Report 76-416.
- Campbell, K. W., 1981, A ground motion model for the central United States based on near-source acceleration data: Proceedings of the Conference on Earthquakes and Earthquake Engineering: the Eastern United States: J. E. Beavers, editor, Ann Arbor Science Publishers, Inc., v. 1, p. 213-232.
- Chang, F. K., 1983, Analysis of strong-motion data from the New Hampshire earthquake of 18 January 1982: Geotechnical Laboratory, U. S. Army Corps of Engineers, Vicksburg, Miss.
- Dwyer, J. J., R. B. Herrmann and O. W. Nuttli, 1983, Spatial attenuation of the Lg wave in the central United States: Bulletin of the Seismological Society of America, v. 73, p. 781-796.
- Fuller, M. B., 1912, The New Madrid earthquake: U. S. Geological Survey Bulletin 494, Washington, D.C.
- Geller, R. J., 1976, Scaling relations for earthquake source parameters and magnitudes: Bulletin of the Seismological Society of America, v. 66, p. 1501-1523.
- Herrmann, R. B., 1977, Analysis of strong motion data from the New Madrid seismic zone: 1975-1976: Department of Earth and Atmospheric Sciences, Saint Louis University, St. Louis, Mo.
- Herrmann, R. B. and J. A. Canas, 1978, Focal mechanism studies in the New Madrid seismic zone: Bulletin of the Seismological Society of America, v. 68, p. 1095-1102.
- Herrmann, R. B. and O. W. Nuttli, 1980, Strong motion investigations in the central United States: Proceedings 7th World Conference on Earthquake Engineering, Geoscience Aspects, Part II, Istanbul, Turkey, p. 533-536.

- Hopper, M. G. and S. T. Algermissen, 1980, An evaluation of the effects of the October 31, 1895, Charleston, Missouri, earthquake: U. S. Geological Survey Open-File Report 80-778.
- Hopper, M. G., S. T. Algermissen and E. C. Dobrovolsky, 1983, Estimation of earthquake effects associated with a great earthquake in the New Madrid seismic zone: U. S. Geological Survey Open-File Report 83-179 and Federal Emergency Management Agency CUSEPP no. 82-3.
- Joyner, W. B. and D. M. Boore, 1981, Peak horizontal acceleration and velocity from strong-motion records including records from the 1979 Imperial Valley, California, earthquake: Bulletin of the Seismological Society of America, v. 71, p. 2011-2038.
- Kanamori, H. and D. L. Anderson, 1975, Theoretical basis of some empirical relations in seismology: Bulletin of the Seismological Society of America, v. 65, p. 1073-1095.
- Murphy, J. R. and L. J. O'Brien, 1977, The correlation of peak ground acceleration amplitude with seismic intensity and other physical parameters: Bulletin of the Seismological Society of America, v. 67, p. 877-915.
- Nuttli, O. W., 1973, The Mississippi Valley earthquakes of 1811 and 1812: Intensities, ground motion and magnitudes: Bulletin of the Seismological Society of America, v. 63, p. 227-248.
- Nuttli, O. W., 1974, Magnitude recurrence relations for central Mississippi Valley earthquakes: Bulletin of the Seismological Society of America, v. 64, p. 1189-1207.
- Nuttli, O. W., 1979, State-of-the-Art for Assessing Earthquake Hazards in the United States: The relation of sustained maximum ground acceleration and velocity to earthquake intensity and magnitude: Miscellaneous Paper S-73-1, Report 16, U. S. Army Corps of Engineers, Vicksburg, Miss.
- Nuttli, O. W., 1983a, Average seismic source-parameter relations for mid-plate earthquakes: Bulletin of the Seismological Society of America, v. 73, p. 519-535.
- Nuttli, O. W., 1983b, Empirical magnitude and spectral scaling relations for mid-plate and plate-margin earthquakes: Tectonophysics, v. 93, p. 207-223.
- Nuttli, O. W. and R. B. Herrmann, 1984, Ground motion of Mississippi Valley earthquakes: Journal of Technical Topics in Civil Engineering, American Society of Civil Engineers, v. 110, p. 54-69.

- Savage, J. C., 1972, Relation of corner frequency to fault dimension: *Journal of Geophysical Research*, v. 77, p. 1073-1095.
- Street, R., 1982a, A contribution to the documentation of the 1811-1812 Mississippi Valley earthquake sequence: *Earthquake Notes*, v. 53, n. 2, p. 39-52.
- Street, R., 1982b, Ground motion values obtained for the 27 July 1980 Sharpsburg, Kentucky, earthquake: *Bulletin of the Seismological Society of America*, v. 72, p. 1295-1307.
- Trifunac, M. D. and A. G. Brady, 1975, On the correlation of seismic intensity scales with the peaks of recorded strong ground motion: *Bulletin of the Seismological Society of America*, v. 65, p. 139-162.
- Weichert, D. H., P. W. Pomeroy, P. S. Munro and P. N. Mork, 1982, Strong motion records from Miramichi, New Brunswick, 1982 aftershocks: *Earth Physics Branch Open File Report 82-31*, Ottawa, Canada.

**EARTHQUAKE-INDUCED LANDSLIDES IN THE
CENTRAL MISSISSIPPI VALLEY, TENNESSEE AND KENTUCKY**

Randall W. Jibson and David K. Keefer

U.S. Geological Survey

Menlo Park, California

ABSTRACT

The New Madrid earthquakes of 1811-12 caused widespread landsliding from the bluffs along the Mississippi River in western Tennessee and Kentucky. To determine what areas may be susceptible to landsliding in future earthquakes a regional analysis was made of the bluffs from Cairo, Ill., to Memphis, Tenn., using airphotos and field reconnaissance. The morphologies and apparent ages of most large landslides suggest a seismic origin dating to the 1811-12 earthquakes. Statistical analyses of the landslide distribution to determine possible relations between landslides and bluff height, slope angle, and estimated peak ground acceleration (PGA) from the 1811-12 earthquakes indicate that landslides in the area are related most strongly to bluff height and PGA.

The field and statistical evidence show that most landslides in the study area are related to the 1811-12 earthquakes; thus the bluffs in the study area would probably be susceptible to landsliding in future major earthquakes. At present, the best index of the potential for earthquake-induced landsliding along the bluffs is bluff height. According to the data presented, bluffs below 40 ft (12 m) are probably stable in earthquakes; above 40 ft (12 m) potential for earthquake-induced landsliding increases with increasing bluff height.

INTRODUCTION

Among the most dramatic of the geologic phenomena which accompanied the New Madrid earthquakes of 1811-12 were the numerous landslides which occurred along the bluffs bordering the Mississippi alluvial plain in western Tennessee and Kentucky. In his report of a field investigation of the New Madrid earthquakes conducted in 1904, Fuller (1912, p. 59) states:

Probably no feature of the earthquake is more striking than the landslides developed in certain of the steeper bluffs ***. From the vicinity of Hickman in southwestern Kentucky at least to the mouth of the Obion River, about halfway across the state of Tennessee *** the landslides are a striking feature. Skirting the edge of the bluffs, in the vicinity of Reelfoot Lake, a characteristic landslide topography is almost constantly in sight ***.

To determine what areas may be susceptible to landsliding in future earthquakes, it is important to know the extent of landsliding due to past events. This report presents a landslide inventory map of a portion of the central Mississippi Valley along with field observations and statistical analyses to identify landslides of probable seismic origin. It then discusses methods for assessing earthquake-induced landslide potential in the study area.

Description of Study Area

The study area includes 192 mi (310 km) of bluffs which form the eastern edge of the Mississippi alluvial plain from Barlow, Ky., 7 mi (11 km) east of Cairo, Ill., to Walls, Miss., 12 mi (20 km) south of Memphis, Tenn. (fig. 1). The bluffs are as much as 230 ft (70 m) in height. The Eocene Jackson

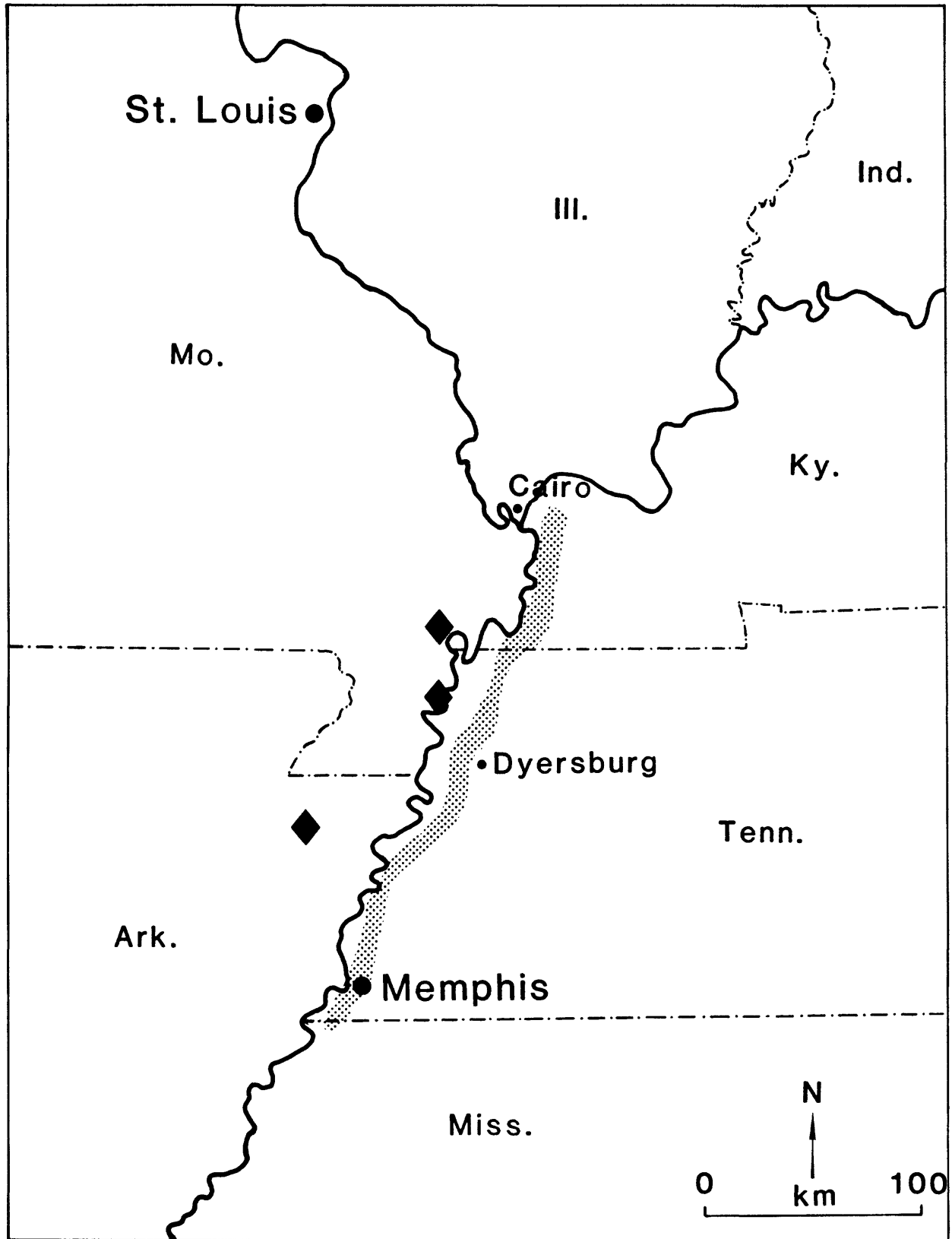


Figure 1. Location map showing study area (shaded) and epicenters of 1811-12 earthquakes (diamonds).

Formation (Conrad, 1856) forms the base of the bluffs throughout the study area. It is highly variable in composition, generally consisting of discontinuous layers of soft to stiff clay and silt from a few centimeters to many tens of meters thick. In some areas clean, uncemented sands with interbedded soft clays are present in layers tens of meters thick; in other areas lignitic clays are present. Some clay layers are saturated, whereas others are desiccated and fissured. The clays are also subject to seasonal variation in ground-water level. The Jackson Formation is highly erodible and few well-exposed outcrops are present. Lying unconformably on the Jackson is as much as 40 ft (12 m) of Pliocene gravel and sand of the Lafayette Formation (McGee, 1891; Potter, 1955). The lenses of gravel and sand are uncemented in many areas but can have very hard concretionary beds as much as 6 ft (2 m) thick. This unit is locally saturated where perched water tables are present and is subject to large seasonal fluctuations in ground-water conditions. The unit pinches out in some areas. The bluffs are capped by 10 to 100 ft (3 to 30 m) of Pleistocene loess, which lies unconformably on the Lafayette Formation. Loess is a slightly cohesive silt, which forms vertical faces owing to the presence of vertical fractures.

The study area has a humid climate and is thickly vegetated. Most of the bluffline is undeveloped and is covered by a dense deciduous forest and a thick undergrowth of smaller brush and trees. Portions of the bluffs in some areas have been cleared for buildings or pasture.

The bluffline is sub-parallel to a line connecting the estimated epicenters of the 1811-12 earthquakes; the two lines are between 12 and 30 mi (20 and 50 km) apart except at the extremities of the study area where the bluffs extend beyond the epicentral line. The proximity of the bluffs to epicenters of earthquakes which had estimated surface-wave magnitudes (M_s) between 8.4 and 8.8 (Nuttli and Herrmann, 1984) means that these bluffs were

subjected to very strong ground shaking. Keefer (1984) related earthquake magnitude to maximum epicentral distance at which landslides caused by an earthquake are likely to occur; the study area lies well within this boundary (fig. 2).

LANDSLIDE INVENTORY MAP

Method of Compilation

Aerial Photographic Mapping. A landslide inventory map was compiled on 1:24,000-scale topographic base maps using black and white 1:20,000-scale aerial photographs taken in 1970-71 by the U.S. Department of Agriculture. Landslides having minimum dimensions of 200 ft (60 m) were the smallest mappable features. Landslides were identified by the presence of arcuate scarps, disrupted or hummocky topography, and ponded drainage.

Landslides were classified according to their morphology and our level of confidence in identification. Three morphological classes were used (Varnes, 1978): (1) translational block slides and rotational slumps which have been revegetated and eroded, together classified as **old coherent slides** (OC), (2) **young rotational slumps** (YS), which have fresh features, and (3) **earth flows** (EF), most of which are inactive but some of which have active portions. Three levels of confidence were used for all classes which indicate whether the identification is **definite** (D), **probable** (P), or **questionable** (Q). This procedure is similar to that recommended by Wieczorek (1984) for the compilation of landslide inventory maps.

Each landslide feature was identified by a two-letter designation followed by an ordinal number. For example, EFP-14 signifies a probable landslide which is the 14th of the earth flow type as counted from the north end of the study area.

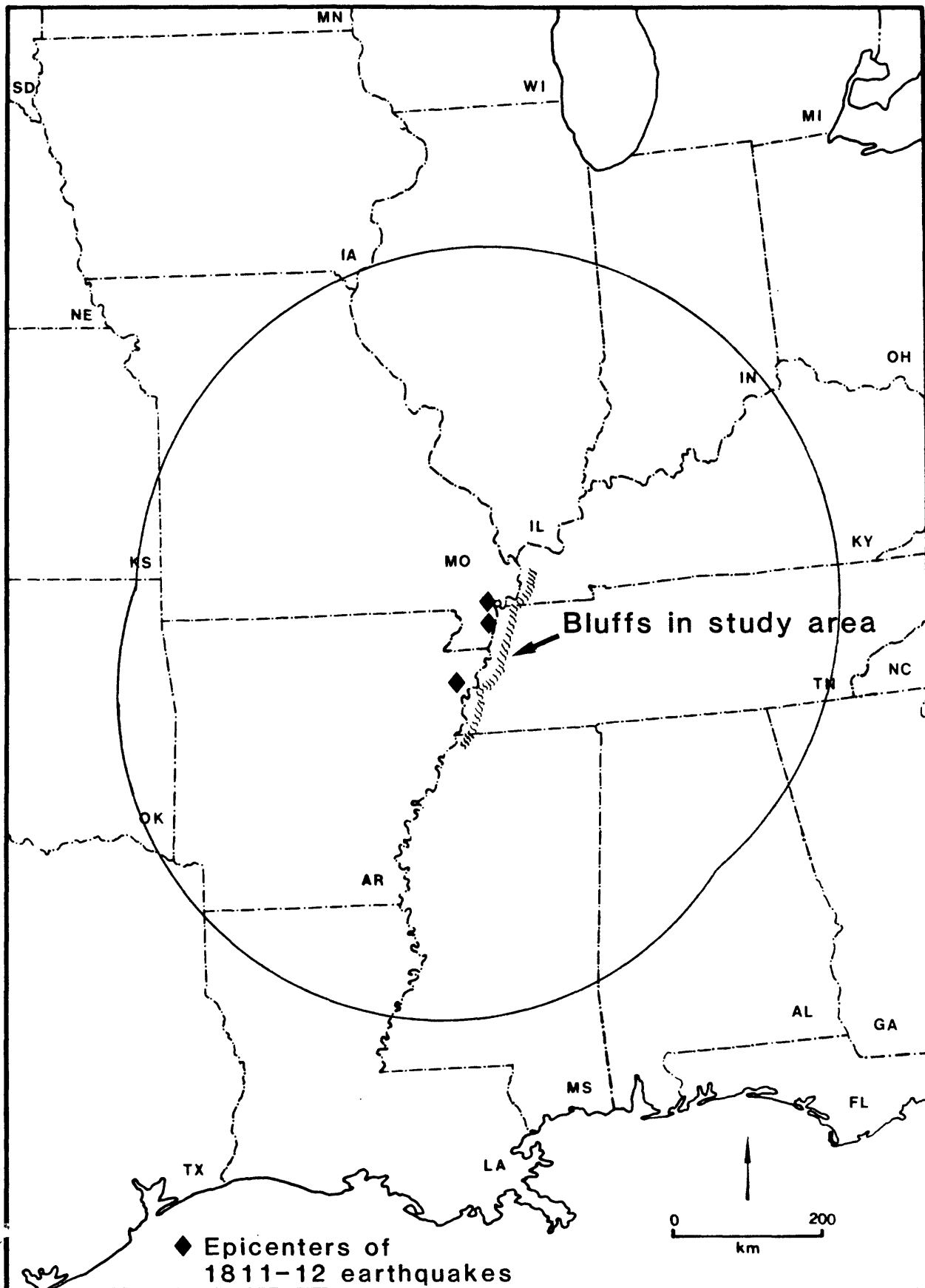


Figure 2. Map showing maximum distance at which landslides could be expected to have occurred during the 1811-12 earthquakes (Keefer, 1984).

Field Reconnaissance. After completion of the initial airphoto mapping, accessible landslides were visited and examined on the ground. More than 75 percent of the originally mapped landslide sites were accessible. Of these, approximately 20 percent were upgraded in level of confidence; only four percent were downgraded or deleted.

The field reconnaissance allowed calibration of the accuracy of the airphoto mapping. Taking the field observations into account, the airphotos were re-examined and the sites which were not visited were reclassified as appropriate.

Results of Mapping

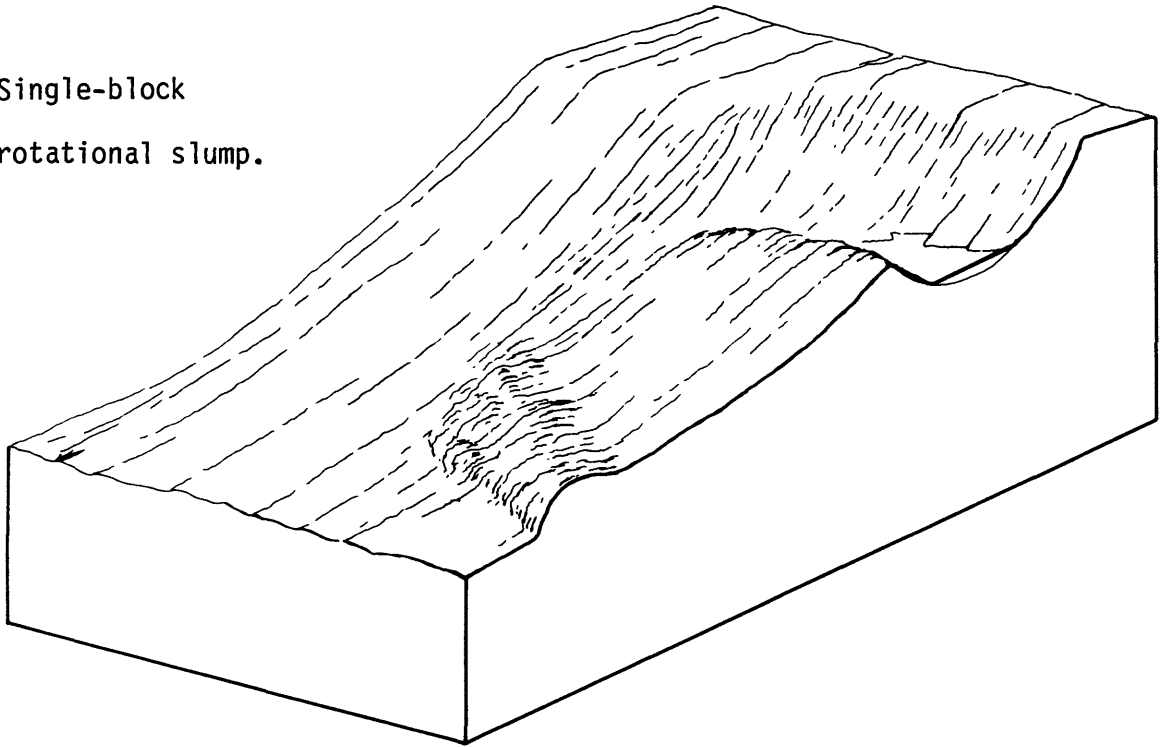
Plate 1 is a strip map of the bluffs at 1:62,500 scale showing the locations and letter designations of the 221 landslides mapped. The bluffs are divided into 2500-ft-long (762 m) segments for this study; every tenth segment is numbered on the map (plate 1) for reference. The number and characteristics of the landslides according to our classification are recorded in table 1.

Old coherent slides constitute 65 percent of the total. Idealized drawings of these types of landslides are shown in figure 3, and airphotos showing typical examples are shown in figure 4. Old translational and rotational landslides were grouped together because heavy tree cover and eroded features often made it impossible to distinguish between them. In areas where a distinction could be made, similar numbers of translational and rotational slides were present. Both types of landslides in this class are deep-seated (greater than 25 m), none of which have fresh features. These occur throughout the area except in locations where earth flows are concentrated.

Table 1. Landslide characteristics.

| | Old Coherent | Young Rotational | Earth |
|-------------------------|--------------|------------------|-------|
| | Slides | Slumps | Flows |
| NUMBER | | | |
| Definite | 73 | 16 | 26 |
| Probable | 43 | 5 | 11 |
| Questionable | 30 | 3 | 14 |
| Total | 146 | 24 | 51 |
| LENGTH (m) | | | |
| Minimum | 60 | 60 | 90 |
| Median | 185 | 150 | 185 |
| Maximum | 4175 | 245 | 455 |
| WIDTH (m) | | | |
| Minimum | 75 | 170 | 75 |
| Median | 395 | 505 | 365 |
| Maximum | 2345 | 2455 | 3535 |
| SLOPE HEIGHT (m) | | | |
| Minimum | 10 | 10 | 15 |
| Median | 35 | 40 | 30 |
| Maximum | 75 | 60 | 75 |
| SLOPE ANGLE (°) | | | |
| Minimum | 6 | 13 | 6 |
| Median | 18 | 23 | 15 |
| Maximum | 31 | 34 | 28 |

a. Single-block rotational slump.



b. Multiple-block rotational slump.

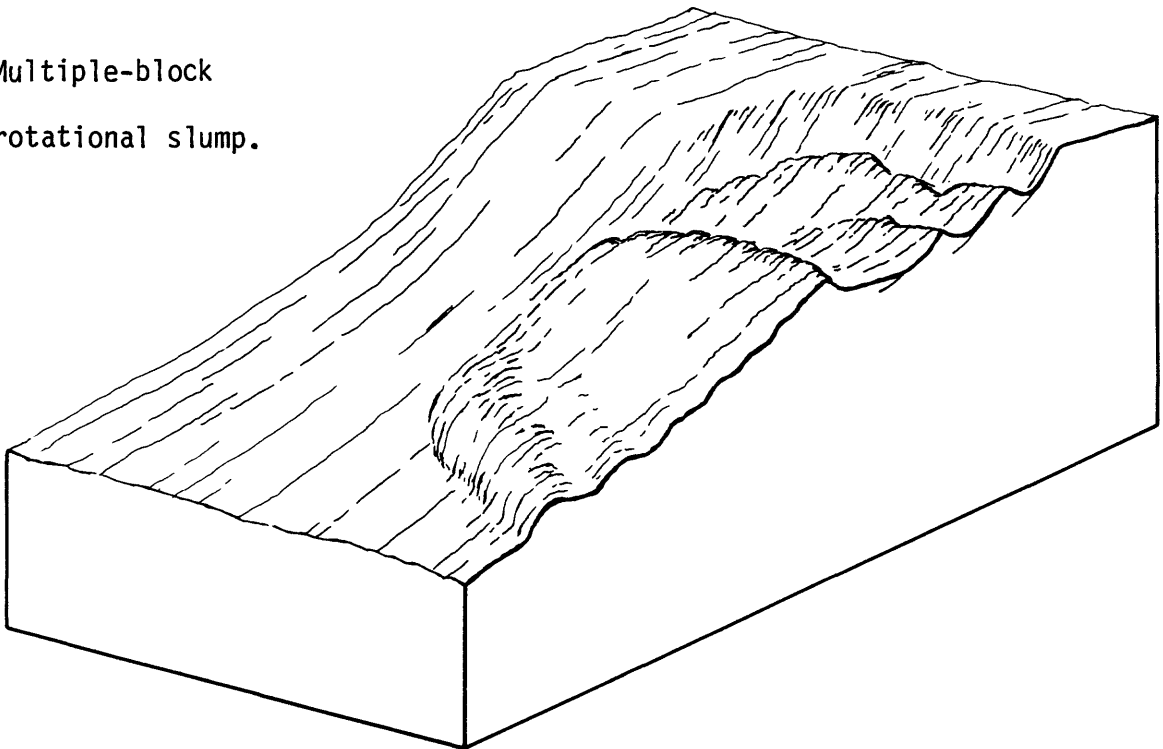


Figure 3. Idealized drawings of types of old coherent slides in study area.

c. Translational block slide.

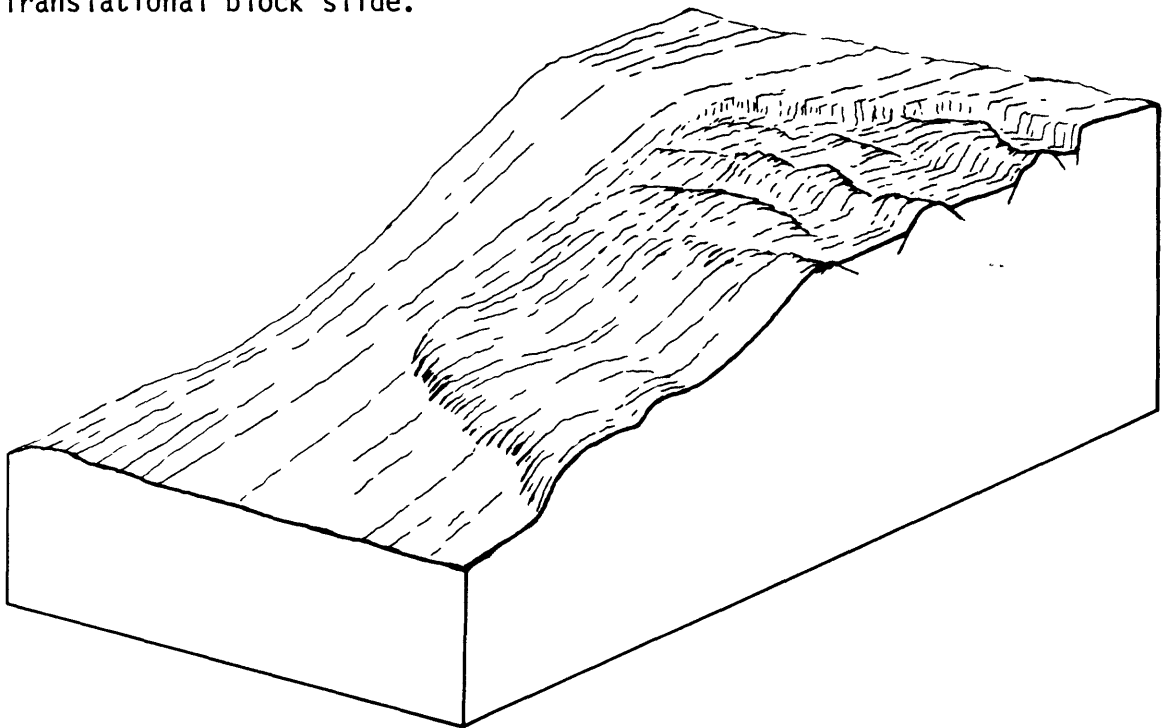
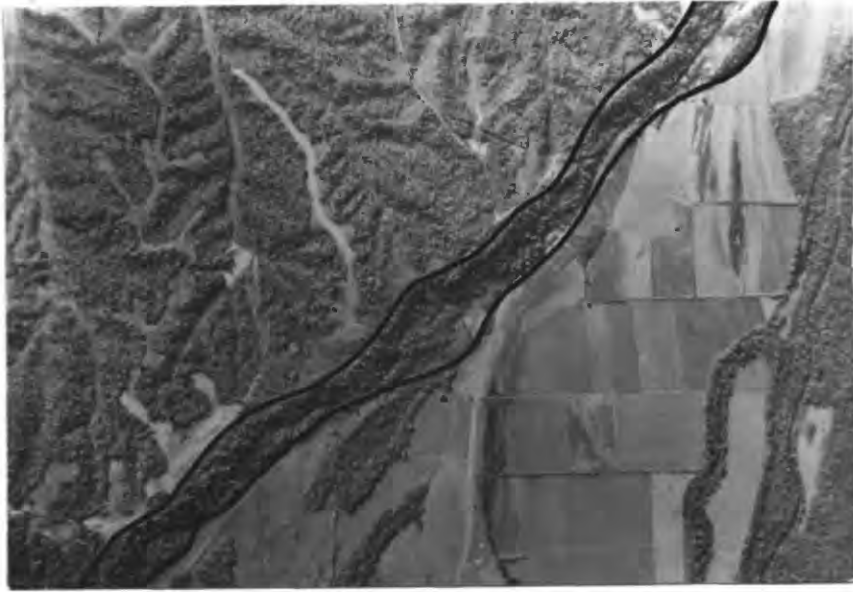


Figure 3. Idealized drawings of types of old coherent slides in study area. (cont.)



a. Series of old coherent slides northeast of Reelfoot Lake, Tenn.



b. Translational block slide near Dyersburg, Tenn.

.24 /
1.50

Figure 4. Airphotos of old coherent slides in study area (outlined).

The translational block slides are characterized by horst and graben topography consisting either of one or a few large horst blocks with broad intervening grabens, or of several smaller horst and graben blocks arranged in stair-step fashion. The toe areas commonly have pressure ridges where soil at the base of the slope was compressed and deformed as the landslide blocks moved down and out from the parent slope. These landslides have basal shear surfaces inclined between 4° and 25° and have moved as much as 300 ft (90 m). Rotational slumps in the OC class are characterized by either single or multiple rotational blocks. The blocks in most cases appear to have rotated a large amount. Erosion and revegetation have subdued the features of both block slides and slumps in the OC class; locating the rare exposures which show the attitude of the bedding is often the only means of distinguishing between them.

A large majority of the translational block slides and old rotational slumps appear to be of similar age. The degree of erosion of landslide ridges is similar for the two types, as is the apparent age and density of vegetation on scarps and disrupted areas. Scarp retreat and incision also appear similar.

Earth flows, schematically depicted in figure 5, constitute 24 percent of the landslides. Earth flows in the study area occur on the lowest and gentlest slopes, on the average, of the three landslide classes. Characteristic features are gently hummocky topography and ridges of accumulated material in the toe area (fig. 6a). Some earth-flow complexes contain active earth flows which have fractured ground and show evidence that downslope movement of soil has occurred in the last several years (fig. 6b). The earth flows are primarily concentrated in the central portion of the area between segments 120 and 240 (plate 1).

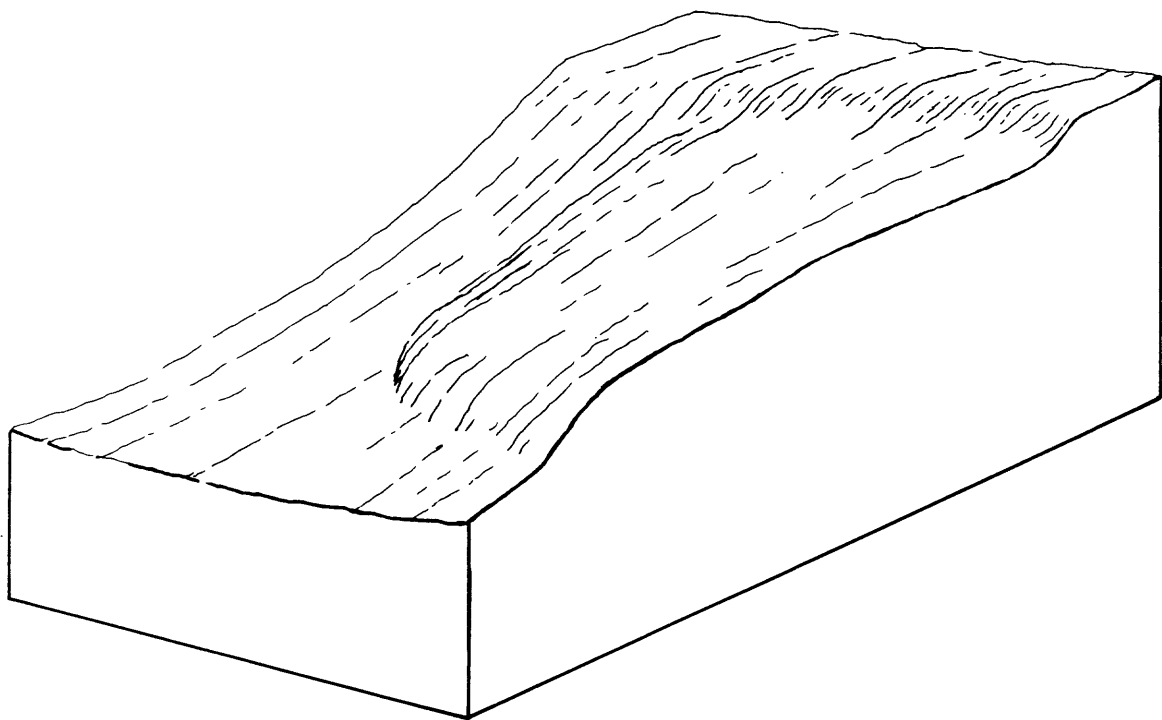


Figure 5. Idealized drawing of earth flow in study area.



a. Hummocky topography on inactive earth flow south of Lenox, Tenn.



b. Active portion of earth-flow complex south of Lenox, Tenn.

.09
/ 1.70

Figure 6. Photographs of earth flows in study area.

The remaining 11 percent of the landslides are young rotational slumps, an example of which is shown in figure 7. Photographs of these slumps are shown in figure 8. These landslides occur exclusively in areas where the Mississippi River has impinged on the bluff since 1820. Approximately 20 mi (33 km) of bluffs, or 11 percent of the overall length, has been subject to fluvial erosion since that time (Fisk, 1944). The young rotational slumps occur on the steepest, highest slopes, on the average, of the three landslide classes and are characterized by massive single slump blocks which form where the river has undercut the bluffs. They are differentiated from old slumps on the bases of less rotation, less eroded scarps and heads, absence of multiple blocks, and, in some instances, lack of vegetation.

FIELD EVIDENCE OF LANDSLIDE AGE AND ORIGIN

Young Rotational Slumps

The only landslides present in areas where the river has impinged on the bluffs since 1820 are single-block rotational slumps; neither translational block slides, multiple-block rotational slumps, nor earth flows are present in such areas. In addition, these near-river portions of the bluffs are the only places where deep-seated landslides have fresh features. Thus it appears that under aseismic conditions the only large-scale, deep-seated landsliding along the bluffs results from the fluvial activity which triggers these single-block rotational slumps. Though the 1811-12 earthquakes probably caused landslides on the bluffs along the river, fluvial erosion and consequent landsliding has likely destroyed evidence of the earthquake-induced landslides; hence these slumps are judged to be young, occurring after the 1811-12 earthquakes.

Old Coherent Slides

If the old rotational slumps in the study area were triggered by fluvial

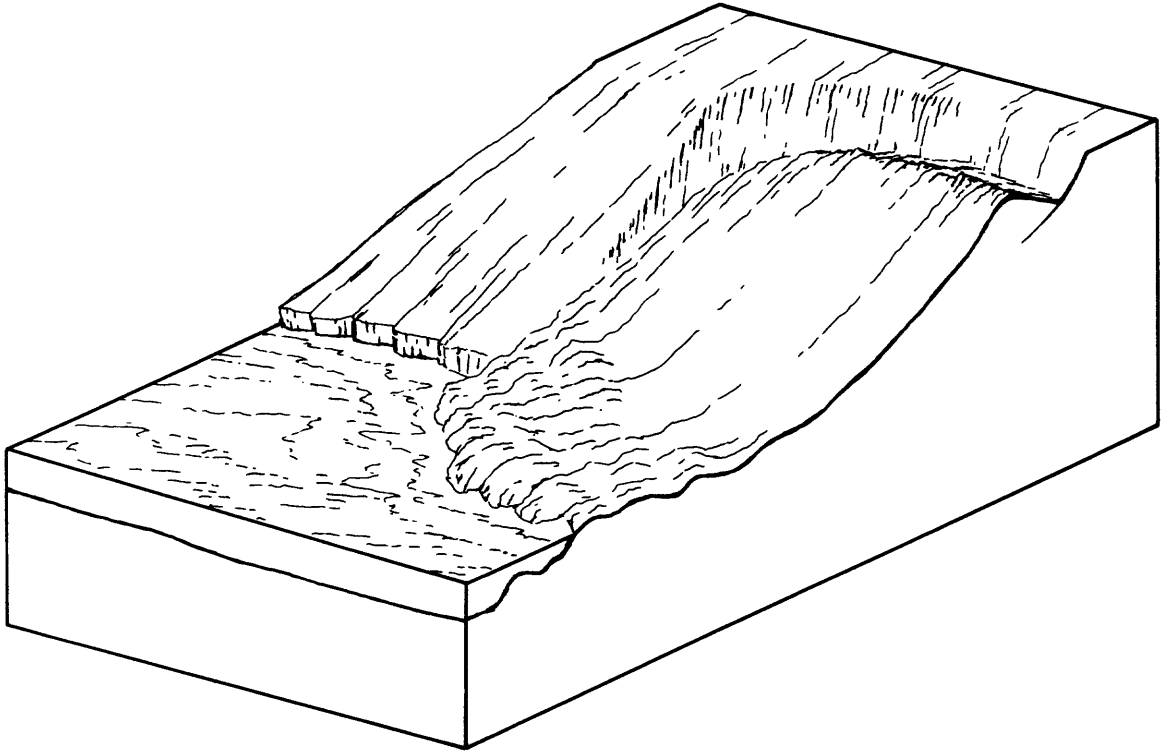


Figure 7. Idealized drawing of young rotational slump in study area.



a. Series of young rotational slumps with scallop-shaped scarps.



b. Oblique airphoto of young rotational slump.

.10/
/1.50

Figure 8. Airphotos of young rotational slumps in study area.

activity, we would expect to see a continuous variation in their ages corresponding to the length of time since the river impinged on that portion of the bluffs. As noted above, most old coherent slides, both rotational and translational, appear to be of similar age. Thus most or all landslides of both types probably occurred as a result of the same triggering event; moreover, this event was not related to fluvial activity.

Though no definitive method for establishing absolute ages of the old coherent slides was found, several lines of evidence suggest ages consistent with triggering by the 1811-12 earthquakes. McGee (1892) studied the ages of straight and tilted trees on landslides along the bluffs near Reelfoot Lake in Tennessee in 1891 and determined that "a trustworthy and fairly accurate date for the production of the landslide features--a date determined by much counting of annual rings lies between seventy-five and eighty-five or ninety years ago." This conclusively brackets the age of the landslides he studied to within five years of the 1811-12 earthquakes. Fuller (1912) used the same technique in 1904 and determined that "the greater part of the upright growth on the disturbed surfaces is fairly uniform and a little less than 100 years of age, trees of greater age being in general tilted and partly overthrown." From this he concluded that the major landslides in the area occurred at the time of the 1811-12 earthquakes. The bluffs have been logged several times since McGee and Fuller made their observations; no tilted trees were observed during our field investigation. According to Fuller's descriptions, the landslide features 75 years ago were much less degraded than those present in 1983. He described sharp ridges, steep-walled grabens, and numerous sag ponds. The present features are much more subdued; few sag ponds remain, presumably because headward erosion in grabens has drained most ponds. Horst and graben blocks are rounded and vegetated. The significant degradation of

landslide features in the last 75 years indicates that the landslides are still young enough to be geomorphically unstable and susceptible to relatively rapid degradation. If they were several hundred or thousand years old, the geomorphic changes which would occur in 75 years would probably not be as pronounced as those observed (Colman and Watson, 1983).

During the field investigation, we spoke with several long-time residents of the area. These conversations indicated that the landslide features have changed considerably during the last century. For example, Paul Stoddard (oral commun., 1983) of Lenox, Tenn., stated that his grandfather, who had grown up in that area in the 1850's, recalled seeing open fractures and steep-walled grabens on the local landslides, features that would indicate a relatively young age. At present there are no open fractures on these landslides, and the walls of the grabens have gentle slopes. In another locality, a trail dating at least to the 1870's (Ferron Stewart, oral commun., 1983) extends along the crown of a translational block slide near Dyersburg, Tenn., suggesting that the landslide was present when the trail was built. The stair-step arrangements of displaced blocks in the head region of some of the landslides are generally referred to as "shakedown" in the local vernacular because of local historical accounts that they resulted from the earthquakes.

The morphologies and stratigraphies of many of the old coherent slides are consistent with seismic origin. Translational block slides in the area are not associated with current fluvial activity, so another causative factor is probably involved. Several of these landslides have basal shear surfaces with dips as gentle as 4° and have translated great distances (as much as 90 m). In aseismic conditions it is unlikely that deep-seated blocks would move such great distances on such gently sloping shear surfaces. However, such

block slides have occurred in recent earthquakes (Davis and Karzulovic, 1963; Hansen, 1965). Landslides caused by the 1964 Alaska earthquake (Hansen, 1965), the Turnagain Heights landslide in particular, have morphologies and stratigraphies strikingly similar to many of the old coherent slides in the study area. Many of the landslides caused by the Alaska earthquake failed along sensitive* silt and clay layers. Preliminary shear-strength tests on subsurface samples from a translational block slide near Dyersburg, Tenn. (OCD-77, plate 1), show materials are present with sensitivities between four and ten; these are classified as "very sensitive" materials (Mitchell, 1976, p. 208). Thus, the morphologies and stratigraphies of the translational block slides in the study area are consistent with those of landslides which occurred in another major earthquake.

The morphology of old multiple-block rotational slumps suggests they were caused by severe, long-duration ground shaking. Such shaking would likely cause successive slump blocks to fail after the formation of the initial steep scarp and would account for the large amount of rotation in both single- and multiple-block old slumps. In addition, multiple-block rotational slumps do not occur along the riverbanks in the study area, which suggests that these landslides were triggered by something other than fluvial undercutting.

Earth Flows

All the active earth flows occur in areas where the trees have been cleared. Some earth flow complexes are partly forested and partly cleared, and active portions of these complexes invariably occur on the cleared areas. None of the forested earth flows that were examined showed evidence of

*Sensitivity is the ratio of peak to remolded undrained shear strength (Mitchell, 1976). Sensitive materials lose a significant amount of their shear strength when disturbed.

recent activity or had any disturbed or tilted trees; trees estimated to be more than one hundred years old were commonly present. Also, no evidence of episodic and (or) continuing movement of various portions of the large forested earth flows was seen, something commonly seen on complexes where movement occurs under nonseismic conditions (Keefer, 1977; Keefer and Johnson, 1983). This suggests that large earth-flow complexes rarely form on heavily forested slopes in this area under normal (aseismic) conditions. Earth flows are relatively uncommon during earthquakes (Keefer, 1984), but silt and clay layers with sensitivities as high as 9.8 and with dips sub-parallel to the bluff face are present in the areas where the earth flows are concentrated. Boreholes drilled on an earth flow near Lenox, Tenn. (EFD-27, plate 1), revealed a disturbed zone, probably the failure surface, located in the sensitive layers. The presence of sensitive materials and the lack of active earth flows in forested areas suggest that the earth flows in the forested parts of the study area may be associated with ground shaking.

STATISTICAL ANALYSIS OF LANDSLIDE DISTRIBUTION

Landslide occurrence is controlled by many interrelated factors. Some of the factors which influence landslide occurrence in the study area are slope height, slope steepness, stratigraphy, geologic structure, shear strength, ground-water conditions, trend and sinuosity of the bluffs, vegetal cover, and proximity to seismic sources. Although this list is not exhaustive, it includes the most important factors.

The general structural geology and stratigraphy are nearly uniform throughout the area. The west-dipping sequence of loess overlying Lafayette Formation overlying, in turn, Jackson Formation is present in virtually the entire study area. As described above, however, the internal stratigraphy,

shear strength, and ground-water conditions of these formations vary considerably. Also, the vegetal cover in some areas has been altered significantly in recent decades, so the character of the vegetal cover present when many of the older landslides occurred is unknown. Some factors, then, cannot easily be quantified for statistical analysis of landslide distribution with the data available at present. The factors chosen for analysis were slope height, slope angle, and proximity to seismic sources.

Method of Analysis

The study area was divided into segments 2,500 ft (762 m) long. The percentage of the length of each bluff segment which was occupied by deposits of various types of landslides was recorded. Average values of slope height and slope angle were determined from the 1:24,000-scale topographic base maps. For those segments occupied by landslides, the pre-landslide heights and angles were estimated from adjacent segments. The estimated locations of the epicenters of the three main shocks of the New Madrid earthquake sequence of 1811-12 were also located (Nuttli, 1973; Hopper and others, 1983) and distances from each of the epicenters to each bluff segment were measured (fig. 1). Peak ground accelerations (PGA) at each segment from each of the three earthquakes were then calculated using the following equation of Nuttli and Herrmann (1984):

$$\log a_h = 0.57 + 0.50(m_b) - 0.83 \log(R^2 + h^2)^{\frac{1}{2}} - 0.00069(R)$$

where,

a_h is the peak horizontal ground acceleration (cm/sec²),

m_b is the body-wave magnitude,

R is the epicentral distance (km),

h is the depth of focus (km).

Nuttli's (1973) estimated body-wave magnitudes for the three main events are 7.2 for the southern epicenter, 7.1 for the middle epicenter, and 7.4 for the northern epicenter. The estimated focal depth for all these events is 40 km (Nuttli and Herrmann, 1984). Using these values the maximum PGA and the sum of the three PGA's were determined for each site. The sum of the PGA's was used because it may be a more complete characterization of the strong ground motion from the earthquake sequence.

For each segment, values of slope height, slope angle, maximum PGA, and the sum of the PGA's were treated as the independent variables. The dependent variables were the percentages of bluff length occupied by landslides of various classes. The MINITAB program (Pennsylvania State University, 1982) was used to conduct the statistical analysis. Analyses were carried out for several combinations of landslide classes and levels of confidence.

Discriminant Analysis. A discriminant analysis was first conducted by separating the bluff segments into two populations: (1) those which contained landslides or portions of landslides, and (2) those which did not contain landslides. The independent variables from these two populations were then statistically compared to see which of them, if any, would enable discrimination between the two populations. The means and standard deviations of the two populations and a t-statistic were calculated using the formula given by Ryan and others (1976, p. 141). From the t-statistic the attained significance, P, which is the probability that the two populations are statistically identical, was determined (Ryan and others, 1976).

The results are shown in table 2. Each of the four independent variables enabled discrimination between the populations of landslide occurrence and no landslide occurrence at very high levels of statistical significance. Slope height was the best discriminator, followed in decreasing order by sum of the PGA's, slope angle, and maximum PGA. This shows that these four

Table 2. Results of discriminant analysis.

| | Mean | St. Dev. | t | P |
|-------------------|-------|----------|-------|--------|
| SLOPE HEIGHT (m) | | | | |
| Landslides | 128.0 | 41.2 | 11.71 | 0.0000 |
| No Landslides | 72.4 | 43.7 | | |
| SLOPE ANGLE (°) | | | | |
| Landslides | 17.0 | 4.8 | 4.80 | 0.0000 |
| No Landslides | 14.0 | 6.1 | | |
| SUM OF PGA S (%g) | | | | |
| Landslides | 120.0 | 21.8 | 6.17 | 0.0000 |
| No Landslides | 102.8 | 27.2 | | |
| MAXIMUM PGA (%g) | | | | |
| Landslides | 53.4 | 11.7 | 4.53 | 0.0000 |
| No Landslides | 47.2 | 12.5 | | |

characteristics of the bluffs differ significantly between areas where landslides occur and areas where they do not.

Linear Regression. Linear regression analyses, which correlated each independent variable singly with each dependent variable, were next conducted. Coefficients of determination (R^2) and t-statistics were calculated for all analyses. R^2 is the percentage of variation in the dependent variable explained by the independent variable. The t-statistic is used to test the hypothesis that there is actually no correlation between the variables ($R^2=0$), that the data are randomly distributed. For the sample size in this study, values of the t-statistic greater than 2.00 indicate, at the 97.5 percent confidence level, that the data are not randomly distributed,

that some correlation exists. Equations for calculating R^2 and t are given by Ryan and others (1976).

Results of the linear regression analyses are given for four data sets, including the definite and probable landslides from each of the three morphological classes and the definite and probable landslides from the combined old coherent (OC) slide and earth flow (EF) classes. The combined class is used because (1) these landslides are not restricted to bluffs recently undercut by the river as are the young rotational slumps, and (2) the OC and EF landslides comprise all the old landslides in the area and are the classes most likely associated with the 1811-12 earthquakes. The results of linear regression of these data sets on the four independent variables are shown in table 3.

Table 3. Results of linear regression.

| | OLD COHERENT SLIDES | | EARTH FLOWS | | YOUNG ROTATIONAL SLUMPS | | OLD COHERENT SLIDES AND EARTH FLOWS | |
|--------------|---------------------|-------|-------------|-------|-------------------------|-------|-------------------------------------|--------|
| | $R^2(\%)$ | t | $R^2(\%)$ | t | $R^2(\%)$ | t | $R^2(\%)$ | t |
| SLOPE HEIGHT | 15.1 | 7.70* | 11.6 | 6.61* | 2.4 | 3.03* | 33.8 | 13.04* |
| SLOPE ANGLE | 7.7 | 5.27* | 0.1 | 0.41 | 13.4 | 7.64* | 7.3 | 5.10* |
| MAXIMUM PGA | 4.1 | 3.78* | 1.0 | 1.86 | 0.3 | 1.14 | 6.3 | 4.73* |
| SUM OF PGA'S | 3.7 | 3.59* | 7.1 | 5.05* | 0.5 | 1.44 | 12.5 | 6.88* |

*this t -value indicates high probability (greater than 97.5 %) that R^2 is not actually zero.

With one exception, the R^2 -values for the data range from 0 to 15 percent, which indicates that no single independent variable has a particularly strong correlation with any class of landslide occurrence. Nevertheless, t-values greater than 2.00 for 12 of the 16 analyses show that these correlations are statistically significant at the 97.5 percent confidence level. The only large R^2 -value, 33.8 percent, is for the regression of slope height on the combined class of old coherent slides and earth flows. This indicates that approximately one-third of the variation in the distribution of the old coherent slides and earth flows is accounted for by slope height. The large t-values associated with small R^2 -values for the other variables in this combined class indicate that, though there is considerable scatter in the data, some linear trend may be present. To test this hypothesis, the independent variables were grouped into increments and the corresponding values of combined old coherent slide and earth flow incidence were averaged for each increment.

The incrementally averaged plots are shown in figure 9. Slope height was grouped into 10-foot (3 m) height increments, slope angle into 5° increments, sum of the PGA's into 0.20 g increments, and maximum PGA into 0.10 g increments. All of the plots have good best-fit lines, indicating that an increase in any of the variables corresponds to an increase in the incidence of old coherent slides and earth flows. The effect of slope angle is more accurately characterized by a two-segment line, shown dashed in the plot (fig. 9b). This suggests that for slopes steeper than about 16 degrees the average incidence of these landslides appears to be independent of slope angle, whereas for slopes less than 16 degrees slope angle affects landslide occurrence.

For the two classes of landslides most likely associated with

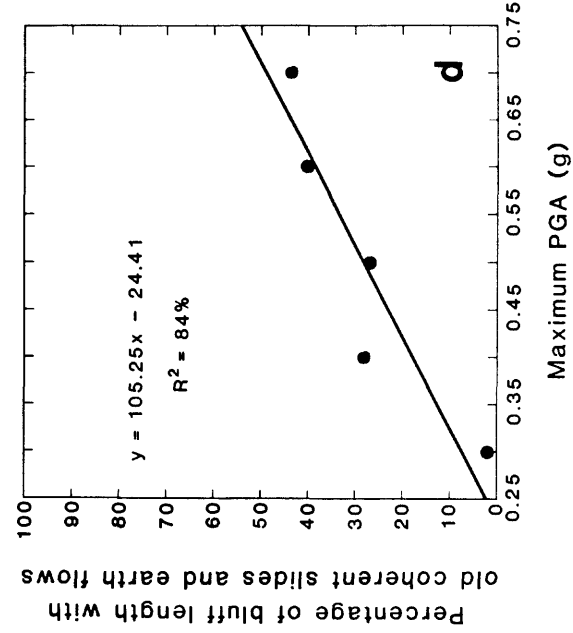
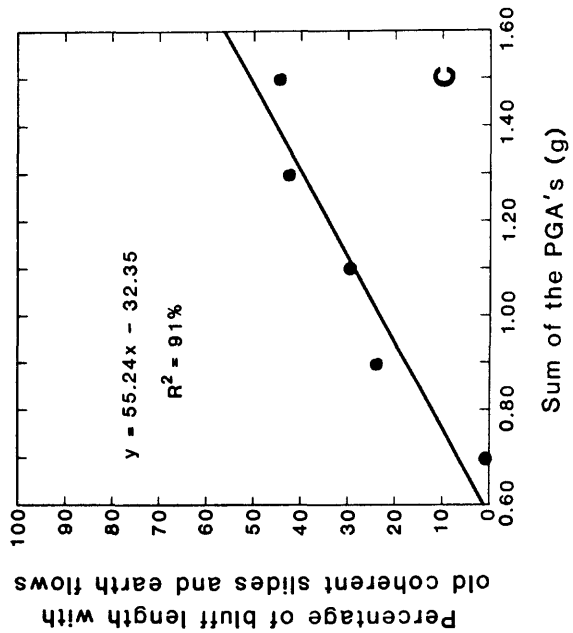
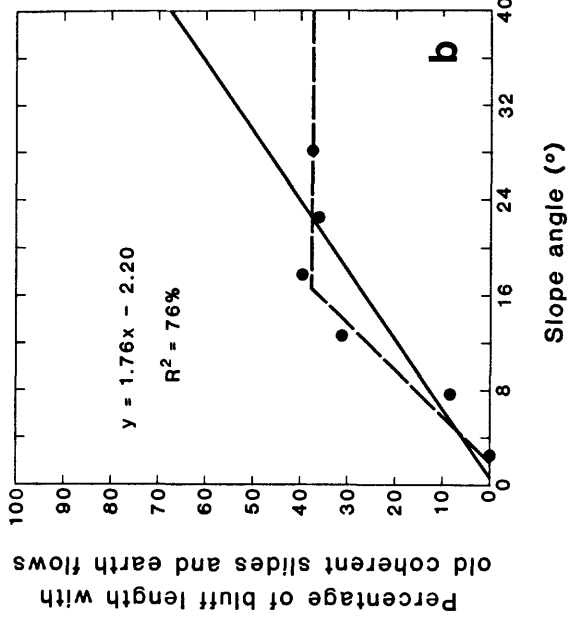
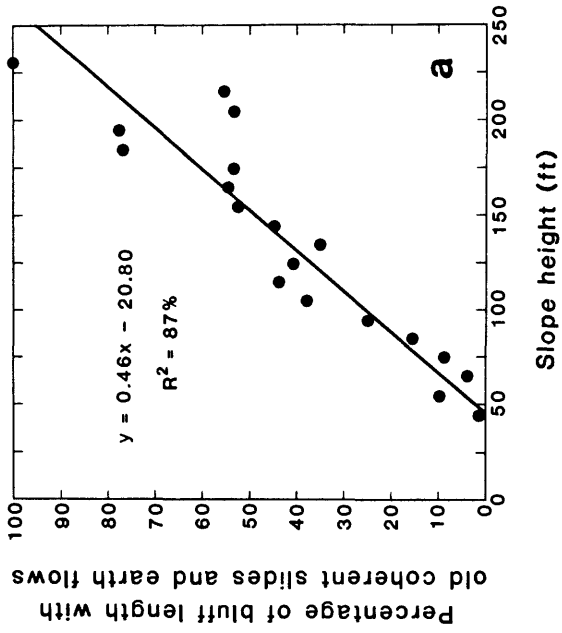


Figure 9. Incrementally averaged plots of slope height, slope angle, sum of the PGA's, and maximum PGA.

earthquakes, old coherent slides and earth flows, one or both of the ground-motion variables have significant t-values (table 3). In the combined class both ground-motion variables have significant t-values and strongly linear trends for the incrementally averaged plots (fig. 9), as do slope height and slope angle. Young rotational slumps, however, whose distribution is controlled by the location of the river, do not have significant correlation with the ground-motion variables, but are correlated with slope angle, which is probably related to undercutting due to fluvial erosion. Slope height is correlated with young rotational slumps to a much lesser degree than is slope angle.

Stepwise Multiple Linear Regression. A stepwise multiple linear regression analysis was next conducted to determine the combined effects of the four independent variables. In this approach, a test statistic is calculated for each variable in the regression equation. If any are below the 97.5 percent confidence level, then the smallest one is removed and a new regression equation is calculated. If no variable can be removed, a test statistic is calculated for each variable not in the equation and the largest one is then added provided it is above the 97.5 percent confidence level. When no more variables can be added or deleted, the procedure ends. R^2 - and t-values are calculated at each step.

The multiple linear regression analysis is appropriate only if the variables included are truly independent. Cross-correlation analyses between the four independent variables indicates that only the correlation between the two PGA variables is of practical significance ($R^2=74.3\%$). This cross-correlation between maximum PGA and sum of the PGA's means that, in the multiple linear regression analysis, the effect of one of these variables may mask the effect of the other. To see if this is the case, the results of the

multiple linear regression can be compared to those of the simple linear regression, where the individual effects of both variables are evident.

The results of the multiple linear regression are shown in table 4. Each of the individual landslide classes have R^2 -values near the 20 percent level. As in the simple linear regression, only the combined class had a large amount of correlation, 36.5 percent, with the independent variables. The significant variables for the combined class were slope height and sum of the PGA's. Also, as in the simple linear regression, only the young rotational slumps are not correlated with either of the ground-motion variables.

In both multiple and simple linear regression analyses, slope height is the dominant variable in the old coherent slide and earth flow classes. In order to see how the ground-motion variables behave when slope height is constant, the bluff segments were grouped into 10-foot (3 m) height increments and the occurrence of landslides in the combined old coherent slide and earth flow classes were plotted against maximum PGA and sum of the PGA's for each height increment.

When landslide occurrence was plotted against sum of the PGA's, 16 of the 19 slope-height increments in which landslides occurred had best-fit lines with non-negative slopes, indicating the data were not randomly distributed. There was a remarkable concordance of slope values among all the data; of the 15 positive slope values the average was 1.41 and the standard deviation was only 0.92. If there were little or no correlation between landslide occurrence and sum of the PGA's, approximately half the slopes would be positive and half negative and there would probably be very large variations in the slope values. Thus, the predominantly positive and concordant slope values suggest a significant positive correlation between increased ground

motion and occurrence of old coherent slides and earth flows when slope height is constant

For the maximum PGA plots, 14 of the 19 increments have non-negative slopes; the average of the positive slopes is 2.45 with a standard deviation of 1.79. Though not as consistent as the previous data, this result also suggests a positive correlation between increased ground motion and occurrence of old coherent slides and earth flows.

These slope values (landslide incidence / PGA) can be used to approximate the effect of increasing the PGA on landslide incidence at a given slope height. The slope values for sum of the PGA's suggest that, for a given slope height, landslide incidence increases about 1.4 percent for every one-percent-g increase in sum of the PGA's. For maximum PGA, the slope values suggest that landslide incidence increases about 2.5 percent for every one-percent-g increase in maximum PGA. Refinement of these approximations is possible by plotting the slopes of the best-fit lines against the bluff-height increment from which they were derived, as shown in figure 10. Slope values determined by regression analyses with t-values significant at the 95 percent confidence level are indicated. Both plots have reasonable best-fit lines; R^2 is 62 percent for sum of the PGA's, 78 percent for maximum PGA. The fact that the slopes of the best-fit lines increase with increasing bluff height suggests that sensitivity to seismic shaking increases with increasing bluff height.

Discussion of Statistical Analysis

The statistical analyses show that there are definite correlations between landslide occurrence and slope height, slope angle, and ground motion. The discriminant analysis shows the significant differences in all of these variables between areas of landslide occurrence and no landslide occurrence. The linear regression analyses and the incrementally averaged plots show that

Table 4. R^2 - and t-values from stepwise multiple linear regression.

| | Step | 1 | 2 | 3 | 4 |
|-------------------------------------|------|-------|----------|------|------|
| | | | t-values | | |
| OLD COHERENT SLIDES | | | | | |
| Slope Height | | 7.70 | 6.02 | 5.43 | |
| Slope Angle | | | 2.58 | 2.64 | |
| Maximum PGA | | | | 2.45 | |
| R^2 (%) | | 15.1 | 16.8 | 18.3 | |
| EARTH FLOWS | | | | | |
| Slope Height | | 6.61 | 5.23 | 4.51 | 5.07 |
| Sum of PGA's | | | 3.17 | 5.84 | 5.73 |
| Maximum PGA | | | | 4.86 | 4.78 |
| Slope Angle | | | | | 2.27 |
| R^2 (%) | | 11.6 | 14.2 | 19.9 | 21.2 |
| YOUNG ROTATIONAL SLUMPS | | | | | |
| Slope Angle | | 7.64 | | | |
| R^2 (%) | | 13.4 | | | |
| OLD COHERENT SLIDES AND EARTH FLOWS | | | | | |
| Slope Height | | 13.04 | 11.23 | | |
| Sum of PGA's | | | 3.79 | | |
| R^2 (%) | | 33.8 | 36.5 | | |

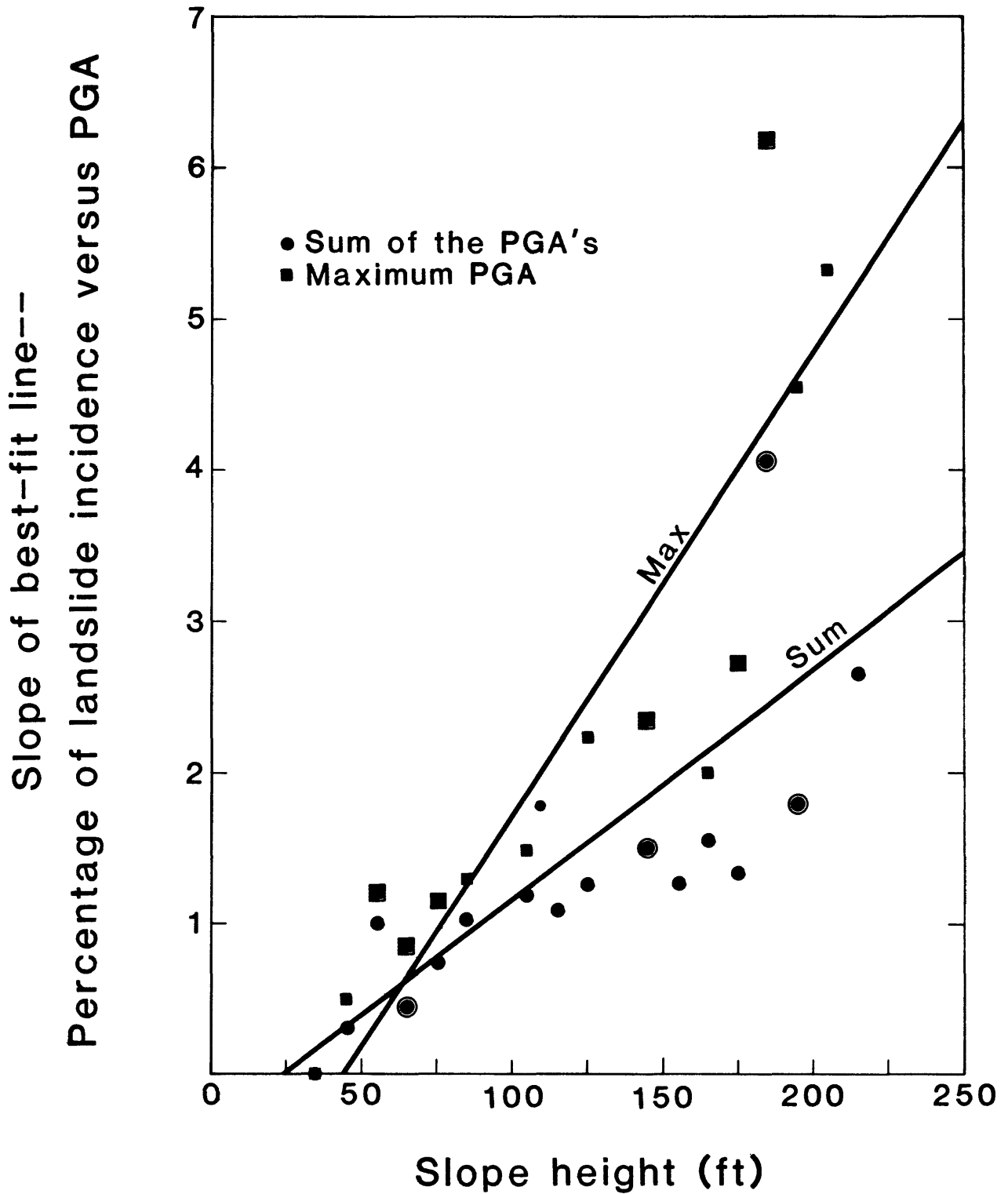


Figure 10. Plot of slope height vs. slope of the best fit line for percentage of old coherent slide and earth flow incidence vs. PGA.

old coherent slides and earth flows are related most strongly to slope height, sum of the PGA's and maximum PGA; whereas young rotational slumps are related most strongly to slope angle.

A linear model was used in all the regression analyses because it is a simple first approach to the problem of landslide distribution. Though non-linear models may yield more accurate predictive equations, we judge the linear models to be sufficient to show the general trends.

Peak ground acceleration was used as an index of earthquake ground motion; it is easily calculated from available equations and is widely used in seismic hazard evaluation. The other ground-motion parameters which probably have the greatest effect on the types of landslides present in the study area are duration and frequency of strong ground motion (Wilson and Keefer, 1983). The lack of strong-motion records for large earthquakes in the central United States makes it infeasible to appraise the quality of peak ground acceleration as an index of these parameters.

In the statistical analyses the sum of the estimated peak ground accelerations from the 1811-12 earthquakes was used as a predictive variable. It often appeared to have the stronger correlation of the two ground-motion parameters, but its physical significance is uncertain. If the sum of the PGA's is a valid parameter and does have stronger correlation to landslide incidence than maximum PGA, it suggests that successive occurrences of strong ground motion from events of similar magnitudes weaken the bluffs and make them increasingly susceptible to slope failure. The first episode may not cause catastrophic failure, but may induce a small amount of displacement or disturbance of the bluff material which would reduce its shear strength. A subsequent earthquake, though of similar or even lower magnitude, or some other event such as a major rainstorm could then cause catastrophic

failure in the weakened material. Such occurrences have been documented in other earthquakes (Wright and Mella, 1963; Seed, 1968; Saleem, 1977; N. Oyagi, 1979, oral commun.; G. Rodolfi, 1980, oral commun.; Ambraseys and others, 1981, Harp and others, 1981). The presence of sensitive soil layers in the area increases the likelihood of this scenario. Even so, using the sum of the PGA's directly to predict future landslide occurrence is difficult because it would require predicting the character of an entire earthquake sequence rather than a single event.

From the low but statistically significant correlations between the four independent variables and landslide occurrence, it is concluded that these four factors have a measurable influence on the occurrence of various types of landslides, but that other factors are also important. We judge that site geology and ground-water conditions are probably the most critical of these factors, based on field observations in the study area and studies of other landslide-prone areas (Keefer, 1984).

The smallest peak ground acceleration estimated to have occurred at any bluff segment in the study area was 0.278 g. This is a large value and represents a severity of ground motion well above that required for the onset of landsliding in the types of materials present in the bluffs (R. C. Wilson, oral commun., 1984). This suggests that the entire study area may have been subjected to ground motions strong enough to initiate landsliding along the bluffs, so much of the variation in landslide occurrence is more probably related to variations in other factors.

EARTHQUAKE-INDUCED LANDSLIDE POTENTIAL

Both field and statistical evidence indicates that, except for areas undergoing active fluvial erosion, most of the large-scale landsliding along

the bluffs in the study area is related to the 1811-12 earthquakes. From this we conclude that these bluffs are susceptible to large-scale landsliding in future major earthquakes. In all probability, other areas in the central United States are also susceptible to earthquake-induced landslides because the area enclosed by the maximum distance line in figure 2 extends well beyond the study area.

Assessment of the susceptibility of specific portions of the bluffs to landsliding requires quantitative information about the site geology, material properties, and hydrology along the bluffs. Our research is continuing in order to evaluate these effects. Seasonal ground-water fluctuations may make the timing of an earthquake critical to landslide susceptibility. Also, the lack of information concerning the nature of strong ground-motion in major earthquakes in the area limits our confidence in using peak ground acceleration as a predictive tool.

For the purposes of regional hazard evaluation in the study area, slope height is a good predictive tool. The equation of the best fit line in fig. 9a indicates that slopes lower than 40 ft (12 m) are not likely to undergo seismically induced landsliding whereas slopes higher than 220 ft (67 m) are likely to experience major failure in a large earthquake comparable to the 1811-12 events.

CONCLUSIONS

The observations and analyses presented in this report lead to the following conclusions:

1. Under normal (aseismic) conditions most or all of the large-scale landsliding in the study area occurs where the river impinges on the bluffs. Landslides caused by fluvial action are single-block rotational slumps.

2. Most of the landslides in areas where the river has not recently impinged on the bluffs are of similar age and include translational block slides, single- and multiple-block rotational slumps, and earth flows. Apparent ages, morphologies, and historical descriptions of these landslides indicate a probable seismic origin dating to the 1811-12 earthquake sequence.

3. Statistical analyses of landslide distribution using linear models shows that, for the older block slides, slumps, and earth flows, slope height explains a significant amount of the variation in areal distribution. By averaging the incidence of these landslides over increments of slope height, slope angle, maximum PGA, and sum of the PGA's, strong correlations show that an increase in any of these variables corresponds to an increase in landslide incidence. When combined in a multivariate model, slope height and sum of the peak ground accelerations from the 1811-12 events combine to explain a large amount of the variation in the incidence of older block slides, slumps and earth flows. Distribution of young rotational slumps associated with fluvial activity is best predicted by slope angle, most likely related to undercutting of the bluffs by fluvial erosion.

4. The variation unexplained by the four independent variables in the statistical analysis is probably accounted for largely by variations in site geology, material properties, and ground-water conditions. These properties vary significantly throughout the area and are important in any slope stability analysis.

5. The bluffs in the study area are susceptible to landsliding in future earthquakes. At present the best parameter for predicting the relative severity of landsliding in a future major earthquake is slope height. Slopes less than 40 ft (12 m) are probably stable in earthquakes; for slopes greater than 40 ft (12 m) high, the potential for earthquake-induced landsliding

increases with increasing slope height. Continued research into the effects of other parameters is needed before a comprehensive method for assessing earthquake-induced landslide potential can be developed.

REFERENCES

- Ambraseys, N., Lensen, G., Moinfar, A., and Pennington, W., 1981, The Pattan (Pakistan) earthquake of 28 December 1974: field observations: Quarterly Journal of Engineering Geology, v. 14, p. 1-16.
- Colman, S. M., and Watson, Ken, 1983, Ages estimated from a diffusion equation model for scarp degradation: Science, v. 221, p. 263-265.
- Conrad, T. A., 1856, Observations on the Eocene deposit of Jackson, Miss., with descriptions of 34 new species of shells and corals: Philadelphia Academy of Natural Science, 1855, Proceedings, 1st series, v. 7, p. 257-258.
- Davis, S. N., and Karzulovic, K. J., 1963, Landslides at Lago Rinihue, Chile: Seismological Society of America Bulletin, v. 53, no. 6, p. 1403-1414.
- Fisk, H. N., 1944, Geological investigation of the alluvial valley of the lower Mississippi River: U. S. Army Corps of Engineers, 78 p.
- Fuller, M. L., 1912, The New Madrid Earthquake: U. S. Geological Survey Bulletin 494, 119 p.
- Hansen, W. R., 1965, Effects of the earthquake of March 27, 1964 at Anchorage, Alaska in The Alaska earthquake, March 27, 1964--effects on communities: U. S. Geological Survey Professional Paper 542-A, 68 p.
- Harp, E. L., Wilson, R. C., and Wieczorek, G. F., 1981, Earthquake-induced landslides from the February 4, 1976, Guatemala earthquake: U. S. Geological Survey Professional Paper 1204-A, 35 p.
- Hopper, M. G., Algermissen, S. T., and Dobrovolsky, E. E., 1983, Estimation of earthquake effects associated with a great earthquake in the New Madrid seismic zone: U. S. Geological Survey Open-File Report 83-179, 94 p.
- Keefer, D. K., 1977, Earthflow: Stanford University, Ph. D. dissertation, 317 p.
- _____, 1984, Landslides caused by earthquakes: Geological Society of America Bulletin, v. 95, no. 4, p. 406-421.
- Keefer, D. K., and Johnson, A. M., 1983, Earth Flows: morphology, mobilization, and movement: U. S. Geological Survey Professional Paper 1264, 56 p.

McGee, W. J., 1891, The Lafayette Formation: U. S. Geological Survey 12th Annual Report, pt. 1, p. 387-521.

_____, 1892, A fossil earthquake: Geological Society of America Bulletin, v. 4, pp. 411-414.

Mitchell, J. K., 1976, Fundamentals of soil behavior: New York, John Wiley and Sons, 422 p.

Nuttli, O. W., 1973, The Mississippi Valley earthquakes of 1811 and 1812: intensities, ground motion, and magnitudes: Seismological Society of America Bulletin, v. 63, p. 227-228.

Nuttli, O. W., and Herrmann, R. B., 1984, Ground motion of Mississippi Valley earthquakes: American Society of Civil Engineers, Journal of Technical Topics in Civil Engineering, v. 110, no. 1, p. 54-69.

Pennsylvania State University, 1982, MINITAB statistical program: University Park, Pennsylvania State University Statistics Department.

Potter, P. E., 1955, The petrology and origin of the Lafayette Gravel, part II, geomorphic history: Journal of Geology, v. 63, no. 2, p. 115-132.

Ryan, T. A., Joiner, B. L., and Ryan, B. F., 1976, MINITAB student handbook: North Scituate, Mass., Duxbury Press, 341 p.

Saleem, A. S., 1977, The Khulm (Tashqurghan) earthquake of March 19, 1976, Samangan Province, Afghanistan: Seismological Society of America, Earthquake Notes, v. 48, nos. 1-2, p. 25-33.

Seed, H. B., 1968, Landslides during earthquakes due to soil liquefaction: American Society of Civil Engineers, Journal of the Soil Mechanics and Foundation Division, v. 94, no. SM5, p. 1053-1122.

Varnes, D. J., 1978, Slope movement types and processes, chap. 2 of Schuster, R. L., and Krizek, R. S., eds., Landslides: Analysis and control: U.S. National Academy of Sciences, Transportation Research Board Special Report 176, p. 11-33.

Wieczorek, G. F., 1984, Preparing a detailed landslide-inventory map for hazard evaluation and reduction: Association of Engineering Geologists Bulletin, v. 21, no. 3, p. 337-342.

Wilson, R. C., and Keefer, D. K., 1983, Dynamic analysis of a slope failure from the 6 August 1979 Coyote Lake, California earthquake: Seismological Society of America Bulletin, v. 73, no. 3, p. 863-877.

Wright, C., and Mella, A., 1963, Modifications to the soil pattern of south-central Chile resulting from seismic and associated phenomena during the period May to August 1960: Seismological Society of America Bulletin, v. 53, no. 6, p. 1367-1402.

LIQUEFACTION POTENTIAL IN THE CENTRAL MISSISSIPPI VALLEY

by

Stephen F. Obermeier

U.S. Geological Survey

Reston, Virginia

Abstract

Liquefaction-induced ground failure caused by the 1811-12 New Madrid earthquakes was commonplace over large areas, even far from the epicenters. Recurrence of strong earthquakes would undoubtedly cause severe liquefaction again and lead to the destruction of many bridges and buildings in the central Mississippi Valley. There is a need to predict the circumstances for which unconsolidated materials with differing physical properties and settings will liquefy, for different design earthquake magnitudes.

In this paper, estimated accelerations are presented for the 1811-12 earthquakes, based on the pattern of sand boils from those earthquakes and mechanical properties of sands in the region of liquefaction. From these 1811-12 acceleration data and modern seismic data, accelerations can be estimated for any magnitude earthquake. This permits use of the Simplified Procedure of Seed and Idriss (that is, the acceleration-magnitude) method to evaluate liquefaction potential. Because of uncertainties of accelerations caused by strong earthquakes in the central Mississippi Valley, another method is presented. This method, called the magnitude method, is based on occurrences of liquefaction from scattered sites around the world, the 1811-12 earthquakes, and other historical earthquakes in the central Mississippi Valley. It is recommended that the final judgment of the possibility of

liquefaction be based on the Simplified Procedure of Seed and Idriss and the magnitude method, in consultation with correlations between Modified Mercalli intensity and acceleration data published elsewhere.

Sediments in the central Mississippi Valley susceptible to liquefaction are generally restricted to sands and silts. There are many large terraces and flood plains in the central Mississippi Valley region which contain moderately dense to loose clean sands and silty sands. Evaluating their properties and relating these properties to liquefaction susceptibility is reasonably easy and straightforward. However, there are also many thick glacial lake deposits, eolian deposits, and reworked eolian deposits made up of silt-rich and clay-bearing materials of highly varying liquefaction potential. Field methods for assessing their properties are crude, and there appear to be so few laboratory data available in the central Mississippi Valley that there are no guidelines based on simple criteria such as void ratio, cohesion, and plasticity characteristics. Laboratory testing should be used to supplement field data for silt-rich materials, even for a regional assessment of liquefaction potential.

Liquefaction Potential in the Central Mississippi Valley

I. INTRODUCTION

Both historical accounts of the 1811-12 New Madrid earthquakes and present day evidence show that liquefaction-induced ground failure was very commonplace and widespread in alluvial lowlands, especially between the towns of New Madrid, Missouri, and Marked Tree, Arkansas (fig. 1). This ground failure was typically manifested by sand boils, lateral spreads, ground fissures, and localized distortion and warping of the ground surface (Fuller,

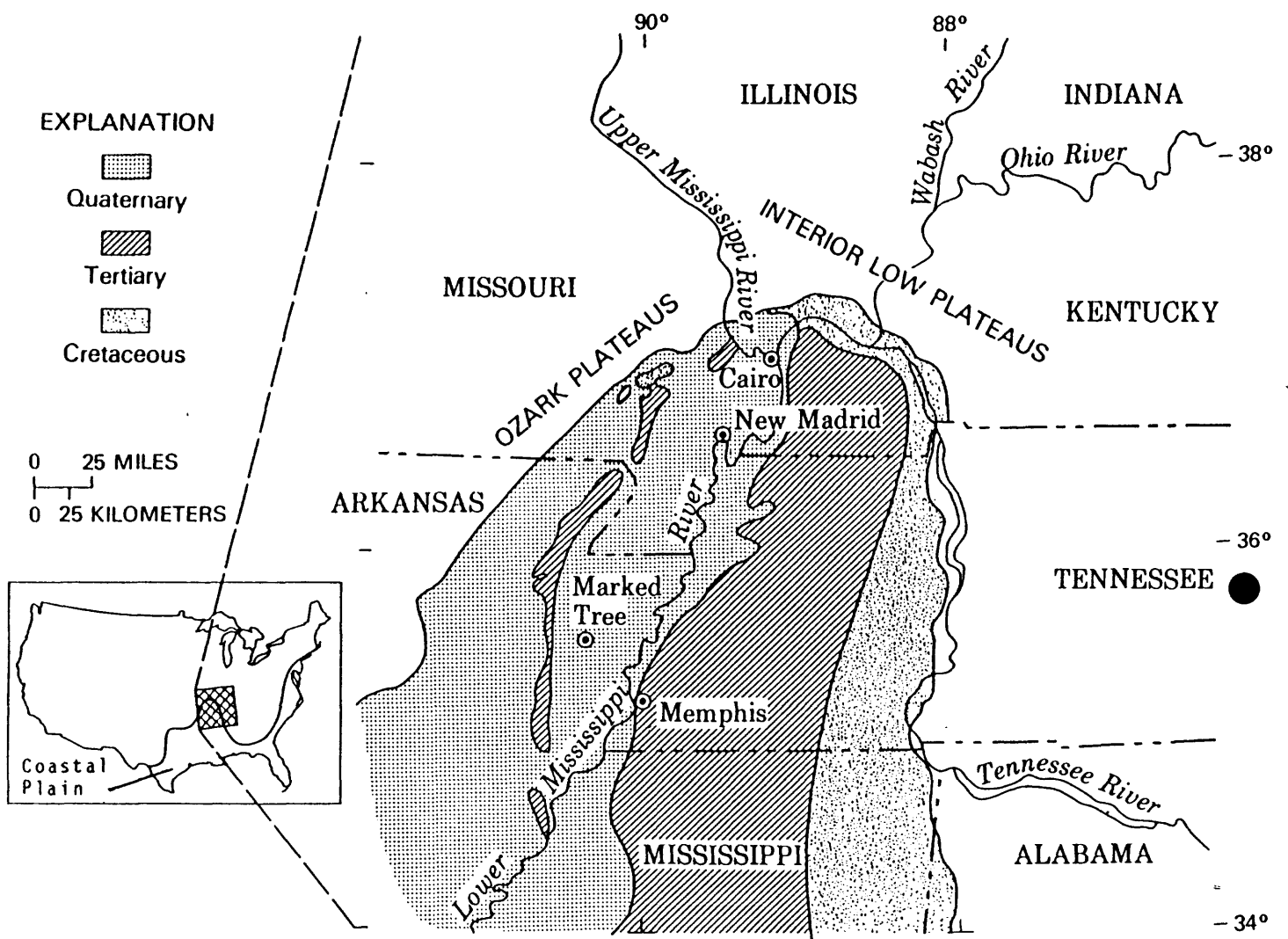


Figure 1. Map of the northern Mississippi Embayment of the Gulf Coastal Plain, showing the major physiographic features of that area, and distribution of Quaternary alluvium, and Tertiary and Cretaceous sediments.

1912). Along streams and in some uplands, many rapid earth flows were doubtlessly caused by liquefaction. If the 1811-12 earthquakes were to recur today, liquefaction-induced ground failure would probably make impassable much of the Interstate highway system in the St. Francis Basin (fig. 2) from Cairo, Illinois, to nearly as far south as Memphis, Tennessee. Many of the bridges would probably be knocked down or badly damaged by lateral spreads or collapse of the stream banks. The pavement would be so damaged by ground fissures and warping that it would be impassable at many places, even to 4-wheel drive vehicles. In addition, there might be widespread flooding (Saucier, 1977) due to expulsion to the ground surface of liquefied sand and water. Many houses and other structures would also be destroyed by effects of liquefaction.

Recounting what took place in 1811-12 and what would take place today given recurrence of such strong earthquakes makes it clear that liquefaction would be responsible for much of the total damage. In what is probably a reasonably analogous situation, the Alaskan earthquake of 1964, liquefaction-induced ground failure caused more than half the economic losses (Mosaic, 1979).

Given the possibility of such dire consequences, exactly where and under what circumstances can liquefaction-induced ground failure be anticipated? Liquefaction generally takes place only in unconsolidated sands or silts, but not all sands or silts have even approximately the same susceptibility. Important factors other than susceptibility are earthquake magnitude and ground response characteristics. It is the purpose of this paper to present information so that one can evaluate the regional susceptibility of different materials in the central Mississippi Valley for different strength earthquakes. To do that, the paper is organized as follows: there is a brief review of factors that cause liquefaction and liquefaction-induced ground

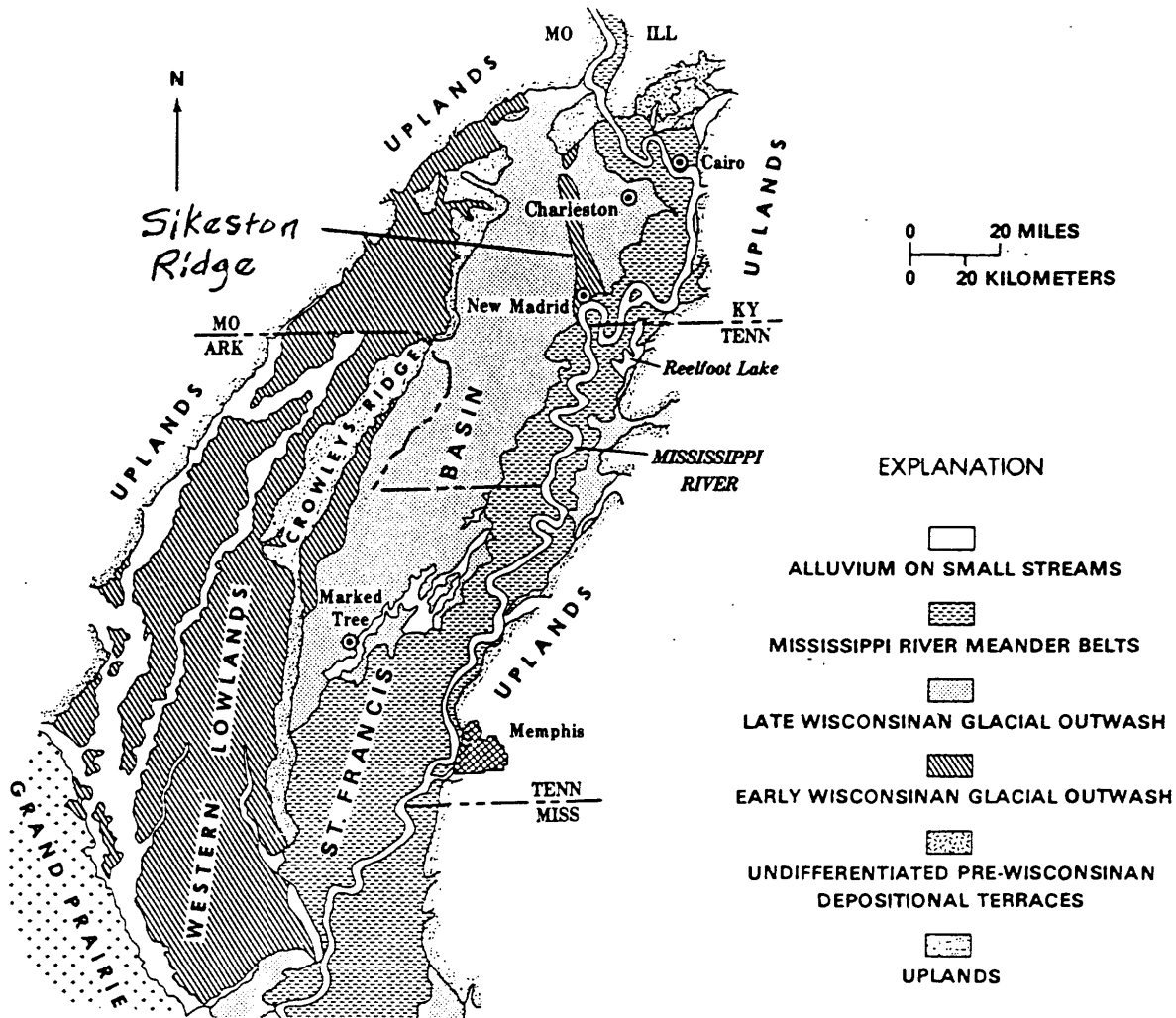


Figure 2. Late Quaternary alluvial deposits in the St. Francis and Western Lowlands Basins (from Saucier, 1974).

failure; the effects of the historical earthquakes in the central Mississippi Valley are examined, to see what data can be extracted; there is an examination and discussion of two methods that can be used to evaluate liquefaction potential; and sediment material properties are presented for the geographic area (basically the alluvial area of fig. 1) where there is a moderate to high probability of liquefaction given recurrence of 1811-12 strength earthquakes. In this way, one can make an assessment of the possibility of liquefaction for any earthquake strength.

The paper is intended to be understandable to geologists, seismologists, and engineers. This necessarily requires some replication of information that is common knowledge within each of these professions. Where words have different meanings within the different professions, such as the word "soil", it is the commonly accepted engineering interpretation that is intended. Important words are defined in the text.

Different earthquake magnitude scales are used in the text. Equivalent values for the different scales are in the following table.

Earthquake Magnitude Scales

The table below shows equivalent earthquakes for the central Mississippi Valley in terms of Richter local magnitude (M_L), body-wave magnitude (m_b), and surface-wave magnitude (M_s). Data are from Nuttli and Herrmann (1982).

| M_L | m_b | M_s |
|-------|-------|-------|
| 5.0 | 5.0 | 4.4 |
| 5.2 | 5.2 | 4.8 |
| 5.4 | 5.4 | 5.2 |
| 5.6 | 5.6 | 5.6 |
| 5.8 | 5.8 | 6.0 |
| 6.0 | 6.0 | 6.4 |
| 6.2 | 6.2 | 6.8 |
| 6.4 | 6.4 | 7.2 |
| 6.6 | 6.6 | 7.6 |
| 6.8 | 6.8 | 8.0 |
| 7.0 | 7.0 | 8.4 |
| 7.2 | 7.2 | 8.7 |

II. OVERVIEW OF LIQUEFACTION

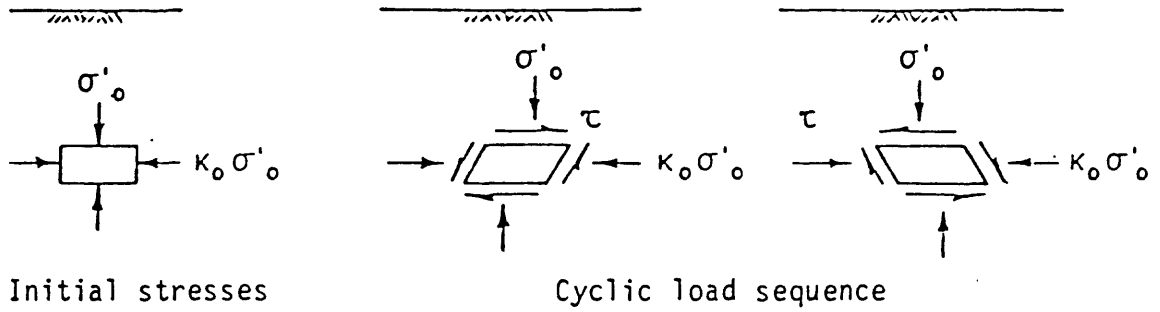
Liquefaction is defined as "the transformation of a granular material from a solid state into a liquefied state as a consequence of increased pore-water pressures" (Youd, 1973). In the liquefied state, the material basically behaves as a fluid mass.

A. Conditions for liquefaction

The application of cyclic shear stresses induced by earthquake ground-motions causes pore-water pressure buildup in saturated cohesionless soils (Seed, 1979). These stresses are due primarily to the upward propagation of shear waves. A soil element on level ground undergoes loading conditions as depicted in figure 3, the shear stress applications being somewhat random but nonetheless cyclic. Because of the shearing, cohesionless soils that are sufficiently loose would become more compact (that is, occupy less volume) if pore water drainage would occur. Because drainage is usually impeded during the short length of an earthquake, there is an increase in the pore-water pressure and a decrease in intergranular stress. With continued application of cyclic shear stresses, the pore pressure of loose sands can approach the initial static confining pressure, even though the shear strains are still small. Further cyclic shearing can cause the pore pressure to increase suddenly to the initial confining pressure, causing large shear straining and even flowage.

Moderately densely packed cohesionless materials^{1/}, while not nearly as susceptible to large shear straining as loose materials, may still develop a residual pore pressure equal to the confining pressure. After the cyclic stress applications stop, this residual pore pressure generally causes an

^{1/} Hereafter, moderately densely-packed, densely-packed, and loosely-packed materials will be referred to as 'moderately dense', 'dense', and 'loose', respectively. These density values are relative to one another, rather than absolute values.



EXPLANATION

- τ - earthquake-induced horizontal shear stress
- σ'_o - initial vertical effective overburden stress
- K_o - ratio of initial lateral/vertical effective stress

Figure 3. Idealized field loading conditions (from Seed and Idriss, 1971).

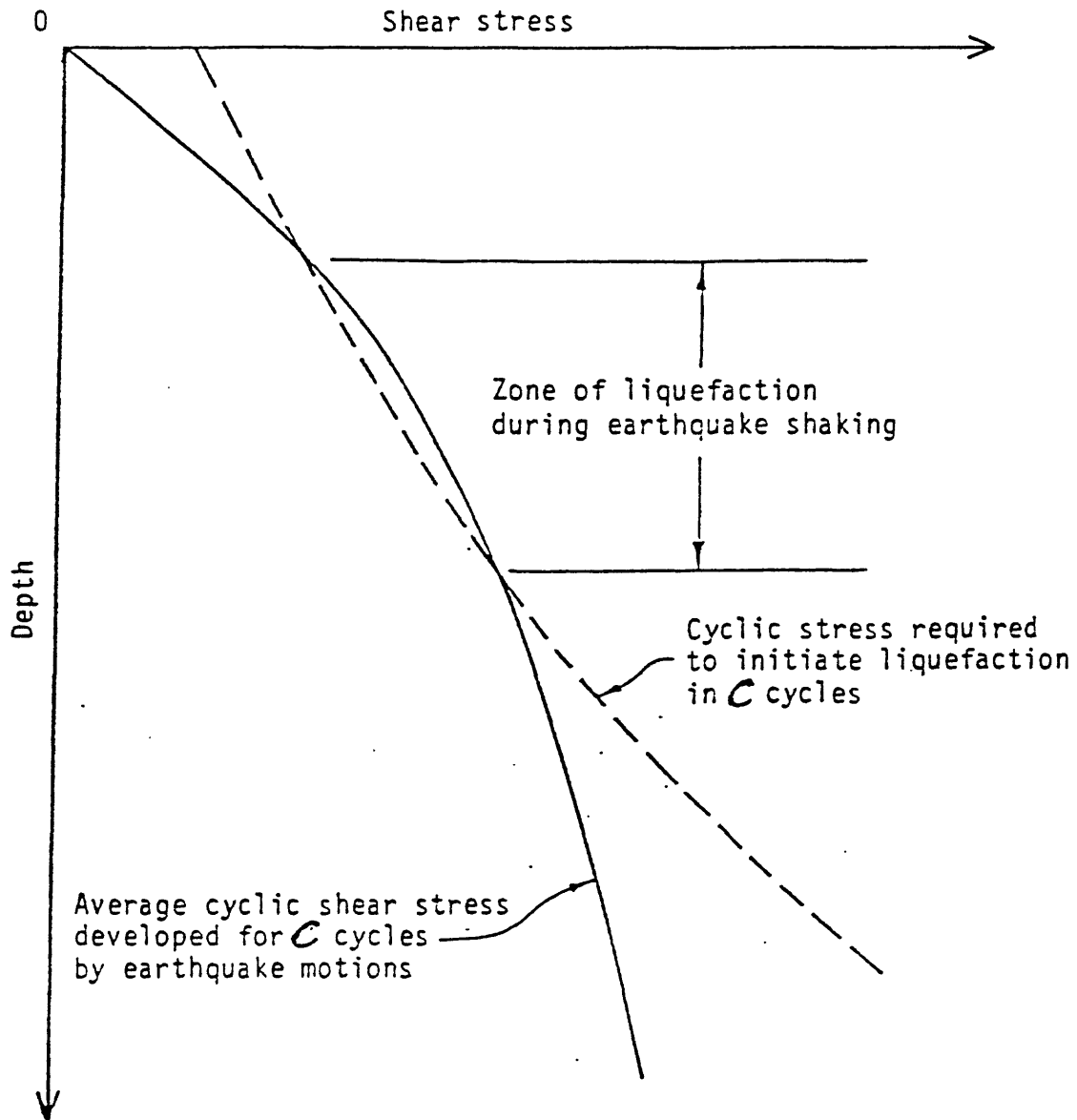
upward flow of water. It is likely that the upward flow of water to the ground surface from an underlying layer having a high pore water pressure is the major causative factor in carrying sand to the ground surface and causing "sand blows" (Housner, 1958) or "sand boils" (Seed, 1979). (Sand blows and sand boils are terms for the same phenomenon.)

Liquefaction during earthquake shaking commonly originates in a zone whose top is 2 to 5 m below the ground surface, but can originate at a depth greater than 20 m (Seed, 1979). Generally, the water table must also be near (say, within 3 to 5 m) the ground surface for there to be very serious problems. Figure 4 illustrates that the zone of liquefaction depends on the relationship between the cyclic shear stresses generated by the earthquake and the resistance to liquefaction of the soil.

Seismological factors of prime importance that control liquefaction during shaking include the amplitude of the cyclic shear stresses and the number of applications of the shear stresses (Seed, 1979). These in turn are related to field conditions of shaking amplitude (that is, peak acceleration) and earthquake magnitude. Analytical engineering methods for evaluating variable cyclic shear stress applications and irregular cyclic stress applications typical of real earthquakes are presently well developed and yield quite acceptable results (Seed and others, 1983), providing shaking amplitude-time records can be predicted with reasonable accuracy.

B. Materials prone to liquefaction

Age and relative density of granular materials are the principal physical controls for liquefaction-susceptibility. As granular materials age, grain-to-grain bonds develop and increase resistance to liquefaction; granular



C is the number of cycles

Figure 4. Schematic depiction of the location of the zone of liquefaction during earthquake loading (from Seed and Idriss, 1971).

materials with high relative densities are much more resistant to liquefaction than loosely-packed granular materials. Very young deposits, less than 500 years in age, are much more susceptible to liquefaction than older, Holocene-age deposits (Youd and Perkins, 1978). As a practical example owing to effects of less aging, deposits on modern flood plain generally are more susceptible than terraces at slightly higher elevations, even if the ground-water table is at the same depth.

In areas strongly shaken by the 1811-12 earthquakes, the most common materials prone to widespread liquefaction are loose to moderately dense clean sands, although there are many deposits of gravelly sands and silty very fine sands that can also liquefy. There are hundreds of river and creek depositional terraces and flood plains in the area of figure 1 which have high water tables and loose sands.

Clean silts with very small amounts of clay and low cohesion are also susceptible to liquefaction, although almost certainly not to the extent of many of the clean sands. Thick, soft, clean silts, deposited as loess, are commonplace in many upland areas near major streams which carried meltwaters from glaciers. Alluvial lowlands adjacent to these loess-covered uplands have a rather thick veneer of soft silt at many places, that originated as loess which was subsequently eroded and redeposited in the lowlands.

Some of the silts in the glacial meltwaters were carried into large lakes and deposited on the lake bottoms. There are vast, thick glacial lake deposits north and northeast of Cairo, Illinois. Many of these old lakes presently have high ground-water tables, and the silts are so clean and soft as to be susceptible to liquefaction. Beneath the silts in these old lake beds, there are very loose sands at many places.

Clay-bearing soils which may also liquefy in the event of a New Madrid-strength earthquake appear to be those with less than 15 percent finer than 0.005 mm, an Atterberg liquid limit less than 35 ^{1/}, and a water content ^{1/} nearly equal to or greater than the liquid limit (Seed and others, 1983). Almost without exception, the only soils with these properties are the silt-rich soils just discussed, and possibly very young sediments in modern flood plains or in very wet swampy areas.

It is also possible that clay-rich sediments which are very young (no older than a few tens or hundreds of years), and extremely soft (so soft that the sediments are mud or an ooze) are prone to liquefaction. Soft sediment deformation features, in the class of "convolute structures", are present in Holocene-age, highly plastic clay strata near Marked Tree, Arkansas. The convolute structures were possibly induced by earthquake shaking. For practical engineering purposes in the central Mississippi Valley, though, liquefaction is potentially a problem for only extremely soft clay-rich soils.

C. Consequences of liquefaction

Liquefaction leads to three basic types of ground failure (Seed, 1968): flow landslides; landslides with limited movement (lateral spreads); and quick-condition failures. In addition, ejection of soil by sand boils and differential loosening and densifying of soil causes differential settling of the ground surface. For sands, Youd (1978) has suggested that the type of ground failure induced by liquefaction is related to the ground surface slope (table 1).

^{1/} The liquid limit is the water content at which a remolded sample has a soft consistency; the liquid limit is the state at which the sample is on the semisolid-liquid boundary. Liquid limit is measured in a standardized test described in any elementary soil mechanics text. Water content is the ratio, (weight of water)/(weight of dry soil), in percent.

Table 1. Ground slope and expected failure mode of coarse-grained deposits liquefied during earthquakes (after Youd, 1978).

| Ground Surface Slope | Failure Mode |
|----------------------|------------------|
| < 0.5 | Bearing capacity |
| 0.5 - 5.0% | Lateral spread |
| > 5.0% | Flow landslide |

The thickness and setting factors such as depth or lateral continuity of the sand deposit also need to be considered in determining the probable mode of ground failure. For example, a thin, loose sand layer at a depth of 10 m in an otherwise non-liquefiable clay deposit is not likely to cause a flow landslide or a bearing capacity failure, irrespective of the ground surface slope. However, this condition might lead to a translational landslide on steep slopes or magnify ground surface movement due to lateral spreading in flat areas (Anderson and others, 1982).

Flow landslides - On slopes steeper than 5 percent, large soil masses can move as viscous fluids or blocks of intact materials riding on liquefied flows. Liquefaction in sands and silts can lead to flows that travel distances of up to hundreds of meters (for example, see figs. 20-22, Youd and Hoose, 1978). Some of the most destructive flows ever recorded originated in loess on hill slopes in Russia (Keefer, 1984).

Lateral-spreading landslides - On slopes between 0.5 to 5 percent, underlain by sands or silts which occur at depth or underlain by sands or silts which are too dense to flow freely, limited flow can take place. Where loose sands are on slope inclinations as low as 0.5 percent, horizontal displacements can still be many meters and leave large open cracks at the surface (Youd, 1978). Generally, lateral spreads develop in alluvial lowlands along streams, where they form parallel to and then move into the stream valley. Lengths of spreads are generally longest parallel to the streams.

Lengths of 150 to 300 m are not unusual (for example, see Fuller, 1912). Rather large lateral spreads can also develop wherever lateral resistance to movement is reduced by removal of only a few meters of soil. Small scarps and man-made ditches are likely locations. Lateral spreads are commonplace in alluvium as a result of moderate to strong earthquakes.

Quick-condition failures - Seepage forces caused by upward percolating pore water can drastically reduce the strength of granular materials, for minutes to days after earthquake shaking. If the strength is reduced to the point of instability, this state is known as a "quick condition" (this is the same as "quicksand" to the general public).

Quick condition failures are generally found only in thick sand deposits that extend from below the water table to the ground surface. Loss of bearing capacity is a common type of quick condition failure. During the 1964 Niigata earthquake in Japan, high-rise apartment buildings had quick-condition, bearing capacity failures and rotated so much that people could walk on the previously vertical exterior; embankments also subsided into the weakened sands. Buoyant rise of buried tanks, and empty swimming pools and water treatment tanks is another common result.

Differential settlements - Wherever seepage forces carry sand and water to the surface, buildings can be undermined. Vertical displacement of the ground surface by compaction of a liquefied soil layer can cause differential settling of buildings. Though probably not often totally destructive of buildings, differential settling can distort and damage structures.

D. Engineering evaluation of liquefaction potential.

Various field methods can be used for regional evaluation of liquefaction potential. Recently developed methods include the electric cone penetration test, the cross-hole seismic velocity test, and the pressuremeter test (Youd and Bennett, 1983). These test methods are still somewhat experimental, and there

are so few data for these methods in the central Mississippi Valley that it is not reasonable to consider their use for regional evaluation. Laboratory dynamic test data on natural soils are virtually non-existent for the central Mississippi Valley, and it would be prohibitively expensive to develop a reasonable data base using dynamic laboratory testing. The only method for which there are abundant data is the Standard Penetration Test.

Evaluation of the liquefaction potential of sand deposits is most commonly done in the field, at least for preliminary analysis, by testing the soil in-place with the Standard Penetration Test (SPT) blow count method (American Society for Testing and Materials, 1978). A sampling tube is driven into the ground by dropping a 140-lb (63.5 kg) weight from a height of 30 inches (176.2 cm). The penetration resistance is reported in number of blows of the weight required to drive the sampler 1 foot (30.5 cm). The SPT blow counts (N values) are then used in conjunction with anticipated earthquake-induced shear stresses and number of repetitions of the shear stress (which is related to earthquake magnitude) to determine if liquefaction may take place. Figure 5 shows boundary curves (by Seed and others, 1983) which define where liquefaction is likely to occur for earthquakes with different magnitudes. The figure applies to clean sands with almost no silt, on level ground. (Figure 5 can be modified for use with silty sands and clean silts that plot below the A-line on the Unified System plasticity chart (Seed and others, 1983, p. 479) by adding 7.5 to the N_1 value before entering the chart). For a given earthquake magnitude, data points below or to the right of the curve will almost certainly not liquefy, and data points above or to the left of the curve have a high probability of liquefying sufficiently to cause sand boils (and landslides and other liquefaction-related ground failure). The curves were developed from field and theoretical studies of earthquake-induced liquefaction at many sites around the world.

The field cyclic stress ratio of figure 5 is the ratio on an element in the sand layer, of the average earthquake-induced horizontal cyclic shear stress ($\tau_{h \text{ avg}}$) to the vertical effective stress (σ'_0) before the cyclic stresses were applied.

The cyclic stress ratio developed in the field due to earthquake shaking is computed from equation (1) (Seed and others, 1983):

$$(1) \quad \frac{\tau_{h \text{ avg}}}{\sigma'_0} = \frac{0.65 (A_{\text{max}} \cdot \sigma_0 \cdot r_d)}{(g \cdot \sigma'_0)}$$

where A_{max} = peak horizontal acceleration at the ground surface; σ_0 = total overburden stress on the sand under consideration; σ'_0 = initial effective overburden stress (total stress minus pore-water pressure) on the sand layer under consideration; r_d = stress reduction factor ranging from a value of 1 at the ground surface to a value near 0.9 at a depth of about 10 m ; and g = the acceleration of gravity.

For one of the most common field conditions on alluvium in the New Madrid earthquake region, where the water table is about 2 m below the ground surface and the weakest sands are at a depth of 4 to 5 m, the field cyclic stress ratio is almost exactly equal to the peak horizontal acceleration; that is, if the peak horizontal acceleration is 0.20g, the cyclic stress ratio is essentially 0.20.

On figure 5, the modified penetration resistance, N_1 , is the SPT blow count value measured in the field multiplied by a correction factor that accounts for the influence of field stress conditions on the measured blow count; for the field conditions in the paragraph above, the multiplication factor is 1.4 (see Seed and others, 1983).

To illustrate use of the curves, assume that the peak horizontal acceleration at the ground surface is 0.20g for an earthquake magnitude (M) of 6³, and the SPT blow count in clean sand is 11 (corrected to $N_1 = 15.4$) on a nearly level terrace for the depth and water table conditions above. These

conditions are given by point A on figure 5; liquefaction and production of sand boil deposits would be very probable.

The accelerations required for liquefaction using figure 5 are both a lower bound, and a most probable bound. Figure 6 shows the curve for M equal to $7/2$, and field data from many earthquakes around the world. The solid circles in figure 6 are for sites where there was evidence of liquefaction-induced ground failure, such as sand boils. Although no evidence for liquefaction was observed for open circles, liquefaction may still have occurred but was not observed because of the field setting. For example, an especially thick fine-grained cap above liquefied sands prevented sand boils from reaching the ground surface at many places in the St. Francis Basin during the 1811-12 earthquakes (Saucier, 1977; Obermeier, unpublished data). As another example, especially coarse, permeable deposits above the zone liquefied during shaking may dissipate pore pressure so fast that sand boils do not develop. The data in figure 6 are for many types of field settings, scattered around the world, and it is not surprising that liquefaction-related features were not observed in some. In summary, the solid line in figure 6 is probably quite a good bound for estimating accelerations, providing attention is given to the field setting; and, it is extremely unlikely that there would not be liquefaction at accelerations 25 percent higher than the solid line bound (see fig. 6).

Figure 5 is strictly applicable only for level or nearly level ground. On steeper slopes, higher accelerations are required to cause liquefaction, and more sophisticated methods must be used to determine if liquefaction may develop. Still, use of figure 5 helps assess if there is the possibility of problems on the slopes; if slope instability is indicated by figure 5, there is a high probability of potential problems.

The procedure sketched above, known as the Simplified Procedure of Seed and Idriss, indicates only where liquefaction is probable. Damaging ground failure

may or may not result from an occurrence of liquefaction. In general, liquefied loose sands are much more likely to flow, move large distances, or cause damage than liquefied medium dense sands; more rigorous methods are necessary for evaluating the complete scenario.

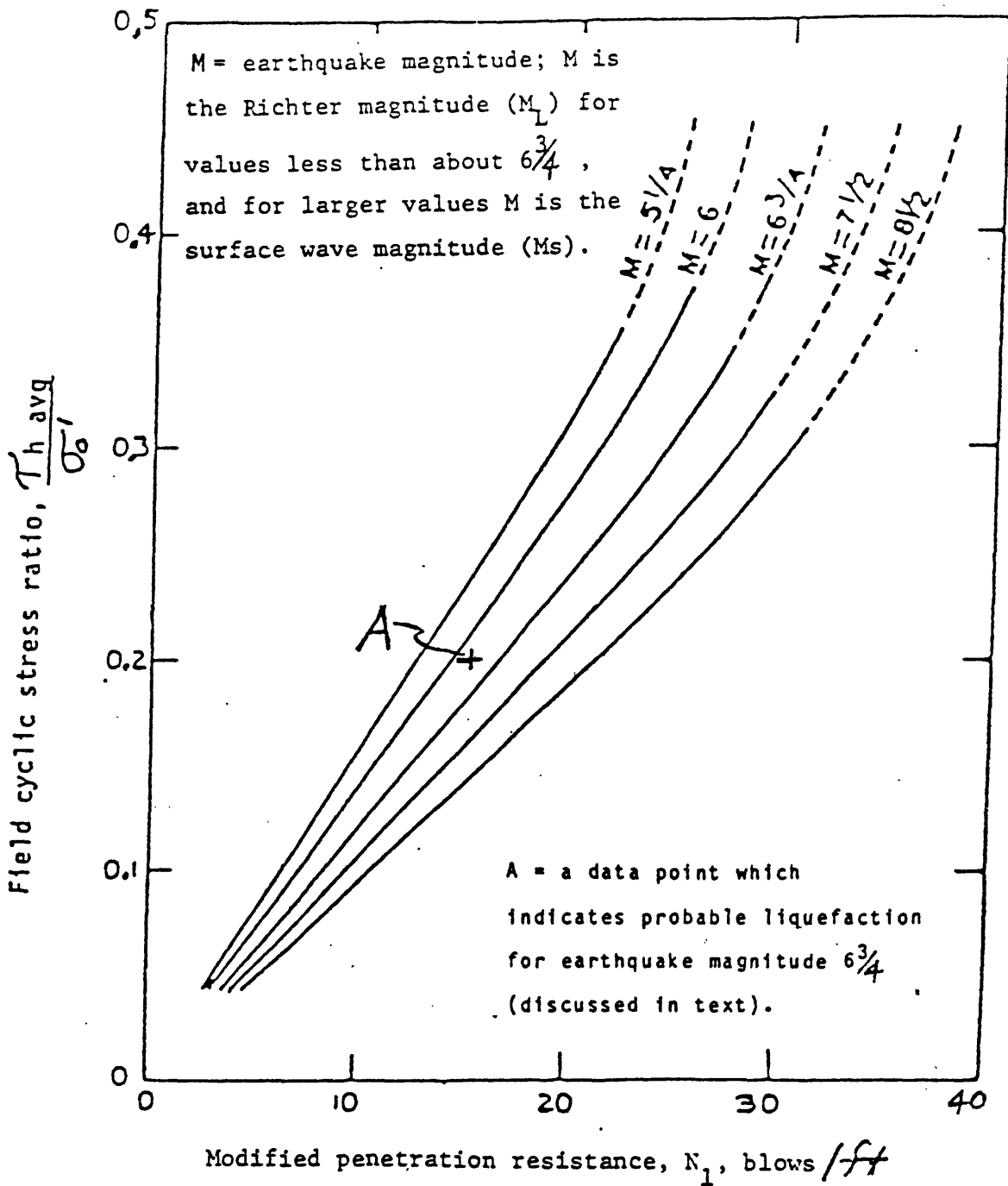
For clay-bearing soils that plot above the A-line on the Unified Classification System plasticity chart (Seed and others, 1983, p. 479), there are no charts analogous to figure 5. Laboratory test methods must be used at the present time to appraise their behavior in any detail. However, it is certain that serious liquefaction can take place in these materials only if they are very soft. The softness of silts and clays can also be crudely estimated by the SPT method. Only very weak clay-bearing soils that have index and physical properties (natural water content, liquid limit, percent clay) in the range discussed previously are candidates for liquefaction.

III. Liquefaction and Historical Earthquakes

Historical earthquakes in the central Mississippi Valley are examined to establish relations between liquefaction, earthquake magnitudes, accelerations, and Modified Mercalli (MM) intensities. Liquefaction effects of the 1811-12 earthquakes are reviewed first, followed by accounts of more recent earthquakes having body-wave magnitudes (m_b) greater than 5.3.

A. 1811-12 Earthquakes

It is well known (Fuller, 1912) that great numbers of liquefaction-induced ground failures (hereafter called "liquefaction") took place many tens of kilometers from the probable epicenters, and locally were as far as 175 km (Keefer, 1984). Accounts of the farthest liquefaction typically describe disappearing islands in rivers, sand boil deposits near streams, and lateral spreads along stream banks. Almost certainly most if not all of these farthest liquefaction features were in very young alluvial sediments.



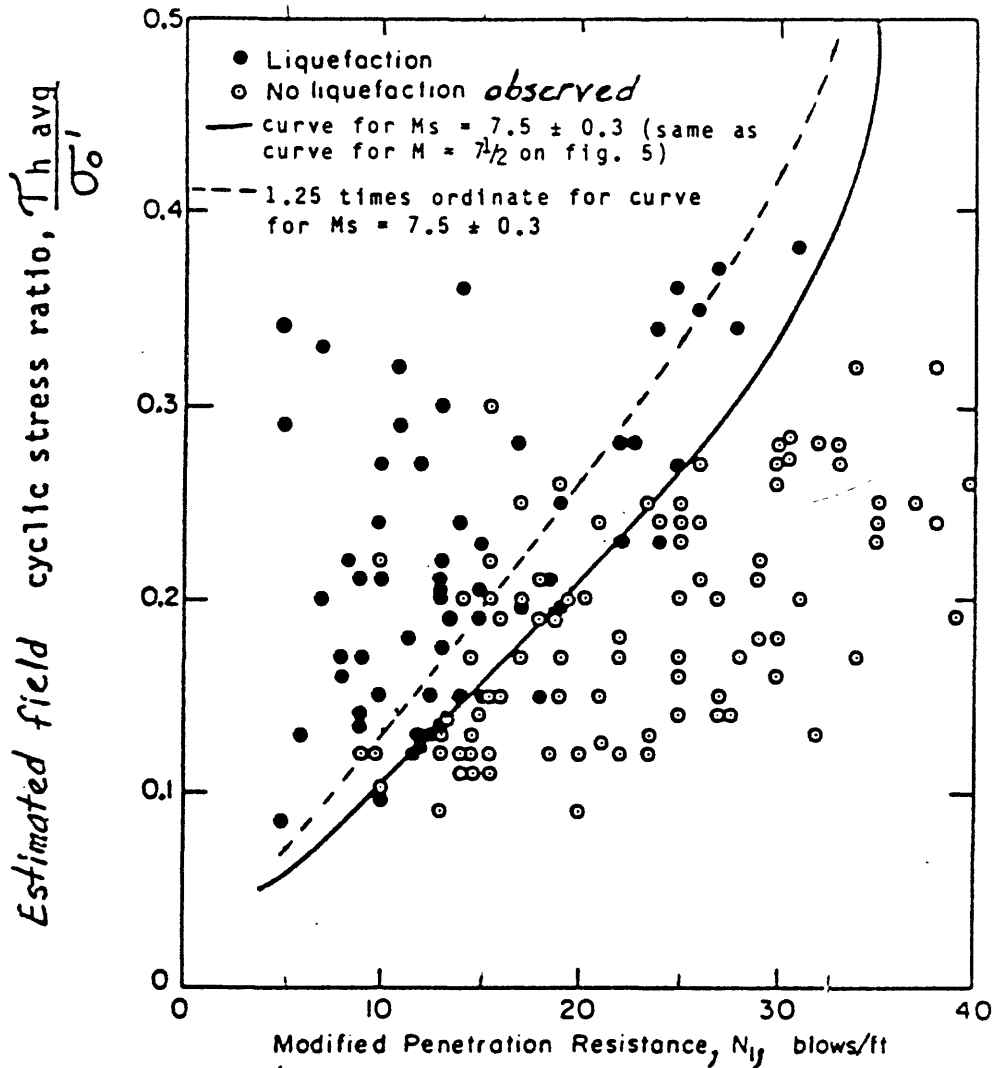
EXPLANATION

$T_h \text{ avg}$ - average earthquake-induced horizontal cyclic shear stress

σ_0^v - vertical effective stress

N_1 - Standard Penetration Test blow count measured in field, modified to blow count resistance at vertical effective stress of 1 ton/ft²

Figure 5. Chart for evaluation on level ground of liquefaction potential of sand deposits (average diameter > 0.25 mm), for different magnitude earthquakes (from Seed and others, 1983).



EXPLANATION

T_h avg - average earthquake-induced horizontal cyclic shear stress.

σ_0^v - vertical effective stress

N_1 - Standard Penetration Test blow count measured in field, modified to blow count resistance at vertical effective stress of 1 ton/ft²

Figure 6. Correlation on level ground between field liquefaction behavior of sand deposits (average diameter > 0.25 mm) and modified penetration resistance, for surface wave magnitude (M_s) = 7.5 ± 0.3 (from Seed and Idriss, 1981).

In general, the youngest sediments are most susceptible to liquefaction, other things being equal (Youd and Perkins, 1978). The stream energy of the depositional environment is another important variable, with the highest relative densities being from the highest energy flow regimes (Bennett and others, 1981). The Holocene sediments in the central Mississippi Valley are from a variety of flow regimes and, in addition, range in thickness from a feather-edge to many tens of meters. This large variation in physical properties and thicknesses causes wide variations in ground response characteristics. Thus, using the regional pattern of liquefaction features to understand earthquake characteristics (such as epicenter locations and accelerations) must be approached very carefully, and is extremely difficult in a highly variable geologic setting. However, the thickness and physical properties of Late Quaternary alluvium in the St. Francis and Western Lowlands Basins presents an almost ideal setting.

Alluvium in St. Francis and Western Lowlands Basins

Figure 2 shows alluvial deposits in the St. Francis and Western Lowlands Basins. Almost all the deposits shown in the eastern two-thirds of the figure are Late Quaternary in age; only locally, generally on modern flood plains, are there significant deposits of much younger alluvium. Total thickness of alluvium is typically between 30 and 50 m throughout the St. Francis Basin (Saucier, 1964), and is only slightly less in the Western Lowlands (Smith and Saucier, 1971). For such thick alluvium, small variations in thickness causes only minor changes in ground response to underlying bedrock accelerations, for a given earthquake magnitude and narrow range of accelerations, providing the physical properties of the alluvium are relatively uniform.

Alluvium of the Western Lowlands and alluvium between the towns of Cairo and Marked Tree is mostly braided stream terraces of glacial outwash or valley train

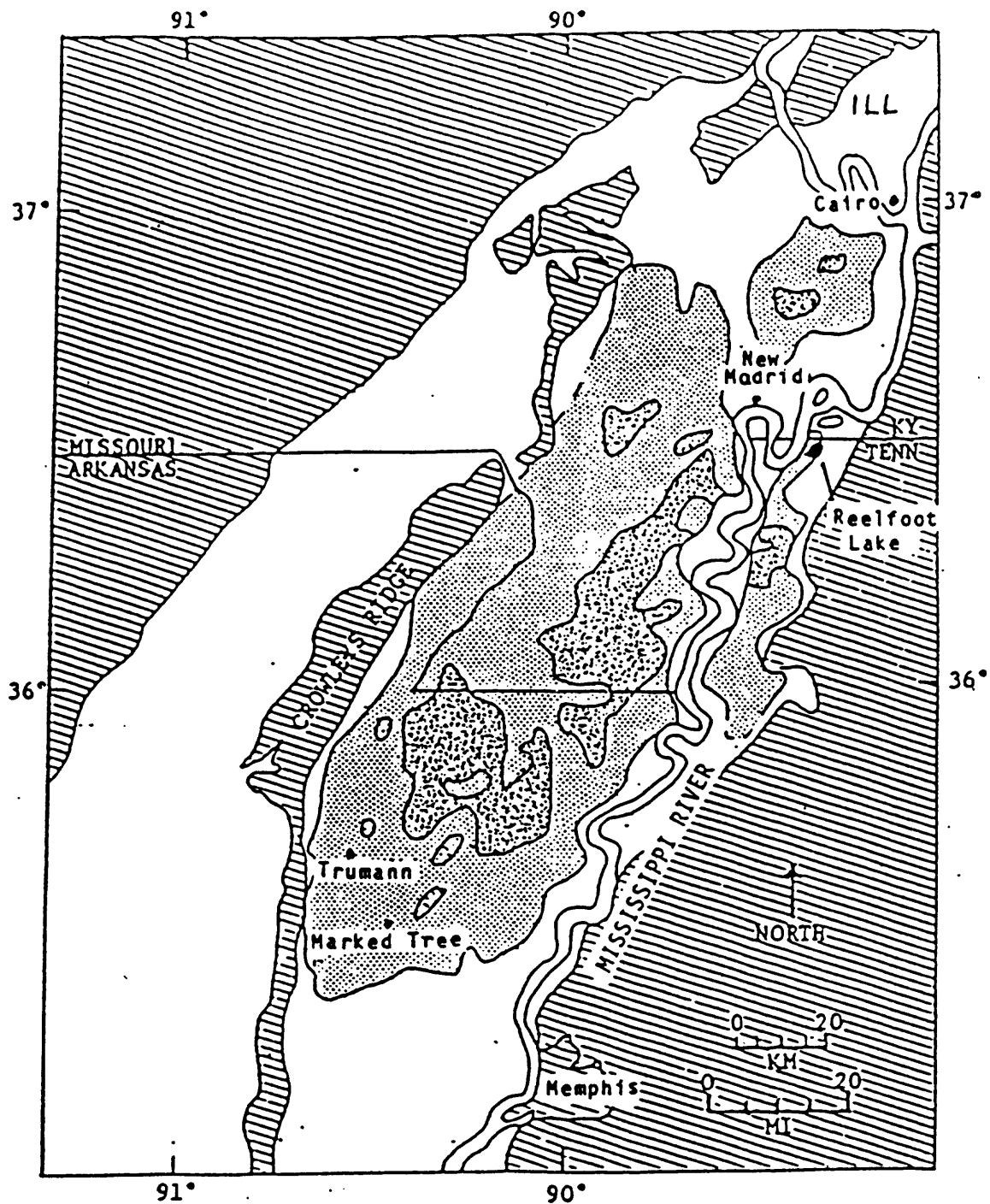
deposits. These terraces are typically a layered sequence of "topstratum" over "bottomstratum" (Saucier, 1964). The topstratum is generally a 2 to 6 m thick overbank deposit, which contains primarily thick to thin strata that are very clay-rich, highly plastic, and black. The clay strata are interspersed with a few strata of silt and very fine sand. The topstratum beds abruptly grade down into the bottomstratum, over a distance typically less than a meter. The bottomstratum is very clean, moderately dense sand, which is generally fine- to medium-grained near the top, and grades downward to a coarse sand with gravel at the base.

Meander belt deposits of the Mississippi River generally have thick strata of clean sand, silty fine sand, and clay within the uppermost 10 to 15 m. Beneath that are clean sands. There is a clay-rich cap of overbank deposits over these meander belt deposits at many places, especially in swales and sloughs. The total thickness of the clay-rich cap rarely exceeds 10 m. Within these meander belts, there are usually many places nearby (within a few hundred meters) where the clay cap is only a few meters thick, and clean sand underlies the cap. Overall, braided stream and meander belt deposits are almost certainly the same with respect to seismic response characteristics.

Sand boil deposits in St. Francis Basin

Figure 7 shows the distribution and concentration (that is, density of areal coverage) of sand boil deposits in the St. Francis Basin, excluding alluvium of modern meander belts. Figure 7 is based on an investigation by the author, using 1938-1940 vintage and more recent airphotos (scale about 1:20,000) in conjunction with field verification. Field and airphoto studies for figure 7 were restricted to the St. Francis Basin and the eastern one-third to one-half of the Western Lowlands Basin. No sand boil deposits were found in the Western Lowlands Basin.

Much of the field and airphoto study was directed to locating the margin of liquefaction effects, which was empirically defined as the outer limit where at



EXPLANATION

- | | |
|--|---|
| <ul style="list-style-type: none">  Upland areas  Alluvium with no observed sand boils | <ul style="list-style-type: none">  Alluvium with recognizable sand boil deposits (> 1 percent ground coverage), but not intense ground coverage  Alluvium with more than 25 percent of ground surface covered by sand boil deposits |
|--|---|

Figure 7. Distribution of sand boil deposits on alluvium excluding modern flood plains, presumably produced by 1811-12 earthquakes.

New

least one percent of the ground surface is covered by sand boil deposits (smaller percents are difficult to determine from airphotos). In that way, the location of the epicenter (more accurately, the "energy release center"^{1/}) could be estimated for the December 16, 1811 earthquake, and earthquake accelerations could be estimated away from near-field effects, using the relations in figure 5.

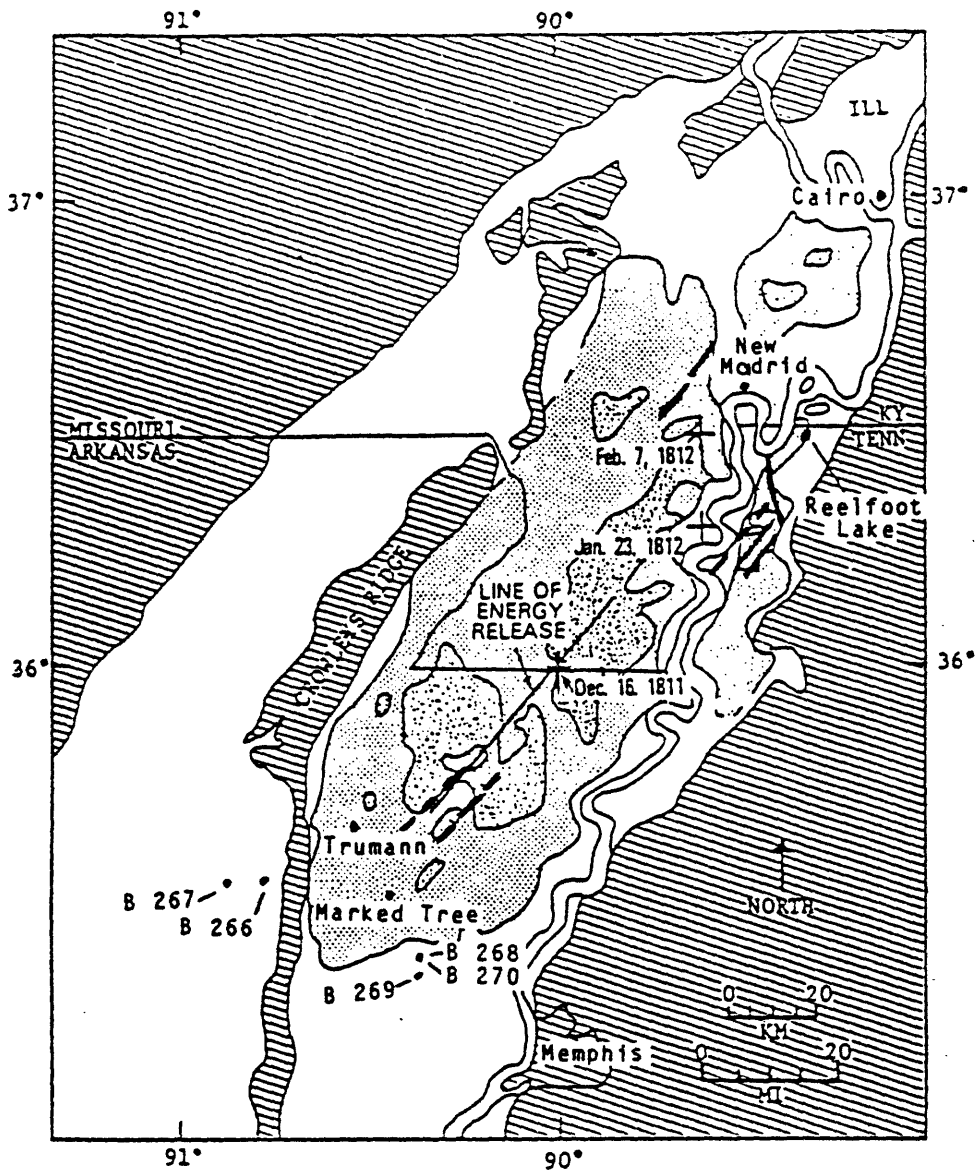
Energy release center

Based on regional earthquake intensity studies, Nuttli (1979) estimated the three largest 1811-12 earthquakes had the epicenters shown on figure 8. Although the epicenter locations are very approximate, it is likely that the first strong earthquake, the December 16 event, was located considerably southwest of the other two. Thus, it seems reasonable to associate the southernmost one-third of sand boil deposits with the December 16 event. Nuttli's estimated epicenters for the other two large events are so close to one another that use of the pattern of sand boil deposits to locate energy release centers would be extremely difficult, if not impossible.

A cursory examination of figure 7 suggests that the energy release center for the December 16 earthquake is a line centrally located to the boundary of sand boil deposits, roughly in the southern one-third of these deposits. In addition, the line trends southwest-northeast, and has a southern terminus that is a little north of Marked Tree (see fig. 8). This energy release center line location is based on the premise that the alluvium in the region, excluding very young alluvium, has about the same physical settings and engineering properties, and thus the same liquefaction potential.

The writer investigated the physical settings and engineering properties of alluvium in the St. Francis and Western Lowlands Basins by compiling some 400

^{1/} The epicenter is the point on the earth's surface directly above the earthquake focus (the focus is the point at which strain energy is first converted to elastic wave energy). Thus, the epicenter may or may not be



EXPLANATION

- | | | | |
|---|---|---|--|
|  | Upland areas |  | Alluvium with recognizable sand boil deposits (> 1 percent ground coverage), but not intense ground coverage |
|  | Alluvium with no observed sand boils |  | Alluvium with more than 25 percent of ground surface covered by sand boil deposits |
|  | • B Standard Penetration Test location and number | | |
|  | + Epicenters for earthquakes according to Nuttli (1979), on adjacent dates. | | |
|  | Fault zone |  | Fault |

Fault zones and faults are from Hamilton and Zoback (1982).

Figure 8. Energy release center line for the December 16, 1811 earthquake, and fault zones, faults, and selected borings.

borings logs. Most of the data were collected from files of the Army Corps of Engineers, Memphis District. About 250 of the logs had SPT data to a depth of about 12 to 15 m. The borings were scattered throughout the area, but most were near levees or large drainage ditches excavated throughout the basins. Data from very young alluvium and alluvium along most small streams were excluded.

The data were separated according to the following geographic-geologic settings: braided stream terraces, Western Lowlands Basin; southern half of braided stream terraces, St. Francis Basin; and Mississippi River meander belt deposits. The southern half of braided stream terraces in the St. Francis Basin was further subdivided into four large areas. It was found that in meander belt deposits, layers of silty very fine sand and very fine sand are much more common than in braided stream terrace deposits, which generally have much coarser sands. This textural difference required making a correction to the SPT blow count (the method of Tokimatsu and Yoshimi (1981) was used) to account for the influence of grain size on liquefaction potential. Also, there are no substantive differences in SPT blow counts or sand textures in braided stream deposits, throughout the southern part of the St. Francis Basin.

Table 2 shows results of the study. The table shows "modified penetration resistance"(N_1) values (see fig. 5), which is the field SPT blow count modified to account for the influence of overburden pressure and water table location. The N_1 values are for the depth range generally most susceptible to liquefaction, 3 to 8 m. Median and lower quartile (that is, the 50 and 25 percent) values are given because they are thought by the writer to realistically bracket the percentage of a sand body in this depth range that must be liquefied to form a significant regional development of sand boil deposits. Requiring that half the coincident with the point or zone of maximum energy release (that is, the 'energy release center').

volume of sand liquefy is a severe requirement, because liquefaction of a single, loose layer can be adequate for production of extensive sand boil deposits. For a significant regional development of sand boil deposits, though, there must be some significant degree of liquefaction, although the lower cut-off is very uncertain and must depend on factors other than N_1 (such as the topstratum thickness or the rate at which the excess pore-water pressure can be dissipated in strata overlying the layer liquefied during shaking).

Table 2. Modified penetration resistance values (N_1) ^{1/} in selected setting in Western Lowlands and St. Francis Basins

| Geologic-geographic setting | Median N_1 | Lower Quartile N_1 |
|---|--------------|----------------------|
| Braided stream terrace deposits, Western Lowlands | 22-23 | 15 |
| Braided stream terrace deposits, southern half, St. Francis Basin | 26 | 19 |
| Meander belt deposits of Mississippi River | 25 | 17-18 |

Irrespective of whether the median or lower quartile is more appropriate, table 2 shows that in the St. Francis Basin, N_1 values are basically the same in braided stream terrace deposits and Mississippi River meander belt deposits, and both types of St. Francis Basin alluvium have higher N_1 values than Western Lowland braided stream terrace alluvium. The topstratum is so thin at many places (less than 3 to 4 m) in both the Western Lowlands and St. Francis Basins that an excessive topstratum thickness could not have been a major factor in determination of the outer bound of sand boil deposits, at least regionally. Thus, the energy release center for the December 16, 1811 should lie approximately in the center of the outer limits of sand boil deposits. From this knowledge, the southern limit and orientation of the energy release center shown ^{1/} 1 is the modified penetration resistance, as discussed in Seed and others (1983).

on figure 8 is established; the length of the energy release center line is based on an estimate of the length of rupture, reported by Nuttli (1983).

Other types of data strongly suggest that the fault that caused the December 16 earthquake was strike-slip, and was parallel to and very close to the energy release center line on figure 8; modern seismic activity (Stauder, 1982) is near the energy release line, and the stress field in lithified rocks is oriented east-west (Hamilton and Zoback, 1982). In addition, the overall style of surface deformation near Reelfoot Lake is consistent with a fault zone extending from the vicinity of Reelfoot Lake toward Marked Tree (Russ, 1982).

Accelerations in alluvium

Sites generally best suited for back-calculating earthquake accelerations based on liquefaction are outer margin locations of sand boil deposits, where liquefaction causes only minor changes in pre- and post-earthquake SPT blow counts. No data were available along the margin of sand boils on figure 7, but 10 STP borings were at scattered sites beyond the margin, where no sand boils were observed. Thus, at these sites, earthquake accelerations determined using the smallest N_1 values are maximum possible accelerations; actual values were somewhat smaller. It is assumed that the December 16 earthquake had a M_s value of 8.5 (Nuttli, 1983).

Three of the borings are in the St. Francis Basin, between Marked Tree and Memphis; these borings are about 40 km south of the energy center line (see table 3). The smallest N_1 values that are relatively common are about 17 to 20. Using the chart in figure 5 to determine the cyclic stress ratio for a M_s value of 8.5, and then calculating the acceleration from equation (1), yields a peak horizontal acceleration of about 0.18g. Two borings in the Western Lowlands (see table 3), 45 and 52 km from the energy center line, yield peak horizontal accelerations of about 0.19g. Thirty-two km north of the energy center line, the data yield 0.19g; the borings north of the energy center line are from sites where it was rather

Table 3. Field boring log data at selected locations in Western Lowlands and St. Francis Basins.

Western Lowlands Basin

Boring log no. 266

Boring log no. 267

| Sample From (ft) To (ft) | Stratum From (ft) To (ft) | Field classification and remarks | N ₁ 1/ | N ₁ 2/ | N ₁ 3/ adjusted | Sample From (ft) To (ft) | Stratum From (ft) To (ft) | Field classification and remarks | N ₁ | N ₁ adjusted |
|--------------------------|---------------------------|---|-------------------|-------------------|----------------------------|--------------------------|---------------------------|---|----------------|-------------------------|
| 15.0 16.5 | 0.0 13.5 | silty clay. thin lenses of f and m and silty sand, and 1 in. lens of clayey silt. m sand. | 12 | 12 | 19-20 | 16.0 17.5 | 0.0 12.0 | clayey silt. | 11 | 18-19 |
| 18.0 19.5 | 13.5 | | 37 | 37 | 37 | 19.0 20.5 | 12.0 16.0 | sandy silt, w/tr clay. f sand. | 18 | 18 |
| 21.0 22.5 | | f and m sand. | 15 | 15 | 15 | 22.0 23.5 | 16.0 | f and m sand. | 20 | 20 |
| 24.0 25.5 | | f and m sand. | 29 | 29 | 29 | 25.0 26.5 | | f and m sand. | 24 | 24 |
| 27.0 28.5 | | f and m sand. | 20 | 20 | 20 | 28.0 26.5 | | f and m sand, w/ some 1/16 in. lenses of clayey silt. | 16 | 16 |
| 30.0 31.5 | | f and m sand. | 30 | 30 | 30 | | >36.5 | f and m sand. | 12 | 12 |
| 33.0 34.5 | | f and m sand. | 29 | 29 | 29 | | | f and m sand. | 18 | 18 |

St. Francis Basin

Boring log no. 268

Boring log no. 269

| Sample From (ft) To (ft) | Stratum From (ft) To (ft) | Field classification and remarks | N ₁ 1/ | N ₁ 2/ | N ₁ 3/ adjusted | Sample From (ft) To (ft) | Stratum From (ft) To (ft) | Field classification and remarks | N ₁ | N ₁ adjusted |
|--------------------------|---------------------------|--|-------------------|-------------------|----------------------------|--------------------------|---------------------------|---|----------------|-------------------------|
| 11.0 12.5 | 0.0 8.0 | silty clay. | 12 | 12 | 19-20 | 18.0 19.5 | 0.0 18.0 | silty clay. | NA | NA |
| 14.0 15.5 | 8.0 10.5 | f sand. | 41 | 41 | 48-49 | | 18.0 | f sand, w/6 in. thick lens of sandy silt. | NA | NA |
| 17.0 18.5 | 10.5 | f sand. | 26 | 26 | 26 | 21.0 22.5 | | sandy silt. | NA | NA |
| | | m sand in upper 6 in., layers of f to m sand in lower 12 in. | 56 | 56 | 56 | 24.0 25.5 | | lost sample. | NA | NA |
| 20.0 21.5 | | m sand, w/layers of 1/2 in. thick f sand. | 26 | 26 | 26 | 27.0 28.5 | | sandy silt, w/6 in. lens of clay. | NA | NA |
| 23.0 24.5 | | m sand, w/lenses of f sand. | 30 | 30 | 30 | 30.0 31.5 | | clayey silt, w/6 in. lens of clay. | 24 | 31-32 |
| 26.0 27.5 | | m sand, w/gravel. | 67 | 67 | 67 | 33.0 34.5 | | sandy silt. | NA | NA |
| 29.0 30.5 | | m sand, w/gravel. | 63 | 63 | 63 | | >37.5 | clayey silt, w/6 in. lens of clay. | NA | NA |
| 32.0 33.5 | | m sand, w/gravel. | | | | | | sandy silt. | | |

Table 3 continued

St. Francis Basin

Boring log no. 270

| Sample From (ft) | To (ft) | Stratum From (ft) | To (ft) | Field classification and remarks | N ₁ | N ₁ adjusted |
|------------------------|------------|-------------------------|------------|--|----------------|----------------------------|
| | | 0.0 | 9.0 | silty clay. | | |
| | | 9.0 | 11.0 | sandy silt. | | |
| 10.0 | 11.5 | 11.0 | 11.5 | lean clay. | NA | NA |
| | | 11.5 | 12.0 | sandy silt. | | |
| 12.0 | 13.5 | 12.0 | 13.5 | silty sand, w/very few thin clayey lenses. | NA | NA |
| | | 13.5 | 15.5 | silty sand. | | |
| 15.0 | 16.5 | 15.5 | 16.0 | f sand. | 10 | 17-18 |
| 19.0 | 21.0 | 19.0 | 21.0 | f and m sand. | 9 | 9 |
| 21.0 | 22.5 | 21.0 | 24.5 | f and m sand, w/ very thin clay lenses. | 16 | 16 |
| 24.0 | 25.5 | 24.5 | 25.5 | f sand. | 16 | 23-24 |

- 1/ The letters f and m are abbreviations for fine and medium, respectively.
- 2/ N₁ values are Standard Penetration Test (SPT) blow counts, adjusted for an overburden stress of 1 ton/ft².
- 3/ Where applicable, N₁ values are adjusted to account for influence of sand grain size on liquefaction potential, by adding 7 to 8 to values in adjoining column. Many of the sands classified in the field as being fine have an average diameter of about 0.25 mm, based on laboratory sieve testing of the composite sample from the SPT sampling tube. The samples in-situ are typically alternating thin layers of very fine and fine to medium sand. Thus, adding 7 to 8 to the N₁ values for the samples designated as fine sand is conservative for back-calculating the 1811 accelerations.
- 4/ NA is abbreviation for 'not applicable' or 'not available'.

difficult to detect sand boil deposits, because of the generally sandy texture of surface soils, and therefore much less confidence can be associated with these accelerations. However, based on the SPT data from south of the energy center line and from the Western Lowlands Basin, it is very probable that at 40 to 45 km from the energy center the peak horizontal accelerations at the ground surface were less than 0.20g.

Accelerations in bedrock

The lack of strong motion ground response data for the New Madrid earthquake region makes it necessary to relate the acceleration in alluvium to bedrock motion by empirical relations elsewhere and semi-quantitative calculations. Seed and Idriss (1982, p. 37) have shown that, on average, at 0.20g, the peak acceleration in rock is nearly the same or only slightly higher than in overlying stiff or thick cohesionless soil. These cohesionless soils presumably range from loosely to densely packed. Sharma and Kovacs (1980), in a microzonation study of the Memphis area using the program SHAKE, found that the moderately thick (about 30 - 40 m), moderately densely packed sands of the area probably have peak accelerations which are about the same as in the underlying bedrock, for strong earthquakes in the New Madrid fault zone (the New Madrid fault zone is located at about the same place as the energy release center line of figure 8); their data show that the peak accelerations in these sands should range from about equal to but not more than about 20 percent higher than in the underlying bedrock^{1/}. All the accelerations back-calculated from SPT-liquefaction relations in the preceding section are from sites where sand is about 30 to 50 m thick. Thus, it is likely that at these sites the peak accelerations at the ground surface were about the same as or only slightly higher than in the bedrock beneath.

^{1/} Sharma and Kovacs made acceleration amplification calculations for both a basal stratum of sand and of gravel. The writer believes the results for sand are most applicable to the St. Francis Basin.

Farthest liquefaction

The farthest lateral spreads or flows were about 175 km from the 1811-12 earthquake epicenters, according to Keefer (1984). O. W. Nuttli (St. Louis University, oral communication, 1983) has found historical accounts of sand boil activity on the flood plain of the Mississippi River, near St. Louis. Street and Nuttli (this volume) report sand blows and fissures in White County, Illinois, along the Wabash River. Both St. Louis and White County are less than 300 km from the probable epicentral region for the February 7, 1812, earthquake. (see fig. 8 for epicenter location). According to Street and Nuttli (this volume), the southernmost limit of the damaged area for the December 16 earthquake was Island 53 or Island 57, on the Mississippi River. It is possible that liquefaction caused the damage on these islands, which are about 350 km south of the probable epicenter for the December 16 earthquake (the probable December 16 epicenter is located later in this paper).

B. Other Historical Earthquakes

Table 4 is a compilation of central Mississippi Valley historical earthquakes having body-wave magnitudes equal to or higher than 5.3, and the associated accounts of liquefaction and Modified Mercalli (MM) intensities. Liquefaction was reported only for the 1895 earthquake (which is also known as the Charleston, Missouri, 1895 earthquake). Sand boils occurred at scattered locations over a region about 16 km in diameter, at places north of Charleston, in Charleston, and south and southwest of Charleston (Powell, 1975). This region where sand boils developed is in braided stream alluvium (see fig. 2) which is only a little less prone to liquefaction than at other places (excluding very young alluvium) in the Western Lowlands and St. Francis Basins. Thus, a reasonable threshold for liquefaction is m_b between 5.5 and 6.0, for braided stream and meander belt deposits in both basins, excluding deposits on modern flood plains. This assumes that back-calculated magnitudes are reasonably accurate.

C. Earthquake intensity and liquefaction

Table 4 has no reports of liquefaction for MM VII ^{1/} or lower. Alternately, the MM VIII area of the 1895 Charleston earthquake, with reports of sand boils, is in an area where the sediments are moderately dense and at least moderately difficult to liquefy. It seems incongruous that in table 4 there are no reports of liquefaction for the 1895 or any other earthquakes in loose flood plain deposits for MM VII, and yet liquefaction in moderately dense materials for MM VIII. The writer thinks it is probable that there were sand boils in the flood plain alluvium, and especially the very young (< 500 years old) alluvium for many of the MM VII-producing earthquakes, but the sand boils were not reported. Sand boils develop in the flood plain behind both natural and artificial levees along the Mississippi River after many of the largest annual floods, because of the large difference in hydraulic head on opposite sides of the levees, and the sand boils are so commonplace as to not receive special attention.

Figure 9 is a map by Nuttli (1981) showing regional intensity data for the December 16, 1811 earthquake. Locations of farthest sand boils (in the Mississippi River flood plain near St. Louis and the Wabash River valley) are in the zone of MM VII intensity. Thus, it is concluded that a regional MM VII is the liquefaction threshold for the loose flood plain sands, irrespective of earthquake magnitude. This intensity conforms to findings by Keefer (1984).

It might seem to follow that MM VIII is the threshold for the moderately dense Wisconsinan-age alluvium in the Western Lowlands and St. Francis Basins, but that does not seem to be true. Comparison of figure 9 with figure 7 shows that the outer bound of sand boils, in the southern third of sand boils deposits, does not extend beyond the boundary for MM X. Part of this discrepancy of MM
Table 4. Central Mississippi Valley historical earthquakes with

^{1/} Values in table 4 are regional, rather than absolute maximum values that are present within a region. At a given site, intensity values are commonly one unit higher or lower than regional values; site MM intensity values are two units higher in exceptional places.

Table 4. Central Mississippi Valley historical earthquakes with body-wave magnitudes greater than 5.2, exclusive of 1811-12 earthquakes: locations, intensities, and liquefaction.

| Location <u>1/</u> | Date | Modified <u>2/</u> Mercalli Intensity | Body-wave <u>1/</u> magnitude | Lique- faction <u>2/</u> |
|--|------------|---|----------------------------------|-----------------------------|
| Miss. Embayment 35.2 N. Lat. 90.5 W. Long. | 1-4-1843 | VIII (minimum) | 6.0 | none reported |
| Miss. Embayment 36.5 N. Lat. 89.5 W. Long. | 8-17-1865 | VII | 5.3 | none reported |
| Miss. Embayment 37.0 N. Lat. 89.4 W. Long. | 10-31-1895 | VIII | 6.2 | common- place |
| Miss. Embayment 36.9 N. Lat. 89.3 W. Long. | 11-4-1903 | VII | 5.3 | none reported |
| Wabash Valley 39.0 N. Lat. 87.6 W. Long. | 9-27-1909 | VII | 5.3 | none reported |
| Miss. Embayment 35.5 N. Lat. 90.3 W. Long. | 10-28-1923 | VII | 5.3 | none reported |
| Miss. Embayment 36.5 N. Lat. 89.0 W. Long. | 5-7-1927 | VII | 5.3 | none reported |
| Wabash Valley 38.0 N. Lat. 88.5 W. Long. | 11-9-1968 | VII | 5.5 | none reported |

1/ Reference: Nuttli and Herrmann, 1978.

2/ Reference: Coffman and von Hake, 1973.

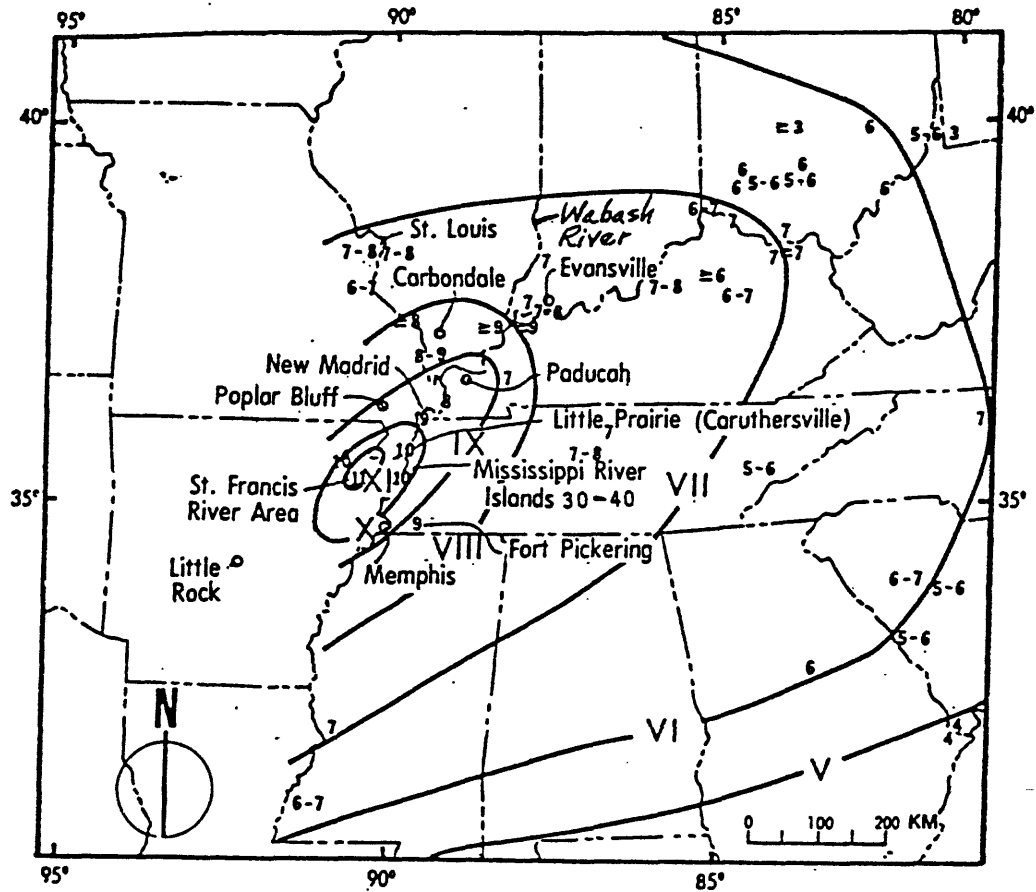


Figure 9. Modified Mercalli Intensities for the December 16, 1811 earthquake (from Nuttli, 1981).

intensity and liquefaction threshold is probably due to the fact that the MM intensity scale is often a crude measure of earthquake acceleration even for a given earthquake.

IV. Suggested Methods for Evaluating Liquefaction Potential

Acceleration, magnitude, intensity and liquefaction data are further evaluated to develop independent approaches for evaluating liquefaction potential.

A. Simplified Procedure of Seed and Idriss

The Simplified Procedure of Seed and Idriss requires an acceleration-epicentral distance relationship for various magnitude earthquakes, in order to be versatile. Data by Nuttli and Herrmann (this volume) are used in combination with the acceleration data at the margin of sand blows (this paper) to develop reasonable interrelations.

Figure 10 is a plot by Nuttli and Herrmann (this volume) showing the peak horizontal acceleration (average of two components) for stiff soil as a function of epicentral distance and body-wave magnitude, for the central United States. Although Nuttli and Herrmann do not state so in their text, their usage also implies that their epicenter is coincident with the point or zone of maximum energy release. The accelerations of figure 10 are based on semi-theoretical calculations, and are mean values. The error of estimate for one standard deviation for the Nuttli-Herrmann curves on figure 10 is a factor of 1.74. Nuttli (oral communication, 1983) has expressed to the writer, that whereas the acceleration values used to develop figure 10 may have a significant error of estimate, the attenuation relations are quite realistic.

The curves in figure 10 are intended to be applicable to stiff soil, (Nuttli and Herrmann, this volume). Stiff soils may amplify (probably amplify, based on calculations by Sharma and Kovacs, 1980) bedrock accelerations a small to moderate amount (that is, by a factor of 1.1 to 1.4) for small to moderate accelerations for earthquakes of the size (mainly $m_b < 5.5$) from which figure

Explanation

The dashed horizontal line is the most probable peak horizontal acceleration in alluvium for the range in possible distances, A and B, from the epicenter of the December 16, 1811, earthquake ($m_b = 7.1$); point C is the most probable distance. Point C' is the maximum possible peak horizontal acceleration in underlying bedrock, at distance C.

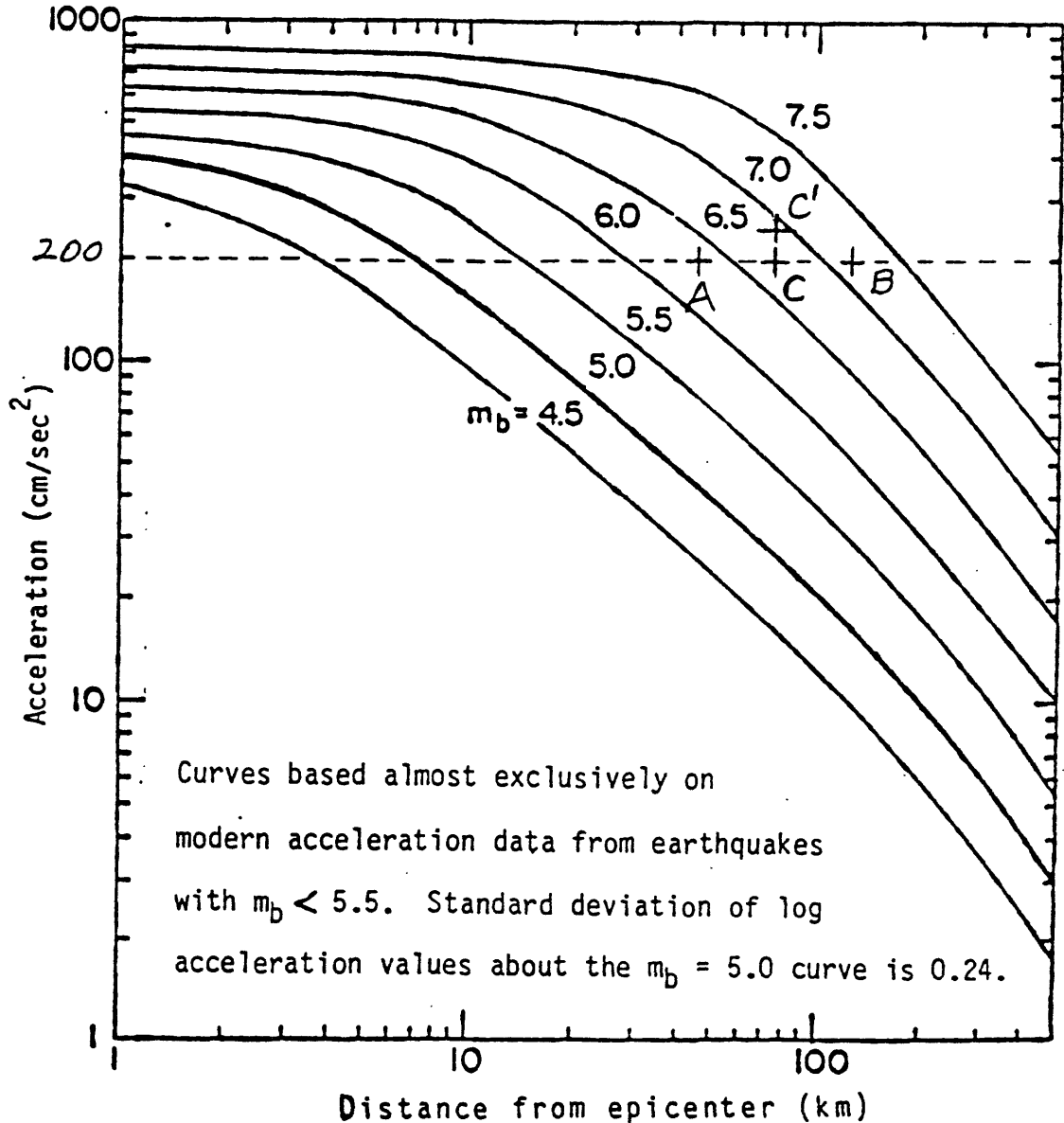


Figure 10. Curves for peak horizontal accelerations on stiff soils (arithmetic average of peak accelerations on the two horizontal components), versus epicentral distance for various body-wave magnitudes (from Nuttli and Herrmann, this volume); and back-calculated December 16, 1811, accelerations for St. Francis Basin alluvium (this paper).

10 was developed. The amount of amplification of unconsolidated materials also varies somewhat as a function of epicentral distance, acceleration level, and layer thickness. Thus, the basis for extrapolation to large earthquakes used for the Nuttli-Herrmann curves of figure 10, and the relations of the curves to bedrock motions are not clearly defined.

It is not possible to make direct comparisons between figure 10 and acceleration versus distance from the energy release center line for the December 16 earthquake, because the energy released may have varied along the fault, and because the epicenter may not have coincided with the zone of maximum energy release. However, for discussion purposes, it is assumed that the epicenter of the December 16 earthquake was coincident with the zone of maximum energy release (which is the matter of major concern for this study of liquefaction). With this constraint on the definition of epicenter, some bounds can be placed on acceleration as a function of distance from the epicenter.

The peak horizontal acceleration in bedrock for the December 16 earthquake, previously determined in this paper near the margin of sand boil deposits, was probably about 0.20g at 40 to 50 km from the southern terminus of the energy release center. Assuming that the energy released was uniformly distributed along the energy release line would conservatively yield a peak horizontal acceleration of 0.20g about 40 km from the epicenter. This is shown as point A in figure 10. Point A is almost certainly a lower bound of acceleration at this distance from the epicenter. The farthest northward location of an epicenter that is possibly associated with the pattern of sand boils is the northern end of the energy release line; if the epicenter was further north there should have been widespread liquefaction further northwest of New Madrid, in the braided stream deposits between Sikeston Ridge and Crowleys Ridge (fig. 2). Thus, as a

maximum, the peak horizontal acceleration was 0.20g at 110 km from the epicenter, along the axis of the energy release line. This is shown as point B on figure 10. This upper bound includes the maximum possible effects of focusing along a strike-slip fault. Point B is the point which the writer considers as the absurd upper limit. Almost certainly the northern limits of sand boils were the result of the February 7, 1812 earthquake, which probably had its epicenter near New Madrid (Nuttli, 1979).

The most reasonable epicenter for the December 16 earthquake is the center of the southernmost large area of very intense sand boil development, shown on figure 8. Throughout much of this large area the volume of liquefied sand that was vented to the surface was so great at most places as to make a continuous sheet of sand, 1 to 1.5 m thick. North of this area of the sand sheet, and northeast of the point showing Nuttli's December 16 epicenter, there are only localized places where the sheet of sand is continuous. This "most reasonable epicenter" is shown as point C on figure 10. The writer believes, therefore, that the most reasonable curve of acceleration as a function of epicentral distance, for m_b equal to 7.1 (equivalent to M_s of 8.5), goes through point C and is parallel to the curves for m_b equal to 7.0 and 6.5; point C is intended for both bedrock and moderately thick (30 - 50 m), moderately dense sand in the St. Francis Basin.

Also shown on figure 10 is a data point (C^1) that represents the upper bound of reasonable peak horizontal accelerations in bedrock at distance C from the epicenter. This upper bound is based on the premise that the accelerations based on figure 5 may be as much as 25 percent too low; this excludes consideration that peak accelerations in sand during the December 16 earthquake may have been 20 percent higher than the underlying rock (based on the study of bedrock-surface acceleration relationships anticipated for Memphis, Tennessee (Sharma and Kovacs,

1980). The acceleration at C^1 is 0.25g. Even assuming that for the December 16 earthquake the peak acceleration in sand at the border of sand boils was 20 percent lower than in bedrock, yields an acceleration at C^1 of 0.29g; this point on figure 10 falls almost exactly on the Nuttli-Herrmann curve for $m_b = 7.1$.

In summary, the curves by Nuttli and Herrmann indicate higher accelerations than the liquefaction-based data. It should be also noted that the Nuttli-Herrmann relations on figure 10 are the average of two components. Liquefaction, however, is controlled primarily by the peak component of acceleration (Seed and others, 1975). This again makes the Nuttli-Herrmann values seem too high.

It is suggested that for liquefaction analysis, it is reasonable to adjust the curves on figure 10 for bedrock accelerations for any value of m_b , by some type of simple scaling scheme. (For example, it would not seem unreasonable to reduce the acceleration by a factor of 20 percent; the set of curves would be for peak horizontal accelerations on bedrock.) The type of scaling method that one uses depends on the conservatism that is intended. Then, using the adjusted curves to determine the acceleration for the magnitude and epicentral distance in question, and adjusting the accelerations for local seismic response conditions that may affect the values (such as thickness of alluvium and dynamic modulus properties), the liquefaction potential can be assessed from figure 5. This assessment would be for movement along a strike-slip fault, along the axis of the fault, and thus would be an upper limit.

B. Magnitude method

Both theoretical calculations (Youd and Perkins, 1978) and field observations of liquefaction features (Kuribayashi and Tatsuoka, 1975; Youd, 1977; Youd and Perkins, 1978; Davis and Berrill, 1983; Keefer, 1984) demonstrate that there is a reasonably well-defined relationship between the farthest extent of significant liquefaction and distance from the epicenter, for a given

earthquake magnitude and a fixed susceptibility to liquefaction. The field observations were predominantly in Holocene-age silt, silty sand, or sand, which are materials that typically have moderate to high susceptibility to liquefaction during strong shaking (Youd and Perkins, 1978).

Figure 11 shows results based on field observations, and some suggested practical bounds on the limits of localized damaging liquefaction. The solid line is the outer limit of lateral spreads or flows, based on data by Davis and Berrill (1983) and by Keefer ^{1/} (1984) from more than 46 earthquakes scattered around the world. (Keefer's compilation includes both natural deposits and artificial fill.) Very probably, most of these data are from sites where there was at least 40 mm of differential vertical or lateral movement, which is adequate to damage structures that are very deformation-sensitive. Such structures include well-built underground pipes, concrete-lined canals, nuclear reactors, and poorly built buildings (especially old brick bearing-wall buildings). The dashed line is the best fit of data for all types of liquefaction-induced ground failure in Japan, including sand boils, reported by Kuribayashi and Tatsuoka (1975). The dotted line is the outer limit on natural deposits from all data sources for practical purposes, although rarely natural deposit data lie on the solid line, for the outer limit of reported data.

The articles cited with the data for the curves (solid, dashed, and dotted) on predominantly loose sediments do not report the thickness of sediments, and

^{1/} Smallest displacements reported in the paper by Keefer are at least 40 mm; however, at least some very few data points that Keefer shows in his figures could have had smaller displacements (Keefer, personal communication, 1984). For these reasons, it is presumed that for practical purposes the lateral displacements were greater than 40 mm.

In his original compilation, Keefer used moment magnitudes (M_w) for M values greater than 7.5; a replot of Keefer's data for figures 11 and 12 using surface wave magnitudes (M_s) shows basically no change in the curve of outer limit of reported data. Values of M_s for the replot of the 1811-12 earthquakes are from Nuttli (1983).

Explanation

- outer limit of reported data, lateral spreads or flows, very probably > 40 movement, predominantly loose and probably thin sediments; based on data from Davis and Berrill (1983) and Keefer (1984); damage to deformation-sensitive structures.
- - - best fit for all data in Japan, outer limit of marginal liquefaction, predominantly loose and probably thin sediments; curve from Kuribayashi and Tatsuoka (1975).
- ... outer limit on natural deposits for practical purposes, lateral spreads or flows, very probably > 40 mm movement, predominantly loose and probably thin sediments; based on data from Davis and Berrill (1983) and Keefer (1984); damage to deformation-sensitive structures. Curve applies to M_L values up to 5 and possibly slightly higher.
- data points, outer limits of sand boil deposits in St. Francis Basin alluvium exclusive of modern flood plain and very young meander deposits along Mississippi River and small streams.
- - - conservative outer limit for marginal liquefaction, moderately thick (30 - 50 m) sand deposits; data from this paper; damage to deformation-sensitive structures. Curve applies to M_L values equal 15 to 20.
- × data point, outer limit of reported damage possibly due to liquefaction for Dec 16, 1811, earthquake; data from Street and Nuttall (this volume).
- ⊙ data point, outer limit of reported sand boil deposits for Feb 7, 1812, earthquake; data from Street and Nuttall (this volume).
- + outer limit of reported data, lateral spreads or flows, very probably > 40 mm movement, predominantly loose sediments, 1811-12 earthquakes; based on data from Keefer (1984).

Magnitude greater than 5.5 are surface wave magnitudes (M_s); values less than 5.5 are Richter local magnitudes (M_L).

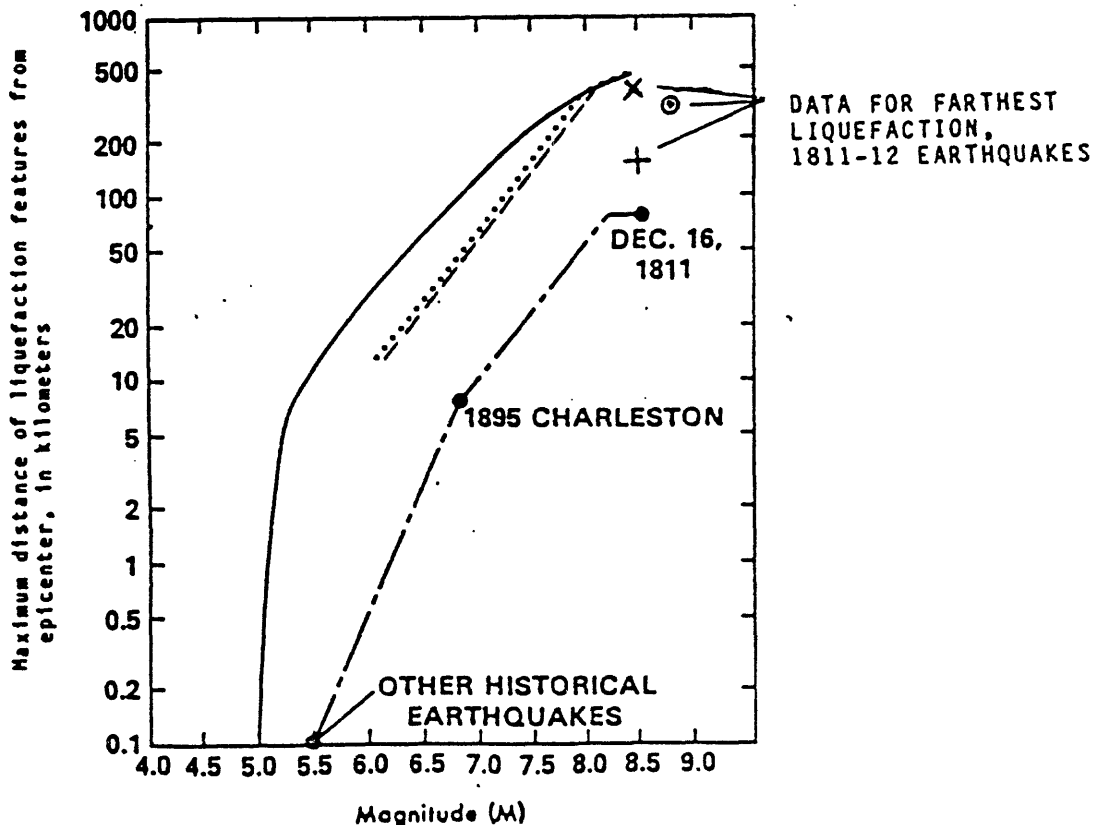


Figure 11. Maximum distance from epicenter of liquefaction in sand, as a function of earthquake magnitude (part of this figure is modified from Keefer, 1984).

possible bedrock acceleration amplifications. It is likely, though, that very considerable amplification (by a factor of 1.5 or more) occurred at many of the liquefaction sites, particularly where the sediments were thin.

Figure 11 also shows the farthest liquefaction from the 1811-12 earthquake epicenters. Three data points show the outer limit of damage possibly due to liquefaction, the outer limit of reported sand boil deposits, and the outer limit of lateral spreads or flows. Figure 11 shows that for the 1811-12 earthquakes, the outer limits of liquefaction did not extend an unusually large distance compared to other large earthquakes scattered around the world. This seems surprising at first, because of the huge area over which the 1811-12 earthquakes caused high MM intensities. It is possible that occurrences of sand boils and other liquefaction-induced features took place much further than 350 km from the epicenter (the farthest distance on fig. 11) and were not observed, but the writer does not believe that to be the case. In 1811, there were many settlers in western Kentucky and along the Ohio River valley, which has a wide flood plain westward from the mid-longitude of Indiana. This flood plain contains thick deposits of clean sand at many places. Natural levees along the Ohio River are generally small features and not very high, and sand boils caused by flooding are not commonplace. Surely, because they are unusual, sand boils caused by the 1811-12 earthquakes would have been noticed and reported. Instead, it is more likely that the alluvium in these flood plains is not as loose as at many of the other localities with liquefaction in figure 11. Probably, only sand bar, very young point bar and abandoned meander deposits less than 500 years old in the central Mississippi Valley region typically have very high susceptibility, and these would be the only materials liquefied at the outer limits from the epicenters. The dotted line in figure 11 is, therefore, believed to be a practical outer limit for very loose sands in the central Mississippi Valley.

Figure 11 also shows a conservative, yet not extremely conservative, outer limit for marginal liquefaction of alluvial deposits in the Western Lowlands and St. Francis Basin; modern flood plain and very young deposits are excluded. These limits were determined by using distance C on figure 10 as the maximum distance from the epicenter to the outer bound of liquefaction features for the December 16 earthquake (this is believed by the writer to be conservative because it is the distance on figure 8 from the center of high intensity sand boil development to the southwestward limit of sand boils). The distance from the center to the outer limit of sand boils near Charleston is used as distance from the epicenter for the 1895 earthquake; the Charleston data are based on a maximum diameter of 16 km for sand boils (based on information reported by Powell, 1975). The data from historical earthquakes in table 4 provide a third point at M equal to 5.5. The shape of the curve has also been chosen to be conservative. For magnitudes less than 8.2 and larger than 6.8, the slope is the same as for much weaker sands; the overall shape conforms to that of the outer limit (solid) line. This curve, for the limits of marginal liquefaction, probably represents the outer limits where there would be some serious structural damage to poorly built, old commercial or residential brick or block buildings and other deformation-sensitive structures, but well-built masonry buildings and houses would only be cracked. The curve applies to sands at least 30 m thick, with N_1 values equal to approximately 15 to 20.

As pointed out by Youd and Perkins (1978), epicentral distance is not a very good measure for the type of correlation in figure 11 because the epicenter does not define the entire zone of energy release, particularly for large earthquakes. They suggested, therefore, that the seismic source zone (or fault rupture zone) is a better point of reference. A plot showing the maximum distance of lateral spreads and flows from the fault-rupture zone by Keefer

(1984) is the primary basis for figure 12. Figure 12 shows the following: for practical purposes the outer limit for lateral spreads or flows with greater than 40 mm of movement in predominantly loose sediments (solid line); the outer limit (from Youd and Perkins, 1978) for greater than 100 mm of movement in predominantly loose sediments (dashed line); and the practical outer limit for marginal liquefaction in St. Francis and Western Lowlands Basins alluvium, exclusive of modern flood plain and very young deposits (long-and short-dashed line). Youd and Perkins selected 100 mm as the minimum displacement required to cause significant damage to most structures.

Fault rupture locations for the 1811-12 earthquakes were estimated from fault zones on figure 8. For the December 16 earthquake, the fault zone north of Marked Tree was used as the reference point from which to measure the farthest liquefaction, which was taken to be the outer bound of sand boils southwest of Marked Tree. For the February 7 earthquake, the fault zone at Reelfoot Lake was used as the reference point, and the farthest liquefaction was taken to be northernmost bound of sand boils in the braided stream deposits between Sikeston Ridge and Crowleys Ridge. The fault rupture for the 1895 Charleston earthquake was the location central to the margin of sand boils.

Because the bound by Youd and Perkins is based on so few data, especially for M values less than about 7, it is suggested that the dashed line is a moderately but not highly conservative limit for potentially damaging liquefaction in natural loose deposits (N_1 values equal to about 5 or less). The dashed-dotted line is thought to be a rather conservative bound for the alluvium in the St. Francis and Western Lowlands Basins alluvium, except for deposits on modern flood plains and very young alluvium. The dashed or solid line should be used for the very young alluvium.

Explanation

- outer limit of reported data, lateral spreads or flows, very probably > 40 mm movement, predominantly loose and probably thin sediments; based on data from Keefer (1984); damage to deformation-sensitive structures.
- - - practical outer limit, lateral spreads or flows, > 100 mm movement, predominantly loose and probably thin sediments; curve from Youd and Perkins (1978); damage to most structures. Curve applies to N_1 values up to 5 and possibly slightly higher.
- data points and practical outer limit for marginal liquefaction, moderately thick (30 - 50 m) sand deposits; data from this paper; damage to deformation-sensitive structures. Curve applies to N_1 values equal (5 to 20).

Magnitude greater than 5.5 are surface wave magnitudes (M_s); values less than 5.5 are Richter local magnitudes (M_L).

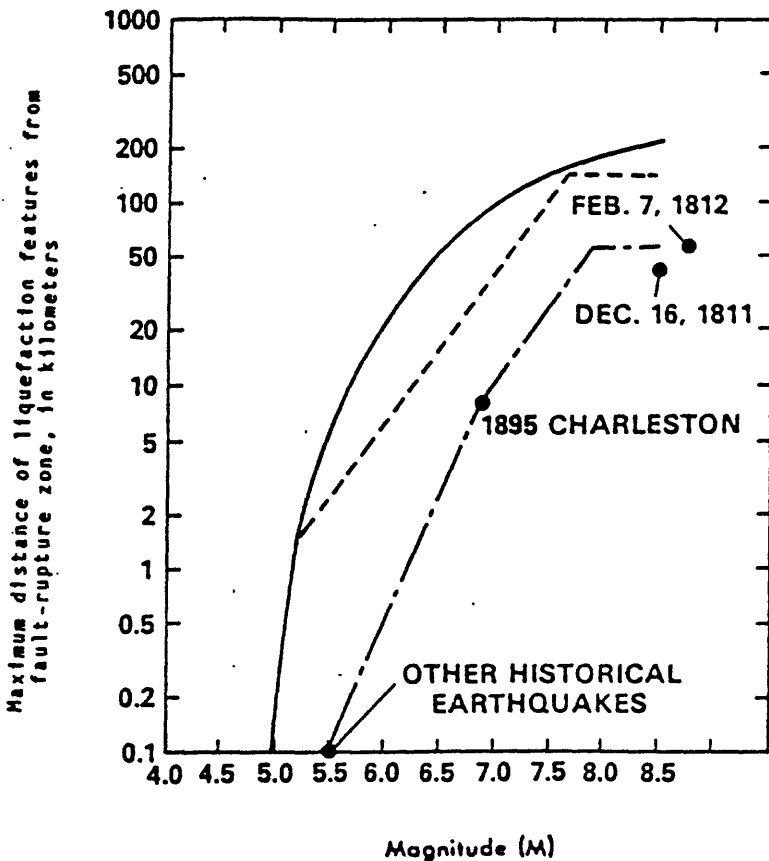


Figure 12. Maximum distance from fault-rupture zone of liquefaction in sand, as a function of earthquake magnitude (part of this figure is modified from Keefer, 1984).

New

V. Application of methods

Both the Simplified Procedure of Seed and Idriss (with acceleration-epicentral distance curves on fig. 10) and the magnitude method are conservative approaches for estimating where liquefaction is likely to occur, in that they over-estimate the geographic region. Both methods show only the farthest limits, accounting for effects such as focusing of energy from the epicenter or source fault. Focusing can cause a major distortion in the pattern of ground shaking, as illustrated by the Modified Mercalli intensity contours on figures 9 and 13. Figure 9 shows regional intensity contours for the December 16 1811, earthquake, with intensity values which are approximately average values; figure 13 is a hypothetical maximum regional intensity map for an 1811-size earthquake having an epicenter anywhere in the New Madrid seismic zone (that is, the zone of present intense microseismicity).

Figure 13 is based on data from earthquakes listed in table 4. Intensity data from all the larger historical earthquakes (1811, 1843, 1895) with epicenters roughly in the zone of most frequent modern seismic activity (Stauder, 1982), extending from approximately Marked Tree to Cairo, have MM intensity values VII and higher that are consistently strongly focused in much the same geographic area. Hopper and others (1983) found that the largest MM intensities are in a region oriented approximately parallel to the zone of modern seismicity, and in addition there is some focusing near the Mississippi River, extending from near Cairo toward St. Louis. The map for figure 13 was made by drawing MM intensity contour maps for the 1843 and 1895 earthquakes, and then scaling them to the 1811 earthquake. For example, the highest MM intensity for the 1895 earthquake was VIII, and the highest for 1811 was XI; thus a value of III was added to all the 1895 values. Intensity values in figure 13 approach being the

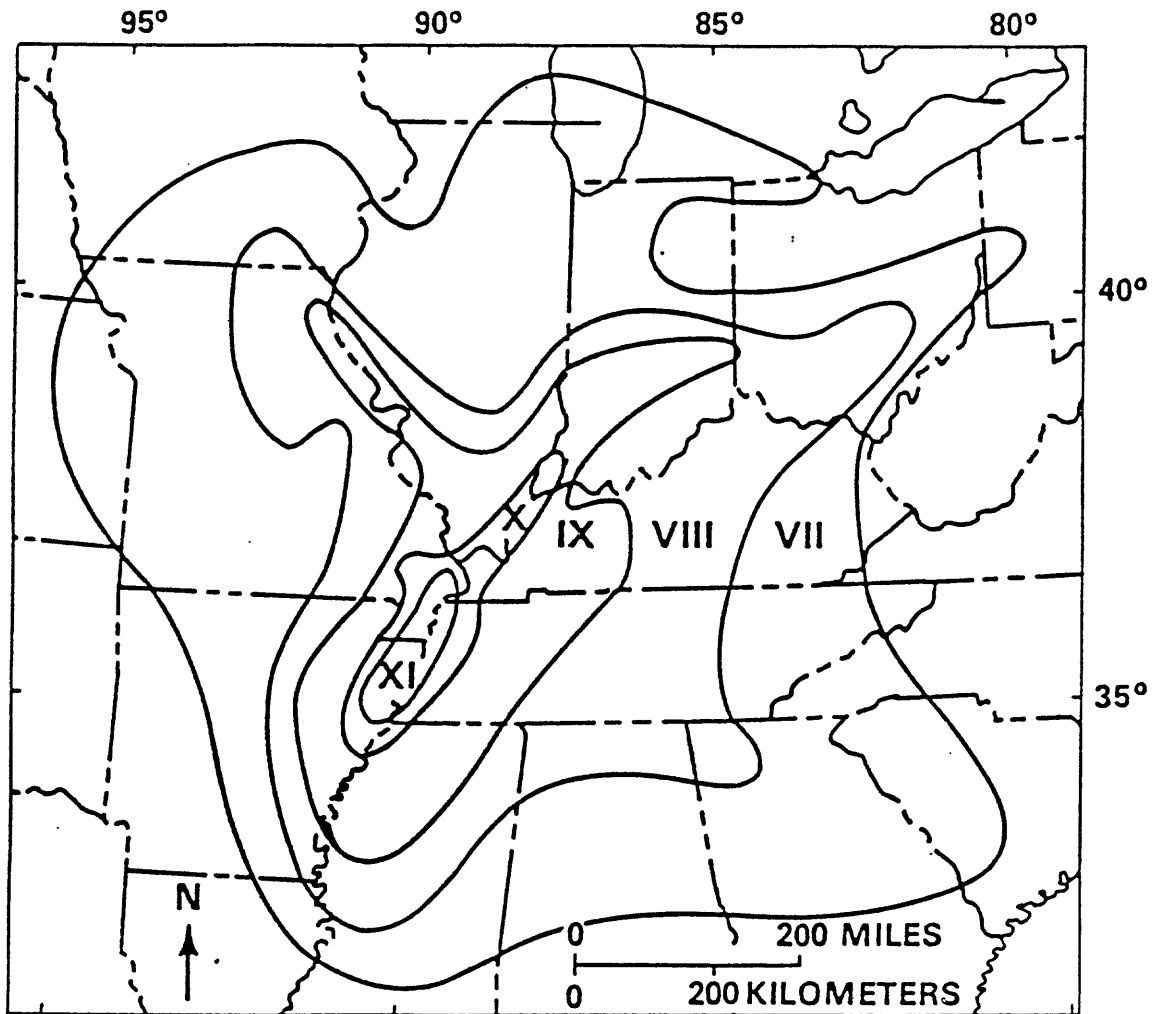


Figure 13. Hypothetical regional intensity map showing maximum intensity values for an 1811-size earthquake having an epicenter anywhere along the New Madrid seismic zone (from Hopper and others, 1983).

highest that can be expected in a region, accounting for the influence of both focusing of energy and amplification of bedrock motions in weak soil.

Although figure 9 and 13 show that there are large variations in shaking severity as a function of distance from the epicenter, presently it does not seem practical or realistic to try to quantify these variations for other than 1811-size earthquakes. Instead, it is suggested that estimates of the farthest limits of liquefaction be based on both the Simplified Procedure of Seed and Idriss and the magnitude method; in addition, relations between epicentral distance, MM intensity, and acceleration published elsewhere (for example, Nuttli and Herrmann, this volume; Krinitzsky and Marcuson, 1983) should be consulted.

Where MM intensity relations are used, it should be kept in mind that for practical purposes, an average regional value of MM VII is the liquefaction threshold for modern flood plain deposits, which have loose sands. For a map of maximum intensity values, such as figure 13, MM VIII is the threshold for minor occurrences of liquefaction of extremely loose sediments with highly amplified bedrock motion; for figure 13, MM IX is probably the intensity threshold where damaging liquefaction is relative commonplace in loose sands.

The final judgment of whether or not potential problems exist must be based on the consequences of an occurrence of liquefaction. For example, if all methods show a high probability of liquefaction exists, and a critical structure is involved, then some sort of mitigation is in order. For other than critical structures, the decision may be quite subjective.

VI. Liquefaction Susceptibility and Geologic Origin

The texture, mode of deposition, and age of deposits affect liquefaction potential in a generally predictable way (Youd and Perkins, 1978), as discussed in earlier sections. Based on these criteria, sediments in the central Mississippi Valley can be categorized for susceptibility to liquefaction on a

regional basis, using surficial geologic map units. Surficial geologic maps are available in all States at a scale of 1:1,000,000, and in some States at scales which show much more detail. Maps at a scale of 1:62,000 or 1:24,000 are more optimal, but are generally available only for localized areas.

Many of the deposits on the State maps have formation names, which may change at a State boundary. For that reason, names are not used in this discussion, but rather the geologic origin and age are used as a basis. Liquefaction potential is given in terms of N_1 values whenever possible.

A. Braided stream and meander belt deposits.

The properties of Wisconsinan-age braided stream terraces made up of glacial deposits and Mississippi River meander belt deposits on figure 2 have been described previously in the text and in table 2, and will only be summarized here. Median N_1 values are generally near 25 in the upper 15 m, and increase slightly with depth. Rarely, N_1 values are as low as 10 to 12 in the upper 15 m. There are abundant thick, clean sands which fine-upward to a thin stratum of fine or silty sand just beneath a clay-rich cap, 3 to 6 m thick. Glacial deposits having about the same properties are present at many places along many of the larger streams which carried glacial outwash. The Wabash, and Ohio Rivers laid down especially large volumes of clean sand in Illinois and Indiana. Thicknesses of 30 m are not unusual.

Although rivers further south did not carry glacial outwash, many have terraces Late Wisconsinan in age or older, that are dominantly thick clean sands. The Obion River in Tennessee has some especially large terraces. The terrace deposits along the southern rivers probably have about the same resistance to liquefaction as the braided stream deposits in the St. Francis and Western Lowlands Basins, because they are all about the same age and all have minerals with about the same physical properties.

B. Glacial lake deposits.

Large glacial lakes formed along many rivers carrying glacial meltwater, particularly in Indiana, Illinois, and Kentucky. Many of these glacial lakes laid down thick deposits of sand, silt, and clay. At many places there is a fining-upward tendency from a basal sand. Thicknesses of 15 m are commonplace.

Near large streams, thick and unusually loose sands (N_1 about 8) about 6 m deep are at many places. At most other places the sands are denser and have much higher N_1 values. Very soft silts and clays with SPT blow counts of 2 to 3 are relatively common in lower elevation places near streams throughout Indiana, Illinois, and Kentucky. The higher, better drained sites typically have much higher blow counts due to effects of dessication and a lower ground water table.

C. Modern flood plain deposits, exclusive of very young sediments.

Very young sediments less than about 500 years old are excluded from the class of modern flood plain deposits. Modern flood plains along major streams generally have thick strata of clean sand, silt, and clay. The sands generally have median N_1 values of about 20, though locally median N_1 values of 15 are commonplace. Silt-rich strata in some abandoned channels are so soft as to be potentially subject to liquefaction.

D. Very young sediments.

Very young sediments are defined as being less than 500 years old, because older sediments generally have much greater resistance to liquefaction (Youd and Perkins, 1978). Very young sediments typically border streams as point bars, or are sand bars in streams. However, very young meander cut-offs can be far from large streams. N_1 values less than 10 are very common, in sands. Very young meander cut-offs also contain very loose and very soft sediments at many places.

E. Eolian deposits.

Thick loess deposits are present in upland areas near the major streams that carried large volumes of glacial meltwater.

The Wabash and Mississippi Rivers have especially thick deposits on nearby uplands, especially east of the rivers. Near the rivers, thicknesses of 20 to 25 m are not unusual. The loess is predominantly silt, with almost no cohesion at some places. Even clayey silt loess can have an extremely low cohesion and sensitivity ^{1/} as high as 10, and is potentially subject to liquefaction with large shear straining or flowing (Randall Jibson, U. S. Geological Survey, personal communication, 1984). Locally, and especially near large rivers, loess has lenses of clean, very loose dune sand or water-deposited strata of clean sand. In the highly dissected upland areas with thick loess, the loess may be only locally or partly saturated far beneath the ground surface, and thus not very prone to liquefaction at most places. It is probable, though, that where the ground water table is high, slopes in loess are potentially subject to flowing failure during earthquakes. The writer is unaware of any soil mechanics, dynamic laboratory test data on loess in the area.

F. Reworked eolian deposits.

At the base of the high loess bluffs along major rivers, there is generally a veneer of silt washed down from the hills. This veneer is 6 m thick at many places, and in lowland areas is commonly very soft. Clearly many of these sediments are weak enough to liquefy in moderate to severe shaking, though in most cases liquefaction would probably be accompanied by limited straining. To the writer's knowledge, the only data relevant to evaluation of dynamic behavior of reworked eolian materials is in Puri (1983).

^{1/} Sensitivity is defined as the ratio of undisturbed unconfined compressive strength divided by the remolded unconfined compressive strength.

VII. Summation

There are so few data on strong earthquakes that all the methods most commonly used for evaluating liquefaction potential, based on accelerations, magnitudes, or intensities are somewhat suspect. Even a regional assessment should be based on results from more than one method and requires a considerable amount of judgment.

There are many large terraces and flood plains in the central Mississippi Valley region which contain moderately dense to loose clean sands and silty sands. Evaluation of their liquefaction potential is reasonably easy and straightforward, providing the acceleration-magnitude relations are known. However, there are also many thick glacial lake deposits, eolian deposits, and reworked eolian deposits made up of silt-rich materials of highly varying liquefaction potential. Field methods for assessing their properties are extremely crude at best, and there appear to be so few laboratory data that there are no guidelines based on simple criteria such as void ratio, cohesion, and plasticity characteristics. It should be a relatively simple matter to do such a thing.

Earthquake accelerations have a very important role in liquefaction. The back-calculated accelerations presented in this paper for the 1811 earthquake have some degree of uncertainty, but the writer believes they are accurate within 25 percent.

References Cited

- American Society for Testing and Materials, 1978, Annual book of ASTM standards, pt. 19, Designation D 1586-67 (Reapproved 1974), Standard method for penetration test and split barrel sampling of soils: Philadelphia, Pa., p. 235-237.
- Anderson, L. R., Keaton, J. R. Aubry, K., and Ellis, S. J., 1982, Liquefaction potential map for Davis County, Utah: Dames and Moore Consulting Engineers, Salt Lake City, Utah, 49 p.

- Bennett, M. J., Youd, T. L., Harp, E. L., and Wieczorek, G. F., 1981, Subsurface investigation of liquefaction, Imperial Valley Earthquake, California, October 15, 1979: U.S. Geological Survey Open-file report 81-502, 83 p.
- Coffman, J. J., and von Hake, C. A., 1973, Earthquake history of the United States: U.S. Department of Commerce, National Oceanic and Atmospheric Administration, Publication 41-1, 208 p.
- Davis, R. O., and Berrill, J. B., 1983, Comparison of a liquefaction theory with field observations: The Institution of Civil Engineers, London, Geotechnique, vol. XXXII, no. 4, p. 455-460.
- Fuller, M. L., 1912, The New Madrid earthquake: U.S. Geological Survey Bulletin 494, 119 p.
- Hamilton, R. M., and Zoback, M. D., 1982, Tectonic features of the New Madrid seismic zone from seismic reflection profiles: in McKeown, F. A. and Pakiser, L. C., ed., Investigatins of the New Madrid, Missouri, earthquake region: U.S. Geological Survey Professional Paper 1236, Chapter F.
- Hopper, M. G., Algermissen, S. T., and Dobrovolny, E. E., 1983, Estimation of earthquake effects associated with a great earthquake in the New Madrid seismic zone: U.S. Geological Survey, Open-file report 83-179, 94 p.
- Housner, G. W., 1958, The mechanism of sandblows: Bulletin of the Seismological Society of America, v. 48, p. 155-161.
- Keefer, D. K. (1984), Landslides caused by earthquakes: Geological Society of America Bulletin, v. 95, p. 406-421.
- Krinitzsky, E. L., and Marcuson, W. F., 1983, Principles for selecting earthquake motions in engineering design: Bulletin of the Association of Engineering Geologists, v. xx, no. 3, p. 253-265.
- Kuribayashi, E., and Tatsuoka, F., 1975, Brief review of liquefaction during earthquakes in Japan: Soils and Foundations, v. 15, no. 4, p. 81-92.
- Mosaic, July/August, 1979, When soils start to flow, v. 10, no. 4, p. 26-34.
- Nuttli, O. W., 1979, Seismicity of the central United States: in Geology in the siting of nuclear power plants; Reviews in Engineering Geology (Hatheway, A. W., and McClure, C. R. Jr., eds.), v. 4, The Geological Society of America, p. 67-93.
- Nuttli, O. W., 1981, Evaluation of past studies and identification of needed studies of the effects of major earthquakes occurring in the New Madrid fault zone: A report submitted to Federal Emergency Management Agency Region VII, Kansas City, Missouri, 28 p.
- Nuttli, O. W., 1983, Empirical magnitude and spectral scaling relations for mid-plate and plate-margin earthquakes: in Quantification of earthquakes (Duda, S. J., editor; et. al.), Tectonophysics, v. 93, no. 3-4, p. 207-223.

- Nuttli, O., and Herrmann, R. B., 1978, State-of-the-art for assessing earthquake hazards in the United States--Credible earthquakes for the central United States: U.S. Corps of Engineers, Papers 5-13-1, report 12, 99 p.
- Nuttli, O. W., and Herrmann, R. B., 1981, Consequences of earthquakes in the Mississippi Valley: Preprint 81-519, American Society of Civil Engineers, Conference at St. Louis, Missouri, Oct. 26-31, 1981, 13 p.
- Nuttli, O. W., and Herrmann, R. B., 1982, Earthquake magnitude scales: American Society of Civil Engineers Proceedings, Journal of the Geotechnical Engineering Division, v. 103, no. GT 5, p. 783-786.
- Nuttli, O. W., and Herrmann, R. B., 1984, Ground motion of Mississippi Valley earthquakes: Journal of Technical Topics in Civil Engineering, American Society of Civil Engineers, v. 110, v. no. 1, p. 54-69.
- Powell, B. F., 1975, History of Mississippi County, Missouri, beginning through 1972: BLN Library Service, Independence, Missouri.
- Puri, V., 1983, Liquefaction behavior and dynamic properties of loessial (silty) soils, unpublished Ph. D. thesis, University of Missouri-Rolla, Rolla, Missouri, 295 p.
- Russ, D. P., 1982, Style and significance of surface deformation in the vicinity of New Madrid, Missouri: in McKeown, F. A. and Pakiser, L. C., ed., Investigations of the New Madrid, Missouri, earthquake region: U.S. Geological Survey Professional Paper 1236, Chapter H.
- Saucier, R. T., 1964, Geological Investigation of the St. Francis Basin, lower Mississippi Valley: U.S. Army Corps of Engineers, Waterways Experiment Station Technical Report 3-659.
- Saucier, R. T., 1974, Quaternary geology of the lower Mississippi Valley: Arkansas Archeological Survey, Research Series No. 6, 26 p.
- Saucier, R. T., 1977, Effects of the New Madrid earthquake series in the Mississippi alluvial valley: U.S. Army Engineer Waterways Experiment Station, Miscellaneous paper S-77-5, 10 p.
- Seed, H. B., 1968, Landslides during earthquakes due to soil liquefaction: American Society of Civil Engineers Proceedings, Journal of the Soil Mechanics and Foundations Division, v. 93, no. SM 5, p. 1055-1122.
- Seed, H. B., 1979, Soil liquefaction and cyclic mobility for level ground during earthquakes: American Society of Civil Engineers Proceedings, Journal of the Geotechnical Engineering Division, v. 105, no. GT2, p. 201-255.
- Seed, H. B., and Idriss, I. M., 1971, Simplified procedure for evaluating soil liquefaction potential: American Society of Civil Engineers Proceedings, Journal of the Soil Mechanics and Foundations Division, v. 97, no. SM9, p. 1249-1273.
- Seed, H. B., and Idriss, I. M., 1982, Ground motions and soil liquefaction during earthquakes: Earthquake Engineering Research Institute; Monograph series: Engineering monographs on earthquake criteria, structural design, and strong motion records; Berkeley, California, 134 p.

- Seed, H. B., Idriss, I. M., and Arango, I., 1983, Evaluation of liquefaction potential using field performance data: American Society of Civil Engineers Proceedings, Journal of the Geotechnical Engineering Division, v. 109, no. 3, p. 458-482.
- Seed, H. B., Idriss, I. M., Makdisi, F., and Bannerjee, N. 1975, Representation of irregular stress time histories by equivalent uniform stress series in liquefaction analyses: Earthquake Engineering Research Center, University of California, Berkeley, California, Report no. EERC 75-28, 13 p.
- Sharma, Sunil; and Kovacs, W. D., 1980, Microzonation of the Memphis, Tennessee, area: Report no. 14-08-0001-17752, Purdue University, West Lafayette, Indiana, 129 p.
- Smith, F. L. and Saucier, R. T., 1971, Geological investigations of the Western Lowlands area, lower Mississippi valley: U.S. Army Engineer Waterways Experiment Station, Corps of Engineers, Vicksburg, Mississippi, Technical Report No. S-71-5.
- Stauder, W., 1982, Present day seismicity and identification of active faults of the New Madrid seismic zone: in McKeown, F.A. and Pakiser, L. C., eds., Investigations of the New Madrid, Missouri, earthquake region: U.S. Geological Survey Professional Paper 1236, Chapter C.
- Tokimatsu, K., and Yoshima, Y., 1981, Field correlation of soil liquefaction with SPT and grain size: Proceedings of International Conference on Recent Advances in Geotechnical Earthquake Engineering and Soil Dynamics, University of Missouri-Rolla, April 26 - May 3, 1981, v. 1, p. 203-208.
- Youd, T. L., 1973, Liquefaction, flow, and associated ground failure: U.S. Geological Survey Circular 688, 12 p.
- Youd, T. L., 1977, Discussion of brief review of liquefaction during earthquakes in Japan by Eiichi Kuribayashi and Fumio Tatsuoka, 1975, in (Soils and Foundations, v. 15, no. 4, p. 81-92): Soils and Foundations, v. 17, no. 1, p. 82-85.
- Youd, T. L., 1978, Major cause of earthquake damage is ground failure: Civil Engineering, American Society of Civil Engineers, v. 48, no. 4, April, p. 47-51.
- Youd, T. L., and Bennett, M. J., 1983, Liquefaction sites, Imperial Valley, California: American Society of Civil Engineers Proceedings, Journal of the Geotechnical Engineering Division, v. 109, no. 3, p. 440-457.
- Youd, T. L., and Hoose, S. N., 1978, Historic ground failures in northern California triggered by earthquakes: U.S. Geological Survey Professional Paper 993, 177p.
- Youd, T. L., and Perkins, D. M., 1978, Mapping liquefaction-induced ground failure potential: American Society of Civil Engineers Proceedings, Journal of the Geotechnical Engineering Division, v. 104, no. GT4, p. 433-446.

**A LOOK AT THE PRESENT STATE-OF-KNOWLEDGE ON EARTHQUAKE HAZARDS
IN THE NEW MADRID SEISMIC ZONE AND SUGGESTIONS FOR FUTURE RESEARCH**

by

Walter W. Hays

U.S. Geological Survey

Reston, Virginia 22092

INTRODUCTION

Since 1811-1812 when the New Madrid earthquakes occurred, many investigators have contributed to the state-of-knowledge of the earthquake hazards of ground shaking, earthquake induced ground failures, tectonic deformation, and the mechanisms of faulting in the New Madrid seismic zone. Progress, although slow, has come in direct proportion to and as a consequence of multidisciplinary research studies which have synthesized geologic, geophysical, seismological, and engineering data to evaluate individual earthquake hazards and to assess the risk. These studies have focused on complex topical subjects, such as:

- 1) The relation of seismicity to ancient rifts and aulacogens.
- 2) The relation of seismicity to plutons.
- 3) The relation of the gravity and magnetic fields of the Mississippi embayment to thick masses of post-Paleozoic sediments and crustal and mantle upwarping.
- 4) The use of seismic reflection and refraction data to define the three dimensional structure and trenching to define recurrence intervals.

- 5) The reason for the contrast in seismicity between northeast trending structures (seismically active) and northwest trending structures (seismically inactive) even though both structure trends are suitably oriented with respect to the east-west stress field.
- 6) The possibility of block uplift and tilting of the Ozarks about a northeast-striking axis as a consequence of contemporary stresses in the embayment rather than as a consequence of ambient stresses associated with interacting continental plates.
- 7) The physical characteristics (amplitude, spectral composition, attenuation rate, and duration) of ground motion.
- 8) The physical processes controlling the spatial and temporal phenomena of ground failure, tectonic deformation, and faulting.

The objective of this paper is to utilize the approach of Janus, the Roman god who could simultaneously look backward to see where he had been and forward to see where he was going. If we had Janus' ability, research in earthquake hazards in the New Madrid seismic zone would be easier. Although we lack this ability we can use the concept and the opportunity provided by this symposium to evaluate our progress in basic research and to suggest the directions of future research that will have the greatest payoff.

CURRENT STATUS OF KNOWLEDGE ON EARTHQUAKE HAZARDS

Although no standard methodology exists for evaluating the earthquake hazards in the New Madrid seismic source zone, (Figure 1) or any other region of the nation, research has produced several methodologies that can be used. The methodology that is used (whether deterministic or probabilistic) seeks answers to the following questions:

- 1) Where have past earthquakes occurred? Where are they occurring now?
- 2) Why are they occurring?
- 3) How big are the earthquakes and what hazards do they cause?
- 4) How often does each hazard occur?
- 5) What are the physical characteristics (amplitude or severity, frequency of occurrence, and duration) of each hazard and their physical effects on buildings and other facilities?
- 6) What are the options for mitigation measures (earthquake-resistant design, land use, and building codes)?

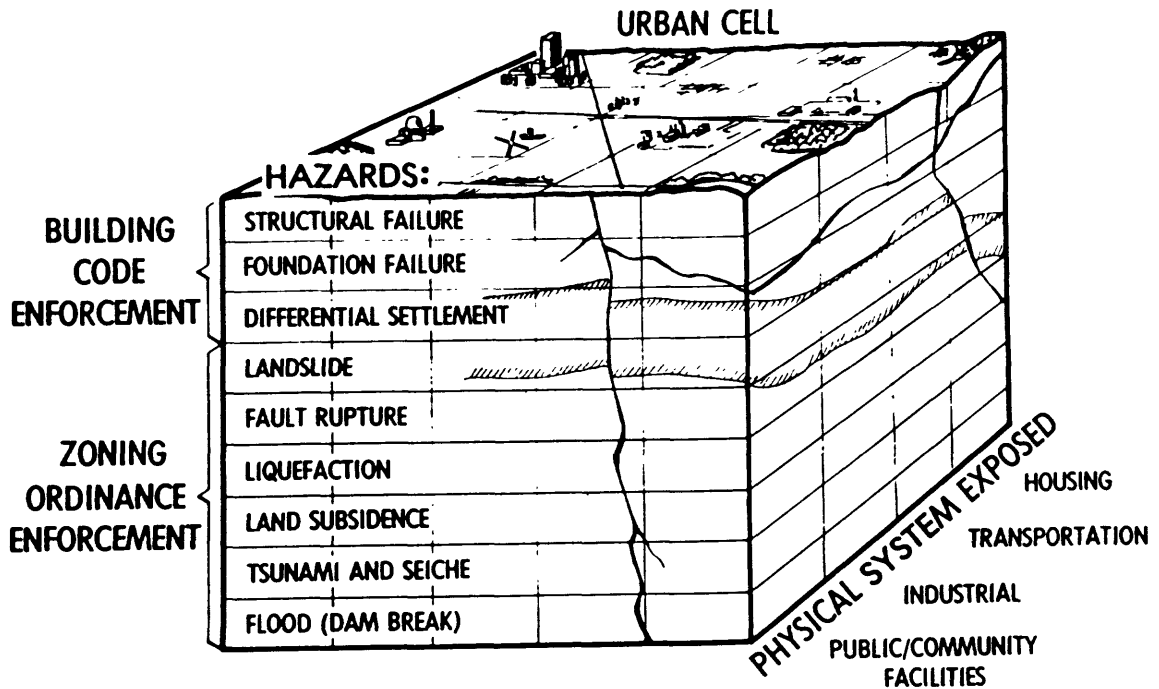


Figure 1.--Schematic illustration of a typical community in the New Madrid seismic zone having physical systems (public/community facilities, industrial, transportation, and housing) exposed to earthquake hazards of ground shaking, earthquake-induced ground failure, tectonic deformation and potential surface faulting. Evaluation of the earthquake hazards provides policy makers with a sound physical basis for choosing mitigation strategies such as: avoidance, land-use planning, engineering design, and distribution of losses through insurance. Because of buried faults, the task of evaluating the earthquake hazards in the New Madrid seismic zone is a complicated research problem.

THE PAST IS THE KEY TO THE PRESENT

When we look back into the past we can clearly see the progress that the scientific community has made in increasing knowledge of earthquake hazards in the New Madrid seismic zone. Portions of 6 publications in the Bulletin of the Seimological Society of America are quoted below to illustrate: a) the types of research questions that have been articulated either explicitly or implicitly since 1911, and b) some of the problems and obstacles that have been successfully met. These quotations, combined with the results presented at this symposium, show that:

- 1) The state-of-knowledge of earthquake hazards in the New Madrid seismic zone has increased substantially.
- 2) Better research questions are being asked today and detailed answers are still needed for: a) vulnerability studies, b) specification of seismic design parameters for buildings, lifeline systems and critical facilities, and c) the assessment of risk (chance of loss).

Quotation from "Seismology in the United States" by Andrew C. Lawson, March 1911.

"Until within a very few years, the United States was far behind many other countries in its equipment for the study of earth vibrations, their rate of propagation, and their paths and in the number of men interested in it. . . . We are not bestirring ourselves. This awakening interest in the phenomena of earthquakes dates chiefly from the California earthquake of 1906.

There is an important department of seismology which can be pursued to advantage only by world-wide cooperation. I refer to the instrumental study of earthquakes . . . of such great violence that their vibrations extend to all parts of the earth's surface and may be recorded by suitable apparatus. The determination of the time of arrival, intensity of the components of motion and duration of the different phases of these vibrations, at a sufficient number of stations distributed over the face of the earth) affords data of the highest importance. . . ."

Now when we stop to review the spread of these installations in the United States during the past few years, we cannot fail to be impressed with the fact that it is due to local spontaneity and that the distribution of the stations is guided by no guiding principle. Their position has been determined by accident rather than by design. . . . It is evident . . . that our seismological activities are unorganized.

Another . . . phase of seismological work which has received but little attention in this country is that which is concerned with seismically active regions. . . . In such regions where small earthquakes occur frequently and disastrous shocks occasionally, the proper investigation of the conditions which obtain in the earth's crust necessitates a combination of geological field work with instrumental observations recorded at numerous stations. . . . The work requires a corps of observers who shall give about an hour daily to the apparatus. . . . It requires also a small number of active field geologists who are specialists in structural and physiographic geology. . . . The work . . . would result in not only the precise location of all the various faults which by recurrent movement produce earthquakes with the region, but it would also enable us to become familiar with the progress of fault movements.

For such an undertaking, having to do with natural conditions and processes which affect humanity so seriously, it might be supposed that funds would be readily forthcoming. But such is not the case. In the present State of public opinion in California, for example, it is practically impossible to secure state aid for the study of earthquakes. . . . An appeal was made to Congress to establish a Bureau of Seismology under the Smithsonian Institution with support of \$20,000; the bill which was introduced for the purpose was killed in committee.

Another phase of seismological research which would be greatly advanced by a proper organization . . . would comprise those studies which are necessary on the occurrence of a first class earthquake anywhere within our borders, . . . as in the case of the 1886 Charleston and 1906 California earthquakes."

Quotation from "The Observation of Earthquakes," by H. O. Wood.

"From the point of human welfare, the problems of first importance are these: when and where will strong shocks occur in the future, and what conditions, which are subject to human control, tend to mitigate their disasterous consequences.

At the present state of knowledge, we are, in general, unable even roughly to foretell the time of occurrence of shocks. There is hope of progress in this direction, but no immediate solution of the problem is expected.

The place where shocks will occur, however, and what the conditions are which may modify or control their behavior, we can already determine in

advance with considerable accuracy. We know something, however little, about the geological causes of earthquakes and of their action under diverse geological and structural conditions. In order to determine more precisely when they are most likely to originate and to cause disaster, as well as the conditions which lessen or increase their dangers, we must carry on investigations in greater detail than has yet been done regarding the relations between the places of origin and the distribution of the perceptible effects of shocks; the relation between these effect and the geological character of the ground where they occur; how the character of structures affects the degree of the disaster--in short, the inter-relationship of all these things, place of orgin, phenomena, character of ground and of structures, through the whole area in which the shocks is felt perceptibly.

In regions where earthquakes occur frequently, we need to correlate their place of origin, to compare their significant surface phenomena, to determine their distribution in time and space, all with relation to the geologic structure in the district,--seeking thus to bring to light the immediate geological cause of the whole series of shocks and its mode of operation, whether this cause is acting permanently or only temporarily in the human sense, and whether the shocks come periodically or in a wholly sporadic way."

Quotation from "The New Madrid and Other Earthquakes in Missouri," by F. A. Sampson, June 1913.

"James MacFarlane of Towanda, Pennsylvania, presented a paper in 1883 to the American Association for the Advancement of Science holding "The Earthquake at New Madrid in 1811 Probably not an Earthquake." His arguments were that the locality did not show any indication of volcanic action, and he thought the disturbance was from subsidence due to solution of underlying strata. His evidence was the long continuance from 1811-1813; the progression from place to place to place, ending nearly 100 miles from the place of beginning; that they were never repeated in the same place; that none of the ordinary phenomena of earthquakes occurred, except subsidence; that no great alluvial region like this had ever been visited by an earthquake; that earthquakes do not occur so far from seashore."

Quotation from "Discussion of Fundamental Factors Involved in the Underwriting of Earthquake Insurance," by Alton C. Chick, October 1934.

"Since the occurrence of several severe earthquakes (e.g., St. Lawrence Valley, Long Beach, Santa Barbara) in the United States and Canada within the past 10 years, the average citizen is becoming more interested in earthquakes and their effects. Moreover, insurance companies are more generally being requested to cover damage caused by earthquakes.

Studies made by well-known authorities show that there are definite regions of seismic activity, and that no region can be considered immune from earthquake shocks. Therefore, every property owner should realize that his structures may some day be called upon to resist the forces of an

earthquake. . . . Much can be accomplished by educating the public to appreciate that severe earthquakes will occur in the future as in the past, and to recognize that it is possible practically to eliminate the loss of life and the damage to buildings by proper design and construction.

These are five main factors which must be considered in determining a premium rate for earthquake insurance: 1) frequency of occurrence of earthquakes in any particular region, 2) expected loss ratio for any given type of construction, 3) the amount of insurance coverage in relation to the sound value of the structure, 4) underwriting expenses, and 5) factor of safety and reserve. . . . The first two of these factors are more or less uncertain and must be considered with judgment. . . . The type of ground upon which a building rests has an important effect upon the amount of damage suffered by any particular type of structure. It has been found by careful investigation that often 5-10 times greater proportional damage has been done to structures built on soft, moist sands and sediments near the shoreline or on filled ground over old swamps than to similar buildings only a short distance away build on hard, firm ground, or on bedrock."

Quotation from "A Contribution to the Seismic History of Missouri," by Ross R. Heinrich.

"Published contemporaneous accounts of the first great shock of the New Madrid series, which occurred on December 16, 1811, are the first tangible evidence of earthquake study in this region. During the period of the New Madrid earthquakes and in the century following, such studies were essentially macroseismic in method, since scientists investigated principally the surface effects of these shocks. . . .

Macroseismic studies of the seismicity of Missouri date from the time the first local earthquake was recorded on the Wiechert seismograph of St. Louis University on October 23, 1909. . . . In 1925, Father Macelwane introduced a plan for a more detailed earthquake study of the Ozark region. This plan had four main objectives:

- 1) to establish seismograph stations,
- 2) to determine, if possible by suitable research, the influence of local structure on the seismic waves generated by near earthquakes,
- 3) to utilize the data . . . in detailed studies of strong local earthquakes and those with unusual characteristics and to combine, with investigations of this type, questionnaire surveys to determine the limit of affected areas.
- 4) to compile a regional seismic history showing the frequency, intensity, and distribution of Missouri earthquakes.

Contrary to a popular impression, the earthquake series of 1811-1812 was not the first evidence of seismicity in the New Madrid region."

Quotation from "Focal Mechanism Studies in the New Madrid Seismic Zone" by Robert B. Herrmann and Jose-Antonio Canas, August 1978.

"As part of a continuing studies of the nature of earthquake sources in the New Madrid seismic zone, this paper reports on recent focal mechanism studies. . . . Previous focal mechanism studies were presented by Street et al (1974) and Nuttli et al (1974). . . . The previous studies were an initial attempt at inferring something about regional tectonics and did serve to point out the complexity within the region. . . . The present study indicates a consistent picture of the nature of faulting (right lateral fault motion) on the northeast-southwest Arkansas-Tennessee trends. This is important because numerical ground motion studies can progress using the observed right-lateral motion on the trend as a starting point. . . . Recent gravity and magnetic studies (Hildenbrand et al, 1977) indicate that crustal structure along the Arkansas-Tennessee trend is rift-like or graben-like. An intriguing explanation may be that we are witnessing a reactivation of an ancient zone of weakness under the action of a stress system completely different from that which formed the zone."

SUGGESTIONS FOR FUTURE RESEARCH

Just as a mason builds a brick wall by laying one brick on top of another, future research in the New Madrid seismic zone must also build on the present state-of-knowledge. Figure 2 shows the broad range of multidisciplinary research topics that must be considered in the evaluation of earthquake hazards. The recommended priorities are:

- 1) To increase fundamental knowledge about the New Madrid seismic zone in the broader context of seismicity in the Eastern United States, focusing on the ground-shaking hazard (the physical phenomena occurring in a major earthquake that cause spectacular damage, partial failure and collapse of nonearthquake-resistant buildings, and large loss of life and injuries) and the ground-failure hazard (the "quiet" physical phenomena that cause damage through landslides, liquefaction, lateral spread failures, and flow failures).
- 2) To foster an environment for implementation of loss reduction measures (e.g., building codes, land-use planning, and zoning ordinances in urban areas located in or near the New Madrid seismic zone).

| | | |
|----------------------------|---|---|
| I. REGIONAL STUDIES | { | Where are earthquakes occurring? Why are they occurring? How often do they occur? |
| II. URBAN AREA STUDIES | { | What are the physical effects? How do they vary spatially? |
| III. RECOMMENDATIONS | { | What are the best options for reducing losses from earthquake hazards? |
| IV. TRANSFER OF TECHNOLOGY | { | How can existing knowledge be transferred and used? |

Figure 2.--When evaluating earthquake hazards in the New Madrid seismic source zone, answers to these questions are complex.

Each recommendation will be discussed briefly below.

RESEARCH ON EASTERN SEISMICITY: GROUND SHAKING AND GROUND FAILURE HAZARDS

Research on earthquake hazards in the New Madrid seismic zone will be enhanced if it is considered in the broader context of eastern seismicity. The need is for an integrated, multidisciplinary research program. Such program should build on past accomplishments, focusing on scientific and technical issues which include, but are not limited, to the following:

Issue 1: What is the relationship between the historic earthquake record, pre-existing structures, and earthquake potential?

- A) What is the contemporary distribution of seismicity?
 - 1) What part of the crust is seismogenic, and what is its physical character?
 - 2) What are the distinctive physical characteristics of eastern earthquakes?
- B) Is there a relationship between small and large earthquakes in intraplate environments?
 - 1) What are their spatial and temporal relationships?
 - 2) What are their source parameter relationships?
- C) What is the recurrence behavior of intraplate earthquakes?
 - 1) Is there evidence of progressive deformation?
 - 2) Have any events had a recurrence?
- D) What is the association between earthquakes and geologic features?
 - 1) At specific locations, is there a systematic relationship between earthquake hypocenters, their focal mechanisms, and geologic structures.

Issue 2: What is the relationship between the state-of-stress, rate of deformation, and earthquake potential?

- A) What is the rate of contemporary crustal deformation?
 - 1) Is the rate of crustal deformation spatially uniform in both the Eastern and Central United States?
 - 2) Is there a correlation between contemporary crustal deformation and the geologic and seismogenic record?

- B) What is the distribution of crustal stresses?
- 1) Is there an "Atlantic Coast Stress Province," and, if so, what is its origin?
 - 2) Is the stress field in areas of large eastern earthquakes (e.g., New Madrid and Charleston) similar or different from that in the surrounding areas.
 - 3) How does the pattern of crustal stress correlate with crustal structure, geology, and contemporary strain?
- C) What is the long-term rate of deformation as indicated in the geologic record?
- 1) What part of the crust is seismogenic and what is its physical character?
 - 2) What are the physical characteristics of eastern earthquakes?

Issue 3: What is the relationship between the strong ground motions recorded in the Western United States and those which may be expected in the Eastern United States?

- A) Are there significant differences in source characteristics of earthquakes in the Eastern United States?
- 1) What is the average stress drop expected for earthquakes in the Eastern United States?
 - 2) What is the appropriate scaling of source and ground motion characteristics with magnitude?
- B) What are the source dynamics of seismogenic failure in the Eastern United States?
- 1) What does the combination of source mechanisms, and location imply about the nature of crustal stresses in the Eastern United States?

- 2) Can source parameters and source mechanisms studies be utilized to predict seismogenic failure on a larger scale?
- C) How does the marked difference between the geology and tectonics of the Eastern and Western United States affect the expected strong ground motion?
- 1) What are the appropriate attenuation relations for peak acceleration, peak velocity, etc.?
 - 2) What properties of the Lg waveguide are relevant to predicting damaging strong ground motion?
 - 3) Can high-frequency site response be predicted from a knowledge of the near-surface velocity structure at the site?
- D) What geologic hazards tend to be triggered by ground shaking?
- 1) What are the controlling physical mechanisms?

Issue 4: How do earthquake effects correlate with local geology?

Issue 5: Can probabilistic procedures be used to model the earthquake ground-shaking hazard in the East? Are they realistic?

- A) How is uncertainty in the median value of the most important physical parameters incorporated in the model?

IMPLEMENTATION OF RESEARCH RESULTS

An important task for the future is the effective use of scientific information to reduce loss of life and damage to property caused by earthquake hazards. Successful implementation requires **COMMUNICATION** of **TRANSLATED SCIENTIFIC INFORMATION** to **RESPONSIBLE OFFICIALS** and **INTERESTED PARTIES** seeking to **REDUCE HAZARDS** by use of one or more **REDUCTION TECHNIQUES**.

The first priority is to determine the needs of policy makers in the New Madrid seismic zone area for earthquake hazards information. The second priority is to produce translated (i.e., interpreted information derived from basic scientific data) scientific information that meets the needs of these user groups. The third priority is to foster an environment for implementation of research results by local governments, utilizing workshops, training classes, questionnaires and other procedures to communicate the scientific information.

The objective of implementation activities is to make it easy for local government, engineers, architects, planners, emergency preparedness planners, and emergency responders to use the technical information generated in this program. A key strategy is to build on past successful activities such as this symposium. Partnerships between the research community and those who will ultimately use the information to implement hazard-reduction plans are necessary for success, and the strongest possible effort must be made to achieve effective partnerships.

Translated scientific information is a prerequisite to its transfer to a user and its use in a loss-reduction measure or technique. While a great deal of scientific information can be used directly by engineers or other scientists, some information must be translated to enhance its understanding and effective use by nonscientists. Examples of translated information include: locations of potential fault-rupture with forecasts of recurrence intervals and anticipated displacement, locations of liquefaction potential with levels of relative susceptibility, locations of potential landslide hazard with levels of relative susceptibility, locations of potential

inundation caused by hypothetical dam failures, and locations of potential building failures caused by ground shaking. The following actions are likely to improve use of scientific information by nonscientists:

- 1) Identify and catalog existing hazard maps and reports.
- 2) Identify the hazard maps and reports needed for hazard-reduction measures.
- 3) Estimate cost and determine responsibility, funding, and delivery of the information that can be provided.
- 4) Assure that new information is prepared in the detail and at the scales needed by the users.
- 5) Make special efforts to present the information in a format and language suitable for use by engineers, planners, and decisionmakers.
- 6) Assure that information (including discoveries, advances, and innovative uses) is released promptly through appropriate communicators and communication techniques.

CONCLUSIONS

A significant increase in knowledge about earthquake hazards in the New Madrid seismic zone has resulted from the integrated, multidisciplinary research studies of many individuals. The progress has been rapid in the past decade as research studies matured. Every effort must be made to continue the momentum that has been achieved, seeking to attain a broader understanding of eastern seismicity and to foster implementation of research results.

REFERENCES

Chick, Alton, C., (1934), Discussion of fundamental factors involved in the underwriting of earthquake insurance: Bulletin of the Seismological Society of America, v.24, p. 385-397.

Heinrich, Ross R., (1941), A contribution to the seismic history of Missouri: Bulletin of the Seismological Society of America, v. 31, p. 187-224.

Herrmann, Robert B. and Canas, Jose-Antonio, (1978), Focal mechanism studies in the New Madrid Seismic Zone: Bulletin of the Seismological Society of America, v. 68, p. 1095-1102.

Lawson, Andrew C., (1911), Seismology in the United States: Bulletin of the Seismological Society of America, v.1, p. 1-4.

Sampson, F. A., (1913), The New Madrid and other earthquakes of Missouri: Bulletin of the Seismological Society of America, v.2, p. 57-71.

Wood, H. O., (1911), The observation of earthquakes: Bulletin of the Seismological Society of America, v.1, p. 48-82.

PARTICIPANTS LIST
SYMPOSIUM ON "THE NEW MADRID SEISMIC ZONE"

Mr. Dallali Ali
Department of Plant Pathology
University of Missouri
108 Waters Hall
Columbia, Missouri 65211

Dr. Clarence R. Allen
California Institute of Technology
Pasadena, California 91125

Mr. Warren H. Anderson
Kentucky Geological Survey
Room 311 Breckinridge Hall
University of Kentucky
Lexington, Kentucky 40504

Ms. Dorothy Ank
2628 Azalea Lane
Cape Girardeau, Missouri 63701

Ms. Karen A. Ansell
3012 B. Themis
Cape Girardeau, Missouri 63701

Mr. Donald V. Babcock
1711 East Melles
Jefferson City, Missouri 65101

Mrs. Joyce Babcock
1711 East Melles
Jefferson City, Missouri 65101

Mr. James E. Beal, Jr.
University of Louisville
1135 Milton Street
Louisville, Kentucky 40217

Dr. Max E. Bell
Northeast Missouri State University
Kirksville, Missouri 63501

Dr. Terrill R. Berkland
Department of Geology
Central Missouri State University
Warrensburg, Missouri 64093

Mr. Kenneth Black
Department of Geology
Southern Illinois University
Carbondale, Illinois 62901

Dr. Robert F. Blakely
Indiana Geological Survey
611 North Walnut Grove
Bloomington, Indiana 47405

Mr. John Blattner
R.O. Hawkins Jr. High School
Highway 61
Jackson, Missouri 630752

Mr. James H. Bollwerk
Tennessee Earthquake Information Center
Memphis State University
Memphis, Tennessee 38104

Dr. Lawrence W. Braile
Department of Geosciences
Purdue University
West Lafayette, Indiana 47907

Mr. Kent M. Bratton
Southeast Missouri Regional
Planning Commission
1 West St. Joseph Street
P.O. Box 366
Perryville, Missouri 63775

Ms. Carol A. Bressan
School of Medicine
Southern Illinois University
P.O. Box 3926
801 North Rutledge
Springfield, Illinois 62708

Dr. Kenneth G. Brill, Jr.
St. Louis University
P.O. Box 8099
St. Louis, Missouri 63156

Mr. Larry Brooks
Southeast Missouri State University
Cape Girardeau, Missouri 63701

Mr. Wallace E. Brumfield
Missouri Department of Conservation
P.O. Box 233
New Madrid, Missouri 63869

Mr. Chauncy D. Buchheit
Southeast Missouri Regional
Planning Commission
P.O. Box 366
1 West St. Joseph Street
Perryville, Missouri 63775

Dr. Charles G. Bufe
U.S. Geological Survey
905 National Center
Reston, Virginia 22092

Mr. David W. Burney
Amax Lead Company of Missouri
Buick Mine
Route KK
Boss, Missouri 65440

Dr. Tom C. Buschbach
St. Louis University
St. Louis, Missouri 63103

Dr. James R. Carr
Department of Geological Engineering
University of Missouri
Rolla, Missouri 65401

Mr. Paul E. Chaplin
Department of Natural Sciences & Math
Lincoln University
Jefferson, Missouri 65101

Mr. C. W. Clendenin, Jr.
Amax Exploration
Route 5, P.O. Box 9
Salem, Missouri 65560

Mr. Bennie L. Cooper
Department of Safety and Health
Murray State University
Murray, Kentucky 42071

Mr. Brian Alexander Cowan
Federal Emergency Management Agency
500 C Street, S.W.
Washington, D.C. 22024

Mr. William R. Cramer
6642 Trebeck
Spring, Texas 77373

Dr. Loren Denney
Southwest Missouri State University
Springfield, Missouri 65804-0095
Dr. William H. Diment
U.S. Geological Survey
MS 966, P.O. Box 25046
Denver Federal Center
Denver, Colorado 80225

Mr. Richard D. Dunlap
Southeast Missouri State University
College of Science
Magil Hall
Cape Girardeau, Missouri 63701

Mr. Eric A. Durham
State Emergency Management Agency
P.O. Box 116
Jefferson City, Missouri 65102

Dr. Russell R. Dutcher
Department of Geology
Southern Illinois University
Carbondale, Illinois 62901

Dr. Tim Errol Eckstein
P.O. Box A
409 Mott Street
New Madrid, Missouri 63869

Dr. Dale Elifrib
University of Missouri
Rolla, Missouri 65401

Mr. Robert J. Ellison
Department of Geology
Southern Illinois University
Parkinson Laboratory
Carbondale, Illinois 62901

Ms. Dorothy Emery
55 York Drive
Brentwood, Missouri 63144

Dr. Edward M. Emery
Monsanto Company
800 N. Lindbergh Boulevard
St. Louis, Missouri 63167

Mr. Lewis M. Evans, P.E.
Evans Engineering, Inc.
1406 Warde Roko
P.O. Box 449
Charleston, Missouri 63834

Ms. Sharon L. Everett
Tennessee Earthquake Information Center
Memphis State University
Memphis, Tennessee 38152

Mr. Lee E. Evinger
Department of Geology
Missouri Western State College
4525 Downs Drive
St. Joseph, Missouri 64506

Dr. Stan Fagerlin
Department of Geography & Geology
P.O. Box 87
Southwest Missouri State University
Springfield, Missouri 65804-0089

Dr. Dorothy Feir
Department of Biology
St. Louis University
St. Louis, Missouri 63103

Dr. George H. Fraunfelter
Department of Geology
Southern Illinois University
Carbondale, Illinois 62901

Ms. Dee French
Charleston R-1 Schools
South Main
Charleston, Missouri 63834

Dr. D. H. Froemsdorf
College of Science and Technology
Southeast Missouri State University
Cape Girardeau, Missouri 63701

Mr. Mark H. Frumhoff
Southeast Missouri State University
825 Goodhope, Box 228B
University Hall
Cape Girardeau, Missouri 63701

Mr. Clyde E. Graham
P.O. Box 133, Route 1
Whitewater, Missouri 63785

Mr. Richard Hackett
Northwest Missouri State University
117 Garret-Strong
Maryville, Missouri 64468

Dr. Richard D. Hagni
Department of Geology & Geophysics
University of Missouri-Rolla
Rolla, Missouri 65401

Mr. Robert H. Hansman
Missouri Geological Survey
P.O. Box 250
Rolla, Missouri 65401

Dr. Syed E. Hasan
Department of Geosciences
University of Missouri
Kansas City, Missouri 64110-2499

Dr. Paul C. Heigold
Illinois State Geological Survey
615 East Peabody Drive
Champaign, Illinois 61820

Mr. Paul Hemmer
1718 Park Tree
St. Louis, Missouri 63138

Mr. Greg Hempen
USAED-St. Louis
Corps of Engineers
210 Tucker Boulevard, North
St. Louis, Missouri 63101

Dr. Sherman Henry
The School of the Ozarks
Pt. Lookout, Missouri 65726

Dr. Robert B. Herrmann
Department of Earth & Atmospheric
Sciences
St. Louis University
P.O. Box 8099
St. Louis, Missouri 63156

Ms. Donna E. Higginbotham
1549 Breezeridge Drive
St. Louis, Missouri 63131

Mr. Thomas G. Hildenbrand
U.S. Geological Survey
MS 964, P.O. Box 25046
Denver Federal Center
Denver, Colorado 80225

Mr. Steve Hohensee
322 Phillips
Maryville, Missouri 64468

Mr. Ron Hornberger
711 Washington Avenue
Cairo, Illinois 62914

Mr. John T. Howard
126 Sunset Drive
Piedmont, Missouri 63957

Mr. George Huffstutter
Charleston High School
South Thorn Street
Charleston, Missouri 63834

Ms. Sarah Lee Hunter
170 St. Thomas
New Madrid, Missouri 63869

Ms. Cynthia L. Hutchinson
Route 2, P.O. Box 139
Cabool, Missouri 65689

Mr. Max D. Hutchison
Natural Land Institute
RR 1
Belknap, Illinois 62908

Dr. Yogendra M. Kapoor
Lincoln University
Jefferson City, Missouri 65101

Mr. Robert L. Kelley
1171 Ascot Lane
Kickwood, Missouri 63112

Mr. Ernest L. Kern
Department of Earth Sciences
Southeast Missouri State University
Cape Girardeau, Missouri 63701

Dr. John D. Kiefer
Assistant State Geologist
Kentucky Geological Survey
University of Kentucky
311 Breckinridge Hall
Lexington, Kentucky 40506

Ms. Eva Kirkpatrick
Fox C-6-Seckman Jr. High
2811 Seckman Road
Imperial, Missouri 63052

Mr. R. K. Kirkpatrick
3511 Stonebrook Forest Drive
Imperial, Missouri 63052

Mrs. E. B. Kisvarsanyi
Missouri Geological Survey
P.O. Box 250
Rolla, Missouri 65401

Dr. Ray Knox
Department of Earth Sciences
Southeast Missouri State University
Cape Girardeau, Missouri 63701

Mr. Keith Koepf
Route 1, Box 563
Benton, Missouri 63736

Dr. Ellis L. Krinitzsky
Waterways Experiment Station
Corps of Engineers
Vicksburg, Missouri 39180

Ms. Dorothy Lell
Department of Earth Sciences
Southeast Missouri State University
118 Rhodes Hall
Cape Girardeau, Missouri 63701

Mr. Herbert F. Levy
901 South Hanley
St. Louis, Missouri 63105

Mr. Paul M. Long
Millers Mutual Insurance
111 E. 4th
Alton, Illinois 62052

Dr. Gary R. Lowell
Department of Earth Sciences
Southeast Missouri State University
Cape Girardeau, Missouri 63701

Mr. D. K. Lumm
Illinois State Geological Survey
207 Natural Resources Building
615 E. Peabody Drive
Champaign, Illinois 61820

Ms. Rosemary F. Lumsden
Route 4, P.O. Box 295
Poplar Bluff, Missouri 63901

Ms. Jennifer W. Mac Adam
University of Missouri
205 Waters Hall
Columbia, Missouri 65211

alinconico, Jr.
logy
University
ois 62901

rod III
ergy Systems, Inc.

IS 2
iee 37831

ieson
llege
63435

Cash

Rolla, Missouri 65401

Ms. Elizabeth Whitlow McCoy
Chillicathe Jr. High School
1529 Calhoun
Chillicathe, Missouri 64601

Ms. Mary H. McCracken
926 West 10th Street
Rolla, Missouri 65401

Mr. John David McFarland III
Arkansas Geological Commission
3815 W. Roosevelt Road
Little Rock, Arkansas 72204

Ms. Ann G. Metzger
Tennessee Earthquake Information
Center
Memphis State University
Memphis, Tennessee 38152

Dr. Brian J. Mitchell
Department of Earth and
Atmospheric Sciences
St. Louis University
P.O. Box 8099, Laclede Station
St. Louis, Missouri 63156

Dr. Thomas D. Moeglin
Geosciences Department
Southwest Missouri State University
Springfield, Missouri 65804

Ms. Linda Ann Moore
Windsor High School
6208 Highway 61-67
Imperial, Missouri 63012

Dr. Ken Moxey
Department of Psychology
Southeast Missouri State University
Cape Girardeau, Missouri 63701

Dr. Richard H. Moy
School of Medicine
Southern Illinois University
801 North Rutledge
Springfield, Illinois 62704

Ms. Susan J. Nava
Tennessee Earthquake Information Center
Memphis State University
Memphis, Tennessee 38152

Mr. John Nelson
Illinois State Geological Survey
615 E. Peabody
Champaign, Illinois 61820

Ms. Linda Nelson
1007 S.W. Boulevard, Suite A
Jefferson City, Missouri 65101

Mr. Paul W. Nelson
Natural History Program
P.O. Box 176
Jefferson City, Missouri 65102

Dr. Eldon Null
Wappapello Lumber
Wappapello, Missouri

Dr. Otto W. Nuttli
St. Louis University
P.O. Box 8099, Laclede Station
St. Louis, Missouri 63156

These
have been
Replaced

Ms. Margaret Ann Scott Odom
1 Clar Mar Place
Sikeston, Missouri 63801

Mr. James R. Palmer
Division of Geology and Land Survey
P.O. Box 250
Rolla, Missouri 65401

Professor Robert W. Parkinson
Department of Earth Science
Southeast Missouri State University
Cape Girardeau, Missouri 63701

Mr. Mark Powers
Tennessee Earthquake Information Center
Memphis State University
Memphis, Tennessee 38152

Dr. B. G. Ramsey
Department of History
Southeast Missouri State University
Cape Girardeau, Missouri 63701
Mr. Charles O. Rauch
205 East Sarno Drive
Morehouse, Missouri 63868

Dr. John Rockaway
Department of Geological Engineering
University of Missouri-Rolla
Rolla, Missouri 65401

Dr. Rene Rodriguez
St. Louis University
P.O. Box 8099 Laclede Station
St. Louis, Missouri 63156

Dr. Dean Rosebery
Northeast Missouri State University
Kirksville, Missouri 63501

Mr. James A. Roth
University of Missouri
P.O. Box 1
Malden, Missouri 63863

Dr. David P. Russ
U.S. Geological Survey
905 National Center
Reston, Virginia 22092

Mr. Bruce D. Schecater
Tennessee Valley Authority
400 West Summit Hill Drive, 174LB-K
Knoxville, Tennessee 37902

Mr. Peter Scheffler
Tennessee Valley Authority
Division of Land & Economic Resources
2A14 Old City Hall Building
Knoxville, Tennessee 37902

Mr. Robert J. Schumer
City Hall
120 N. Jackson Street
Perryville, Missouri 63775

Mr. Howard Schwalb
615 E. Peabody Drive
Illinois State Geological Survey
Champaign, Illinois 61820

Dr. Gary Sells
Northeast Missouri State University
Kirksville, Missouri 63501

Dr. Stanley D. Sides
14 Doctor's Park
Cape Girardeau, Missouri 63701

Mr. Gary D. Siville
Parkinson Laboratory
Southern Illinois University
Carbondale, Illinois 62901

Dr. Richard G. Stearns
Vanderbilt University
P.O. Box 1615, STAB
Nashville, Tennessee 37235

Ms. Sheila Steele
Earth Science Research & Consulting
Union-Hall Route 4
Carbondale, Illinois 62901

Mr. Gregory Steiner
Tennessee Earthquake Information
Center
Memphis State University
Memphis, Tennessee 38152

Dr. J. Carl Stepp
Electric Power Research Institute
3412 Hillview Avenue
Palo Alto, California 94303

Ms. M. Merrill Stevens
Department of Geological Engineering
125 Mining Building
University of Missouri-Rolla
Rolla, Missouri 65401

Dr. Edward C. Stoeber, Jr.
Department of Earth Sciences
Southeast Missouri State University
Cape Girardeau, Missouri 63709

Ms. Margaret A. Stratton
7373 Landi Court
Hazelwood, Missouri 63042

Dr. David R. Docks Tader
Department of Geology
University of Louisville
Louisville, Kentucky 40292

Mr. Jefferson Tallent
United Way of Greater St. Louis
915 Olive Street
St. Louis, Missouri 63101

Mr. Charles A. Telker
Charleston R-1 Schools
South Main Street
Charleston, Missouri 63834

Ms. Joan M. Thomas
1835 Stoddard
Cape Girardeau, Missouri 63701

Dr. Nicholas H. Tibbs
Department of Earth Sciences
Southeast Missouri State University
Cape Girardeau, Missouri 63701

Sr. Margaret E. Tucker
Fontbonne College
6800 Wydown Boulevard
St. Louis, Missouri 63105

Mr. Charlie A. Tucker, Jr.
Meramec Community College
11333 Big Bend Boulevard
Kirkwood, Missouri 63122

Mr. C. Scott Turner
2347 Belleridge Pike
Cape Girardeau, Missouri 63701

Professor Louis Unfer, Jr.
Department of Earth Science
Southeast Missouri State University
Cape Girardeau, Missouri 63701

Mr. James D. Vaughn
Division of Geology & Land Survey
P.O. Box 250
Rolla, Missouri 65401

Mr. Christopher Vierrether
3012 B. Themis
Cape Girardeau, Missouri 63701

Mr. Jerry D. Vineyard
Assistant State Geologist of Missouri
Missouri Geological Survey
P.O. Box 250
Rolla, Missouri 65401

Mr. John T. Waltrip
309 Salcedo Road
Sikeston, Missouri 63801

Dr. Peter W. Whaley
Murray State University
Murray, Kentucky 42071

Mr. Heyward M. Wharton
Missouri Geological Survey
P.O. Box 250
Rolla, Missouri 65401

Ms. Corinne Whitehead
League of Women Voters Kentucky
P.O. Box 25, Route 9
Benton, Kentucky 42025

Dr. James Hadley Williams
Division Geology & Land Survey
P.O. Box 250
Rolla, Missouri 65401

Mr. Jim Henry Wilson
Endangered Species Coordinator
P.O. Box 180
Jefferson City, Missouri 65102

Dr. Jeanene Yackey
Natural Sciences Department
Fontbonne College
6800 Wydown Boulevard
St. Louis, Missouri 63105